YOLLA 3

T/L1 OFFSHORE BASS BASIN

WELL COMPLETION REPORT
INTERPRETIVE DATA

D.M. Brooks & K. Bierbrauer

Origin Energy Resources Ltd
339 Coronation Drive
MILTON QLD 4064
Australia

MAY 2005

Distribution List:

Chief Geologist

Chief Geophysicist

Subsurface Manager BassGas

Contents

1. WELL INDEX SHEET

Permit Interests:	Origin Energy Resources Ltd (32.5%) - OPERATOR Origin Energy Northwest Pty Ltd (5%) AWE Petroleum Pty Ltd (30%) CalEnergy Gas (Australia) Ltd (20%) Wandoo Petroleum Pty Ltd (12.5%)
Rig on Location:	06/06/2004
Spud:	11/08/2004
Reached TD:	04/09/2004
Rig Released:	30/09/2004
Total Rig Days:	56
Rig Name:	ENSCO 102
Drilling Contractor:	ENSCO
Total Depth:	3497m MDRT (Drillers) 3057.3 mSS (Drillers)
Well Status:	Cased Gas Producer

Well Name:	Yolla 3
Basin:	Offshore Bass
Permit:	T/L1
Type:	Deviated Production Well
Water Depth:	80.8m (MSL to seabed)
Elevation:	43m (RT-sea level)
Latitude:	39° 50' 40.4707"S
Longitude:	145° 49' 06.0849"E
Easting:	398 905.69metres
Northing:	5 588 825.22metres
(GDA 94; UTM Zone 55S, Central Meridian 147° East).	
Seismic Reference:	In-line 480, X-line 1000 Yolla 3D survey
Actual Well Cost:	A$ 23,329,727

FORMATION TOPS

FORMATION / *SEISMIC MARKER*	**TOPS (m)**				**REMARKS/SHOWS**
	m MDRT	m TVDSS	THICK (rel to TVD)	TWT (ms)	
Torquay Group	123.8	80.8	963.3	128	No Returns 123.8 – 1017.0 mMDRT. Claystone, calcareous.
Upper Angahook Formation	1221.6	1044.1	191.6	868	Claystone, calcareous in part
Angahook Volcanics	1486.0	1235.7	130.0	1028	Volcanic Tuff interbedded with claystone and sandstone and minor siltstone
Angahook Oligocene	1659.0	1365.7	292.3	1136	Interbedded sandstone, siltstone and claystone, grain size decreasing with depth
Demons Bluff Formation	2034.0	1658.0	129.6	1378	Siltstone with minor interbedded sandstone and occasional dolomite
Eastern View Coal Measures	2184.8	1787.6	1233.4	1487	Interbedded Sandstone, coal, siltstone and minor claystone
TEV4	*2217.5*	*1816.0*	*8.2*	1510	Sandstone (oil and gas)
TEV4 OWC	*2234.7*	*1831.0*	*NA*		
2458 sand	*2902.8*	*2464.4*	*16.3*	*1922*	*Water bearing sand (oil in Yolla 4)*
Igneous Intrusive	*2994.5*	*2555.5*	*64.4*	1974	*Gabbro*
2718 sand	*3145.3*	*2705.8*	*8.2*	*2043*	*Water bearing sandstone*
2755 sand	*3179.8*	*2740.2*	*16.2*	*2061*	*Gas-bearing sandstone*
2809 sand	*3236.5*	*2796.9*	*23.4*	*2090*	*Gas-bearing sandstone*
2844 sand	*3269.6*	*2830.0*	*11.0*	*2107*	*Tight Sandstone*
2873 sand	*3300.6*	*2861.0*	*10.3*	*2123*	*Tight sandstone*
2952 sand	*3383.0*	*2943.3*	*10.4*	*2164*	*Tight sandstone*
2973 sand	*3404.1*	*2964.4*	*19.5*	*2174*	*Gas-bearing sandstone*
Basal Volcanics	3460.7	3021.0	36.3+	2202	Volcanics: basalt and weathered basalt
TOTAL DEPTH	3497.0	3057.3			

FORMATION EVALUATION WHILE DRILLING

Hole Size (inches)	Interval (mMDRT)	MWD services	LWD services
16	215 - 1012	DWD with PCD-R	none
12.25	1017 – 1593	P4M-DIR-FE	DGR - EWR-P4
12.25	1593 – 2216	P4M-DIR-FE	DGR - EWR-P4
12.25	2216 – 2347	P4M-DIR-FE	DGR - EWR-P4
8.5	2347 – 3497	P4M-DIR-FE	DGR – EWR-P4

WIRELINE LOGS

Suite #	Run #	Interval (mMDRT)	Logs Acquired
1	1	3474 m - surface	PEX-HRLA-CMR-SP-GR-LEHQT
1	2	3494 – 1000 m (HNGS-DSI to 120)	FMI-DSI-HNGS-ECS-LEHQT
1	3	3479.5 – 3148.6 m	MDT-GR (pre-tests)
1	4	3420.6 – 3149 m	MDT-GR (sampling)
1	5	3453 – 2281 m	USIT-CBL-VDL-GR-CCL
1	6	2265 – 1350 m	USIT-CBL-VDL-GR-CCL
1	7-11	3248.5 – 2210.2 m	4 ½", 12 spf, HSD 34JL, Pure Perforating Record
1	12-13	3258 - 3258	CPST Packer Set, Packer Setting Record

CORES

CONVENTIONAL

Core #	Interval (mMDRT)	Cut (m)	Rec (m)	Formation
1	2216.00 – 2234.10	18	18.1 (100%)	Top EVCM TEV4 sand

SIDEWALL

Suite#	Run#	Type	Interval (mMDRT)	Bullets	Mud	Empty	Low Rec	Recovered
None Taken								

PRESSURE TESTING AND FLUID SAMPLING

Suite#	Run#	Type	Interval (mMDRT)	Total Tests	Valid Tests	Supercharged	Tight Tests	Retests	Lost Seal	Samples Collected
1	4	MDT	3479.5 – 3148.6	65	25	15	24	0	1	5

HOLE & CASING DETAILS

Hole Size	Interval (mMDRT)	Casing Size	Shoe Setting Depth (mMDRT)
		20"	215
16 "	124 - 1012	13 $^{3}/_{8}$ "	1007
12 ¼ "	1012 - 2347	9 $^{5}/_{8}$ "	2340
8 ½ "	2347 - 3497 (TD)	6 $^{5}/_{8}$ "	3497

2. WELL SUMMARY

Yolla 3 was drilled as a deviated development well in the northern part of the Yolla Gas Field in the offshore Bass Basin, Tasmania within Production Licence T/L1. The well is located approximately 120 kilometres offshore from Tasmania and 200 kilometres south south-east of Melbourne, Victoria (Figure 1). The well was drilled using the ENSCO 102 jack up drilling rig, which was temporarily cantilevered over the top of the Yolla A permanent production platform. The well was directionally drilled in a northwest direction from the platform. Yolla 3 was designed to target the sandstone reservoirs of the Eastern View Coal Measures (EVCM) previously intersected and evaluated in Yolla 1 and Yolla 2.

Yolla 3 spudded on the 11th August 2004. Primary objectives within the Paleocene, termed 2718, 2755, 2809 and 2973 sand units, were intersected close to prognosed depth. The secondary objective, the Eocene TEV4 sand at the top of the EVCM was also encountered close to predicted depth. All primary objectives were production tested and flowed gas and condensate. The secondary objective flowed oil and gas on test. The well reached total depth of 3497 mRT (3057.3 mTVDSS) on 4th September 2004. Following production testing, the rig was skidded back to Yolla 4 for further testing on 30th September 2004.

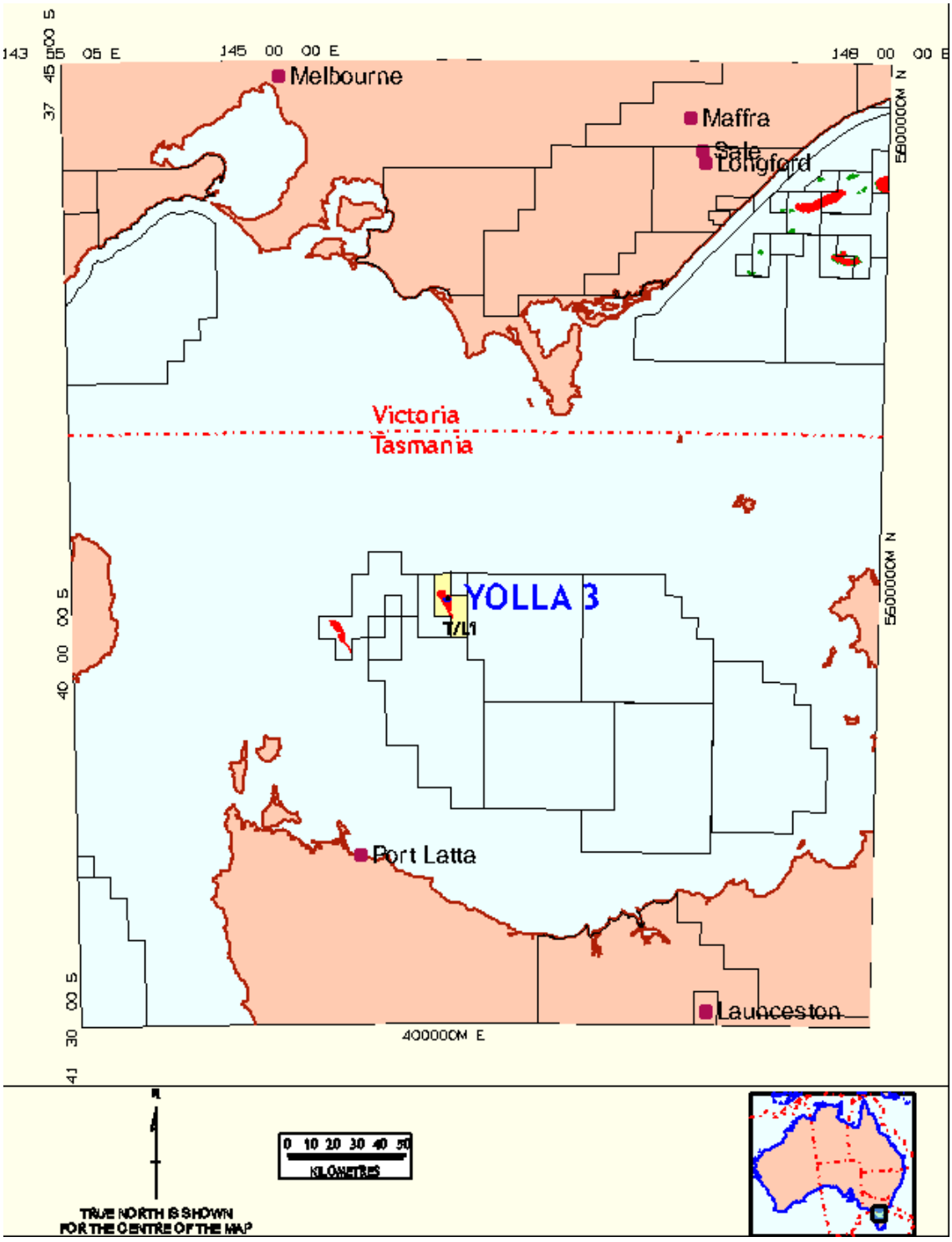

Figure 1: Yolla 3 location map

3. WELL RESULTS

3.1 Hydrocarbons Encountered

Mudlog gas readings commenced from 1017mRT. Background gas readings in Yolla 3 remained fairly steady down to the base of the Miocene section of the upper Angahook Formation (total gas range 1 – 65 units). No significant gas peaks were recorded and no fluorescence was observed.

The first sandstone in the well was intersected at a depth of 1544mRT, within the Miocene age Angahook volcanics. At this depth a gas peak of 748 units, including up to C5, was recorded. Gas readings dropped to lower levels (average 147 units total gas) below 1555mRT. Three more gas peaks were seen within this unit, one at 1583m reached total gas of 216 units. The zone of elevated gas readings between 1593 – 1607mRT reached 295 units total gas. The last gas peak in the volcanics units between 1625 – 1635mR recorded maximum total gas of 277 units.

Throughout the remainder of the Angahook Formation and the underlying Demons Bluff Formation, background gas readings steadily increased from average 50 units to 111 units, with one gas peak recorded within sandstone interbeds at 2140mRT (1069 units total gas).

Immediately upon entering the Eastern View Coal Measures gas readings climbed sharply to a total gas peak of 472 units at 2216mRT. The interval from 2216 – 2234mRT was cored. The total gas readings remained high during coring, ranging from 331 to 491.6 units. Fluorescence was noted in the core chip descriptions between 2221mRT and 2234mRT. The fluorescence is described as trace to 60% dull yellow to bright blue-green, pinpoint to very slow even direct cut, no to blooming bright green/cream crush cut and no to moderately bright green/cream broken residue ring. Strong hydrocarbon odour was present in the samples containing fluorescence down to 2229mRT. The well is interpreted to have encountered 7m of the gas column and 9.7m of the oil column which was first discovered in Yolla 1. The GWC is interpreted to be at a depth of 1822mTVDSS and the OWC at 1831.7mTVDSS.

Gas readings reduced to high background levels averaging 230 units between 2234mRT – 2279mRT. Total gas remained at lower background levels averaging between 4 and 41 units from 2279mRT to 3144mRT, except for minor peaks at coal beds.

Between 2904 and 2946mRT 3 to 5% fluorescence in sandstone cuttings was recorded. The fluorescence is dull yellow to very dull green, patchy to pinpoint slow direct cut, fast to trace crush cut, moderately bright green/cream broken residue ring. Gas readings remained at low levels ranging form 27 – 48 units. This unit is stratigraphically correlated to the oil-bearing sand in Yolla 4 which is informally referred to as the 2458 sand.

The 2718 sand was encountered between 3145.3 to 3153.5mRT. Total gas readings rose to a peak of 176 units and fluorescence was noted in this sand. The fluorescence consisted of 5 – 8% dull cream, spotted, slow direct cut, moderately bright white fast streaming crush cut, moderately bright yellow green thick residue ring.

Below the 2718 sand, but above the 2755 sand, total gas readings averaged 64 units within a mainly siltstone unit. However a sandy interval between

3154 – 3159m contained fluorescence and had an associated total gas peak of 119 units. The fluorescence is described as 5 – 8% dull cream, spotted, slow direct cut, moderately bright white fast streaming crush cut with a moderately bright yellow green thick residual ring.

At 3179.8mRT the 2755 gas zone was intersected and total gas readings rose to 351 units, dropping to background levels at 3195mRT. Within this sand, fluorescence in cuttings between 3183mRT – 3195mRT is described as trace – 20% moderately bright yellow, spotted slow direct cut, moderately bright white fast streaming crush cut, bright cream/green thick residue ring. Log analysis, MDT and production test results indicate a 6.4m (relative to TVD) net gas column was intersected with the GWC at 3272.7mRT (2833mTVDSS).

Between the 2755 gas zone and the 2809 gas zones (3195 – 3235.5mRT), gas levels generally remained at background levels averaging 57 units.

The 2809 gas zone had average total gas readings of 308 units and fluorescence occurred intermittently between 3237 and 3240mRT. The fluorescence was trace dim green spotted direct cut, fast off-white crush cut, moderately bright green / cream thin residue ring. Log analysis, MDT and production test results indicate a 11.9m (relative to TVD) net gas column was intersected with the GWC at 3266.2mRT (2826.5mTVDSS).

Below the 2809 gas zone, from 3235 – 3382mRT total gas levels within the predominantly siltstone and claystone interval averaged around 30 to 55 units. One small sandstone unit (termed the 2873 zone) contained a gas peak of 119 units between 3001 – 3308.5mRT.

The 2952 sand was intersected from 3383.0 to 3393.4mRT where gas peaked at 153 units. Background gas readings remained moderately high (19 to 89 units) from 3384mRT to the top of the 2973 gas zone at 3404.1mRT.

The 2973 gas zone exhibited two zones of high gas peaks. The upper one from 3402 – 3406mRT had total gas readings up to 343 units. The total gas in the lower zone between 3414.5 and 3422mRT peaked at 317 units. Fluorescence in the interval 3383 – 3390mRT consisted of pale olive, slow, pin-point direct cut, moderately bright white fast even crush cut and bright white thin residue ring. Log analysis, MDT and production test results indicate 2 gas columns within the 2973 sand. The respective GWCs are interpreted at 3426.2mRT (2986.5mTVDSS) and 3429.7mRT (2990.0mTVDSS).
The net pay of the combined sand units is 8.2m (relative to TVD).

From the base of the 2973 gas zone to top of the volcanics (3459mRT) total gas readings remained low averaging 45 units. Between the top of the volcanics to total depth (3497mRT) gas readings slowly decreased from 10.9 to 4.8 units.

3.2 Stratigraphy

The generalised stratigraphy of the Bass Basin is illustrated in Figure 2 and the stratigraphic section intersected by Yolla 3 in Figure 3. As can be seen in Figure 3, the actual stratigraphy encountered was very similar to the prognosed stratigraphy.

Lithological descriptions from ditch cuttings and conventional core (see Appendices 1 and 2, Yolla 3 Well Completion Report Volume 1, Basic Data), together with the MWD and wireline log interpretation (Appendix 1, this volume), provide the basis for the stratigraphic breakdown in the

Composite Well Log (Enclosure 1). All thicknesses quoted are referenced to TVDSS depths.

Torquay Group
(123.8 to 1221.6mRT, 80.8 to 1044.1mTVDSS)

The Torquay Group in Yolla 3 is approximately 963.5mTVD thick. The unit is interpreted to be deposited under shallow marine conditions and can be seismically divided into two upper units separated by a prominent seismic marker called the 'Lower Miocene Seismic event'. This event separates the Pliocene to Miocene mainly calcareous dominated lithology from the underlying Miocene age claystone. The third and lowermost unit of the group is the Angahook Formation, which itself can be divided into 3 sub-units.

Returns were established from 1017mRT therefore lithology above this depth is assumed to be similar to the offset well Yolla 1. In Yolla 1 the top portion of the Torquay Group consists of a bioclastic limestone. This upper limestone section comprises white to mid-grey, coarse- to fine-grained unconsolidated bioclastic calcarenite to calcirudite composed of friable and loosely cemented skeletal debris consisting of pelecypods, bryozoans, foraminifera and gastropods. The fragment size decreases with depth with biocalcirudites grading to biocalcarenites and calcarenites and finally calcilutites. Quartz grains appear in the lower portion of the limestone interval. There is a general increase in the proportion of clay in silt towards the base of this interval.

The lower portion of the Torquay Group is described in Yolla 3 as a claystone which is light grey to medium grey and olive grey, trace cream, soft to very soft, sub-blocky, 10% calcareous clay size grains, 80 to 90% clastic clay grains and 0 to 10% clastic silt size grains with trace amounts of: fossil fragments, forams and disseminated pyrite.

Angahook Formation
(1221.6 to 2034.0mRT, 1044.1 to 1658.0mTVDSS)

Overall the thickness of the Miocene to Oligocene Angahook Formation in Yolla 3 is 613.9mTVD. This unit is distinctive from the overlying upper units of the Torquay Group due to reworking and presence of volcanics and sediments proximal to centres of Miocene volcanism (*Lennon et al, 1999*).

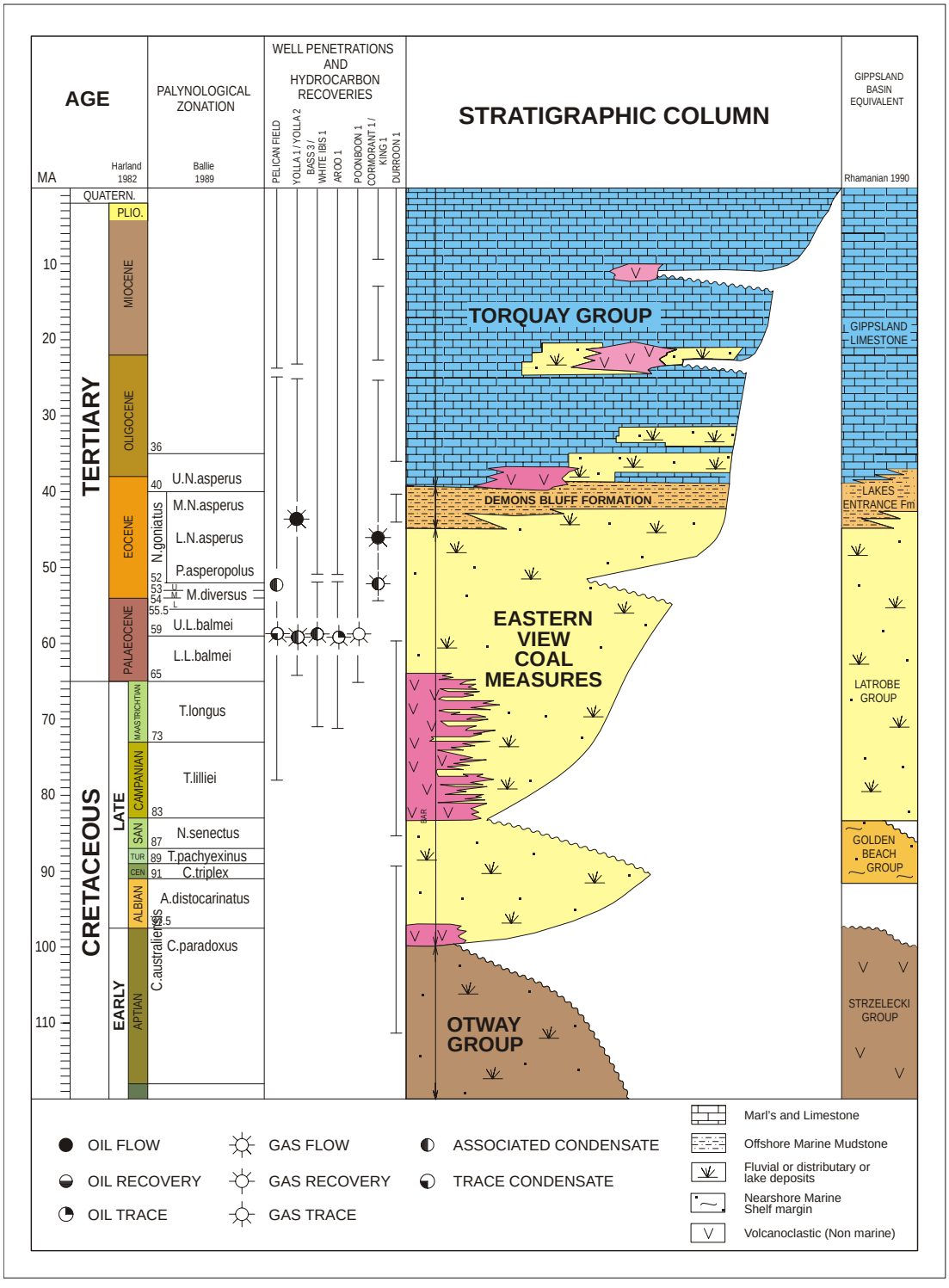

Figure 2: Generalised Stratigraphy of the Bass Basin

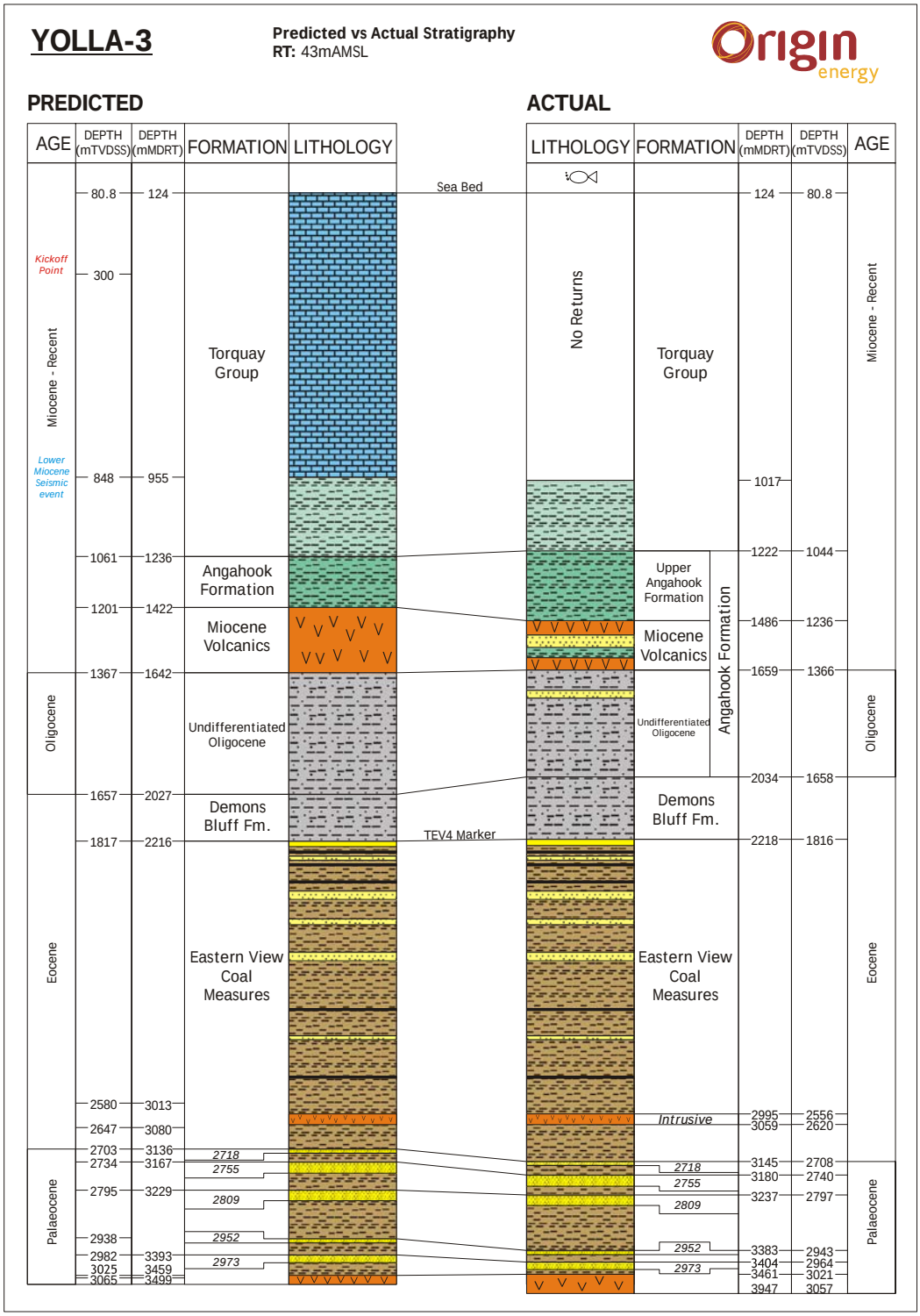

Figure 3: Yolla 3 Predicted versus Actual Stratigraphy

Upper Angahook Formation
(1221.6 to 1486.0mRT, 1044.1 to 1235.7 mTVDSS)

In Yolla 3 the upper 157.7m (drilled thickness) of the Angahook Formation consists of calcareous claystone with minor interbedded siltstone. The claystone is light to medium grey, very soft to dispersive, sub-blocky, is up to 20% calcareous and contains 20% silt, and trace pyrite and fossil fragments, including forams and bryozoans. The siltstone is composed of medium grey/brown coloured silt grains which are very soft to firm, sub-blocky and include 5 to 10% calcareous clay size grains, 10% clastic clay grains and 10 to 20% fine grained sand. Accessories include up to 10% calcite, trace pyrite and fossils and forams. The basal interval from 1380 to 1486mRT is still predominantly claystone but overall there is an increase in siltstone and trace sandstone compared to the overlying sequence. The claystone in the basal section consists of medium to dark grey and olive grey clastic clays which are very soft, amorphous to sub-blocky and contain up to 10% calcareous clay size grains, 20% clastic silt grains and traces of fossil fragments and pyrite. The siltstone is the same as the overlying zone but with trace carbonaceous matter appearing near the base of the formation. The sandstone is light grey and yellow/grey, friable to firm, blocky, contains 5% calcareous clay size grains, 30 to 40% clastic clay grains, 0 to 10% silt and 50 to 60% very fine sand, very well sorted, well rounded, spherical with 5% moderately hard calcite cement, trace fossils and bryozoans and 3% visual intergranular porosity.

The log response through this interval is a fairly uniform GR and resistivity response with a slight decrease in GR from the top of the unit to the base suggesting a gradual fining upward trend in grainsize. The mudlog shows a minor but consistent increase in gas and wet gas from the top to the base.

Angahook Volcanics
(1486.0 to 1659.0mRT, 1235.7 to 1365.7mTVDSS)

The volcanic-rich interval within the Angahook Formation in Yolla 3 is described as interbedded volcanic tuff, claystone, sandstone and minor siltstone. The top of the unit is distinctive on logs due to the gamma-ray (GR) response of the tuffs compared to the overlying claystone. The top of the unit is picked on the first low GR response (which overall is 35 m drilled thickness in Yolla 3). This feature is correlatable to Yolla 1 and Yolla 4. The tuff is assumed to be sourced from the Miocene volcano which is evident on seismic and located just to the north of the Yolla Field.

The volcanic tuff is light bluish grey and off-white in colour, very soft and amorphous to firm, with tuffaceous texture in part with a predominantly silt to very fine sand size quartz and glassy ground mass, commonly the tuff is weathered to claystone. The claystone is brownish grey to light medium grey colour, very soft, amorphous containing 5% calcareous grains, 20% silt and trace amounts of fossils and pyrite. The sandstone is described as volcanoclastic, light to medium mottled brown, very soft to soft, sub-blocky with trace to 10% calcareous clay and 30% clastic clay, 40% very fine sand, 20% fine sand, well sorted, rounded, sub-spherical, weak argillaceous matrix, trace calcite and trace visual intergranular porosity. The siltstone is medium to light brown to cream, soft, sub-blocky and contains trace to 10% calcareous clay size grains and 30 to 40% clay, 50% silt, 10% very fine sand grains, trace to 10% calcite and trace pyrite.

Undifferentiated Oligocene
(1659.0 to 2034.0mRT, 1365.7 to 1658.0mTVDSS)

The remaining basal interval of the Angahook Formation is a clastic dominated marine unit of interbedded sandstone, siltstone and rare claystone, within increasing percentage of siltstone and decreasing sand content down hole.

An apparent increase in sandiness from the GR response, compared to the overlying unit, characterises the top of this interval. There is a gradual decrease in grain size down hole. The overall GR and resistivity log responses (from the LWD tools) is fairly bland.

Siltstone is the dominant lithology in this interval and consists of light to dark, predominantly medium brown colour, soft to friable to firm, sub-blocky to blocky, 10 to 30% calcareous clay size grains, 30% clastic clay grains, 50% silt and 10% very fine sand size grains, abundant loose quartz grains and trace glauconite, trace pyrite. The sandstone is light brown to off-white, sometimes mottled brown, friable to firm, sub-blocky to blocky, with 0 to 10% calcareous clay grains, 5 to 10% clay size grains, 10 to 30% silt, 40 to 50% very fine sand and 0 to 10% fine sand grains, well to moderately sorted, sub-angular to sub-rounded, sub-spherical grains with a weak calcareous cement moderately strong argillaceous matrix in part and accessories are 0 to trace glauconite, abundant kaolinite, trace to abundant calcite and trace to 3% intergranular porosity. The rare claystone interbeds are light brown to cream coloured, very soft, dispersive, and is made up of 20% calcareous clay grains, 60% siliciclastic clay, 20% silt grains.

Offset well palynological analysis suggests this zone was deposited in a very nearshore marine environment.

Demons Bluff Formation
(2034.0 to 2184.8mRT, 1658.0 to 1787.6mTVDSS)

The Demons Bluff Formation lithology is dominated by siltstone within minor interbedded sandstone and trace dolomite. This formation forms a thick regional seal over the EVCM.

The GR logs at the top of the unit show a distinct baseline shift indicating a reduction in overall grainsize compared to the Angahook Formation. The LWD GR and resistivity log responses throughout the interval is very uniform.

The siltstone is dark grey to greyish black and medium dark grey to brown, soft to moderately hard, sub-fissile, trace calcareous clay grains, 15 to 30% clay, 70 to 80% silt, 5 to 10% very fine sand, 0 to 5% fine sand size grains with traces of mica, carbonaceous matter and foraminifera. The sandstone consists of medium brown to light brown and grey coloured grains, soft to moderately hard, mainly firm, blocky made up of 5% calcareous clay, 25 to 30% siliciclastic clay, 20 to 30% silt, 40% very fine sand and 0 to 10% fine sand, well to moderately well sorted, sub-angular to sub-rounded, sub-spherical, argillaceous matrix with moderate to weak strength, strong dolomitic and calcareous cement in top part of the formation, moderately strong siliceous cement at the base, trace glauconite, forams and pyrite and trace visual intergranular porosity. The minor dolomite is described as light brown to tan, hard, blocky occasional sub-conchoidal fracture.

Yolla 4 palynological information indicates marginal marine conditions prevailed during Demons Bluff Formation deposition.

Eastern View Coal Measures
(2184.8 to 3460.7mRT, 1787.6 to 3021.0mTVDSS)

The Eastern View Coal Measures (EVCM) is a very thick succession of non-marine fluvio-lacustrine deposits at the base to nearshore and marginal marine sediments at the top of the formation. Younger volcanic related intrusives are also present within this formation. The formation ranges in age from Eocene to Paleocene in Yolla 3 (based on palynological age dating from Yolla 1).

The formation can be split into 3 broad lithological units. The top unit dated as Eocene based on the presence of the lower *N.asperus* spore pollen zone in Yolla 1, is sandstone-rich and is interpreted to be deposited in a marginal marine to near-shore marine environment. The middle unit is a highly thinly interbedded coal, siltstone and minor sandstone and is also Eocene as it includes the *P.asperopolus* to middle *M.diversus* spore pollen zones. These sediments are interpreted to have been deposited in a marginal marine to non-marine lacustrine/lagoonal settings. The basal interval is dominated by thick beds of siltstone and sandstone and was deposited in a fluvial setting. The age of these sequences is Paleocene, as they span the spore-pollen zones lower *M.diversus* to lower *L.balmei*.

The topmost unit of the EVCM spans the drilled depth range 2184.8 to 2492mRT in Yolla 3. This interval is dominated by sandstone within interbedded siltstone, and minor thin coal beds appearing near the base of the unit.

The topmost sand of the EVCM is termed TEV4 and is gas and oil bearing in Yolla 3. The entire hydrocarbon zone was cored from 2216 – 2234m. Five thin sections from core plugs which represented end members in the permeability, porosity and grain density measured within the TEV4 sand were submitted for petrological analysis (Appendix 4). The samples are variably argillaceous to clean, very fine grained quartzarenites in which framework grains are mainly quartz and, below 2216.70m, peloidal glauconite. Detrital clay forms dispersed matrix and is concentrated into irregular patches, along discontinuous thin laminae and around sandy burrow fills. Sandstone at 2230.27m is clean. Authigenic clay is almost entirely kaolinite. Diagenetic effects include siderite and pyrite replacement, glauconite compaction, authigenic kaolinite formation and incipient quartz overgrowth precipitation. Clean, quartzose sandstone is poorly compacted and uncemented. Visible macroporosity ranges from 0.6% to 30.8% and varies mainly according to detrital clay + siderite content. Being little affected by diagenesis, sandstone is highly permeable where it is clean and quartzose. High grain density at 2219.36m reflects the presence of significant amounts of siderite that is associated with detrital clay.

The sandstone over the remainder of the upper EVCM is described as medium brown to light yellow brown, light brown grey, light brown to cream and off-white, clear to translucent, soft and friable to firm, sub-blocky to dispersive and is composed of 0 to 30% clay, 0 to 30% silt, 0 to 50% very fine sand grains, 0 to 15% fine sand and 0 to 50% medium sand grains, 0 to 50% coarse sand grains, 0 to 30% very coarse sand grain size, which are poorly to well sorted, rounded to angular, sub spherical to sub-elongate, weakly argillaceous and weak calcareous cement, occasionally trace pyrite cement, trace forams and trace to 15% intergranular visual porosity. The interbedded siltstone is medium to dark brown to brown grey to dark grey and medium grey to grey-black, friable to firm, sub-blocky to sub-fissile, consisting of 10 to 40% clay, 55 to 80% silt and 5 to 20% very fine

sand grains, and traces of pyrite, mica and fossils, and trace to 10% carbonaceous grains. The coals are described as black to very dark brown, firm to friable, blocky, vitreous to sub-vitreous, trace to 15% clay, nil to 30% silt and nil to trace very fine sand.

The middle EVCM unit was intersected between 2492 to 2994.5mRT. This portion of the EVCM is composed of thinly bedded siltstone, coals, sandstone and minor claystone. The siltstones intersected are light to medium brown to brown black and grey black and becoming light to medium to dark brown and dark grey to grey brown with depth, firm to soft, sub-fissile to blocky, composed of 10 to 30% clay, 50 to 90% silt, nil to 30% very fine sand grains, 0 to trace fine sand grains with traces of micro mica and trace carbonaceous grains, grading to carbonaceous siltstone in part. The coals are dull black to black to dark brown, friable to firm, blocky, sub-vitreous to vitreous, with trace to 10% clay and nil to 5% silt. The sandstones are all very fine grained and silty and are described as off-white to light brown and light grey-brown, very soft to friable, dispersive to sub-blocky and composed of 10 to 40% clay, 10 to 40% silt, 30 to 50% very fine sand, nil to 20% fine sand grains, moderately to well sorted, rounded to sub-angular, sub-spherical, and 10 to 30% kaolinite matrix, weak argillaceous cement, trace carbonaceous grains and trace to 3% intergranular visual porosity.

The oil bearing 2458 Sandstone that was encountered in Yolla 4 is water wet in Yolla 3 and was intersected between 2902.9 and 2919.2mRT.

At the base of this middle section, from 2994.5 to 3059.1mRT, a thick igneous sill has intruded into the sediment pile. The intrusive is a dolerite/gabbro described as mottled green, grey, black and off-white with occasional yellow and tan grains, hard, irregular, clear crystalline definition, common olivine, pyroxene, hornblende, plagioclase, and trace disseminated pyrite.

Below the intrusive, the lowermost portion of the EVCM was intersected between 3059.1 to 3460.7RT. This interval is dominated by thickly bedded siltstones and sandstones, minor claystone and rare coal. This section contains the primary targets of the well which are the gas-bearing reservoirs of the Yolla Field known as the 2755, 2809 and 2973 sands.

Above each of the reservoir zones are thick siltstone units which are providing top seal over the gas pay. The siltstones are described as medium to very dark grey to grey/brown, trace light brown, friable to hard, sub-fissile to sub-blocky, composed of 10 - 30% clay, 60 - 90% silt, 5 - 10% very fine sand grains with traces of micro mica and pyrite, occasionally very carbonaceous (up to 20%). Claystone within the sealing intervals is off-white to light brown, soft, sub-blocky and consists of 40% clay, 30% silt, 30% very fine sand and trace fine sand, up to 25% kaolinite and trace coal. The rare coal is black, vitreous, firm, blocky and brittle.

The first sand unit encountered in this interval is the 2718 sand. This sand is 6.4m thick (relative to TVD) and present between 3145.3 to 3153.5mRT. The sand had previously been interpreted as gas-bearing in Yolla 1 but was clearly water saturated and very tight in Yolla 3. The sandstone is described as cream, light to medium brown, soft, sub-blocky consisting of 15% clay, 20% silt, 50% very fine sand and 15% fine sand grains which are well sorted, sub-angular, sub-spherical and weak argillaceous matrix, 5% visual intergranular porosity.

The topmost major sand unit to be drilled was the 2755 sand between 3179.8 to 3196.0mRT. This gas-bearing sand consists of mainly sandstone

with minor siltstone. The sandstone colour varies from off white to light grey and is friable and sub-blocky, composed of 20% clay, 10% silt, 10% very fine sand, 50% fine sand and trace medium sand grains, well sorted, sub-rounded, sub-spherical, weak argillaceous matrix, trace carbonaceous grains with 10% visual intergranular porosity.

The 2809 gas-charged sand is the third sand encountered in this section and is present between 3236.5 – 3259.9mRT with a vertical thickness of 23.4m. The sands in this interval are described as off-white to very light grey and clear to translucent and minor brown-stained grains, loose to friable and sub-blocky comprising 0 – 10% clay, 0 to 10% silt, 0 to 50% very fine sand, 0 to 30% fine sand grain size, 0 to 10% medium sand, trace to 50% coarse sand and 0 - 40% very coarse sand size grains, which is mainly poorly to moderately sorted, sub-angular to angular, elongate to sub-elongate grains with weak argillaceous and weak to moderately strong siliceous cement, 5 to 25% visual intergranular porosity.

Below the 2809 sand, two coarsening upward sequences are present which and culminate in 2 sand units at the top. The higher unit is termed the 2844 sand and the deeper is called the 2873 sand. In Yolla 3 the 2844 and 2873 sand units are both water bearing and tight. The sandstones of these 2 units consist of off-white to very light grey, friable and sub-blocky, 10% clay, 10% silt, 40% very fine sand, 40% fine sand, and trace coarse sand, well sorted, sub-rounded, sub-spherical, trace siliceous cement and up to 20% weak argillaceous matrix and 5% visual intergranular porosity.

A very thick siltstone is present between the 2873 and the deepest sandstone units in the well. The siltstone is dark grey and brown grey, firm and friable, sub-fissile, composed of 20% clay, 80% silt, trace very fine sand and trace mica.

The 2952 and 2973 sand units are the deepest gas-bearing unit in Yolla 3. The 2952 sand occurs between 3383.0 and 3393.5mRT and the 2973 sand between 3404.1 – 3423.6mRT. The thin 2952 sandstone is light brown, firm, sub-blocky and 20% clay, 10% silt, 50% very fine sand and 20% fine sand, well sorted, sub-rounded, sub-spherical, with up to 20% weak argillaceous matrix and 5% visual intergranular porosity. The thicker and coarser sands of the 2973 gas zone are off-white with clear and translucent grains, loose and dispersive composed of 30% medium sand, 40% coarse sand and 30% very coarse sand size grains which are moderately sorted, angular and sub-spherical with trace of argillaceous matrix and 20% visual intergranular porosity. The 2973 zone also contains an argillaceous sandstone which is described as cream to off white coloured, very soft, sub blocky, 40% clay, 20% silt, 40% very fine sand, well sorted, sub angular, sub spherical, weak argillaceous cement, 40% kaolinite with trace intergranular porosity.

Below the gas-bearing zones in the well, the basal 37m of the EVCM consists of interbedded argillaceous very fine sandstone and siltstone. The sandstone is cream to light to medium brown, soft, sub-blocky comprising 30% clay, 30% silt, 30% very fine sand and 10% fine sand which is well sorted, sub-rounded and sub-spherical grains with 30% weak argillaceous (kaolinite) matrix and 3% visual intergranular porosity. The siltstone is dark to medium brown, friable to firm, sub fissile, 30% clay, 70% silt, trace very fine sand, trace carbonaceous material, mica and coal.

Basal Volcanics
(3460.7 to 3497.0mRT, 3021.0 to 3057.3mTVDSS)

Between the base of the EVCM and total depth in Yolla 3 a basalt sequence was drilled. The basalt intersected in Yolla 3 varies from relatively fresh to weathered. The age of the basalts is interpreted to be Late Cretaceous or Early Paleocene.

The weathered basalt is described as white, green grey and dark grey coloured with minor mottled orange, dull red, orange read, light brown and mottled dark red grains, very soft, sub blocky to amorphous, trace weathered pyroxene and olivine, often weathered to clay. The unaltered basalt is green black, medium to coarse crystals of olivine, feldspar, pyroxene, biotite, olivine partially weathered to serpentinite

3.3 Reservoir Evaluation

3.3.1 Petrophysical Summary

A comprehensive petrophysical review was conducted to assess the reservoir quality and hydrocarbon saturation of all zones which displayed good hydrocarbon shows while drilling (Appendix 1).

A summary of the reservoir net sand and net pay is given in Table 1.

The Upper EVCM reservoir was penetrated in the 12 ¼" hole section and cored throughout. Unfortunately, wireline logs could not be obtained across this interval and the evaluation is based upon the core data, LWD GR and resistivity and cased hole (and then reprocessed) wireline GR and sonic. The core net sand porosity was 29.8% with a geometric average permeability of 35 mD. Hydrocarbon saturation was measured from the core using the Dean Stark technique and was used as the minimum possible value for the saturation calculated from the logs. 11.9 mMD of the interval was determined from the logs to be net pay with an average porosity of 31%, geometric average (ga) permeability of 57 mD and average water saturation of 46%.

The 2718 sand was found to be water-bearing and is now considered not to be a pay interval in the field. The 2755, 2809, 2952 and 2973 sands were found to be gas bearing. Net pay intervals were estimated from the wireline logs. These reservoirs contained 26.9 mMD of net pay with an average porosity of 17.7%, (ga) permeability of 173 mD and an average water saturation of 25%.

Overall, the well is interpreted to have encountered 39.0 mMD of net pay, with an average porosity of 22.0%, (ga) permeability of 137 mD with an average water saturation of 33%.

GROSS INTERVAL				NET PAY				
Reservoir Zone	Top mRT	Base mRT	Thickness* mMD (mTVDSS)	Thickness* mMD (mTVDSS)	Net / Gross [%]	Phi [%]	K [m]D	Sw [%]
UEVCM	2218.2	2231.5	13.3 (8.2)	12.1 (7.5)	91.0	31.5	55.1	44.0
2458	2902.8	2919.2	16.4 (16.3)	0 (0)	NA	NA	NA	NA
2718	3145.3	3153.5	8.2 (8.2)	0 (0)	NA	NA	NA	NA
2755	3179.8	3196.0	16.2 (16.2)	6.4 (6.4)	39.0	16.5	62	33.0
2809	3236.5	3259.9	23.4 (23.4)	11.9(11.9)	51.0	18.9	284	19.9
2844	3269.6	3280.6	11.0 (11.0)	0 (0)	NA	NA	NA	NA
2952	3383.0	3393.4	10.4 (10.4)	0.4 (0.4)	3.9	15.4	30	58.2
2973	3404.1	3423.6	19.5 (19.5)	8.2 (8.2)	42.0	17.1	106	24.1
2718 - 2973 inclusive								
Total Gas Zone	**3145.3**	**3423.6**	**278.3**	**26.9(26.9)**	**9.7**	**17.7**	**173**	**24.6**
All reservoirs			60.9	39.0 (34.4)	NA	22.0	137	33.1

* note: thickness calculation ignores effects of structural dip which is in the order of 0 to 5 degrees (see dip meter interpretation in Appendix 10 for local dip variation and azimuth)

Cut-offs applied				
Reservoir Zone	**shale volume**	**Porosity**	**permeability**	**Water saturation**
2458 (oil zone)	< 40%	Not directly applied	> 1 mD (oil)	< 60%
2718 – 2973	< 40%	Not directly applied	> 0.1 mD (gas)	< 60%

Table 1: Yolla 3 Net Pay Summary

3.3.2 Core Analysis Summary

One 18m core was acquired between 2216 – 2234.1mRT in Yolla 3 within the top sandstone unit (informally named TEV4) of the upper EVCM which is gas and oil bearing. The core covered the entire net hydrocarbon column and both the GOC and OWC were intersected by the core. No SWC or MSCT's were attempted in this well. The average ambient measured porosity is 30.4% and average permeability 86.6mD.

A plot of the porosity versus permeability, displayed by hydrocarbon zone, is presented in Figure 4. The summary of the average porosity and permeability values for the gas and oil zones is shown in Table 2 below.

Routine Core Analysis (RCA) and Special Core Analysis (SCAL) were performed by ACS Laboratories Pty Ltd. The RCA report is included in Appendix 3 of the Basic WCR report for Yolla 3. The special core analysis (SCAL) report is included in Appendix 6 of this volume.

Zone Name	Average Porosity	Average Permeability
TEV4 Gas	32.5%	117.2 mD
TEV4 Oil	32.5%	118.4 mD
TEV4 Water	29.0%	15.9mD

Table 2: Yolla 3 Average Porosity and Permeability Data

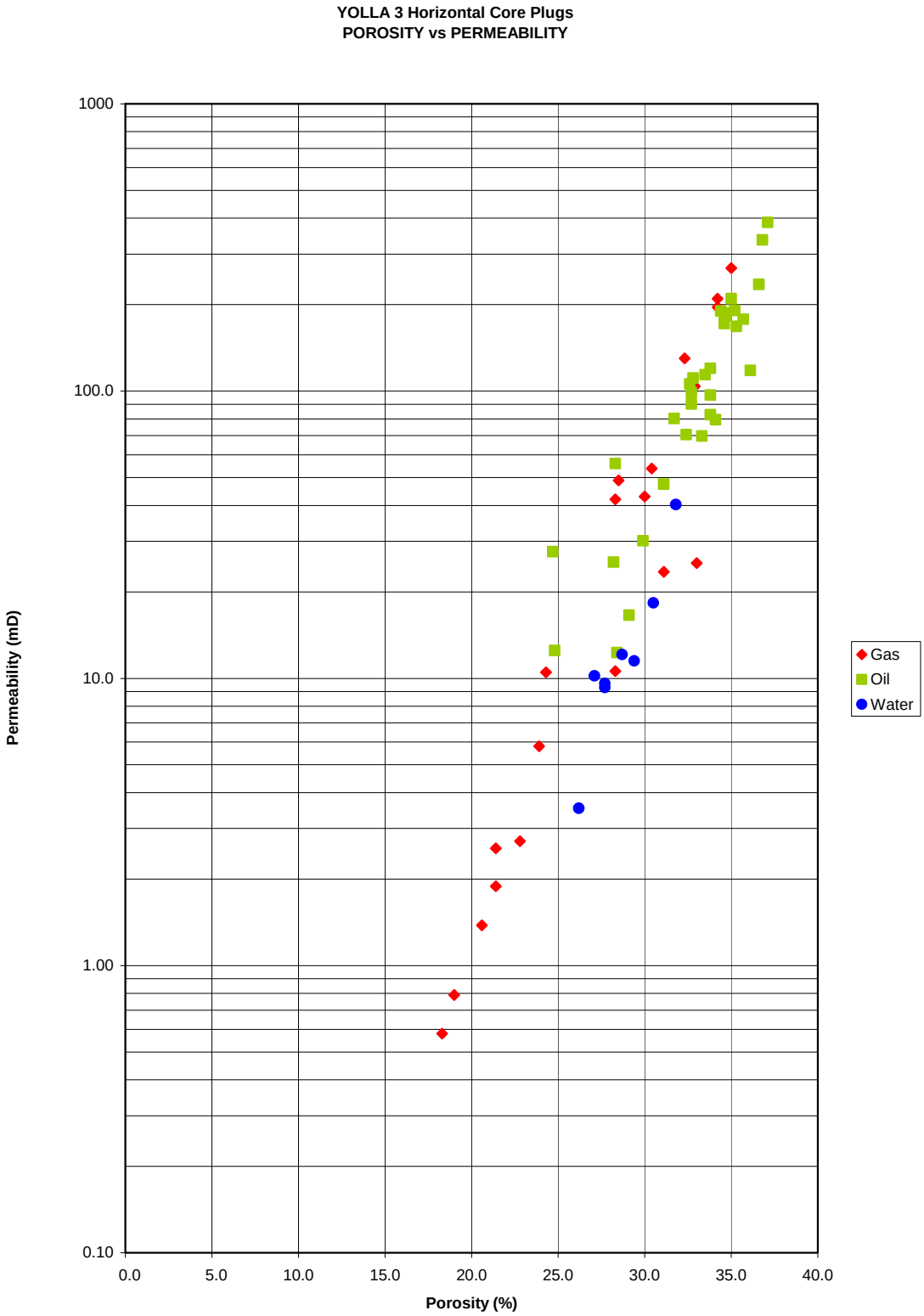

Figure 4: Yolla 3 Measured Porosity vs Permeability

3.3.3 Facies Interpretation

A sedimentological study of Core 1 from the upper Eastern View Coal Measures in Yolla 3 indicates that this interval was deposited in a marine / marginal marine setting. Interpreted depositional environments include distal lower shoreface, sandy embayment / tidal flat, wave influenced proximal delta and offshore marine / wave influenced prodelta transition. The degree and diversity of bioturbation in the distal lower shoreface indicate that fully marine conditions prevailed, whereas in the other environments, stresses such as fluctuating salinity, low oxygen levels and turbidity resulted in more restricted ichnofacies assemblages.

High resolution sequence stratigraphy and ichnofacies analysis has been used to subdivide the cored interval into high-order systems tracts and, a longer period, lower-order sequence. Key surfaces; sequence boundaries (SB) and transgressive surfaces of erosion (TSE); are marked by a characteristic ichnofacies assemblage of robust, sharp walled, passively filled, vertical to sub-vertical domichnia (dwelling burrow), that is excavated into semi-consolidated (firmground) substrates (*Glossifungites* ichnofacies). This surface demarcates discontinuity surfaces that reflect pauses in sedimentation, generally accompanied by erosion.

The succession is dominated by intervals in which the rate of base level change was balanced with the sediment supply, producing aggradational stacking. These intervals are separated by periods of rapid relative base level change causing juxtaposition of differing depositional settings. A sequence boundary (SB) separates the distal lower shoreface from the sandy embayment / tidal flat setting indicating a fall in relative base level. The distal lower shoreface represents a highstand systems tract and the overlying sandy embayment / tidal flat, comprises a lowstand / transgressive systems tract. TSEs separate the sandy embayment / tidal flat from the wave influenced proximal delta front and the delta front from the offshore / prodelta sediments, indicating rapid base level rise. The delta front and offshore / prodelta sediments comprise a transgressive systems tract.

Reservoir quality is strongly influenced by facies with the highest permeability occurring in the sandy embayment / tidal flat facies, and to a lesser extent, the wave influenced proximal delta. The degree of bioturbation does not have a strong control on the reservoir quality; original depositional environment is the overall control on the distribution of permeability. The core analysis and facies study report including core photographs and graphical core log representations are included in Appendix 5.

3.4 MDT Pressure Data Interpretation

The Yolla-3 MDT program was conducted over the interval 3149 to 3480 mRT
on 7/9/2004 and 8/9/2004. A total of 65 pre-tests were attempted of which 27 tests were valid, 15 were supercharged, 22 were tight tests and one lost seal to formation. A summary of the pre-test data is included in Appendix 8 of the Yolla-3 WCR Basic Data.

A total of 7 samples ware attempted, with 6 samples successfully recovered. The descriptions of these samples are as follows:

1 x 450 CC Water sample from 2718 Sand (3149.3 mRT)
1 x 450 CC Gas sample from 2755 Sand (3181.7 mRT)
1 x 450 CC No recovery from 2755 Sand (3181.7 mRT)
1 X 450 CC Gas sample from 2809 Sand (3249.0 mRT)
1 X 1gallon Gas sample from 2809 Sand (3249.0 mRT)
1 X 450 CC Gas sample from 2973 Sand (3420.0 mRT)
1 X 450 CC Gas sample from 2973 Sand (3420.0 mRT)

Fluid compositions are included in Appendix 15 of the Yolla-3 Basic WCR report.

The interpretation and graphical representation of the MDT pressure data is included in Appendix 2 this volume. A summary of the results are shown in the Table 3 below.

Sand	Fluid	Yolla 3 GWC (TVDSS)	Yolla 4 GWC (TVDSS)	Recommended GWC (TVDSS)
2718	water	NA	NA	NA
2755	gas	2832.9	2834.0	2832.9
2809	gas	2826.8	2828.2	2826.8
2973 (upper)	gas	2990.2	2990.2	2990.2
2973 (lower)	gas	2986.6	unknown	2986.6
2458	oil	NA	2470.0 (estab. OWC)	2470.0 (estab. OWC)

Table 3: Yolla 3 MDT Summary of Results

3.5 Production Testing Interpretation Results

A flow test program was carried out as a part of the Yolla 3 completion procedure using the drilling rig facilities and surface testing equipment (Appendix 3). Completion fluids, such as brine and diesel, had to be removed from the wellbores before they can be produced into the Yolla-A platform process facilities. All the completion intervals were opened to flow as part of the clean up operation in order to remove completion brine from all annular spaces and from the formation. This also provided a good opportunity to conduct a short flow test to clean up the well, estimate productivity, and obtain samples of produced fluids from each sand unit.

The table 4 summarises the results of the testing.

Yolla 3 Initial Clean-Up Flows - Estimates of Zone Productivity

Sand	Perfs Top m RT	Perfs Bot m RT	Flow Rate mmcfd/bopd	CGR stb/mmscf	FWHP psia	FWHT deg C	Choke /64"	SIWHP psia	Mid Perfs m SS	FBHP psia@gauge	Gauge m SS	Gradient psi/m	FBHP psia@MPP	Pi (MDT) psia@MPP	k.h (est.) md.ft	D (est.)
UEVCM	2210.2	2225.2	16.7	48	1710	58	48	2477	-1816.2	2200	-1842.6	0.25	2193	2709	1180	0.00015
2755	3180.0	3196.0	16.5	19	2221	65	40	3122	-2748.4	2960	-2836.4	0.331	2931	4151	290	0.00010
2809	3236.5	3248.5	17.6	36	3018	70	36	leak	-2802.9	3992	-2836.4	0.35	3980	4162	7300	0.00030
2973U	3404.0	3407.0	6.9	17==>7	682	33	48	3091	-2965.8	1060	-2982.3	1.5	1035	4386	860	0.00030

Notes:
1 Results for the UEVCM, 2809 and 2755 tests affected by leaking production from the 2973U Sand
2 Flowing bottomhole pressures, FWHP and FWHT were rising slowly during the 2809 sand test indicating the well was still cleaning up and stabilising
3 The k.h estimates are from the log interpretation model for 2973U (probably too high), from core for UEVCM (Krg=0.7), and approx. FBU analysis for 2755 and 2809 Sands
4 D coefficients from Woodside correlation except 2755 and 2809 Sands (FBU)
5 Skin factors are based on the currently available test data and do not account for future condensate dropout effects

Table 4: Yolla 3 Estimates of Zone Productivity from Initial Clean-up Flows

4. GEOPHYSICAL DISCUSSION

4.1 Seismic Data

Yolla 3 was located on the basis of the structure mapping derived from the reprocessing of the Yolla 3D seismic survey in 2000. The survey was reprocessed to improve resolution in the lower EVCM which suffered from severe multiple contamination and limited energy penetration below the coal seams which overlay the main reservoir sands. The final reprocessed data set improved attenuation of multiple energy and yielded better imaging of faults and dykes than the original data. Hence the main reservoir horizon reflectors, (coinciding with the 2718 and 2809 sands), while still weak, could be mapped with relative confidence. Detailed velocity analysis was conducted to yield depth maps. These provided the framework for constructing a detailed geological model prior to the field development decision. The Yolla 3 well path was designed on the basis of this model. A full account of the seismic reprocessing and final data quality can be found in the Yolla 3D 2000 Reprocessing and Interpretation Report, (Taylor, 2001).

4.2 Structure

The Yolla structure is a Paleocene-Eocene aged tilted fault block bounded by faults on two sides, one striking NW and the other approximately N-S. The faults intersect at approximately 120 degrees. An additional NW striking fault sets up a second culmination south of the main northern bounding fault, (Figure 5). The top EVCM is a secondary hydrocarbon bearing closure formed by drape and some late fault movement over the deeper fault block, (Figure 6). Yolla 3 was drilled to drain gas reserves from the western portion of the main fault block, and to appraise the oil bearing top EVCM reservoir.

There was considerable igneous activity in the area during the Miocene, during which time a suite of dykes and sills developed that intersect the structure. The dykes are shown as dashed lines in Figure 5. The main sill in Yolla 3 has been intersected in all wells in the field at about the same depth (2600m SS TVD). It is believed that this depth at the time of emplacement, represented the changeover in point where the vertical stress became the minor stress, (P. Boult, pers comm. 2004) The dyke is more than 60 metres thick, but is relatively seismically transparent.

4.3 Well Tie

No VSP was recorded in Yolla 3 due to is close proximity to the bottom hole location of Yolla 1, which had a VSP. An acceptable well tie was achieved by deriving a synthetic seismogram using check-shots from Yolla 1 and applying the same 28ms bulk shift required in the other wells to tie the Yolla 3D reprocessed seismic volume, figure 7.

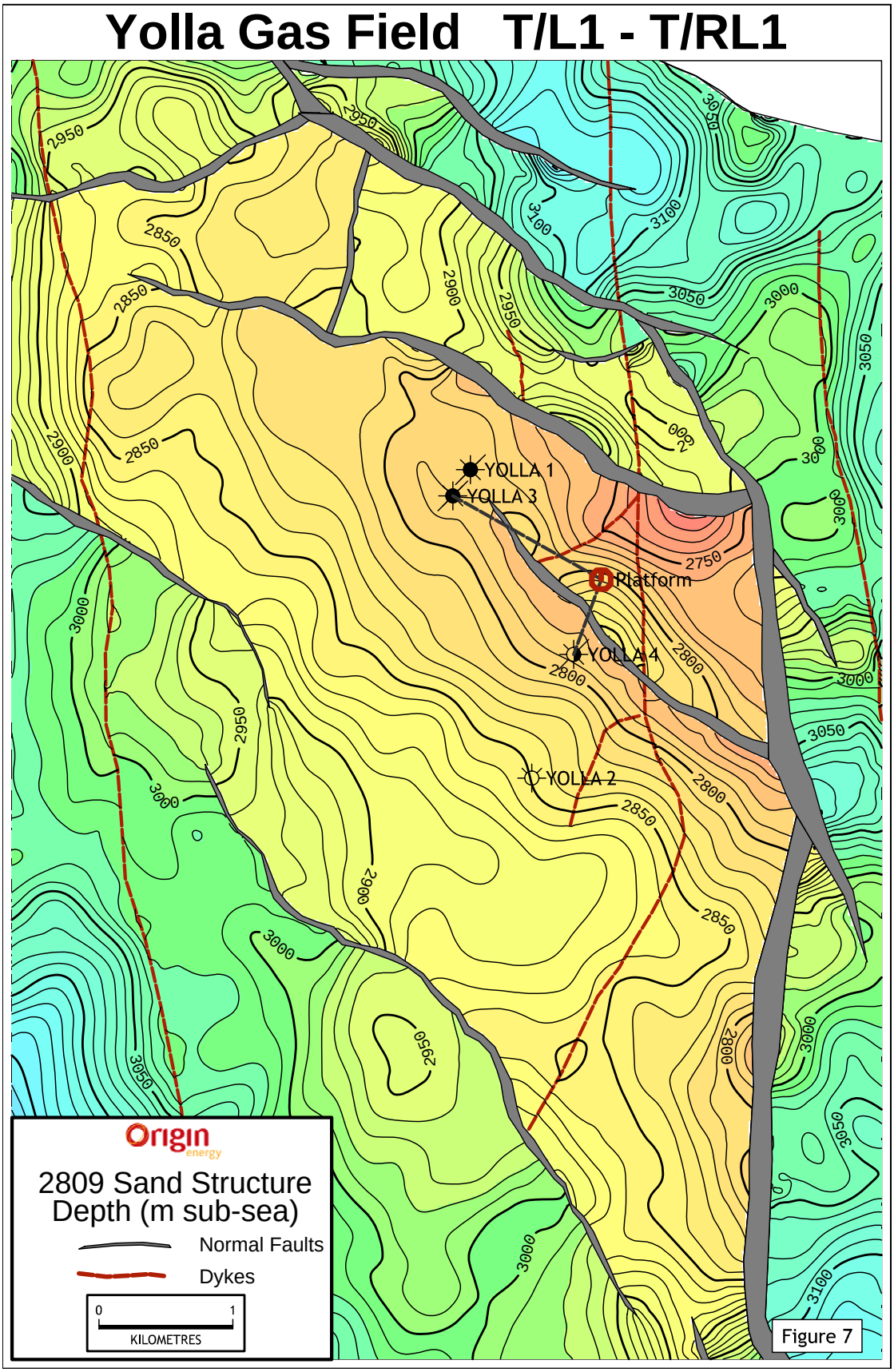

Figure 5: Top 2809 Sand - Depth Structure Map

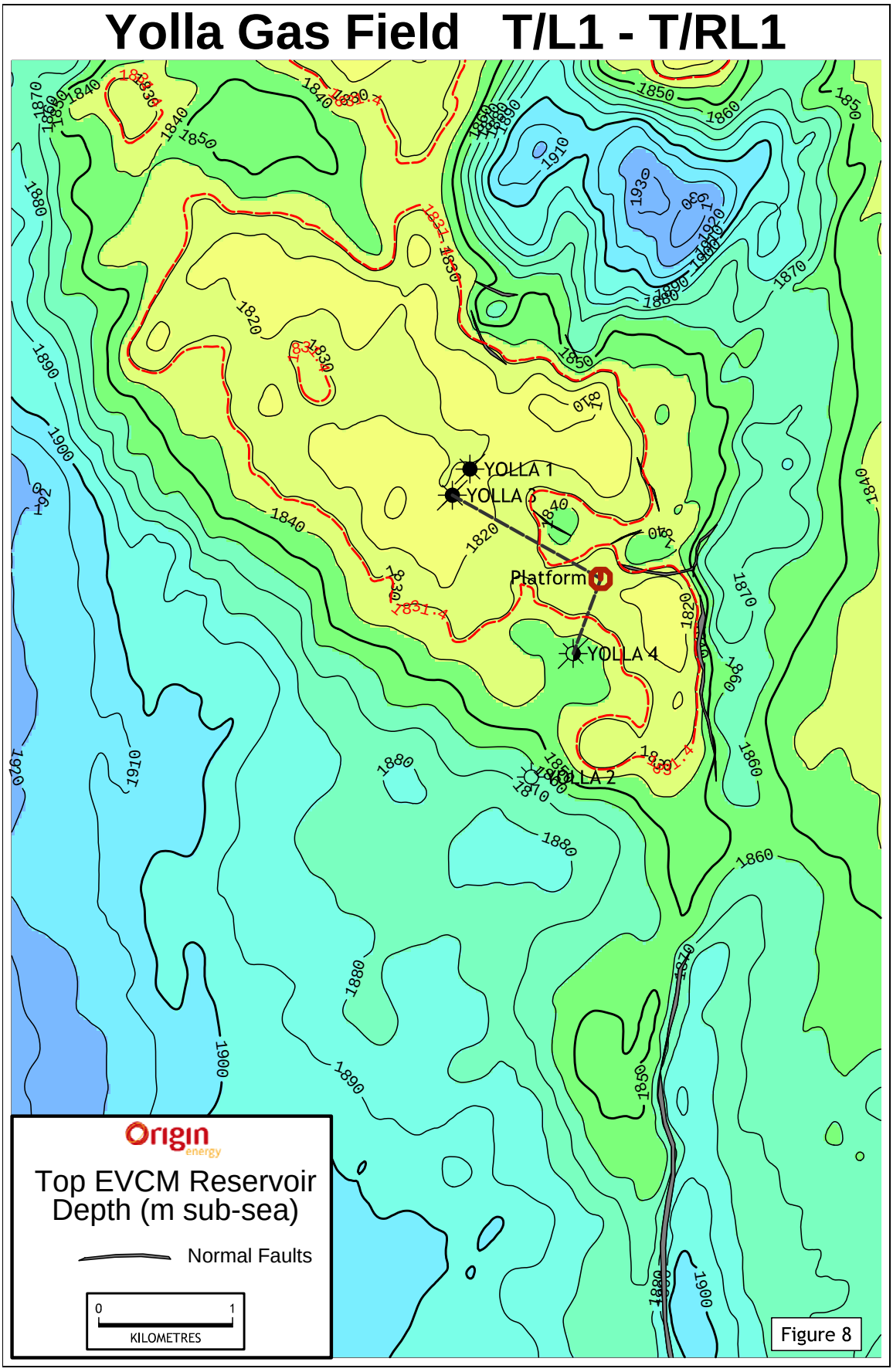

Figure 6: Top EVCM Reservoir - Depth Structure Map

4.4 Actual vs Predicted Depths

Figure 3 shows the actual versus predicted formation tops. Tops based on the top EVCM and 2809 seismic markers were within 1 and 2m of prognosis respectively. Other tops through the main reservoir section were generally within 5m of prognosis. The discrepancy between actual and predicted is mostly attributed to stratigraphic variation and possibly some effect from the emplacement of the 60m thick sill above the main reservoir.

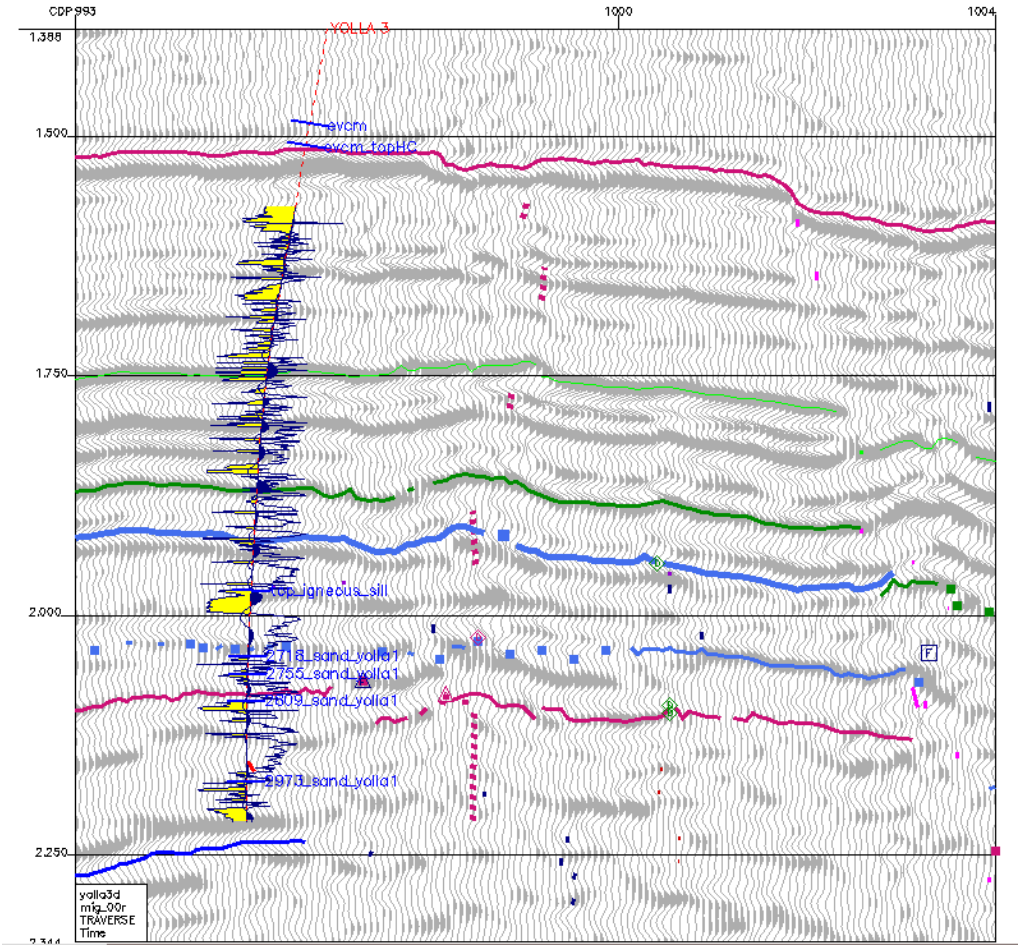

Figure 7: 3D Seismic Traverse through Yolla 3 showing gamma ray log and synthetic seismogram

5. GEOLOGICAL DISCUSSION

5.1 Exploration History

The Yolla Gas Field is a large northwest-southeast trending fault bounded structure which has been compartmentalised by major faults.

Three wells have been previously drilled in the Yolla Field. Yolla 1 was drilled in June 1985 by AMOCO Ltd and encountered gas in both the Intra-Eastern View Coal Measures (EVCM) between 2700 and 3000mRT, and also in the Upper-EVCM at approximately 1830mRT. Gas Pay was encountered in 5 separate zones within the Intra-EVCM, and these provide the main reserves for the BassGas development. DST 1 in Yolla 1 tested gas and liquids from the 2809 Sand of the Intra-EVCM at rates of up to 425 000 m^3/day and 92 kl/day respectively (15.1 mmscfd and 580 bcpd). Yolla 1 was suspended for possible future re-entry.

A 3D seismic survey was acquired over the Yolla Field in mid 1994 with the aim of enabling more accurate depth mapping for the purpose of reserves estimation and appraisal/development planning. These data were subsequently reprocessed in early 2000. Updated depth maps were produced in December 2000 and January 2001 and form the basis for the latest field review and basis for the development plan issued in September 2002.

The Yolla 2 appraisal well was drilled in April and May 1998. The well was drilled 2.35km SSE of Yolla 1, and approximately 45m downdip at the intra-EVCM reservoir level. The well demonstrated good correlation to the sands intersected in Yolla 1, although many were intersected below the gas-water contact due to the low structural location of the well. Pressure data allowed confident interpretation of GWC levels in the different Intra-EVCM units. Yolla 2 was plugged and abandoned.

Yolla 4 development well was drilled immediately prior to Yolla 3. Yolla 4 was directionally drilled to intersect the intra-EVCM gas zones between the Yolla 1 and Yolla 2 wells. This well successfully appraised and completed the main gas zones in preparation for production. A thin oil sand was discovered in Yolla 4 within the EVCM above the main gas zones.

5.2 Regional Geology

5.2.1 Structure

The Bass Basin is located offshore in southeastern Australia between Victoria and Tasmania. It is one of a series of sedimentary basins that were formed in response to rifting during the Late Jurassic to Early Cretaceous between Australia and Antarctica (Williamson et al, 1987). The Bass Basin covers approximately 65,000 km2 and water depths range from 30 to 90 m.

The Bass Basin is a failed intra-cratonic rift basin with structural features which highlight three separate phases of evolution: 1) initial northeast-southwest extension during the early Cretaceous, 2) Late Cretaceous to Pliocene thermal subsidence and 3) Miocene compression. The rifting created a series of northwest-southeast oriented grabens offset by associated east-west wrench movement. The Pelican, Yolla and Cormorant Troughs comprise the major depocentres in the Bass Basin (Fig. 3). The Yolla Field is located on the flank of the Yolla and Cormorant Troughs. These depocentres are fault-bounded half-grabens that progressively developed via growth faulting during the active rifting and thermal

subsidence phases of basin evolution. The dominant structural trend in the basin is northwest-southeast, highlighted by the orientation of the major faults and troughs.

5.2.2 Stratigraphy

The stratigraphic succession in the Bass Basin comprises sediments ranging in age from Early Cretaceous to Recent (Fig. 2)

The Early Cretaceous Otway Group rests unconformably on pre-rift Palaeozoic black shales and quartzites and consists of clastic, volcaniclastic, fluvial and deltaic sediments ranging from coarse-grained sandstone to shale and coal. The Otway Group was deposited as a very thick sequence of sediments (*C.australiensis* to *C.paradoxus*) that have been intersected in the Bass Basin at only one locale, Durroon-1, in the extreme southeast.

Localised uplift and erosion then occurred on the basin margins as the initial rifting phase subsided (Middle Cretaceous). The Otway Drift phase then began along the southern margin of Australia, which was largely contemporaneous with the start of the Tasman Rifting event on the eastern edge of the southern margin. This recommenced rifting in the Bass Basin, which resulted in deposition of the prospective Early Cretaceous to Late Eocene Eastern View Coal Measures (EVCM) which comprise a thick succession of sandstone, siltstone, shale and coal, deposited primarily within fluvial, deltaic and lacustrine depositional environments. Seismic data suggests that the EVCM is over 4000m thick in the Troughs. The EVCM thins markedly towards the basin margins and exhibits both onlap onto basement and erosional truncation. In a broad sense, the EVCM can be divided into three sequences separated by erosional unconformities. The middle sequence was penetrated in Bass-1 and Yolla 1 and –2 and contains the major gas accumulations in the Yolla Field. This sequence is bounded at the base by the N. senectus unconformity and at the top by the upper M. diversus unconformity.

The Lower Eastern View Coal Measures (EVCM) depositional sequence was deposited from Cenomanian to Santonian times (*A.distocrinatus* to *N.senectus*). These units have only been intersected in Durroon-1 in the southeast of the Bass Basin and are equivalent to the Golden Beach Group in the Gippsland Basin.

An angular unconformity is identified over localised highs on the basin margins at the top of the *N.senectus* zone. The boundary is marked in places by significant extrusive volcanism, similar to that observed in the Gippsland Basin. This event signals the termination of Tasman rifting, which was followed by sea floor spreading in conjunction with the already active drift in the Otway region. During this time, thermal subsidence dominated throughout the basin and thick, ubiquitous deposition of the Late Cretaceous to Paleocene Lower EVCM occurred (*T.lillei* to Lower *M.diversus* / *P.asperopolus*).

The Late Cretaceous sediments are restricted mainly to the basin depocentres and axial reaches where accommodation space was sufficient for deposition and subsequent preservation. The section is missing on the basin margins due to sediment bypass. The Paleocene section is extensive throughout with the greatest thickness of sediments in the basin depocentres and significant thinning towards the basin flanks, as a result of both condensing of the section and basement onlap.

The Late Cretaceous/Paleocene Lower EVCM has been intersected in numerous wells in the basin, identifying it as a continuos sequence of late low stand sediments grading through a transgressive systems tract and finally capped by high stand sediments. Environments are gradational both laterally and temporally from alluvial through fluvio-deltaic and nearshore to deeper restricted lacustrine. Primary sediment input to the basin was from the southeast with minor localised input also deposited transversely from the flanks of the troughs. Extensive coal measures dominate the sedimentary sequence in the southeast of the basin (Pelican Trough) with increasingly thicker homogeneous shale units occurring through the Yolla and Cormorant Troughs.

The top of the Lower EVCM is identified by localised uplift and inversion of the pre-existing sedimentary sequence, caused by mild regional compression. The effects of this uplift are variable with the degree of erosion extending from the Mid *M.diversus* through to the *P.asperopolus* in places.

The Eocene upper EVCM (Mid *M.diversus* / *P.asperopolus* to Mid *N.asperus*) was then deposited under a regime of slower subsidence, resulting in more widespread, highly variable facies development. Fluctuating conditions of alluvial, fluvio-deltaic and shallow marine processes resulted with more extensive deposition of coal measure sediments. A regional marine transgression then occurred, resulting in the basin-wide deposition of the Demons Bluff, the base of which is marked by a locally very thick transgressive sand.

Conformably overlying the EVCM is the Late Eocene Demon's Bluff Formation. Lithologically this unit consists of a basal sequence of fine-grained carbonaceous shale and siltstone deposited in an open marine environment. The unit has an average thickness over the basin of approximately 120 m, but thins toward the basin margins. The Demon's Bluff Formation provides a regional top seal to hydrocarbons reservoired in the top-most sandstone units of the EVCM as demonstrated in Yolla 1.

The Demon's Bluff Formation is overlain by the Late Eocene to Pliocene age Torquay Group which broadly consists of a basal sequence of marls and calcareous shales which grade upwards into a succession of bioclastic limestones. The Torquay Group signifies continual deposition under pervasive marine conditions. The Torquay Group is punctuated in places by episodes of minor uplift and/or erosion accompanied by varying effects of volcanism. Large-scale extrusives (volcanoes) are observable on the seismic data with extensive sill and dyke networks also resulting from these events (Yolla 1, Cormorant 1 and Aroo 1).

5.3 Contributions to Geological Concepts and Conclusions

Yolla 3 confirmed the presence of a gas and an oil column within the top sands of the upper EVCM. Prior to drilling this well the exact nature of the reservoired hydrocarbons, the hydrocarbon-water contact and reservoir quality within this zone was poorly understood. The core taken in this unit in Yolla 3 has proven, better than predicted, good reservoir quality within the top EVCM reservoir sandstones which improves the prospectivity of this zone to be included in future production.

The 2718 gas bearing sand in Yolla 1 is found to be water bearing in Yolla 3 and 4 and is now considered not to be pay interval in the field.

In addition to that, the MDT data from Yolla 3 have shown that two separate gas columns exist within the 2973 zone (Table 5). These zones are now referred to as the upper and lower 2973 sands. In Yolla 4 only the upper zone is present or developed as reservoir indicating the spatial variability of facies types and reservoir architecture.

The oil bearing 2458 sand unit which was encountered in Yolla 4 is water bearing in Yolla 3 where the unit was penetrated 3.7 metres deeper with respect to Yolla 4 (relative to TVDSS). This is consistent with a very thin 2.7 metres of net pay present in the top portion of the 2458 sand in Yolla 4. The results from Yolla 3 confirm a very thin oil column with an OWC at approximately 2464mTVDSS.

Depth units	TEV4 sand OWC		2718 sand GWC		2755 sand GWC		2809 sand GWC		2973 sand GWC		
	Pre-drill	Post drill	Pre-drill	Post drill	Pre-drill	Post drill	Pre-drill	Post drill	Pre-drill	Post drill Upper	Post drill Lower
mTVDSS	1831.5	1831.7	2727.0	Water	2834.0	2833.0	2834.0	2826.5	2997.0	2986.5	2999.0
mMDRT		2235.5		Water		3272.7		3266.2		3426.2	3429.7

Table 5: Yolla 3 Hydrocarbon-Water contacts, pre- vs post-drill

6. REFERENCES

Amoco Australia Petroleum Company, 1986 – Yolla 1 Final Well Report, Volume 1 – Geology, Appendix 9, Part 2: Vitrinite reflectance Determinations and Organic Petrology

Boreham, C.J., Blevin, J.E., Radlinski, A.P. and Trigg, K.R., 2003 – *Coal as a source of oil and gas: A case study from the Bass Basin, Australia*. APPEA Journal 43 (1) 117 - 148

Lennon, R.G., Suttill, R.J., Guthrie, D.A. and Waldron, A.R., 1999 - *The renewed search for oil and gas in the Bass Basin: Results of Yolla 2 and White Ibis 1*. APPEA Journal 39 (1) 248 – 262.

Taylor, R., 2001 - *Yolla 3D 2000 Reprocessing and Interpretation Report*, Origin Energy Resources Ltd, unpublished report.

Williamson, P.E., Pigram, C.J., Colwell, J.B., Scherl, A.S., Lockwood, K.L. and Branson, J.C., 1987 – *Review of stratigraphy, structure and hydrocarbon potential of Bass Basin, Australia*. AAPG Bulletin V.71, No.3, 253 - 280

APPENDIX 1: PETROPHYSICS REPORT

TRL/1, BASS BASIN, TASMANIA

YOLLA - 3

PETROPHYSICAL INTERPRETATION

EASTERN VIEW COAL MEASURES

2100 – 3500 mRT

FINAL

Origin Energy Resources Limited
Second Floor, South Tower, John Oxley Centre
339 Coronation Drive
MILTON QLD 4064

Andy Hall, March 2005

EXECUTIVE SUMMARY

Yolla-3 was drilled as the 4th well on the Yolla Field after the Yolla-1 exploration well in 1985, Yolla-2 appraisal well in 1999 and the Yolla-4 development well, which immediately preceded Yolla-3. The objective of the well is to produce from the Intra-EVCM 2755, 2809 and 2973 Sandstones (named after their measured depth penetrations in Yolla-1).

A summary of the reservoir net sand and net pay is given in Table 1.

The Upper EVCM reservoir was penetrated in the 12 ¼" hole section and cored throughout. Unfortunately, wireline logs could not be obtained across this interval and the evaluation is based upon the core data, LWD GR and resistivity and cased hole (and then reprocessed) wireline GR and sonic. The core net sand porosity was 29.8% with a geometric average permeability of 35 mD. Hydrocarbon saturation was measured from the core using the Dean Stark technique and was used as the minimum possible value for the saturation calculated from the logs. 11.9 mMD of the interval was determined from the logs to be net pay with an average porosity of 31%, geometric average (ga) permeability of 57 mD and water saturation of 46%.

The 2718 Sst was found to be water-bearing and is now considered not to be a pay interval in the field.

The 2755, 2809, 2952 and 2973 Sandstone (Sst) were found to be gas bearing. Net pay intervals were estimated from the wireline logs. These reservoirs contained 26.9 mMD of net pay with an average porosity of 17.7%, ga permeability of 173 mD and water saturation of 25%.

Overall, the well is interpreted to have encountered 39.0 mMD of net pay, with an average porosity of 22.0%, ga permeability of 137 mD and water saturation of 33%.

Table 1: Net Sand and Net Pay Summary for Yolla-3

	Gross Interval			Net Sand				Net Pay				
Reservoir Zone	Top mRT	Base mRT	Thickness mMD	Thickness mMD	NTG Fraction	Porosity Fraction	Permeability mD	Thickness mMD	NTG Fraction	Porosity Fraction	Permeability[1] mD	Sw Fraction
UEVCM	2218.2	2231.5	13.3	13.3	1.000	0.311	47.2	12.1	0.909	0.315	55.1	0.438
2458 Sst	2902.8	2919.2	16.4	7.9	0.485	0.190	14.2	0	0	-	-	-
2718 Sst	3145.3	3153.5	8.2	4.4	0.529	0.155	37.0	0	0	-	-	-
2732 Sst	3160.6	3162.1	1.5	0	0	-	-	0	0	-	-	-
2755 Sst	3179.8	3196.0	16.2	6.5	0.401	0.164	60.2	6.4	0.394	0.165	62.0	0.331
2809 Sst	3236.5	3259.9	23.4	15.6	0.668	0.171	86.3	11.9	0.508	0.189	284	0.199
2844 Sst	3269.6	3280.6	11.0	2.9	0.268	0.139	9.7	0	0	-	-	-
2952 Sst	3383.0	3393.4	10.4	1.2	0.112	0.133	6.4	0.4	0.039	0.154	30.0	0.582
2973 Sst	3404.1	3423.6	19.5	9.1	0.469	0.163	59.7	8.2	0.420	0.171	106	0.241
2718 Sst to 2973 Sst Inclusive												
Gas zone	**3145.3**	**3423.6**	**278.3**	**39.7**	**0.143**	**0.163**	**62.5**	**26.9**	**0.097**	**0.177**	**173**	**0.246**
All reservoirs				**60.9**		**0.199**	**52.9**	**39.0**		**0.220**	**137**	**0.331**

	Net Sand Parameters			*Net Pay (Net Sand + ...)*
Reservoir Zone	*Shale Volume*	*Porosity*	*Permeability*	*Water Saturation*
U EVCM	*< 40%*	*Not directly applied*	*> 1 mD (oil & gas zone)*	*< 60%*
2718 – 2973 Sst	*< 40%*	*Not directly applied*	*> 0.1 mD (gas zone)*	*< 60%*

TABLE OF CONTENTS

Figures

Tables

Enclosures

BOREHOLE DATA

Hole / Casing Diameters

Borehole			Casing OD		
Inches	**mm**	**Section TD (mDDRT)**	**Inches**	**mm**	**Casing Shoe (mDDRT)**
Casing driven into sea-bed			20	508	215
16	406	1012	13 3/8	340	1007
12 ¼	311	2347	9 5/8	244	2340
8 ½	216	3497	168 mm (6.625") liner run post logging to 3497 mRT		

Hole Deviation

The Yolla-3 well was drilled to about 250mRT and then deviated at an azimuth of 300° and an inclination of approximately 44° to 1270mRT. The well was then allowed to drop to a final inclination of less than 1° to encounter the reservoir targets close to vertically.

The hole plan and cross-section are given in Figure 1 and Figure 2.

Drilling Mud Properties

The following mud properties were read off the Schlumberger log plot for Run 2 / 1 of the TD logging suite.

Rm		Rmf		Rmc		Mud Weight
(Ω.m)	(Deg C)	(Ω.m)	(Deg C)	(Ω.m)	(Deg C)	lb / gal
0.184	25.8	0.147	25.5	0.229	23.6	9.45

Logging While Drilling (LWD) Data

LWD gamma ray and resistivity was acquired by Sperry Sun from the 340 mm (13 3/8") casing shoe at 1000 mRT to final TD at 3497 mRT.

The 311 mm (12 ¼") section was drilled in three bit runs, due to core being taken in the Upper EVCM reservoir. LWD logging comprised the dual gamma ray (DGR) and four-phase Electromagnetic Resistivity (EWR-P4) tool. This yielded the Smoothed Gamma ray log (SGRC)

and the micro, shallow, medium and deep resistivity curves (SEXP, SESP, SEMP and SEDP respectively). The cored sections were wiped with the tools when drilling recommenced after coring.

LWD DGR & EWR-P4 was acquired throughout the 216 mm (8 ½") hole section.

Wireline Log Data

A comprehensive logging suite (PEX-CMR-HRLA, FMI-DSI-HNGS, MDT, MSCT) was planned in the 311 mm (12 ¼") hole section to appraise the Upper EVCM reservoir (and any other reservoirs encountered). The first logging suite (PEX), would not, however, pass deeper than 1143 mRT, even when various tool configurations and lengths were tried. After several attempts, wireline logging operations in this hole section were abandoned. Sonic and gamma logs were acquired through casing in the TD logging suite. The sonic log has been reprocessed by Schlumberger to remove the effects of the casing.

The wireline log runs acquired by Schlumberger over the section from the 244 mm (9 $^{5}/_{8}$") casing to TD are given below.

Run	Log Suite	Top (mRT)	Base (mRT)	Maximum Temperature (^{o}C)
2 / 1	SP-HRLA-PEX-CMR-GR	124	3491	132
2 / 2	FMI-DSI-HNGS	2337	3474	143
2 / 3	MDT - GR	3148.6	3479.5	148
2 / 4	MDT - GR	3149	3420.6	146

The MDT was used to obtain 79 pre-test pressures in the first run. An equipment failure resulted in the tool not being able to take samples. The tool was pulled to surface and repaired. The MDT was then rerun and acquired five fluid samples:

Depth (mRT)	Reservoir	Comment
3149.3	2718 Sst	1 x 450 cc water sample
3181.7	2755 Sst	1 x 450 cc gas sample 1 misfire
3249.0	2809 Sst	1 x 450 cc gas sample 1 x 1 gallon gas sample
3420.6	2973 Sst	2 x 450 cc gas samples

Core Data

One 18 metre core was acquired in the Upper EVCM reservoir in Yolla-3.

Core #1 was taken in the Upper EVCM sandstone between 2216 - 2234 mDDRT with 100% recovery. Comparison of the core GR to the wireline GR suggests that the core depths were 0.9 mMD deep of the wireline depth datum for the well.

- 181 probe permeability measurements were acquired
- 60 plugs were cut and used to measure porosity, grain density and permeability.
- 20 overburden porosities and permeabilities were measured using an overburden pressure of 3200 psi
- 6 plugs were submitted for SCAL analysis. Measurements were made on these to determine Archie 'm' and 'n', cation exchange capacity and capillary pressure

Borehole Temperature

Bottom hole temperature (BHT) was measured in each of the logging runs. The temperature range was from 132^{o}C in Run 2 / 1 to 149.4^{o}C (corrected to logging TD) in Run 2 / 4. The Horner plot suggests a corrected BHT of 156.7^{o}C, equivalent to a temperature gradient of 49.3^{o}Ckm^{-1}, assuming a sea bed temperature of 8^{o}C (Figure 3).

The temperature from Run 2 / 1 SP-HRLA-PEX-CMR (132^{o}C at 3491.0 mRT) was used in the petrophysical analysis.

Figure 1: Plan View of the Yolla-3 Well Deviation

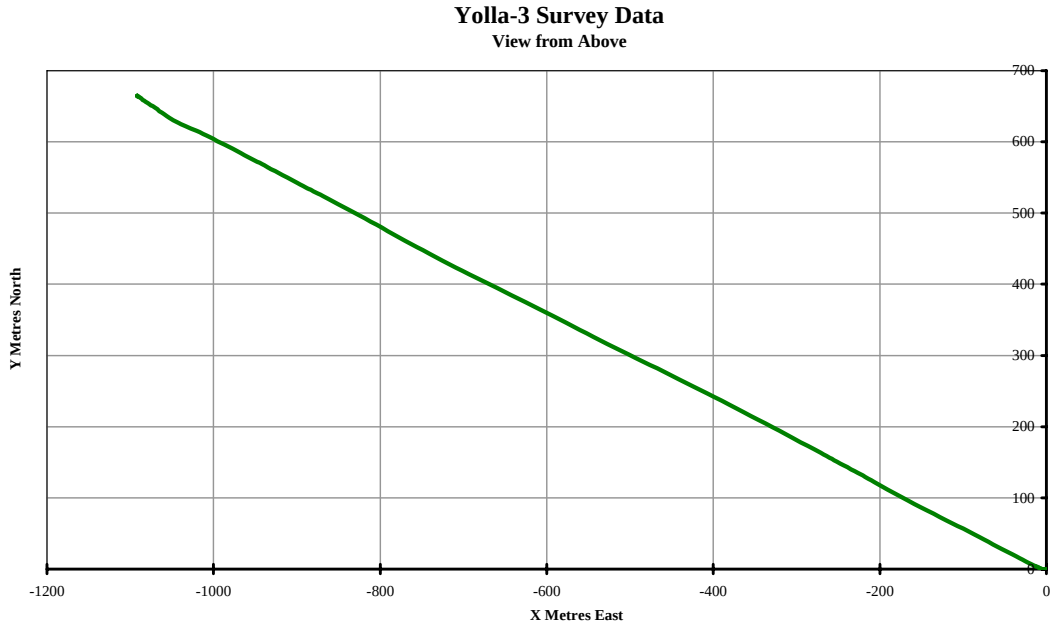

Figure 2: Cross-section View of the Yolla-3 Well

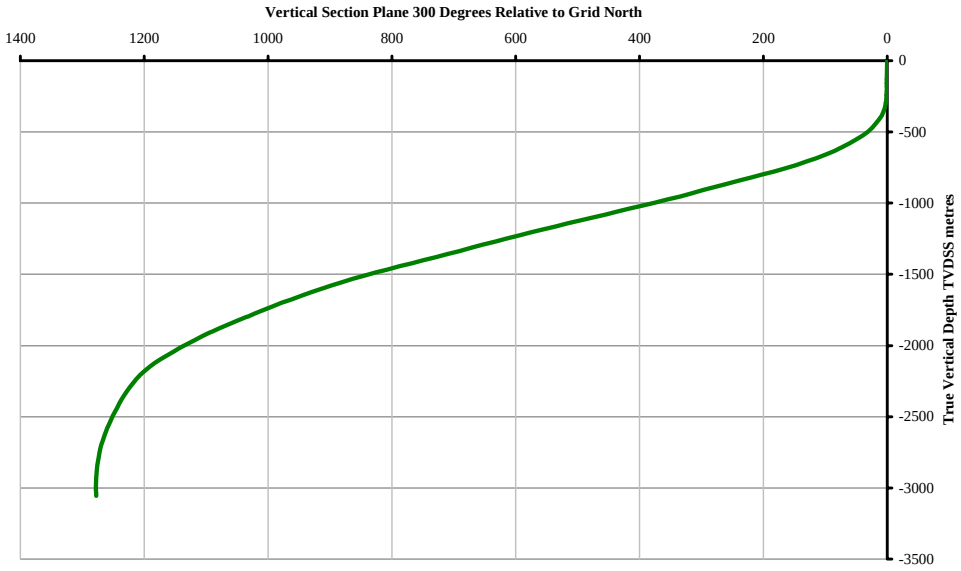

Figure 3: Horner Temperature Plot for the TD Logging Suite at Yolla-3

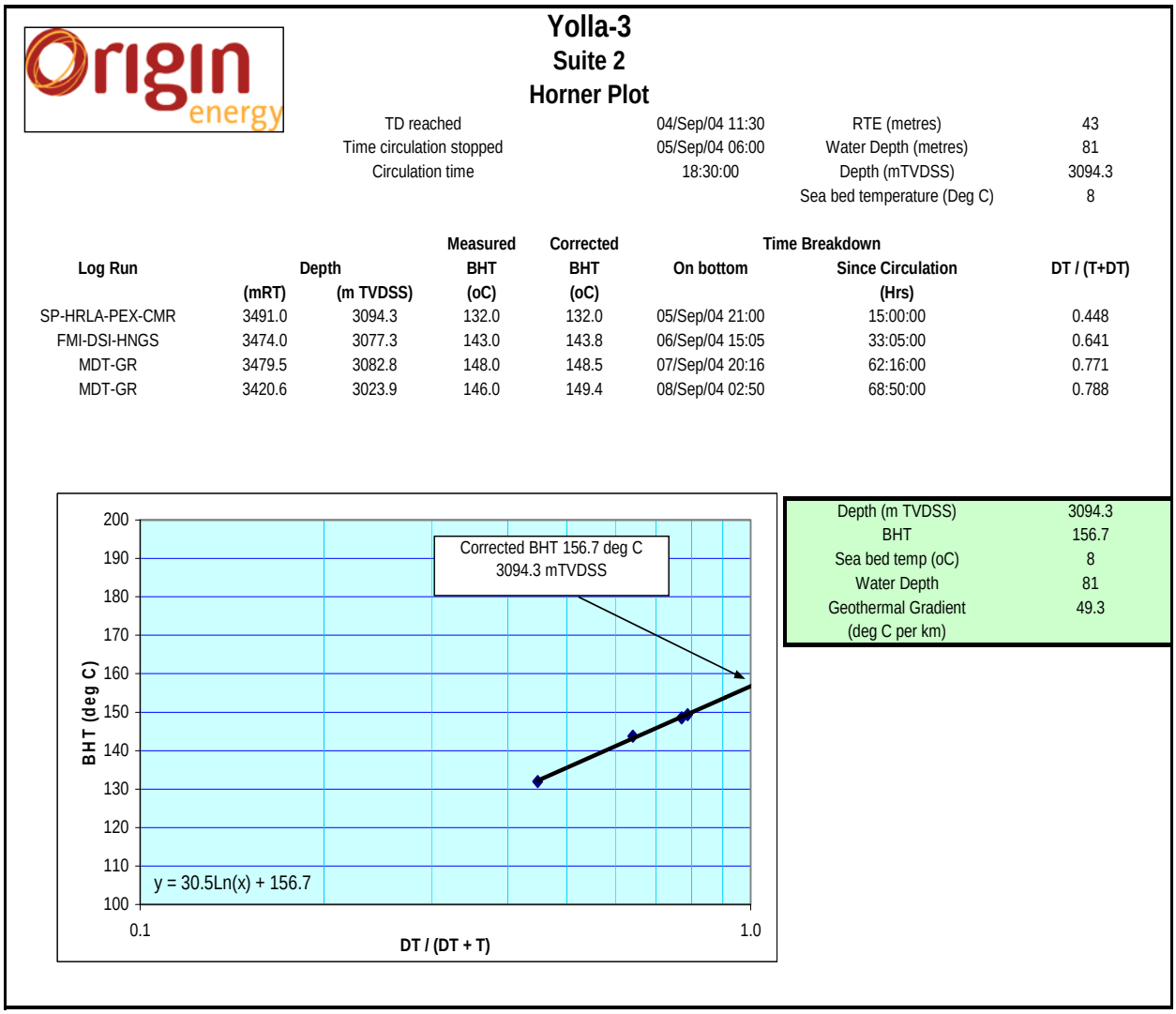

LOG ANALYSIS METHODOLOGY

The Terrastation II macro used to process the Yolla-3 well is given in Appendix A. This contains all the details of log corrections etc applied. The procedure was similar to that applied to the logs for Yolla-4 (Reference 2).

Shale Volume

Shale volume in the Upper EVCM was calculated from the gamma ray log alone using a linear transform. The petrology suggests that the sandstone contains a significant volume of radioactive minerals (8-16% glauconite, 1 – 1.5% K-feldspar, 0.5 – 1.0% mica). Hence the shale volume in this interval will be over-estimated. Shale volume was not used as a parameter in the determination of net sand in this reservoir.

Shale volume in the 8 ½" hole section was determined from the minimum of the gamma ray using a linear transform and the neutron-density logs.

Porosity

Porosity in the Upper EVCM was derived from the sonic log, calibrated directly to the core porosity.

Porosity in the 8 ½" hole section was derived from the neutron (lithology and shale corrected), density, density-neutron, sonic and CMR logs. Reservoir properties were taken from the equivalent reservoirs in the cored wells. A good agreement between the logs was observed throughout most of the section.

The density-CMR (DMR) porosity log was assumed to be the most accurate and was used in the determination of net sand and net pay for the 8 ½" hole section.

Permeability

Permeability in the Upper EVCM was derived from the relationship between the core overburden corrected porosity and permeability as follows:

$$\text{Permeability} = 0.0013\, e^{\text{PHI\_S}*100 * 0.3379}$$

The overburden corrected porosity / permeability transform, from the Yolla-4 cores in the 2755 and 2809 Sst shows a fairly reliable trend of increasing permeability with porosity.

A log of permeability data was created using

$$P1 = 0.0193 * e^{(PHI\_ND*100*0.5168)}$$

$$Permeability = P1 - P1*(VSH*0.064)$$

Permeability in the shales was set to the CMR permeability KTIM. There is no core in Yolla-3 to correlate this response to.

Water Saturation

Water saturation was derived from the Archie and Waxman Smits equations for all the reservoirs. Parameters were as determined from the wells where core was taken.

The formation water resistivity used in the main reservoirs was the same as used in the Yolla-4 interpretation (Table 2). The water resistivity for the 2755, 2809, 2952 and 2973 Sst were derived in Yolla-2, where the sands are below the GWC. The water resistivity from Pickett Plot analysis at Yolla-4 was used in the 2718 Sst.

Net Sand / Net Pay Cut-offs

A similar approach to that used in Yolla-4 was followed. The net sand permeability was set to 0.1 mD in gas sands and 1 mD in oil bearing sandstones. No direct porosity cut-off is applied. The porosity / permeability relationship applied in the Upper EVCM suggests that this would correspond with an OB porosity of about 19.7%. In the main reservoirs, this would correspond with a porosity of about 8%.

Net sand was assumed to have a shale volume of less than 40%.

Coal and volcanic filters, generated by manual inspection of the wireline logs, were applied to ensure that no non-clastic intervals were included in the net sand interval.

Net pay was determined to be present where net sand is determined and water saturation is less than 60%.

Table 2: Formation Properties Used in the Interpretation

Sandstone	Grain Density	Fluid Density	Water Resistivity	Rw Temperature	CEC	Archie Parameters		
	(gcm^{-3})	(gcm^{-3})	(ohm.m)	(^oC)		a	m	n
2718	2.716	1.00	0.689	25	0.14	1.00	1.762	1.748
2755	2.697	1.00	0.468	25	0.10	1.00	1.762	1.748
2809	2.663	1.00	0.468	25	0.18	1.00	1.770	1.748
2952	2.724	1.00	0.401	25	0.14	1.00	2.000	1.633
2973	2.679	1.00	0.576	25	0.14	1.00	2.000	1.633

INTERPRETATION

Upper EVCM (2218.2 – 2231.5 mRT)

The data for the interpretation of this reservoir consists of full core coverage and LWD Gamma / resistivity logs (acquired when the Bottom Hole Assembly (BHA) was run after coring). Due to the tools hanging up higher in the hole, open hole wireline logs were not acquired across the interval. Cased hole sonic and gamma were acquired in the TD logging suite and have been reprocessed to remove the effect of the casing.

60 core plugs were submitted for RCA analysis. Twenty of these plugs were submitted for overburden (OB) analysis.

Five core plugs were submitted for petrographic analysis (Reference 1). The samples are variably argillaceous / clean, very fine grained quartz arenites in which the framework is largely quartz and, in all but the uppermost sample, peloidal glauconite.

The inclusion of a significant volume (8 – 16%) of radioactive glauconite in the sandstone will cause the gamma ray to over-estimate shale volume. No other shale volume log is available. Shale volume was, therefore, calculated from the gamma ray log calibrated to the authigenic and detrital clay percentage determined in the XRD petrology (Figure 4). No conversion was made between clay and shale volume.

Porosity was determined for the three cored intervals using core / log correlation plots (Figure 5). Note that in these plots, the sonic has not been shale corrected and the fluid slowness is simply a correction factor between sonic and porosity, not an estimate of true fluid property.

A strong correlation between core OB porosity and OB permeability was observed (Figure 6). This suggests that a net sand permeability cut-off of 1 mD is likely to correspond to 19.7% porosity. The porosity / permeability relationship was used to calculate permeability from sonic porosity in the reservoir.

$$\text{Permeability} = 0.0013\, e^{0.3379 * \text{Porosity}}$$

Oil and water saturations were measured for 19 plugs through the core and used to determine the likely formation fluid (Figure 7). This suggests three fluid zones. A gas zone was inferred between 2215.5 – 2224.6 mRT from the low log-derived water saturation and low oil saturation, an oil zone between 2224.6 – 2231.1 mRT and a water zone below 2231.1 mRT.

The Archie parameters 'a' and 'm' have been derived from the core data to be 0.80 and 2.27 respectively (Figure 8). If 'a' is assumed to equal 1.0, then 'm' = 1.85. Resistivity index data to derive 'n' is not currently available.

The Cation Exchange Capacity (CEC) was calculated on six core plugs. The top plug has an uncrushed CEC of 0.7 meq/100g, but the deeper plugs are all above 2.3 meq/100g and average 3.26 meq/100g. The calculated Qv for the interval was derived from the following total porosity / Qv relationship:

$$Qv = 11562 * \Phi_{sonic}^{-3.1819}$$

With the porosity being very high throughout the interval, the Qv is low and has negligible effect on the calculated water saturation.

Formation water resistivity for the Upper EVCM was taken to be the minimum formation water resistivity to honour or exceed all the measured oil saturations from the core data. This corresponds with a water resistivity of 0.05 Ω.m at 80°C (60,140 ppm NaCl equiv), which is similar to observations in other wells.

Results

The interpreted section is shown in Figure 9.

Net sand can be calculated from the log response or directly from the core data. If a 1 mD cut-off is applied to the OB corrected core data, then 96.7% of the interval (2 non-net plugs) is net sand with an average (OB corrected) porosity of 29.8% and geometric average (ga) permeability of 34.6 mD. Using the log data, all the interval qualifies as net sand with an average porosity of 31.1% and ga permeability of 47.4 mD.

Net pay was calculated from the Waxman Smits derived water saturation, 11.9 mMD of the interval qualifies as net pay, with an average log derived total porosity of 31.6%, water saturation of 46.4% and ga permeability of 57 mD.

2718 Sst (3145.3 – 3153.5 mRT)

The WSG described the interval as a very fine, well sorted sandstone with a weak silica cement and common silty / argillaceous matrix. 8% dull green spotty fluorescence with moderate bright white streaming crush cut and a moderately bright pale yellow / green solid ring residue was observed in the lower interval of the sandstone.

11 mDT pre-tests were acquired in and immediately surrounding the 2718 Sst. These indicated a water gradient (Figure 11) and a maximum mobility of only 10 mD/cp.

The interval has 4.4 mMD of net sand (NTG = 53%) with an average porosity of 15.5% and ga permeability of 37 mD (Figure 10). The sands were water saturated throughout and no net pay is calculated to be present.

2755 Sst (3179.8 – 3196.0 mRT)

The WSG described the interval as a very fine, well sorted sandstone with a weak silica cement and common silty / argillaceous matrix. The siltstones were dark gray, micro-micaceous and moderately hard to hard. Good drilling gas shows were recorded. Dull to moderately bright green fluorescence was observed.

11 MDT pre-tests were acquired in the 2755 Sst. These indicated a variable mobility (range 0.6 – 108 mD/cp). Some of the points appear to be super-charged and there is no clear gradient that can be extrapolated from the data (Figure 12).

The interval has 6.5 mMD of net sand (NTG = 40%) with an average porosity of 16.4% and ga permeability of 60 mD (Figure 10). Pay was divided into two zones with an intervening shaly sequence. 6.4 mMD of the interval qualifies as net pay, with an average porosity of 16.5%, ga permeability of 62 mD and water saturation of 33%.

2809 Sst (3236.5 – 3259.9 mRT)

The WSG described the sandstone as very fine, well sorted, with a weak silica cement. There are occasional loose coarse or very coarse grains and a silty / argillaceous matrix. Good drilling gas shows were recorded. Only a trace of fluorescence was observed.

10 MDT pre-tests were acquired in this interval. 4 were tight or super-charged. The remainder had a mobility between 6 – 153 mD/cp. The pressures indicate a gas gradient throughout and suggest communication throughout the reservoir (Figure 12).

The interval has 15.6 mMD of net sand (NTG = 67%) with an average porosity of 17.1% and ga permeability of 86 mD (Figure 10). 11.9 mMD of the interval qualifies as net pay, with an average porosity of 18.9%, ga permeability of 284 mD and water saturation of 19.9%.

2952 Sst (3383.0 – 3393.4 mRT)

The WSG described the interval as a very fine to fine sandstone, moderately well sorted with common kaolinite cement, trace quartz overgrowths and trace lithics. Trace - 20% moderately bright yellow fluorescence was observed. There was a slow direct cut and instantaneous crush cut with a thin residual ring.

Three MDT pre-tests were acquired in this interval. Two were tight and the remaining point had a mobility of only 1 mD/cp.

Only 1.2 mMD of the interval qualifies as net sand (Figure 14) and less than a metre could be considered net pay.

2973 Sst (3404.1 – 3423.6 mRT)

The WSG geologist described this interval as a medium to very coarse sandstone, with loose unconsolidated grains, good to very good inferred porosity. Good gas shows were seen but no fluorescence was observed.

7 MDT pre-tests were taken in the 2973 Sst. There ranged between super-charged and 297 mD/cp mobility. The pressure gradient (Figure 13) shows that the two sandstones in the 2973 interval are not in communication. The Upper sandstone (3404 – 3407 mRT) is on the same pressure line as the 2973 Sst in Yolla-4 and is, presumably, in communication with that interval. The deeper sandstone (3417 – 3423 mRT) is on a different pressure gradient and not in communication with either the sandstone in Yolla-4 or the upper sandstone in this well.

The interval has 9.1 mMD of net sand (NTG = 47%) with an average porosity of 16.3% and ga permeability of 60 mD (Figure 14). 8.2 mMD of the interval qualifies as net pay, with an average porosity of 17.1%, ga permeability of 106 mD and water saturation of 24%. The pay is divided into two discrete intervals:

Figure 4: Correlation Between Gamma Ray and Core XRD Clay Volume

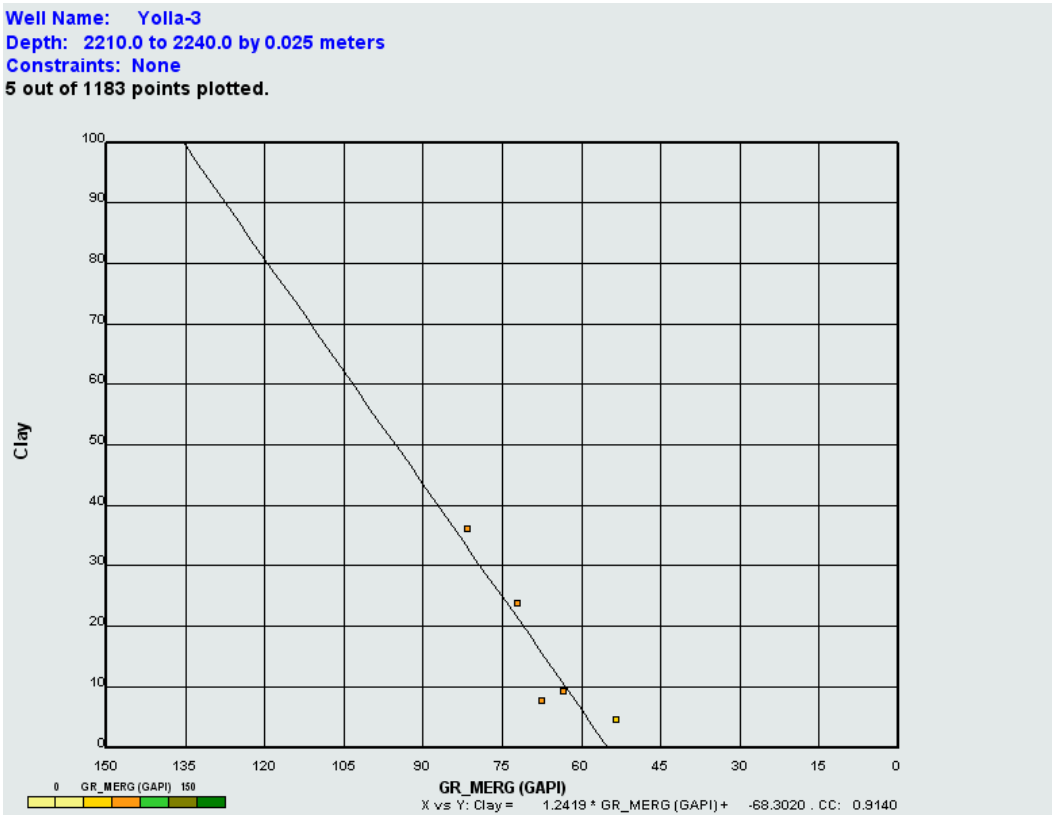

Figure 5: Sonic / Core Porosity Correlation Plots for the Upper EVCM

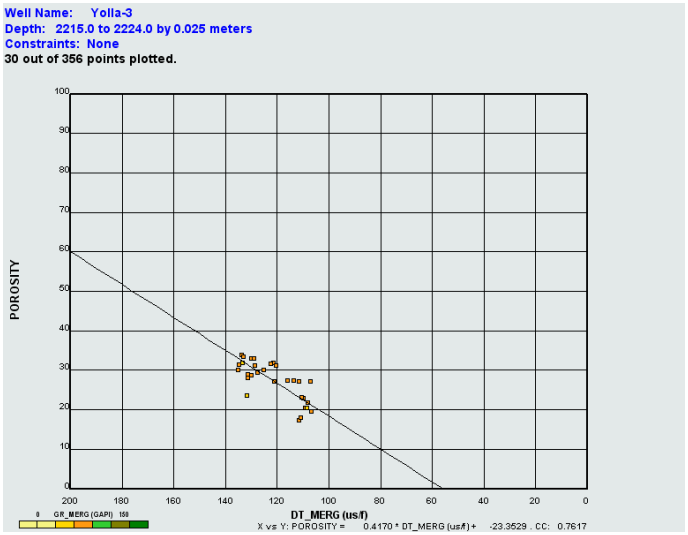

Gas Zone (2215 – 2224 mRT)

DT_{ma} = 56 usec/ft

DT_{fl} = 296 usec/ft

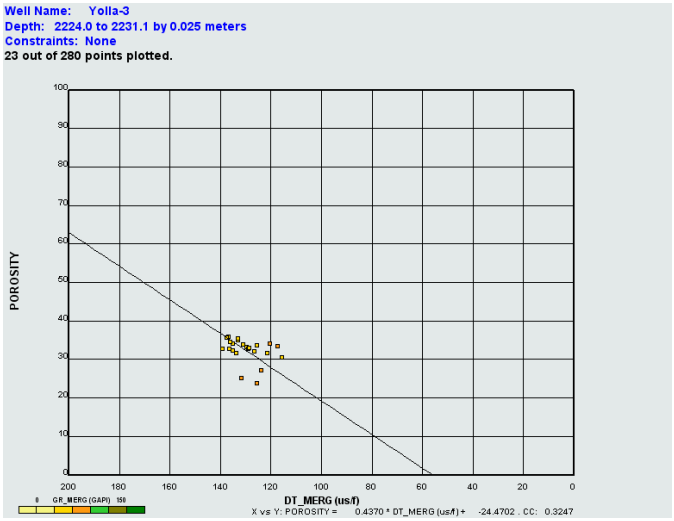

Oil Zone (2224 – 2231 mRT)

DT_{ma} = 56 usec/ft

DT_{fl} = 285 usec/ft

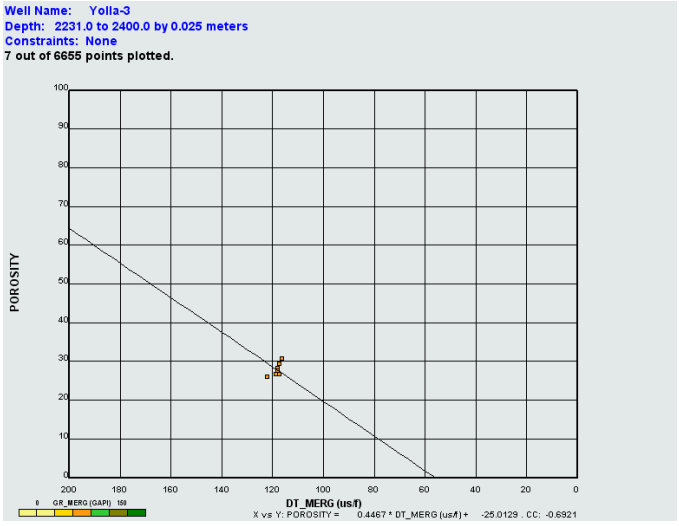

Water Zone (>2231 mRT)

DT_{ma} = 56 usec/ft

DT_{fl} = 280 usec/ft

Figure 6: Core Porosity / Permeability Relationship for the Upper EVCM Reservoir

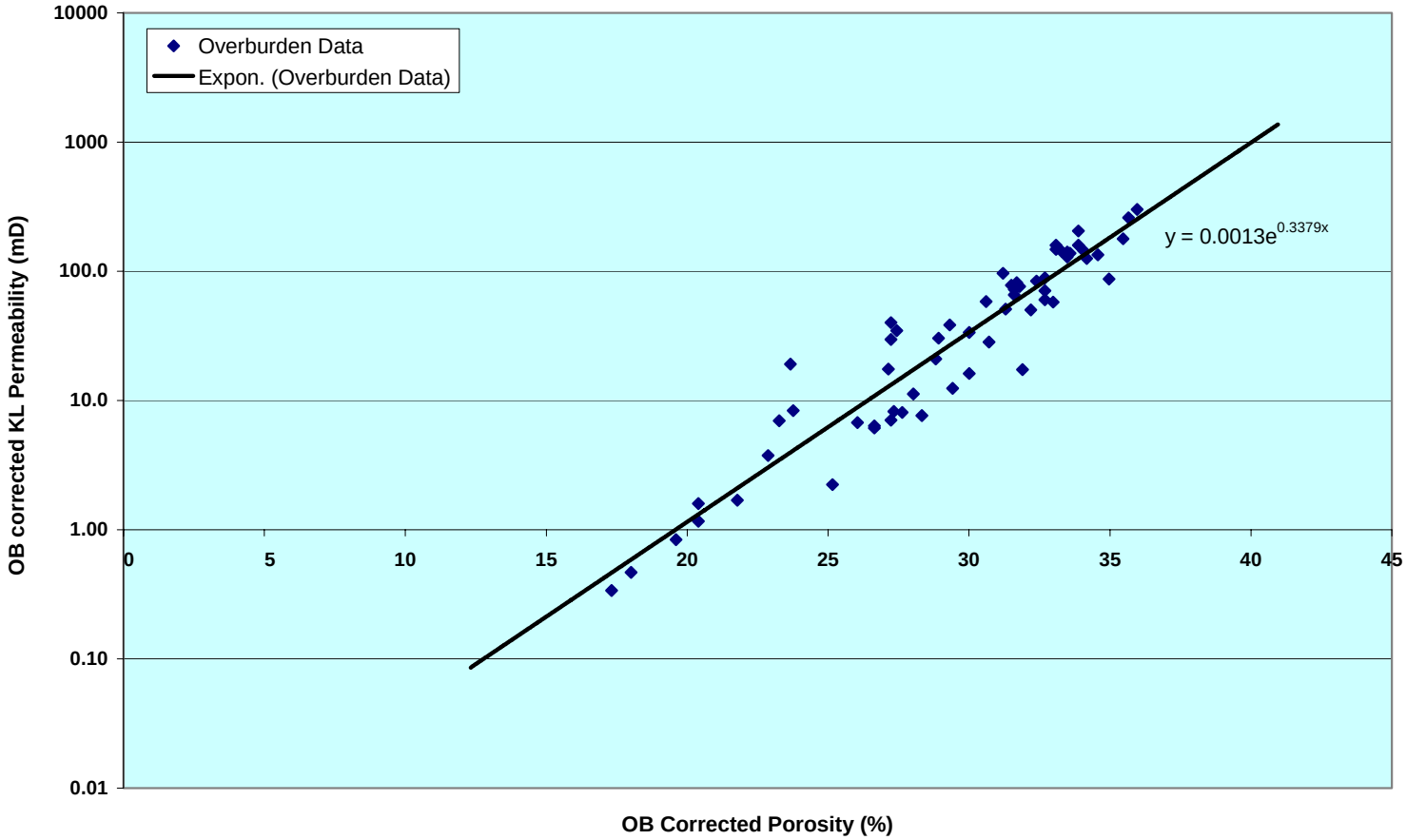

Figure 7: Measured Oil and Water Saturations from the Upper EVCM Core in Yolla-3

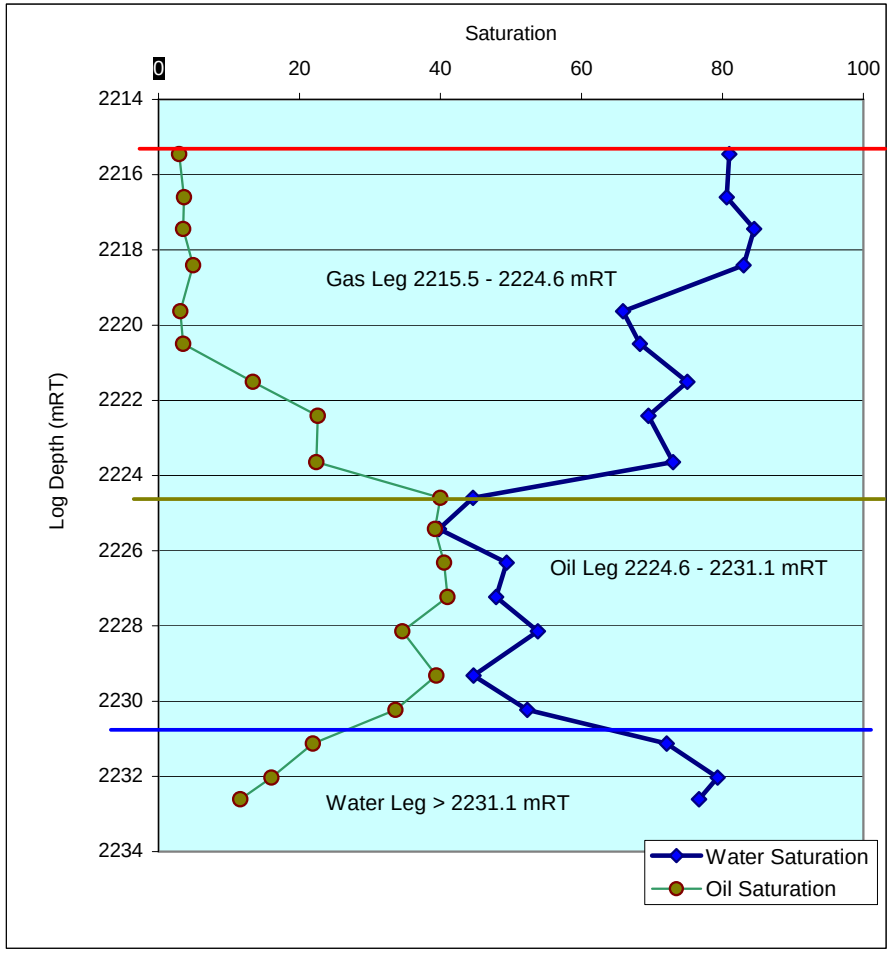

Core Depth (m)	Log Depth (mRT)	Fluid Saturation So (percent)	Sw (percent)
2216.40	2215.45	2.9	81.0
2217.55	2216.60	3.6	80.6
2218.39	2217.44	3.5	84.5
2219.36	2218.41	4.9	83.0
2220.58	2219.63	3.1	65.9
2221.45	2220.50	3.5	68.3
2222.46	2221.51	13.4	75.0
2223.36	2222.41	22.6	69.5
2224.59	2223.64	22.4	73.0
2225.54	2224.59	40.0	44.6
2226.37	2225.42	39.2	39.8
2227.27	2226.32	40.5	49.4
2228.18	2227.23	41.0	47.9
2229.09	2228.14	34.6	53.8
2230.27	2229.32	39.4	44.7
2231.18	2230.23	33.6	52.3
2232.08	2231.13	21.9	72.1
2232.98	2232.03	16.0	79.3
2233.56	2232.61	11.6	76.7

Figure 8: Core Formation Factor vs Core Porosity for the UEVCM Reservoir in Yolla-3

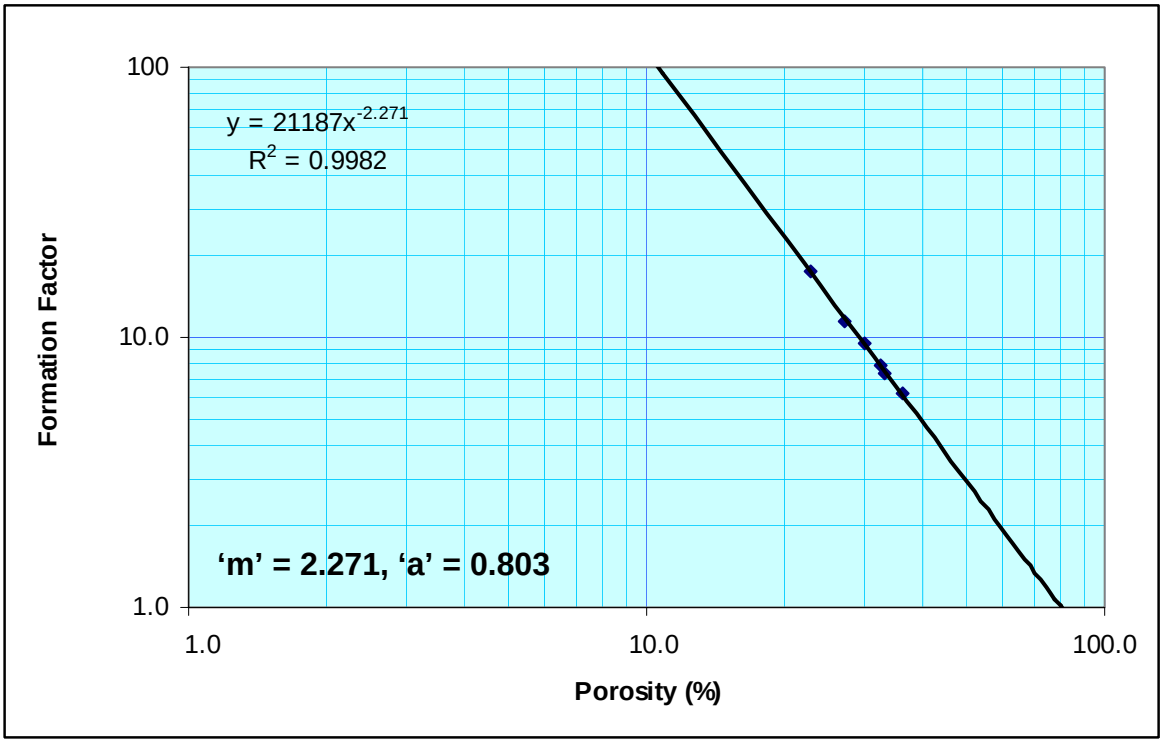

Figure 9: Interpreted Section Through the Upper EVCM in Yolla-3

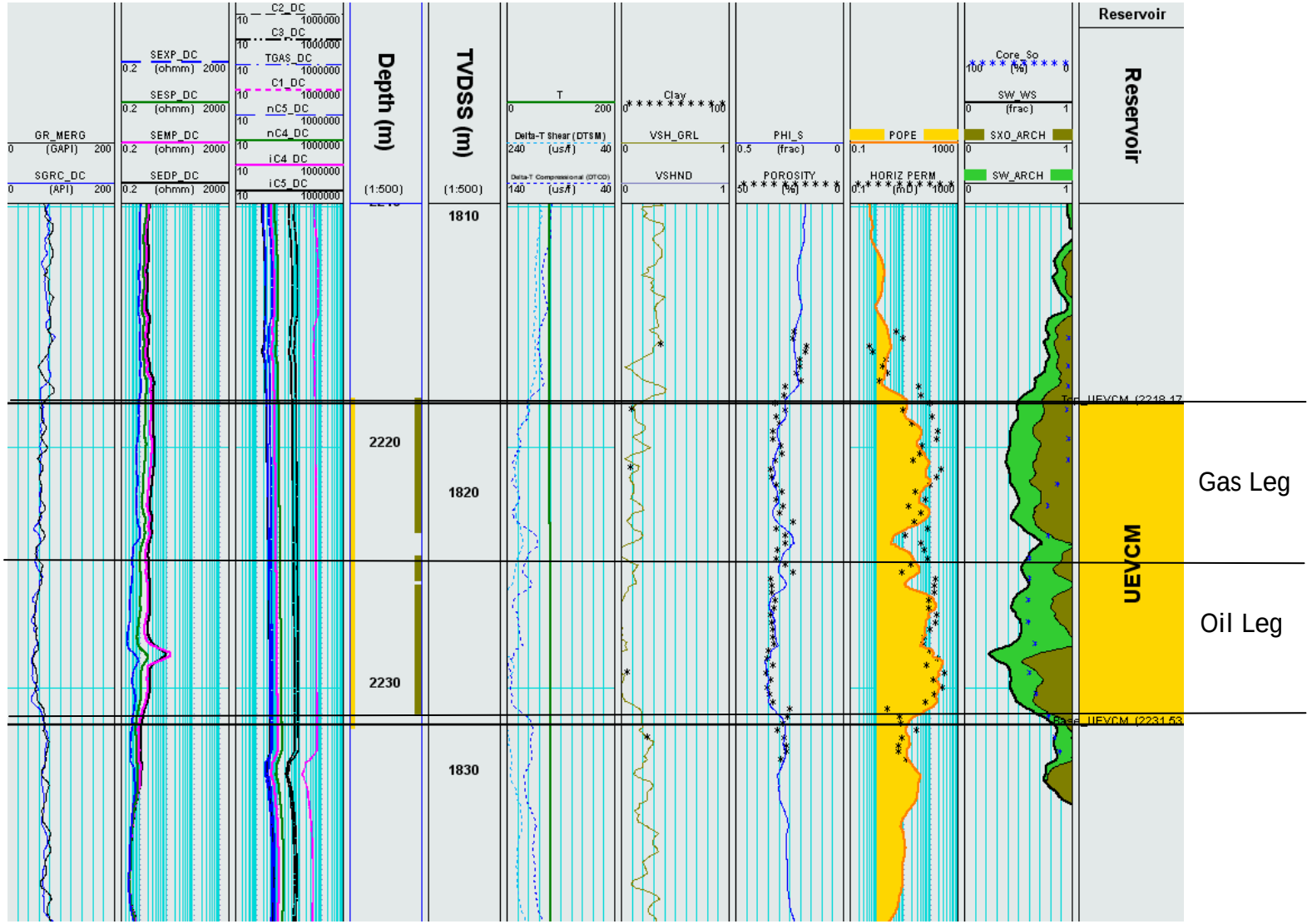

Figure 10: Interpreted Section through the 2718, 2755 and 2809 Sst

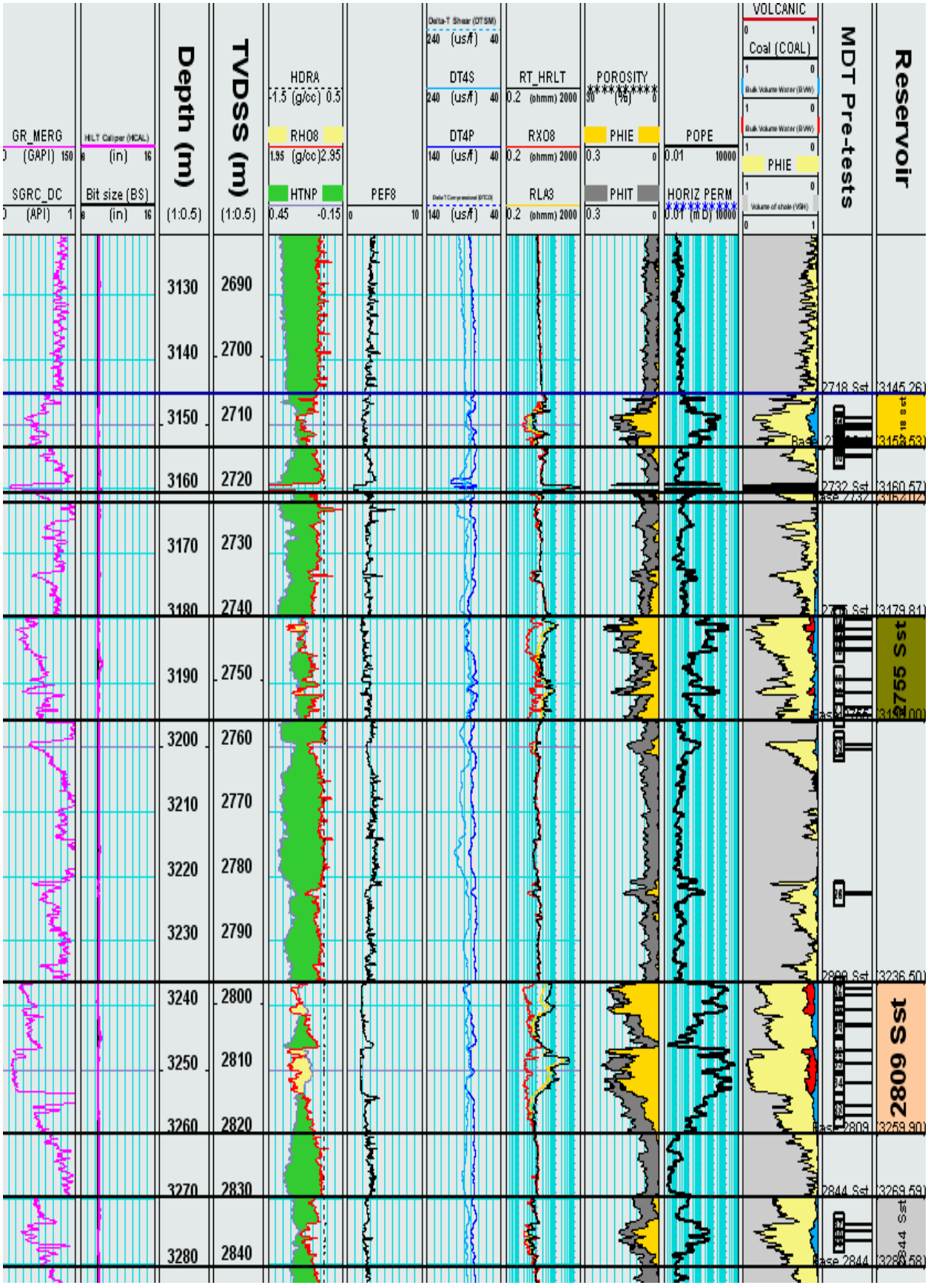

Figure 11: MDT Pressure Profile for the 2718 Sst

(By Mark Mussared)

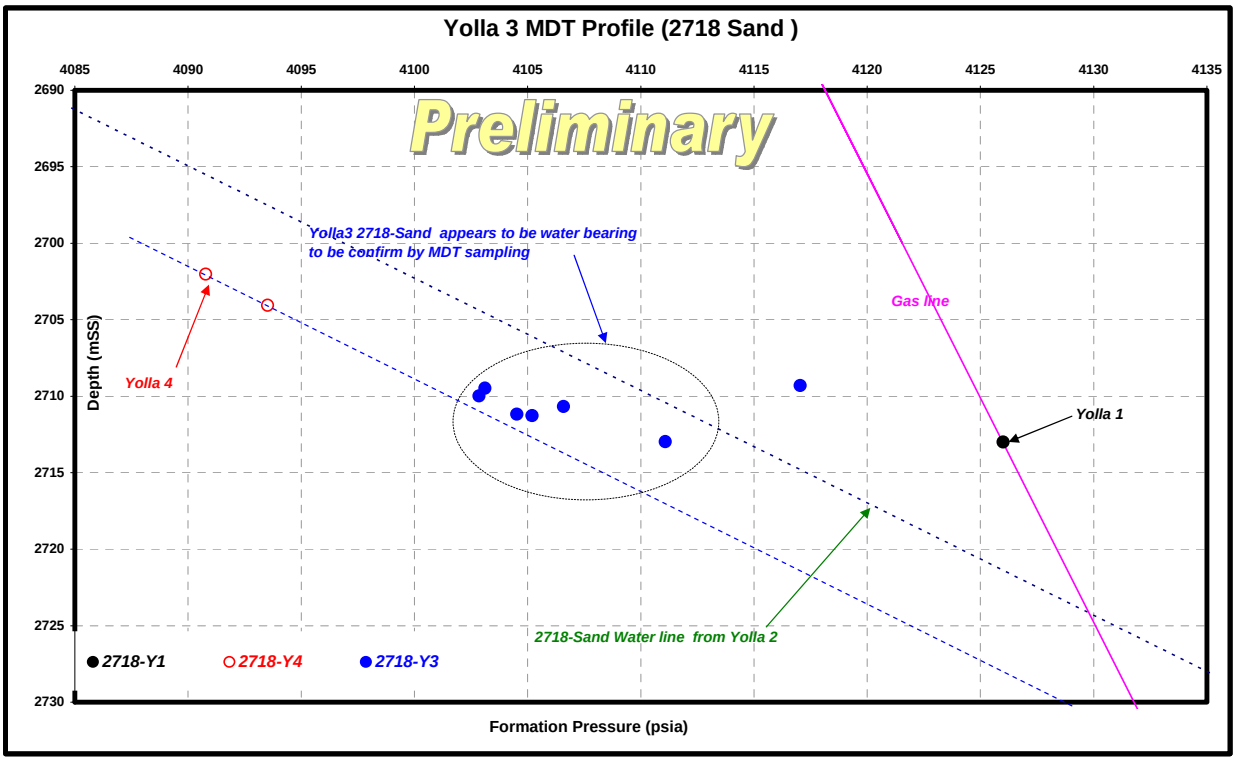

Figure 12: MDT Pressure Profile for the 2755 and 2809 Sst

(By Mark Mussared)

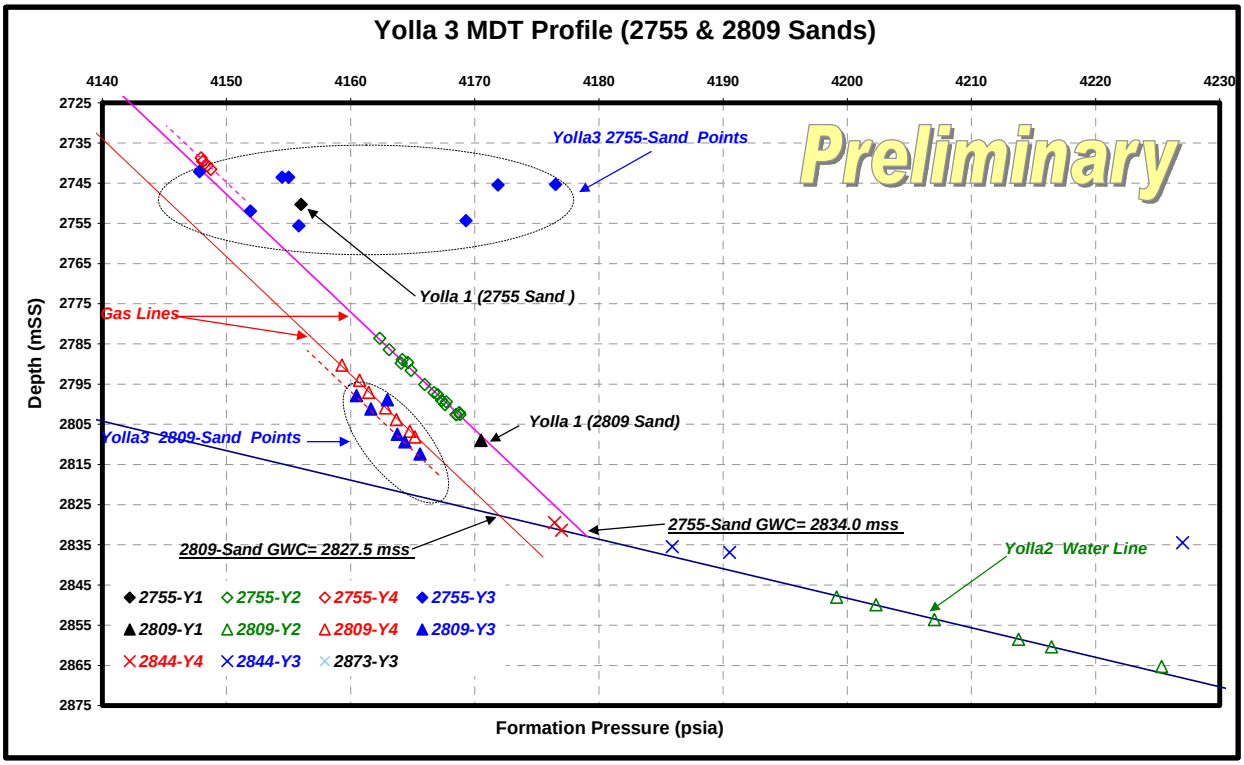

Figure 13: MDT Pressure Profile for the 2973 Sst

(By Mark Mussared)

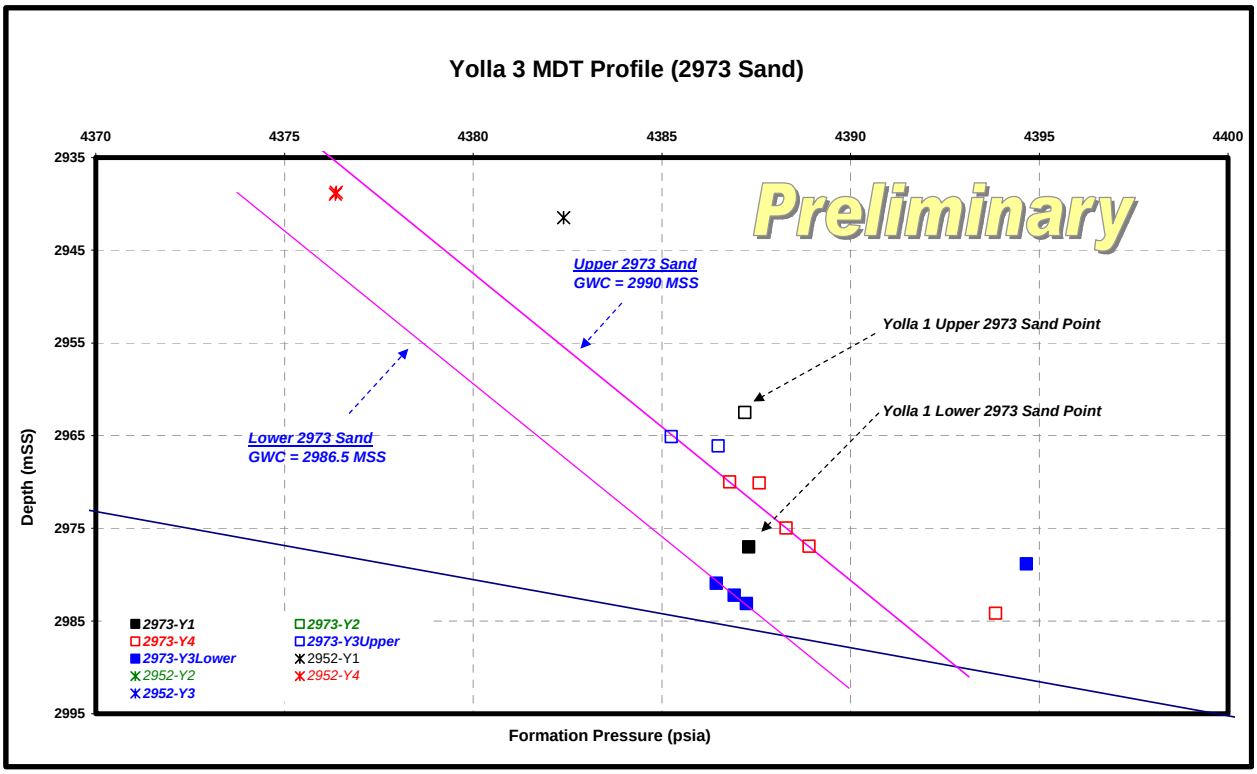

Figure 14: Interpreted Section through the 2952 and 2973 Sst

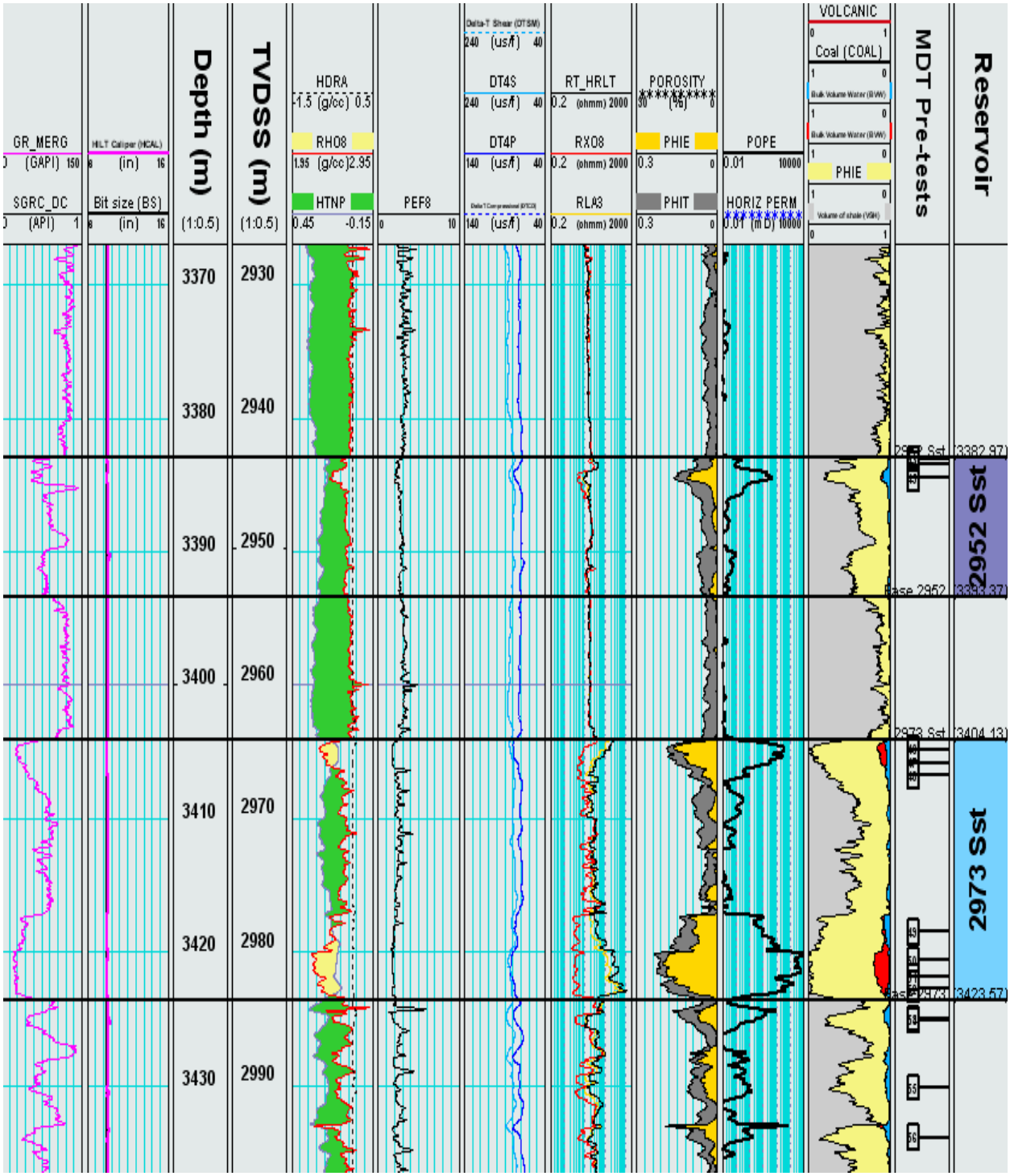

REFERENCES

1. Petrology, Diagenesis and Reservoir Quality of Core Samples from Yolla-3, Julian Baker, November 2004.
2. Yolla-4 Petrophysical Interpretation, Eastern View Coal Measures, 2590 – 3235 mRT, Andy Hall, Origin Energy, December 2004.

Appendix A: Terrastation Macro Used to Interpret the Yolla-3 Well

```
**********************************************
STANDARD_REPORT_TEXT OFF
*
CLEAR CHANNEL 70
SET CHANNEL NAME 70 VSH_GRL
*
CLEAR CHANNEL 57
SET CHANNEL NAME 57 VSHND
*
CLEAR CHANNEL 80
SET CHANNEL NAME 80 VSH
*
CLEAR CHANNEL 1375
SET CHANNEL NAME 1375 TEMPA
*
CLEAR CHANNEL 1376
SET CHANNEL NAME 1376 TEMPB
*
CLEAR CHANNEL 700
SET CHANNEL NAME 700 T
*
CLEAR CHANNEL 701
SET CHANNEL NAME 701 RW_T
*
CLEAR CHANNEL 702
SET CHANNEL NAME 702 RMF_T
*
CLEAR CHANNEL 328
SET CHANNEL NAME 328 SW_ARCH
*
CLEAR CHANNEL 340
SET CHANNEL NAME 340 SXO_ARCH
*
CLEAR CHANNEL 360
SET CHANNEL NAME 360 BVW
*
CLEAR CHANNEL 703
SET CHANNEL NAME 703 BVXO
*
* Waxman Smits terms
*
CLEAR CHANNEL 674
SET CHANNEL NAME 674 QV
*
CLEAR CHANNEL 675
SET CHANNEL NAME 675 B
*
CLEAR CHANNEL 676
SET CHANNEL NAME 676 F_STAR
*
CLEAR CHANNEL 677
SET CHANNEL NAME 677 N_STAR
*
CLEAR CHANNEL 678
SET CHANNEL NAME 678 M_STAR
*
CLEAR CHANNEL 679
SET CHANNEL NAME 679 TERM1
*
CLEAR CHANNEL 680
SET CHANNEL NAME 680 SW_TP
*
CLEAR CHANNEL 681
SET CHANNEL NAME 681 NWS
*
CLEAR CHANNEL 682
SET CHANNEL NAME 682 A_STAR
*
CLEAR CHANNEL 683
SET CHANNEL NAME 683 RI_STAR
*
```

```
CLEAR CHANNEL 481
SET CHANNEL NAME 481 TEST
*
CLEAR CHANNEL 482
SET CHANNEL NAME 482 POPE
*
CLEAR CHANNEL 483
SET CHANNEL NAME 483 PHI_DW
*
CLEAR CHANNEL 484
SET CHANNEL NAME 484 PHI_DMR
*
CLEAR CHANNEL 485
SET CHANNEL NAME 485 PHIT
*
CLEAR CHANNEL 486
SET CHANNEL NAME 486 PHIE
*
CLEAR CHANNEL 713
SET CHANNEL NAME 713 SXO_DMR
*
CLEAR CHANNEL 714
SET CHANNEL NAME 714 LEV_J
*
CLEAR CHANNEL 715
SET CHANNEL NAME 715 SW_CP
*
CLEAR CHANNEL 716
SET CHANNEL NAME 716 HEIGHT
*
CLEAR CHANNEL 717
SET CHANNEL NAME 717 PG
*
CLEAR CHANNEL 718
SET CHANNEL NAME 718 L
*
*------------------------------
* Net sand and net pay outputs
*
CLEAR CHANNEL 760
SET CHANNEL NAME 760 VSH_NP
*
CLEAR CHANNEL 762
SET CHANNEL NAME 762 PHIT_NP
*
CLEAR CHANNEL 763
SET CHANNEL NAME 763 PHIT_NS
*
CLEAR CHANNEL 764
SET CHANNEL NAME 764 PHIE_NP
*
CLEAR CHANNEL 765
SET CHANNEL NAME 765 POPE_NP
*
CLEAR CHANNEL 766
SET CHANNEL NAME 766 POPE_NS
*
CLEAR CHANNEL 767
SET CHANNEL NAME 767 SW_NP
*
CLEAR CHANNEL 768
SET CHANNEL NAME 768 PHIE_NS
*
************************************************
* Mud properties RM (C7), RMF (C9), RMC (C5), MW (C25)
* Temperatures RM (C8), RMF (C10), RMC (C6)
* From Yolla-3 Run 2/1
* MW
            C25= 9.45
* Rm
            C7 = 0.184
            C8 = 25.8
* Rmf
            C9 = 0.147
```

```
            C10 = 25.5
* Rmc
            C5 = 0.229
            C6 = 23.6
PRINT Mud Properties entered
*-------------------------------------------------------------------
* Temperature Log
*
* SET BHT (C13) and Depth (C20), Surface Temp (C14) and Depth (C34)
            C13 = 132
            C20 = 3491
            C14 = 8
            C34 = 124
C47 = @KEY(TVDSS)
if (C47 > 0)
            C50 = @SETDEPTH (C20)
            C50 = @GETVALUE (TVDSS)
            BEGIN
                        VT= C14 + (C13 - C14) * (VTVDSS - C34) / (C50 - C34)
            ENDBEGIN
            PRINT Temperature calculated in mTVDSS
else
            BEGIN
                        VT= C14 + (C13 - C14) * (VDEPTH - C34) / (C20 - C34)
            ENDBEGIN
            PRINT Temperature calculated in mMD
endif
*****************************************************************************
* Upper EVCM and the 12 1/4" hole section
* LWD GR and resistivity, sonic processed through casing
*
* Matrix GR (C61), Sonic (C63)
            C61 = 20
            C63 = 56
*
* Shale GR (C65), Sonic (C67), Resistivity (C19)
* Shale compaction factor (C57), Cut-off (C41)
            C65 = 135
            C67 = 80
            C19 = 15
            C57 = 25
            C59 = 0.24
*
* Fluid GR (C69), Density (C70), Sonic (C71), Neutron (C72)
            C69 = 10
            C71 = 189
* Permeability
* Exponential function terms from core (C55, C56)
            C55 = 0.0013
            C56 = 0.3379
*
* Net sand and net pay cut-offs
* VSH (< C40), Porosity (> C41), Permeability (> C42), Sw (< C43)
            C40 = 0.40
            C41 = 0.01
            C42 = 1.00
            C43 = 0.60
*
* Archie Parameters
* Set a (C16), m (C17), n (C18)
            C16= 0.803
            C17= 2.271
            C18= 1.840
*
* Water Resistivity
* Set Rw (C11) and RWT (C12)
            C11 = 0.115
            C12 = 25
*
*
SET DEPTH INTERVAL 2150 2340
BEGIN
*
* Shale Volume ----------------------------------------------
```

```
* Above EVCM
        if (VDEPTH < 2210)
                C61 = 40
                C65 = 120
        endif
* Above EVCM
        if (VDEPTH > 2210 & VDEPTH < 2240)
                C61 = 55
                C65 = 135
        endif
* Below EVCM
        if (VDEPTH > 2240)
                C61 = 40
                C65 = 120
        endif
        VVSH_GRL = (VGR_MERG-C61)/(C65 - C61)
        VVSH = VVSH_GRL
*
* Sonic Porosity ------------------------------------------------
* Overburden
        if (VDEPTH < 2184)
                VPHI_S = 0.05
        endif
* Gas Zone
        if (VDEPTH > 2184 & VDEPTH < 2224)
                C71 = 296
                VPHI_S = (VDT_MERG - C63) / (C71 - C63)
        endif
* Oil Zone
        if (VDEPTH > 2224 & VDEPTH < 2231)
                C71 = 285
                VPHI_S = (VDT_MERG - C63) / (C71 - C63)
        endif
* Water Zone
        if (VDEPTH > 2231 & VDEPTH < 2340)
                C71 = 280
                VPHI_S = (VDT_MERG - C63) / (C71 - C63)
        endif
        VPHIT = VPHI_S
        VPHIE = VPHIT - VVSH*0.17
*
* Permeability ------------------------------------------------
*
        VPOPE = (C55*@EXP((VPHIT*100)*C56))
*
* Water saturation ------------------------------------------------
*
* Temperature correct Rw and Rmf
*
        VRW_T = C11 * (C12 + 21.5) / (VT + 21.5)
        VRMF_T = C9 * (C10 + 21.5) / (VT + 21.5)
*
* Archie Water saturation
        VSW_ARCH = ((C16/VPHIT^C17)*(VRW_T/VSEDP_DC))^(1/C18)
        VSXO_ARCH = ((C16/VPHIT^C17)*(VRMF_T/VSEXP_DC))^(1/C18)
        if (VSW_ARCH > 1)
                VSW_ARCH = 1
        endif
        if (VSXO_ARCH < VSW_ARCH)
                VSXO_ARCH = VSW_ARCH
        endif
*
* Waxman Smits water Saturation ------------------------------------------
        VQV= 11562*(VPHIT*100)^-3.1819
*
* B = (0.225 * T  - 1.28 + 0.0004059*T^2) / 1+Rw^1.23*(0.045T-0.27)
        VB=(0.225*VT-1.28+0.0004059*VT^2)/(1+((VRW_T^1.23)*(0.045*VT-0.27)))
*
        VNWS=VRW_T*VB*VQV
*
* F* = F (1+Rw*B*Qv)
        VF_STAR=(C16/(VPHIT^C17))*(1+VNWS)
*
* m* = m - LOG10(1+RwBQv)/LOG10(PORO)
```

```
            VM_STAR=C17-@LOG10(1+VNWS)/@LOG10(VPHIT)
*
* a* = F* * PORO^m*
            VA_STAR = VF_STAR * VPHIT ^ VM_STAR
*
* RI* = RI ((1+(RwBQv/Sw))/(1+RwBQv))
*
            VSW_TP=VSW_ARCH
* ------------------------------------------------------------
            C47=0
:LOOP1
*
* RI* = RI ((1+(RwBQv/Sw))/(1+RwBQv))
            VRI_STAR=VSW_TP^(-1*C18)*((1+(VNWS/VSW_TP))/(1+VNWS))
            VN_STAR = -1 * @LOG10(VRI_STAR)/@LOG10(VSW_TP)
            if (VN_STAR = FALSE)
                        VN_STAR = C18
            endif
*
            VTERM1=((C16*VRW_T)/(VSEDP_DC*VPHIT^VM_STAR))
*
            C47=C47+1
            if (C47>20)
                        OUTPUT NUMBER 10 3 VDEPTH
                        OUTPUT TEXT Did not converge
                        PRINT OUTPUT
                        GOTO ENDLOOP1
            endif
            VSW_WS = ( VTERM1 * (1 / (1+(VNWS/VSW_TP))))^(1/VN_STAR)
            VTEST=@ABS(VSW_WS-VSW_TP)
*
            if (VTEST < 0.01)
                        GOTO ENDLOOP1
            else
                        VSW_TP=VSW_WS
                        GOTO LOOP1
            endif
:ENDLOOP1
* Net Sand / Net Pay Flags
            if (VVSH < C40 & VPOPE > C42)
                        VNETSAND = 1
            else
                        VNETSAND = 0
            endif
            if (VNETSAND = 1 & VSW_WS < C43)
                        VNETPAY = 1
            else
                        VNETPAY = 0
            endif
* Calculate BVW
            VBVW=VSW_WS*VPHIT
            if (VBVW > VPHIE)
                        VBVW = VPHIE
            endif
ENDBEGIN
************************************************************************
************************************************************************
************************************************************************
SET DEPTH INTERVAL 2340 3507
BEGIN
* Set COAL FLAG
            if (VRHO8 < 2.20 & VHTNP > 0.35)
                        VCOAL = 1
            else
                        VCOAL = 0
            endif
*------------------------------------------------------------
*2458 Sst Interval
            if (VDEPTH < 2980)
* Matrix GR (C61), Density (C62), Sonic (C63), Neutron (C64)
            C61 = 25
            C62 = 2.690
            C63 = 51.5
            C64 = -0.06
```

```
*
* Shale GR (C65), Density (C66), Sonic (C67), Neutron (C68), Resistivity (C19)
        C65 = 160
        C66 = 2.60
        C67 = 80
        C68 = 0.35
        C19 = 15
        C57 = 25
        C59 = 0.04
*
* Fluid GR (C69), Density (C70), Sonic (C71), Neutron (C72)
        C69 = 10
        C70 = 1.0
        C71 = 189
        C72 = 1.00
* Permeability
        C55 = 0.0242
        C56 = 0.3356
*
* Net sand and net pay cut-offs
* VSH (< C40), Porosity (> C41), Permeability (> C42), Sw (< C43)
        C40 = 0.40
        C41 = 0.01
        C42 = 1.00
        C43 = 0.60
*
* Archie Parameters
* Set a (C16), m (C17), n (C18)
        C16= 1.000
        C17= 1.762
        C18= 1.748
*
* Capillary Pressure Water Saturation
* Gas Gradient (C74), Water Gradient (C75), Oil Gradient (C60)
* J functions related to SW (C44, C45) and GWC (C35)
*
        C74 = 0.10
        C75 = 0.45
        C60 = 0.295
        C44 = 63.919
        C45 = -0.4864
        C35 = 2470.0
        if (VDEPTH < 2962.6 | VDEPTH > 2984.9)
                C44 = 0
                C45 = 0
        endif
*
* Water Resistivity
* Set Rw (C11) and RWT (C12)
        C11 = 0.347
        C12 = 25
* Nominate best porosity
* 1 = PHI_DMR, 2 = PHI_D, 3 = PHI_ND, 4 = PHI_S
        C22 = 1
        GOTO PAR_DONE
        endif
*-----------------------------------------------------------------
*2718 Sst
        if (VDEPTH < 3179)
* Matrix GR (C61), Density (C62), Sonic (C63), Neutron (C64)
        C61 = 25
        C62 = 2.716
        C63 = 51.5
        C64 = -0.06
*
* Shale GR (C65), Density (C66), Sonic (C67), Neutron (C68)
        C65 = 130
        C66 = 2.66
        C67 = 80
        C68 = 0.33
        C19 = 15
*
* Fluid GR (C69), Density (C70), Sonic (C71), Neutron (C72)
        C69 = 10
```

```
            C70 = 1.0
            C71 = 189
            C72 = 1.00
* Permeability
            C55 = 0.0080
            C56 = 0.5443
*
* Net sand and net pay cut-offs
* VSH (< C40), Porosity (> C41), Permeability (> C42), Sw (< C43)
            C40 = 0.40
            C41 = 0.01
            C42 = 0.10
            C43 = 0.60
*
* Archie Parameters
* Set a (C16), m (C17), n (C18)
            C16= 1.000
            C17= 1.762
            C18= 1.748
*
* Capillary Pressure Water Saturation
* Gas Gradient (C74), Water Gradient (C75), Oil Gradient (C60)
* J functions related to SW (C44, C45) and GWC (C35)
*
            C74 = 0.10
            C75 = 0.45
            C60 = 0.295
            C44 = 0
            C45 = 0
            C35 = 0
*
* Water Resistivity
* Set Rw (C11) and RWT (C12)
            C11 = 0.689
            C12 = 25
* Nominate best porosity
* 1 = PHI_DMR, 2 = PHI_D, 3 = PHI_ND, 4 = PHI_S
            C22 = 1
            GOTO PAR_DONE
            endif
*-----------------------------------------------------------------
*2755 Sst
            if (VDEPTH < 3236)
* Matrix GR (C61), Density (C62), Sonic (C63), Neutron (C64)
            C61 = 25
            C62 = 2.697
            C63 = 51.5
            C64 = -0.06
*
* Shale GR (C65), Density (C66), Sonic (C67), Neutron (C68)
            C65 = 130
            C66 = 2.66
            C67 = 80
            C68 = 0.33
            C19 = 15
*
* Fluid GR (C69), Density (C70), Sonic (C71), Neutron (C72)
            C69 = 10
            C70 = 0.6
            C71 = 350
            C72 = 0.6
* Permeability
            C55 = 0.0080
            C56 = 0.5443
*
* Net sand and net pay cut-offs
* VSH (< C40), Porosity (> C41), Permeability (> C42), Sw (< C43)
            C40 = 0.40
            C41 = 0.01
            C42 = 0.10
            C43 = 0.60
*
* Archie Parameters
* Set a (C16), m (C17), n (C18)
```

```
            C16= 1.000
            C17= 1.762
            C18= 1.748
*
* Capillary Pressure Water Saturation
* Gas Gradient (C74), Water Gradient (C75), Oil Gradient (C60)
* J functions related to SW (C44, C45) and GWC (C35)
*
            C74 = 0.10
            C75 = 0.45
            C60 = 0.295
            C44 = 62.736
            C45 = -0.4977
            C35 = 2832.9
            if (VDEPTH < 3179.8 | VDEPTH > 3196.0)
                  C44 = 0
                  C45 = 0
            endif
*
* Water Resistivity
* Set Rw (C11) and RWT (C12)
            C11 = 0.468
            C12 = 25
* Nominate best porosity
* 1 = PHI_DMR, 2 = PHI_D, 3 = PHI_ND, 4 = PHI_S
            C22 = 1
            GOTO PAR_DONE
            endif
*-----------------------------------------------------------------
*2809 Sst
            if (VDEPTH < 3269)
* Matrix GR (C61), Density (C62), Sonic (C63), Neutron (C64)
            C61 = 15
            C62 = 2.663
            C63 = 51.5
            C64 = -0.06
*
* Shale GR (C65), Density (C66), Sonic (C67), Neutron (C68)
            C65 = 140
            C66 = 2.65
            C67 = 80
            C68 = 0.31
            C19 = 15
*
* Fluid GR (C69), Density (C70), Sonic (C71), Neutron (C72)
            C69 = 10
            C70 = 0.6
            C71 = 189
            C72 = 0.6
* Permeability
            C55 = 0.00080
            C56 = 0.67768
*
* Net sand and net pay cut-offs
* VSH (< C40), Porosity (> C41), Permeability (> C42), Sw (< C43)
            C40 = 0.40
            C41 = 0.01
            C42 = 0.10
            C43 = 0.60
*
* Archie Parameters
* Set a (C16), m (C17), n (C18)
            C16= 1.000
            C17= 1.770
            C18= 1.748
*
* Capillary Pressure Water Saturation
* Gas Gradient (C74), Water Gradient (C75), Oil Gradient (C60)
* J functions related to SW (C44, C45) and GWC (C35)
*
            C74 = 0.10
            C75 = 0.45
            C60 = 0.295
            C44 = 63.919
```

```
            C45 = -0.4864
            C35 = 2826.8
            if (VDEPTH < 3236.5 | VDEPTH > 3259.9)
                  C44 = 0
                  C45 = 0
            endif
*
* Water Resistivity
* Set Rw (C11) and RWT (C12)
            C11 = 0.468
            C12 = 25
* Nominate best porosity
* 1 = PHI_DMR, 2 = PHI_D, 3 = PHI_ND, 4 = PHI_S
            C22 = 1
            GOTO PAR_DONE
            endif
*-----------------------------------------------------------------
*2844 Sst
            if (VDEPTH < 3350)
* Matrix GR (C61), Density (C62), Sonic (C63), Neutron (C64)
            C61 = 25
            C62 = 2.663
            C63 = 51.5
            C64 = -0.06
*
* Shale GR (C65), Density (C66), Sonic (C67), Neutron (C68)
            C65 = 130
            C66 = 2.66
            C67 = 80
            C68 = 0.33
            C19 = 15
*
* Fluid GR (C69), Density (C70), Sonic (C71), Neutron (C72)
            C69 = 10
            C70 = 1.0
            C71 = 189
            C72 = 1.00
* Permeability
            C55 = 0.00080
            C56 = 0.67768
*
* Net sand and net pay cut-offs
* VSH (< C40), Porosity (> C41), Permeability (> C42), Sw (< C43)
            C40 = 0.40
            C41 = 0.01
            C42 = 0.10
            C43 = 0.60
*
* Archie Parameters
* Set a (C16), m (C17), n (C18)
            C16= 1.000
            C17= 1.770
            C18= 1.748
*
* Capillary Pressure Water Saturation
* Gas Gradient (C74), Water Gradient (C75), Oil Gradient (C60)
* J functions related to SW (C44, C45) and GWC (C35)
*
            C74 = 0.10
            C75 = 0.45
            C60 = 0.295
            C44 = 0
            C45 = 0
            C35 = 0
*
* Water Resistivity
* Set Rw (C11) and RWT (C12)
            C11 = 0.468
            C12 = 25
* Nominate best porosity
* 1 = PHI_DMR, 2 = PHI_D, 3 = PHI_ND, 4 = PHI_S
            C22 = 1
            GOTO PAR_DONE
            endif
```

```
*-----------------------------------------------------------------
*2952 Sst
            if (VDEPTH < 3404)
* Matrix GR (C61), Density (C62), Sonic (C63), Neutron (C64)
            C61 = 25
            C62 = 2.724
            C63 = 51.5
            C64 = -0.06
*
* Shale GR (C65), Density (C66), Sonic (C67), Neutron (C68)
            C65 = 130
            C66 = 2.66
            C67 = 75
            C68 = 0.33
            C19 = 6
*
* Fluid GR (C69), Density (C70), Sonic (C71), Neutron (C72)
            C69 = 10
            C70 = 1.0
            C71 = 189
            C72 = 1.00
* Permeability
            C55 = 0.0003
            C56 = 0.7493
*
* Net sand and net pay cut-offs
* VSH (< C40), Porosity (> C41), Permeability (> C42), Sw (< C43)
            C40 = 0.40
            C41 = 0.01
            C42 = 0.10
            C43 = 0.60
*
* Archie Parameters
* Set a (C16), m (C17), n (C18)
            C16= 1.000
            C17= 2.000
            C18= 1.633
*
* Capillary Pressure Water Saturation
* Gas Gradient (C74), Water Gradient (C75), Oil Gradient (C60)
* J functions related to SW (C44, C45) and GWC (C35)
*
            C74 = 0.10
            C75 = 0.45
            C60 = 0.295
            C44 = 0
            C45 = 0
            C35 = 0
*
* Water Resistivity
* Set Rw (C11) and RWT (C12)
            C11 = 0.401
            C12 = 25
* Nominate best porosity
* 1 = PHI_DMR, 2 = PHI_D, 3 = PHI_ND, 4 = PHI_S
            C22 = 1
            GOTO PAR_DONE
            endif
*-----------------------------------------------------------------
*2973 Sst
            if (VDEPTH > 3404)
* Matrix GR (C61), Density (C62), Sonic (C63), Neutron (C64)
            C61 = 25
            C62 = 2.679
            C63 = 51.5
            C64 = -0.06
*
* Shale GR (C65), Density (C66), Sonic (C67), Neutron (C68)
            C65 = 130
            C66 = 2.66
            C67 = 69
            C68 = 0.33
            C19 = 15
*
```

```
* Fluid GR (C69), Density (C70), Sonic (C71), Neutron (C72)
        C69 = 10
        C70 = 0.6
        C71 = 189
        C72 = 0.6
* Permeability
        C55 = 0.0003
        C56 = 0.7493
*
* Net sand and net pay cut-offs
* VSH (< C40), Porosity (> C41), Permeability (> C42), Sw (< C43)
        C40 = 0.40
        C41 = 0.01
        C42 = 0.10
        C43 = 0.60
*
* Archie Parameters
* Set a (C16), m (C17), n (C18)
        C16= 1.000
        C17= 2.000
        C18= 1.633
*
* Capillary Pressure Water Saturation
* Gas Gradient (C74), Water Gradient (C75), Oil Gradient (C60)
* J functions related to SW (C44, C45) and GWC (C35)
*
        if (VDEPTH < 3410)
                C74 = 0.10
                C75 = 0.45
                C60 = 0.295
                C44 = 58.221
                C45 = -0.3534
                C35 = 2990.2
        else
                C74 = 0.10
                C75 = 0.45
                C60 = 0.295
                C44 = 39.588
                C45 = -0.3744
                C35 = 2986.6
        endif
        if (VDEPTH < 3404 | VDEPTH > 3423.6)
                C44 = 0
                C45 = 0
        endif
*
* Water Resistivity
* Set Rw (C11) and RWT (C12)
        C11 = 0.576
        C12 = 25
* Nominate best porosity
* 1 = PHI_DMR, 2 = PHI_D, 3 = PHI_ND, 4 = PHI_S
        C22 = 1
        GOTO PAR_DONE
        endif
:PAR_DONE
*-------------------------------------------------------
* Determine shale volume
        VVSH_GRL = (VGR_MERG-C61)/(C65 - C61)
        V1375 = (C62 - C70) * (C72 - VHTNP) - (VRHO8 - C70) * (C72 - C64)
        V1376 = (C62 - C70) * (C72 - C68) - (C66 - C70) * (C72 - C64)
        VVSHND=V1375 / V1376
*
        if (VVSH_GRL<=VVSHND)
                VVSH = VVSH_GRL
        else
                VVSH= VVSHND
        endif
        if (VVSH < 0)
                VVSH=0
        endif
        if (VVSH > 1)
                VVSH=1
        endif
```

```
*-------------------------------------------------------------
* Porosity
*
        VPHI_D = (C62 - VRHO8) / (C62 - C70)
        VPHI_DW = (C62 - VRHO8) / (C62 - 1.00)
        VNPSC = VHTNP_SS - VVSH * (0.41 - 0.06)
        VPHI_ND = @SQT((VPHI_D^2 + VNPSC^2) / 2)
        if (VPHI_DW > VTCMR)
                VPHI_DMR = (VPHI_DW*0.6)+(0.4*VTCMR)
        else
                VPHI_DMR = VTCMR
        endif
*
        VDTSC = VDT_MERG - VVSH * 29
        VPHI_S = (C63 - VDTSC) / (C63 - C71)
*
        if (VCOAL=1)
                VPHI_D=0
                VPHI_S=0
                VPHI_ND=0
                VPHI_DMR=0
        endif
        if (VVOLCANIC=1)
                VVSH=0
                VCOAL=0
                VPHI_D=0
                VPHI_S=0
                VPHI_ND=0
                VPHI_DMR=0
        endif
* Nominate best porosity for each zone
        if (C22 = 1)
                VPHIT = VPHI_DMR
        endif
        if (C22 = 2)
                VPHIT = VPHI_D
        endif
        if (C22 = 3)
                VPHIT = VPHI_ND
        endif
        if (C22 = 4)
                VPHIT = VPHI_S
        endif
        VPHIE = VPHIT - (VTCMR - VCMFF)
*-------------------------------------------------------------
* Water saturation
* Rw and Rmf correction
*
        VRW_T = C11 * (C12 + 21.5) / (VT + 21.5)
        VRMF_T = C9 * (C10 + 21.5) / (VT + 21.5)
*
* Archie Water saturation
        VSW_ARCH = ((C16/VPHIT^C17)*(VRW_T/VSEDP_DC))^(1/C18)
        VSXO_ARCH = ((C16/VPHIT^C17)*(VRMF_T/VSEXP_DC))^(1/C18)
*
* Indonesia -----------------------------------------------------------
        C54 = (C16*VRW_T)/(VPHIE^C17)
        VSW_IND= ((VVSH^(0.5*(2-VVSH)))/(C19/VRT_HRLT)^0.5+(VRT_HRLT/C54))^(-2/C18)
        C54 = (C16*VRM_HRLT)/(VPHIE^C17)
        VSXO_IND=((VVSH^(0.5*(2-VVSH)))/(C19/VRXO8)^0.5+(VRXO8/C54))^(-2/C18)
        VSW_IND = ((VSW_IND * VPHIE) + (VPHIT-VPHIE)) / VPHIT
        VSXO_IND = ((VSXO_IND * VPHIE) + (VPHIT-VPHIE)) / VPHIT
*
* DMR SGXO ------------------------------------------------------------
        if (VTCMR > 0)
                VL = (1.00 - 0.25) / (C62 - 1.00)
                VPG = 1 - @EXP(-1*(5/3))
                C58 = 0.4
                VSXO_DMR = 1 - (VPHI_DW - VTCMR)/((VPHI_DW*(1-C58*VPG))+(VL*VTCMR))
        endif
*
* Permeability ------------------------------------------------
*
        VPOPE = (C55*@EXP((VPHIT*100)*C56))
```

```
            if (VVOLCANICS =  1)
                        VPOPE = 0
            endif
*
* Capillary Pressure Sw calculation ------------------------------------
            VHEIGHT = C35 - VTVDSS
            if (VHEIGHT < 0)
                        VSW_CP = 1
                        GOTO END_CP
            endif
            VLEV_J = ((VHEIGHT * (C75 - C74)*3.28084) / 50) * (VPOPE / VPHIT)^0.5
            VSW_CP = (C44 * VLEV_J^C45) / 100
:END_CP
* Waxman Smits water Saturation ----------------------------------------
* QV = CEC * RHOG * (1-PORO) / (100* PORO)
            VQV= 3.256 * C62 * (1 - VPHIT) / (100 * VPHIT)
*
* B = (0.225 * T  - 1.28 + 0.0004059*T^2) / 1+Rw^1.23*(0.045T-0.27)
            VB=(0.225*VT-1.28+0.0004059*VT^2)/(1+((VRW_T^1.23)*(0.045*VT-0.27)))
*
            VNWS=VRW_T*VB*VQV
*
* F* = F (1+Rw*B*Qv)
            VF_STAR=(C16/(VPHIT^C17))*(1+VNWS)
*
* m* = m - LOG10(1+RwBQv)/LOG10(PORO)
            VM_STAR=C17-@LOG10(1+VNWS)/@LOG10(VPHIT)
*
* a* = F* * PORO^m*
            VA_STAR = VF_STAR * VPHIT ^ VM_STAR
*
* RI* = RI ((1+(RwBQv/Sw))/(1+RwBQv))
*
            VSW_TP=VSW_ARCH
* ------------------------------------------------------------
            C47=0
:LOOP2
*
* RI* = RI ((1+(RwBQv/Sw))/(1+RwBQv))
            VRI_STAR=VSW_TP^(-1*C18)*((1+(VNWS/VSW_TP))/(1+VNWS))
            VN_STAR = -1 * @LOG(VRI_STAR)/@LOG(VSW_TP)
            if (VN_STAR = FALSE)
                        VN_STAR = C18
            endif
*
            VTERM1=((C16*VRW_T)/(VSEDP_DC*VPHIT^VM_STAR))
*
            C47=C47+1
            if (C47>20)
                        OUTPUT NUMBER 10 3 VDEPTH
                        OUTPUT TEXT Did not converge
                        PRINT OUTPUT
                        GOTO ENDLOOP2
            endif
            VSW_WS = ( VTERM1 * (1 / (1+(VNWS/VSW_TP))))^(1/VN_STAR)
            VTEST=@ABS(VSW_WS-VSW_TP)
*
            if (VTEST < 0.01)
                        GOTO ENDLOOP2
            else
                        VSW_TP=VSW_WS
                        GOTO LOOP2
            endif
:ENDLOOP2
* Calculate BVW
            VBVW=VSW_IND*VPHIE
            if (VBVW > VPHIE)
                        VBVW = VPHIE
            endif
*
*-------------------------------------------------------------
*
* Net Sand / Net Pay Flags
            if (VVSH < C40 & VPOPE > C42)
```

```
                VNETSAND = 1
        else
                VNETSAND = 0
        endif
        if (VNETSAND = 1 & VSW_IND < C43)
                VNETPAY = 1
        else
                VNETPAY = 0
        endif
ENDBEGIN
PRINT STARS
OUTPUT TEXT Well Name:
OUTPUT WELLNAME
PRINT OUTPUT
PRINT SPACES
OUTPUT TEXT RESERVOIR    GROSS INTERVAL        NET SAND            NET PAY
PRINT OUTPUT
OUTPUT TEXT GROSS Top, Base, Thickness
PRINT OUTPUT
OUTPUT TEXT NETSAND Thickness, NTG, PHIT, PHIE, PERMEABILITY
PRINT OUTPUT
OUTPUT TEXT NETPAY Thickness, NTG, PHIT, PHIE, PERMEABILITY, Sw
PRINT OUTPUT
SET CURRENT ZONE IUEVCM
C26 = 1
:AVERAGES
IF (C26 = 1)
        OUTPUT TEXT UEVCM___
ENDIF
IF (C26 = 2)
        OUTPUT TEXT 2458_Sst
ENDIF
IF (C26 = 3)
        OUTPUT TEXT 2718_Sst
ENDIF
IF (C26 = 4)
        OUTPUT TEXT 2732_Sst
ENDIF
IF (C26 = 5)
        OUTPUT TEXT 2755_Sst
ENDIF
IF (C26 = 6)
        OUTPUT TEXT 2809_Sst
ENDIF
IF (C26 = 7)
        OUTPUT TEXT 2844_Sst
ENDIF
IF (C26 = 8)
        OUTPUT TEXT 2952_Sst
ENDIF
IF (C26 = 9)
        OUTPUT TEXT 2973_Sst
ENDIF
C37 = 0
C36 = 0
C54 = 0
C74 = 0
PRINT SPACES
BEGIN
        C36 = C36 + 1
        if (C36 = 1)
                C75 = VDEPTH
        endif
        if (VNETSAND = 1)
                C37 = C37 + 1
                VVSH_NS = VVSH
                VPHIT_NS = VPHIT
                VPHIE_NS = VPHIE
                VPOPE_NS = VPOPE
        endif
        if (VNETPAY = 1)
                C54 = C54 + 1
                VVSH_NP = VVSH
                VPHIT_NP = VPHIT
```

```
                    VPHIE_NP = VPHIE
                    VPOPE_NP = VPOPE
                    VSW_NP = VSW_IND
          endif
          C47 = VDEPTH
ENDBEGIN
                    C48 = C47 - C75
                    C49 = C37 / C36
                    C50 = C49 * C48
                    C51 = C54 / C36
                    C52 = C51 * C48
                    C38 = @AMEAN(VSH_NS)
                    C39 = @AMEAN(PHIT_NS)
                    C40 = @AMEAN(PHIE_NS)
                    C41 = @GMEAN(POPE_NS)
                    C42 = @AMEAN(VSH_NP)
                    C43 = @AMEAN(PHIT_NP)
                    C44 = @AMEAN(PHIE_NP)
                    C45 = @GMEAN(POPE_NP)
                    C46 = @AMEAN(SW_NP)
*
* Gross Interval
OUTPUT NUMBER  7 1 C75
OUTPUT NUMBER  7 1 C47
OUTPUT NUMBER  6 1 C48
* Net Sand Parameters
OUTPUT NUMBER  6 1 C50
OUTPUT NUMBER  6 3 C49
OUTPUT NUMBER  6 3 C39
OUTPUT NUMBER  6 3 C40
OUTPUT NUMBER  8 2 C41
* Net Pay Parameters
OUTPUT NUMBER 6 1 C52
OUTPUT NUMBER 6 3 C51
OUTPUT NUMBER 6 3 C43
OUTPUT NUMBER 6 3 C44
OUTPUT NUMBER 8 2 C45
OUTPUT NUMBER 6 3 C46
PRINT OUTPUT
SET NEXT ZONE
          if (C26 = 9)
                    PRINT STARS
                    STOP
          else
                    C26 = C26+1
          endif
GOTO AVERAGES
STOP
```

ENCLOSURE-1
Petrophysical Summary Plot
Upper EVCM
2150-2250 mRT (1:200)

Yolla-3

Permit: Yolla	**RTE:** 43.0 m	**TD (logs):** 3507.0 m
Latitude : 39 50’ 40.4707’ S	**Bit Size:** 8.5 in	**BHT:** 132.0 degC
Longtitude : 145 49’ 06.0849’ E	**Rm:** 0.184 ohmm at: 25.8 degC	**Vertical Scale** 1:200 m
Easting : 398905.69	**Rmf:** 0.030 ohmm at: 77.4 degC	**Interpreter :** Andy Hall
Northing : 5588825.22	**Rmc:** 0.229 ohmm at: 23.6 degC	
Datum : Rotary Table (RT)	**Plot created on:** 23/Dec/04 at: 14:30:16	

GR_MERG 0 (GAPI) 200 — SGRC_DC 0 (API) 200

SEXP_DC 0.2 (ohmm) 2000 — SESP_DC 0.2 (ohmm) 2000 — SEMP_DC 0.2 (ohmm) 2000 — SEDP_DC 0.2 (ohmm) 2000

C2_DC 10 1000000 — C3_DC 10 1000000 — TGAS_DC 10 1000000 — C1_DC 10 1000000 — nC5_DC 10 1000000 — nC4_DC 10 1000000 — iC4_DC 10 1000000 — iC5_DC 10 1000000

Depth (m) (1:200)

TVDSS (m) (1:200)

T 0 200 — Delta-T Shear (DTSM) 240 (us/f) 40 — Delta-T Compressional (DTCO) 140 (us/f) 40

Clay 0 100 — VSH_GRL 0 1 — VSHND 0 1

PHI_S 0.5 (frac) 0 — POROSITY 50 (%) 0

POPE 0.1 1000 — HORIZ PERM 0.1 (mD) 1000

Core_So 100 (%) 0 — SW_WS 0 (frac) 1 — SXO_ARCH 0 1 — SW_ARCH 0 1

Reservoir

Top_UEVCM (2218.5

UEVCM

Base_UEVCM (2231.5

ENCLOSURE-2
Petrophysical Summary Plot
Upper EVCM
2150-2250 mRT (1:500)

Yolla-3

Permit: Yolla	**RTE:** 43.0 m	**TD (logs):** 3507.0 m
Latitude : 39 50’ 40.4707’ S	**Bit Size:** 8.5 in	**BHT:** 132.0 degC
Longtitude : 145 49’ 06.0849’ E	**Rm:** 0.184 ohmm at: 25.8 degC	**Vertical Scale** 1:500 m
Easting : 398905.69	**Rmf:** 0.030 ohmm at: 77.4 degC	**Interpreter :** Andy Hall
Northing : 5588825.22	**Rmc:** 0.229 ohmm at: 23.6 degC	
Datum : Rotary Table (RT)	**Plot created on:** 23/Dec/04 at: 14:27:33	

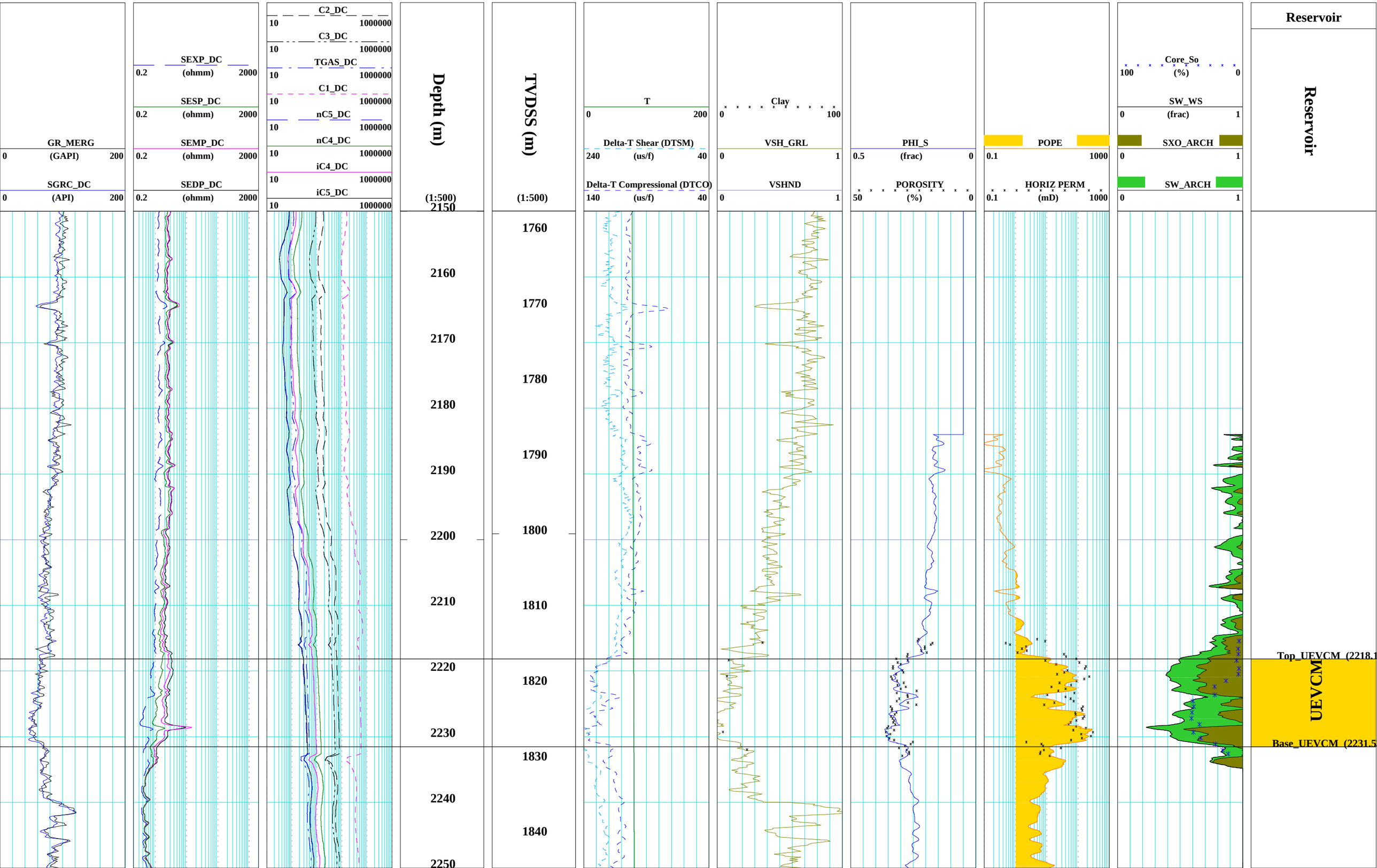

ENCLOSURE-3
Petrophysical Summary Plot
Main EVCM Reservoirs
3100-3500 mRT (1:200)

YOLLA-3

Permit: Yolla	RTE: 43.0 m	TD (logs): 3507.0 m
Latitude : 39 50' 40.4707' S	Bit Size: 8.5 in	BHT: 132.0 degC
Longtitude : 145 49' 06.0849' E	Rm: 0.184 ohmm at: 25.8 degC	Vertical Scale 1:200 m
Easting : 398905.69	Rmf: 0.147 ohmm at: 25.5 degC	Interpreter : Andy Hall
Northing : 5588825.22	Rmc: 0.229 ohmm at: 23.6 degC	
Datum : Rotary Table (RT)	Plot created on: 16/Mar/05 at: 10:46:39	

ENCLOSURE-4
Petrophysical Summary Plot
Main EVCM Reservoirs
3100-3500 mRT (1:500)

YOLLA-3

Permit: Yolla	**RTE:** 43.0 m	**TD (logs):** 3507.0 m
Latitude : 39 50’ 40.4707’ S	**Bit Size:** 8.5 in	**BHT:** 132.0 degC
Longtitude : 145 49’ 06.0849’ E	**Rm:** 0.184 ohmm at: 25.8 degC	**Vertical Scale** 1:500 m
Easting : 398905.69	**Rmf:** 0.147 ohmm at: 25.5 degC	**Interpreter :** Andy Hall
Northing : 5588825.22	**Rmc:** 0.229 ohmm at: 23.6 degC	
Datum : Rotary Table (RT)	**Plot created on:** 16/Mar/05 at: 10:27:55	

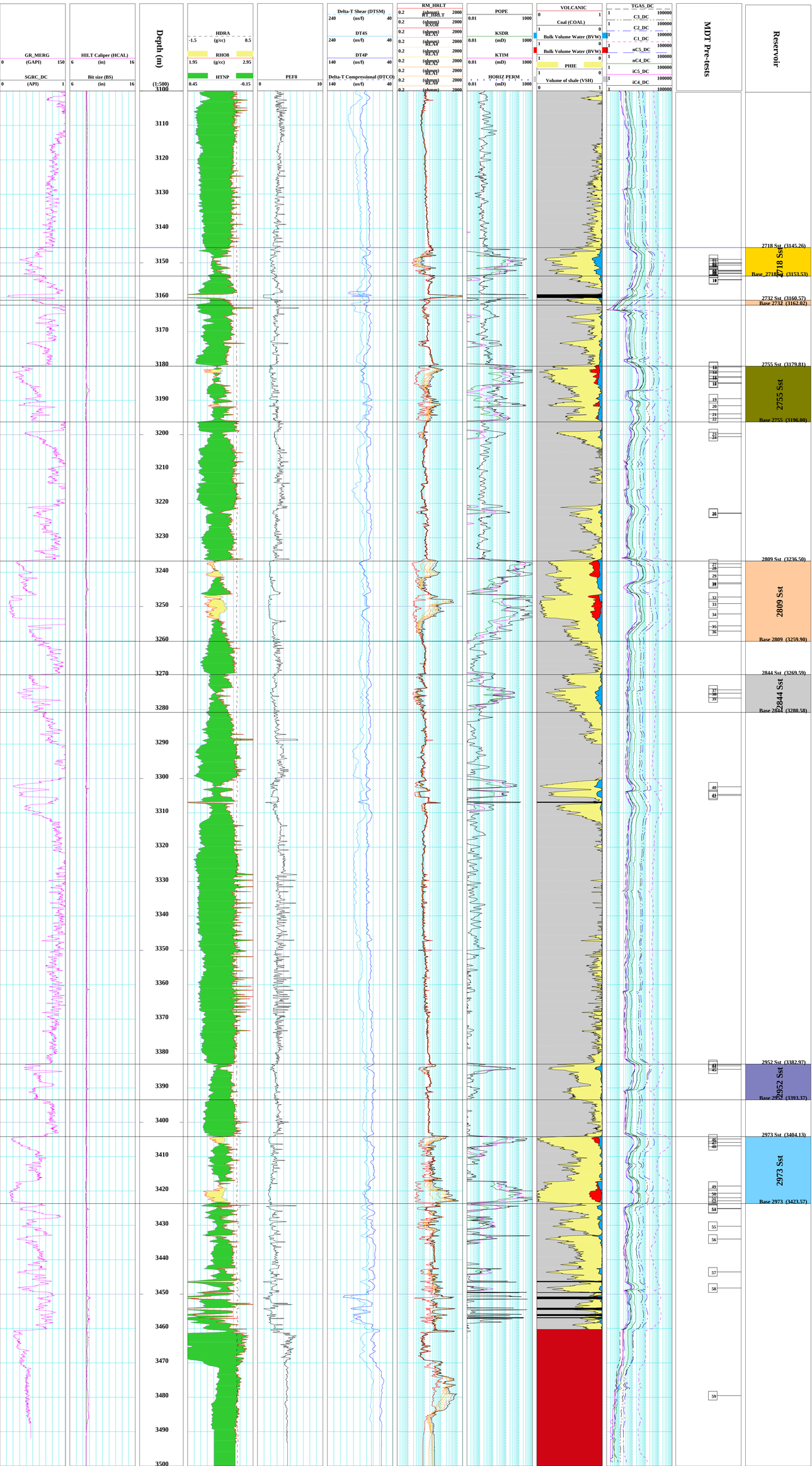

APPENDIX 2: MDT INTERPRETATION REPORT

YOLLA 3

MDT INTERPRETATION

FEBRUARY 2005

DATE OF SURVEY:07/9/2004

by Joe Parvar

A Schlumberger MDT tool with pump out module, resistivity tool, optical analyser, quartz and strain gauges was used to obtain pressure data and collects reservoir fluid samples from Yolla-3. The tool was also fitted with 6x450cc and a 1 gallon sample chambers.

The Yolla-3 MDT program was conducted over the interval 3149 to 3480 mRT on 7/9/2004 and 8/9/2004. A total of 65 pre-tests were attempted of which 27 tests were valid, 15 were supercharged, 22 were tight tests and one lost seal to formation.

A summary of the pre-test data is included in Appendix 8 of the Yolla-3 WCR Basic Data.

A total of 7 samples ware attempted, with 6 samples successfully recovered. The descriptions of these samples are as follows.

1 x 450 CC Water sample from 2718 Sand (3149.3 mRT)
1 x 450 CC Gas sample from 2755 Sand (3181.7 mRT)
1 x 450 CC No recovery from 2755 Sand (3181.7 mRT)
1 X 450 CC Gas sample from 2809 Sand (3249.0 mRT)
1 X 1gallon Gas sample from 2809 Sand (3249.0 mRT)
1 X 450 CC Gas sample from 2973 Sand (3420.0 mRT)
1 X 450 CC Gas sample from 2973 Sand (3420.0 mRT)

The fluid composition and analysis of these samples are included in Appendix 15 of the Yolla-3 WCR Basic Data.

Meanwhile the pump out sub with optical fluid analyser (OFA) was used to identify the reservoir fluid in the 2952, 2873 and 2844 sands (and also at 3222.7 mRT depth) but the formation was too tight as summarised below.

OFA at 3384.5 mRT (2952 Sand) …..(too tight)
OFA at 3302.1 mRT (2873 Sand) …..(too tight)
OFA at 3275.1 mRT (2844 Sand) …..(too tight)
OFA at 3222.7 mRT …..(too tight)

The interpretation of the MDT data is presented in figures 4 to 7 while figures 1 to 3 demonstrate the data validation process (quality check).

Figure1 shows the initial mud hydrostatic pressure recorded by the quartz gauge. The data indicates a slope of 0.483 psi/ft equivalent to a mud density of 9.3 ppg at the down hole condition.

Figure2 illustrates the difference between the initial and final mud hydrostatic pressures recorded by the quartz gauge. As shown in this plot this variance is mainly close to zero (+/- 1.0 psi).

Figure3 shows the difference between reservoir pressure recorded by the quartz and strain gauges. The variance for most of the points (including all the valid points) is close to zero (+/- 1psi).

Figure4 shows the pressure vs. depth plot of all the zones within the Intra-EVCM. A water line with a gradient of 0.415 psi/ft, based on the Yolla-2 RFT data, was established for the Intra-EVCM sands (with the exception of 2718 Sand which is now confirmed to be water saturated and has a separate water line).

Figure5 shows the MDT profile for the 2718 Sand. The MDT data indicates that this zone is water saturated confirming the Yolla-4 results. A MDT sample taken at 3149.3 mRT also recovered formation water backing up the above results. The single Yolla-1 RFT point, from which a gas column has been inferred in the past, should have been supercharged.

The 2718 Sand has a separate water line which indicates that this zone is not connected to the hydrodynamic system of the main Intra-EVCM sands.

Figure6 Illustrates the pressure vs. depth profile for the 2755 and 2809 sands. The plot shows that these two sands have separate gas water contacts confirming the Yolla-4 results. A single good MDT point from the Yolla-3 2755 Sand does not lie on the Yolla-4 trend and is offset by approximately 1.1 psi (3.2 m). Similarly the Yolla-3 2809 MDT points do not lie on the Yolla-4 trend and are offset by approximately 1.3 psi (3.7 m). This variance is thought to be due to imprecision in the Yolla 4 depth measurements.

A gas line with a gradient of 0.105 psi/ft (consistent with the measured gas density) fitted through the Yolla-2 RFT data and the single good Yolla-3 2755 Sand MDT point defines a GWC of 2832.9 mss with the established water line (1.1 metre shallower than Yolla 4).

A gas line with a gradient of 0.109 (consistent with the measured gas density for this zone) fitted through the Yolla-3 2809 Sand MDT data defines a GWC of 2826.8 mss (1.4 metre shallower than Yolla-4).

The only two points from Yolla-1 2755 and 2809 sands (from which gas columns have been defined in the past) are both offset by approximately 5 psi. This offset is likely due to a gauge error in the 1985 data.

Figure7 Shows the MDT profile for the 2973 Sand. The interpretation of the combined Yolla-3 and 4 MDT data indicates that there are two separate gas columns (Upper and Lower Sands) within the 2973 zone. The relative positions of the two Yolla-1 2973 MDT points (to

each other) is also consistent with the above separation theory even though both the points are offset by about 2 to 3 psi from the Yolla-3 and 4 trends by what is likely to be gauge error.

A single good MDT point from the Yolla-3 2973 Upper Sand lies on the Yolla-4 established gas line (with a gradient of 0.097 psi/ft) which defines a GWC of 2990.2 mss. This MDT point (unless slightly supercharged) does not appears to suffer from the depth discrepancies seen at the 2755 and 2809 levels.

A gas line with a gradient of 0.097 psi/ft (consistent with the measured gas density) fitted through the Yolla-3 2973 Lower Sand data points defines a GWC of 2986.6 mss with the water line from Yolla-2.

A summary of the results are shown in the following table. Where there is a discrepancy in inferred GWC depth, recommended GWC levels are taken from those inferred from Yolla-3 due to the indicated depth shift in Yolla-4 data relative to the other wells.

Yolla-3 MDT Summary of Results					
Sands	**MDT Profile**	**Fluid**	**Y3 GWC (mss)**	**Y4 GWC (mss)**	**Recommended GWC (mss)**
2718	**Figure 5**	**Water**	**-**	**-**	**-**
2755	**Figure 6**	**Gas**	**2832.9**	**2834.0**	**2832.9**
2809	**Figure 6**	**Gas**	**2826.8**	**2828.2**	**2826.8**
2973 (Upper)	**Figure 7**	**Gas**	**2990.2**	**2990.2**	**2990.2**
2973 (Lower)	**Figure 7**	**Gas**	**2986.6**	**-**	**2986.6**
2458	**NA**	**Oil**	**NA**	**2470.0 (est OWC)**	**2470.0 (est OWC)**

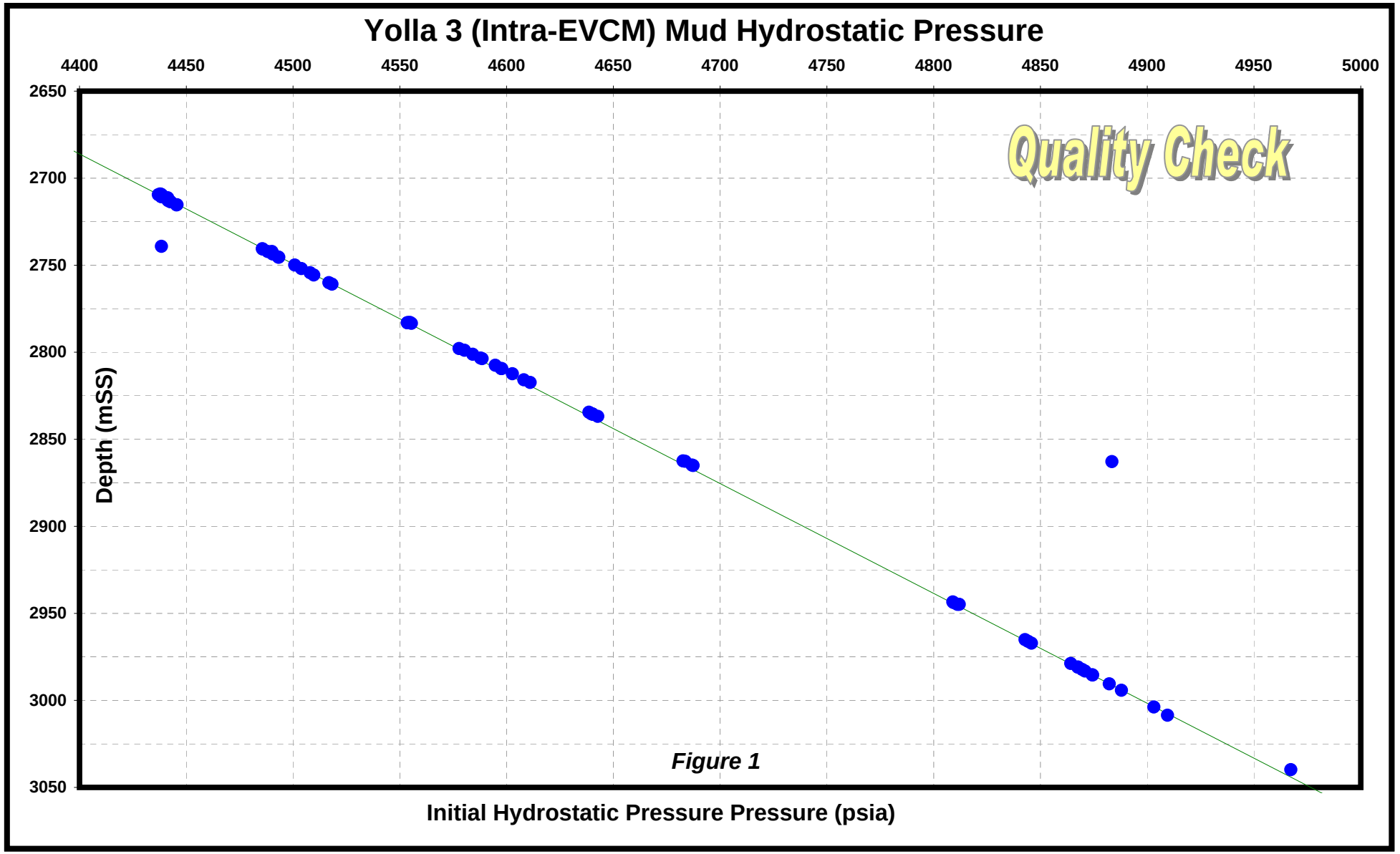
Yolla 3 (Intra-EVCM) Mud Hydrostatic Pressure
Quality Check
Depth (mSS)
Initial Hydrostatic Pressure Pressure (psia)
4400
4450
4500
4550
4600
4650
4700
4750
4800
4850
4900
4950
5000
2650
2700
2750
2800
2850
2900
2950
3000
3050

Figure 1

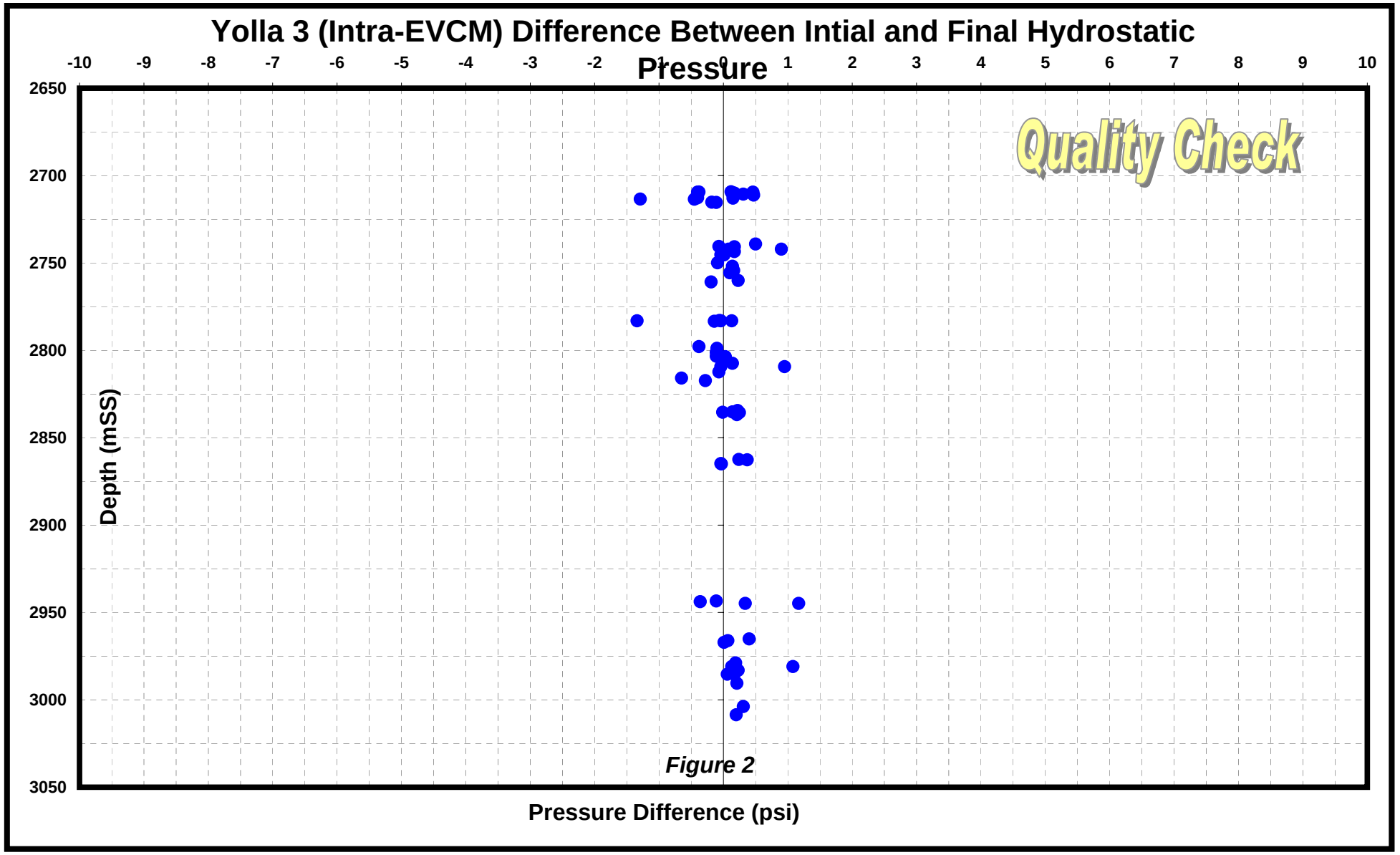
Yolla 3 (Intra-EVCM) Difference Between Intial and Final Hydrostatic Pressure
Quality Check
-10
-9
-8
-7
-6
-5
-4
-3
-2
-1
0
1
2
3
4
5
6
7
8
9
10
2650
2700
2750
2800
2850
2900
2950
3000
3050
Depth (mSS)
Pressure Difference (psi)

Figure 2

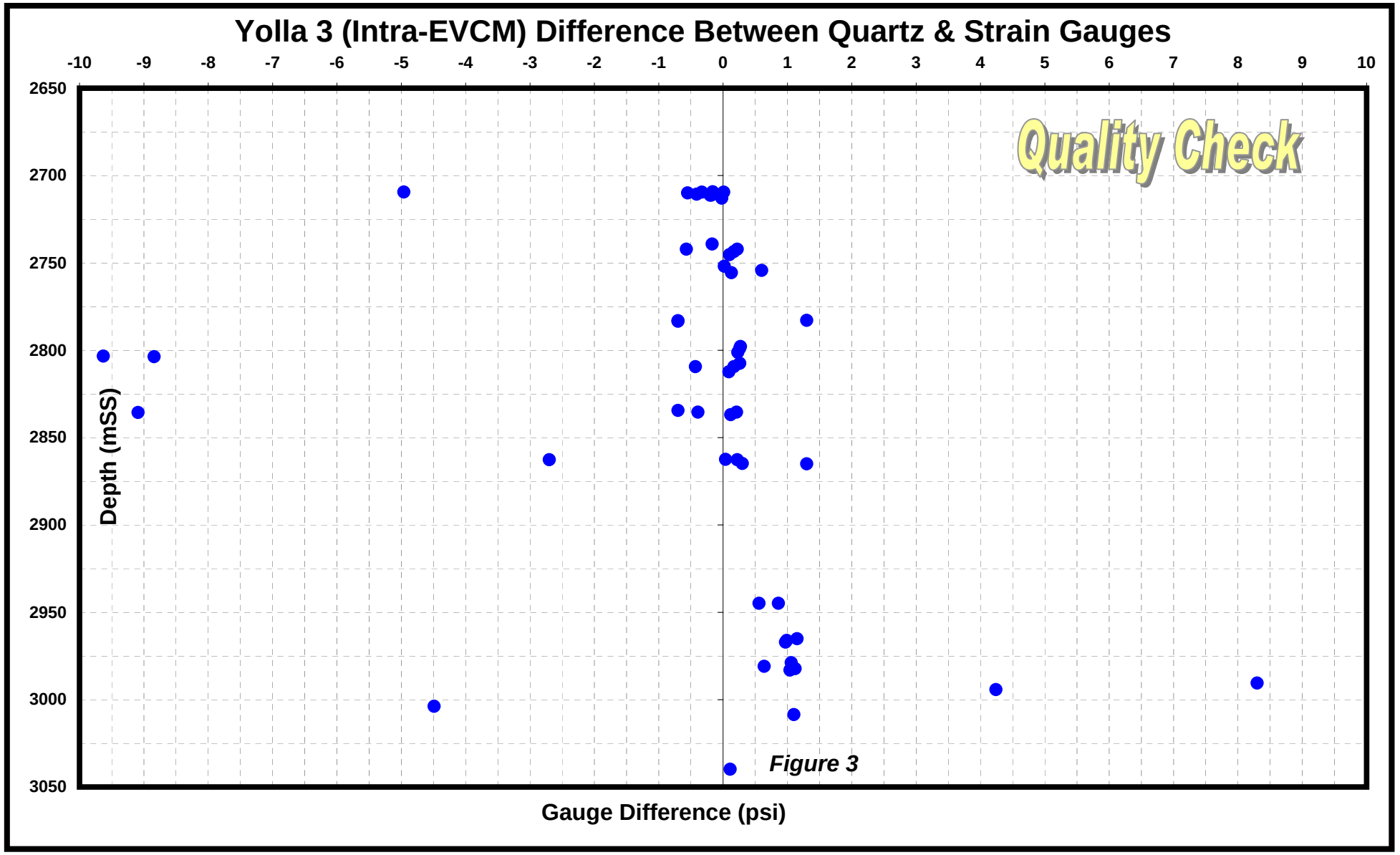
Yolla 3 (Intra-EVCM) Difference Between Quartz & Strain Gauges
-10
-9
-8
-7
-6
-5
-4
-3
-2
-1
0
1
2
3
4
5
6
7
8
9
10
2650
2700
2750
2800
2850
2900
2950
3000
3050
Depth (mSS)
Quality Check
Gauge Difference (psi)

Figure 3

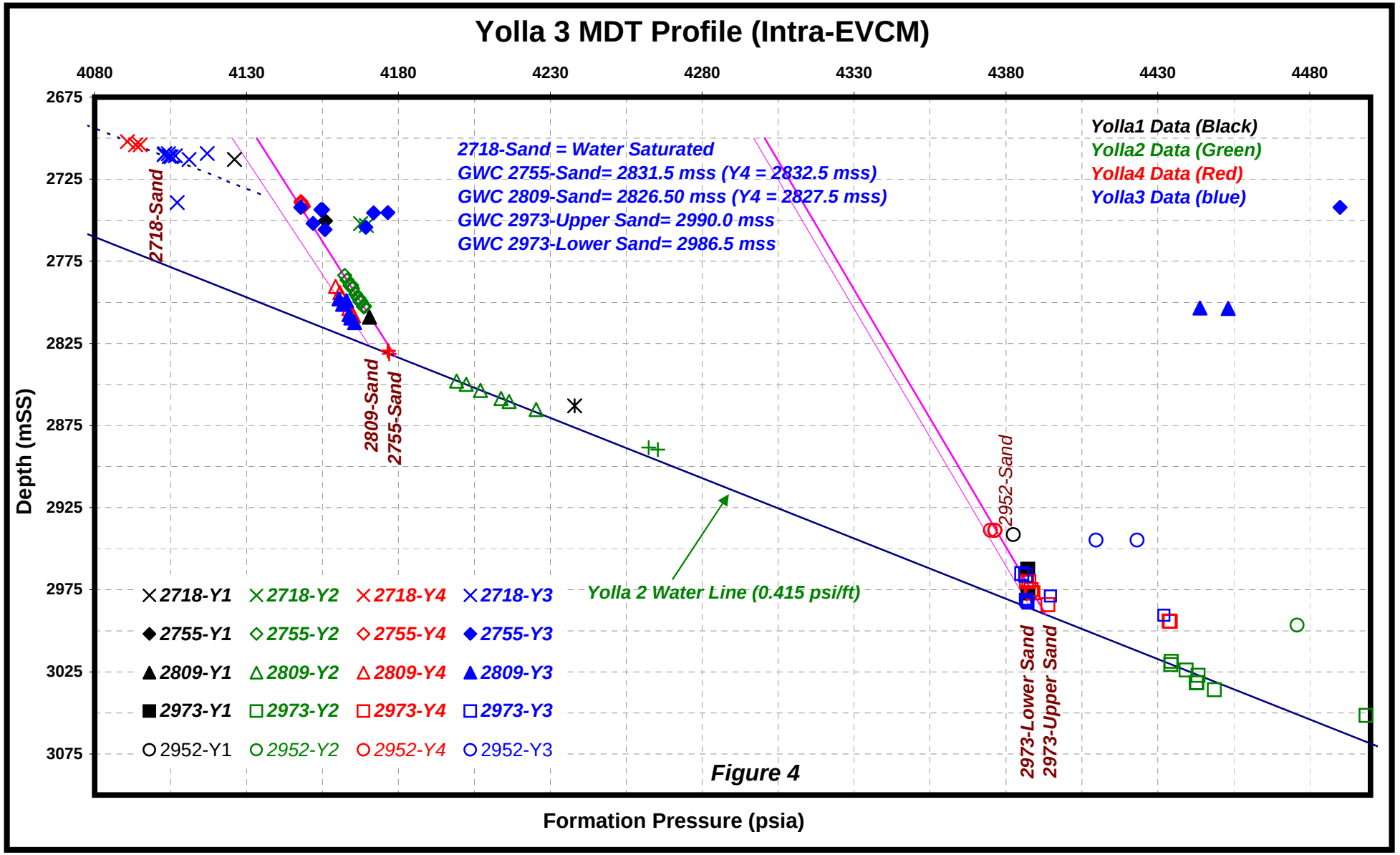
Yolla 3 MDT Profile (Intra-EVCM)
4080
4130
4180
4230
4280
4330
4380
4430
4480
2675
2725
2775
2825
2875
2925
2975
3025
3075
Depth (mSS)
Formation Pressure (psia)
2718-Sand = Water Saturated
GWC 2755-Sand= 2831.5 mss (Y4 = 2832.5 mss)
GWC 2809-Sand= 2826.50 mss (Y4 = 2827.5 mss)
GWC 2973-Upper Sand= 2990.0 mss
GWC 2973-Lower Sand= 2986.5 mss
Yolla1 Data (Black)
Yolla2 Data (Green)
Yolla4 Data (Red)
Yolla3 Data (blue)
2718-Sand
2809-Sand
2755-Sand
2952-Sand
2973-Lower Sand
2973-Upper Sand
Yolla 2 Water Line (0.415 psi/ft)
2718-Y1 2718-Y2 2718-Y4 2718-Y3
2755-Y1 2755-Y2 2755-Y4 2755-Y3
2809-Y1 2809-Y2 2809-Y4 2809-Y3
2973-Y1 2973-Y2 2973-Y4 2973-Y3
2952-Y1 2952-Y2 2952-Y4 2952-Y3

Figure 4

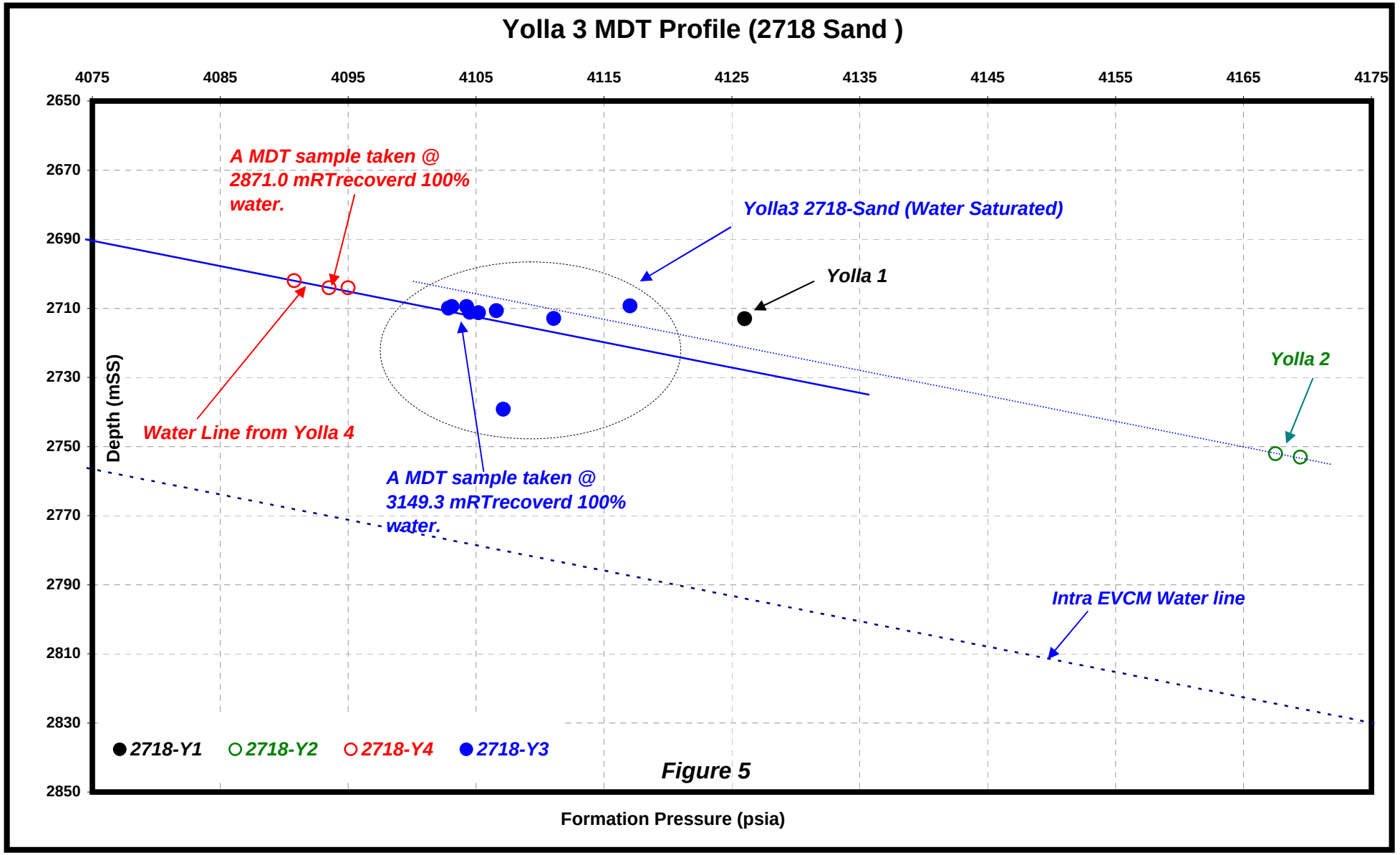
Yolla 3 MDT Profile (2718 Sand)
4075
4085
4095
4105
4115
4125
4135
4145
4155
4165
4175
2650
2670
2690
2710
2730
2750
2770
2790
2810
2830
2850
Depth (mSS)
A MDT sample taken @ 2871.0 mRTrecoverd 100% water.
Yolla3 2718-Sand (Water Saturated)
Yolla 1
Yolla 2
Water Line from Yolla 4
A MDT sample taken @ 3149.3 mRTrecoverd 100% water.
Intra EVCM Water line
2718-Y1
2718-Y2
2718-Y4
2718-Y3
Figure 5
Formation Pressure (psia)

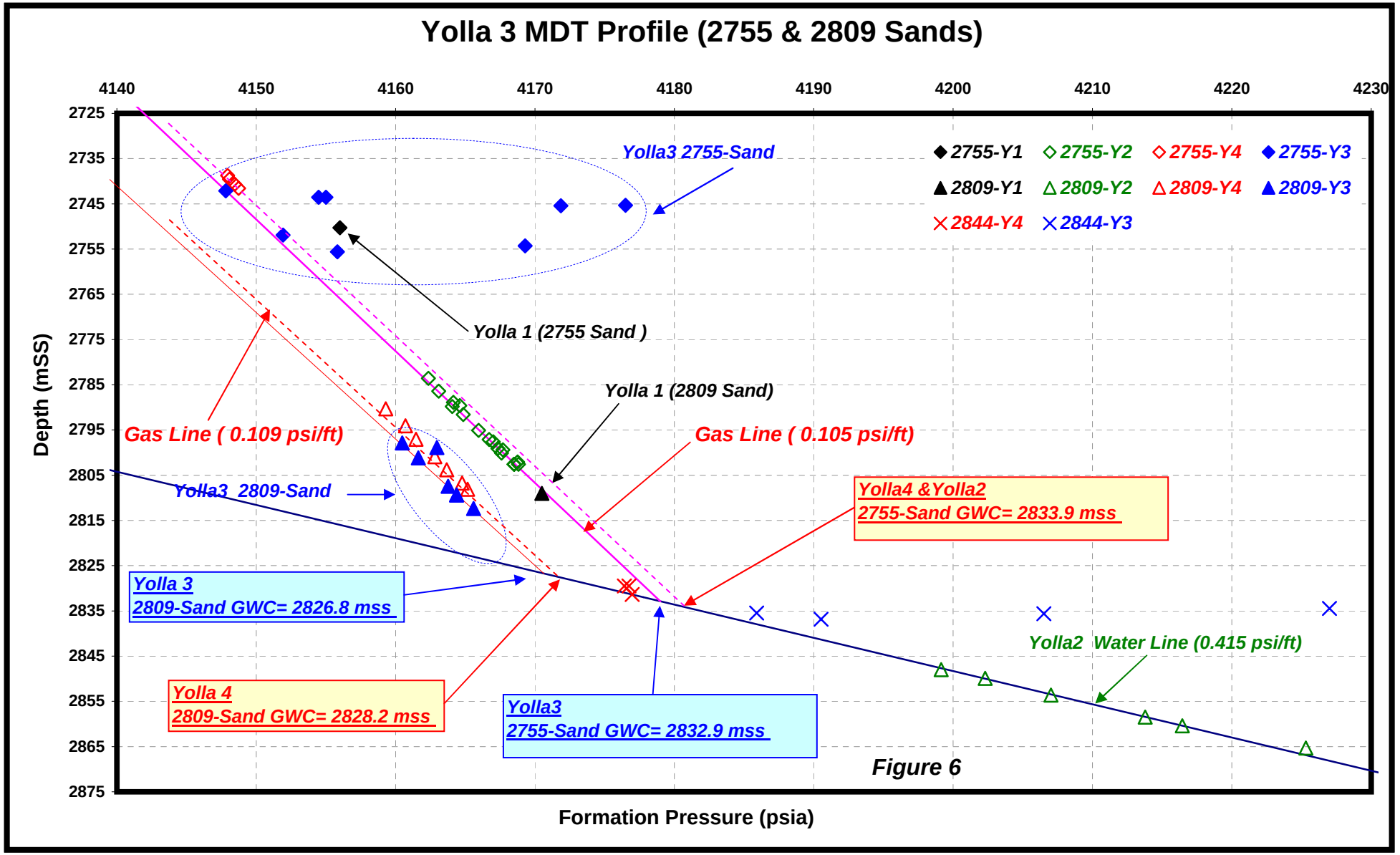
Yolla 3 MDT Profile (2755 & 2809 Sands)
4140
4150
4160
4170
4180
4190
4200
4210
4220
4230
2725
2735
2745
2755
2765
2775
2785
2795
2805
2815
2825
2835
2845
2855
2865
2875
Depth (mSS)
Formation Pressure (psia)
2755-Y1
2755-Y2
2755-Y4
2755-Y3
2809-Y1
2809-Y2
2809-Y4
2809-Y3
2844-Y4
2844-Y3
Yolla3 2755-Sand
Yolla 1 (2755 Sand)
Yolla 1 (2809 Sand)
Gas Line (0.109 psi/ft)
Gas Line (0.105 psi/ft)
Yolla3 2809-Sand
Yolla4 &Yolla2
2755-Sand GWC= 2833.9 mss
Yolla 3
2809-Sand GWC= 2826.8 mss
Yolla2 Water Line (0.415 psi/ft)
Yolla 4
2809-Sand GWC= 2828.2 mss
Yolla3
2755-Sand GWC= 2832.9 mss
Figure 6

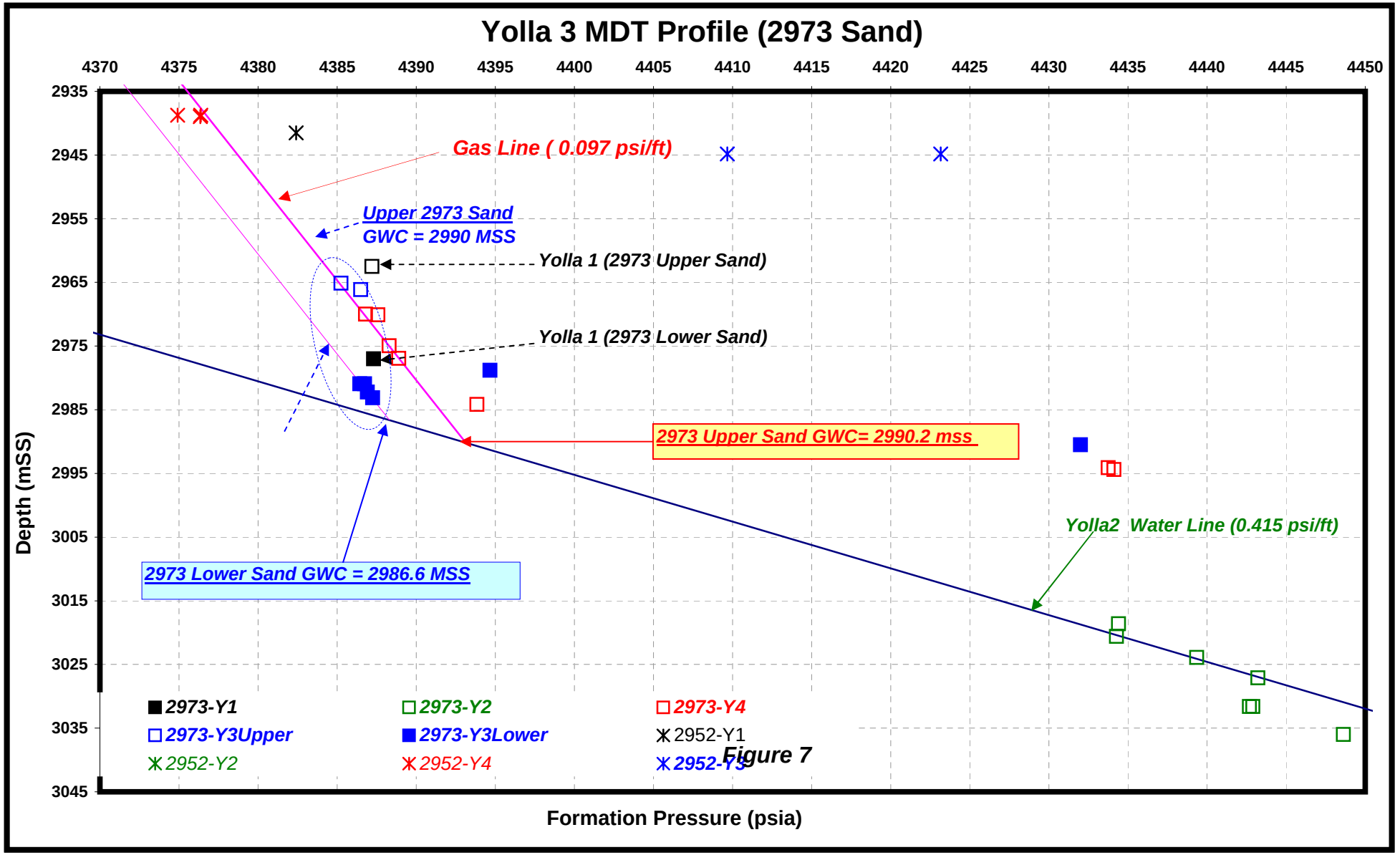
Yolla 3 MDT Profile (2973 Sand)
4370
4375
4380
4385
4390
4395
4400
4405
4410
4415
4420
4425
4430
4435
4440
4445
4450
2935
2945
2955
2965
2975
2985
2995
3005
3015
3025
3035
3045
Depth (mSS)
Formation Pressure (psia)
Gas Line (0.097 psi/ft)
Upper 2973 Sand
GWC = 2990 MSS
Yolla 1 (2973 Upper Sand)
Yolla 1 (2973 Lower Sand)
2973 Upper Sand GWC= 2990.2 mss
Yolla2 Water Line (0.415 psi/ft)
2973 Lower Sand GWC = 2986.6 MSS
2973-Y1
2973-Y2
2973-Y4
2973-Y3Upper
2973-Y3Lower
2952-Y1
2952-Y2
2952-Y4
2952-Y3

Figure 7

APPENDIX 3: PRODUCTION TESTING INTERPRETATION REPORT

(A) Test Interpretation

Yolla 3 Initial Clean-Up Flow Tests – Interpretation Report by Henry Irrgang of AWE

Introduction

As part of the completion procedure, the Yolla 3 well was flowed from each zone to clean up the well, estimate productivity, and obtain samples of produced fluids. Table 1 summarises the results of the testing by completion zone and the sections below describe the operational sequence, and the main test results and interpretations.

Surface production testing operations were carried out by Schlumberger (WCR Basic data Appendix 16) surface sampling was carried out by Petrolab (conventional) and Petrotech (isokinetic), the downhole gauges were provided by Halliburton (WCR Basic data Appendix 16), and programme preparation and technical supervision of testing operations was provided by AWT. The flow rates reported in this document are from the Schlumberger test report, which used tank dips to estimate the condensate flow rates (except for the 2809 sand which used uncorrected Floco meter data). The Petrotech report includes additional measurements of CGR and provides estimated correction factors for the Schlumberger liquid and gas metering based on condensate shrinkage factor and gas stream properties respectively. The Petrolab report also includes measured condensate shrinkage factors and gas stream properties for correcting the field CGR to lab conditions for recombination. It should be noted that due to low FBHP (2973U Sand), and a leaking plug above the 2973 sand during the later tests, the MDT sampling is considered more representative of reservoir fluids.

Operational Summary

The comments below summarise the testing operations and results in the sequence they were carried out – further details are available in the Schlumberger test report The bottomhole and surface pressure data plots are included in Figures 1 – 8 in this document. Pressure gauge data quality was high with good agreement between the gauges.

Test of the 2973U Sand: Following completion of the well, the surface test equipment was set up and pressure tested and the liquid meter calibrated to the surge tank (calibration factors not used however). At 11:45 on 26 September 2004, the 2973 Upper Sand was perforated with 3m of 2 1/8" Enerjet guns at 6 spf from 3404 – 3407m RT while the well was open on 24/64" choke. The well was beaned up gradually to 64/64" choke and the guns were pulled to surface. The FTHP rose to 3067 psia by 16:00 and the well was shut-in at 16:10, the spent gun was retrieved, and the Halliburton memory pressure gauges were run in to hang at 3422m RT = -2982.3m SS (15m MD below perforations). The reservoir pressure measured prior to re-opening the well was 4370 psia (adjusted to mid perforation depth of -2965.8m ss) and rising slowly (compared to 4386 psia from MDT). At 23:30 the well was opened on a series of increasing chokes up to the final 48/64" choke at 06:45 on 27 September. Metering through the test separator started at 09:00 with flow rate declining slightly from 7.2 mmcfd to 6.9 mmcfd and FTHP slowly falling from about 700 psia to 682 psia, with FTHT 33 deg C. The measured CGR was not steady but on average fell from about 17 stb/mmscf early to 7 stb/mmscf near the end of flow, with about 3-4 bbls/mmscf of condensed water. The well was shut in at the choke manifold at 15:31 on 27 September, the gauges were pulled and a plug was set in the bottom RN nipple to isolate the 2973U sand. The THP built up to a maximum 3091 psia over 3.5 hours before the plug was set. The plug was tested by bleeding off 300 psi and pressure rose only 10 psi in 52 minutes.

During the main flow period on 48/64" choke, the FBHP fell from about 1100 psia to 1060 psia over the last 7 hours and the FBHP had not quite stabilised by the end of the flow. There was evidence of some liquid slugging but comparison of the FBHP and FTHP showed no evidence of increasing liquid holdup. The falling CGR was therefore likely to have been mainly due to retrograde condensation in the near wellbore area, resulting in a progressively leaner produced gas, and surface recombination of the samples taken late in the flow period would not be expected to be representative of the original reservoir gas. The final bottomhole temperature was 305 deg F and still rising slowly. There was insufficient pressure buildup duration to allow analysis of permeability and skin.

Test of the UEVCM Sand: The UEVCM SSD was opened at 21:15 on 27 September 2004, production from the UEVCM Sand was started at 22:16 and the well was gradually beaned up to 52/64" choke. The well was SI at 00:21 on 28 September to run in the gauges to hang at 2248m RT (-1842.6m RT), 22.8m MD below the base of perforations and 17m below the sliding sleeve. The pressure recorded prior to re-opening the well was 2675

psia and still rising. The well was re-opened at 01:11 and gradually beaned up to 60/64" choke for 4 hours before beaning back to 48/64" choke at 07:15 for the sampling flow period. Production on 48/64" choke was metered via the test separator between 08:00 and 12:00. The flow rate gradually declined from 17.2 mmcfd to 16.7 mmcfd with FTHP falling from 1740 psia to 1710 psia and the FTHT was 58 deg C. There was a large discrepancy between the Floco condensate meter and the tank dips and the latter were used for reporting. The average CGR was 48 stb/mmscf.

The reported water rate increased towards the end of the test, finishing at about 11 bbls/mmscf. The salinity of the separator water was high (TDS 50,264 mg/l). Review of the composition of the produced water composition versus formation water (55,680 mg/l from Yolla 1 DST 2), mud filtrate (41,920 mg/l from Yolla 4), condensed water and completion brine (~170,000 mg/l NaCl) did not indicate clearly whether or not some formation water had been produced, though this appears likely.

The flowing bottomhole pressures were reasonably steady during the flow on 60/64" choke (1955 psia) and for the final flow on 48/64" (2200 psia). Comparison of the FBHP and FWHP trends indicated increasing liquid holdup in the tubing towards the end of the final flow and some liquid slugging.

The well was SI at 12:02 and after 5 minutes of SI, the gauge was RIH to the 2809 SSD. Consequently, there was insufficient buildup data recorded to allow analysis of permeability and skin. The gauges were retrieved and the UEVCM SSD closed at 15:44 with SITHP 2477 psia. SITHP rose to 2577 psia over the next half hour and was 2835 psia (higher than the UEVCM reservoir pressure) just before the 2809 SSD was opened (at 17:40), indicating a leak in the lower IEVCM completion (probably from the 2973U sand). The maximum bottomhole temperature was 220 deg F, but was probably affected by the leak.

Test of the 2809 Sand: The 2809 SSD was opened and pressure gauges were run in and hung off in the 2973 zone sliding sleeve (below the bottom packer) with the sensing point at approximately 3276m RT (-2836.4m SS). The measured bottomhole pressure was rising and reached 4265 psia prior to opening the well. This pressure is higher than the initial 2809 pressure, even assuming a water gradient above the gauges, indicating communication with the 2973U Sand (e.g. leaking plug or SSD?).

The well was opened up at 21:07 on 28 September 2004 and gradually beaned up to 48/64" choke. The FBHP was rising throughout the 1 ½ hours of flow on 48/64" choke, indicating that the 2809 Sand was still cleaning up. The well was beaned up to 52/64" choke briefly then gradually beaned back to 36/64" for the main 6 hour sampling flow period through the test separator. The separator flow rate was stable at 17.6 mmcfd with an oscillating CGR averaging 36 stb/mmscf, and 2-3 bbls/mmscf of condensed water, with a final FTHP of 3018 psia and FTHT of 70 deg C. The well was shut in at 09:50 on 7 August 2004 and the 2809 SSD was closed at 13:20.

The FBHP during the sampling flow was rising slightly up to 3992 psia, indicating cleanup was continuing. The pressure buildup was irregular and could not be reliably analysed. The diagnostic log-log plot of the first 20 minutes of buildup (see Figure 6) suggested a k.h similar to the log derived value, but the MTR was largely masked by a partial gas hump (wellbore phase segregation). The linear pressure plot showed a buildup slope increase after 20 minutes of SI, indications of some well flow after 48 minutes, a period with pressure noise, and another slope increase at 12:55, with continued rising pressure to higher than the 2809 Sand pressure. The 2809 SSD was closed but pressure continued to rise afterwards. The slope changes did not correspond to recorded events at surface. A possible explanation for some of the pressure buildup irregularities is that the plug/SSD isolating the 2973U Sand, which was leaking during/after the UEVCM test, had become an intermittent leak.

The maximum bottomhole temperature was 299 deg F, but was probably affected by the leak from the 2973U sand.

Test of the 2775 Sand: The 2755 sliding sleeve was opened with little pressure response (the SIBHP was higher than the 2755 pressure). The well was opened up at 16:31 on 29 September 2004 and gradually beaned up to 56/64" choke for 2 hours before settling back to 40/64" for the main 7 ½ hour sampling flow period through the test separator. The flow rate was stable at 16.5 mmcfd with a CGR averaging 19 stb/mmscf, and 2-3 bbls/mmscf of condensed water, with a final FTHP of 2221 psia and FTHT of 65 deg C. The well was shut in at 04:31 on 30 September 2004 and the gauges were pulled at 05:45.

The FBHP on 56/64” choke was 2270 psia and still falling after 2 hours, while on 40/64” choke the FBHP was 2960 psia and falling slowly. The temperature response during the flow period (the temperature gauge was about 90m below the perforations but responded to flow rate changes) confirmed that the 2973U sand was also flowing. The pressure buildup (see Figure 8) was reasonably smooth but the extrapolated pressure was close the 2973U Sand pressure. However, an approximate estimate of permeability-thickness was made (which is probably too high, due to some flow from the 2973U Sand).

Well Test Data Interpretation Summary

Table 1 summarises the well test data including estimates of well productivity. The apparent intermittent leak from the 2973U Sand may have affected the measured gas flow rates and CGR’s for the subsequent tests, resulting in possible small overestimation of well deliverability, underestimation of skins and underestimation of CGR’s. For the 2809 Sand, the FBHP data showed that the zone was still cleaning up at the end of the drawdown phase (rising FBHP), indicating that the skin factor would fall with continued production. Although there is data uncertainty, comparison of the skin factors to Yolla 4 suggests there may have been a significant benefit from use of the Pure perforation system in Yolla 3.

None of the tests had buildup data that could be confidently interpreted due to a combination of short buildups, leaking plug/SSD and/or surface operations affecting the SIBHP. However, the early buildup data from the 2809 and 2755 tests allowed rough estimates of reservoir permeability.

Figures 1 - 8 show the bottomhole and surface pressure and temperature data for the entire test sequence and for the individual zone tests.

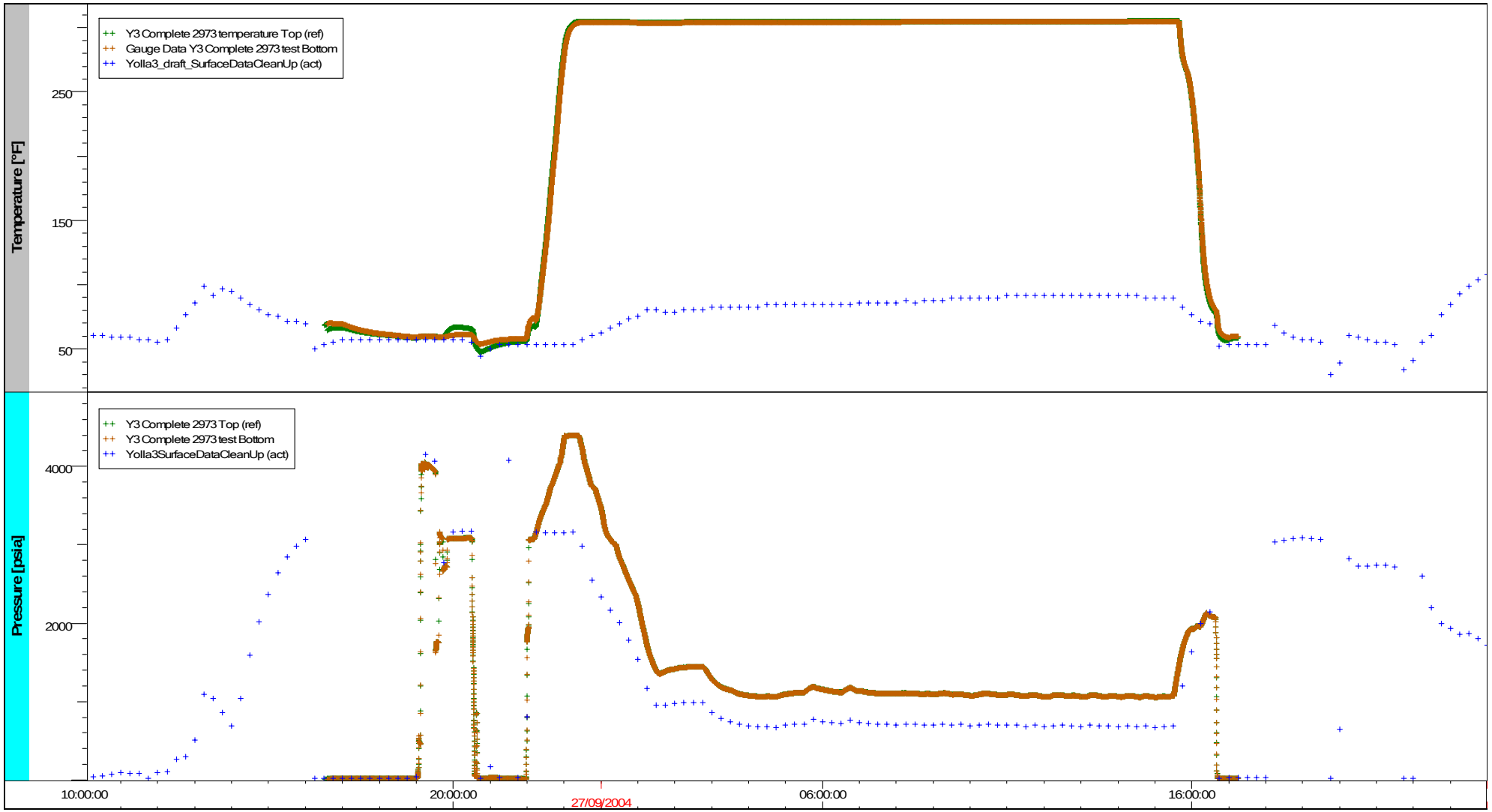

Figure 1 - Cleanup Flow Test of Yolla 3 2973U Sand

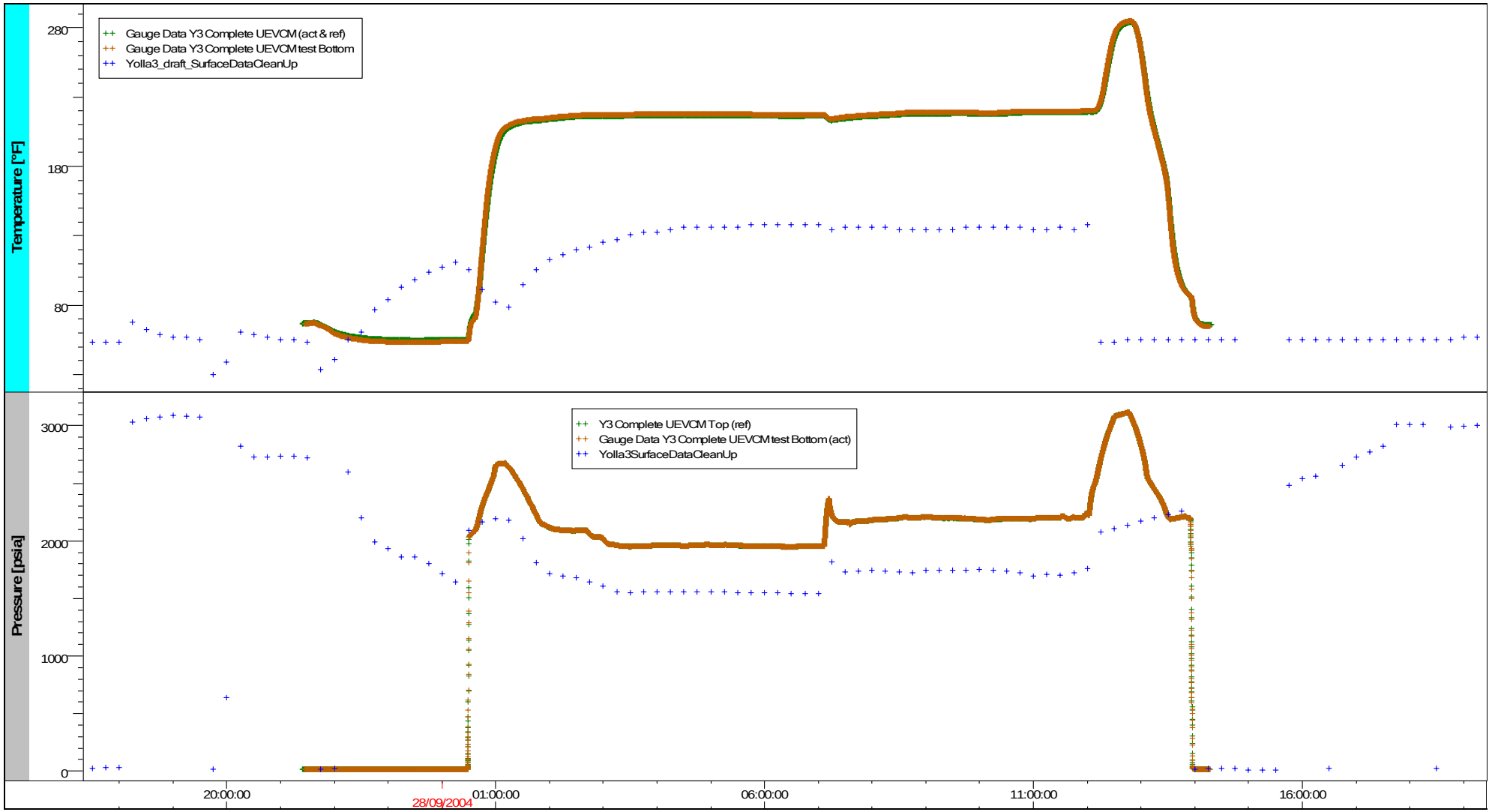

Figure 2 - Yolla 3 Cleanup Flow UEVCM Completion

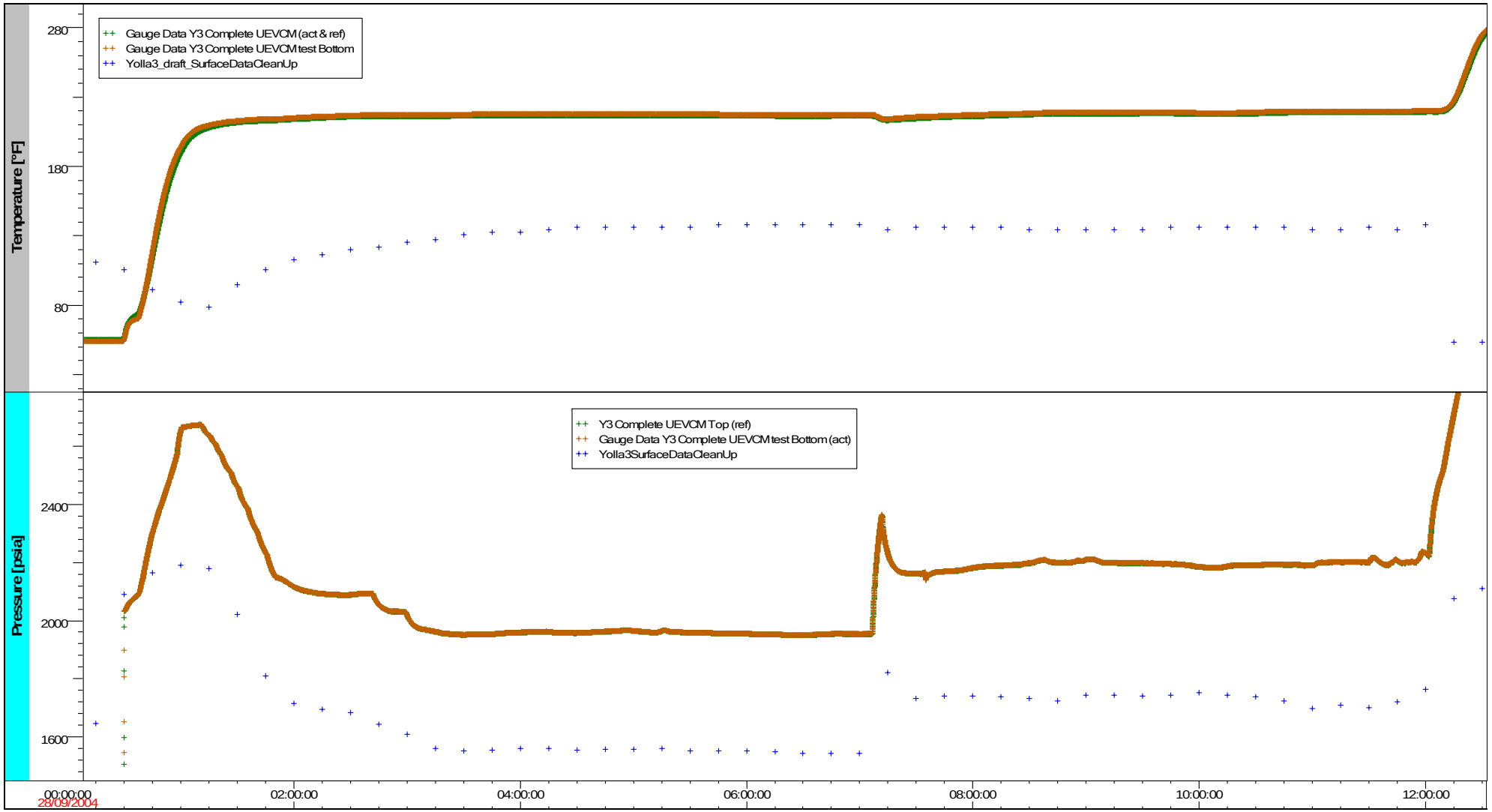

Figure 3 - Yolla 3 Cleanup Flow UEVCM Completion (detail)

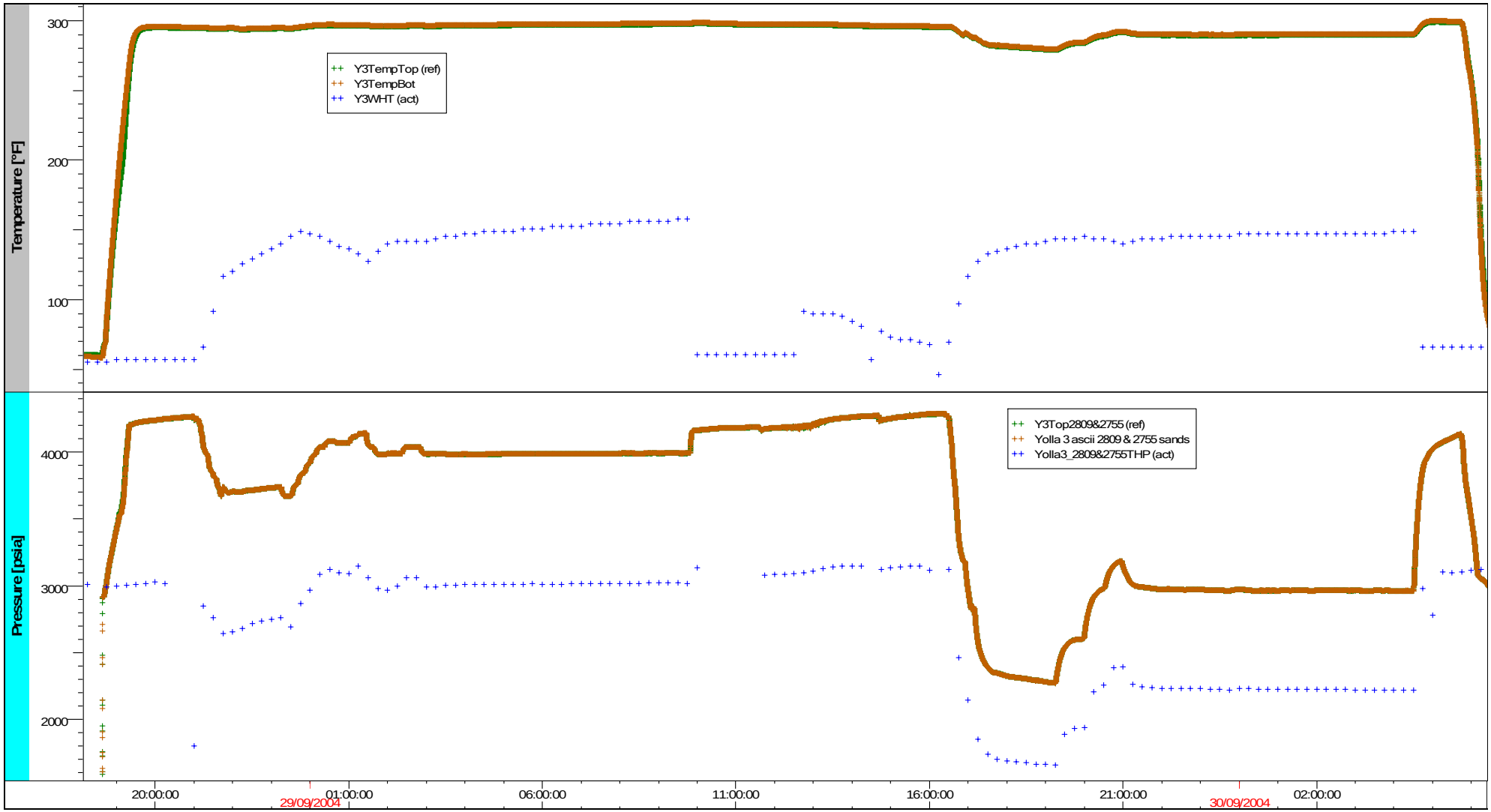

Figure 4 – Yolla 3 2809 and 2755 Cleanup Flow Tests

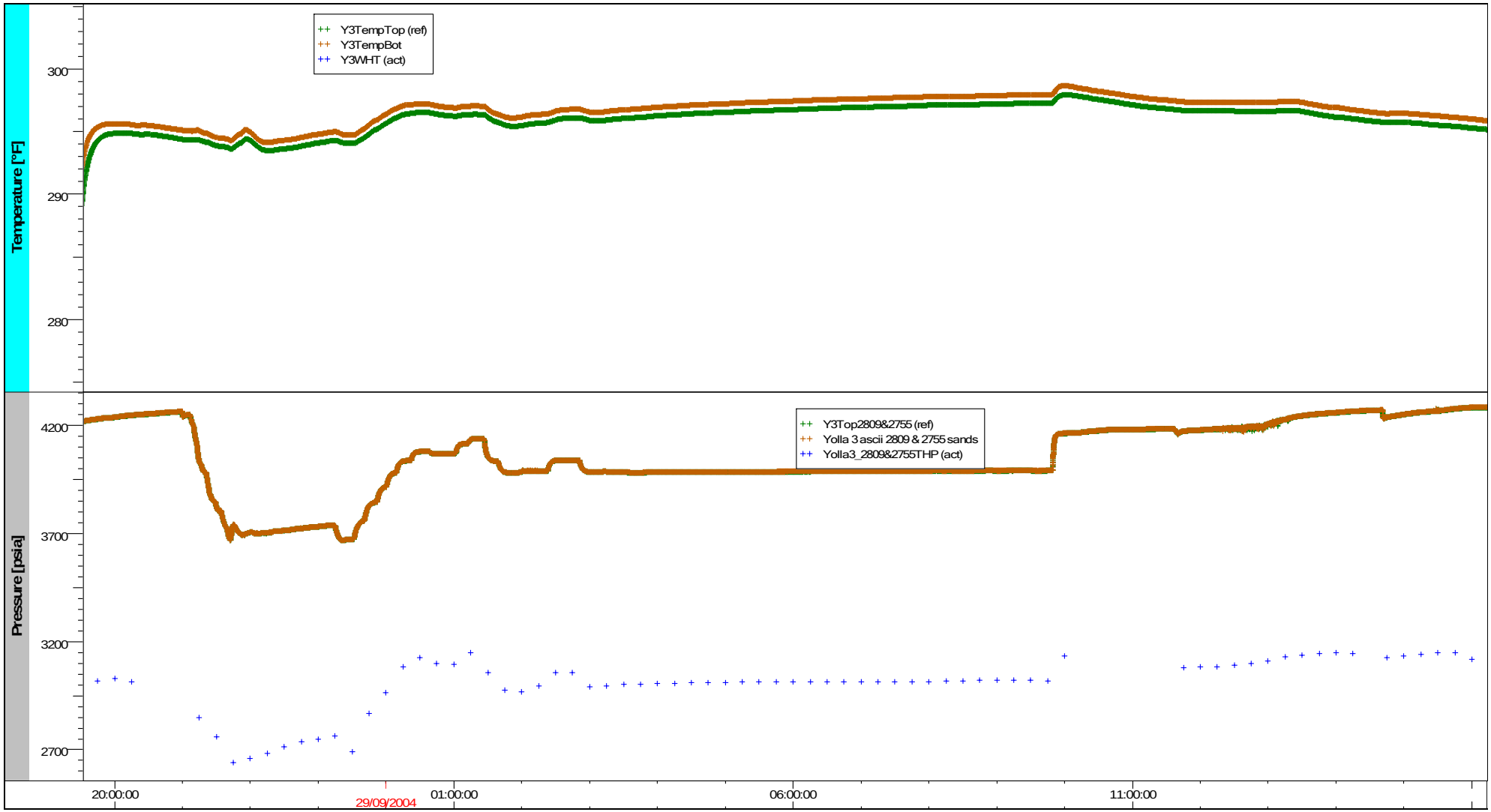

Figure 5 – 2809 Cleanup Flow Test – Detail

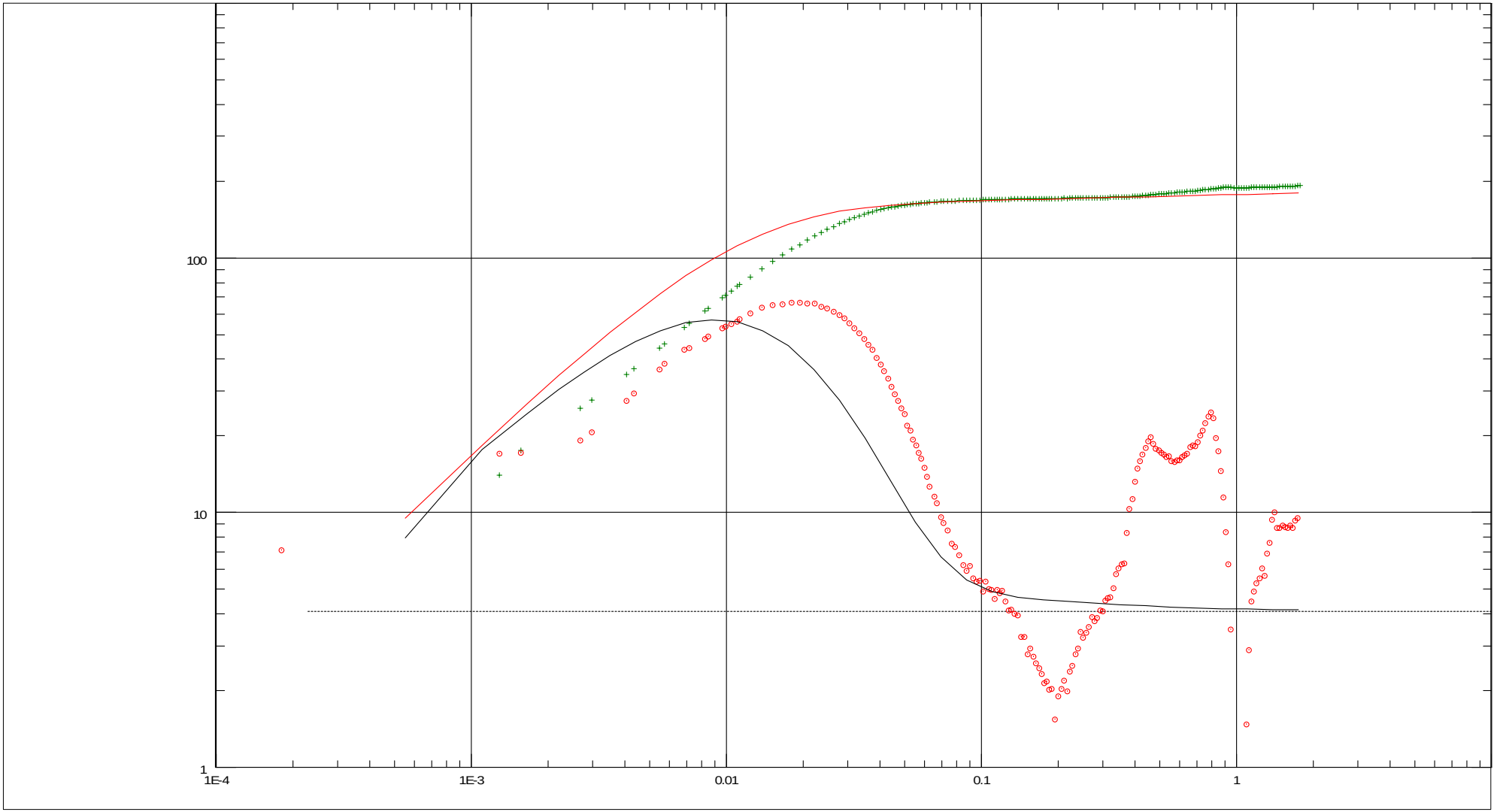

Figure 6 - 2809 Sand Buildup - showing short MTR, gas hump and late wellbore effects

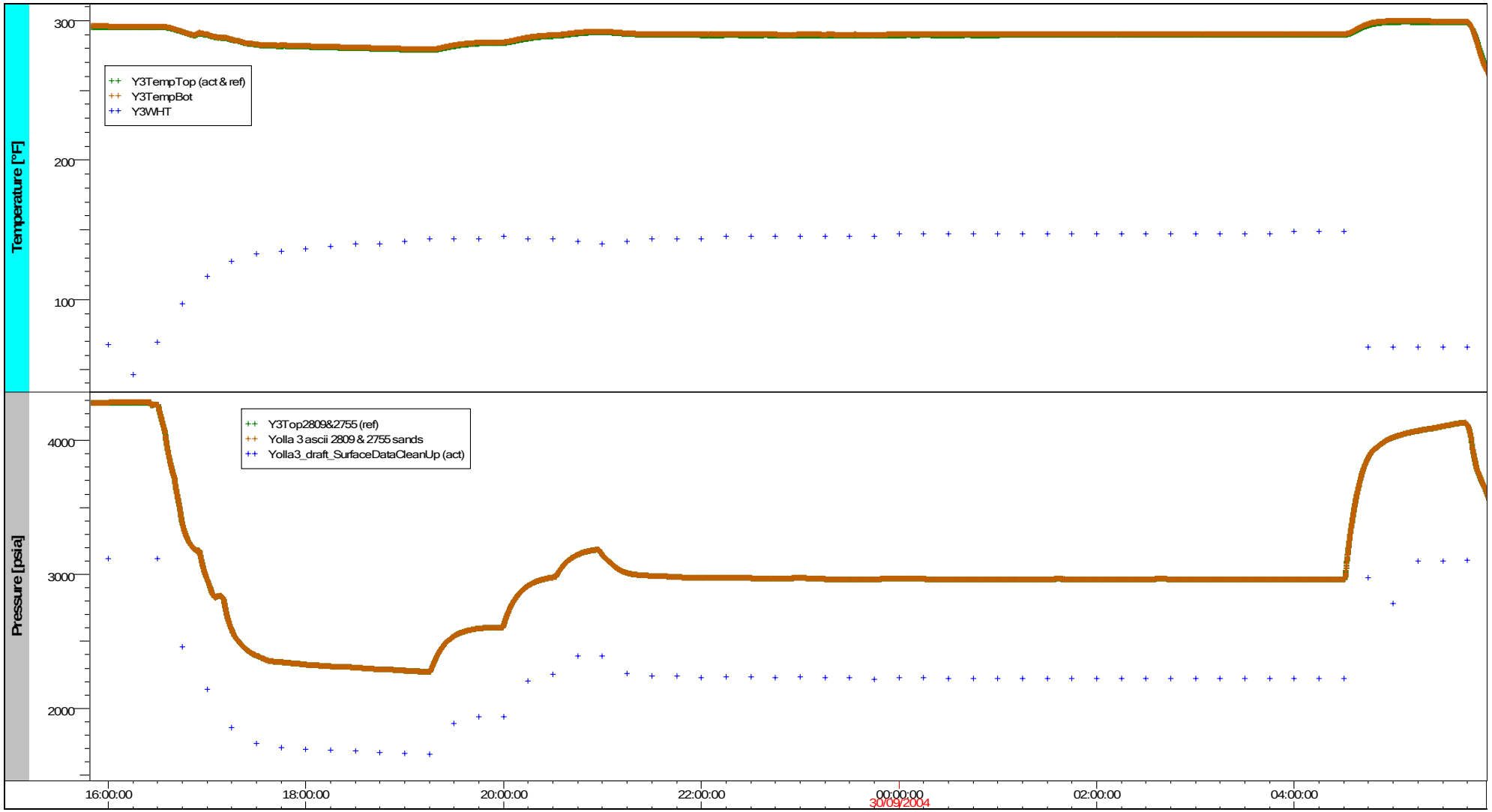

Figure 7 - Yolla 3 - 2755 Sand Cleanup Test (detail)

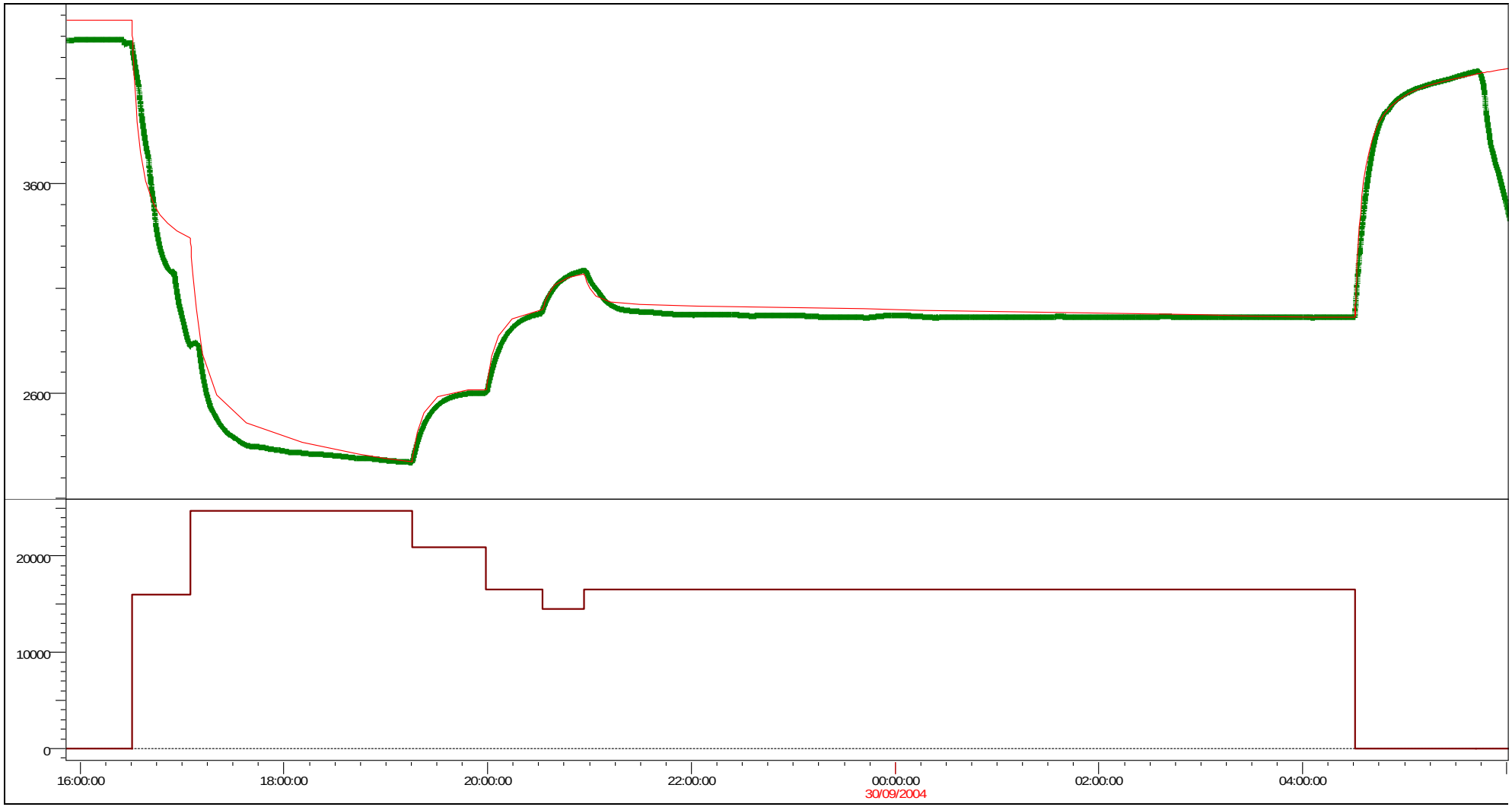

History plot (Pressure [psia], Liquid Rate [STB/D] vs Time [hr])

Figure 8 - 2755 Sand Buildup - Approximate Model Match (Showing Gas Rate in MSCF/D)

Yolla 3 Initial Clean-Up Flows - Estimates of Zone Productivity

Sand	Perfs Top m RT	Perfs Bot m RT	Flow Rate mmcfd/bopd	CGR stb/mmscf	FWHP psia	FWHT deg C	Choke /64"	SIWHP psia	Mid Perfs m SS	FBHP psia@gauge	Gauge m SS	Gradient psi/m	FBHP psia@MPP	Pi (MDT) psia@MPP	k.h (est.) md.ft	D (est.)	Darcy Skin
UEVCM	2210.2	2225.2	16.7	48	1710	58	48	2477	-1816.2	2200	-1842.6	0.25	2193	2709	1180	0.00015	0.0
2755	3180.0	3196.0	16.5	19	2221	65	40	3122	-2748.4	2960	-2836.4	0.331	2931	4151	290	0.00010	-1.7
2809	3236.5	3248.5	17.6	36	3018	70	36	leak	-2802.9	3992	-2836.4	0.35	3980	4162	7300	0.00030	9.0
2973U	3404.0	3407.0	6.9	17==>7	682	33	48	3091	-2965.8	1060	-2982.3	1.5	1035	4386	860	0.00030	80.0

Notes:

1 Results for the UEVCM, 2809 and 2755 tests affected by leaking production from the 2973U Sand
2 Flowing bottomhole pressures, FWHP and FWHT were rising slowly during the 2809 sand test indicating the well was still cleaning up and stabilising
3 The k.h estimates are from the log interpretation model for 2973U (probably too high), from core for UEVCM (Krg=0.7), and approx. FBU analysis for 2755 and 2809 Sands
4 D coefficients from Woodside correlation except 2755 and 2809 Sands (FBU)
5 Skin factors are based on the currently available test data and do not account for future condensate dropout effects

Table 1 – Summary of Yolla 3 Initial Clean-up Flow Tests

(B) Sand Production

CLAMPON
ULTRASONIC SAND DETECTION

WELL TESTING REPORT

YOLLA - 3

Performed by: Aquip Systems

Test Engineer: Simon Mason

Test Date: 26/09/04 – 2/10/04

Sand 2973 Flow (26/09/04 – 27/09/04):
The zone was opened at 23:23 and stabilized at a production rate of @ 7 Mscfeet/day. Minor sand production was indicated at the initial stage of the clean up flow. After diverting to the separator at 08:12 (28/09/04) no further significant sand was produced from this zone. (See fig 1.)
Total sand produced for the period = 2.87kg.

Sand UEVCM Flow (28/09/04):
The zone was opened at 01:11 with the production rate then stabilized at @ 24 Mscfeet/day. At 07:36 flow was switched to a 48/64 fixed choke giving a production rate of @17 Mscfeet/day. The data indicates the well consistently slugging with a moderate amount of particle production.
Total sand production = 7.70Kg. (See fig 2.)

Sand 2809 Flow (28/09/04 – 29/09/04):
The zone was opened at 21:06 on the 28/09/04 and cleaned up at a production rate of @ 32 Mscfeet/day. Production was then decreased to @ 17Mscfeet/day with negligible particle production observed.
Sand production for this period totaled 3.04Kg. (See fig 3.)

Sand 2755 Flow (29/09/04 – 30/09/04):
The zone was opened to a production rate of @ 29 Mscfeet/day with a successful indication of well clean up. Production was then decreased to around 17 Mscfeet/day with no further sand production observed.
Total mass of sand produced was 3.97kg. (See fig 4.)

Yolla 3 Sand 2089 Flow, Re-test (01/10/04 – 02/10/04):
The zone was opened at 22:07 and stabilized at a production rate of @ 18 Mscfeet/day. Initial sand production was minimal with the trend declining to zero.
Total sand produced for the flow was 1.81kg. (See fig 5.)

Tel: 08 9472 0122
Fax: 08 9472 5122
4/5 Brodie Hall Drive
Bentley WA 6102
simon@aquip.com.au

Fig 1. Sand 2973 Flow Period:

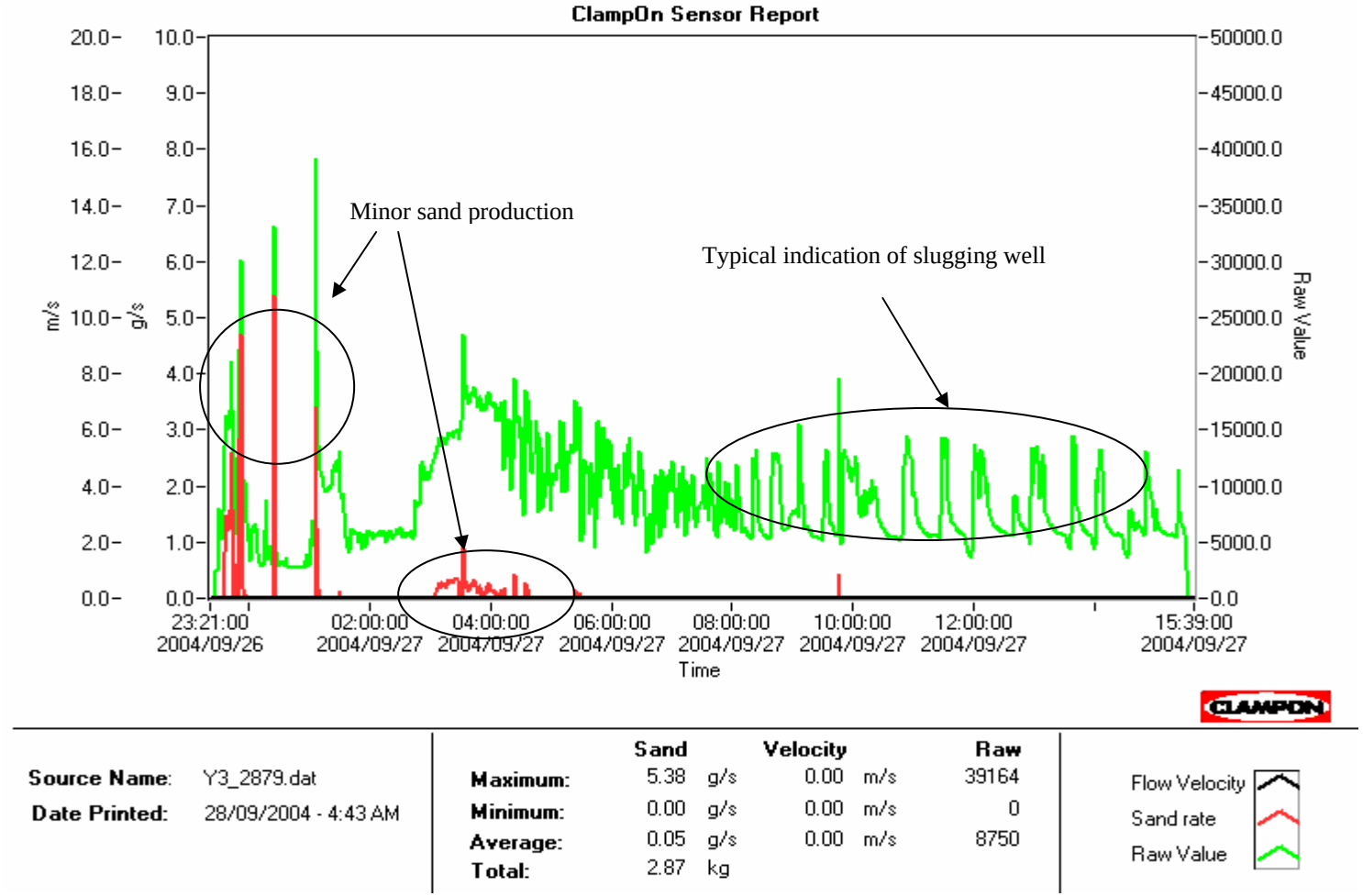

Fig 2. Sand UEVCM Flow:

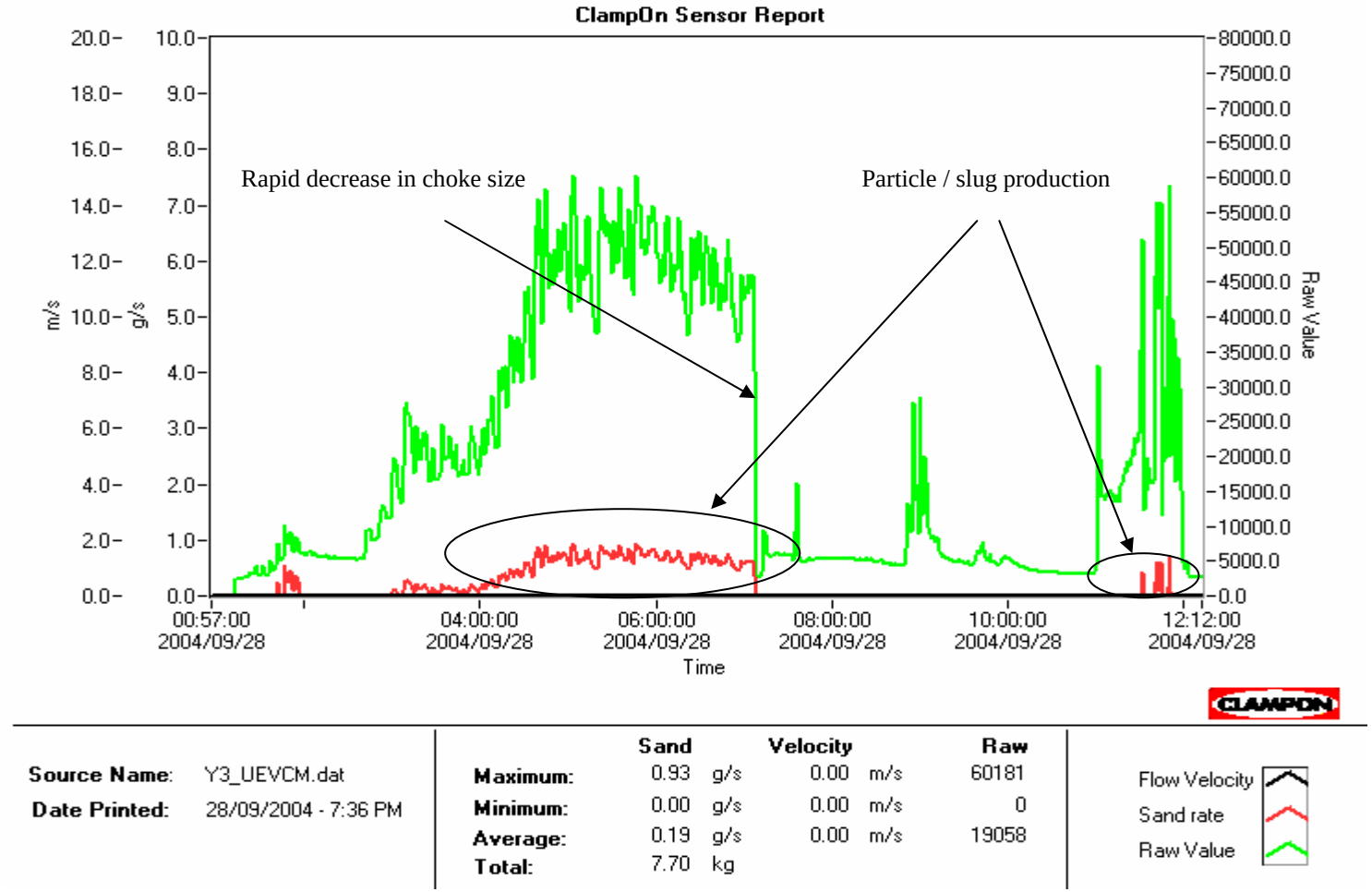

Fig 3. Sand 2809 Flow:

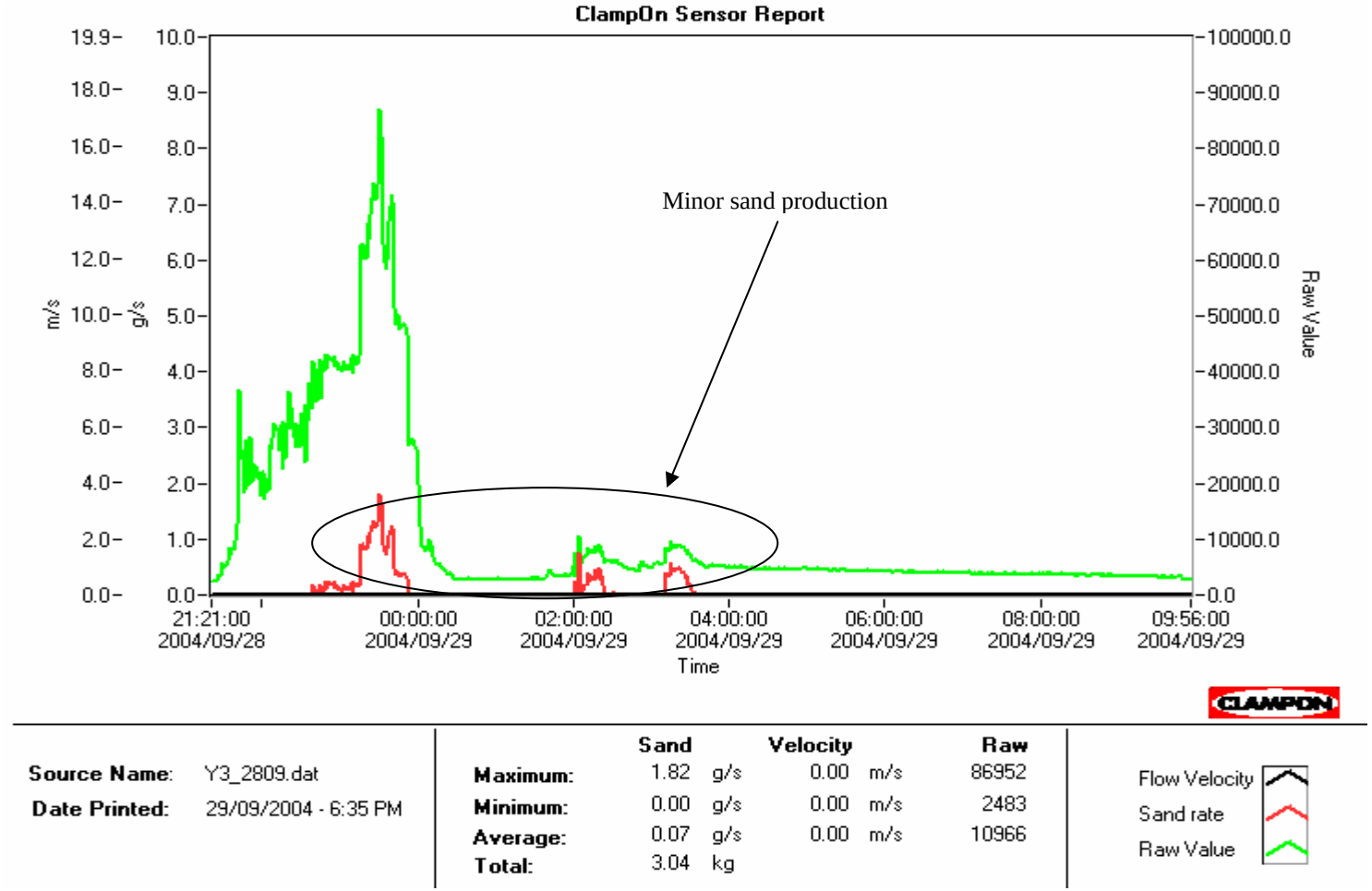

Fig 4 Sand 2755:

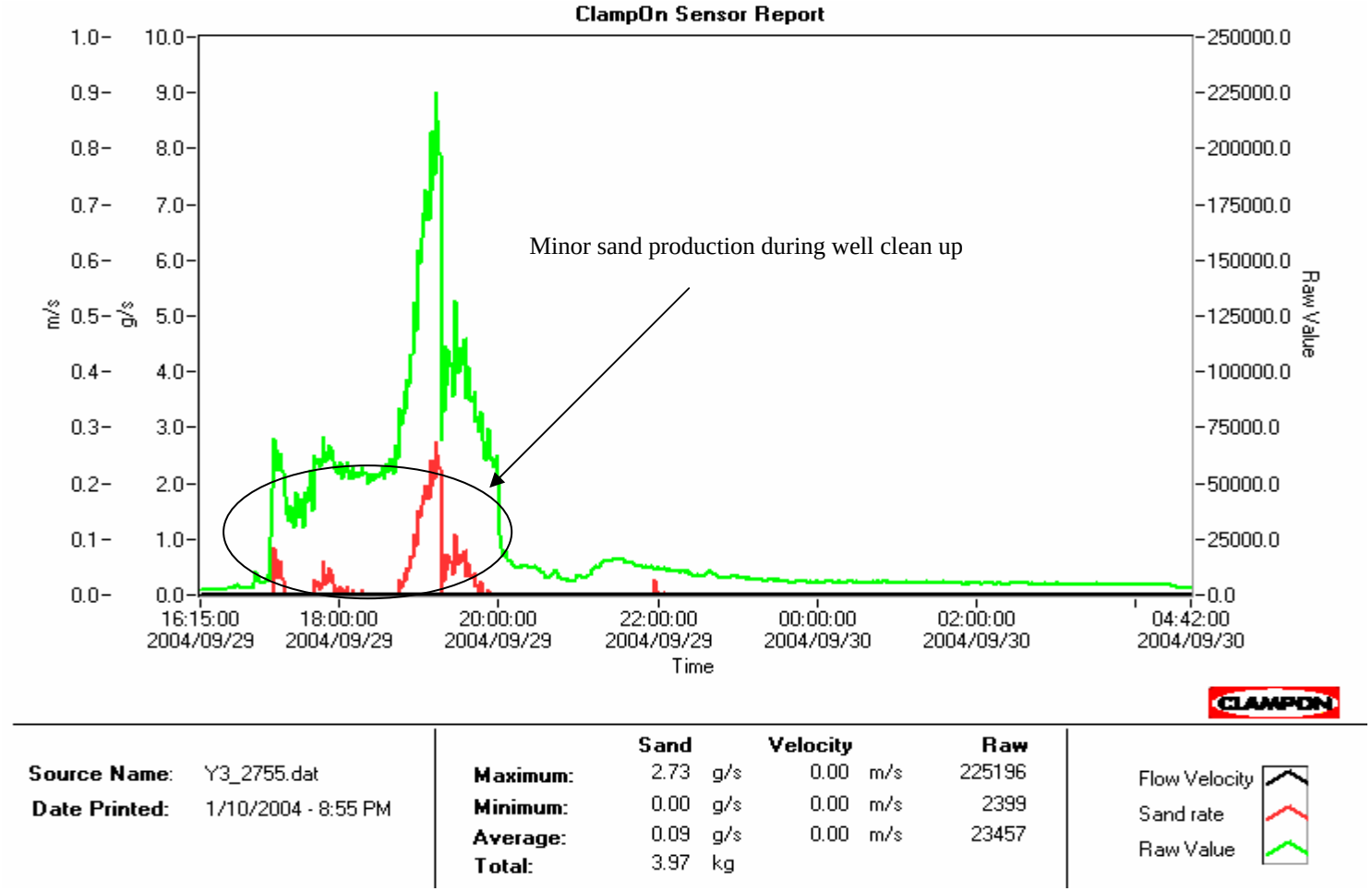

Fig 5 Yolla 4 Sand 2809 Flow – Re test:

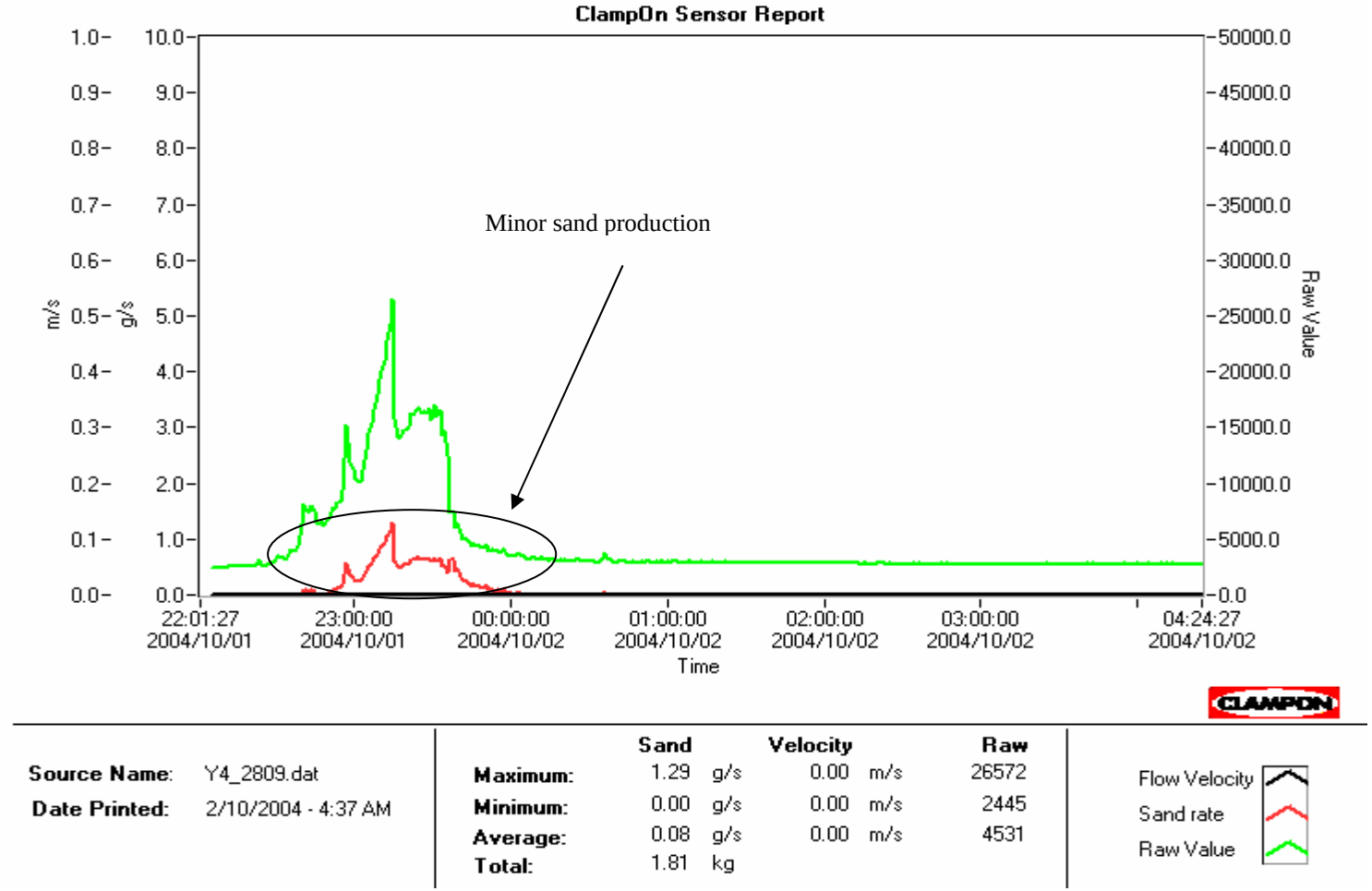

(C) Petrotech Report

WELL: YOLLA-4

ANALYSIS OF PRODUCTION RATES

REPORT TYPE: Final

Client	:	Origin Energy Resources Ltd
Well	:	Yolla-4
Permit	:	T/RL-1
Client Representative	:	Mark Mussared
Date of reporting	:	November 2004
Project number	:	55760
Project co-ordinator	:	Robyn Tamke
Report prepared by	:	Hans Petter Hjermstad
Report reviewed by	:	Robyn Tamke
Number of issues	:	7
Distribution Petrotech	:	1
Distribution Origin	:	6

Petrotech a.s
PO Box 575
N-5501 HAUGESUND
NORWAY
Phone: +47 52 70 07 00
Fax: +47 52 73 71 10

Petrotech Australia
PO Box 61
MELVILLE WA 6956
AUSTRALIA
Phone: +61 8 9314 2050
Fax: +61 8 9314 7424

SUMMARY

The production test data of test # 1 in the well Yolla-4 has been analysed and corrected. A total of three sands (2755, 2809 and 2973) were tested. There is no indication of communication between the sands. Each sand was tested at only one rate and flowed for 3 hours.

The condensate rate was measured by a 2" Floco meter. Meter calibration runs were performed during only two of the three tests. The condensate rate during the test of the 2973 sand was well below the range of the meter. Furthermore, the meter calibration factor obtained for this test is incorrect, leading to a significant underestimation of the condensate production. As the condensate production to the gauge tank has not been reported for this test, it is not possible to accurately give the condensate-gas ratio (CGR). Therefore an estimate has been provided, based on extrapolation of the meter-factor calibration curve using the typical performance of a 2" Floco meter. The CGR value has been predicted to be 17.5 bbl/mmscf with reference to separation at 500 psi and 50 ºC. This corresponds to a CGR value for 23.6 stb/mmscf with a theoretical split at C_5. The uncertainty in this prediction is large.

The corrected CGR values obtained for the two other sands were 24.4 bbl/mmscf @ 500 psi, 50 ºC for the 2755 sand and 29.3 bbl/mmscf @ 500 psi, 50 ºC for the 2809 sand. This corresponds to C_5 CGR values of 31.3 and 34.5 stb/mmscf, respectively.

All three tests are too short to identify any time dependency in the producing CGR of the well streams. Also the uncertainty related to the corrected CGRs for the three sands cannot be given. This would require that each test had consisted of more than one flow period. Additionally, for this reason liquid carry over can be accurately determined. However, it is thought that it did not make a significant contribution to CGR error, as the rates were below the threshold value.

TABLE OF CONTENTS

1. INTRODUCTION

The test separator data (ref 1) from the production test # 1 of Yolla-4 has been analysed. Condensate production rates were measured with a meter for all flows. Equilibrium gas and condensate samples were taken from the test separator. The compositions of these samples have been used to obtain the properties of the flowing phases that are used in the flow rate calculations. The test separator efficiencies during the test were not measured.

2. PRODUCTION RATES MEASURED AT THE TEST SEPARATOR

2.1 Correction of gas rates

The measured gas rates for the flow periods have been corrected by substituting the gravity and compressibility used in the flow calculations during the test with the values calculated from the laboratory composition of the recombined well stream (ref 2). Corrected properties have been achieved by use of an equation of state package (EOS) with good documented predictive capability (ref 3). Flash calculations were also used, in order to account for the change in gas properties with the change in separator pressure and temperature. The measured gas rates have been calculated as 15 minute averages.

2.2 Corrected separator condensate flow rates

A 2" Floco meter was used to measure the condensate production rates for all three sands tested. Only one meter calibration run was performed during the tests of the 2973 sand and the 2809 sand. No meter factor calibration was completed for the test of the 2755 sand. Ideally, it is strongly recommended that, two calibration runs should be performed for each flow. Two meter-factors from the pre-test water calibration were also available. The lack of meter factor data introduces uncertainties in the liquid flow measurements since the meter factor, to some extent, will be dependent on both the fluid rheology and the flow rate. Furthermore, the combined meter-factor will be dependent on the operating conditions of the test separator.

An EOS package (ref 3) was used to calculate the shrinkage of the condensate from separator to standard condition by a flash process. The calculation accounts for the change in separator conditions throughout the test and the EOS will predict the shrinkage within +/- 2 %. The shrinkage from a flash process will correctly represent the volume change of the fluid from separator to gauge tank. Condensate production during the test of the 2973 sand was well below the range of the 2" Floco meter and, additionally, the measured combined meter factor was incorrect (Table 2.4). The true meter factor was deduced from the valid calibration run and the pre-test water factors and exhibited the typical rate dependency of decreasing with increasing volumetric rate, see Figure 2.1.

The meter factor for the test of the 2973 has been obtained by extrapolation from the linear part of Figure 2.1, using the typical rate dependency for a 2" Floco meter, see Figure 2.2. This extrapolation provides only a rough estimate of the condensate production rate during the test of the 2973 sand.

The corrected condensate rates are presented in Tables 2.5 – 2.7.

3. DISCUSSION

The effect of the gas rate corrections is insignificant. The dominating uncertainty in CGRs obtained from test # 1 of Yolla-4 is related to the measurement of the condensate flow rates. Only two meter calibration runs were performed. This is too few to obtain the rate dependency of the true mechanical meter factor. Furthermore, one of the meter factors was obviously incorrect and was also measured outside the linear range of the meter. The pre-test water calibration factors had to be included in order to establish the rate dependency of the meter factor and this neglects any effect of rheology on the meter performance. It is always strongly recommended to make two meter calibration runs for each flow rate.

The true meter factors were obtained from the calibration runs by removing the shrinkage from the measured values. An EOS was used to calculate the shrinkage of the condensate from separator to standard condition by a flash process. This calculation accounts for the change in separator conditions throughout the test. The shrinkage from a flash process will correctly represent the volume change of the fluid from separator to gauge tank. An excellent agreement was demonstrated between the experimental and the calculated shrinkage factors for the separator condensate samples that have been analysed by Petrolab (ref. 2), see Table 2.8. The difference is not larger than the experimental uncertainty.

The meter factor analysis is presented in Table 2.4. The true meter factors showed the typical rate dependency, decreasing with increasing volumetric rate, see Figure 2.1. The extrapolation made in Figure 2.2 is uncertain. However, it is in agreement with measured rate dependency of the meter factor for 2" Floco meters and will give a much better estimate of the CGR of the fluid produced from the 2973 sand than the value provided in the test report (ref. 1).

The condensate rates have not been corrected for the volume change due to the temperature difference between the separator and the position of the meter and any loss of condensate from carryover. The meter temperatures from the tests were not recorded and separator efficiency not measured. Both are believed to be decidedly insignificant compared to the uncertainty in the meter calibration. Typically the gas rate at separator conditions (i.e. the residence time of the separator gas phase) has to be above 1.3 mmcf/d before the performance of a 1440 psi 42" x 10’ test separator starts to decline.

The corrected test separator gas and condensate rates have been used to calculate corrected test separator CGR values. Corrected CGR values have been used to calculate an adjusted separator gas-condensate ratio at a chosen common reference. By use of this procedure the CGR values obtained for the individual flow periods can be directly compared independently of drift or changes in the separator conditions. These adjustments have been obtained by flash simulations with an EOS package (ref 3) and the expression given below:

$$CGR(P_r,T_r) = CGR(P_s,T_s) \cdot CGR^*(P_r,T_r)/CGR^*(P_s,T_s)$$

where:

$CGR\ (P_r,T_r)$ = CGR corrected to reference conditions
$CGR\ (P_s,T_s)$ = Measured CGR at separator conditions
$CGR^*(P_r,T_r)$ = Simulated CGR at reference conditions
$CGR^*(P_s,T_s)$ = Simulated CGR at separator conditions

The reference conditions represent some average conditions during the test, 500 psi and 50 ^{o} C. The corrected values for the test are presented in Tables 3.1 - 3.3 and in Figures 3.1-3.3. The internal consistency in the CGRs for the three sands is only fair with standard deviations between 10 and 15 %, taking the 15 minute averaging period into account. The uncertainty in the CGR values for the three tests cannot be assessed. This would require that each sand had been flowed on more than one rate.

The obtained CGR values at reference conditions for the three sands have been used to recalculate the composition of the test separator samples. A corrected recombination ratio was calculated, by correcting the value at reference conditions to the actual conditions in the separator at the time of sampling, see Tables 3.4 – 3.5. The corrected recombination ratio should also be used if PVT studies will be performed with any of the samples. The tables also present the theoretical condensate yield for the reservoir fluid in the three sands as C_5 CGR values. In the calculation of this value, all components heavier than C_4 are assumed to be condensate and the component lighter than C_5 gas.

4. REFERENCES

1) Schlumberger: Well testing report – Yolla/Yolla 4/Test#1
Report 2004-007

2) Petrolab : Compositional analysis of separator samples –
Yolla 4 O-24035

3) Calsep: PVTsim v.14.0
August 2004

TABLES AND FIGURES

Table 2.1: Corrected gas rates for 44/64" choke flow – 2973 sand

Time	Choke (64ths)	Separator Pressure (psi)	Separator Temp. (°C)	Gas rate test (mmscf/d)	Gas gravity test	Gas Z-factor test	Gas gravity (PVTsim)	Gas Z-factor (PVTsim)	Corr. factor[1]	GasRate corrected (mmscf/d)
30.07.2004 (Test 2973 Sand)										
13:45	44	495.0	42.0	27.187	0.825	0.926	0.818	0.925	1.005	27.324
14:00	44	496.0	44.0	27.107	0.825	0.928	0.819	0.926	1.005	27.233
14:15	44	496.0	45.0	27.117	0.825	0.929	0.819	0.927	1.005	27.240
14:30	44	496.0	47.0	27.078	0.820	0.931	0.820	0.929	1.002	27.121
14:45	44	497.0	48.0	27.243	0.820	0.932	0.820	0.929	1.001	27.280
15:00	44	498.0	49.0	27.219	0.820	0.932	0.820	0.930	1.001	27.249
15:15	44	498.0	50.0	27.166	0.820	0.933	0.820	0.931	1.001	27.190
15:30	44	499.0	50.0	27.192	0.820	0.933	0.820	0.931	1.001	27.218
15:45	44	499.0	51.0	27.140	0.820	0.934	0.821	0.931	1.001	27.157
16:00	44	501.0	52.0	27.212	0.820	0.934	0.821	0.932	1.000	27.224
16:15	44	501.0	53.0	27.158	0.820	0.935	0.821	0.933	1.000	27.164
16:30	44	501.0	54.0	27.107	0.820	0.935	0.822	0.934	1.000	27.107

Table 2.2: Corrected gas rates for 52/64" choke flow – 2755 sand

Time	Choke (64ths)	Separator Pressure (psi)	Separator Temp. (°C)	Gas rate test (mmscf/d)	Gas gravity test	Gas Z-factor test	Gas gravity PVTsim	Gas Z-factor PVTsim	Corr. factor[1]	GasRate corrected (mmscf/d)
01.08.2004 (Test 2755 Sand)										
22:35	52	497.0	36.0	32.480	0.846	0.919	0.816	0.920	1.018	33.052
22:45	52	497.0	38.0	32.291	0.846	0.921	0.817	0.921	1.017	32.850
23:00	52	497.0	38.0	32.291	0.846	0.921	0.817	0.921	1.017	32.850
23:15	52	496.0	39.0	32.349	0.846	0.922	0.817	0.922	1.017	32.905
23:30	52	495.0	40.0	32.247	0.846	0.923	0.817	0.923	1.017	32.794
23:45	52	496.0	41.0	32.322	0.846	0.923	0.818	0.924	1.017	32.865
00:00	52	497.0	42.0	32.344	0.846	0.924	0.818	0.925	1.017	32.882
00:15	52	497.0	43.0	32.226	0.846	0.925	0.818	0.925	1.017	32.758
00:30	52	497.0	43.0	32.126	0.856	0.923	0.818	0.925	1.021	32.811
00:45	52	495.0	44.0	31.939	0.856	0.924	0.819	0.926	1.021	32.614
01:00	52	495.0	44.0	32.096	0.856	0.924	0.819	0.926	1.021	32.774
01:15	52	496.0	44.0	32.235	0.856	0.924	0.819	0.926	1.021	32.915

Table 2.3: Corrected gas rates for 52/64" choke flow – 2809 sand

Time	Choke (64ths)	Separator Pressure (psi)	Separator Temp. (°C)	Gas rate test (mmscf/d)	Gas gravity test	Gas Z-factor test	Gas gravity PVTsim	Gas Z-factor PVTsim	Corr. factor[1]	GasRate corrected (mmscf/d)
07.08.2004 (Test 2809 Sand)										
01:45	52	474.0	42.0	32.003	0.854	0.925	0.818	0.928	1.020	32.641
02:00	52	472.0	43.0	32.053	0.854	0.926	0.819	0.929	1.020	32.685
02:15	52	471.0	45.0	31.981	0.854	0.927	0.819	0.930	1.019	32.601
02:30	52	487.0	45.0	32.097	0.854	0.925	0.819	0.928	1.019	32.715
02:45	52	481.0	45.0	32.063	0.854	0.926	0.819	0.929	1.019	32.681
03:00	52	471.0	45.0	32.011	0.852	0.928	0.819	0.930	1.018	32.599
03:15	52	504.0	47.0	32.320	0.852	0.924	0.820	0.928	1.018	32.887
03:30	52	511.0	47.0	32.139	0.852	0.923	0.819	0.927	1.018	32.708
03:45	52	516.0	48.0	32.344	0.852	0.923	0.820	0.927	1.017	32.909
04:00	52	513.0	49.0	31.987	0.852	0.925	0.820	0.928	1.017	32.543
04:15	52	506.0	49.0	32.039	0.852	0.926	0.820	0.929	1.017	32.598

Table 2.4: Meter factor from calibration runs – 2" Floco

Test	Time	Liquid rate (bbl/d)	Pressure (psi)	Temp. C	Comb. meter fact.	(1-shr)*K (stb/bbl)	Meter factor
Test 2973 Sand	15:45						
	16:11	401	501.0	52.0	0.807	0.876	0.921
Test 2809 Sand	02:20						
	02:32	961	487.0	45.0	0.871	0.835	1.043
Pretest water calibration							
		1440					0.986
		720					1.056

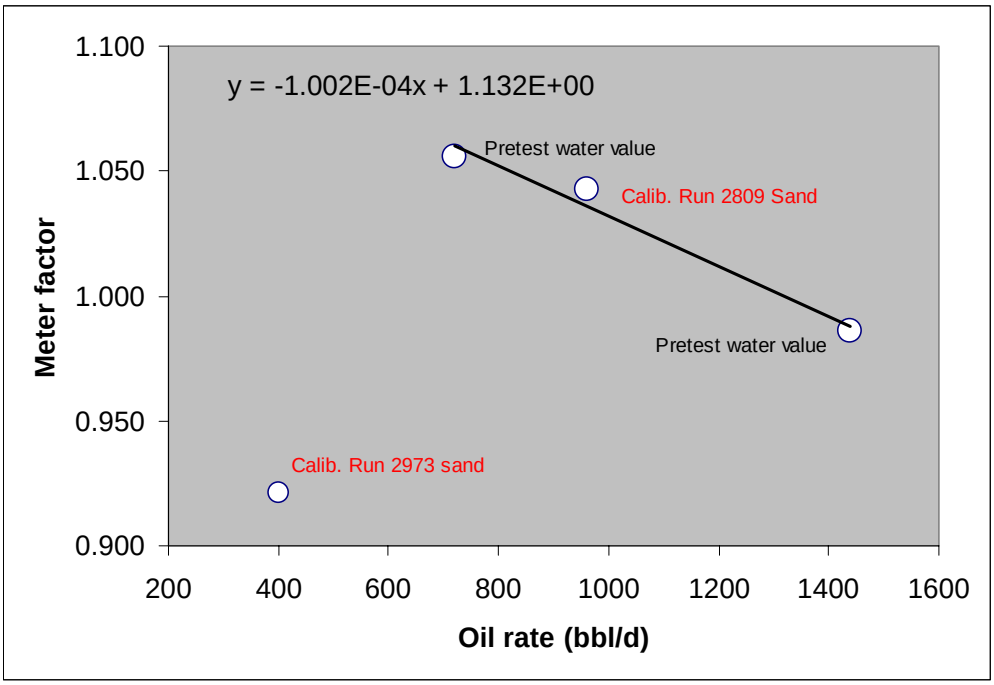

Figure 2.1: Rate dependence of mechanical meter factor - 2" Floco

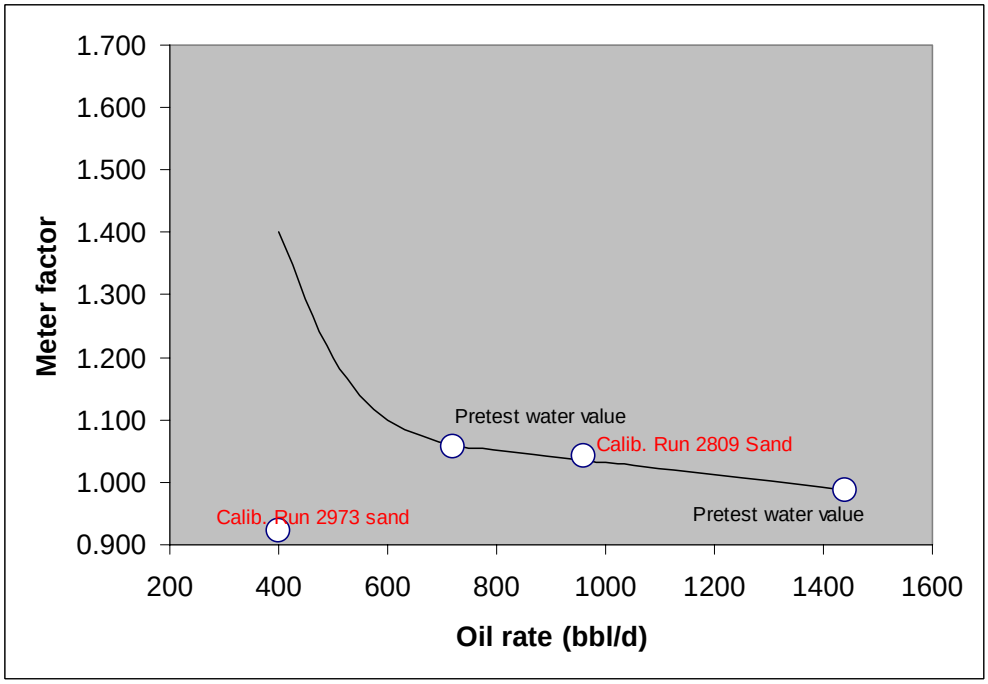

Figure 2.2: Extrapolated rate dependence of mechanical meter factor below range of meter - 2" Floco

Table 2.5: Corrected oil rates for 44/64" choke flow – 2973 sand

Time	Separator pressure (psi)	Separator temp. (ºC)	Meter temp. (ºC)	BSW (%)	(1-shr)*K (stb/bbl)	Meter factor	Oil Rate (bbl/d)	Oil Rate (stb/d)
30.07.2004 (Test 2973 Sand)								
13:45	495.0	42.0	42.0	30.0	0.870	1.300	450.8	392.0
14:00	496.0	44.0	44.0	25.0	0.871	1.300	535.3	466.3
14:15	496.0	45.0	45.0	25.0	0.872	1.300	518.6	452.1
14:30	496.0	47.0	47.0	25.0	0.873	1.300	542.0	473.3
14:45	497.0	48.0	48.0	25.0	0.874	1.300	506.4	442.5
15:00	498.0	49.0	49.0	24.0	0.874	1.300	436.3	381.5
15:15	498.0	50.0	50.0	24.0	0.875	1.300	370.9	324.6
15:30	499.0	50.0	50.0	24.0	0.875	1.300	489.4	428.2
15:45	499.0	51.0	51.0	24.0	0.876	1.300	483.6	423.5
16:00	501.0	52.0	52.0	25.0	0.876	1.300	471.7	413.2
16:15	501.0	53.0	53.0	25.0	0.877	1.300	467.2	409.7
16:30	501.0	54.0	54.0	25.0	0.878	1.300	465.0	408.0

Table 2.6: Corrected oil rates for 52/64" choke flow – 2755 sand

Time	Separator pressure (psi)	Separator temp. (ºC)	Meter temp. (ºC)	BSW (%)	(1-shr)*K (stb/bbl)	Meter factor	Oil Rate (bbl/d)	Oil Rate (stb/d)
01.08.2004 (Test 2755 Sand)								
22:35	497.0	36.0	36.0	27.0	0.838	1.074	623.6	522.9
22:45	497.0	38.0	38.0	27.0	0.841	1.035	1004.5	844.6
23:00	497.0	38.0	38.0	27.0	0.841	1.083	527.5	443.6
23:15	496.0	39.0	39.0	12.0	0.842	1.048	880.7	741.8
23:30	495.0	40.0	40.0	12.0	0.844	1.047	884.7	746.5
23:45	496.0	41.0	41.0	12.0	0.845	1.049	869.3	734.3
00:00	497.0	42.0	42.0	14.0	0.846	1.055	813.4	687.8
00:15	497.0	43.0	43.0	14.0	0.847	1.052	838.3	709.8
00:30	497.0	43.0	43.0	16.0	0.847	1.053	832.8	705.2
00:45	495.0	44.0	44.0	16.0	0.849	1.052	835.1	708.6
01:00	495.0	44.0	44.0	16.0	0.849	1.055	811.6	688.6
01:15	496.0	44.0	44.0	13.0	0.848	1.058	784.5	665.4

Table 2.7: Corrected oil rates for 52/64" choke flow – 2809 sand

Time	Separator pressure (psi)	Separator temp. (ºC)	Meter temp. (ºC)	BSW (%)	(1-shr)*K (stb/bbl)	Meter factor	Oil Rate (bbl/d)	Oil Rate (stb/d)
07.08.2004 (Test 2809 Sand)								
01:45	474.0	42.0	42.0	14.0	0.839	1.046	899.6	755.0
02:00	472.0	43.0	43.0	14.0	0.841	1.010	1230.6	1035.4
02:15	471.0	45.0	45.0	14.0	0.845	1.051	854.2	721.6
02:30	487.0	45.0	45.0	11.0	0.840	1.039	964.1	809.5
02:45	481.0	45.0	45.0	11.0	0.842	1.037	983.5	827.7
03:00	471.0	45.0	45.0	11.0	0.845	1.046	901.4	761.4
03:15	504.0	47.0	47.0	11.0	0.837	1.038	977.8	818.8
03:30	511.0	47.0	47.0	12.0	0.835	1.044	920.4	768.8
03:45	516.0	48.0	48.0	12.0	0.835	1.044	915.6	764.7
04:00	513.0	49.0	49.0	12.0	0.838	1.034	1014.5	849.8
04:15	506.0	49.0	49.0	12.0	0.840	1.044	915.8	769.1

Table 2.8 : Comparison between predicted and measured oil volume factors

Sample	Pressure (psi)	Temp (ºC)	Bo lab (bbl/stb)	Bo PVTsim (bbl/stb)	Deviation (%)
L-209	499	57.5	1.132	1.145	-1.1
L-442	501	59.4	1.134	1.144	-0.8
L-033	497	47.5	1.167	1.185	-1.5
L-412	497	48.1	1.169	1.184	-1.3
L-611	516	53.8	1.188	1.199	-1.0
L-610	506	55.0	1.193	1.195	-0.2

Table 3.1: Corrected CGR at separator and reference conditions, 44/64" choke flow – 2973 sand

Time	Choke (64ths)	Separator Pressure (psi)	Separator Temp. (°C)	Gas Rate (mmscf/d)	Oil Rate (stb/d)	CGR (stb/mmscf)	CGR 500psi, 50°C (stb/mmscf)	CGR 500psi, 50°C (bbl/mmscf)
30.07.2004 (Test 2973 Sand)								
13:45	44	495.0	42.0	27.324	392.0	14.3	14.3	16.4
14:00	44	496.0	44.0	27.233	466.3	17.1	17.1	19.5
14:15	44	496.0	45.0	27.240	452.1	16.6	16.6	18.9
14:30	44	496.0	47.0	27.121	473.3	17.5	17.4	19.9
14:45	44	497.0	48.0	27.280	442.5	16.2	16.2	18.5
15:00	44	498.0	49.0	27.249	381.5	14.0	14.0	16.0
15:15	44	498.0	50.0	27.190	324.6	11.9	11.9	13.6
15:30	44	499.0	50.0	27.218	428.2	15.7	15.7	18.0
15:45	44	499.0	51.0	27.157	423.5	15.6	15.6	17.8
16:00	44	501.0	52.0	27.224	413.2	15.2	15.2	17.3
16:15	44	501.0	53.0	27.164	409.7	15.1	15.1	17.2
16:30	44	501.0	54.0	27.107	408.0	15.1	15.1	17.2
						Avg	15.4	17.5
						St. dev	9.8	9.8

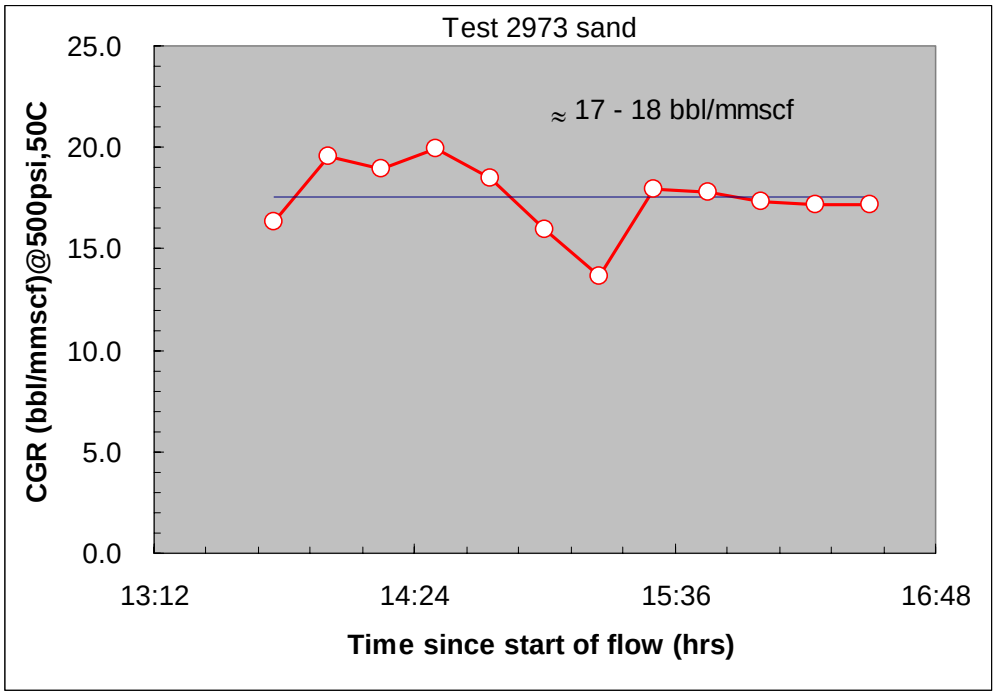

Figure 3.1: Corrected test separator CGRs – 2973 sand

Table 3.2: Corrected CGR at separator and reference conditions, 52/64" choke flow – 2755 sand

Time	Choke (64ths)	Separator Pressure (psi)	Separator Temp. (°C)	Gas Rate (mmscf/d)	Oil Rate (stb/d)	CGR (stb/mmscf)	CGR 500psi, 50°C (stb/mmscf)	CGR 500psi, 50°C (bbl/mmscf)
01.08.2004 (Test 2755 Sand)								
22:35	52	497.0	36.0	33.052	522.9	15.8	15.8	18.5
22:45	52	497.0	38.0	32.850	844.6	25.7	25.7	30.1
23:00	52	497.0	38.0	32.850	443.6	13.5	13.5	15.8
23:15	52	496.0	39.0	32.905	741.8	22.5	22.5	26.4
23:30	52	495.0	40.0	32.794	746.5	22.8	22.8	26.6
23:45	52	496.0	41.0	32.865	734.3	22.3	22.3	26.2
00:00	52	497.0	42.0	32.882	687.8	20.9	20.9	24.5
00:15	52	497.0	43.0	32.758	709.8	21.7	21.7	25.4
00:30	52	497.0	43.0	32.811	705.2	21.5	21.5	25.2
00:45	52	495.0	44.0	32.614	708.6	21.7	21.7	25.4
01:00	52	495.0	44.0	32.774	688.6	21.0	21.0	24.6
01:15	52	496.0	44.0	32.915	665.4	20.2	20.2	23.7
						Avg	20.8	24.4
						St. dev	15.5	15.5

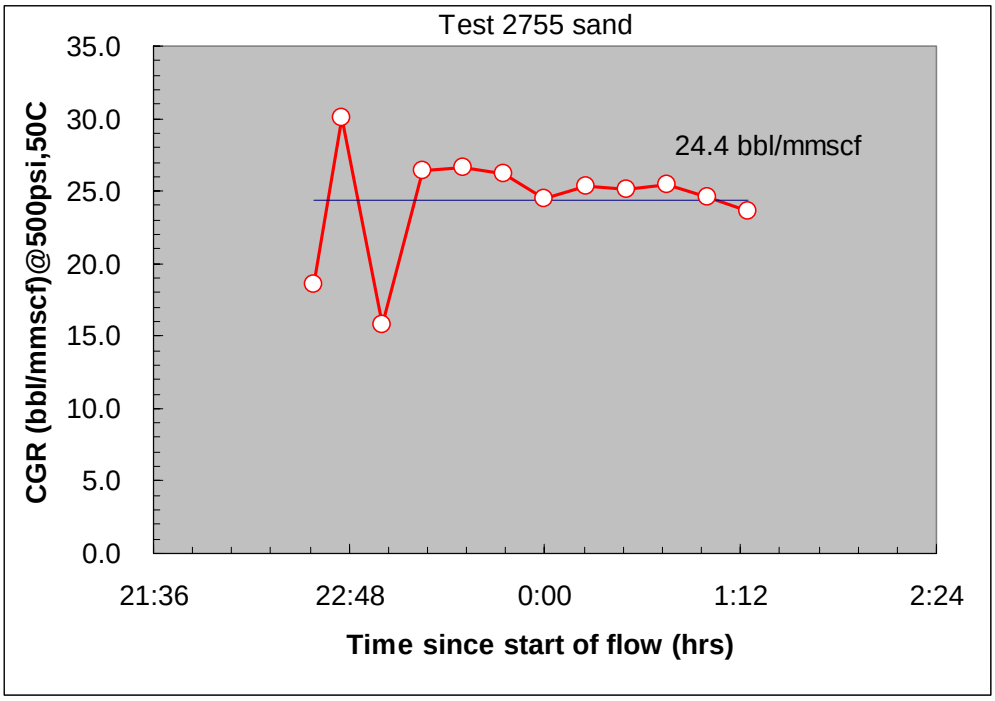

Figure 3.2: Corrected test separator CGRs – 2755 sand

Table 3.3: Corrected CGR at separator and reference conditions, 52/64" choke flow – 2809 sand

Time	Choke (64ths)	Separator Pressure (psi)	Separator Temp. (°C)	Gas Rate (mmscf/d)	Oil Rate (stb/d)	CGR (stb/mmscf)	CGR 500psi, 50°C (stb/mmscf)	CGR 500psi, 50°C (bbl/mmscf)
07.08.2004 (Test 2809 Sand)		**500.0**	**50.0**					
01:45	52	474.0	42.0	32.641	755.0	23.1	23.1	27.4
02:00	52	472.0	43.0	32.685	1035.4	31.7	31.6	37.5
02:15	52	471.0	45.0	32.601	721.6	22.1	22.1	26.2
02:30	52	487.0	45.0	32.715	809.5	24.7	24.7	29.3
02:45	52	481.0	45.0	32.681	827.7	25.3	25.3	30.0
03:00	52	471.0	45.0	32.599	761.4	23.4	23.3	27.6
03:15	52	504.0	47.0	32.887	818.8	24.9	24.9	29.5
03:30	52	511.0	47.0	32.708	768.8	23.5	23.5	27.9
03:45	52	516.0	48.0	32.909	764.7	23.2	23.3	27.6
04:00	52	513.0	49.0	32.543	849.8	26.1	26.2	31.0
04:15	52	506.0	49.0	32.598	769.1	23.6	23.6	28.0
						Avg	24.7	29.3
						St. dev	10.4	10.4

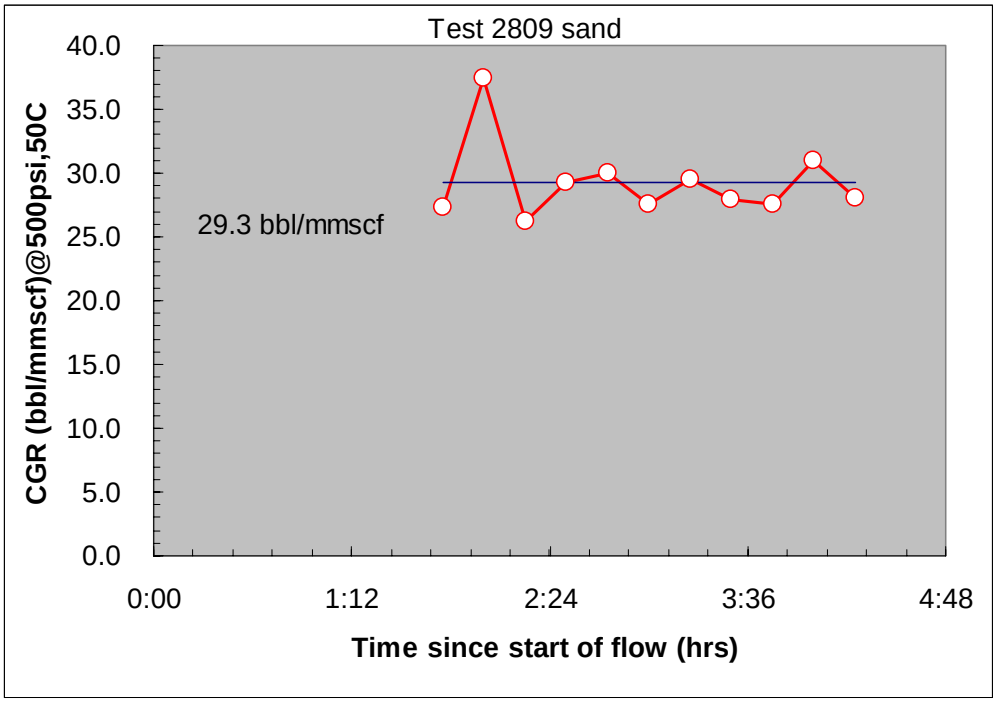

Figure 3.3: Corrected test separator CGRs – 2809 sand

Table 3.4: Recalculated composition of reservoir fluid, 44/64" choke flow – 2973 sand

Test	2973 sand	L-209 and PA-3418	
CGR_{ref}	17.5	bbl/mmscf @ 500psi, 50C	
CGR_{test}	16.3	bbl/mmscf @ test cond.	
CGR_{C5+}	23.3	stb/mmscf	
	Sep. gas mole-%	**Sep. oil mole-%**	**Well stream mole-%**
N_2	0.22	0.05	0.22
CO_2	20.17	5.28	19.97
C_1	71.23	9.32	70.40
C_2	5.15	2.95	5.12
C_3	1.74	2.87	1.76
iC_4	0.42	1.14	0.43
nC_4	0.50	1.99	0.52
iC_5	0.14	1.39	0.16
nC_5	0.13	1.54	0.15
C_6	0.14	5.34	0.21
C_7	0.10	13.81	0.28
C_8	0.03	11.16	0.18
C_9	0.02	11.62	0.18
$C_{10}+$	0.01	31.54	0.43
SUM	100.00	100.00	100.00

Test	2973 sand	L-442 and EC-9460	
CGR_{ref}	17.5	bbl/mmscf @ 500psi, 50C	
CGR_{test}	16.0	bbl/mmscf @ test cond.	
CGR_{C5+}	23.8	stb/mmscf	
	Sep. gas mole-%	**Sep. oil mole-%**	**Well stream Mole-%**
N_2	0.20	0.04	0.20
CO_2	20.16	5.21	19.96
C_1	71.25	9.19	70.44
C_2	5.13	2.90	5.10
C_3	1.70	2.86	1.72
iC_4	0.40	1.13	0.41
nC_4	0.49	2.09	0.51
iC_5	0.16	1.49	0.18
nC_5	0.15	1.63	0.17
C_6	0.16	5.34	0.23
C_7	0.12	13.92	0.30
C_8	0.04	11.20	0.19
C_9	0.03	11.70	0.18
$C_{10}+$	0.01	31.30	0.42
SUM	100.00	100.00	100.00

Average	2973 sand
CGR_{ref}	17.5
CGR_{C5+}	23.6
	Well stream mole-%
N_2	0.21
CO_2	19.97
C_1	70.42
C_2	5.11
C_3	1.74
iC_4	0.42
nC_4	0.52
iC_5	0.17
nC_5	0.16
C_6	0.22
C_7	0.29
C_8	0.18
C_9	0.18
$C_{10}+$	0.43
SUM	100.00

Table 3.5: Recalculated composition of reservoir fluid, 52/64" choke flow – 2755 sand

Test	2755 sand	L-033 and EE-8593	
CGR_{ref}	24.4	bbl/mmscf @ 500psi, 50C	
CGR_{test}	24.9	bbl/mmscf @ test cond.	
CGR_{C5+}	31.5	stb/mmscf	
	Sep. gas mole-%	**Sep. oil mole-%**	**Well stream mole-%**
N_2	0.19	0.02	0.19
CO_2	20.64	6.17	20.32
C_1	68.52	9.63	67.24
C_2	6.41	4.04	6.36
C_3	2.56	4.52	2.60
iC_4	0.42	1.50	0.44
nC_4	0.63	2.97	0.68
iC_5	0.18	1.66	0.21
nC_5	0.16	1.93	0.20
C_6	0.15	6.55	0.29
C_7	0.09	14.12	0.40
C_8	0.04	10.13	0.26
C_9	0.01	9.94	0.23
C_{10}+	0.00	26.82	0.58
SUM	100.00	100.00	100.00

Test	2755 sand	L-412 and PA-3421	
CGR_{ref}	24.4	bbl/mmscf @ 500psi, 50C	
CGR_{test}	24.8	bbl/mmscf @ test cond.	
CGR_{C5+}	31.2	stb/mmscf	
	Sep. gas mole-%	**Sep. oil mole-%**	**Well stream Mole-%**
N_2	0.22	0.02	0.22
CO_2	20.64	6.14	20.32
C_1	68.53	9.60	67.25
C_2	6.43	4.06	6.38
C_3	2.55	4.52	2.59
iC_4	0.40	1.50	0.42
nC_4	0.62	2.97	0.67
in_5	0.17	1.66	0.20
NC_5	0.16	1.93	0.20
C_6	0.15	6.55	0.29
C_7	0.09	14.12	0.40
C_8	0.03	10.13	0.25
C_9	0.01	9.94	0.23
C_{10}+	0.00	26.86	0.58
SUM	100.00	100.00	100.00

Average	2755 sand
CGR_{ref}	24.4
CGR_{C5+}	31.3
	Well stream mole-%
N_2	0.20
CO_2	20.32
C_1	67.24
C_2	6.37
C_3	2.60
iC_4	0.43
nC_4	0.68
iC_5	0.21
nC_5	0.20
C_6	0.29
C_7	0.40
C_8	0.25
C_9	0.23
C_{10}+	0.58
SUM	100.00

Table 3.6: Recalculated composition of reservoir fluid, 52/64" choke flow – 2809 sand

Test	2809 sand	L-611 and PA-3429	
CGR_{ref}	29.3	bbl/mmscf @ 500psi, 50C	
CGR_{test}	28.4	bbl/mmscf @ test cond.	
CGR_{C5+}	34.1	stb/mmscf	
	Sep. gas mole-%	**Sep. oil mole-%**	**Well stream mole-%**
N_2	0.17	0.02	0.17
CO_2	19.89	5.65	19.53
C_1	67.79	9.22	66.33
C_2	7.31	4.35	7.24
C_3	3.10	5.27	3.15
iC_4	0.45	1.78	0.48
nC_4	0.73	3.57	0.80
iC_5	0.18	1.87	0.22
nC_5	0.16	2.22	0.21
C_6	0.12	7.04	0.29
C_7	0.07	14.71	0.44
C_8	0.02	9.92	0.27
C_9	0.01	9.53	0.25
$C_{10}+$	0.00	24.85	0.62
SUM	100.00	100.00	100.00

Test	2809 sand	L-610 and PA-3419	
CGR_{ref}	29.3	bbl/mmscf @ 500psi, 50C	
CGR_{test}	28.0	bbl/mmscf @ test cond.	
CGR_{C5+}	35.0	stb/mmscf	
	Sep. gas mole-%	**Sep. oil mole-%**	**Well stream mole-%**
N_2	0.15	0.01	0.15
CO_2	19.97	5.83	19.62
C_1	67.57	9.67	66.14
C_2	7.30	4.44	7.23
C_3	3.12	5.23	3.17
iC_4	0.46	1.69	0.49
nC_4	0.76	3.50	0.83
iC_5	0.19	1.78	0.23
nC_5	0.18	2.10	0.23
C_6	0.15	6.87	0.32
C_7	0.09	14.41	0.44
C_8	0.04	9.74	0.28
C_9	0.02	9.37	0.25
$C_{10}+$	0.00	25.36	0.63
SUM	100.00	100.00	100.00

Average	2809 sand
CGR_{ref}	29.3
CGR_{C5+}	34.5
	Well stream mole-%
N_2	0.16
CO_2	19.58
C_1	66.23
C_2	7.23
C_3	3.16
iC_4	0.49
nC_4	0.81
iC_5	0.23
nC_5	0.22
C_6	0.30
C_7	0.44
C_8	0.27
C_9	0.25
$C_{10}+$	0.62
SUM	100.00

APPENDIX 4: PETROLOGY REPORT

RESERVOIR SOLUTIONS PTY LTD
LEVEL 2, 2 PARK RD, MILTON, 4064, QLD
PO BOX 2098, MILTON, 4064, QLD
ABN 27 088 995 073

PETROLOGY, DIAGENESIS AND RESERVOIR QUALITY OF CORE SAMPLES FROM YOLLA-3

Julian C. Baker PhD

A report to:

Origin Energy Resources Ltd
339 Coronation Drive
Milton QLD 4064

23 November, 2004

C O N T E N T S

C O N T E N T S cont.

EXECUTIVE SUMMARY

A petrological study was carried out on five core samples from 2216.70-2232.98m in Yolla-3. Analytical techniques used were thin-section analysis, bulk-rock/fine-fraction X-ray diffraction analysis and scanning electron microscopy.

Samples are variably argillaceous/clean, very fine grained quartzarenites in which framework grains are mainly quartz and, below 2216.70m, peloidal glauconite.

Detrital clay forms dispersed matrix and is concentrated into irregular patches, along discontinuous thin laminae and around sandy burrow fills. Sandstone at 2230.27m is clean. Authigenic clay is almost entirely kaolinite that forms scattered patches and mica-like grains where mica has altered. Clay minerals detected by XRD are kaolinite, illite/mica and, below 2216.70m, illitic mixed-layer illite/smectite (glauconite).

Diagenetic effects include siderite and pyrite replacement, glauconite compaction, authigenic kaolinite formation and incipient quartz overgrowth precipitation. Clean, quartzose sandstone is poorly compacted and uncemented.

Visible macroporosity ranges from 0.6% to 30.8% and varies mainly according to detrital clay + siderite content. Visible porosity is mostly primary and intergranular and also includes widely scattered secondary pores that result from K-feldspar dissolution.

Porosity reduction results mainly from pore filling by pyritic/sideritic detrital clay matrix and, in areas where glauconite is concentrated, glauconite compaction.

Variable reservoir quality (0.58-387mD) reflects large differences in detrital clay and siderite content. Being little affected by diagenesis, sandstone is highly permeable where it is clean and quartzose.

High grain density at 2219.36m reflects the presence of significant amounts of siderite that is associated with detrital clay.

1. INTRODUCTION

A petrological study was carried out on five core samples from 2216.70-2232.98m in Yolla-3 in order to provide information on mineralogy, diagenetic effects and controls on reservoir quality. Sample depths and core analyses performed by ACS Laboratories Pty Ltd are given in Table 1.

2. ANALYTICAL PROGRAM

2.1 THIN-SECTION ANALYSIS

Thin-sections were cut in kerosene, impregnated with blue-dyed epoxy resin to aid porosity recognition, and stained with sodium cobaltinitrite to aid feldspar identification. Mineral composition and visible porosity were determined by a count of 400 points, and mean grain size and sorting were estimated in thin-section with the aid of an eyepiece graticule. Photomicrographs were taken of each thin-section to illustrate texture, composition, clay distribution, diagenetic effects and porosity.

2.2 X-RAY DIFFRACTION ANALYSIS

Bulk-rock X-ray diffraction (XRD) analysis was carried out on each sample in order to quantify mineral abundance. The XRD analysis used a finely ground whole rock powder sample and the SIROQUANT processing technique was used to calculate mineral abundance.

XRD analysis was carried out on the fine fraction of each sample in order to precisely determine clay mineralogy. The fine fraction was separated from each sample by disaggregation and settling in distilled water and was air dried on glass discs to produce oriented specimens for XRD analysis. Samples were analysed in air dried condition and also following treatment with ethylene glycol.

2.3 SCANNING ELECTRON MICROSCOPY

Scanning electron microscopy (SEM) was carried out on each sample in order to provide information on clay distribution, diagenetic effects and porosity characteristics. Analyses were done on freshly exposed surfaces that had been thoroughly washed in shellite to remove any volatile hydrocarbons.

3. TEXTURE

Thin-section texture is given in Table 1. Samples are variably argillaceous and clean, grain/matrix supported, well sorted, very fine grained sandstones with a mean quartz grain size of 0.08-0.10mm. In the two most argillaceous sandstones (#3, 2216.70m; #57, 2232.98m), abundant detrital clay forms widely dispersed matrix and is concentrated into irregular patches and along discontinuous thin laminae, the distribution of which has been influenced by intense burrowing. In the other two argillaceous sandstones (#12, 2219.36m; #20, 2221.81m), minor detrital clay forms scattered, irregular patches and thin laminae and also rims sandy burrow fills. The one clean sandstone (#48, 2230.27m) is massive. Where detrital clay is lacking, framework grains are loosely packed, with all juxtaposed quartz grains having point and, much less commonly, long grain contacts, although glauconite peloids are commonly compactionally deformed, particularly in areas where glauconite is concentrated. Most quartz grains are angular to subrounded.

4. THIN-SECTION COMPOSITION

Thin-section composition is given in Table 1, QFR composition is plotted in Figure 1, and annotated photomicrographs are presented in Appendix 2.

4.1 FRAMEWORK GRAINS

Samples are quartzarenites ($Q_{97}F_2R_1$ mean) in which framework grains are mainly quartz and, below 2216.70m, glauconite.

Total detrital quartz content ranges from 49.0% to 53.7% and averages 52.0%. Quartz is mainly monocrystalline. Quartz grains are locally enveloped by incipient quartz overgrowths, the amount of which does not exceed 0.3%.

Feldspar does not exceed 1.5% and is almost entirely K-feldspar (orthoclase) that is generally fresh to slightly altered and locally corroded and partly dissolved. Plagioclase is rare.

Lithic grains do not exceed 0.7% and include quartzose/micaceous/illitic, low-grade metasedimentary rock fragments and rare silicified volcanic rock fragments.

Glauconite, which is common (8.0-15.5%) in all samples except the top sample (#3, 2216.70m), forms fine sand-sized, pale green peloids that are commonly compactionally deformed between adjacent quartz grains, particularly in argillaceous areas, where glauconite tends to be concentrated.

Other detrital grains include chert, mica (fresh and variably kaolinitised muscovite and subordinate biotite), rare siliceous forams (#3, 2216.70m), and accessory heavy minerals (tourmaline, zircon, monazite, sphene, opaque Ti-oxides). In the argillaceous sandstones, fine pyritic organic fragments are associated with detrital clay matrix. Monazite grains are rimmed by radiogenically-immobilised bitumen in #20 (2221.81m) and #57 (2232.98m).

TABLE 1. THIN-SECTION AND CORE ANALYSES

Sample #	3	12	20	48	57
Depth (mRT)	2216.70	2219.36	2221.81	2230.27	2232.98
Quartz (monocrystalline)	51.8	50.8	48.5	51.9	53.4
Quartz (polycrystalline)	1.9	0.3	0.5	0.5	0.3
Quartz overgrowths	-	-	0.3	-	-
Chert	0.7	-	0.3	0.3	0.3
K-feldspar	0.3	1.0	1.5	1.0	1.0
Plagioclase	-	0.3	-	-	-
Volcanic rock fragments	-	0.3	-	-	-
Metamorphic rock fragments	0.7	-	0.5	0.3	0.3
Sedimentary rock fragments	-	-	-	-	-
Mica	0.3	1.0	0.5	0.5	0.8
Heavy minerals	-	-	-	0.7	-
Organic fragments	1.3	-	-	-	0.3
Glauconite	0.7	15.5	11.6	8.0	11.0
Pyrite	4.8	0.3	0.5	-	1.4
Siderite	-	6.0	1.5	0.7	1.8
Anatase/leucoxene	0.7	0.5	0.7	0.7	0.3
Authigenic kaolinite	0.3	1.5	1.3	4.6	3.3
Detrital clay	35.9	7.7	6.5	-	20.5
Primary porosity	0.6	13.5	24.0	29.3	5.3
Secondary porosity	-	1.3	1.8	1.5	-
Q (quartz + chert)	98.2	97.0	96.1	97.5	97.7
F (feldspar)	0.5	2.4	2.9	1.9	1.8
R (rock fragments)	1.3	0.6	1.0	0.6	0.5
Mean grain size (mm)	0.10	0.08	0.09	0.08	0.09
Grain size class	v fine	v fine	v fine	v fine	v fine
Sorting class	well	well	well	well	well
He-injection porosity (%)*	18.3	28.3	35.0	37.1	28.7
Permeability (mD) *	0.58	10.6	268	387	12.1
Grain density (g/cm^3)	2.65	2.74	2.67	2.67	2.67

*ambient; horizontal direction

FIGURE 1. QFR COMPOSITION

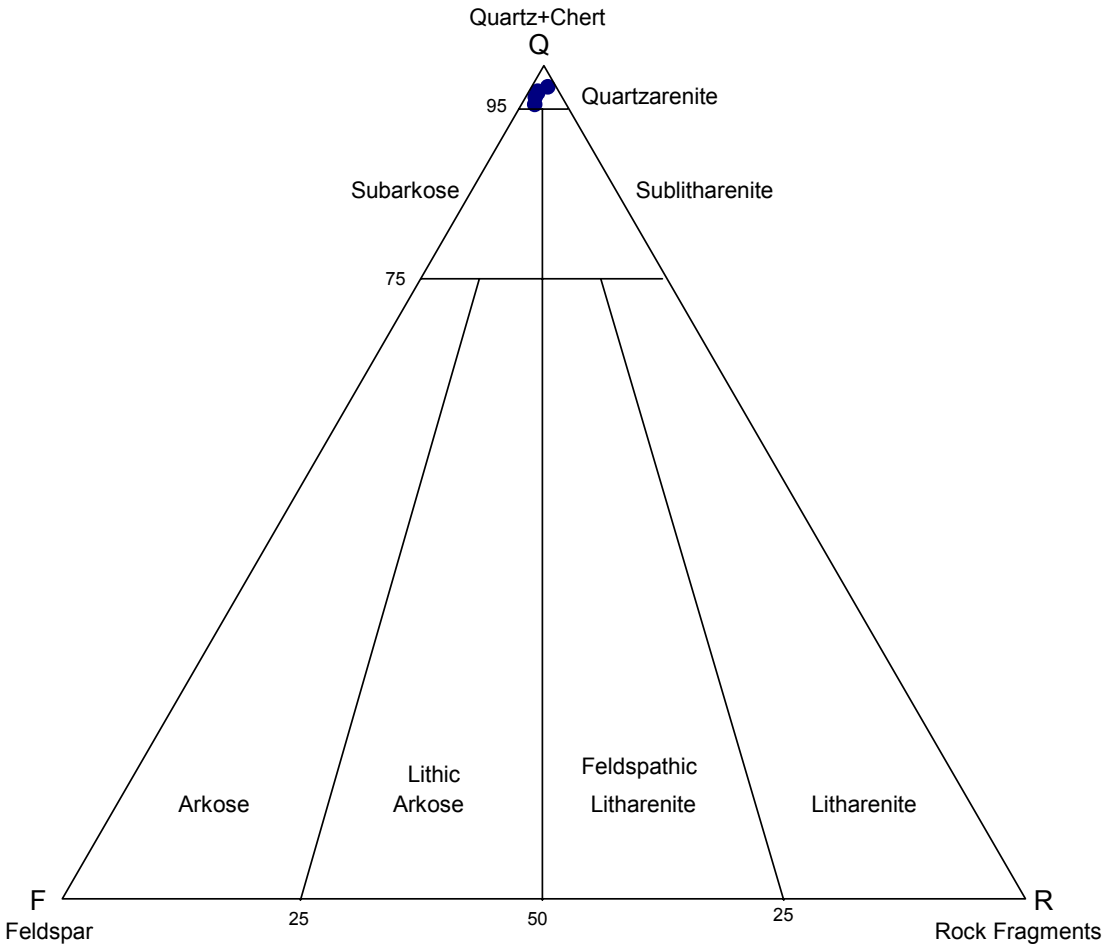

4.2 CLAYS

Detrital clay content ranges from less than 0.3% to 35.9%. In #3 (2216.70m) and #57 (2232.98m), which are the most argillaceous sandstones, detrital clay forms widely dispersed matrix and is concentrated into irregular patches and along discontinuous thin laminae, the distribution of which has been influenced by intense burrowing. In #12 (2219.36m) and #20 (2221.81m), detrital clay forms scattered, irregular patches and thin laminae and also rims sandy burrow fills. Sample #48 (2230.27m) is clean. Pyrite and siderite are commonly associated with detrital clay, particularly in #3 (pyrite) and #12 (siderite).

Authigenic clay ranges up to 4.6% and is almost entirely kaolinite that forms scattered patches and mica-like grains where mica has altered. Mica grains are commonly partly altered to kaolinite.

4.3 CEMENTS

Siderite content does not exceed 1.8%, except in #12 (2219.36m), which contains 6.0% siderite that is finely disseminated throughout detrital clay matrix.

Sample #3 (2216.70m) contains 4.8% pyrite that forms finely-crystalline patches and fine framboids that are disseminated throughout detrital clay matrix and that locally occupy intergranular spaces. Fine pyrite that is associated with detrital clay in the other samples does not exceed 1.4%.

Quartz grains are locally partly enveloped by incipient quartz overgrowths, the amount of which does not exceed 0.3%.

Clean sandstone is uncemented.

4.4 VISIBLE POROSITY

Visible macroporosity ranges from 0.6% to 30.8% and varies mainly accordingly to detrital clay + siderite content (see Fig. 2), with least visible porosity occurring in the highly argillaceous sandstones (#3, 2216.70m; #57, 2232.98m) and most visible porosity occurring in the clean sandstone (#48, 2230.27m). Visible porosity is mainly primary and intergranular and also includes widely scattered secondary pores that result from partial to complete dissolution of K-feldspar grains.

5. X-RAY DIFFRACTION ANALYSES

Quantitative bulk-rock and fine-fraction XRD analyses were carried out on each sample. Quantitative XRD analyses are given in Table 2, clay mineralogy is given in Table 3, and annotated XRD traces are presented in Appendix 1.

Quantitative XRD analyses complement the thin-section analyses but cannot be compared directly. This is because thin-section clay, glauconite and siderite include microporosity, and therefore total thin-section clay, glauconite and siderite are elevated relative to other components. In addition, XRD analyses do not include visible porosity. Therefore, in the case of those sandstones that contain significant amounts of visible porosity, component amounts as determined by XRD analysis will be higher than those determined by thin-section analysis. Finally, the thin-section detrital clay component includes quartz, kaolinite and illite/mica that are recorded as these phases by XRD.

Quantitative XRD analyses show that sandstones are dominated by quartz (72.8-84.1%) and also include clay minerals (13.8-23.4%), K-feldspar (0.5-1.2%), siderite (0-4.3%), pyrite (0-3.8%), anatase (<1.0%) and contaminant halite (<0.4%). Clay minerals are mainly kaolinite (9.8-17.1%) and also include illite/mica (1.8-4.6%) and, in all samples except #3 (2216.70m), mixed-layer illite/smectite (1.1-4.4%).

Fine-fraction XRD analyses (Table 3) show that kaolinite dominates over illite/mica in all samples and that minor to major, illitic (75-80% illite interlayers) mixed-layer illite/smectite occurs in all samples except #3 (2216.70m). Chlorite and smectitic clays are absent.

Detected kaolinite has a detrital and authigenic origin. Detected illite is present as a constituent of detrital clay matrix and as fine detrital mica. The appearance of mixed-layer illite/smectite below 2216.70m coincides with the appearance of significant amounts of glauconite, indicating that detected mixed-layer illite/smectite is present as glauconite. Glauconite peloids may be partly kaolinitic given that 10.9% kaolinite was detected by XRD in #48 (2230.27m), even though thin-section and SEM analyses show that this sandstone is clean and contains only minor authigenic kaolinite.

TABLE 2. BULK-ROCK XRD ANALYSES

Sample # **Depth (mRT)**	3 2216.70	12 2219.36	20 2221.81	48 2230.27	57 2232.98
Quartz	75.5	72.8	80.7	84.1	73.6
K-feldspar	1.2	0.8	0.8	0.5	0.5
Plagioclase	T	-	-	-	-
Kaolinite	15.2	11.9	9.8	10.9	17.1
Illite/mica	3.4	4.6	3.2	1.8	3.0
Illite/smectite	-	4.4	3.5	1.1	3.3
Siderite	-	4.3	0.9	1.0	0.8
Pyrite	3.8	0.8	0.4	-	1.2
Anatase	0.9	0.4	0.4	0.4	0.3
Halite	-	-	0.3	0.2	0.2

TABLE 3. FINE-FRACTION CLAY MINERALOGY

Sample # **Depth (mRT)**	3 2216.70	12 2219.36	20 2221.81	48 2230.27	57 2232.98
Kaolinite	A	A	A	A	M
Illite/mica	m	m	m	m	m
Illite/smectite	-	m	m	m	M
Smectite	-	-	-	-	-
Chlorite	-	-	-	-	-
I/S illite content (%)	-	75-80	75-80	75-80	75-80

A = abundant; M = major; m = minor; T = trace

I/S = mixed-layer illite/smectite

6. DIAGENESIS

Diagenetic effects are minor and include siderite/pyrite replacement, glauconite compaction and authigenic kaolinite formation.

Siderite occurs below 2216.70m, where it forms disseminated, fine (<40μm) crystals that replace detrital clay matrix (Plates 3, 11), particularly at 2219.36m (#12).

Pyrite is common only at 2216.70m (#3), where it forms finely-crystalline patches and fine framboids that are disseminated throughout detrital clay matrix and that locally occupy intergranular spaces.

Authigenic kaolinite forms scattered patches and mica-like grains where mica has altered (Plate 4, Fig. 2; Plate 8). Mica grains are commonly partly altered to kaolinite.

Glauconite peloids are commonly compactionally deformed between adjacent rigid grains, particularly in argillaceous areas below 2216.70m, where they tend to be concentrated (Plates 3, 5, 11). Mica grains and authigenic kaolinite are also commonly compactionally deformed.

Other diagenetic effects include incipient quartz overgrowth precipitation (Plates 2, 4; Plate 6, Fig. 2; Plate 7; Plate 9, Fig. 2; Plate 10), grain contact dissolution to form long grain contacts (most quartz grains have point grain contacts) (Plate 8), K-feldspar dissolution to form widely scattered secondary pores (Plate 9, Fig. 2), and alteration of detrital Fe-Ti oxide grains to leucoxene/anatase. Quartz overgrowth content does not exceed 0.3%. Radiogenically-immobilised bitumen encases monazite grains in #20 (2221.81m) and #57 (2232.98m).

Having been little affected by diagenesis, clean, quartzose sandstone is weakly consolidated and retains abundant primary intergranular porosity (Plates 4-10).

There are no differences in diagenetic effects between samples from the gas zone (#3, 2216.70m; #12, 2219.36m; #20, 2221.81m), oil zone (#48, 2230.27m) and water zone (#57, 2232.98m).

7. RESERVOIR QUALITY

Samples have variable reservoir quality, with He-injection porosity and permeability ranging from 18.3% to 37.1% and 0.58mD to 387mD (Table 1). Wide porosity and permeability variation reflects large differences in detrital clay and siderite content, as shown by the strong negative correlation (R^2 >-0.9) between detrital clay + siderite and visible porosity (Fig. 2) and between detrital clay + siderite and permeability (Fig. 3). Samples are briefly described in order of increasing reservoir quality.

The shallowest sample (#**3, 2216.70m**) is an intensely burrowed, argillaceous sandstone that contains little (0.6%) intergranular porosity due to almost complete pore filling by pyritic detrital clay matrix and localised pyrite cement. Being almost totally microporous, the sandstone has very low (0.58mD) permeability.

The deepest sample **(#57, 2232.98m**) is an argillaceous sandstone in which intergranular spaces are largely filled by irregularly-distributed (due to bioturbation) detrital clay matrix and common compacted glauconite peloids. The sandstone contains 5.3% visible porosity, most of which is confined to relatively clean burrow fills, where it is not conducive to good permeability on a thin-section scale. The sandstone has only moderate (12.1mD) permeability.

Sample **#12** (**2219.36m**) has a similar permeability (10.6mD) to the previous sample, yet contains far more (13.5%) intergranular porosity, with a large part of the sample being clean, quartzose and highly macroporous. Measured permeability appears to be representative of the argillaceous part of the sample, where significant porosity loss results from pore filling by irregularly-distributed (due to bioturbation), sideritic detrital clay matrix and common compacted glauconite peloids. The sample is distinguished by its relatively high (6.0%) content of finely-crystalline siderite, all of which is confined to argillaceous areas.

In **#20** (**2221.81m**), erratically-distributed, slightly sideritic detrital clay matrix and localised concentrations of compacted glauconite peloids have reduced porosity, but most of the sandstone is clean, quartzose and highly macroporous, and permeability is consequently high (268mD). Burrowing has been effective in cleaning up the sandstone to some extent, with the most quartzose and macroporous parts of the sandstone being large sandy burrow fills.

Unlike the other samples, **#48** (**2230.27m**) contains little detrital clay, and, being clean, quartzose, poorly compacted and uncemented, is highly macroporous. Some intergranular spaces are filled by compacted glauconite peloids, but, throughout most of the sandstone, quartz is sufficiently abundant to have prevented significant glauconite compaction. Intergranular pores are evenly distributed and thus well interconnected. The sandstone has the highest permeability (387mD) of the sample suite, reflecting its relatively low content of detrital clay, compacted glauconite and siderite and correspondingly high content (30.8%) of intergranular porosity.

High grain density within the sampled section reflects the presence of significant amounts of siderite, with the most sideritic sample (#12, 2219.36m) having the highest grain density (Table 1).

FIGURE 2. DETRITAL CLAY + SIDERITE/VISIBLE POROSITY CROSS-PLOT

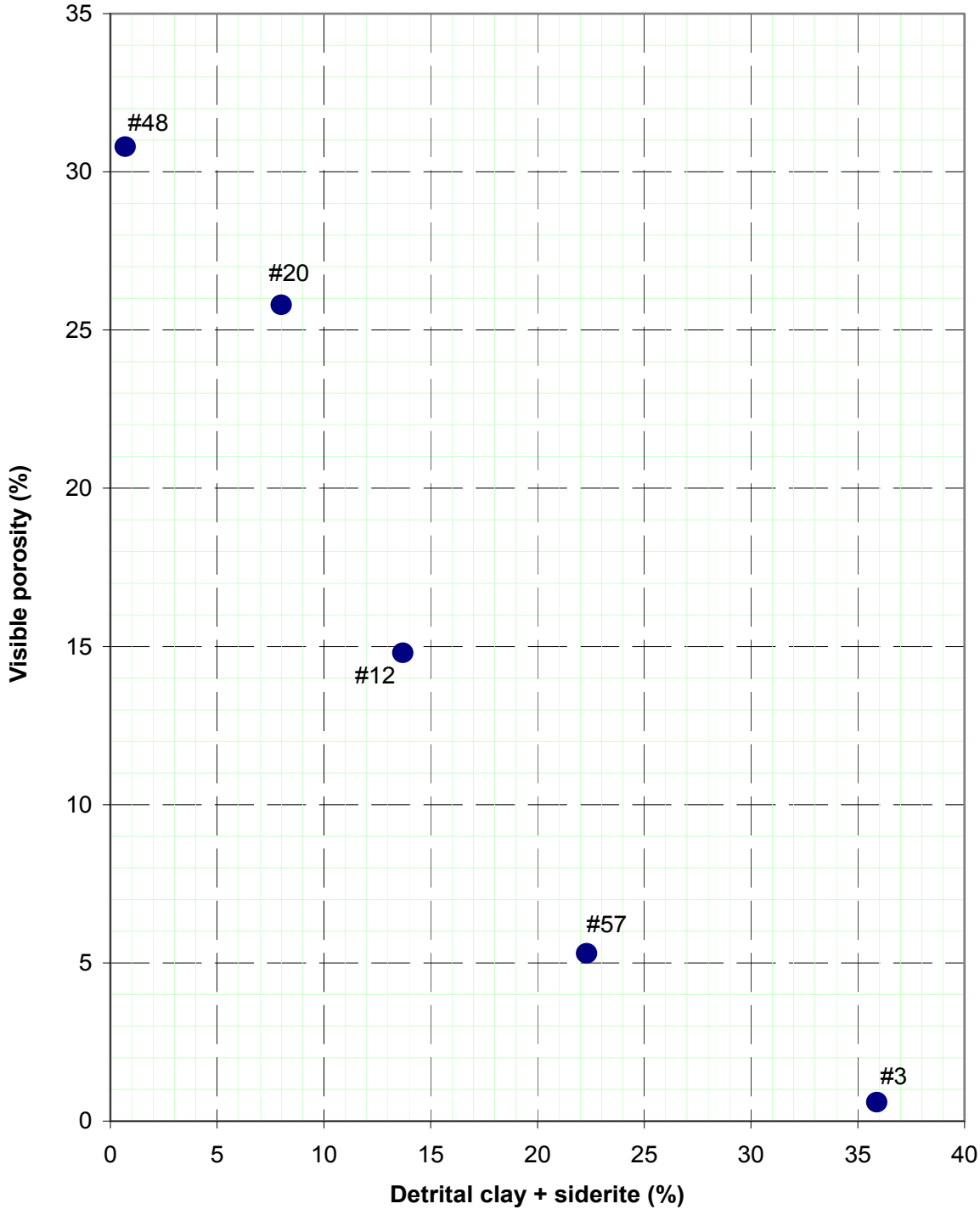

FIGURE 3. DETRITAL CLAY + SIDERITE/PERMEABILITY CROSS-PLOT

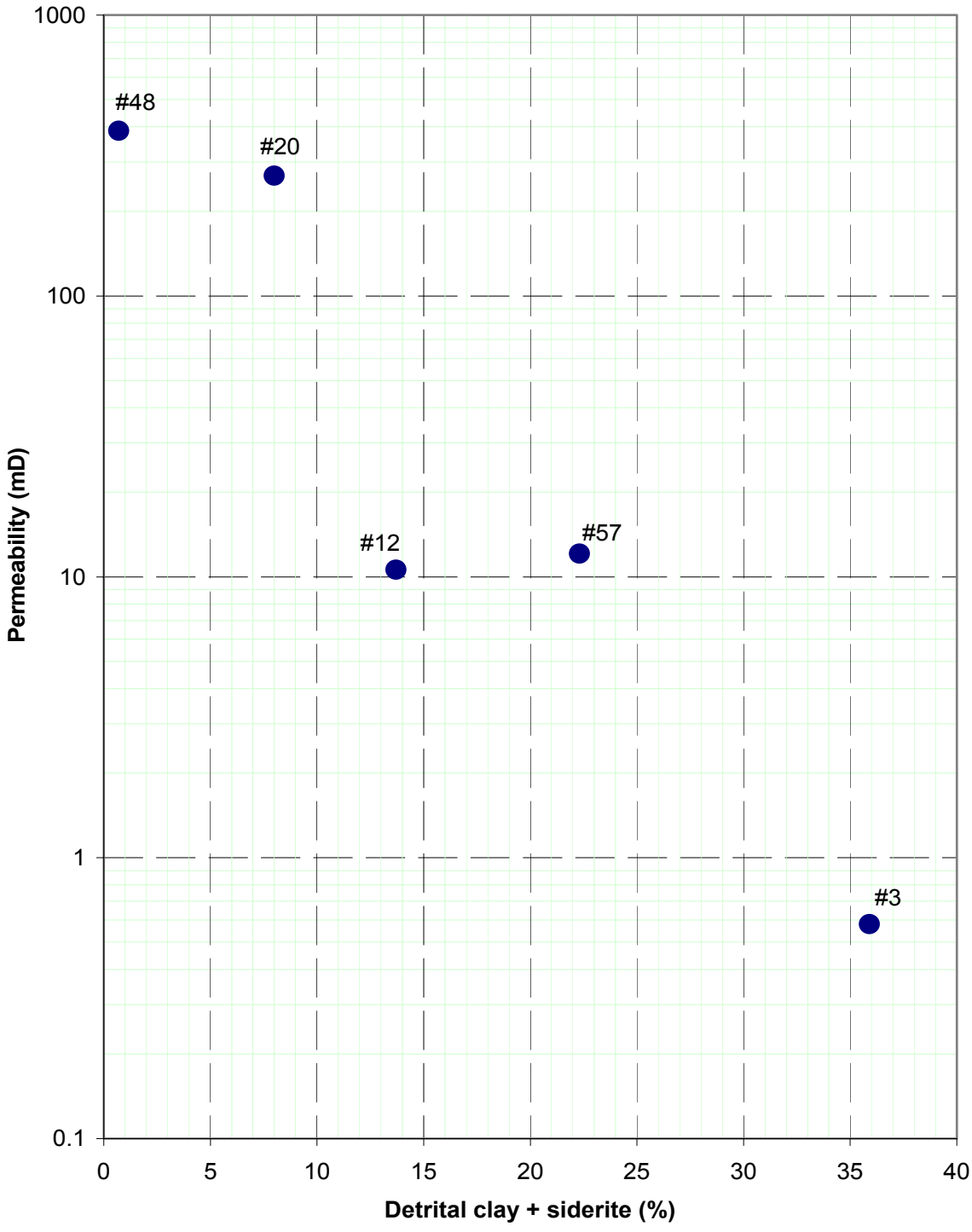

8. SUMMARY AND CONCLUSIONS

- Five core samples from 2216.70-2232.98m in Yolla-3 are variably argillaceous/clean, very fine grained quartzarenites in which framework grains are mainly quartz and, below 2216.70m, peloidal glauconite.

- Detrital clay forms dispersed matrix and is concentrated into irregular patches, along discontinuous thin laminae and around sandy burrow fills. Sandstone at 2230.27m is clean.

- Authigenic clay is almost entirely kaolinite that forms scattered patches and mica-like grains where mica has altered.

- XRD analyses indicate that clay minerals are kaolinite, illite/mica and, below 2216.70m, illitic mixed-layer illite/smectite (glauconite). Smectitic clays are absent.

- Diagenetic effects include siderite and pyrite replacement, glauconite compaction, authigenic kaolinite formation and incipient quartz overgrowth precipitation. Clean, quartzose sandstone is poorly compacted and uncemented.

- Visible macroporosity ranges from 0.6% to 30.8% and varies mainly according to detrital clay + siderite content. Visible porosity is mostly primary and intergranular and also includes widely scattered secondary pores that result from K-feldspar dissolution.

- Porosity reduction results mainly from pore filling by pyritic/sideritic detrital clay matrix and, in areas where glauconite is concentrated, glauconite compaction.

- Variable reservoir quality (0.58-387mD) reflects large differences in detrital clay and siderite content. Being little affected by diagenesis, sandstone is highly permeable where it is clean and quartzose.

- High grain density at 2219.36m (#12) reflects the presence of significant amounts of siderite that is associated with detrital clay.

APPENDIX 1.

X-RAY DIFFRACTOGRAMS

Key to abbreviations:

A = anatase

Ha = contaminant halite

I = illite/mica

I/S = illitic mixed-layer illite/smectite

K = kaolinite

KF = K-feldspar

PF = plagioclase

Py = pyrite

Q = quartz

S = siderite

#3 2216.70m
Bulk rock

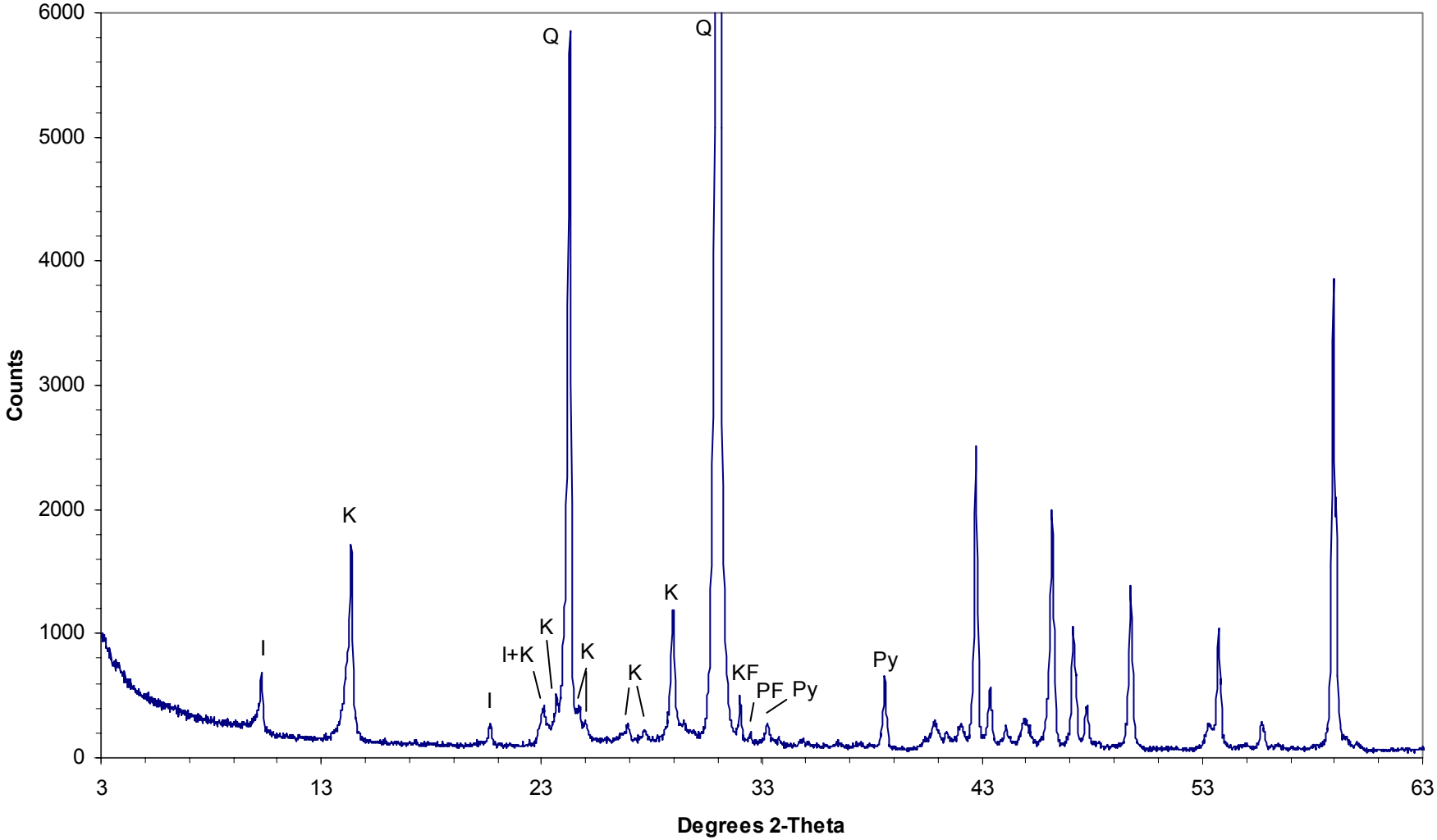

#3 2216.70m
Fine fraction

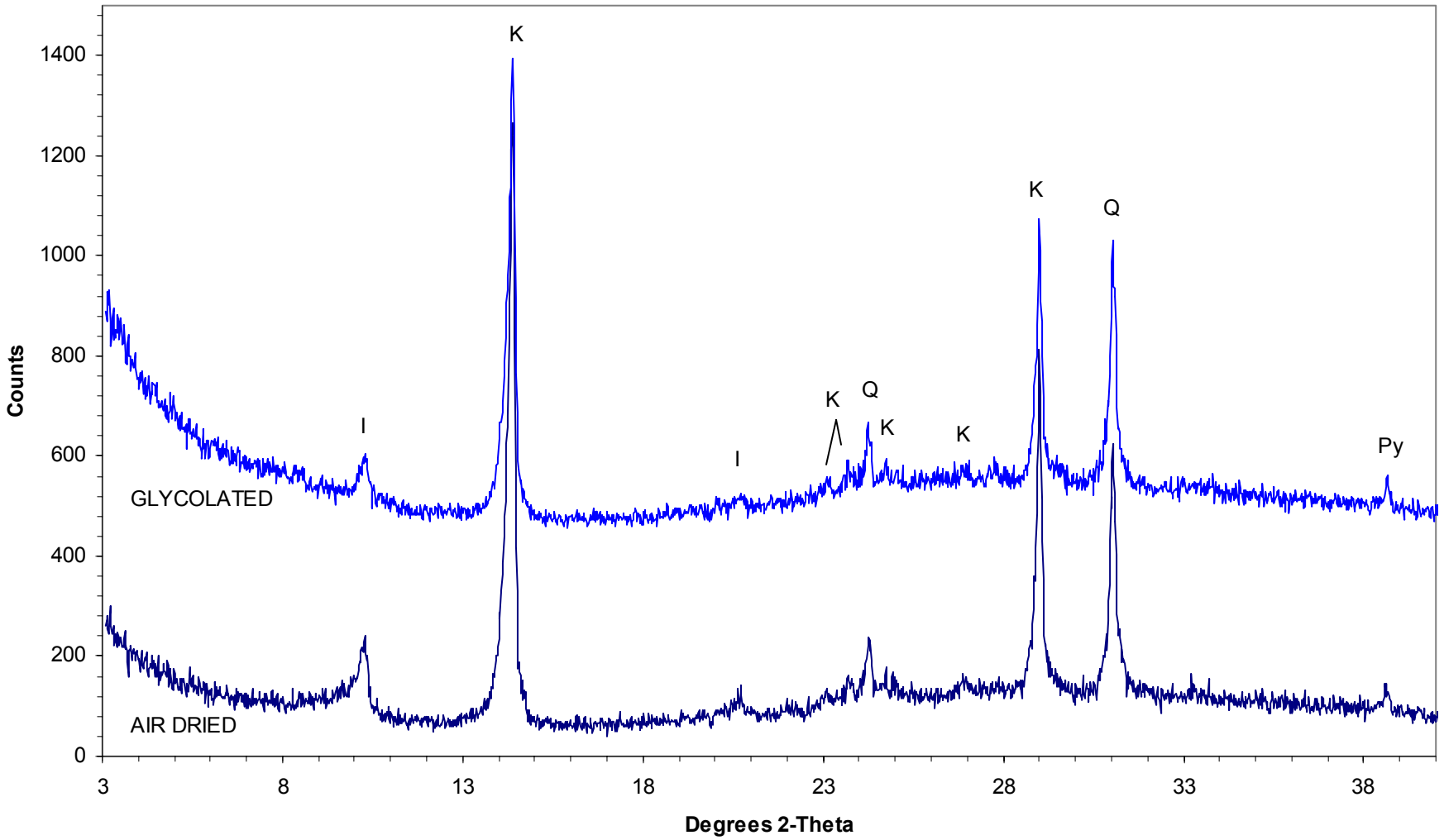

#12 2219.36m
Bulk rock

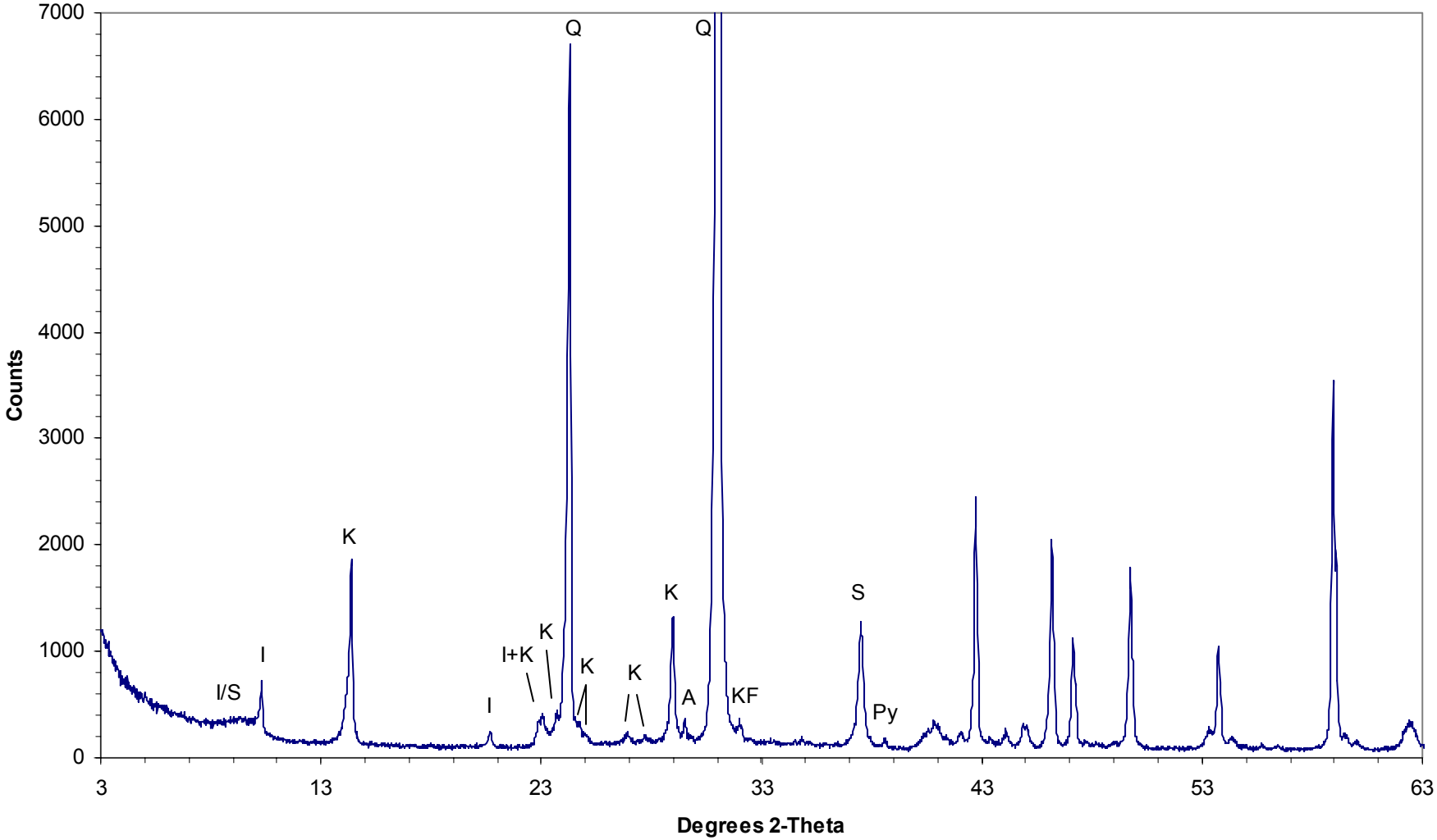

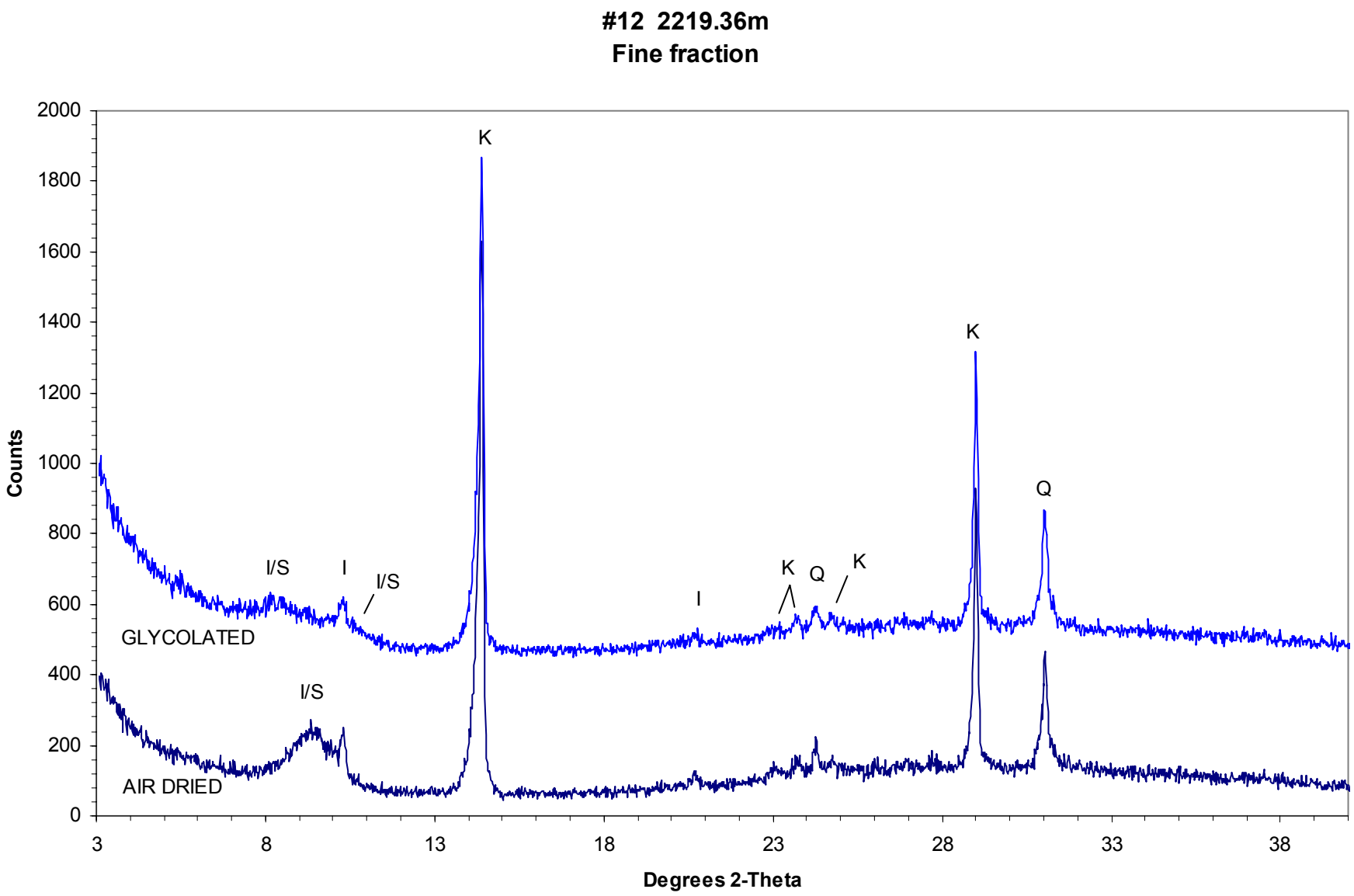
#12 2219.36m
Fine fraction
Counts
Degrees 2-Theta
GLYCOLATED
AIR DRIED
I/S
I
K
Q
2000
1800
1600
1400
1200
1000
800
600
400
200
0
3
8
13
18
23
28
33
38

#20 2221.81m
Bulk rock

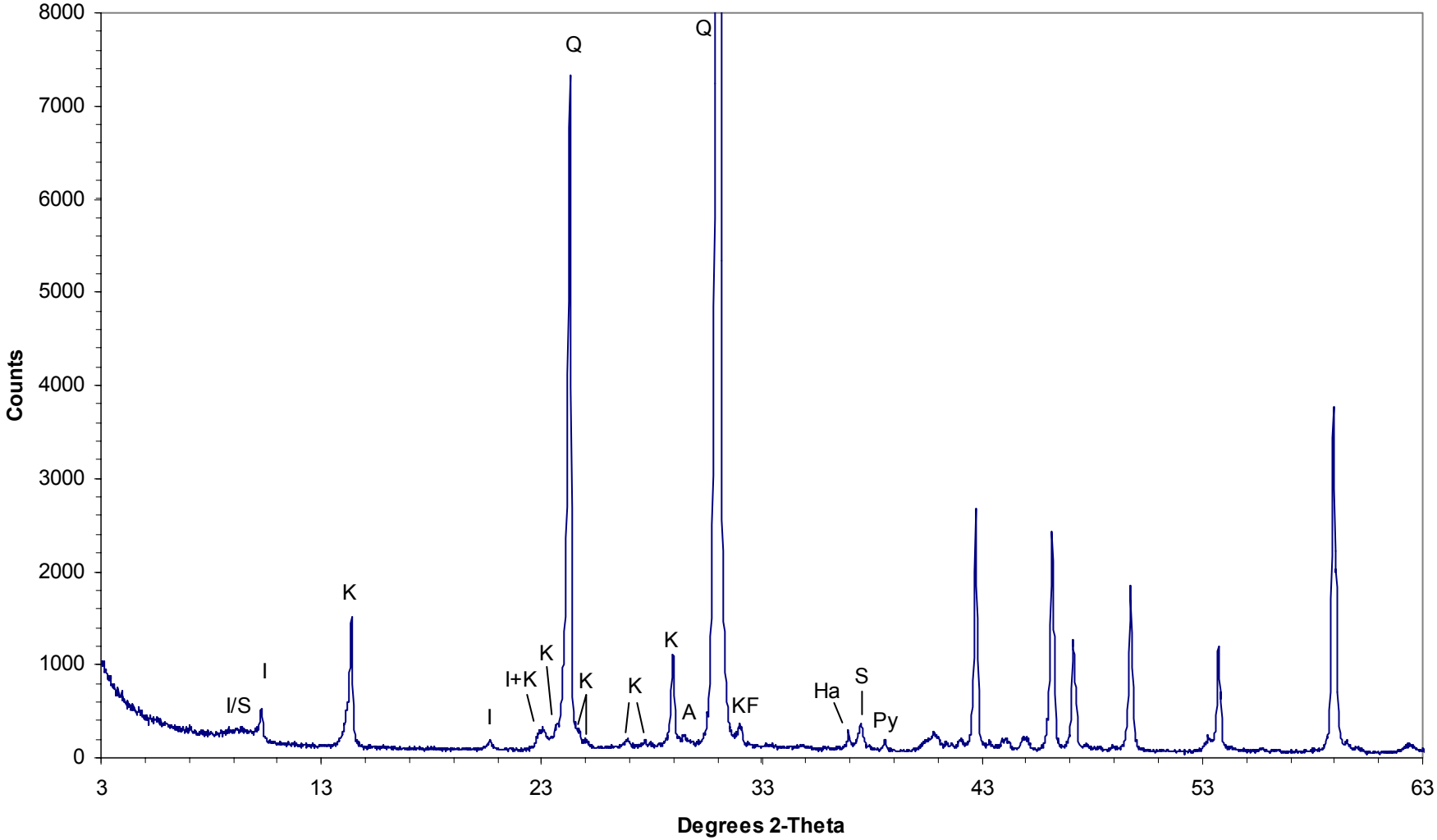

#20 2221.81m
Fine fraction

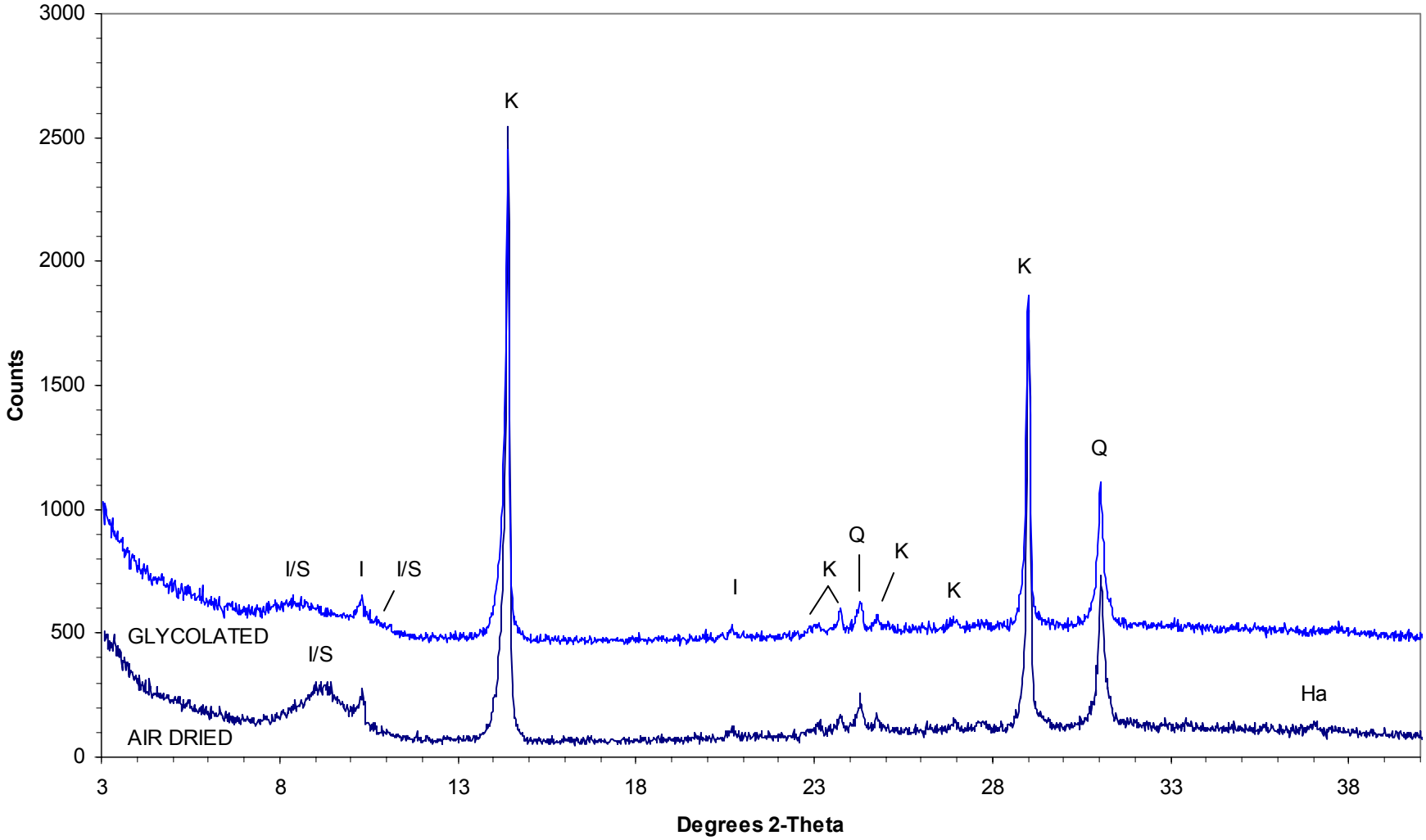

#48 2230.27m
Bulk rock

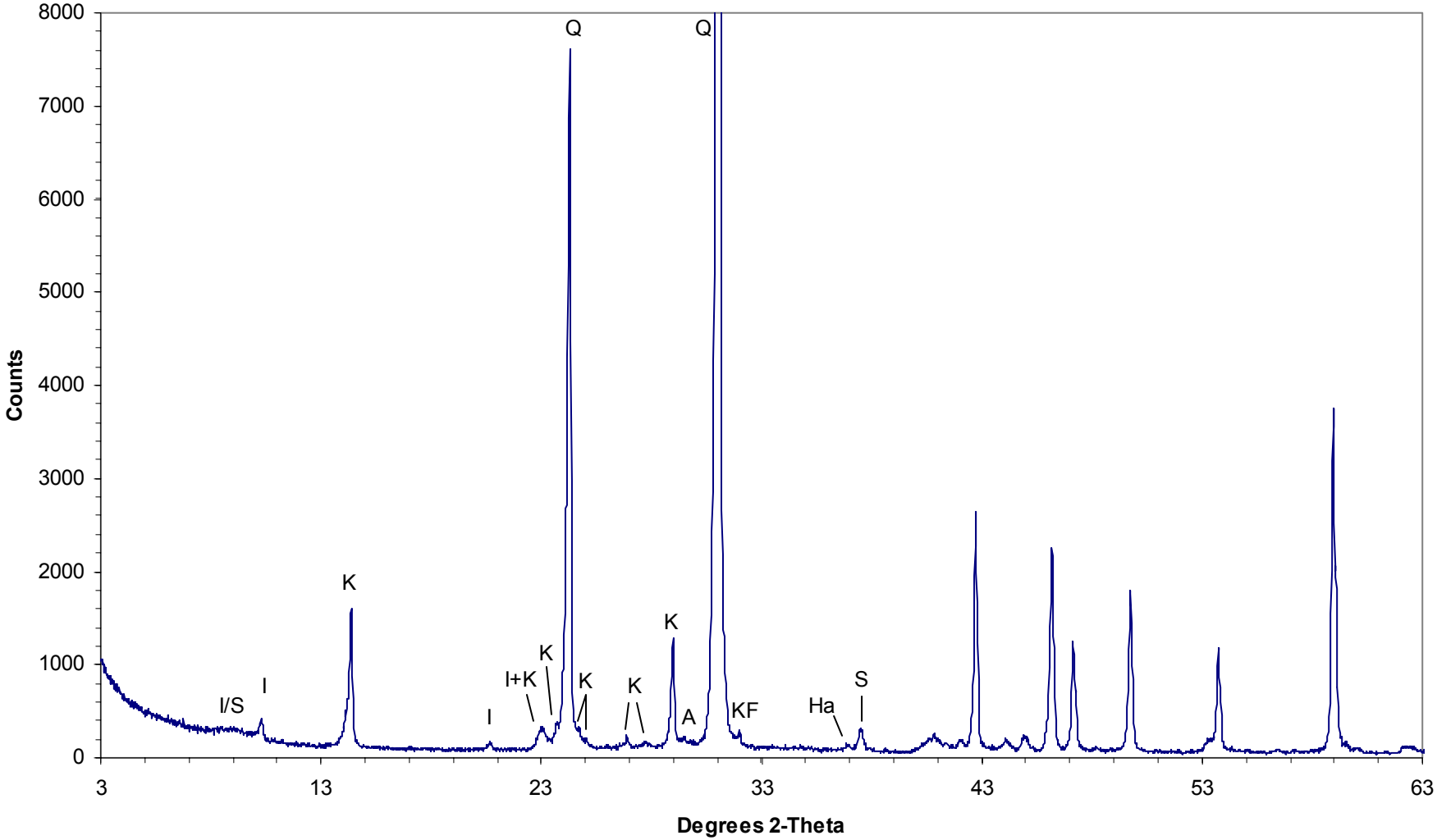

#48 2230.27m
Fine fraction

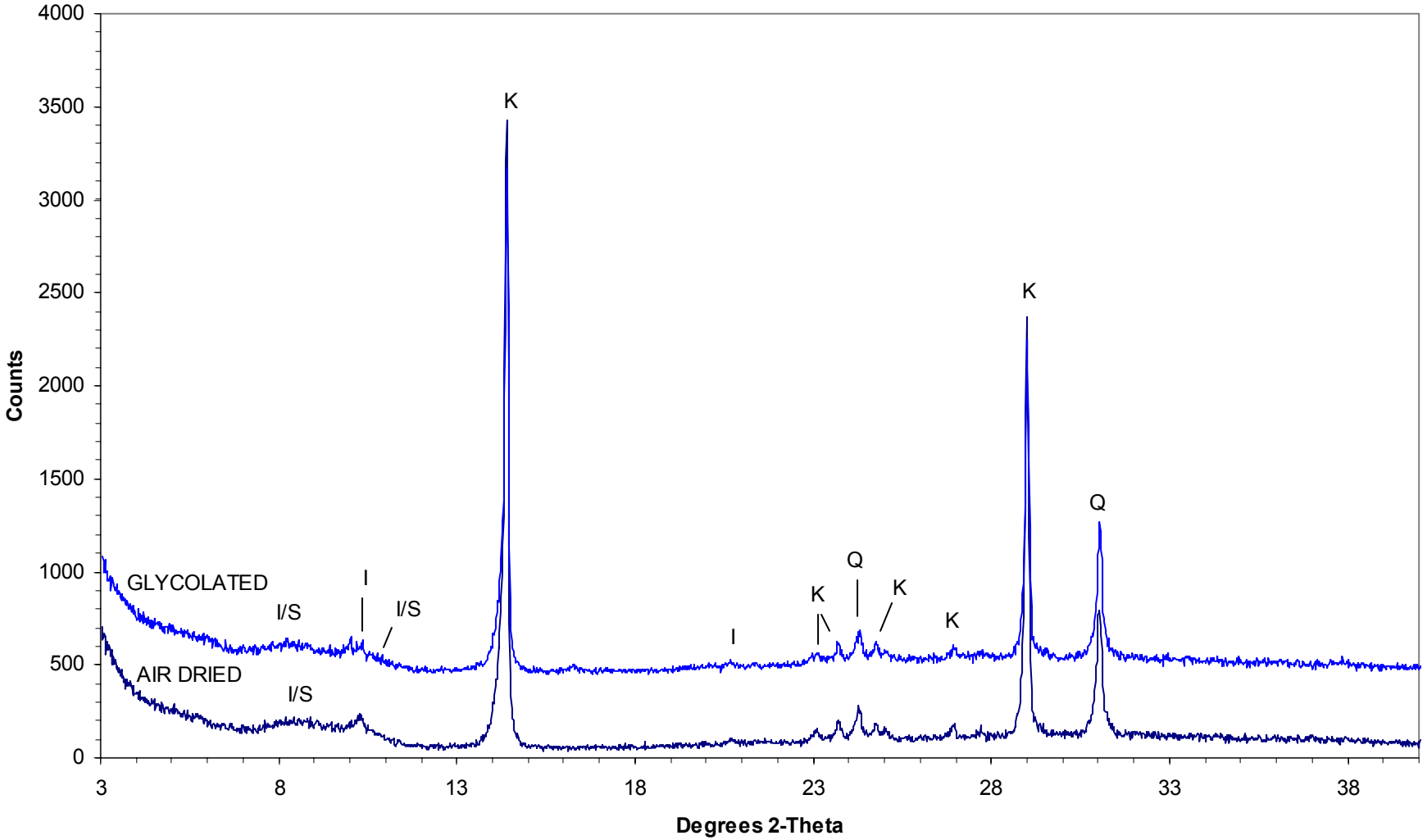

#57 2232.98m
Bulk rock

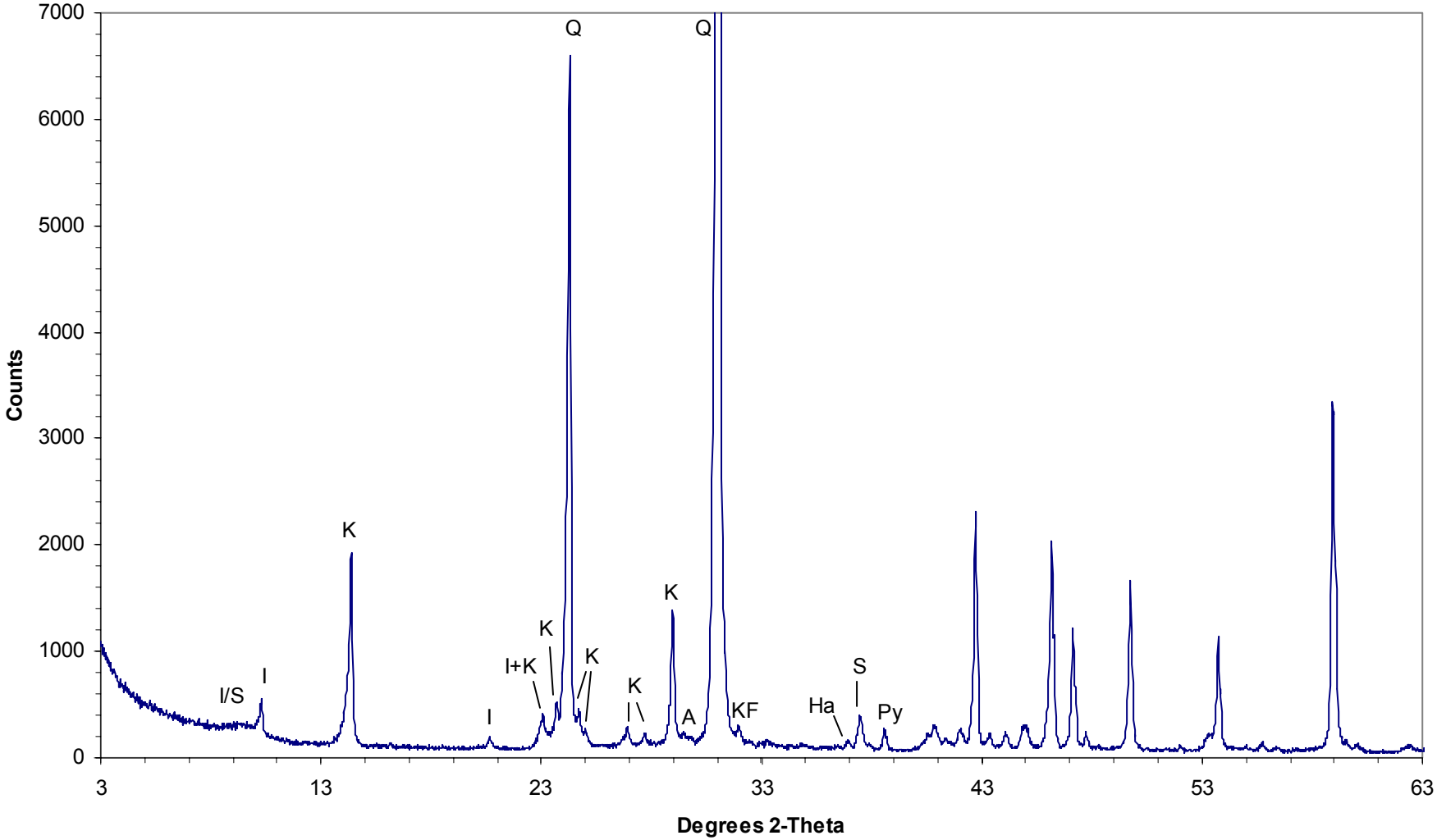

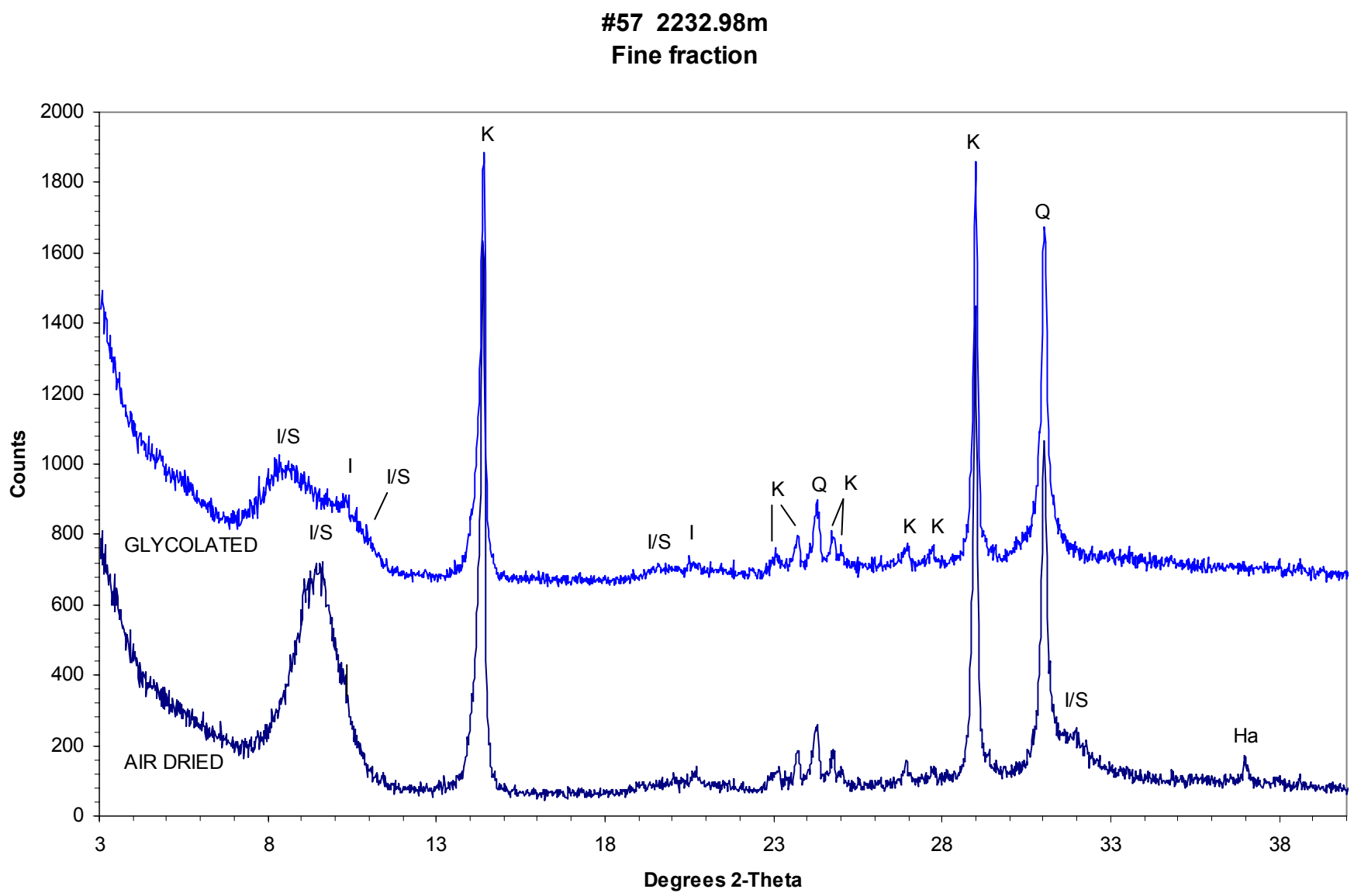
#57 2232.98m
Fine fraction
Counts
Degrees 2-Theta
GLYCOLATED
AIR DRIED
I/S
I
K
Q
Ha
2000
1800
1600
1400
1200
1000
800
600
400
200
0
3
8
13
18
23
28
33
38

APPENDIX 2.

PHOTOMICROGRAPHS

Key to plates

Sample #	Depth (m)	Plate #
3	2216.70	1, 2*
12	2219.36	3, 4*
20	2221.81	5, 6*, 7*
48	2230.27	8, 9*, 10*
57	2232.98	11, 12*

* SEM micrograph

PLATE 1: #3 2216.70m

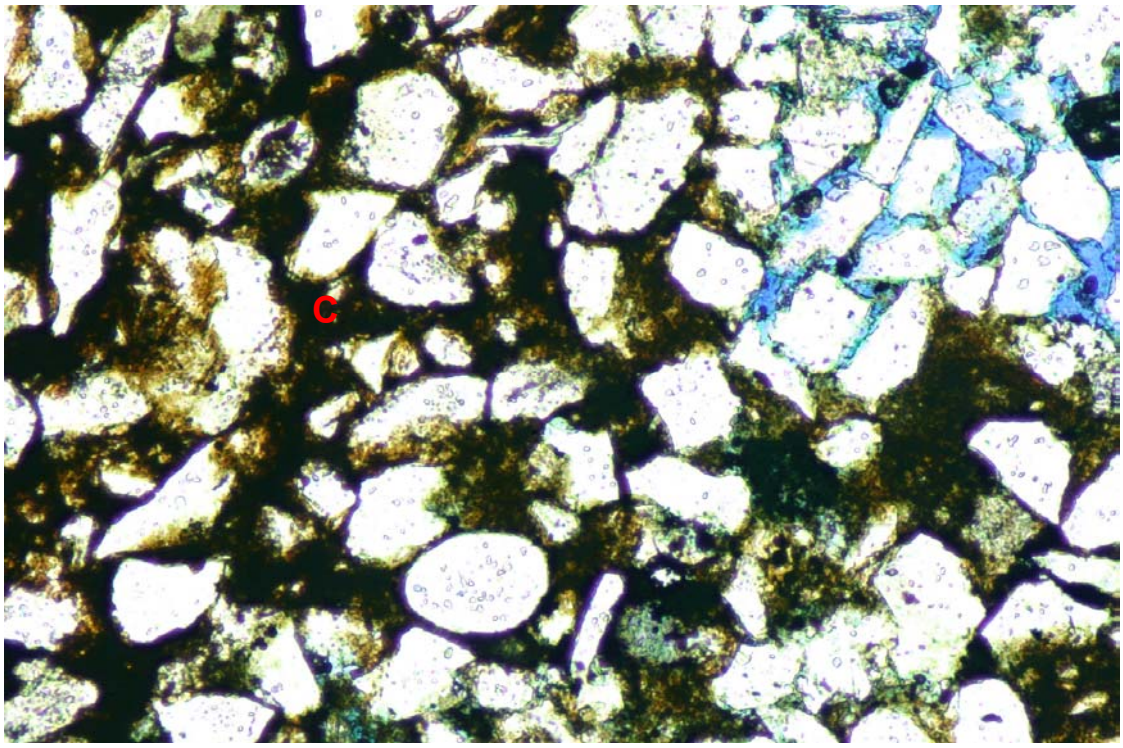

FIGURE 1 Plane polarised light
FIGURE 2 Crossed polarisers

0.2mm

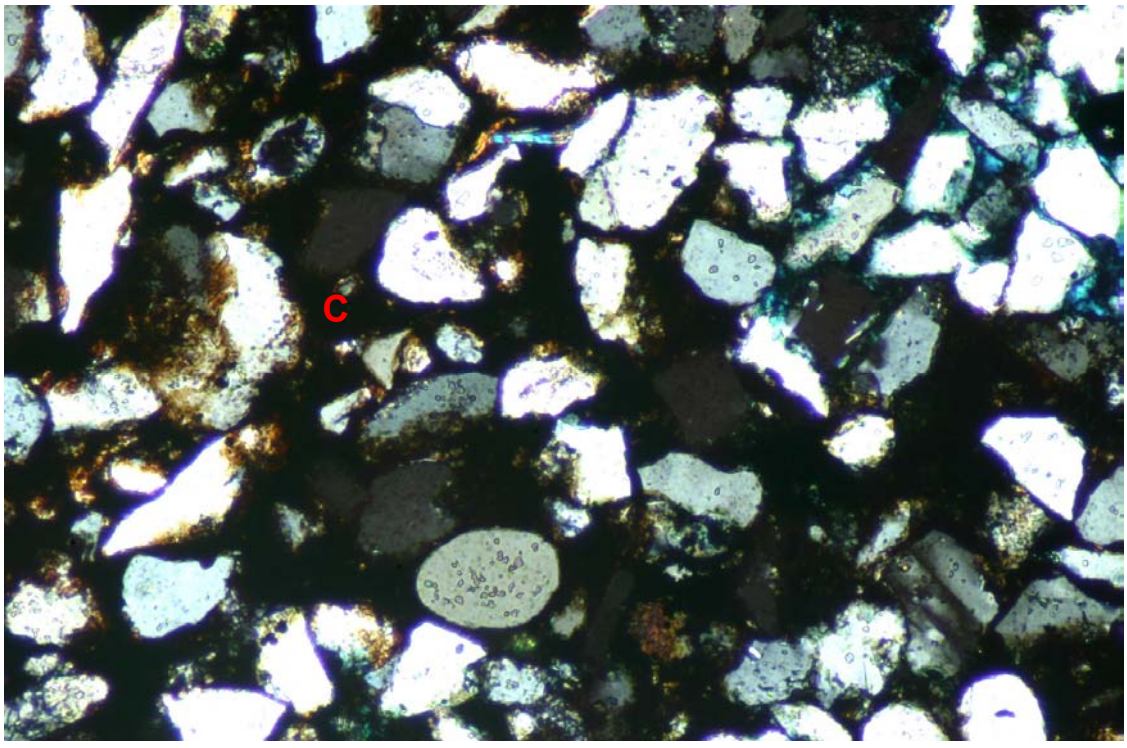

Throughout most of this argillaceous, very fine grained quartzarenite, intergranular spaces are filled by irregularly-distributed (due to bioturbation), pyritic detrital clay matrix (C). Intergranular porosity (blue) is confined to clean sandy burrow fills (upper right), where it is not conducive to permeability on a thin-section scale. K = 0.58mD (Thin-section micrographs)

PLATE 2: #3 2216.70m (cont.)

FIGURE 1

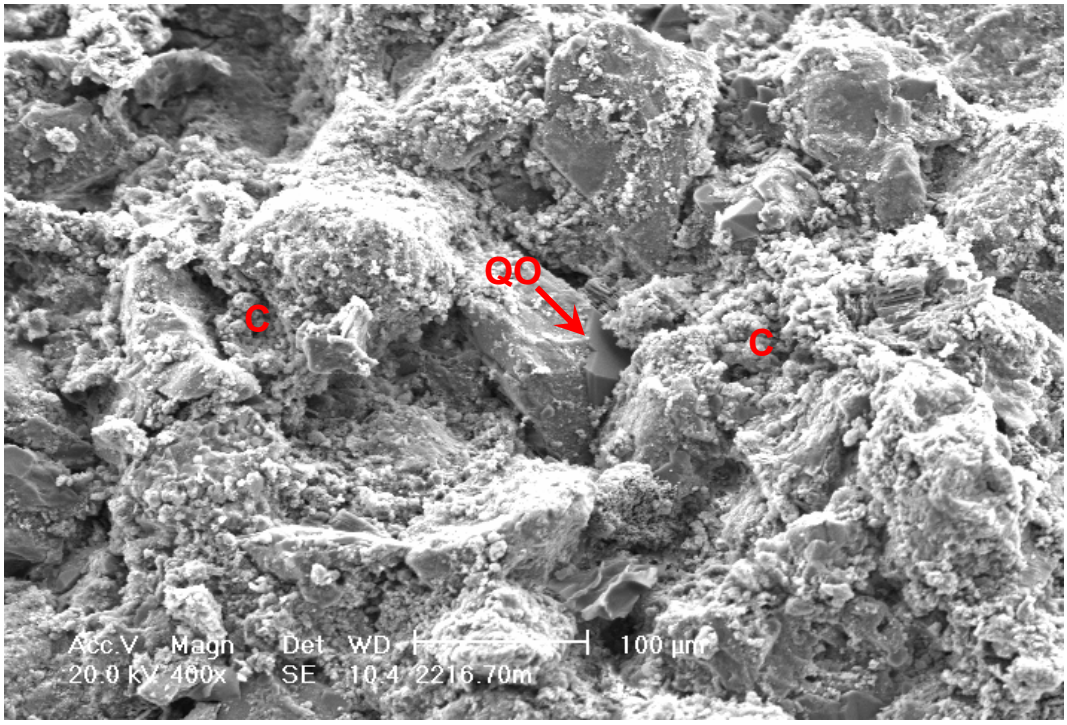

Low permeability (0.58mD) reflects extensive pore filling by detrital clay matrix (C). Small quartz overgrowths (QO) occur where intergranular spaces are incompletely filled by clay. The sandstone is almost entirely microporous. (SEM micrograph)

FIGURE 2

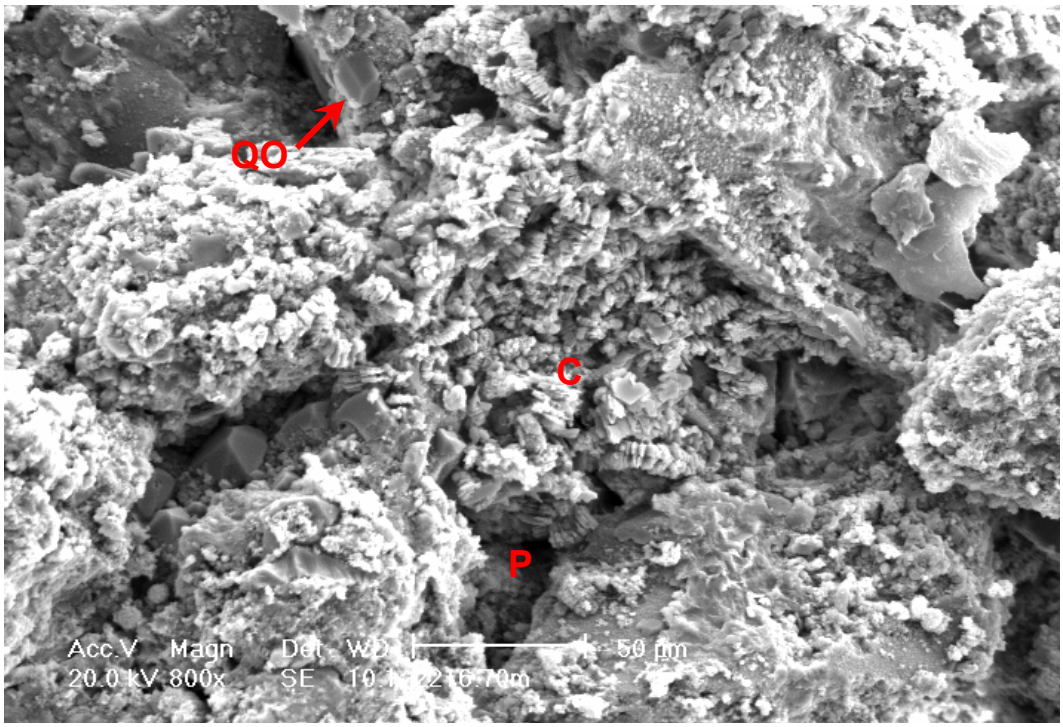

Intergranular spaces are clogged by kaolinitic clay matrix (C) and small quartz overgrowths (QO). Macropores (P) have an erratic distribution throughout the sandstone and therefore are poorly interconnected. (SEM micrograph)

PLATE 3: #12 2219.36m

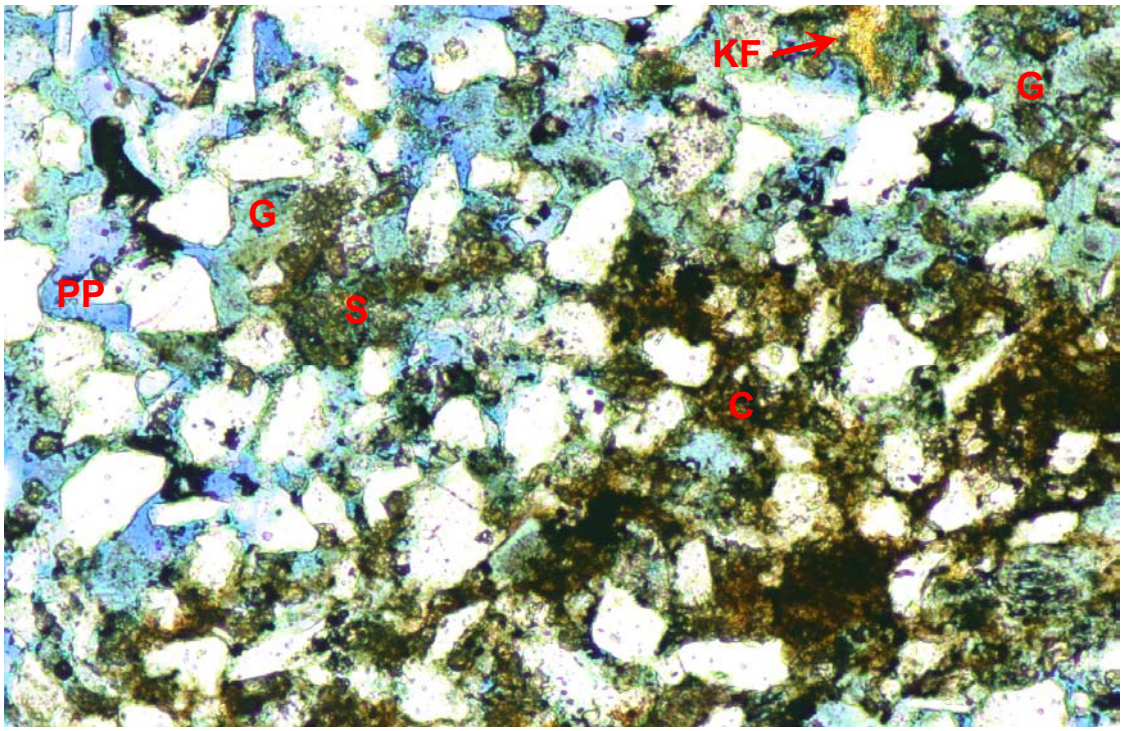

FIGURE 1 Plane polarised light
FIGURE 2 Crossed polarisers

0.2mm

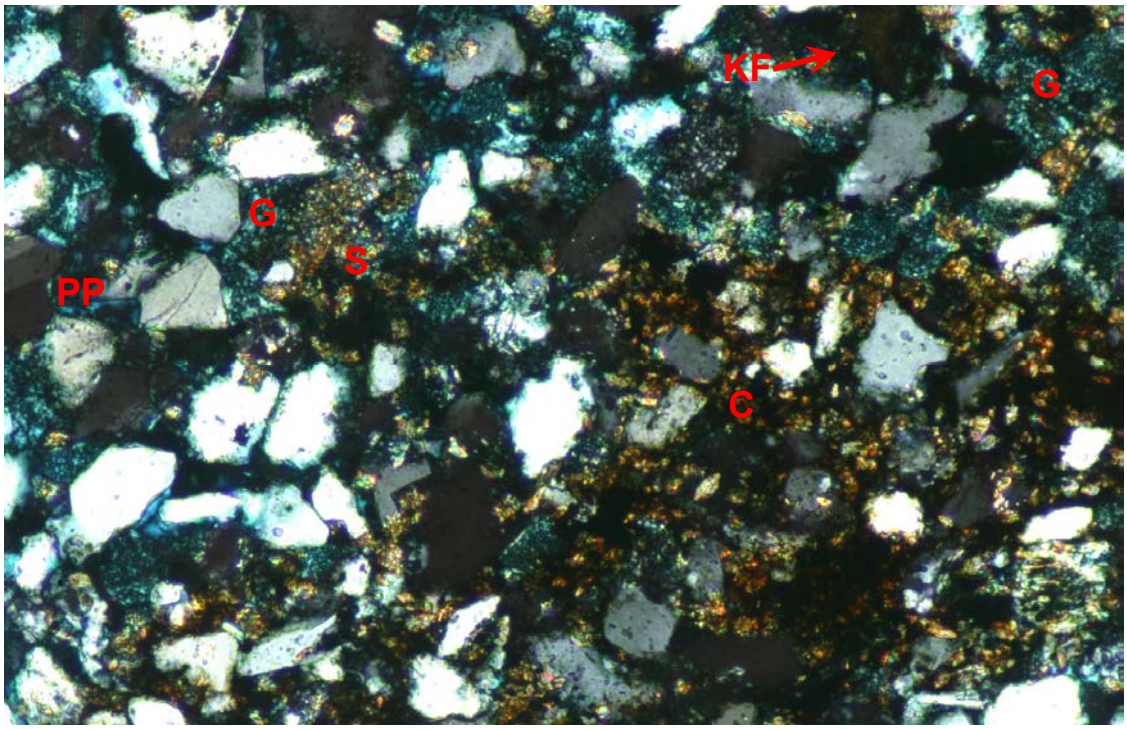

Porosity is reduced in this bioturbated, very fine grained quartzarenite by the presence of irregularly-distributed detrital clay matrix (C) and associated siderite (S). Abundant primary intergranular porosity (PP) is preserved in cleaner areas, despite porosity reduction by the compactional deformation of common glauconite peloids (G). Framework grains include very minor K-feldspar (KF) (stained brown). K = 10.6mD (Thin-section micrographs)

PLATE 4: #12 2219.36m (cont.)

FIGURE 1

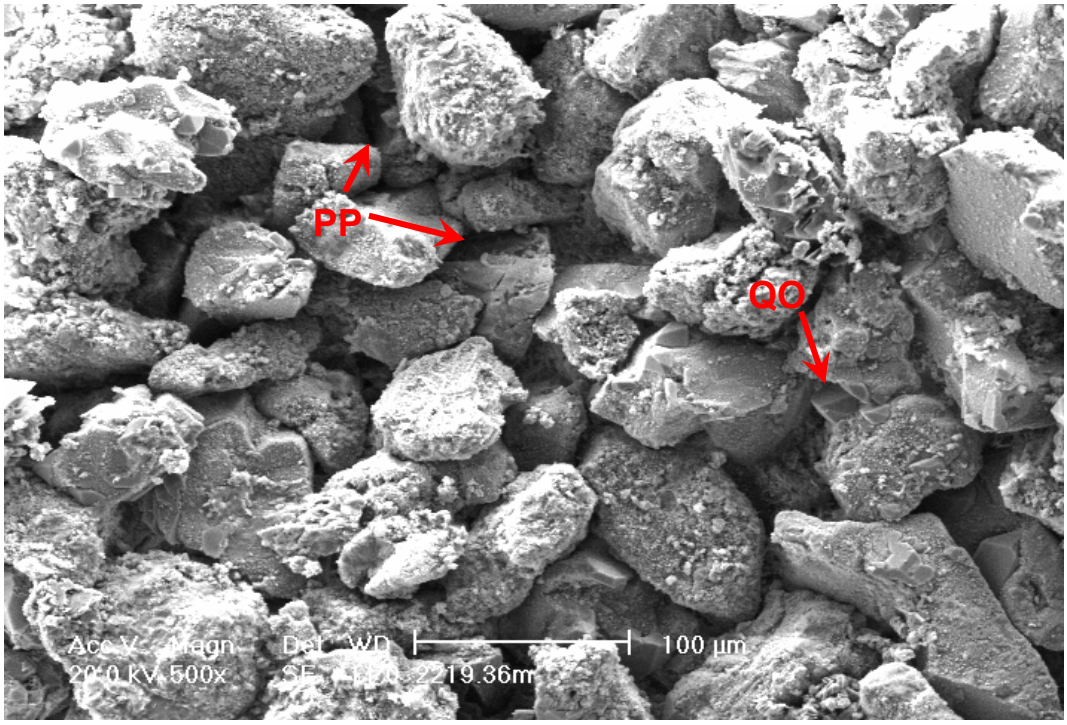

Where detrital clay matrix is absent, abundant primary intergranular porosity (PP) is preserved between loosely packed and uncemented framework grains. Quartz overgrowths (QO) do nothing to reduce permeability and lithify the sandstone. (SEM micrograph)

FIGURE 2

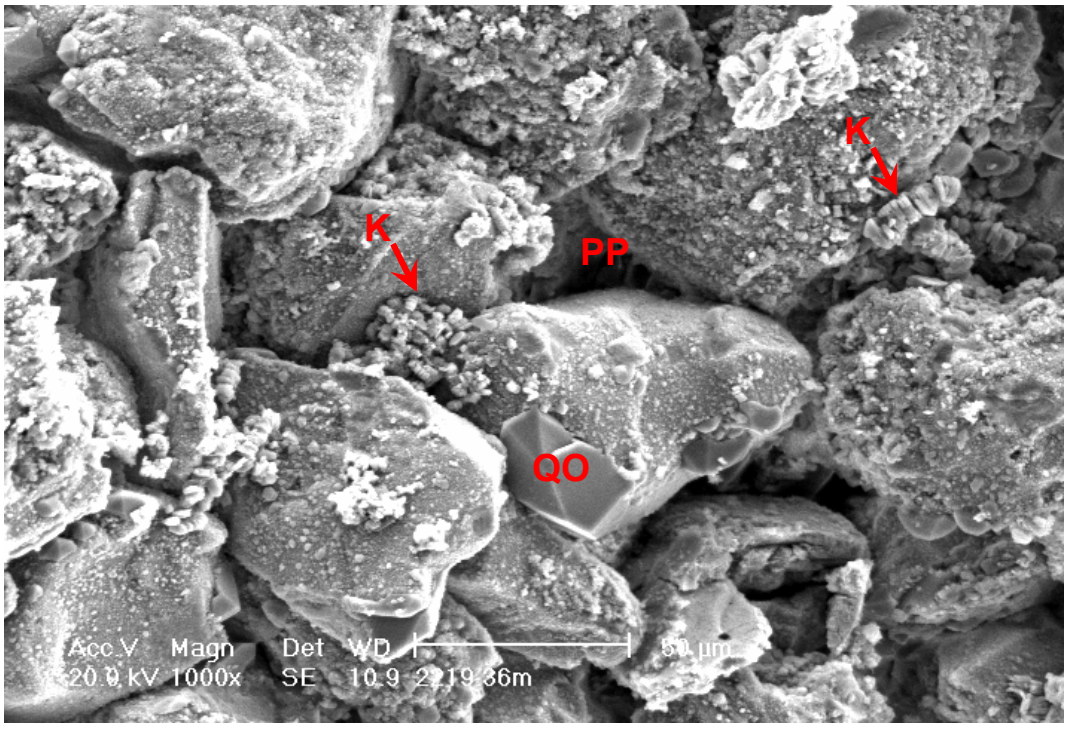

Clay includes authigenic kaolinite (K) that forms isolated patches where micaceous grains have altered. Small, thinly-developed quartz overgrowths (QO) locally occupy primary intergranular pores (PP). (SEM micrograph)

PLATE 5: #20 2221.81m

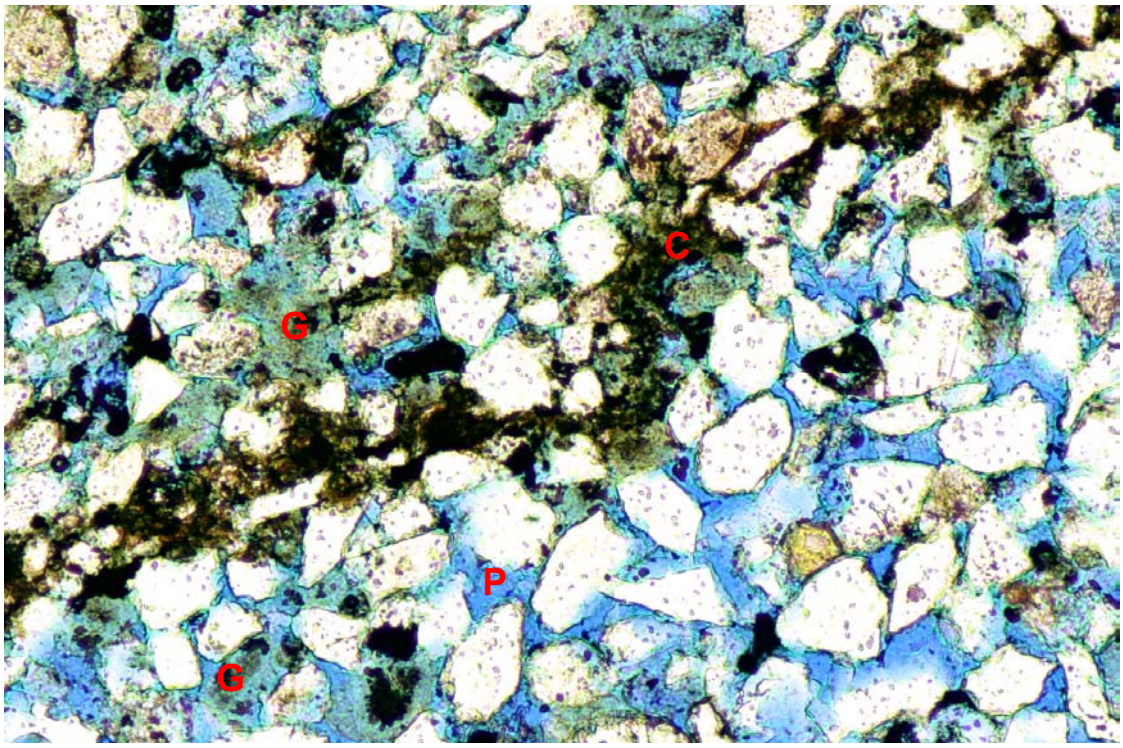

FIGURE 1 Plane polarised light
FIGURE 2 Crossed polarisers

0.2mm

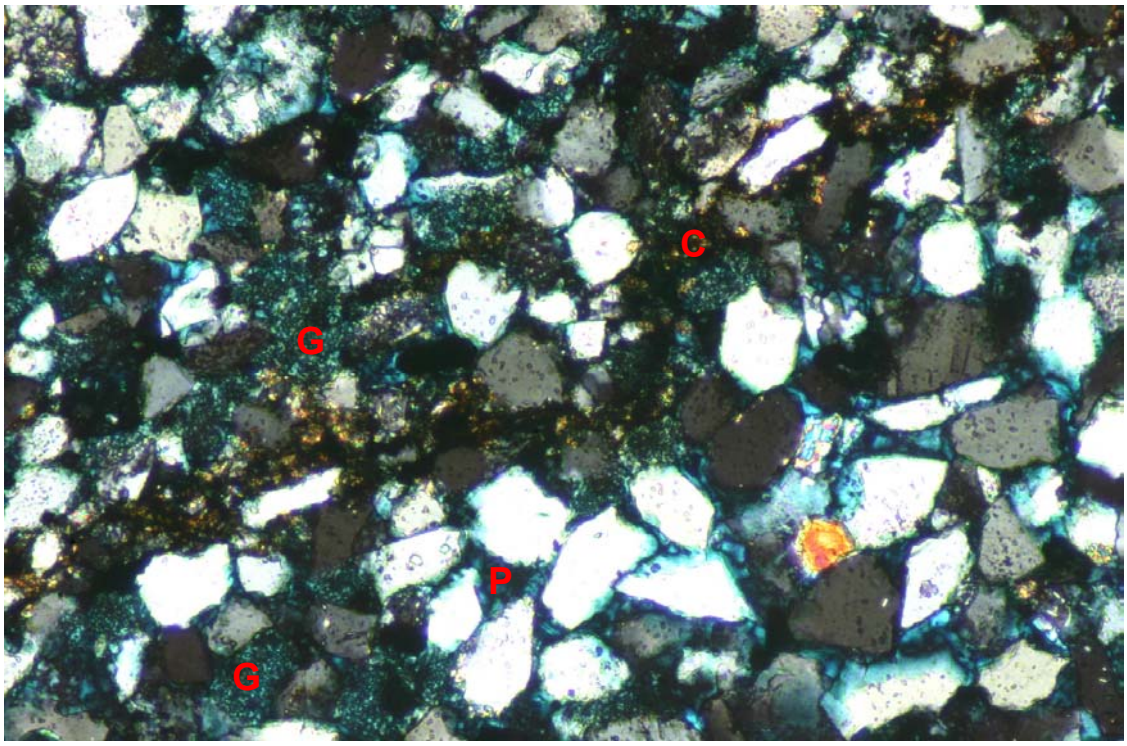

Sideritic detrital clay (C) is concentrated along thin laminae and, outside field of view, into irregular patches, the distribution of which has been influenced by bioturbation. Most of the sandstone is clean and highly macroporous (P). Framework grains include slightly compacted glauconite (G). K = 268mD (Thin-section micrographs)

PLATE 6: #20 2221.81m (cont.)

FIGURE 1

Throughout most of the sandstone, abundant primary intergranular porosity (PP) is preserved between poorly compacted and uncemented framework grains. Detail of marked pore is shown in Plate 7, Figure 2. (SEM micrograph)

FIGURE 2

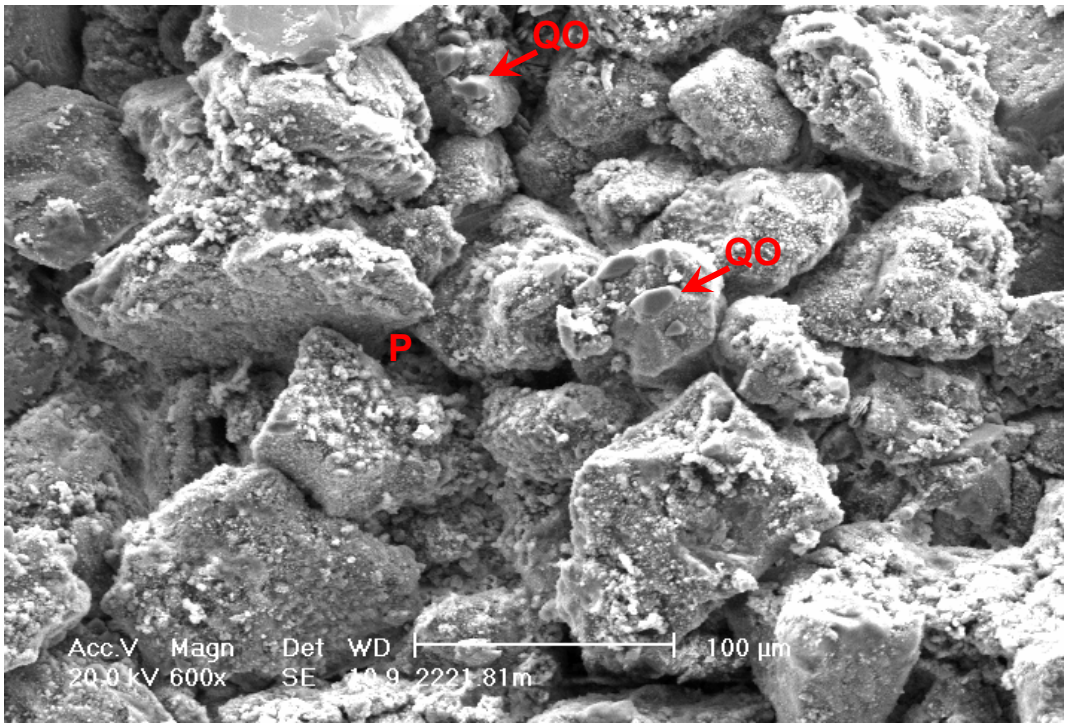

Quartz overgrowths (QO) do little to reduce intergranular porosity (P) between loosely packed framework grains. (SEM micrograph)

PLATE 7: #20 2221.81m (cont.)

FIGURE 1

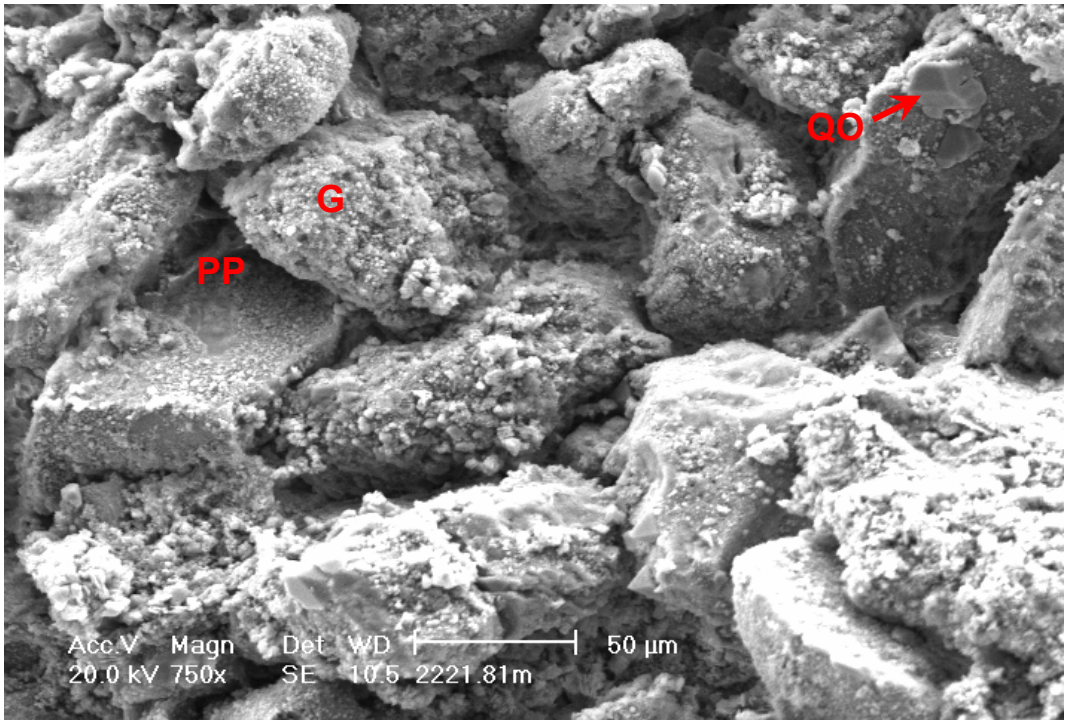

With framework grains being poorly compacted and uncemented, the sandstone contains abundant, evenly distributed, hence well-interconnected primary intergranular porosity (PP). Framework grains are mainly quartz and glauconite (G). Pores are locally occupied by incipient quartz overgrowths (QO). (SEM micrograph)

FIGURE 2

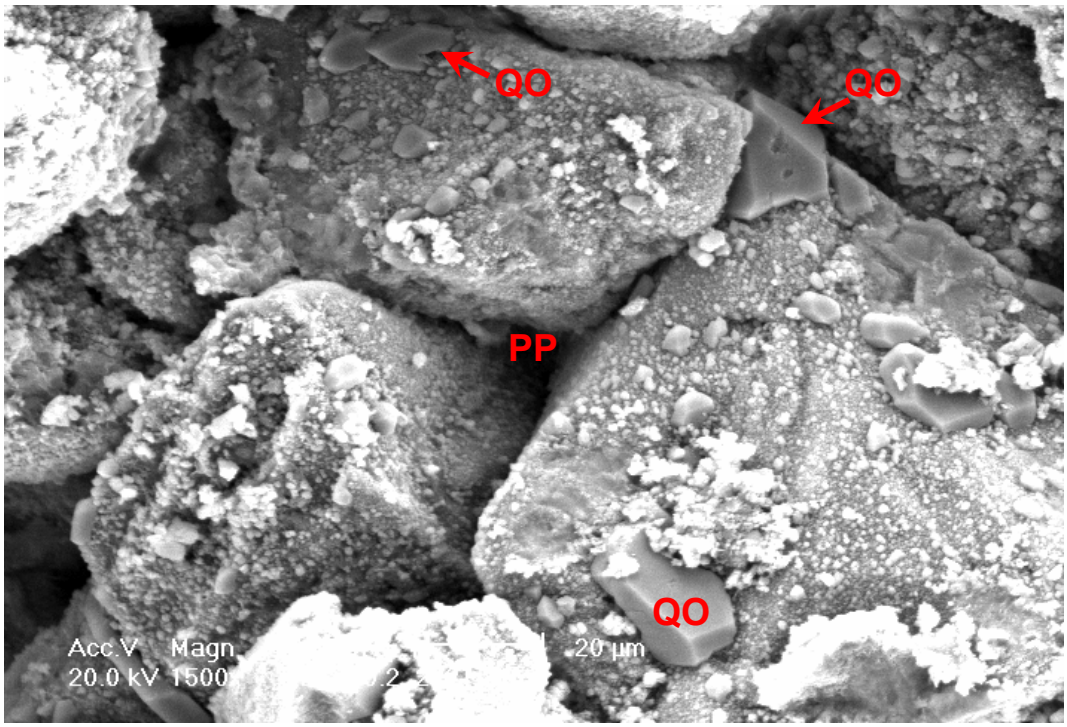

Detail of pore marked in Plate 6, Figure 1. Most macroporosity in the sandstone is accounted for by primary intergranular porosity (PP), the volume of which has been little changed by the precipitation of incipient quartz overgrowths (QO) on pore-bounding grains. (SEM micrograph)

PLATE 8: #48 2230.27m

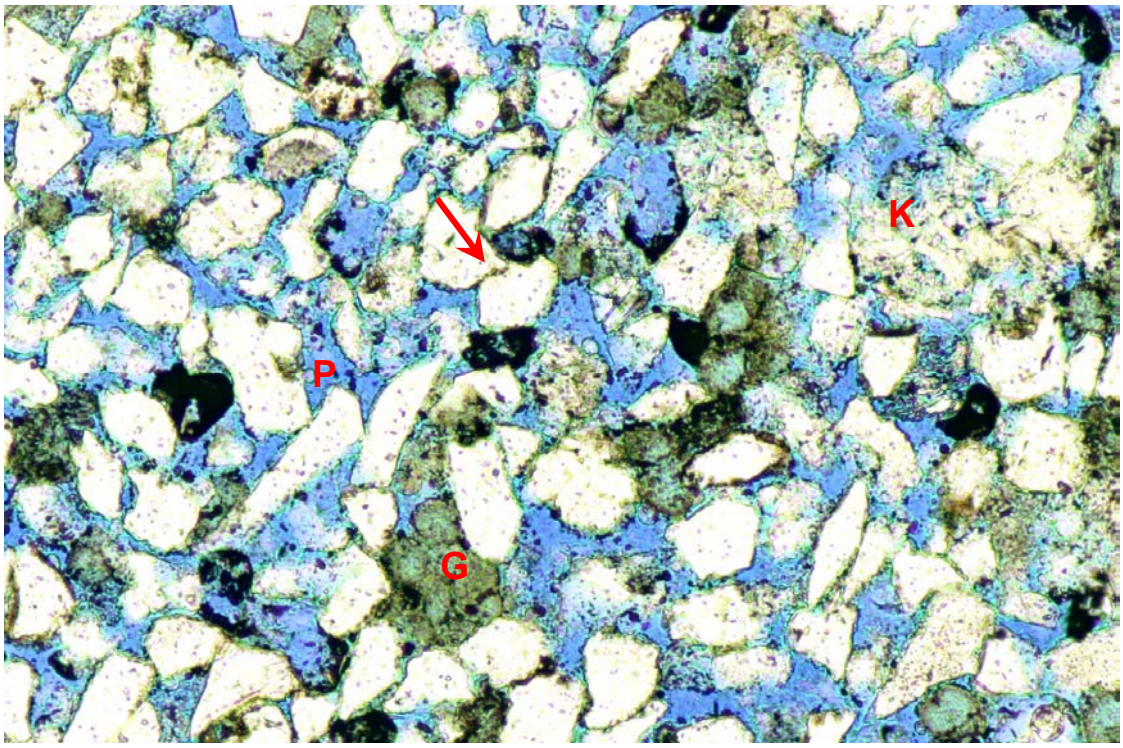

FIGURE 1 Plane polarised light
FIGURE 2 Crossed polarisers

0.2mm

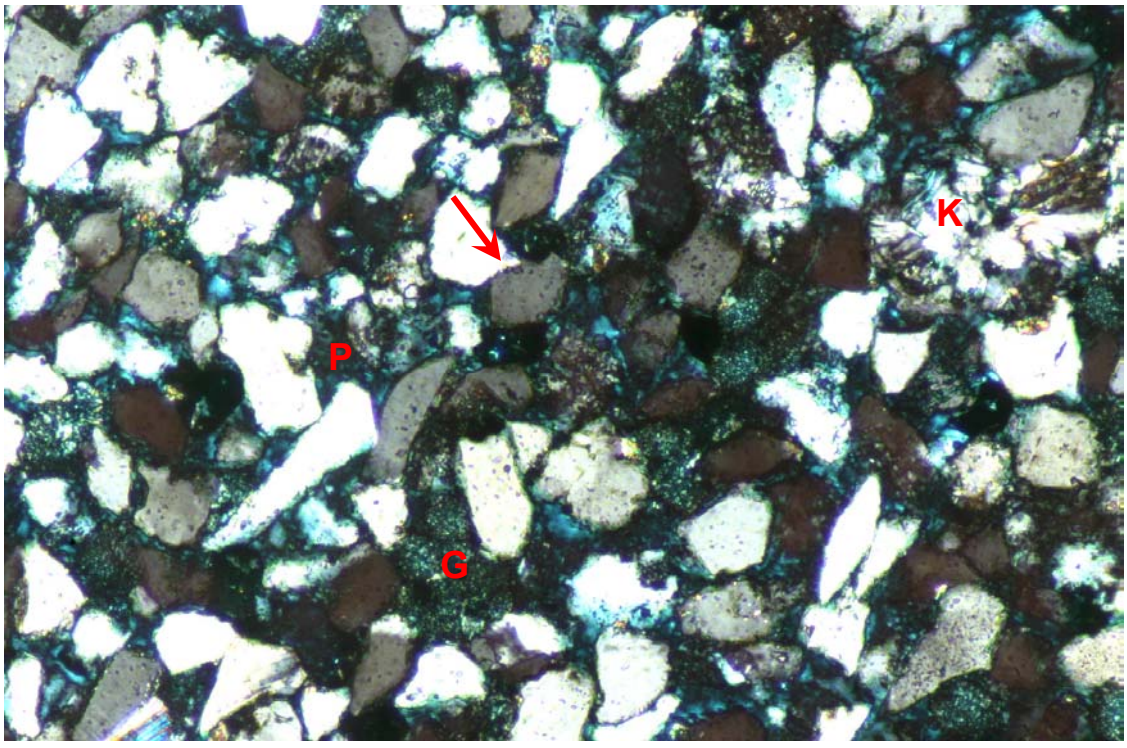

This clean, very fine grained quartzarenite contains abundant intergranular porosity (P), despite porosity reduction by glauconite (G) compaction, grain contact dissolution (arrow) and mica decomposition to kaolinite (K). Unlike the other samples, the sandstone contains little detrital clay matrix and is thus the most permeable of the sample suite. K = 387mD (Thin-section micrographs)

PLATE 9: #48 2230.27m (cont.)

FIGURE 1

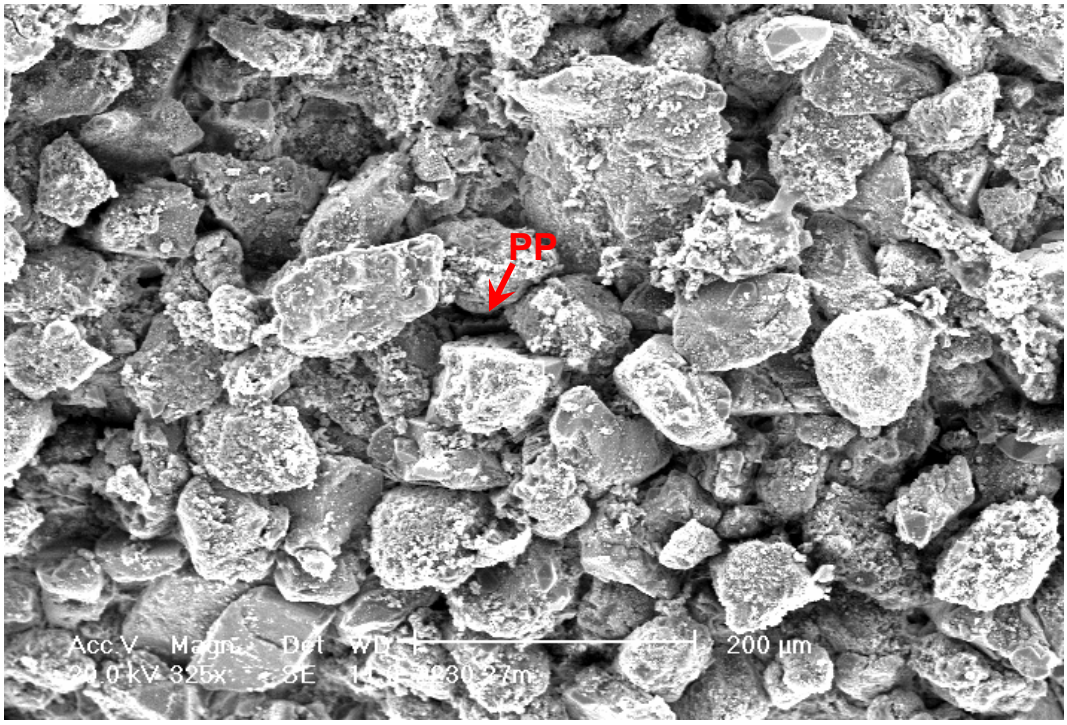

Representative area in which abundant primary intergranular porosity (PP) is preserved between loosely packed and uncemented framework grains. (SEM micrograph)

FIGURE 2

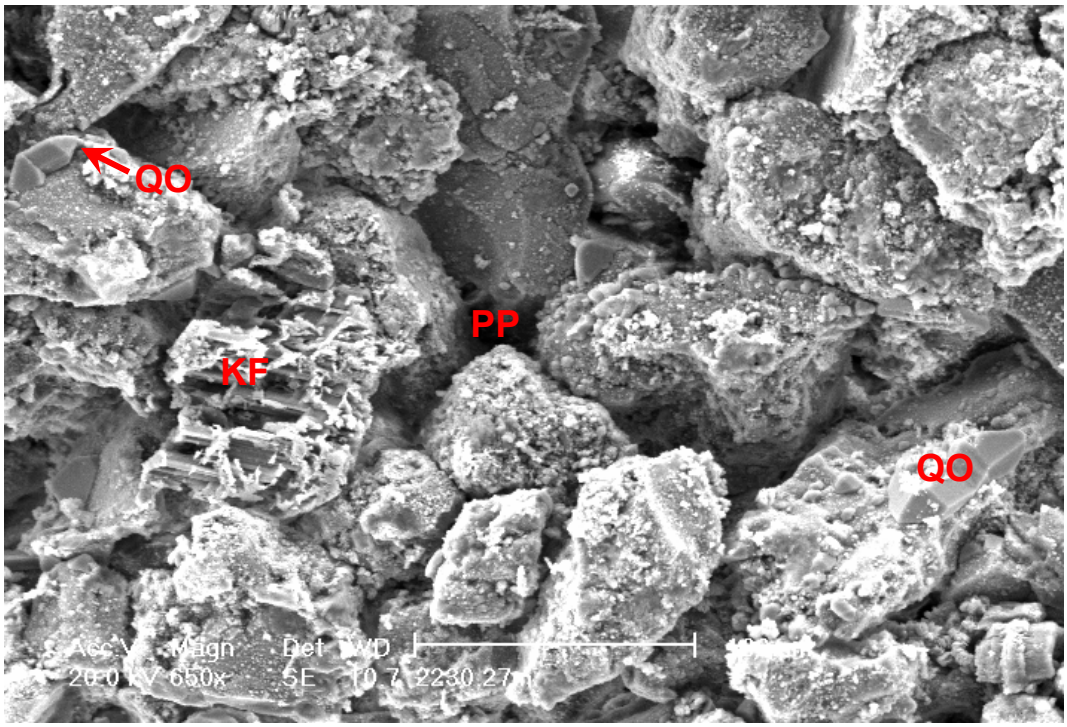

High permeability (387mD) reflects the existence of a system of clean, evenly distributed primary intergranular pores (PP) throughout the sandstone. Framework grains include partly dissolved K-feldspar (KF). Quartz overgrowths (QO) are localised and thinly developed and thus do nothing to reduce permeability and lithify the sandstone. (SEM micrograph)

PLATE 10: #48 2230.27m (cont.)

FIGURE 1

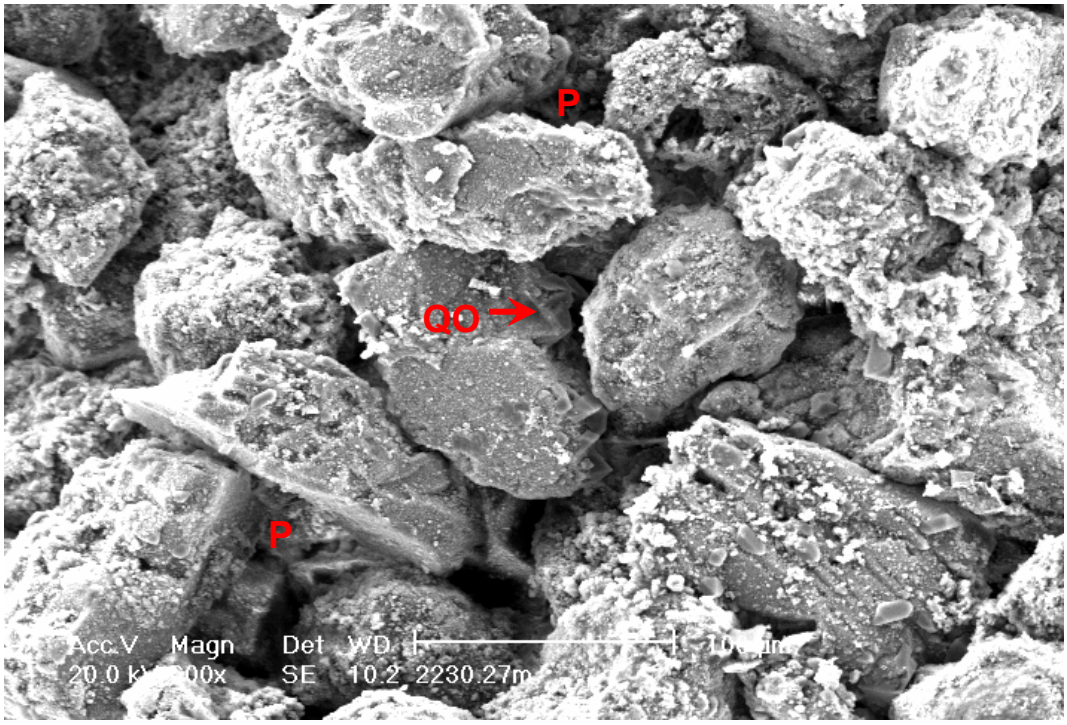

Intergranular pores (P) are evenly distributed and generally free of clay and are consequently conducive to high (387mD) permeability. Compaction and quartz overgrowth (QO) precipitation have done little to reduce intergranular porosity in field of view. (SEM micrograph)

FIGURE 2

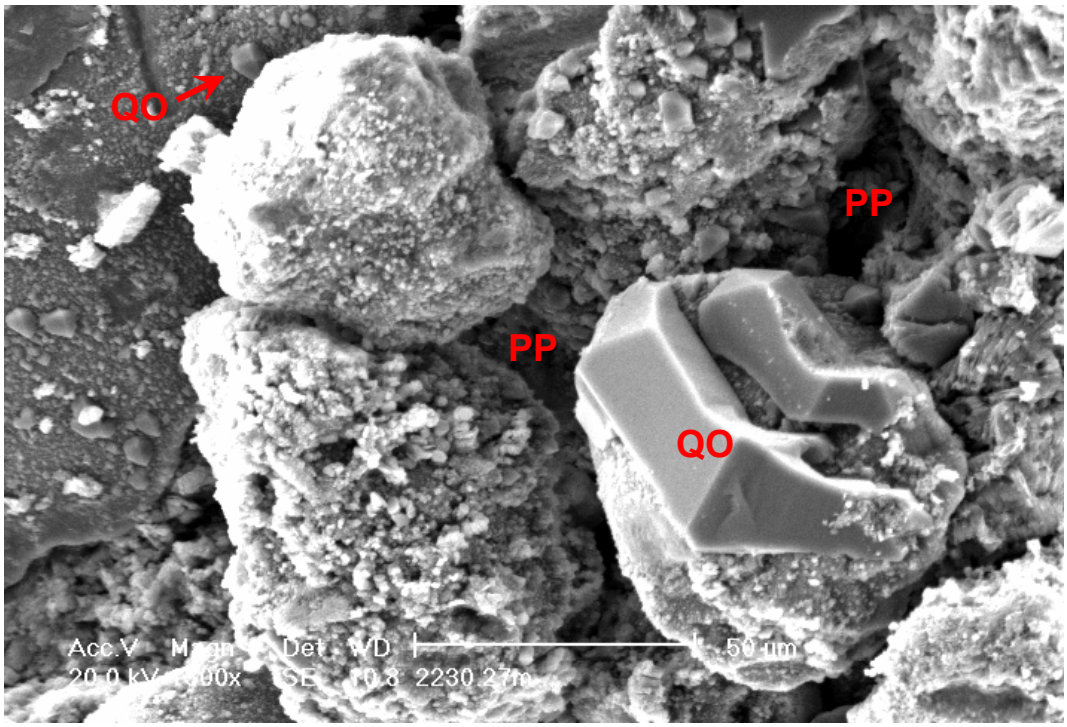

Detail of typical primary intergranular porosity (PP) that is preserved between poorly compacted framework grains. Quartz overgrowths (QO) are volumetrically insignificant and thus do not impact reservoir quality. (SEM micrograph)

PLATE 11: #57 2232.98m

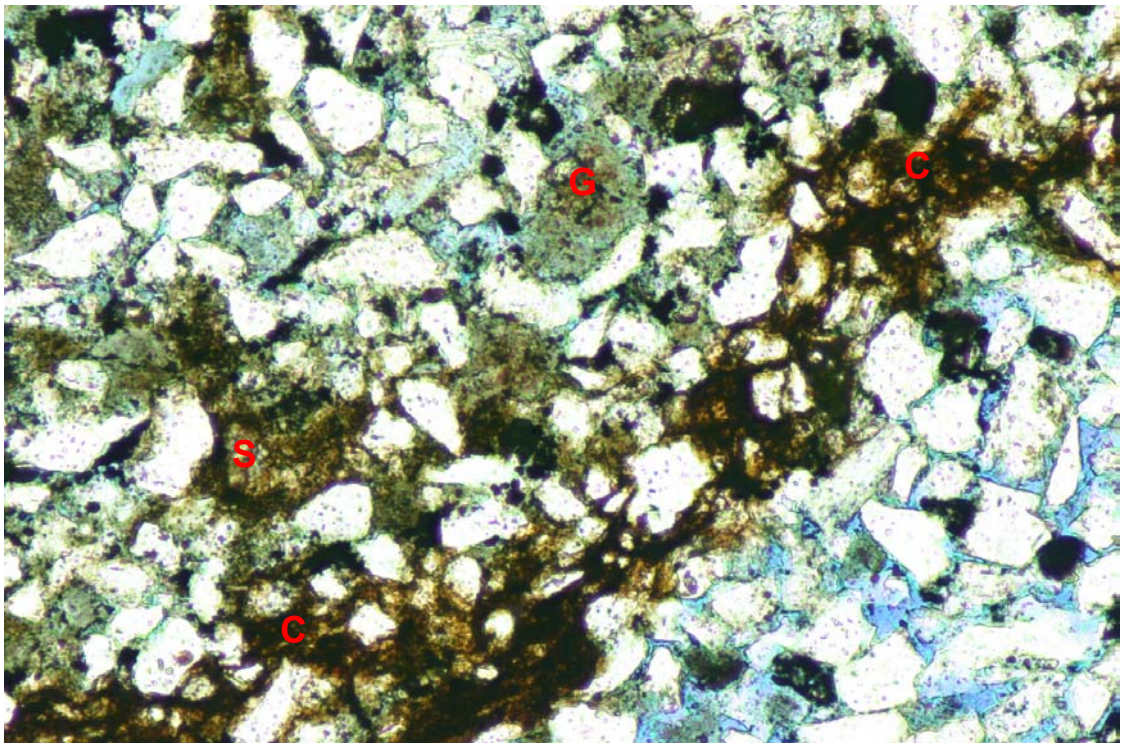

FIGURE 1 Plane polarised light
FIGURE 2 Crossed polarisers

0.2mm

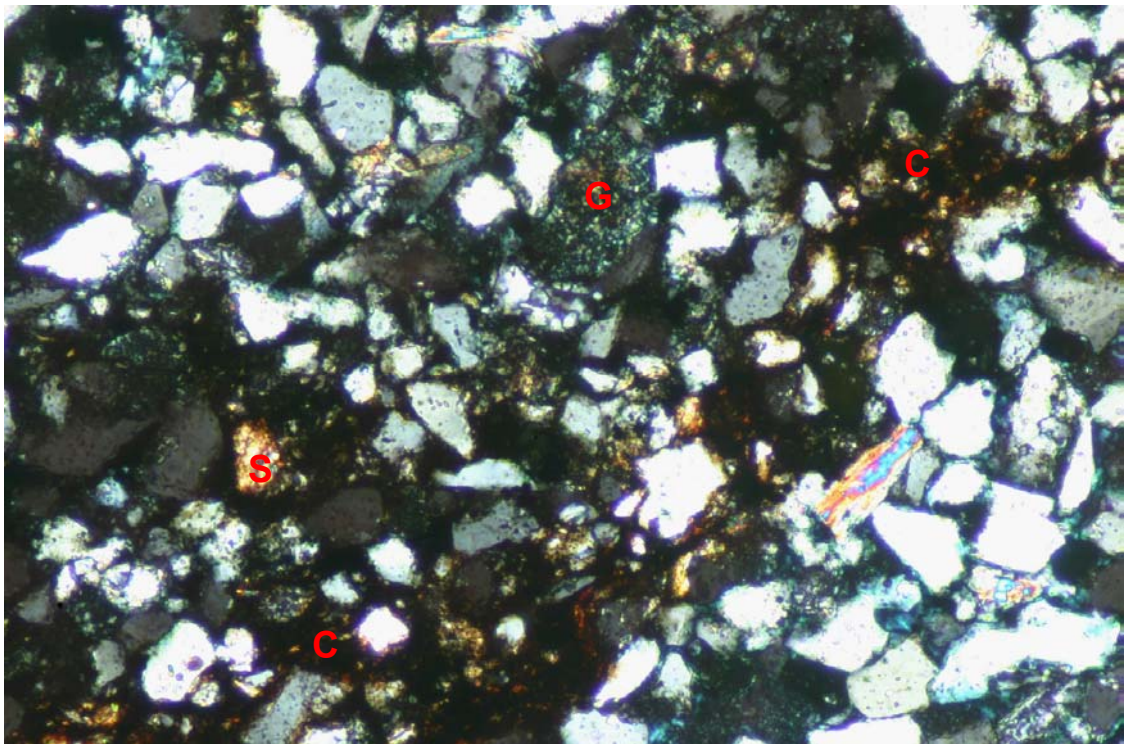

Argillaceous, very fine grained quartzarenite in which intergranular areas are filled by detrital clay matrix (C) and compacted glauconite (G), except within a clean sandy burrow fill (lower right), where abundant primary intergranular porosity (blue) is preserved between poorly compacted quartz grains. Siderite (S) is associated with detrital clay. Low permeability (12.1mD) reflects the presence of abundant, irregularly-distributed (due to bioturbation) detrital clay and compacted glauconite. (Thin-section micrographs)

PLATE 12: #57 2232.98m (cont.)

FIGURE 1

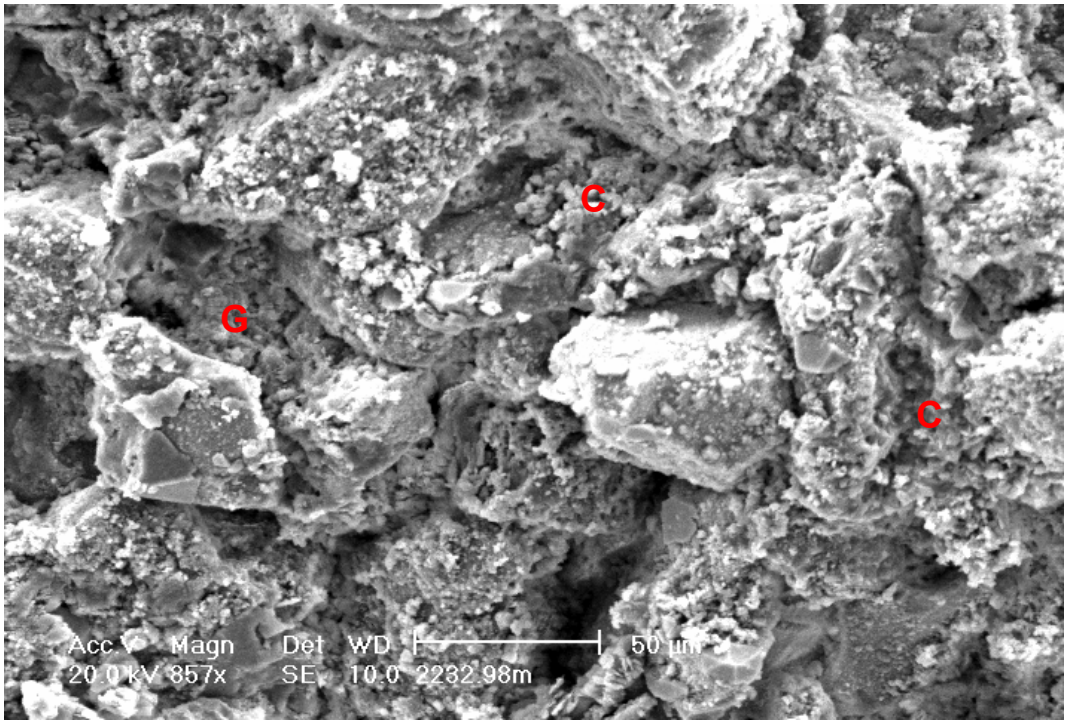

Throughout most of the sample, intergranular areas are clogged by detrital clay matrix (C) and compacted glauconite (G). (SEM micrograph)

FIGURE 2

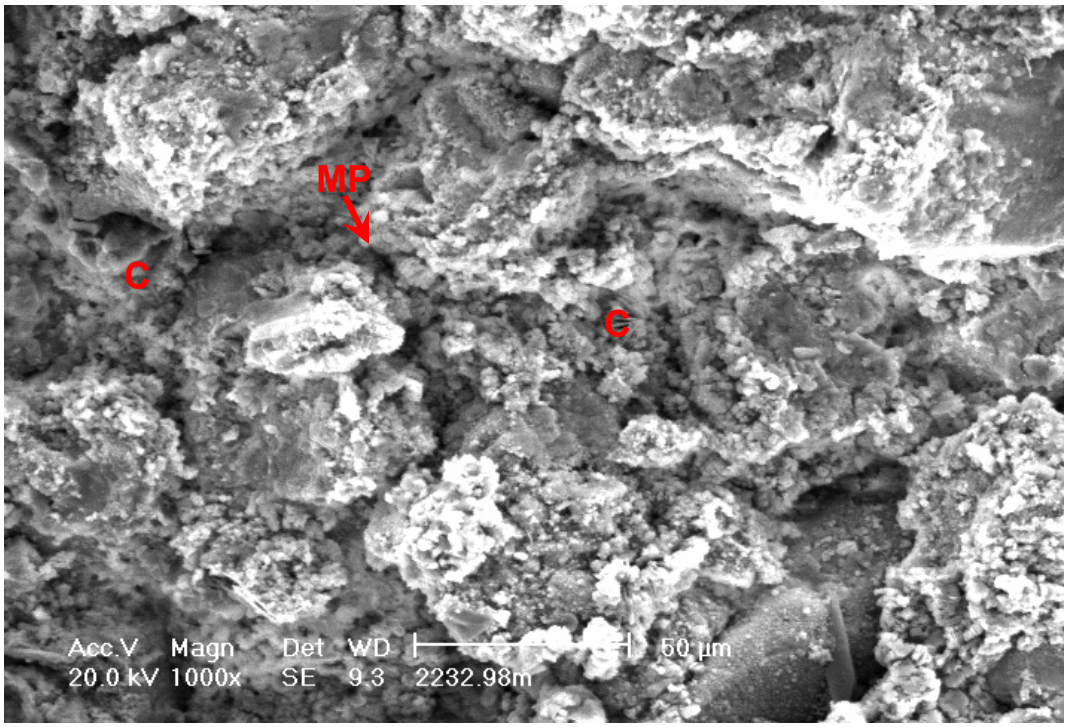

Intergranular porosity is lacking due to complete pore filling by kaolinitic detrital clay matrix (C). Most porosity in the sample is microporosity (MP) that is associated with clay matrix and glauconite. (SEM micrograph)

APPENDIX 5: CORE INTERPRETATION

Yolla 3

Core Description Report

T/L1
BASS BASIN

January 2005

by Brett Pidgeon

EXECUTIVE SUMMARY

A sedimentological study of Core 1 from the upper Eastern View Coal Measures in Yolla 3 indicates that this interval was deposited in a marine / marginal marine setting. Interpreted depositional environments include distal lower shoreface, sandy embayment / tidal flat, wave influenced proximal delta and offshore marine / wave influenced prodelta transition. The degree and diversity of bioturbation in the distal lower shoreface indicate that fully marine conditions prevailed, whereas in the other environments, stresses such as fluctuating salinity, low oxygen levels and turbidity resulted in more restricted ichnofacies assemblages.

High resolution sequence stratigraphy and ichnofacies analysis has been used to subdivide the cored interval into high-order systems tracts and, a longer period, lower-order sequence. Key surfaces; sequence boundaries (SB) and transgressive surfaces of erosion (TSE); are marked by a characteristic ichnofacies assemblage of robust, sharp walled, passively filled, vertical to sub-vertical domichnia (dwelling burrow), that is excavated into semi-consolidated (firmground) substrates (*Glossifungites* ichnofacies). This surface demarcates discontinuity surfaces that reflect pauses in sedimentation, generally accompanied by erosion.

The succession is dominated by intervals in which the rate of base level change was balanced with the sediment supply, producing aggradational, or nearly so, stacking. These intervals are separated by periods of rapid relative base level change causing juxtaposition of differing depositional settings. A sequence boundary (SB) separates the distal lower shoreface from the sandy embayment / tidal flat setting indicating a fall in relative base level. The distal lower shoreface represents a highstand systems tract and the overlying sandy embayment / tidal flat, comprises a lowstand / transgressive systems tract. TSEs separate the sandy embayment / tidal flat from the wave influenced proximal delta front and the delta front from the offshore / prodelta sediments, indicating rapid base level rise. The delta front and offshore / prodelta sediments comprise a transgressive systems tract.

Reservoir quality is strongly influenced by facies with the highest permeability occurring in the sandy embayment / tidal flat facies, and to a lesser extent, the wave influenced proximal delta. The degree of bioturbation does not have a strong control on the reservoir quality; original depositional environment is the overall control on the distribution of permeability.

TABLE OF CONTENTS

INTRODUCTION

Overview

One core, 18.1 m in length, was described in detail from Yolla 3. The core was cut in the upper Eastern View coal Measures (EVCM) (2216 – 2234.11 m) and recovery was 100%. All depths refer to drillers depth unless otherwise stated; note, there is approximately a 1.5 m depth shift between drillers depth and loggers depth. This is the most complete core data for this reservoir and allows detailed sedimentological and sequence stratigraphic interpretation of the depositional environments that can then be used to form facies models for the upper EVCM in the Yolla Field to assist in the reservoir modelling.

Objectives

The main objectives of the core description were the following:

1 Provide a detailed description of the cored intervals
2 Determine lithofacies and ichnofacies
3 Interpret depositional environment
4 Describe sedimentary sequences and key stratal surfaces present within the core
5 Describe the reservoir potential

Methodology

Cores were logged at 1:20 scale. Grainsize, colour, composition, physical sedimentary structures, macro palaeontology, ichnology (including Bioturbation index) were recorded. Bioturbation index (BI) records the intensity of bioturbation within a unit on a scale of 1 to 6. Where 1 indicates sparse bioturbation and disturbance of primary physical sedimentary structures and 6 indicates complete reworking of sediment and removal of all evidence of original sedimentary structures. Other ichnology characteristics including community succession resulting from environmental modification as the habitat becomes less suitable; and tiering in which bioturbation is vertically partitioned, resulting from vertical zoning of physical, chemical and biological parameters.

SEDIMENTOLOGY

The cored interval can be subdivided into four facies on the basis of preserved sedimentary structures and bioturbation that are characteristic of particular depositional environments. The facies, labelled A through D, range from very fine-grained sand to mud. A summary of the main features of the facies is in Table 1 and the ichnofossils assemblages are in Table 2. Interpreted core photographs are included in Appendix 1.

Table 1. Summary of the main features of the sedimentary facies in Yolla 3 Core 1.

Facies	Main features	Inferred depositional process	Depositional environment
A	Thoroughly bioturbated mudstone and sandstone	Suspension settling, infrequent storm activity and low wave energy	Distal lower shoreface
B	Flaser bedding, current, wave & combined flow ripples, tidal bundles, rare bioturbation	Tidal currents with minor wave influence	"Stressed", tidal flat/sandy embayment
C	Low angle lamination, mudstone laminations, rare current ripples. Bioturbation common	Wave activity and rare suspension settling	Wave influenced proximal delta front
D	Thoroughly bioturbated mudstone	Suspension settling, infrequent storm activity and low wave energy	Transitional offshore/wave influenced prodelta

Facies A – Thoroughly bioturbated sandstone and mudstone

Sedimentology

This facies occurs at the base of the core, comprises mudstone and sandy siltstone, with rare silty sandstone, that has been homogenised by bioturbation. The intense bioturbation commonly obscures any vestiges of physical sedimentary structures, although some relict wavy parallel laminae are rarely preserved and these are typically associated with intervals dominated with vertical burrows. Due to the degree of bioturbation, all bed contacts are gradational.

Ichnology

This facies has a bioturbation index of 5 – 6. The high degree of bioturbation commonly obscures the individual biogenic structures, making identification of ichnogenera difficult. Most of the recognised trace fossils are deep tiered structures of the equilibrium community. Softground trace fossils are dominated by deposit feeding and related structures, manifest by abundant *Planolites* and *Chondrites,* common to moderately abundant *Teichichnus* and rare *Terebellina, Asterosoma* and *Thalassinoides*?. Grazing/ foraging structures are also associated, and consist of abundant *Helminthopsis* and *Phycosiphon,* and moderate numbers of *Zoophycos*. *Palaeophycus*, the dwelling structure of a passively predaceous annelid, are locally common. The softground suite does not vary

Table 2. Relative abundance of ichnofossils within the facies observed in the upper EVCM, Yolla 3. The basal zone for the facies represents the *Glossifungites* assemblage.

Ichnofossils	Facies A	Basal Facies B	Facies B	Basal Facies C	Facies C	Basal Facies D	Facies D
Asterosoma	**c**	**-**	**-**	**-**	**-**	**-**	**-**
Bergauria	**-**	**-**	**-**	**-**	**r**	**-**	**-**
Chondrites	**a**	**-**	**c**	**-**	**o**		**a**
Cylindrichnus	**-**	**-**	**r**	**-**	**r**	**-**	**-**
Diplocraterion	**r**	**-**	**r**	**r**	**r**	**r**	
Helminthopsis	**c-o**				**r**		**a**
Macaronichnus	**-**	**-**	**-**	**-**	**a**	**-**	**-**
Ophiomorpha	**r**	**-**	**-**	**c**	**c-o**	**-**	**-**
Palaeophycus	**c-o**	**-**	**r**	**-**	**o-r**	**-**	**r**
Phycosiphon	**a**	**-**	**-**	**-**	**o-r**	**-**	**a-c**
Planolites	**c**	**-**	**r**	**-**	**r**	**-**	**c-o**
Rhizocorallium	**r**	**-**	**-**	**-**	**o-r**	**-**	**-**
Rosselia	**c-o**	**-**	**r**	**-**	**-**	**-**	**-**
Skolithos	**-**	**r**	**-**	**r**	**r**	**-**	**-**
Teichichnus	**c-o**	**-**	**r**	**-**	**-**	**-**	**-**
Terebellina	**r**	**-**	**-**	**-**	**-**	**-**	**c**
Thalassinoides	**o-r**	**-**	**-**	**c**	**r**	**o-c**	**-**
Zoophycos	**c**	**-**	**-**	**-**	**-**	**-**	**c**

significantly with changes in the burrow intensity, with the observed diversity remaining high (MacEachern et al, 1992a). The softground suite is dominated by a resilient, equilibrium community of detritus and deposit feeding organisms that are characteristic of a proximal *Cruziana* ichnofacies (Bann and Fielding, 2004).

The relatively rarer silty sandstone interval is pervasively burrowed and contains *Ophiomorpha, Diplocraterion, Rhizocorallium, Rosselia, Phycosiphon, Palaeophycus, Thalassinoides, Planolites* and *Chondrites*. This does not represent opportunistic colonisation of storm beds as the best preserved ichnogenera (mainly *Ophiomorpha, Diplocraterion* and *Rosselia*) overprint the proximal *Cruziana* ichnofacies. Trace fossils of this assemblage are characteristic of a distal expression of the *Skolithos* ichnofacies. The vertical burrows of suspension feeding organisms represent deep, mud lined, rapidly constructed domiciles able to withstand the unstable conditions (Bann and Fielding, 2004).

Interpretation

Facies A is interpreted to have been deposited in a lower shoreface setting, possibly associated with distal storm events (MacEachern et al, 1992a). The diversity of traces indicates well oxygenated, fully marine conditions. Storms, and to a lesser degree, fair-weather waves are the dominant physical processes operating on the lower shoreface. Therefore, the observed trace fossil variability is attributed to variability in the nature of storm activity. Fluctuations in sedimentary rates are intimately associated with the episodic nature of storm deposition and this controls the ultimate character of the lower shoreface deposits. The intensity of the bioturbation in Facies A, therefore, reflects overall low wave energy with infrequent storm events that favoured more thorough biogenic reworking of fair-weather sediment (MacEachern and Pemberton, 1992). The higher density of the fair-weather assemblage suggests that deposition occurred around or just above maximum fair-weather wave base where offshore processes continue to operate and deposit feeding organisms are still able to dominate the infaunal community during fair-weather periods (Bann and Fielding, 2004).

Fair-weather trace assemblages dominate the succession and under these situations transition from a diverse and abundant *Cruziana* suite (with subordinate grazing/foraging structures and suspension feeding traces) to a *Skolithos* ichnofacies (with rare grazing/foraging structures exploiting muddy zones and a reduced deposit feeding component) may correspond to the transition from distal lower to proximal lower shoreface environments (MacEachern and Pemberton, 1992; Bann and Fielding, 2004). The

Thalassinoides and *Ophiomorpha* are oriented horizontally, indicating low energy conditions as such burrows tend to become progressively more vertically oriented with increasing energy conditions on a shoreface (Raychaudhuri and Pemberton, 1992).

Storm deposits contain a characteristic trace fossil suite that comprises a stable fair-weather (or resident) assemblage, dominated by traces of equilibrium species, and an unstable storm assemblage, dominated by traces of opportunistic species. Storm deposits show the following physical and ichnological characteristics: 1) a fair-weather resident trace fossil suite; 2) a sharp base, with or without a basal lag; 3) parallel to subparallel laminations (hummocky or swaley cross stratification); 4) common escape structures; 5) dwelling burrows of opportunistic organisms that colonise the unexploited storm unit; 6) gradational burrowed tops representative of bioturbation resulting from subsequent burrowing organisms from higher colonisation levels; and 7) a fair-weather resident trace fossil suite indicative of a return to quiescent conditions following storm abatement (Pemberton et al, 1992). Opportunistic communities include organisms that have high reproduction rates, broad environmental tolerances and generalised feeding habits. These organisms rapidly colonise habitats after an abrupt environmental change e.g. storm deposition (Bromley, 1996). The opportunistic community, typically comprising *Skolithos* ichnofacies, are succeeded and overprinted by a resident community generally comprising a *Cruziana* ichnofacies (MacEachern et al, 1992a).

Facies B – Flaser bedded sandstone

Sedimentology

This base of this facies is erosional and overlies Facies A. The facies comprises silty sandstone to very fine-grained sandstone with mudstone occurring as laminations between beds and on foresets. Primary stratification is preserved, predominantly as flaser bedding, internally comprising ripple cross lamination, ripple form sets, flat lamination and micro-hummocky cross stratification (ripple scale). The ripples are current, wave and combined flow (wave modified) generated and there are intervals that suggest the presence of bipolar current ripples that indicate tidal flows. Tidal influence is also inferred from regularly spaced mudstone laminations present on ripple foresets, possibly representing tidal bundles.

Ripple form sets are rare and present in intervals with increased mudstone laminations whereas ripple crests are commonly truncated by the overlying bed base in amalgamated sandstone intervals.

Rare thin intervals (<7 cm) of angular, fine-grained to granule matrix supported mudstone rip up clasts are irregularly distributed throughout the facies and in one case is overlain by a thin, intensely bioturbated interval.

This facies comprises decimetre scale cycles that have sharp, often erosional bases overlain by amalgamated ripple laminated sandstone. Flaser bedding and tidal bundles increase toward the top of the cycles.

Ichnology

The base of this facies is delineated by a *Glossifungites* ichnofacies, comprising rare vertical, passively filled, unlined *Skolithos.* These vertical shafts within the mudstone of Facies A are anomalous as such structures are not capable of being maintained in soft muddy substrates. Further evidence of substrate stability, atypical of soft muddy beds is the passive nature of the burrow fill. This demonstrates that the structure remained open after the tracemaker vacated the burrow, thus allowing material from the succeeding depositional event to passively fill the open structure. If the burrow had been excavated in mud, the domicile would have collapsed upon the burrow vacation unless lined (MacEachern et al, 1992b).

There is a marked decrease in the degree of bioturbation across the contact with Facies A. Bioturbation in Facies B is variable and the Bioturbation Index (BI) ranges from 0 to 6, but is most commonly 1 to 2. Thin intervals (<5 cm) are intensely bioturbated and occur as discrete intervals within intervals of lower BI. Although the high degree of bioturbation commonly obscures the individual biogenic structures, these intervals appear to be dominated by a limited number of ichnospecies. The ichnogenera present are a mixture of dwelling structures of suspension feeders (rare *Diplocraterion* and *Cylindrichnus*) or passive carnivores (*Palaeophycus*) and deposit feeding structures (common *Chondrites,* rare *Planolites, Teichichnus* and *Rosselia*). Escape traces (fugichnia) are locally present. Increased levels of bioturbation, comprising predominantly *Chondrites,* are associated with intervals of mudstone laminations. The deposit feeding strategy of this trace is evident from the preferential concentration of burrows within the mudstone drapes.

Interpretation

A tidal environment is interpreted as the depositional environment of Facies B on the basis of reversing flow structures such as current ripples with reversed asymmetry or symmetrical tops, and mud drapes, interpreted as tidal bundles. Structures typical of

fluctuations in salinity, e.g. synaeresis cracks, are not present due to the lack of thick mudstone units. The small scale cycles are interpreted to represent deposition within a tidal flat/sandy embayment environment (Dalrymple, 1992). From this core it is difficult to determine the exact depositional setting (low gradient, low energy open coast or back-barrier setting), however, the prevalence of *Chondrites* implies reduced oxygen conditions (Bromley, 1996), suggesting a back barrier setting. Interdistributary areas on wave dominated deltas are typically partially or completely closed off by barrier /beach complexes resulting in extensive back barrier areas (Bhattacharya and Walker, 1992).

Tidal flats developed under prograding conditions are characterized by a fining upward sequence. This reflects the decreasing wave action in the progression from subtidal to intertidal to supratidal parts of the tidal flat. Commonly, this sequence is characterised by: 1) a dominantly sandy subtidal zone of channel fill, point bar and shoal sediments; 2) a mixed sand and mud intertidal flat deposit; and 3) a muddy upper intertidal flat, and 4) an algae flat or salt marsh deposit (supratidal flat). The intertidal flat displays a variety of intertidal sand and mud layers, including wavy, flaser and lenticular bedding. Wavy bedding is produced by irregular flow conditions, oscillating flow directions, or relatively high velocity flow. Flaser bedding occurs when thin streaks of mud are deposited between sets of cross-laminated sandy or silty sediment, indicating an environment where the flow has periods of current activity followed by periods of quiescence when mud is deposited. In contrast, lenticular bedding occurs when lenses of sand are preserved in mud, indicating an environment where mud is the favoured mode of deposition. The upper-intertidal flat surfaces are commonly bioturbated or contain slightly laminated mud with thin sand lamina. All of these structures, however, can be modified or completely destroyed by intense burrowing, bioturbation, or profuse tracks and trails (Dalrymple, 1992).

The presence of angular mudstone rip up clasts is interpreted as the deposits of storm events and erosion of desiccation polygons possibly from the upper intertidal flat and supratidal flat (Dalrymple, 1992).

Storm deposits may also be indicated by the thin zones of intense bioturbation that reflect increased levels of food availability in comparison to the background sedimentation rates. The increased organic material incorporated into these beds promoted increased bioturbation by deposit feeding organisms (Beynon and Pemberton, 1992).

Marginal marine environments, including the intertidal zone, shallow lagoons, estuaries, bays and delta platforms, characteristically display steep salinity gradients resulting from variations in 1) amounts of freshwater input from rivers and runoff from land, 2) rainfall, 3) evaporation, 4) tidal range and salinity content in adjacent open ocean coastal waters, 5) morphology of the coastal area, and 6) differences in the wind direction and velocity. Such salinity fluctuations (combined with corresponding changes in temperature, exposure, turbulence, oxygen content, turbidity etc.) result in a physiologically stressful environment for numerous organism groups. In general, the brackish water or stressed marine trace fossil suites are characterised by 1) low diversity, 2) forms typically found in marine environments, 3) simple structures constructed by tropic generalists, 4) suites that are commonly dominated by a single ichnogenus, 5) vertical and horizontal ichnofossils that are common to both the *Skolithos* and *Cruziana* ichnofacies; and 6) some forms may be found in prolific densities (Pemberton and Wightman, 1992).

The mud drape dominated intervals are typified by low diversity ichnofossil assemblages dominated by *Chondrites* and *Planolites* with rare *Teichichnus, Palaeophycus, Diplocraterion* and *Cylindrichnus.* The association is characterised by predominance of horizontal deposit feeding structures (*Chondrites* and *Planolites*) with subordinate occurrences of dwelling structures (*Diplocraterion, Cylindrichnus* and *Palaeophycus*). Although diversity is low, individuals, particularly *Planolites*, may attain high densities in which burrow elements are not always readily apparent. Such ichnofaunal assemblages are characteristic of a mixed *Skolithos-Cruziana* ichnofacies which is characteristic of a stressed marine environment (Beynon and Pemberton, 1992).

The presence of dwelling/suspension feeding structures (*Diplocraterion*) argues against a delta front setting as these structures are rare due to river discharge increasing water turbidity, making suspension feeding difficult or impossible. The filter feeding apparatus of some organisms become clogged, and the high suspended sediment lowers the ratio of food to ingested sediment (Coates and MacEachern, 2000). The monospecific assemblage of *Chondrites* cutting the primary fabric in the mud laminated intervals may indicate reduced oxygen levels as this is typically a deep tier structure. However, as oxygen levels decrease the inhabitants of the deepest tiers will find a niche immediately below the surface (Bromley, 1996).

The *Glossifungites* assemblage represents a substrate controlled assemblage of trace fossils characterised by a robust, sharp-walled, unlined, passively filled, vertical to sub-

vertical domichnia (dwelling burrow), excavated into semi-consolidated (firmground) substrates and demarcates discontinuity surfaces that reflect pauses in sedimentation, generally accompanied by erosion (MacEachern et al, 1992b).

Facies C – Laminated sandstone and mudstone

Sedimentology

Facies C is sharp based and overlies Facies B. This facies comprises mudstone, silty sandstone and very fine-grained sandstone. The facies ranges from 60 to 90% sandstone. There is an increase in the amount of mudstone beds within this facies and lenticular bedded intervals up to 5 cm in thickness are present. There is an overall increase in the amount of mudstone laminations toward the top of the interval. The sandstone beds have a sharp base and contain low angle lamination, wavy laminations and rare ripple laminations. Glauconite is present in rare mudstone dominated intervals.

Ichnology

The base of this facies is again delineated by a *Glossifungites* ichnofacies, comprising passively filled, *Diplocraterion, Ophiomorpha* and *Thalassinoides* that cross cut the background softground trace fossil assemblage of Facies B. The burrows extend up to 70 cm below the contact between Facies B and C. Due to the similarity in grainsize between the facies, *Thalassinoides* is differentiated on the basis of burrow fill texture that truncates the primary textures in Facies B. *Thalassinoides* is the most common ichnofossil associated with this surface and is the deepest tiered structure.

Facies B is characterised by moderate levels of bioturbation, with the BI 2 to 4, which comprises pervasive *Macaronichnus* burrows, with all other trace fossils sporadically distributed. Apart from *Macaronichnus*, identified trace fossils include *Thalassinoides, Palaeophycus, Skolithos, Diplocraterion, Ophiomorpha, Phycosiphon, Planolites, Chondrites, Cylindrichnus, Teichichnus, Helminthopsis* and rare *?Bergauria*. There is a dominance of deposit feeding ichnogenera (*Macaronichnus*, *Thalassinoides, Phycosiphon, Planolites, Chondrites, Cylindrichnus* and *Teichichnus*) with only rare dwelling structures (*Palaeophycus, Skolithos, Diplocraterion, Ophiomorpha* and *Bergauria*) and grazing/foraging structures (*Helminthopsis*). The trace fossils occur in low diversity assemblages; however, the highest trace fossil diversity immediately overlies the *Glossifungites* ichnofacies and comprises *Thalassinoides, Phycosiphon, Planolites, Chondrites* and *Helminthopsis* within a mudstone-sandstone interval. Areas of reduced BI and amalgamated sandstone beds comprise a monospecific assemblage of *Macaronichnus*.

Escape traces (fugichnia) are common in some beds. This comprises a moderately diverse and locally abundant stressed *Cruziana* ichnofacies assemblage.

Interpretation

Thin ripple-laminated sandstone beds are interpreted as representing subtidal deposition under the influence of wave and tidal currents. Facies C is interpreted as being deposited in a wave influenced, proximal deltaic setting on the basis of the low angle and wavy laminated sandstones interstratified with organic rich mudstone. There is a dominance of wave produced structures (such as low angle and wavy laminated intervals representing hummocky cross stratification and amalgamated swaley cross stratification) whereas indicators of high sedimentation rates and freshwater water influence (soft sediment deformation, climbing ripples, synaeresis cracks) are absent. There are tidal indicators, including herringbone cross stratification and potential tidal bundles, implying a mixed wave tidal delta system in the delta front environment (Bhattacharya and Walker, 1992).

Glauconitic minerals are relatively common authigenic constituents of marine sediments, and are good indicators of low sedimentation rate. The water-sediment interface in a marine setting constitutes the ideal place for glauconitisation. The original substrate is gradually replaced by authigenic glauconitic minerals, which evolve through recrystallisation processes (Pasquini et al, 2004). The thickest of the glauconite intervals occurs at 2224.1 m and may represent a hardground where low sedimentation rates prevailed. A palaeodepth range between 60 and 550 m and an open marine environment were originally considered as ideal for glauconisation as these are generally low-energy settings in which accumulation of sediment is relatively slow. However, other depth ranges have been proposed for glauconite formation. Hesselbo and Huggett (2001) have detected autochthonous glaucony pellets formed at 600 - 1000 m water depth, while Chafetz and Reid (2000) described autochthonous glauconitic minerals formed under shallow water to tidal-flat conditions, in a high-energy environment. Thus, the occurrence of glauconitic minerals in the rock record cannot be used a priori as an environmental indicator of water depths greater than 60 m and a slow rate of sedimentation (Pasquini et al, 2004). The presence of glauconite in this facies, and the inferred low rate of sediment deposition, possibly represents autocyclic processes (delta lobe switching etc.) and formation of hardgrounds on the delta front.

The preservation potential of *Macaronichnus* was high despite its apparent deposit feeding mode of life due to the deep tier position that it occupied. In intertidal shoreface

environments, oxygenated surface waters can circulate several metres into the sand, well below the reach of surface wave disturbance. In addition, large volumes of dissolved and finely particulate organic matter, most of which is mineralised at depth, is filtered through the porous sandy sediment. This phenomenon creates a second habitat at depth, separate from the physically controlled habitat at the surface. The deeper habitat is stable, predicable and is constantly replenished with food material (Bann and Fielding, 2004).

Dwelling/suspension feeding structures are rare in this environment and are interpreted to reflect two major factors: 1) river discharge increases the turbidity, making suspension feeding difficult or impossible; 2) storm events are typically accompanied by high rates of precipitation. Near distributaries, large amounts of organic detritus and clay are swept into the basin and, during post storm conditions, this settles onto storm beds, shielding them from opportunistic colonisation. High organic content in the mud may result in rapid oxidation and concomitant 0_2 depletion at the sea floor, diminished the ability of infauna to colonise the bed (Raychaudhuri and Pemberton, 1992; Coates and MacEachern, 2000).

The transition from a moderately diverse stressed *Cruziana* assemblage of deposit feeding ichnogenera to a monospecific assemblage of *Macaronichnus* is attributed to higher energy conditions, producing unstable conditions for shallow tier ichnofossils (Bann and Fielding, 2004).

Facies D – Thoroughly bioturbated mudstone

Sedimentology

Facies D has a sharp erosive base that overlies Facies C and comprises well bioturbated mudstone. No primary structures have been preserved due to the degree of bioturbation.

Ichnology

This facies is dominated by horizontal burrows and the BI is 6. This high degree of bioturbation obscures the individual biogenic structures, making identification of ichnogenera difficult. The softground suite is dominated by deposit feeding structures, containing abundant *Chondrites, Planolites* and *Terebellina*, and rare *Teichichnus*. The assemblage also contains subordinate amounts of grazing/foraging structures such as *Phycosiphon, Helminthopsis* and *Zoophycos*. This represents a moderately diverse, stressed distal *Cruziana* assemblage that is characterised by ichnogenera that are diminutive in size.

The base of this facies is again delineated by a *Glossifungites* ichnofacies, comprising passively filled, *Diplocraterion, Rhizocorallium* and *Thalassinoides,* that extend up to 45 cm below the contact between Facies C and D. *Thalassinoides* is the most common ichnofossil associated with this surface and is the deepest tiered structure.

Interpretation

Facies D is interpreted to have been deposited in an offshore marine/wave influenced prodelta environment. The moderate diversity ichnofacies assemblage and the diminutive size of the traces implies environmental stresses e.g. fluctuating salinity levels, periods of reduced oxygenation etc., however, the presence of grazing/foraging structures indicates that marine conditions were largely maintained. Offshore deposits associated with shoreface successions typically contain diverse and abundant distal and archetypal *Cruziana* suites, though they may display a close affinity with prodelta deposits of wave influenced deltas and may reflect along strike graduation between these systems (Coates and MacEachern, 2000). Therefore, this facies is interpreted to be transitional between a wave influenced prodelta and an offshore marine setting.

This setting was below the fair-weather wave base and fluctuations in sedimentary rates are intimately associated with the episodic nature of storm deposition and this controls the ultimate character of the deposits. The intensity of the bioturbation and the lack of well defined storm deposits therefore, reflects overall low wave energy with infrequent storm events that favoured more thorough biogenic reworking of fair-weather sediment (MacEachern and Pemberton, 1992).

The lack of suspension feeding structures is attributed to high water turbidity and, possibly, post storm mud beds mantling the storm beds (Coates and MacEachern, 2000).

DEPOSITIONAL MODEL

The depositional setting for the succession in the core is marine to marginal marine with facies dislocations separating different environments. The significance of these facies dislocations will be discussed in the Sequence Stratigraphy section.

Distal lower shoreface

The degree and diversity of bioturbation in this setting indicates open marine conditions. There is a lack of identifiable storm deposits implying that overall low wave energy with

infrequent storm events that favoured more thorough biogenic reworking of fair-weather sediment.

Sandy embayment/tidal flat

The presence of tidal structures (possible herringbone cross stratification and tidal bundles) coupled with a stressed ichnofacies comprising deposit feeding and suspension feeding structures implies a low energy sandy embayment/tidal flat environment, developed on a low gradient, low energy shoreface, or in a back barrier setting.

Proximal delta front

The predominance of wave formed structures, a lack of suspension feeding structures and a dominance of deep tier deposit feeding structures implies a high turbidity environment such as a wave influenced proximal delta front.

Offshore/Wave influenced prodelta

The bioturbation is not as diverse as the distal lower shoreface implying environmental stresses e.g. turbidity, low oxygen levels etc. that reflects an offshore/prodelta transition. This setting was below the fair-weather wave base and fluctuations in sedimentary rates are intimately associated with the episodic nature of storm deposition and this controls the ultimate character of the deposits. The intensity of the bioturbation and the lack of well defined storm deposits therefore, reflects overall low wave energy with infrequent storm events that favoured more thorough biogenic reworking of fair-weather sediment.

SEQUENCE STRATIGRAPHY

The stratigraphic record can be subdivided into various scales or orders of cycles, resulting from cyclical variations in sediment supply and relative base level change, on the basis of the periodicities. These cycles occur at different time scales, forming a hierarchy of sequences at differing frequencies and, therefore, longer period sequences contain several shorter period, higher frequency sequences. In this nested periodicity, the longer period sequences influence the stratal patterns within the higher frequency sequences; this is a function of their position within the longer period sequence. The high resolution sequence stratigraphic approach to the analysis of sedimentary successions focuses attention on key stratal surfaces, facies dislocations and parasequence stacking patterns within the context of relative base level changes.

Stratal surfaces

Key stratal surfaces identified in the core include sequence boundaries (SB) and transgressive surfaces of erosion (TSE). The diagnostic features of these surfaces are described below.

Sequence boundaries (SB)

The sequence boundary occurs between Facies A and Facies B and is characterised by an increase in grainsize, a poorly developed *Glossifungites* ichnofacies, and, most noticeably, by a decrease in the degree of bioturbation. The SB separates the offshore/distal lower shoreface from intertidal/subtidal sandy embayment deposits. The facies dislocations indicate a basinward shift in facies associated with a relative base level fall.

Transgressive surface of erosion (TSE)

Transgressive surfaces of erosion (ravinement surfaces) are generated in the marine or marginal marine environments. These surfaces are discontinuity surfaces across which there is a significant deepening in depositional environment and occur between Facies B and Facies C, as well as Facies C and Facies D. In the core it is impossible to determine the degree of erosion associated with these surfaces.

Sequence stratigraphic model

The facies within the cored interval were strongly controlled by changes in relative base level in a marginal marine environment. The relative base level fall within this setting caused a forced regression in which sandy embayment/tidal flat sediments were superimposed onto distal lower shoreface environments. The tidal flat/sandy embayment deposits represent a lowstand systems tract/early transgressive systems tract (LST/TST). These deposits have an aggradational stacking pattern, indicating that relative base level was rising at a rate approximately equal to the sediment deposition rate. The aggradational stacking is more representative of a LST/TST than a Falling Stage Systems Tract (FSST) in which progradational stacking associated with a base level fall (forced regression) is common.

A subsequent rapid rise in relative base level resulted in the formation of a TSE and the deposition of wave influenced, proximal delta front facies. This rise in base level produced a rapid deepening in which the rate of change in base level far outpaced the rate of sediment supply. The TSE separates the LST from the Transgressive Systems Tract

(TST). The wave influenced delta front has an overall slightly retrogradational, almost aggradational stacking; implying that the rate of base level rise and sediment supply were almost balanced. Another TSE separates the proximal delta front sediments from the offshore/prodelta deposits. There is almost an aggradational stacking overlying the TSE, however, it is difficult to determine stacking patterns in bioturbated offshore/prodelta deposits.

The succession in the core is dominated by intervals in which the rate of base level change was balanced with the sediment supply, producing aggradational, or nearly so, stacking. These intervals are separated by periods of rapid relative base level change causing juxtaposition of differing depositional settings.

RESERVOIR QUALITY

Reservoir quality is strongly facies dependent with the sandy embayment/tidal flat and proximal delta front having the highest permeability (Figure 1). The degree of bioturbation has only a limited control on reservoir quality; the greatest control is exhibited by depositional energy. Facies B (sandy embayment/tidal flat) consistently has the highest permeability whereas Facies C (proximal delta front) is more variable but, in places, has permeability values similar to Facies B, possibly reflecting progradation of the delta. Facies A (distal lower shoreface) has variable permeability as a result of differing mudstone content in beds. Facies D (offshore/wave influenced prodelta) has the lowest permeability due to the high mudstone content.

REFERENCES

Bann, K.L. and Fielding, C.R., 2004. Ichnology & Facies Analysis for Petroleum Exploration. Ichnofacies Pty and University of Nebraska Short Course, April 2004.

Beynon, B.M. and Pemberton, S.G., 1992. Ichnological signature of a brackish water deposit: an example from the Lower Cretaceous Grand Rapids Formation, Cold Lake Oil Sands area, Alberta. *In:* Pemberton, S.G., ed: *Applications of Ichnology to Petroleum Exploration: A Core Workshop.* Society for Sedimentary Geology, Tulsa, 199-221.

Bhattacharya, J.P. and Walker, R.G., 1992. Deltas. *In:* Walker, R.G., and James, N.P., eds. *Facies Models: Response to Sea Level Change*. Geological Association of Canada, Newfoundland, 157-177.

Bromley, R.G., 1996. Trace Fossils: Biology, taphonomy and applications. Chapman & Hall, London, 361 pp.

Chafetz, H.S. and Reid, A., 2000. Syndepositional shallow water precipitation of glauconitic minerals. *Sedimentary Geology* 136, 29–42.

Coates, L. and MacEachern, J.A., 2000. Differentiating river- and wave-dominated deltas from shorefaces: examples from the Cretaceous Western Interior Seaway, Alberta, Canada. http://www.cseg.ca/conferences/2000/443.pdf.

Dalrymple, R.W., Tidal depositional systems. *In:* Walker, R.G., and James, N.P., eds. *Facies Models: Response to Sea Level Change*. Geological Association of Canada, Newfoundland, 195-218.

Hesselbo, S.P. and Huggett, J.M., 2001. Glaucony in ocean margin sequence stratigraphy (Oligocene–Pliocene, offshore New Jersey, U.S.A.; ODP LEG 174A). *Journal of Sedimentary Research* 71, 599–607.

MacEachern, J.A. and Pemberton, S.G., 1992. Ichnological aspects of Cretaceous shoreface successions and shoreface variability in the Western Interior Seaway of

North America. *In:* Pemberton, S.G., ed: *Applications of Ichnology to Petroleum Exploration: A Core Workshop.* Society for Sedimentary Geology, Tulsa, 57-84.

MacEachern, J.A., Bechtel, D.J. and Pemberton, S.G., 1992a. Ichnology and sedimentology of transgressive deposits, transgressive related deposits and transgressive systems tracts in the Viking Formation of Alberta. *In:* Pemberton, S.G., ed: *Applications of Ichnology to Petroleum Exploration: A Core Workshop.* Society for Sedimentary Geology, Tulsa, 251-290.

MacEachern, J.A., Raychaudhuri, I. and Pemberton, S.G., 1992b. Stratigraphic applications of the *Glossifungites* ichnofacies: delineating disconformities in the rock record. *In:* Pemberton, S.G., ed: *Applications of Ichnology to Petroleum Exploration: A Core Workshop.* Society for Sedimentary Geology, Tulsa, 169-198.

Pasquini, C., Lualdi, A. and Vercesi, P., 2004. Depositional dynamics of glaucony-rich deposits in the Lower Cretaceous of the Nice arc, southeast France. *Cretaceous Research*, 25, 179-189.

Pemberton, S.G. and Wightman, D.M., 1992. Ichnological characteristics of brackish water deposits. *In:* Pemberton, S.G. ed. *Applications of Ichnology to Petroleum Exploration: A Core Workshop*. Society for Sedimentary Geology, Tulsa, pp141-167.

Pemberton S.G., MacEachern, J.A. and Ranger, M.J., 1992. Ichnology and event stratigraphy: the use of trace fossils in recognising tempestites. *In:* Pemberton, S.G., ed: *Applications of Ichnology to Petroleum Exploration: A Core Workshop.* Society for Sedimentary Geology, Tulsa, 85-117.

Pemberton, S.G., Van Wagoner, J.C. and Wach, G.D., 1992. Ichnofacies of a wave dominated shoreline. *In:* Pemberton, S.G., ed: *Applications of Ichnology to Petroleum Exploration: A Core Workshop.* Society for Sedimentary Geology, Tulsa, 339-382.

Raychaudhuri, I. and Pemberton, S.G., 1992. Ichnologic and sedimentologic characteristics of open marine to storm dominated restricted marine settings within the Viking/Bow Island Formations, south-central Alberta. *In:* Pemberton, S.G., ed:

Applications of Ichnology to Petroleum Exploration: A Core Workshop. Society for Sedimentary Geology, Tulsa, 119-139.

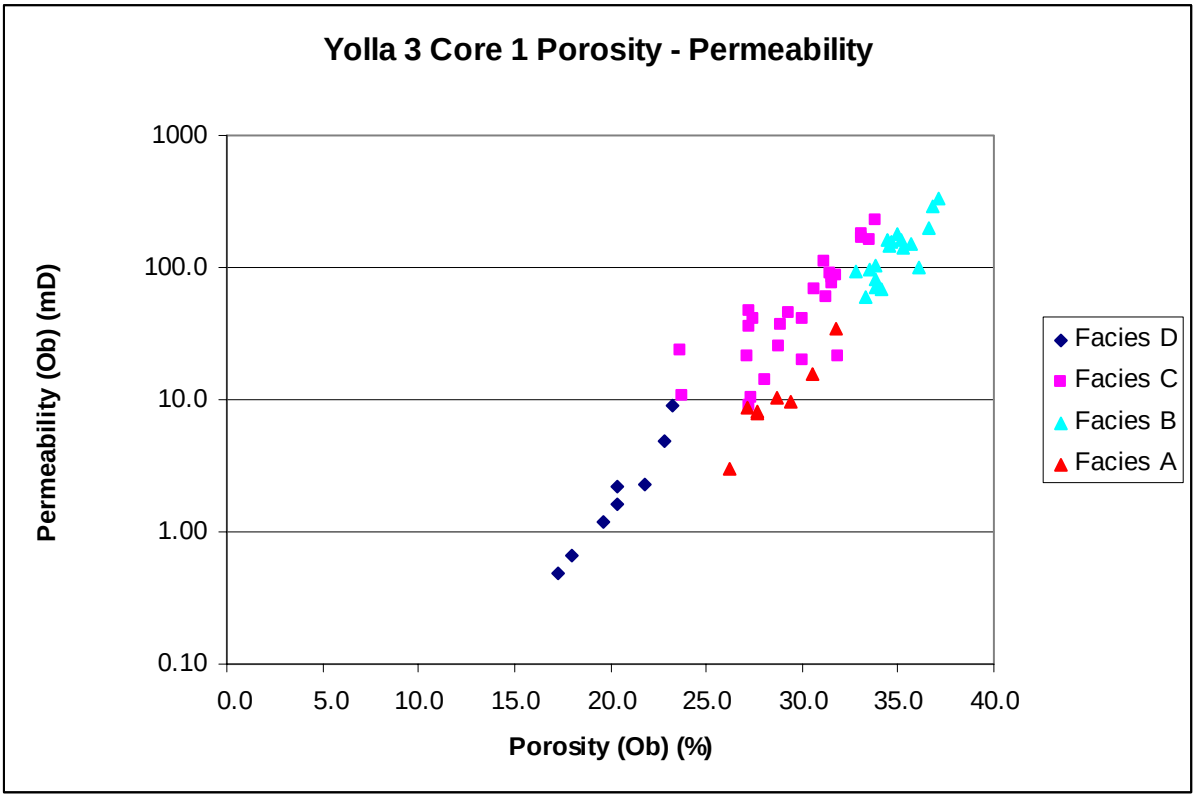

Figure 1. Core porosity and permeability plot. Note the relationship between facies and porosity/permeability.

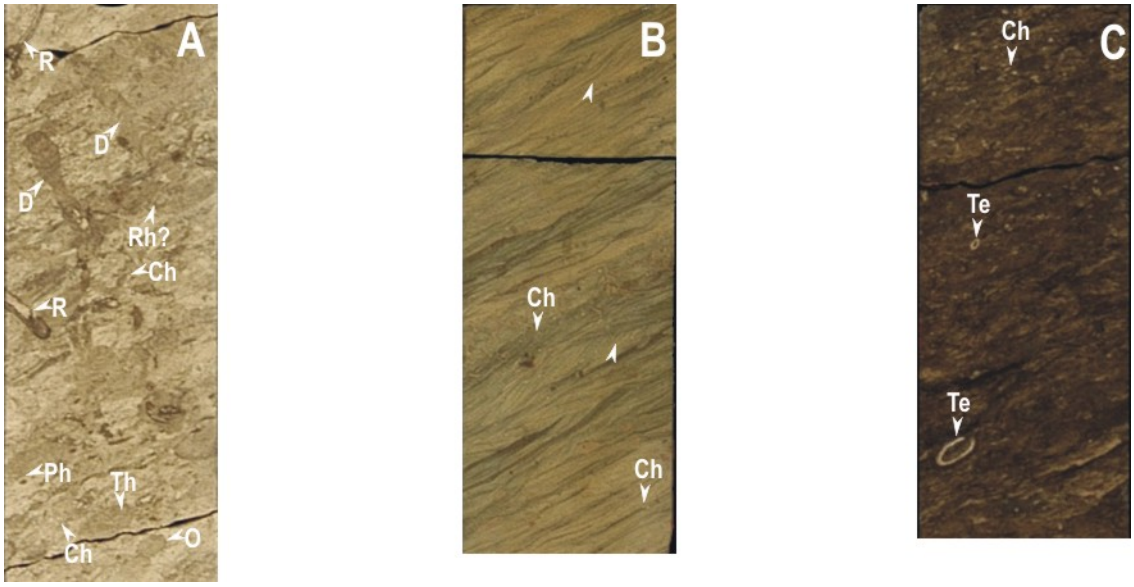

Figure 2. A) Facies A - distal to proximal lower shoreface showing thorough bioturbation, *Chondrites* (Ch), *Diplocraterion* (D), *Ophiomorpha* (O), *Phycosiphon* (Ph), *Rhizocorallium* (Rh), *Rosselia* (R), *Thalassinoides* (Th); 2232.38 – 2232.65 m. B) Facies B – sandy embayment/tidal flat show variable bioturbation, dominated by *Chondrites* (Ch). Tidal influenced is indicated by the presence of tidal bundles (white arrows). The lower tidal bundle set occurs within a wave modified current ripple; 2230.0 – 2230.25 m. C) Facies D – offshore marine/wave influenced prodelta showing the thorough bioturbation of the sediment. Most traces are unrecognisable; *Chondrites* (Ch), *Terebellina* , (Te); 2217.0 – 2217.23 m.

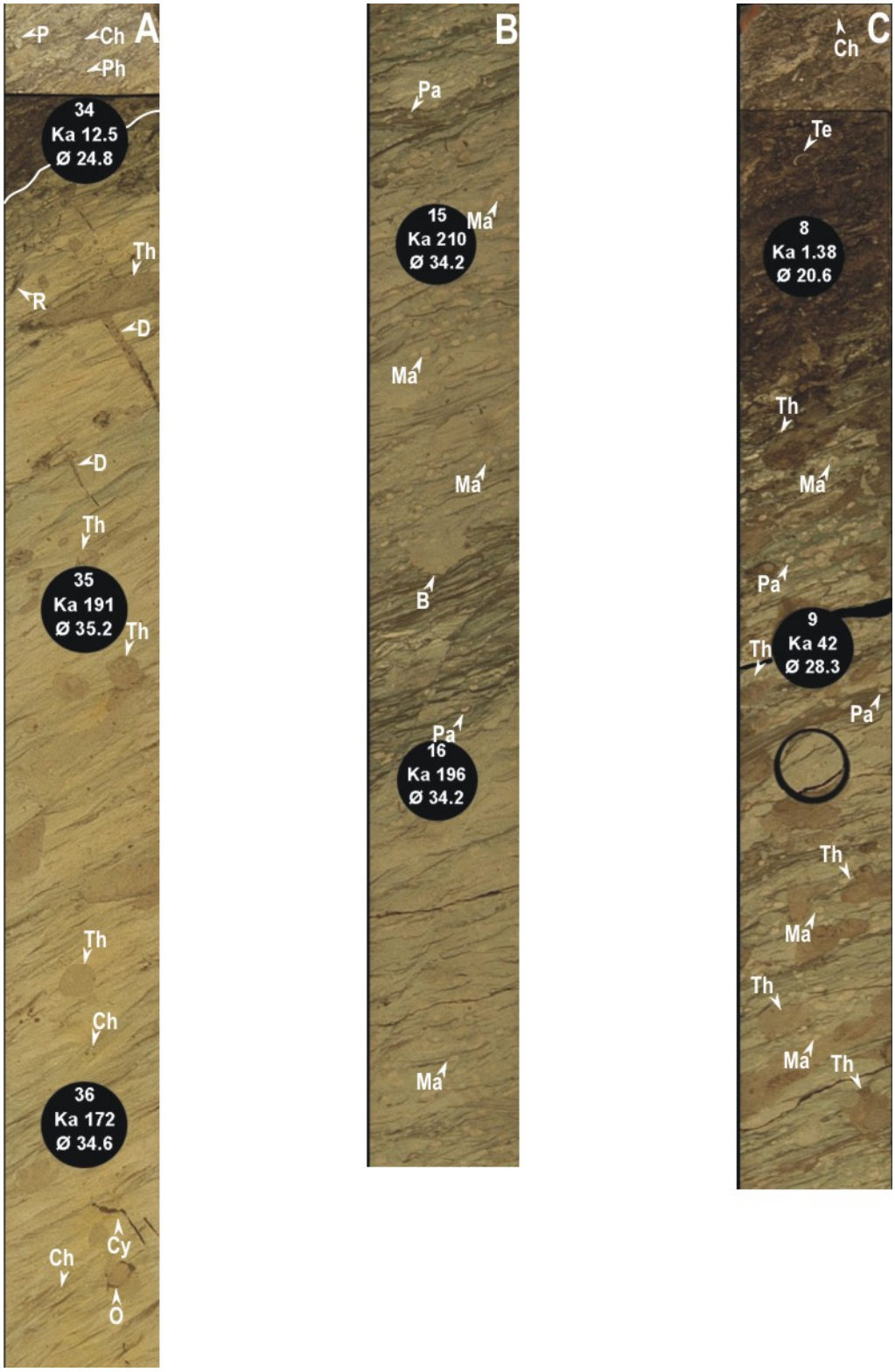

Figure 3. A) Contact (TSE) between Facies B and Facies C demarcated with a *Glossifungites* ichnofacies comprising *Diplocraterion* (D), *Ophiomorpha* (O) and *Thalassinoides* (Th) overprinting a sparse assemblage of *Chondrites* (Ch), *Cylindrichnus* (Cy), *Rosselia* (R). Overlying the TSE is a highly bioturbated zone comprising a moderately diverse assemblage of *Chondrites* (Ch), *Phycosiphon* (Ph), *Planolites* (P); 2226.0 – 2226.78

m. B) Facies C – wave influenced proximal delta front showing pervasive *Macaronichnus* (Ma) bioturbation with rarer *Palaeophycus* (Pa) burrows. Rare *Bergauria*? (B) occur at the base of some beds; 2220.12 – 2220.83 m. C) Contact (TSE) between Facies C and Facies D. A *Glossifungites* ichnofacies, comprising dominantly *Thalassinoides* (Th) is present and overprints the softground assemblage of *Macaronichnus* (Ma) and *Palaeophycus* (Pa). Overlying the contact is a thoroughly bioturbated interval comprising *Chondrites* (Ch) and *Terebellina* (Te), other traces are unrecognisable; 2218.0 – 2218.7 m.

APPENDIX 1

YOLLA 3 INTERPRETED CORE PHOTOGRAPHS

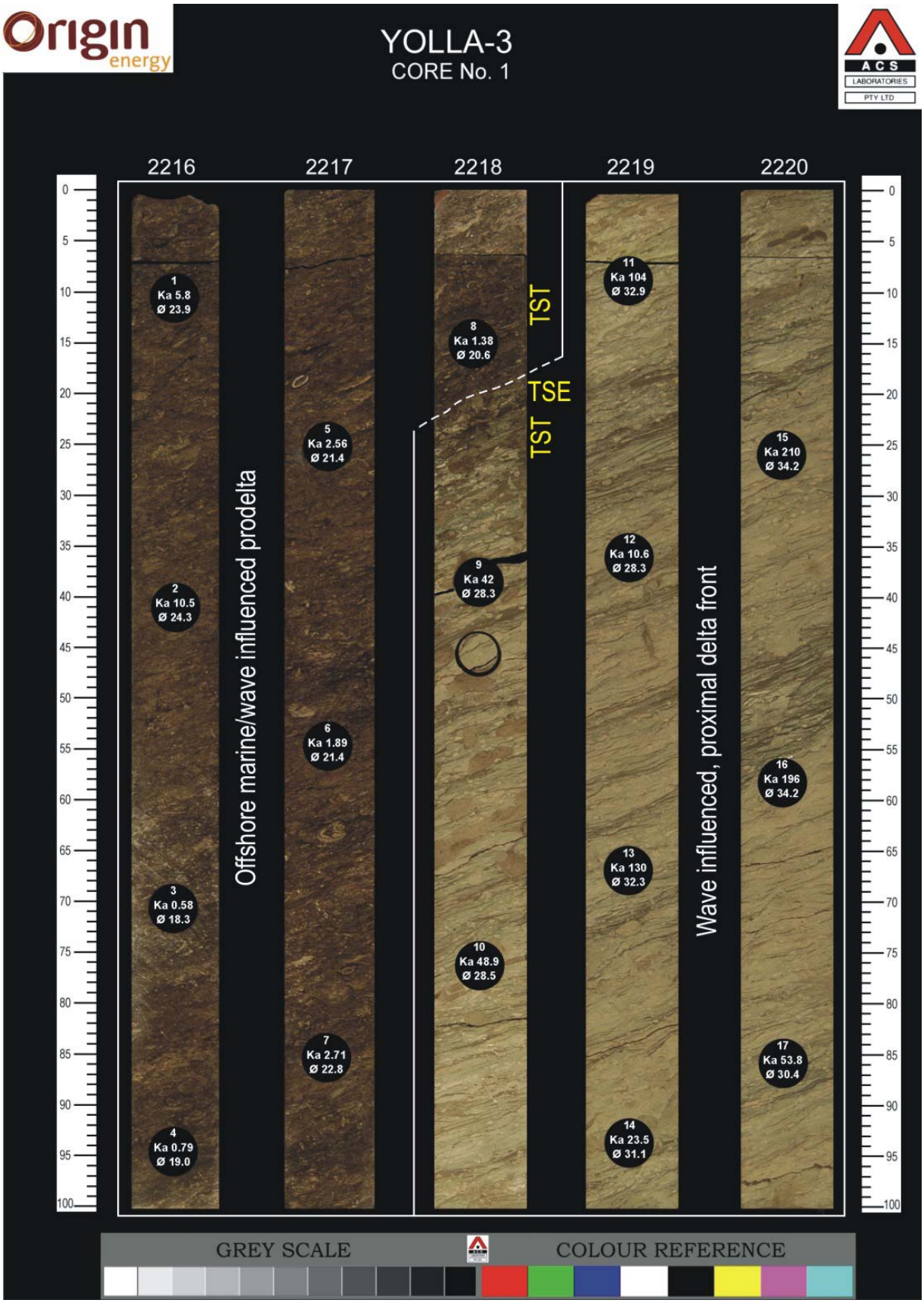
YOLLA-3
CORE No. 1
2216
2217
2218
2219
2220
TST
TSE
TST
Offshore marine/wave influenced prodelta
Wave influenced, proximal delta front
1 Ka 5.8 Ø 23.9
2 Ka 10.5 Ø 24.3
3 Ka 0.58 Ø 18.3
4 Ka 0.79 Ø 19.0
5 Ka 2.56 Ø 21.4
6 Ka 1.89 Ø 21.4
7 Ka 2.71 Ø 22.8
8 Ka 1.38 Ø 20.6
9 Ka 42 Ø 28.3
10 Ka 48.9 Ø 28.5
11 Ka 104 Ø 32.9
12 Ka 10.6 Ø 28.3
13 Ka 130 Ø 32.3
14 Ka 23.5 Ø 31.1
15 Ka 210 Ø 34.2
16 Ka 196 Ø 34.2
17 Ka 53.8 Ø 30.4
GREY SCALE
COLOUR REFERENCE

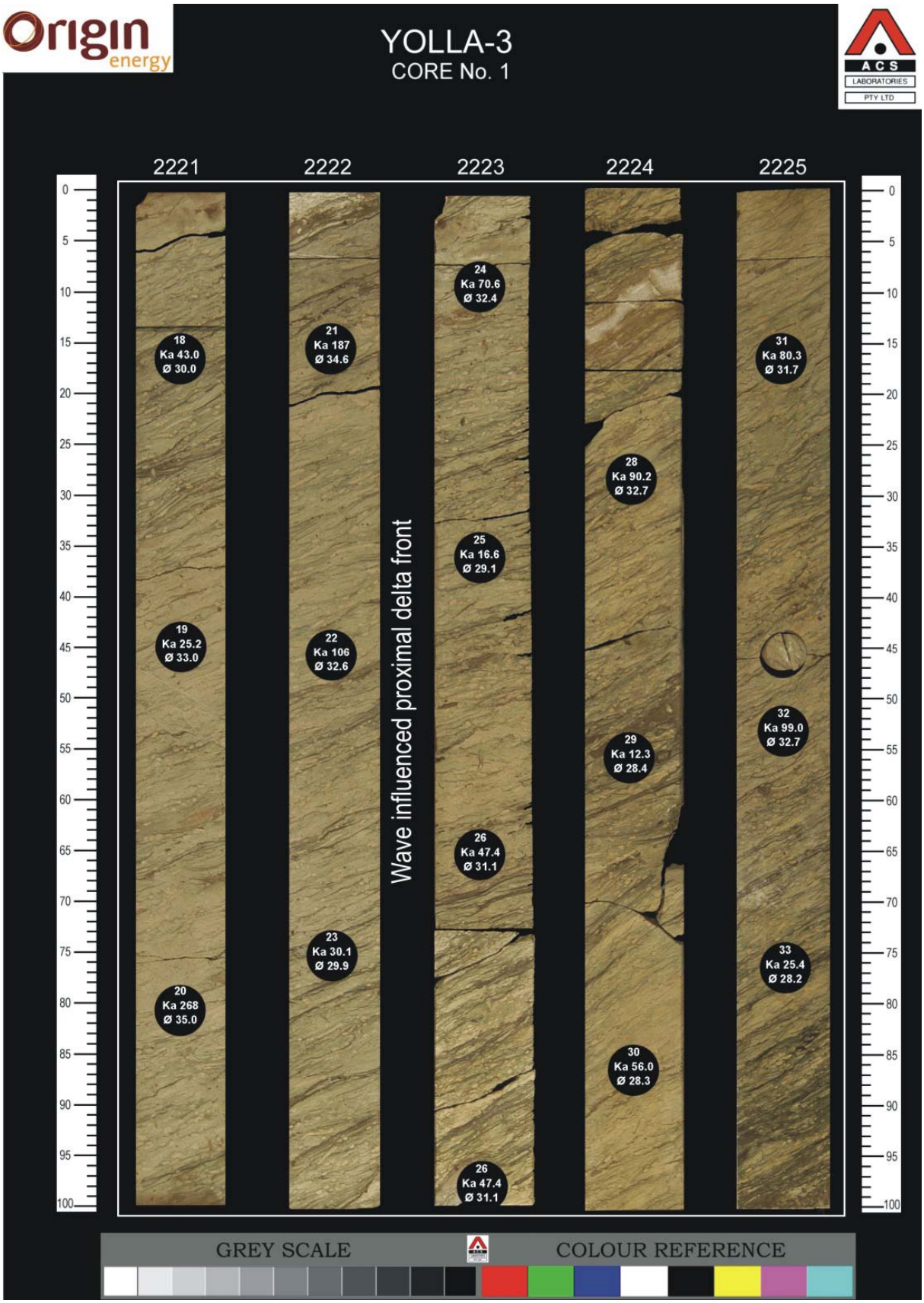
YOLLA-3
CORE No. 1
ACS LABORATORIES PTY LTD
2221
2222
2223
2224
2225
Wave influenced proximal delta front
18 Ka 43.0 Ø 30.0
19 Ka 25.2 Ø 33.0
20 Ka 268 Ø 35.0
21 Ka 187 Ø 34.6
22 Ka 106 Ø 32.6
23 Ka 30.1 Ø 29.9
24 Ka 70.6 Ø 32.4
25 Ka 16.6 Ø 29.1
26 Ka 47.4 Ø 31.1
26 Ka 47.4 Ø 31.1
28 Ka 90.2 Ø 32.7
29 Ka 12.3 Ø 28.4
30 Ka 56.0 Ø 28.3
31 Ka 80.3 Ø 31.7
32 Ka 99.0 Ø 32.7
33 Ka 25.4 Ø 28.2
GREY SCALE
COLOUR REFERENCE

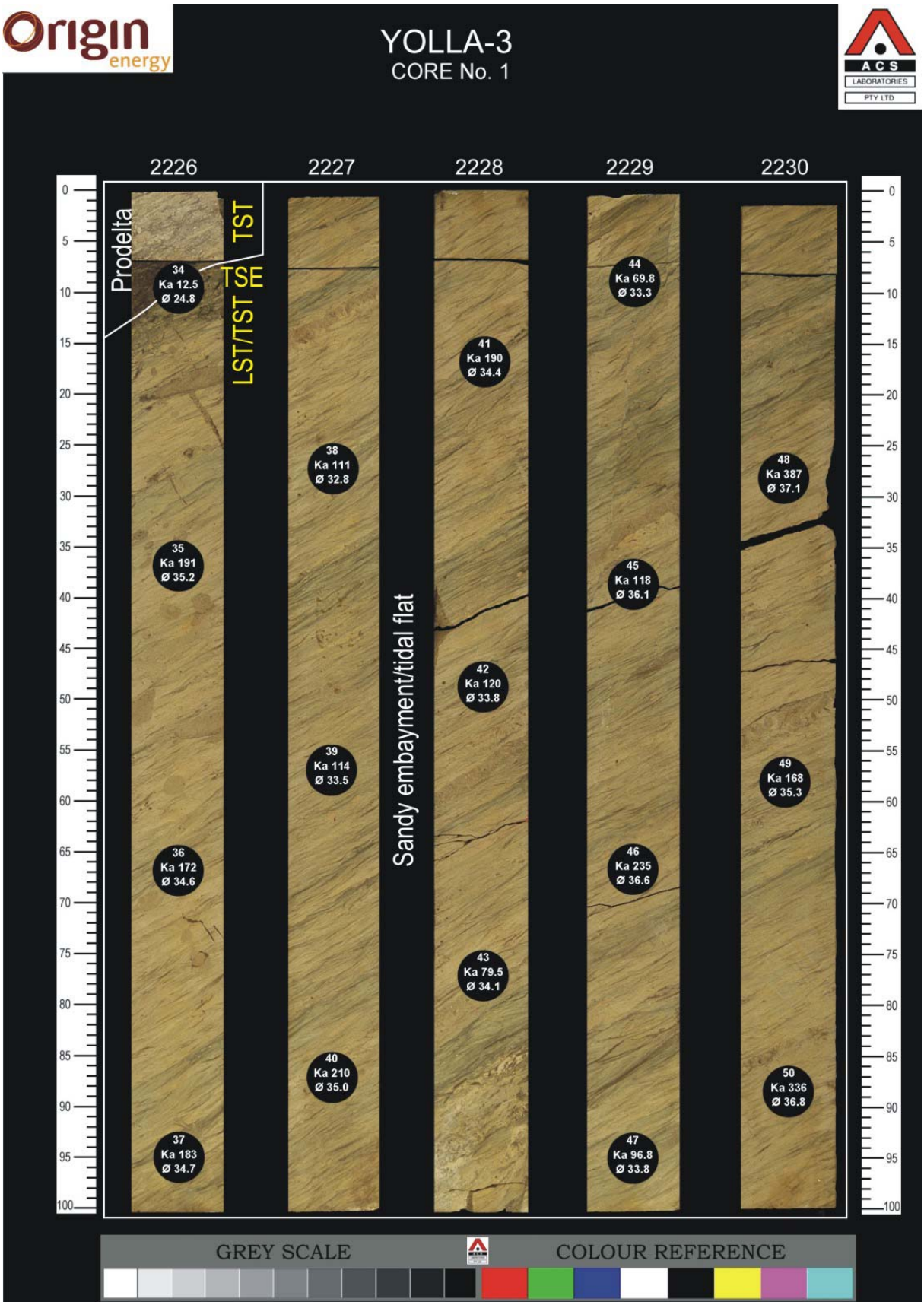
YOLLA-3
CORE No. 1
2226
2227
2228
2229
2230
Prodelta
TST
TSE
LST/TST
Sandy embayment/tidal flat
34 Ka 12.5 Ø 24.8
35 Ka 191 Ø 35.2
36 Ka 172 Ø 34.6
37 Ka 183 Ø 34.7
38 Ka 111 Ø 32.8
39 Ka 114 Ø 33.5
40 Ka 210 Ø 35.0
41 Ka 190 Ø 34.4
42 Ka 120 Ø 33.8
43 Ka 79.5 Ø 34.1
44 Ka 69.8 Ø 33.3
45 Ka 118 Ø 36.1
46 Ka 235 Ø 36.6
47 Ka 96.8 Ø 33.8
48 Ka 387 Ø 37.1
49 Ka 168 Ø 35.3
50 Ka 336 Ø 36.8
GREY SCALE
COLOUR REFERENCE

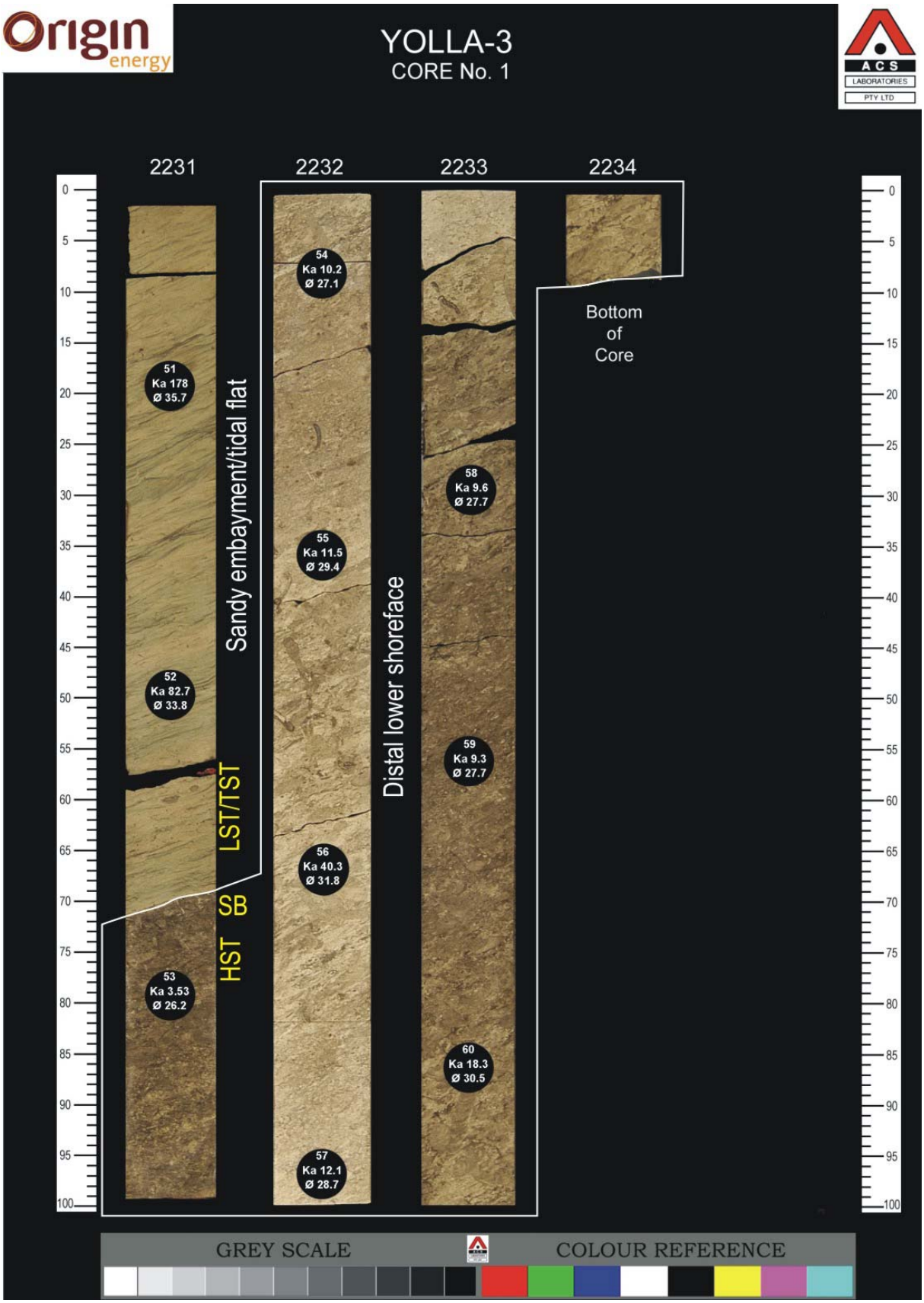
YOLLA-3
CORE No. 1
ACS LABORATORIES PTY LTD
2231
2232
2233
2234
Bottom of Core
Sandy embayment/tidal flat
Distal lower shoreface
LST/TST
SB
HST
51 Ka 178 Ø 35.7
52 Ka 82.7 Ø 33.8
53 Ka 3.53 Ø 26.2
54 Ka 10.2 Ø 27.1
55 Ka 11.5 Ø 29.4
56 Ka 40.3 Ø 31.8
57 Ka 12.1 Ø 28.7
58 Ka 9.6 Ø 27.7
59 Ka 9.3 Ø 27.7
60 Ka 18.3 Ø 30.5
GREY SCALE
COLOUR REFERENCE

APPENDIX 2

TRACE FOSSIL DESCRIPTIONS

The recognition of trace fossils in core is based primarily on their appearance in vertical cross section and due to preservational bias, full relief trace fossils (e.g. *Zoophycos, Teichichnus, Ophiomorpha, Palaeophycus* and *Chondrites*) are more easily recognised in core than epirelief or hyporelief traces (e.g. *Scolicia, Taenidium, Gyrochorte, Cochlichnus* and *Palaeodictyon*). Although it is important to recognise specific types of trace fossils, it is equally important to be able to differentiate between ethological groups, i.e. the behavioural groups traces represent. Such distinction has considerable ramifications for delineating typically depth related ichnofacies and reconstructing depositional histories. Behaviour is modified by prevailing ecological conditions that are dictated by the environment (Pemberton et al, 1992). The following descriptions are taken from Pemberton et al, (1992), Bromley (1996), and Bann and Fielding, (2004).

Asterosoma

Description: star shaped burrow system consisting of radial bulbous arms (15 to 50) tapering inward towards on elevated centre. The arms tend to be circular to irregular in cross sections and consist of very fine concentric laminae of silt and clay packed around a sand filled central shaft. The exterior is generally smooth, but may exhibit longitudinal striae or wrinkles.

Discussion: based on the tubular construction of the galleries and the details of sediment reworking, *Asterosoma* as been interpreted as a feeding burrow of a worm-like organism. The animal appears to have probed repeatedly into the sediment to enlarge the gallery and work more sediment both vertically and horizontally; exact details of the process, however, remain conjectural. The sediment fill may be related to feeding/waste storage functions. *Asterosoma* represents a specialised feeding structure and is more commonly associated with fully marine conditions. It is a common element of the *Cruziana* ichnofacies and can be found in conjunction with *Rosselia* at the top of the lower shoreface.

Bergauria

Description: cylindrical to hemispherical, plug shaped vertical burrows that are circular in cross section. Burrow walls are smooth with unornamented walls. The bases are rounded, with or without a central depression and radial ridges.

Discussion: *Bergauria* is interpreted as the resting or dwelling traces of actinian anemones.

Chondrites

Description: *Chondrites* is a complex burrow system consisting of regularly branching feeding tunnels of uniform diameter. These tunnels never inter-penetrate nor cross-cut one another. Branching typically is in one form of side branches (up to 5 or 6 orders) angling off a previous or main tunnel at 30 – 40°, rather than bifurcating at Y-shaped junctions. In core, *Chondrites* commonly appears as an array of thin elliptical dots where the vertical slice through the core truncates the numerous branching tunnels. In some instances, longitudinal sections through individual tunnels may show actual branches.

Discussion: it has been suggested that *Chondrites* represents tunnels produced by deposit feeding sipunculids, which worked from a fixed centre on the substrate surface and created the tunnels by extending its proboscis. However, some forms of *Chondrites* penetrate so deeply into the substrate that they could only be produced by a vermiform animal dwelling within the structure, moving bodily through the sediment in a similar manner to some modern polychaetes. *Chondrites* is a common element of the *Cruziana* and *Zoophycos* ichnofacies typical of offshore deposits and the trace making organism is considered to be well adapted to low oxygen conditions.

Cylindrichnus

Description: cylindrical to sub-cylindrical gradually conical straight to gently curved burrows with multiple concentrically layered walls. Burrows are typically sub-vertical in which the sediment typically is of the same lithology and texture as the host sediment.

Discussion: *Cylindrichnus* is almost identical to the basal shaft of *Rosselia. Cylindrichnus* fills represent passive, gravity induced sedimentation within open lined burrows and is interpreted as the dwelling burrow of a suspension feeding organism (polychaete or crustacean). The lining of the burrow possibly represents mud filtered from the water column. The burrows show response to gradual sediment aggradation. Although generally associated with the *Skolithos* ichnofacies, *Cylindrichnus* has been found in a wide variety of marine and brackish water environments.

Diplocraterion

Description: vertical, U-shaped spreiten burrows; the spreiten may be retrusive, protrusive, or a combination of both. Aperture of the tubes may be cylindrical or funnel shaped; limbs of the U can be parallel or divergent. Longitudinal sections appear as vertically stacked, menisci bounded by distinct walls and terminating in a distinct burrow that corresponds to the bottom of the U-tube. In some instances, *Diplocraterion* can appear in core as dumbbell shaped burrows on the tops of beds; the paired circular

openings are joined by a horizontal band of reworked sediment corresponding to the spreiten.

Discussion: based on analysis of morphological features, *Diplocraterion* has been interpreted as the dwelling burrow of a suspension feeding organism. Probable originators include polychaetes or other worm-like organisms and amphipod crustaceans. *Diplocraterion* is a common element in the distal portion of the *Skolithos* ichnofacies in middle shoreface settings, it is also common on sandy tidal flats and in estuarine channel deposits.

Helminthopsis

Description: irregularly meandering, smooth walled burrows that never branch, interpenetrate or cut across one another. In cross section, the burrows are elliptical to sub-circular and are generally horizontal. General burrow fill is dissimilar from the surrounding matrix and individual burrows are quite small (1 to 3 mm, on average). In core, *Helminthopsis* commonly appear as tiny dark spots (transverse section) or dark lines (longitudinal section).

Discussion: *Helminthopsis* has been interpreted as a grazing structure produced by a systematic grazing polychaete (or worm-like organism). It is a common element of the distal *Cruziana* ichnofacies and proximal *Zoophycos* ichnofacies on a normal marine shallow shelf.

Macaronichnus

Description: unlined, distinctly walled, predominantly horizontal, randomly curving and meandering to distinctly spiralled cylindrical burrows that rarely interpenetrate, never branch and are characterised by a thin mantle of mafic minerals. The fill is of the same lithology and texture as the host sediment.

Discussion: *Macaronichnus* is distinguished from the similar Ichnological *Planolites* and *Palaeophycus* by the presence of an outer mantle produced by the backfill of a deposit feeder, not a dwelling burrow like *Palaeophycus*. The zoned backfill has been created by particle segregation during the process of feeding with the preferential ingestation of quartz and feldspar sand and avoided mica flakes and mafic grains. If the sediment has few dark grains, the contrast between the sediment and burrow fill may be negligible. *Macaronichnus* occupied a deep tier position and therefore has a high preservation potential and is a common component of the *Skolithos* ichnofacies.

Ophiomorpha

Description: simple to complex burrow systems distinctly lined with agglutinated, pelleted sediment. Burrow lining is near-smooth on the interior and densely to strongly mamillated, or nodose on the exterior of the lining. Individual pellets or pellet masses may be discoid, ovoid, conical, mastoid, bilobate, or irregular in shape. Characteristics of the fill may vary, but in some instances *Ophiomorpha* may be filled actively with meniscoid laminae or well developed floor deposits. Branching is irregular and, where present, is Y- or T-shaped; at bifurcations, burrows become swollen.

Discussion: *Ophiomorpha* has been interpreted as the dwelling burrow of a decapod crustacean (especially thalassinidean shrimp). It is commonly associated with the *Skolithos* ichnofacies. *Ophiomorpha* is also associated with brackish water deposits including estuaries and tidal shoals.

Palaeophycus

Description: infrequently branched, distinctly lined, cylindrical, horizontal to inclined burrows in which the sediment typically is of the same lithology and texture as the host stratum. Wall linings range from very thin to relatively thick, and are either smooth, longitudinally striated, or with transverse annuli. Diameters are variable but commonly range from 3 to 8 mm.

Discussion: *Palaeophycus* is distinguished from morphologically similar ichnogenus *Planolites* primarily by the presence of wall linings and the character of the burrow fill. *Palaeophycus* fills represent passive, gravity induced sedimentation within open, lined burrows; the fillings, therefore, tend to be of the same composition as the surrounding matrix. Passively filled, lined burrows are typically interpreted as dwelling structures. The burrow of the predaceous polychaete, *Glyceria*, has been taken as an excellent modern analogue for *Palaeophycus*. Although, generally associated with *Skolithos* ichnofacies, the morphologically simple *Palaeophycus* has been found in a wide variety of marine and brackish water environments.

Phycosiphon

Description: irregular meandering burrows with a black core and a pale halo of coarser silt particles. In cross section, the burrows are elliptical to sub-circular, U-shaped in the longitudinal profile with an erratic distribution. Extensive bioturbation creates a mottled texture that obscures most traces. In core, *Phycosiphon* commonly has the appearance of tiny dark pin-head size spots (transverse section) or dark U-shaped lines (longitudinal section), which may by discontinuous and surrounded by a pale silt halo.

Discussion: *Phycosiphon* represents the feeding/grazing burrows of polychaetes or other worm-like phyla. It is a common element of the *Cruziana* ichnofacies and is often found as an opportunistic coloniser of storm deposited sands.

Planolites

Description: unlined, rarely branched, straight to tortuous, smooth to irregular walled, burrows in which the structureless fill is different from the host rock. *Planolites* is circular to elliptical in cross section and its dimensions are highly variable (typically 3 to 8 mm).

Discussion: *Planolites* is distinguished from *Palaeophycus* primarily by having unlined walls and burrow fills differing in texture from that of the adjacent rock; fills may also differ in fabric, composition and colour as well. Fills of *Planolites* represent sediment processed by the trace-maker especially through the deposit feeding activities of mobile infaunal polychaetes (or other worm-like organisms). Due to its simple morphology, *Planolites* has been found in virtually every environment, from fluvial overbank to deep sea.

Rhizocorallium

Description: straight to sinuous, U-shaped spreiten burrows. Tubes are generally distinct and more or less parallel; ratio of tube diameter:diameter of spreite is 1:5. Spreite are typically protrusive. Burrow fill is commonly identical to the matrix, but in some cases, is finer grained. In core *Rhizocorallium* is identified by two circular burrows (tube arms) joined by a horizontal band (spreite). Tube walls are commonly ornamented with distinct scratch marks.

Discussion: *Rhizocorallium* has been interpreted as the feeding structure produced by a deposit feeder. The presence of distinct scratch marks on the tube wall is consistent with a crustacean origin. *Rhizocorallium* is generally associated with the distal *Cruziana* ichnofacies that characterises fully marine offshore environments. It is also a common element of the *Glossifungites* ichnofacies that characterises firmground substrates.

Rosselia

Description: single entrance cylindrical, vertical to inclined, straight to gently curved burrows with an expanded, bulbous opening. This bulb is filled with finer grained sediment arranged in poorly developed concentric layers. In transverse section the bulbs are circular to sub-circular and taper at both ends. The cylindrical shaft also displays concentric layering, is commonly curved, and in most cases it penetrates the shaft filled bulb.

Discussion: the basal shaft of *Rosselia* is almost identical to *Cylindrichnus* and complete intergradations among specimens individually referable to *Skolithos*, *Cylindrichnus, Rosselia,* and *Asterosoma* have been noted. *Rosselia* has been interpreted as the feeding burrow of a deposit feeding annelid (or other worm-like phyla), that filtered mud from the water column and packed it into a ball. The bulb was enlarged and may have served a food/waste storage function. *Rosselia* is generally associated with the proximal *Cruziana* ichnofacies in fully marine settings.

Skolithos

Description: single entrance, vertical to inclined, straight to curved burrows that never branch, cross over or interpenetrate. In cross sections the shafts are cylindrical to sub-cylindrical and either lined or unlined. Linings, where present, seldom exceed 1 mm, and consist of either dark organic mud or clean agglutinated sand. The walls are generally smooth, but they may be annulated and the fill is typically massive.

Discussion: ethologically, *Skolithos* represents the dwelling burrow of a suspension feeder or passive carnivore. Probable originators could include a large number of organisms from polychaetes to phoronids, to insect larvae. Because *Skolithos* can be constructed by many different kinds of organisms it is found in virtually every type of environment.

Teichichnus

Description: vertical tubular structures built as a series of tightly packed concave up or (more rarely) concave down crescentic laminae. Longitudinal sections show wavy, long laminae that usually merge upward at the ends. A distinct horizontal, circular to sub-circular, burrow is always present as the upper or lower end of the laminae.

Discussion: *Teichichnus* is generally interpreted as the dwelling/feeding burrow of a deposit feeding organism. Probable originators include annelids, or other worm-like phyla. The *Teichichnus* producing animal appears to be migrating either upward or downward in its burrow. The spreite probably represents an equilibrium response of the trace maker i.e. an attempt to maintain the bottom of its burrow at an optimal depth below the sediment water interface. Although commonly associated with the *Cruziana* ichnofacies, *Teichichnus* is also prevalent in brackish water lagoon/bay environments.

Terebellina

Description: sub-cylindrical, vertical, gently to strongly curved burrows with circular to elliptical cross sections. Diameters are highly variable and the tubes gradually taper distally. The lining is very distinct, ranges in thickness from 1.5 to 5 mm, is composed of

either calcium carbonate or silt grains, and is more resistant to weathering than either the surrounding matrix or the burrow fill. Material filling the burrow is similar in composition to the host rock. In core, specimens generally appear horizontal due to the curvature of the tube.

Discussion: *Terebellina* was originally interpreted as the body fossil of a polychaete, however, because it is a tube constructed by the organism, it must be considered an ichnofossils. Based on its morphological characteristics, *Terebellina* can be interpreted as the dwelling burrow of a suspension feeding organism similar to the sabelliarid polychaetes. *Terebellina* is commonly found in the distal *Cruziana* ichnofacies that characterises offshore marine environments. It represents a special adaptation for constructing an open tube in fine grained argillaceous substrates.

Thalassinoides

Description: relatively large burrow system consisting of smooth walled, essentially cylindrical components. Branches are Y- to T-shaped and are enlarged at points of bifurcation. Burrow dimensions may vary within a given system and cross sections are half moon shaped to elliptical. Although most systems are essentially horizontal, others are irregularly inclined. Structureless to parallel laminated or graded burrow fills represent passive (gravity induced) sedimentation whereas meniscoid or chevron laminated fill represents active backfilling by the trace maker.

Discussion: very thinly lined to essentially unlined burrow systems are characteristic of fine grained coherent substrates that do not require reinforcement. *Thalassinoides* is generally regarded as a dwelling and/or feeding burrow of a decapod crustacean (thalassinid shrimp). It is associated with the *Cruziana* ichnofacies in the lower shoreface to offshore environments and is also found in low diversity, brackish water assemblages. Enlarged junction points are often used as turning points for the organism, or as breeding chambers.

Zoophycos

Description: circular to lobate, flat to curved, horizontal to inclined sheets of spreite wound in a screw-like fashion around a central vertical axis. The spreite consist of closely juxtaposed burrow tunnels that are filled with the host sediment.

Discussion: the *Zoophycos* tracemaker and the purpose are uncertain. It has been interpreted as the feeding and/or grazing structure of a vermiform organism with an extendable/retractable body. *Zoophycos* is a deep tier structure that is common in the *Zoophycos* and *Cruziana* ichnofacies.

ENCLOSURE 1

YOLLA 3 CORE 1 – EVCM

YOLLA 3

CORE 1 - EVCM

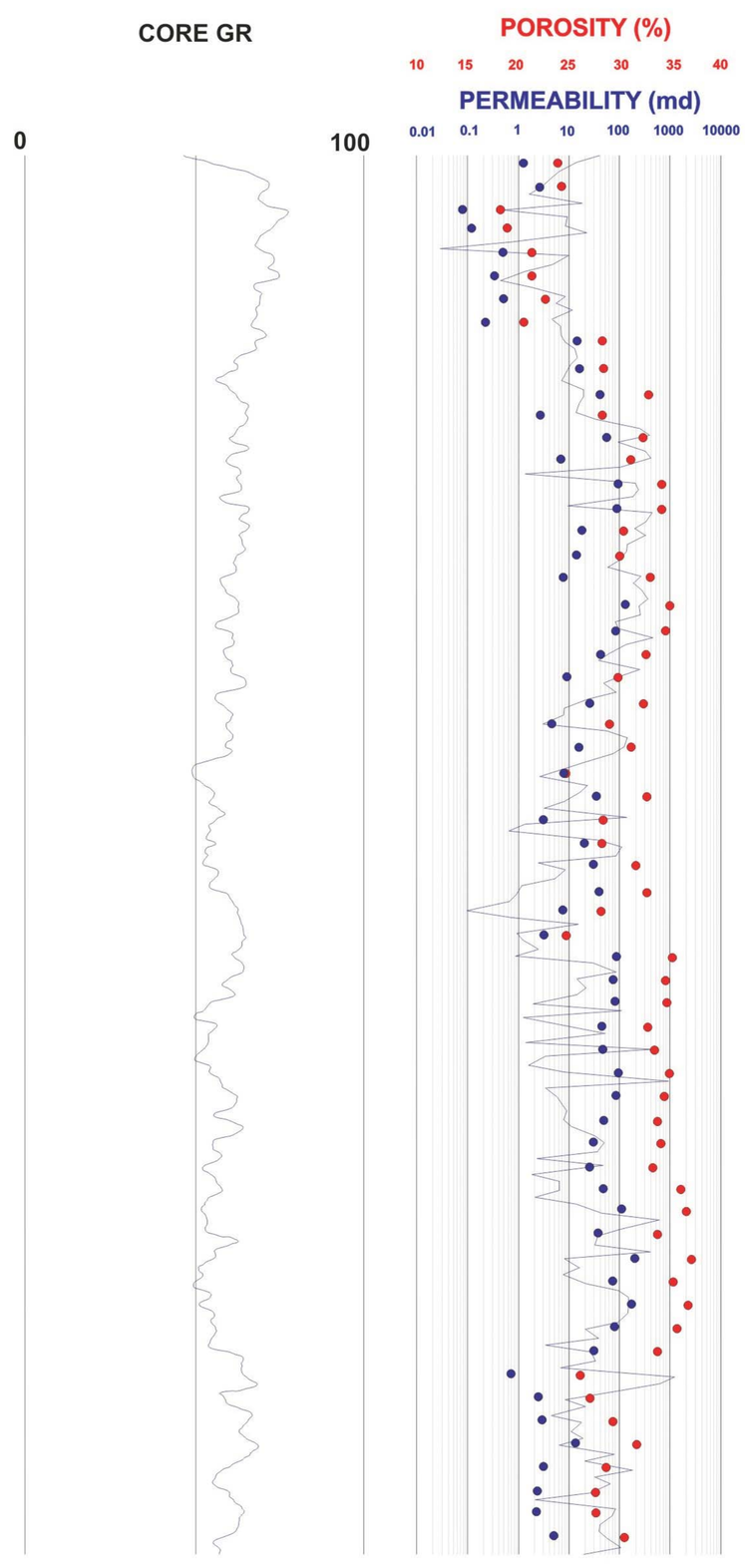

PLUG DATA

- Porosity
- Permeability

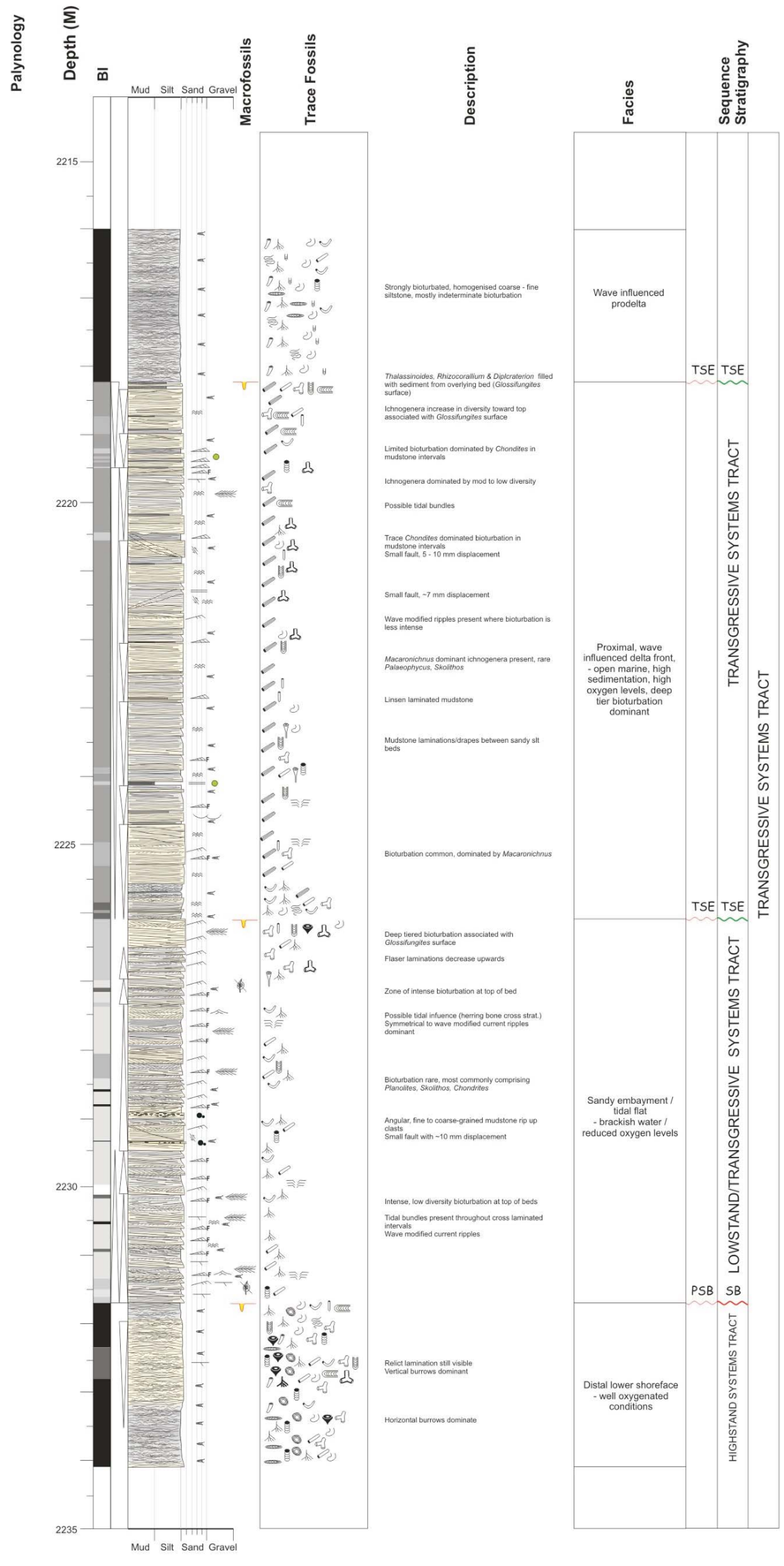

Siliciclastic

- Siltstone - mudstone/anoxic mudstone
- Sandstone
- Conglomerate
- Tuff

Origin energy

delivering the goods

PHYSICAL SEDIMENTARY STRUCTURES

- Trough cross-bedding
- Planar cross-bedding
- Flat lamination
- Plane bedding
- Low-angle lamination
- Current Ripple Cross-lamination
- Wave Ripple Cross-lamination
- Flaser bedding
- Lenticular lamination
- Wavy lamination
- Hummocky cross-stratification
- Bioturbation
- Plant debris
- Wood
- Rip-up clasts
- Extraformational pebbles
- Soft sediment deformation
- Convoluted bedding
- Synaeresis cracks
- Stylolites
- Coaly trace
- Root trace
- Carbonaceous laminae
- Fault
- Erosional base
- Slumped sediment
- Fining upwards
- Coarsening upwards
- Herring bone cross stratification
- Calcite cementation
- Glauconite
- Pyrite
- Siderite/Fe-concretion
- Silica cementation
- Calcite-healed fracture
- Silica-healed fracture
- Fracture/fault with slickensides

ICHNOLOGY

- *Ophiomorpha*
- *Skolithos*
- *Diplocraterion*
- *Macaronichnus*
- *Thalassinoides*
- *Planolites*
- *Palaeophycus*
- *Rhizocorallium*
- *Teichichnus*
- *Phycosiphon*
- *Taedium*
- *Cylindrichnus*
- *Zoophycus*
- *Rosselia*
- *Conichnus*
- *Chondrites*
- *Undifferentiated*
- *Asterosoma*
- *Helminthopsis*
- *Schaubcylindrichnus*
- *Terebellina*
- *Glossifungites surface*
- *Escape burrow*

Bioturbation Index

0 1 2 3 4 5 6

MACROFOSSILS

- *Brachiopods*
- *Molluscs*
- *Bryozoans*
- *Crinoids*
- *Forams*
- *Algae*
- *Stromatolites/stromatoporoids*
- *Unidentified shell fragments*
- *Ammonite*
- *Gastropods*

APPENDIX 6: SPECIAL CORE ANALYSIS

SPECIAL CORE ANALYSIS FINAL REPORT

of

YOLLA-3

for

ORIGIN ENERGY RESOURCES LIMITED

by

ACS LABORATORIES PTY LTD

17 February, 2005

Origin Energy Resources Limited
Level 6
1 King William Street
ADELAIDE SA 5000

Attention: Joe Parver

Origin Energy Resources Limited
1st Floor, John Oxley Centre
339 Coronation Drive
MILTON QLD 4064

Attention: Andy Hall

FINAL REPORT: 0476-08

CLIENT REFERENCE: O4643

MATERIAL: Core Plugs

LOCALITY: Yolla-3

WORK REQUIRED: Special Core Analysis

Please direct technical enquiries regarding this work to the signatories below under whose supervision the work was carried out.

KEVIN H FLYNN
General Manager

CONTENTS

CHAPTERS PAGE

APPENDICES

CHAPTER 1

INTRODUCTION

1. INTRODUCTION

This final report presents the results from a special core analysis study of the Yolla-3 core. The samples utilized were 1½ inch diameter core plugs originally drilled for a routine core analysis study (performed by ACS Laboratories) on the same well.

Following discussions between Origin Energy Resources Limited and ACS Laboratories representatives, the test program was refined to that presented in summary format in Chapter 2 of this report. The subsequent chapters encompass descriptions of procedures and test results. The Appendices include ancillary information pertinent to the study.

CHAPTER 2

SUMMARY OF TEST PROGRAM

FLOW CHART

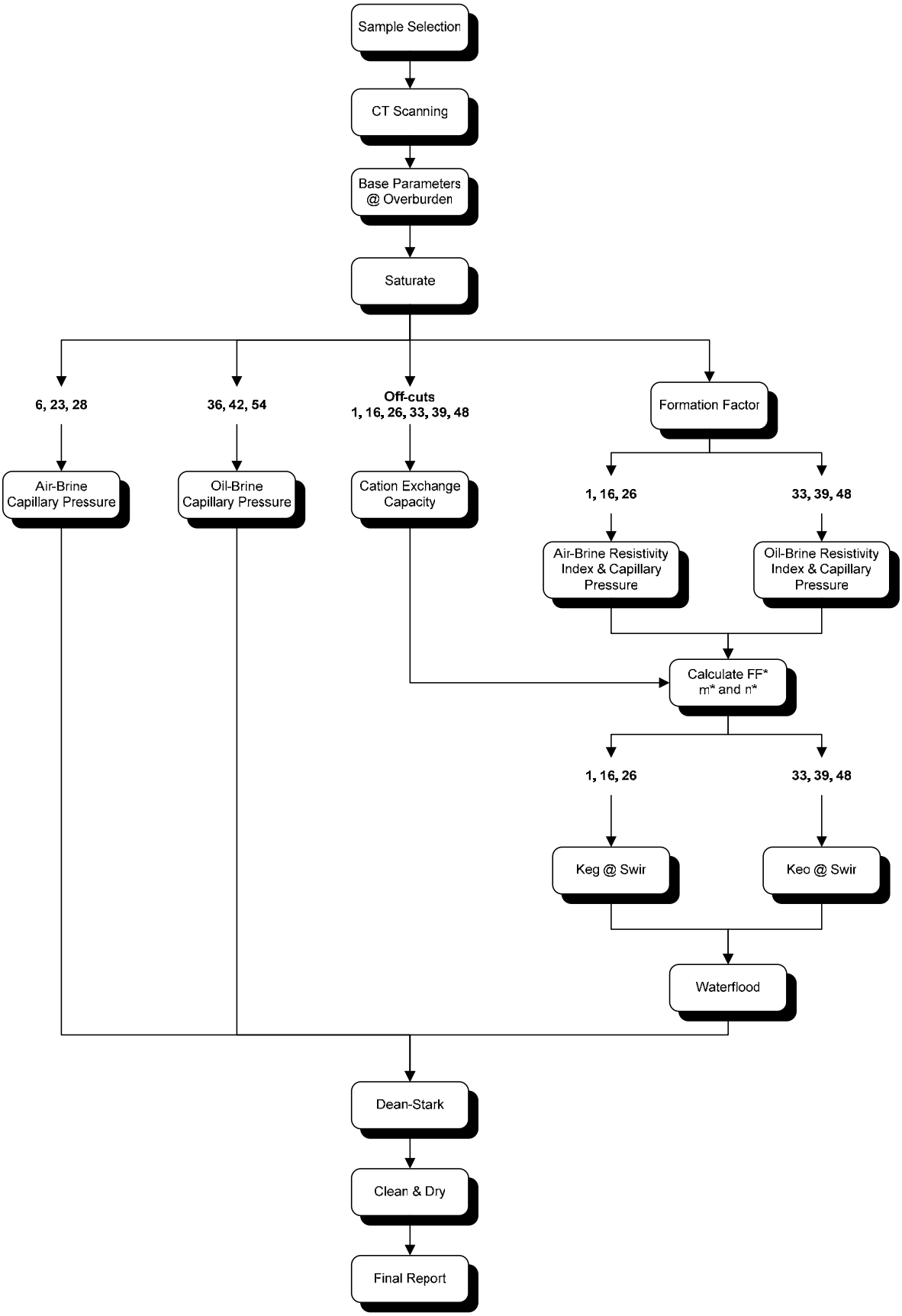
Sample Selection
CT Scanning
Base Parameters @ Overburden
Saturate
6, 23, 28
36, 42, 54
Off-cuts 1, 16, 26, 33, 39, 48
Formation Factor
Air-Brine Capillary Pressure
Oil-Brine Capillary Pressure
Cation Exchange Capacity
1, 16, 26
33, 39, 48
Air-Brine Resistivity Index & Capillary Pressure
Oil-Brine Resistivity Index & Capillary Pressure
Calculate FF* m* and n*
1, 16, 26
33, 39, 48
Keg @ Swir
Keo @ Swir
Waterflood
Dean-Stark
Clean & Dry
Final Report

TEST SCHEDULE

Client: Origin Energy Resources Limited
Well/Project: Yolla-3
ACS File No: 0476-08

F = failed
C = cancelled

		Test Sequence											
Sample	***Depth***	***Overburden Base Parameters***	***CT Scan***	***Saturate***	***Formation Factor***	***Resistivity Index***	***Air-Brine Capillary Pressure***	***Oil-Brine Capillary Pressure***	***Keg @ Swir***	***Keo @ Swir***	***Waterflood***	***Cation Exchange Capacity***	***Clean & Dry***
1	2216.10		X	X	X	X	X		X		X	X	X
6	2217.55	X	X	X			X						X
16	2220.58		X	X	X	X	X		X		X	X	X
23	2222.76	X	X	X			X						X
26	2223.66	X	X	X	X	X	X		X		X	X	X
28	2224.30		X	X			X						X
33	2225.77	X	X	X	X	X		X		X	X	X	X
36	2226.67	X	X	X				X					X
39	2227.57	X	X	X	X	X		X		X	X	X	X
42	2228.49	X	X	X				X					X
48	2230.27	X	X	X	X	X		X		X	X	X	X
54	2232.08	X	X	X				X					X
	Total	9	12	12	6	6	6	6	3	3	6	6	12

CHAPTER 3

SAMPLE PREPARATION AND BASE PARAMETER DETERMINATIONS

3.1 Test and Calculation Procedures

3. SAMPLE PREPARATION AND BASE PARAMETER DETERMINATIONS

3.1 Test and Calculation Procedures

3.1.1 CT Scanning

CT Scanning was undertaken in order that internal inhomogeneities and/or drilling fluid invasion zones may be noted. Typical inhomogeneities may be clasts, bedding sedimentary structures, cementation, fractures and any other discontinuities that may not be readily visible to the naked eye.

The principle of CT Scanning and its applications is presented by Hove et al, 1987 and Wellington and Vinegar, 1987.

CT Scanners generate cross-sectional image slices through the sample by revolving an X-ray tube around the sample and obtaining projections at many different angles (Appendix I). From these image slices, a cross-sectional image was reconstructed by a back projection algorithm in the scanner's computer.

Prior to analysis, an arbitrary orientation line was inscribed onto the sample using a marker to facilitate subsequent re-orientation. The sample was placed vertically within the scanner, with the orientation arrow left to right, and a longitudinal section image obtained. The sample was then rotated through exactly 90^o to the initial orientation, and another section image recorded. These two images are labelled '0' and '90' on the prints.

All images are presented here in a standard ACS format and are stored digitally.

3.1.2 Base Parameters

All ambient base parameters were performed during the routine core analysis study.

Porosity

Porosity was determined in two stages. Initially each sample was placed in a sealed matrix cup. Helium held at 100 psi reference pressure was then introduced to the cup. From the resultant pressure drop the unknown grain volume was determined using Boyle's Law.

$$P_1 V_1 = P_2 V_2$$

$$\Rightarrow P_1 Vr = P_2 (Vr + Vc + Vl - Vg)$$

where

P_1	=	*initial pressure (psig)*
Vr	=	*reference cell volume (cm^3)*
Vc	=	*matrix cup volume (cm^3)*
Vl	=	*line volume (cm^3)*
Vg	=	*grain volume (cm^3)*
P_2	=	*final pressure (psig)*

$$\text{and} \quad \rho = \frac{Wt}{Vg}$$

where ρ = grain density (g/cm^3)
Wt = weight of sample (g)
Vg = grain volume (cm^3)

The samples were then placed into individual thick walled rubber sleeves and the assembly loaded into a hydrostatic cell. With an ambient pressure (400 psi) applied to the sample, helium held at 100 psi reference pressure was released into the samples pore volume. The resultant pressure drop was used to determine pore volume at ambient. The confining pressure was then increased to the overburden pressure of 3200 psi and the resultant change in internal pore pressure was monitored and used to determine pore volume at overburden conditions.

$$Vb = Vp + Vg$$

$$\text{Ambient Porosity \%} = \frac{Vp}{Vb} x\,100$$

$$\text{Overburden Porosity \%} = \frac{Vp - \Delta Vp}{Vb - \Delta Vp} x\,100$$

where Vp = ambient pore volume (cm^3)
Vb = ambient bulk volume (cm^3)
Vg = grain volume (cm^3)
ΔVp = change in pore volume (cm^3)

Permeability to Air

The samples were placed into a hydrostatic cell (Appendix II) with an ambient confining pressure of 400 psi applied. The confining pressure was used to prevent bypassing of air around the sample when the measurement was made. In order to determine permeability a known air pressure was applied to the upstream face of each sample, creating a flow of air through the core plug. Air permeability for each core sample was calculated using Darcy's Law through knowledge of the upstream pressure, flow rate, viscosity of air and sample dimensions.

$$Ka = \frac{2000.BP.\mu.q.L}{(P_1^2 - P_2^2).A}$$

where	*Ka*	=	*air permeability (milliDarcy's)*
	BP	=	*barometric pressure (atmospheres)*
	μ	=	*gas viscosity (cP)*
	q	=	*flow rate (cm^3/s)*
	L	=	*sample length (cm)*
	P_1	=	*upstream pressure (atmospheres)*
	P_2	=	*downstream pressure (atmospheres)*
	A	=	*sample cross sectional area (cm^2)*

The confining pressure was then increased to the overburden pressure of 3200 psi and the above procedure repeated to give permeability at overburden conditions.

3.1.3 Sample Saturation

The selected samples were initially vacuum saturated with 60000 ppm NaCl equivalent brine (Appendix I) followed by pressure saturation at 2000 psi for a minimum of 12 hours. To determine complete saturation, the saturations were determined by mass balance and compared with that of porosimetry. In all cases the samples were deemed suitable to proceed with the test program.

CHAPTER 3

SAMPLE PREPARATION AND BASE PARAMETER DETERMINATIONS

3.2 Test Results

BASE PARAMETERS

Client : Origin Energy Resources Limited
Well : Yolla-3

Overburden Pressure 3200 psi

Sample Number	Depth (metres)	Ambient Porosity (percent)	Overburden Porosity (percent)	Grain Density (g/cm^3)	Ambient Permeability (milliDarcy's)	Overburden Permeability (milliDarcy's)
1	2216.10	23.9	22.9	2.64	5.8	3.90
6	2217.55	21.4	20.3	2.63	1.89	1.01
16	2220.58	34.2	33.1	2.66	196	171
23	2222.76	29.9	28.8	2.72	30.1	23.2
26	2223.66	31.1	30.0	2.70	47.4	38.3
28	2224.30	32.7	31.7	2.73	90.2	78.6
33	2225.77	28.2	27.1	2.68	25.4	20.2
36	2226.67	34.6	33.6	2.67	172	149
39	2227.57	33.5	32.4	2.68	114	97.5
42	2228.49	33.8	32.6	2.67	120	102
48	2230.27	37.1	36.1	2.67	387	333
54	2232.08	27.1	25.8	2.66	10.2	7.9

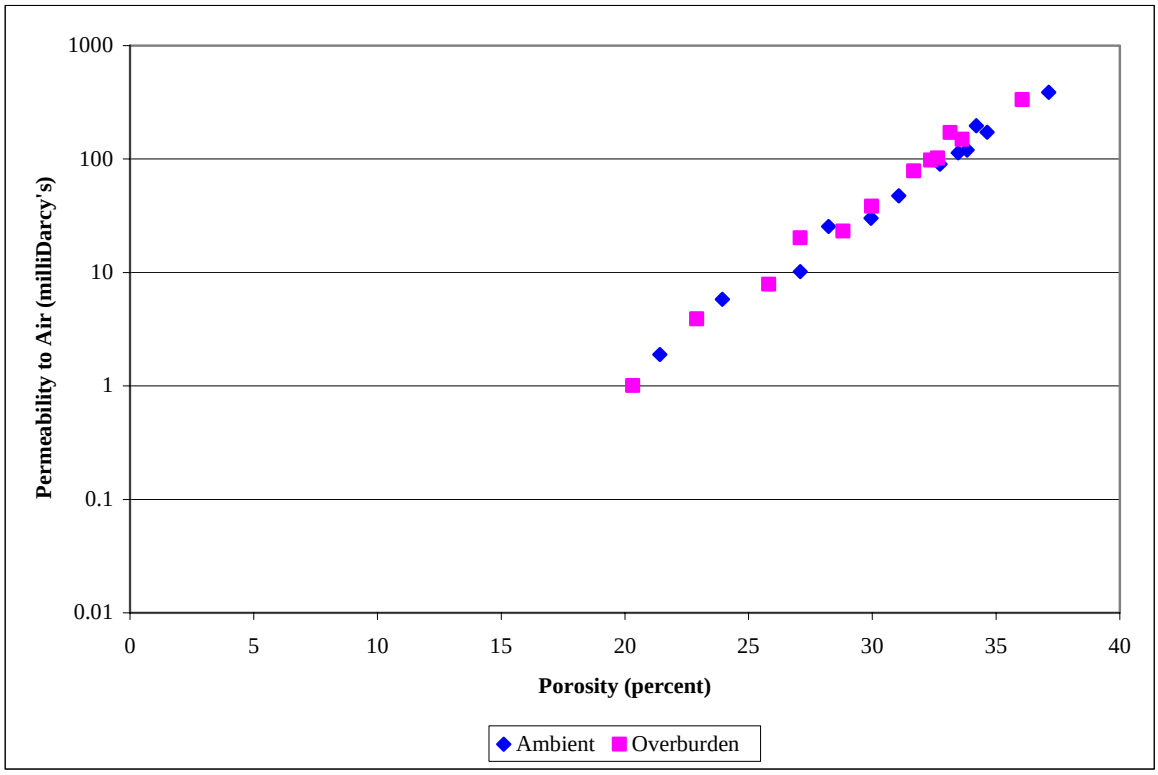

CHAPTER 4

ELECTRICAL PROPERTIES AND CAPILLARY PRESSURE

4.1 Test and Calculation Procedures

4. ELECTRICAL PROPERTIES AND CAPILLARY PRESSURE

4.1 Test and Calculation Procedures

4.1.1 Formation Resistivity Factor

On completion of base parameter and pressure saturation with 60000 ppm brine, the ten selected samples continued on for formation resistivity factor analyses.

Each fully brine saturated sample was sandwiched between a pair of stainless steel core holder platens. These platens also act as the current carrying and potential electrodes. A thin silver leaf was also placed between the plug endfaces and electrodes, to ensure electrical contact. A strongly hydrophilic membrane was placed at the bottom end of the sample. This assembly was placed into a snugly fitting rubber overburden sleeve and then loaded into a Hydrostatic type core holder. A confining pressure was gradually applied as an effective overburden pressure (see Appendix II for schematic).

Synthetic brine (Appendix I) was slowly flowed through each sample at a rate of $0.5 cm^3$/min. During this process sample resistivity was monitored on a digi-bridge capable of measuring sample resistance to 0.001 (ohms) accuracy. In each case the current frequency was selected to yield minimum phase angles, thus ensuring maximum electrical contact (between each sample and the current carrying and potential electrodes). Values of sample resistance (Rc) and effluent brine resistivity (Rw) were recorded daily. Each sample was deemed to be at ionic equilibrium when three consecutive daily readings were recorded within 1%.

From these stable data, the following results were recorded:

$$Ro = \frac{A \,.\, Rc}{100 L}$$

where Ro = *sample resistivity (ohm.m)*
Rc = *sample resistance (ohms)*
L = *electrode gap (sample length - cm)*
A = *cross sectional area (cm^2)*
100 = *units conversion*

Formation resistivity factor was calculated using the following equations:

$$FF = \frac{a}{\Phi^m}$$

and

$$FF = \frac{Ro}{Rw}$$

where Rw = *brine resistivity (ohm.m)*
a = *intercept (assumed = 1)*
m = *cementation exponent*

and Φ = *porosity (fraction)*

The brine resistivity (Rw) was accurately determined by a NATA certified fluids laboratory.

4.1.2 Formation Resistivity Index and Capillary Pressure

Upon completion of the preceding formation resistivity factor analyses, the selected samples continued immediately for formation resistivity index analyses in conjunction with drainage capillary pressure curves. For samples 1, 16 and 26 the top endface port was connected to a supply of humidified air and the bottom port connected to a graduated receiving tube (Appendix II). Samples 33, 39 and 48 were connected to a pressure controlled supply of mineral oil. The samples were desaturated by gradually increasing the displacing fluid pressure to the samples. The actual pressures utilised were inversely proportional to the individual sample permeability data. The air-brine samples proceeded to a maximum pressure of 40 psi and the oil-brine to 20 psi (values supplied by Origin Energy Resources Limited). A small amount of oil was placed into the collection tubes to prevent any potential brine loss by evaporation. Sample resistances were measured at successive decreasing brine saturations, which were calculated from the following equation:

$$\textit{Water Saturation (\%)} = \frac{\textit{Pore Volume @ OB}\left(cm^3\right) - \textit{Brine Expelled}\left(cm^3\right)}{\textit{Pore Volume @ OB}\left(cm^3\right)} \textit{ x 100}$$

Capillary pressure curves plot water saturation (x-axis) against applied displacing fluid pressure. A hyperbolic curve is used to define this relationship. The ratio of the sample resistance (Rc) values to the previously determined FF values (at 100% saturation) were used to calculate the formation resistivity indices.

$$Rt = \frac{A \,.\, Rc}{100L}$$

where Rt = *resistivity of partially brine saturated sample (ohm.m)*
Rc = *sample resistance (ohms)*

and $$RI = \frac{Rt}{Rw \,.\, FF}$$

where RI = *resistivity index*
Rw = *resistivity of brine (ohm.m)*

(modified from standard Archie equation to include Rw).

These RI values (for each sample) were plotted against brine saturation (Sw) on graphs with logarithmic axes and the gradient of the best-fit line through the co-ordinate (1.0, 1.0) was calculated. Each gradient is quoted as the saturation exponent (n) for that sample, in accordance with Archie's formula.

$$RI = \frac{1}{Sw^n}$$

4.1.3 Capillary Pressure

Three samples were selected for air-brine capillary pressure (6, 23 and 28) and three samples for oil-brine capillary pressure (36, 42 and 54). Each fully brine saturated sample was sandwiched between a pair of stainless steel core holder platens with a strongly hydrophilic membrane at the bottom end of the sample. This assembly was placed into a snugly fitting rubber overburden sleeve and loaded into a hydrostatic type core holder and an overburden pressure of 3200 psi applied.

The top endface port was connected to a supply of humidified air or mineral oil and the bottom port connected to a graduated receiving tube (Appendix II). The samples were desaturated by gradually increasing the displacing fluid pressure to the samples. The actual pressures utilised were inversely proportional to the individual sample permeability data. The air-brine samples proceeded to a maximum pressure of 40 psi and the oil-brine to 20 psi. A small amount of oil was placed into the collection tubes to prevent any potential brine loss by evaporation. Sample resistances were measured at successive decreasing brine saturations, which were calculated from the following equation:

$$Water\ Saturation(\%) = \frac{Pore\ Volume\ @\ OB\ (cm^3) - Brine\ Expelled\ (cm^3)}{Pore\ Volume\ @\ OB\ (cm^3)}\ x\,100$$

Capillary pressure curves plot water saturation (x-axis) against applied displacing fluid pressure. A hyperbolic curve is used to define this relationship.

4.1.4 Cation Exchange Capacity

Cation exchange capacity was determined on approximately 5 grams of sample (off-cuts) using the wet chemistry method. The samples were first washed with an ammonium chloride solution to exchange ions with the available clay cations. An exchange reagent was then washed through the sample and the resultant solution titrated. Where a smaller sample is used the limit of detection becomes greater and a minimum value is reported.

Values of exchangeable cations (theoretical minimum of zero) present in the samples are reported as milliequivalents per 100 grams of dry sample (meq/100 g). Values of Q_v have been calculated using the following equation:

$$Q_v = \frac{CEC\,(1-\Phi)\rho}{100\,\Phi}$$

where ρ = *grain density (g/cm^3)*
Φ = *porosity (fraction)*
Q_v = *volume concentration of clay exchange cations (meq/cm^3 pore space)*
CEC = *cation exchange capacity (meq/100 g dry sample)*

Based on these CEC/Qv data, values of shaly sand equivalent formation factor (FF*), cementation factor (m*) and saturation exponent (n*) were calculated using the following equations:

$$FF^* = FF\,.\,(1 + B.Qv.Rw)$$

$$m^* = \frac{\log FF^*}{-\log \Phi}$$

$$n^* = \frac{\log\left[\dfrac{1 + Rw.B.Qv}{1 + Rw.B.Qv/Sw}\right] - \log FRI}{\log Sw}$$

where[1] $B = \dfrac{-1.28 + 0.225.T - 0.0004059.T^2}{1 + Rw^{1.23}\,.\,(0.045.T. - 0.27)}$

FF = *formation resistivity factor*
*FF** = *shaly sand equivalent formation resistivity factor*
*m** = *shaly sand equivalent cementation factor*
Φ = *porosity (fraction)*
*n** = *shaly sand equivalent saturation exponent*
Rw = *brine resistivity (ohm.m @ 25^{o}C)*
T = *temperature of 25°C*
B = *equivalent conductance of clay exchange cations*
Qv = *volume concentration of clay exchange cations*
Sw = *final saturation (fraction)*
FRI = *resistivity index @ saturation Sw*

[1] Juhasz, I., 1981, Normalized Q, - the key to shaly sand evaluation using the Waxman-Smits equation in the absence of core data, paper Z, in 22nd Annual Logging Symposium Transactions: Society of Professional Well Log Analysts, 36p.

CHAPTER 4

ELECTRICAL PROPERTIES AND CAPILLARY PRESSURE

4.2 Test Results

4.2.1 Formation Factor

FORMATION RESISTIVITY FACTOR

Client	Origin Energy Resources Limited	**Saturant**	60000 ppm
Well	Yolla-3	**Rw of Saturant**	0.116 at 25ºC
		Overburden	3200 psi
		Average m	1.85

Sample Number	Depth (metres)	Permeability to Air (milliDarcy's)	Porosity (percent)	Formation Factor FF	Cementation Exponent m
1	2216.10	3.90	22.9	17.5	1.94
16	2220.58	171	33.1	7.4	1.81
26	2223.66	38.3	30.0	9.5	1.87
33	2225.77	20.2	27.1	11.5	1.87
39	2227.57	97.5	32.4	7.9	1.83
48	2230.27	333	36.1	6.2	1.79

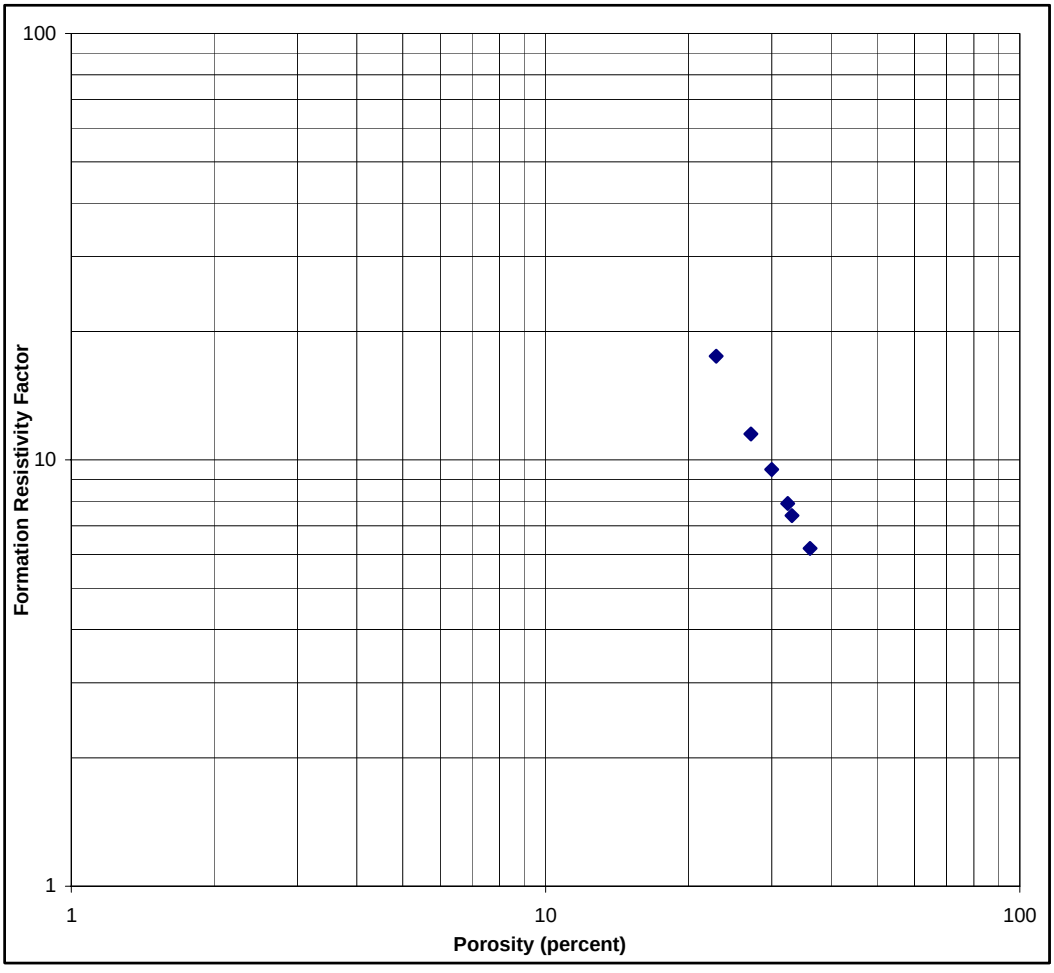

CHAPTER 4

ELECTRICAL PROPERTIES AND CAPILLARY PRESSURE

4.2 Test Results

4.2.2 Resistivity Index

RESISTIVITY INDEX

Client Origin Energy Resources Limited
Well Yolla-3

Rw of Saturant 0.116 at 25ºC
Method Air/Brine Porous Plate @ Overburden

Sample Number	Depth (metres)	Permeability to Air (milliDarcy's)	Porosity (percent)	Formation Factor FF	Brine Saturation (fraction)	Resistivity Index RI	Saturation Exponent n
1	2216.10	3.90	22.9	17.5	1.000	1.00	
					0.996	1.05	
					0.854	1.25	
					0.684	1.87	
					0.628	2.24	
					0.579	2.63	1.72

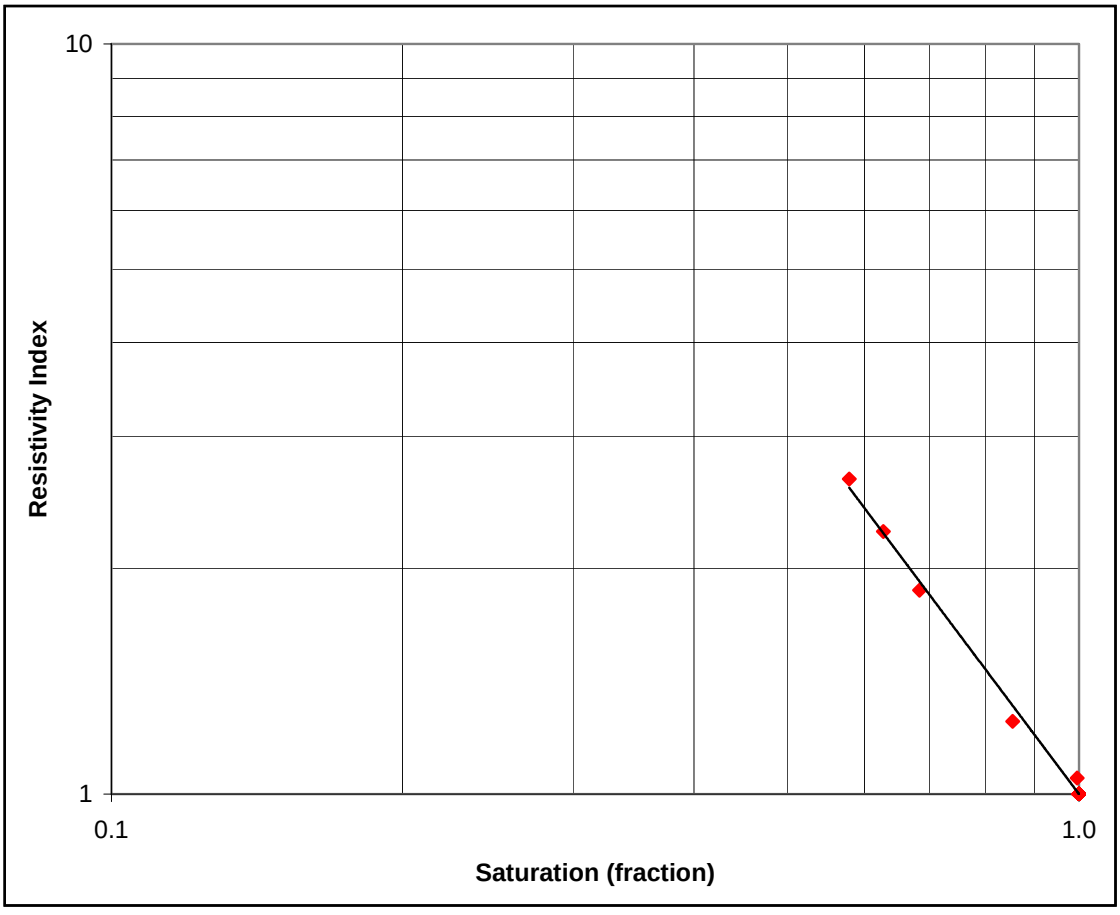

RESISTIVITY INDEX

Client Origin Energy Resources Limited
Well Yolla-3

Rw of Saturant 0.116 at 25ºC
Method Air/Brine Porous Plate @ Overburden

Sample Number	Depth (metres)	Permeability to Air (milliDarcy's)	Porosity (percent)	Formation Factor FF	Brine Saturation (fraction)	Resistivity Index RI	Saturation Exponent n
16	2220.58	171	33.1	7.4	1.000	1.00	
					0.983	1.06	
					0.568	2.61	
					0.452	4.16	
					0.402	5.05	
					0.382	6.11	
					0.355	7.07	1.83

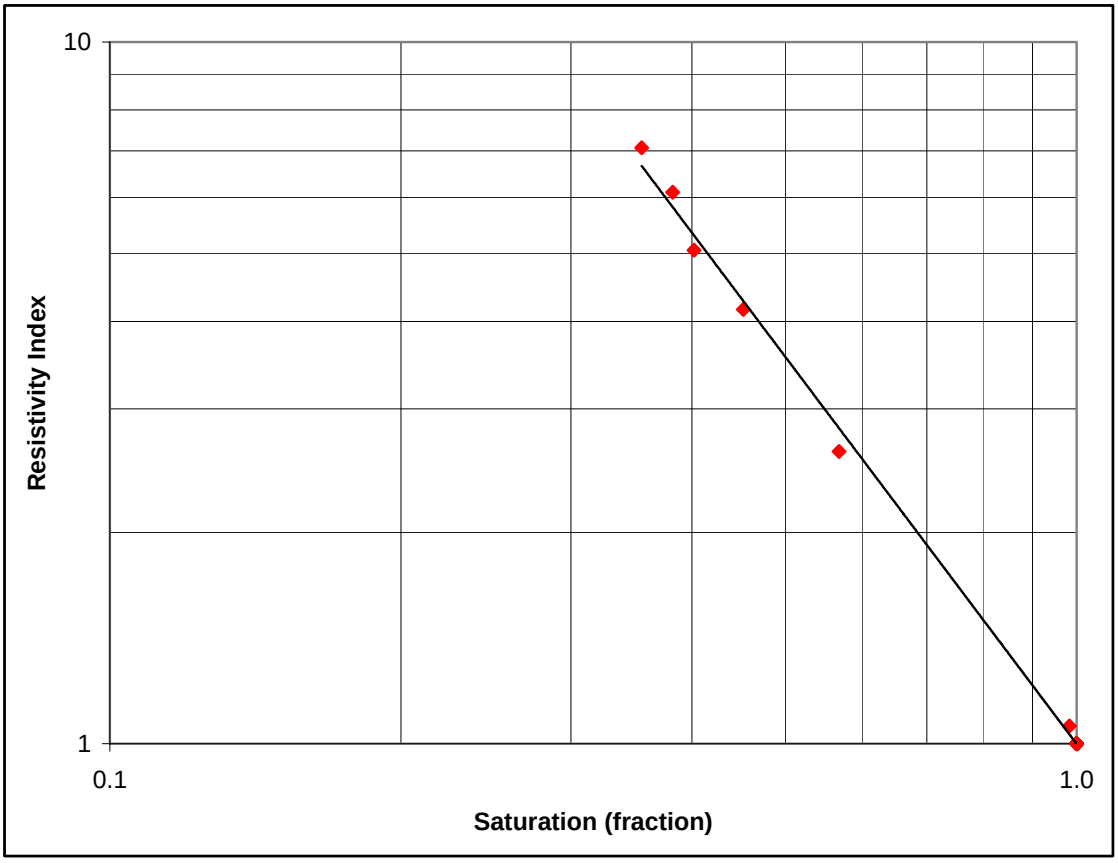

RESISTIVITY INDEX

Client Origin Energy Resources Limited
Well Yolla-3

Rw of Saturant 0.116 at 25ºC
Method Air/Brine Porous Plate @ Overburden

Sample Number	Depth (metres)	Permeability to Air (milliDarcy's)	Porosity (percent)	Formation Factor FF	Brine Saturation (fraction)	Resistivity Index RI	Saturation Exponent n
26	2223.66	38.3	30.0	9.5	1.000	1.00	
					0.994	1.04	
					0.982	1.05	
					0.837	1.37	
					0.657	2.22	
					0.536	3.26	
					0.464	4.10	
					0.428	5.03	1.88

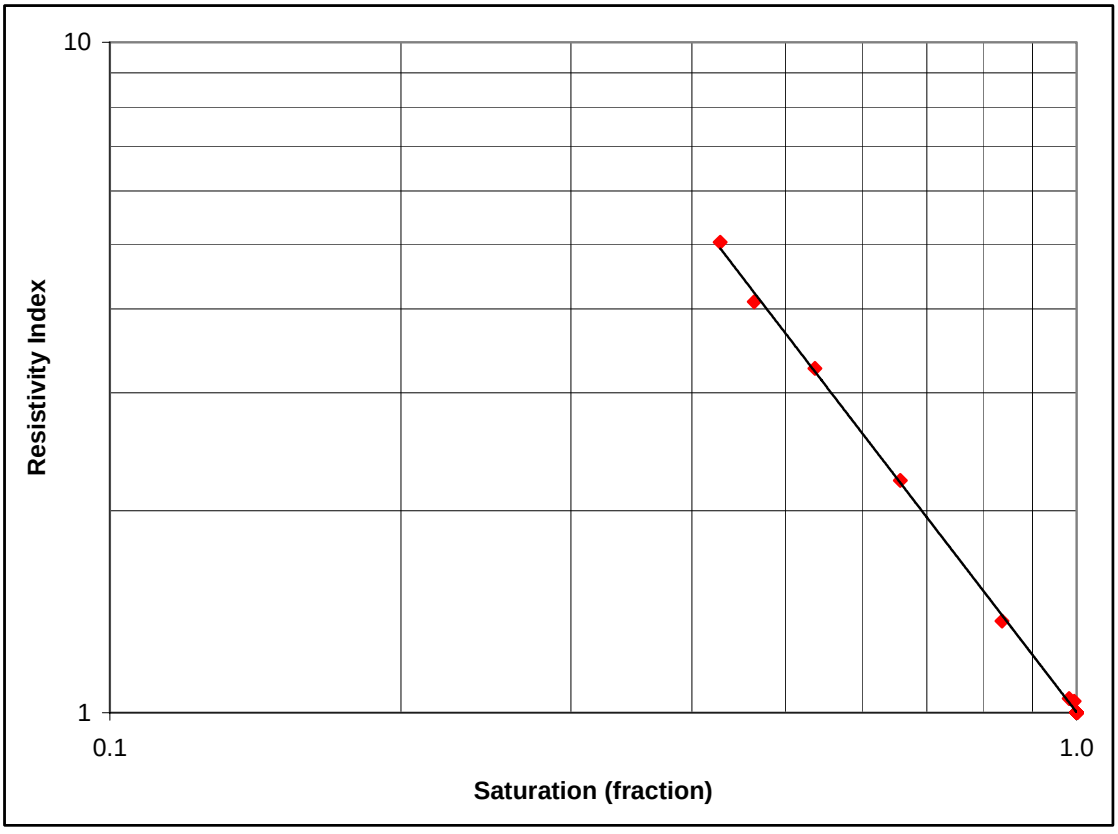

RESISTIVITY INDEX

Client Origin Energy Resources Limited
Well Yolla-3

Rw of Saturant 0.116 at 25ºC
Method Oil/Brine Porous Plate @ Overburden

Sample Number	Depth (metres)	Permeability to Air (milliDarcy's)	Porosity (percent)	Formation Factor FF	Brine Saturation (fraction)	Resistivity Index RI	Saturation Exponent n
33	2225.77	20.2	27.1	11.5	1.000	1.00	
					0.997	1.04	
					0.897	1.24	
					0.695	2.04	
					0.629	2.47	
					0.592	2.86	1.97

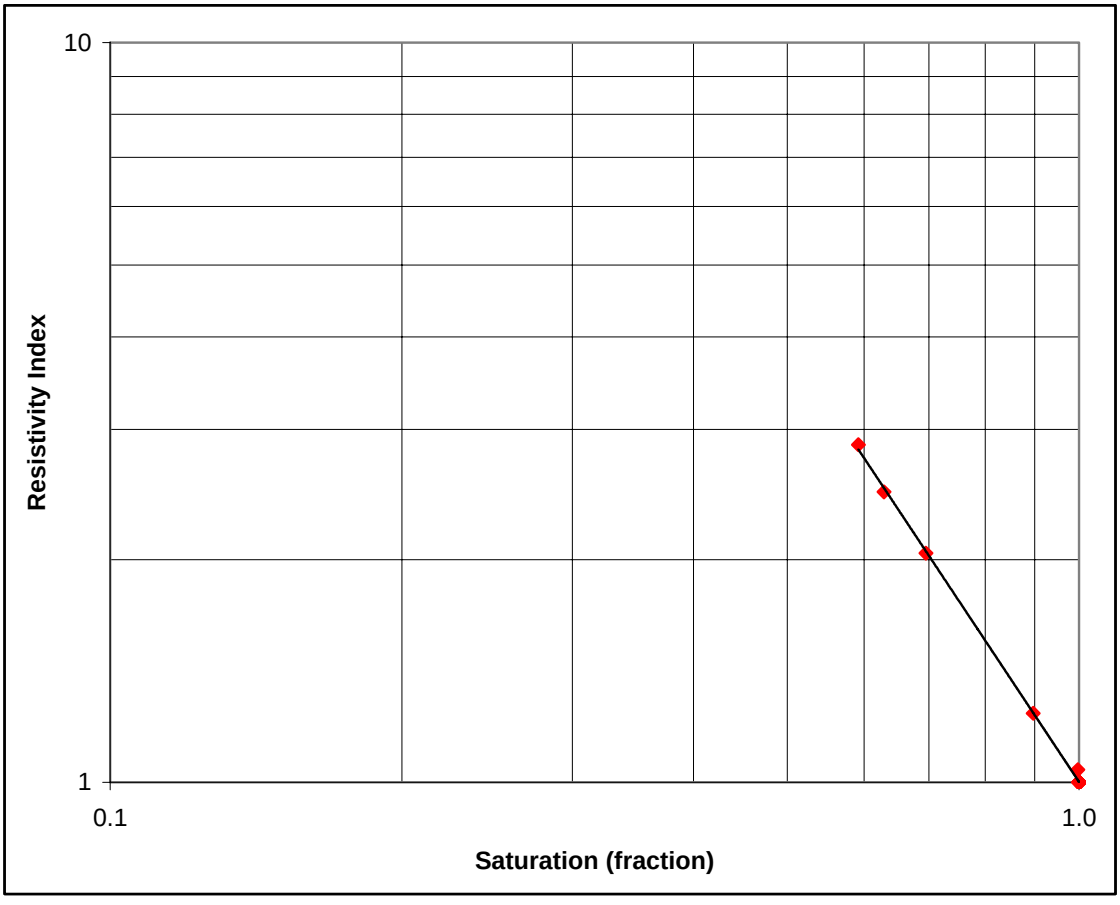

RESISTIVITY INDEX

Client Origin Energy Resources Limited
Well Yolla-3

Rw of Saturant 0.116 at 25ºC
Method Oil/Brine Porous Plate @ Overburden

Sample Number	Depth (metres)	Permeability to Air (milliDarcy's)	Porosity (percent)	Formation Factor FF	Brine Saturation (fraction)	Resistivity Index RI	Saturation Exponent n
39	2227.57	97.5	32.4	7.9	1.000	1.00	
					0.997	1.02	
					0.644	2.22	
					0.503	3.75	
					0.436	5.28	
					0.419	5.55	1.96

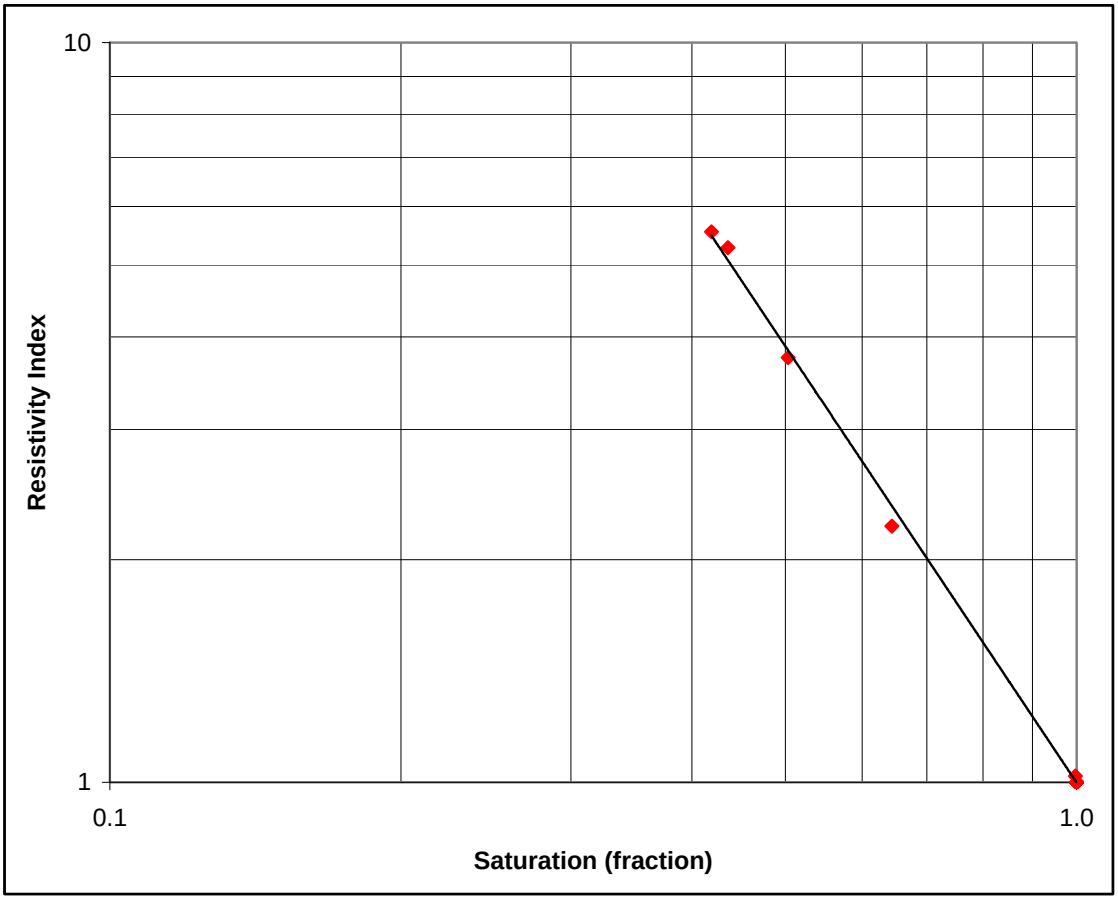

RESISTIVITY INDEX

Client Origin Energy Resources Limited
Well Yolla-3

Rw of Saturant 0.116 at 25ºC
Method Oil/Brine Porous Plate @ Overburden

Sample Number	Depth (metres)	Permeability to Air (milliDarcy's)	Porosity (percent)	Formation Factor FF	Brine Saturation (fraction)	Resistivity Index RI	Saturation Exponent n
48	2230.27	333	36.1	6.2	1.000	1.00	
					0.933	1.10	
					0.749	1.60	
					0.543	2.61	
					0.423	4.11	
					0.313	7.22	
					0.252	9.91	
					0.226	12.2	1.67

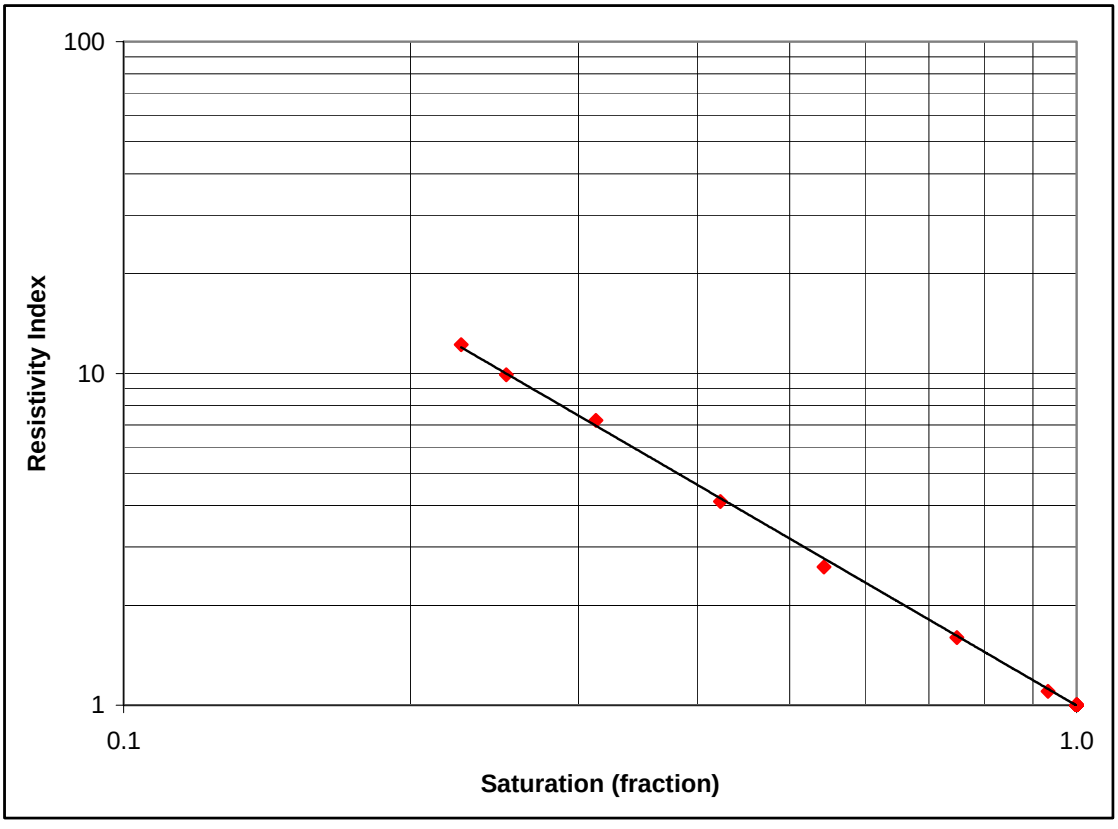

RESISTIVITY INDEX

Client Origin Energy Resources Limited
Well Yolla-3

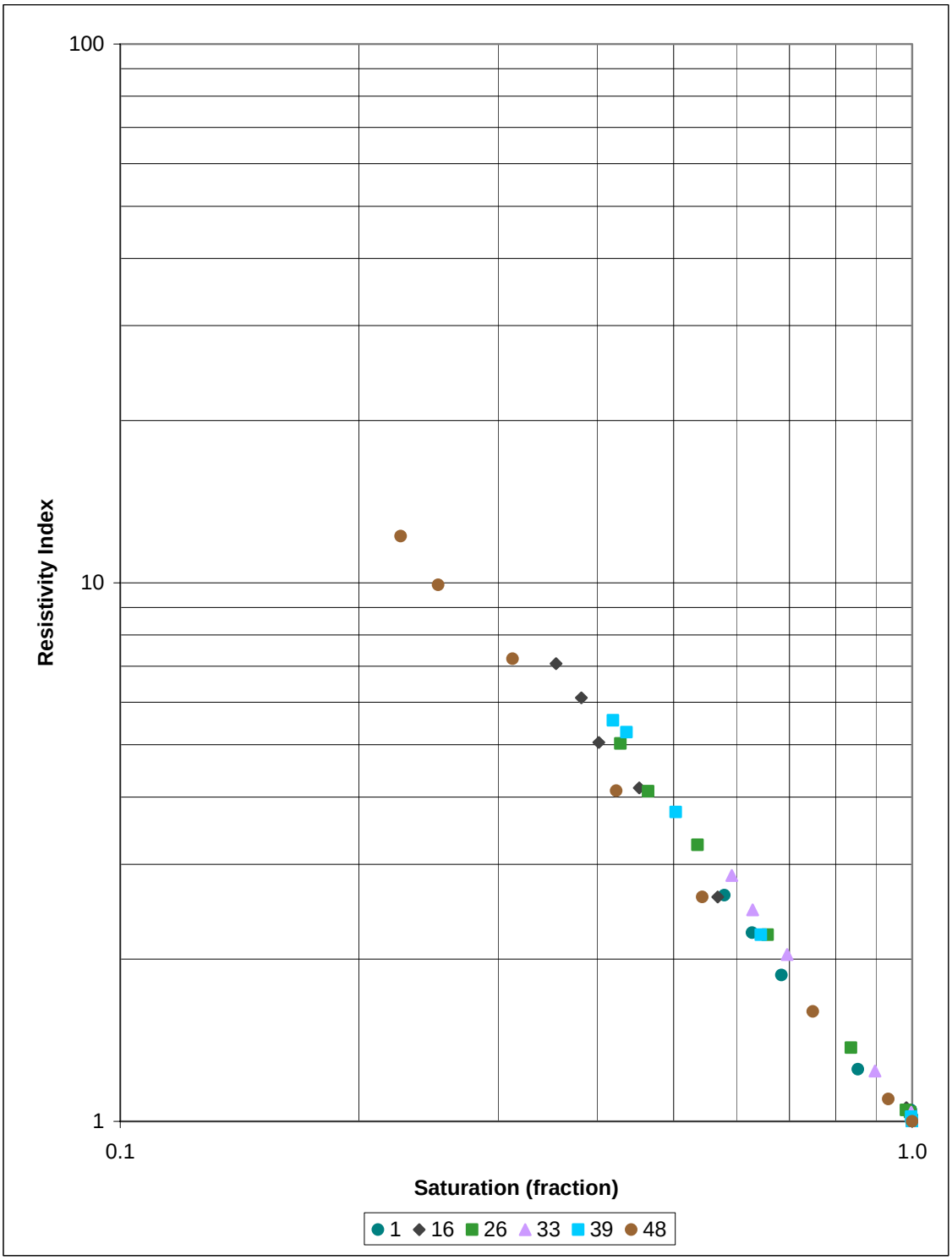

CHAPTER 4

ELECTRICAL PROPERTIES AND CAPILLARY PRESSURE

4.2 Test Results

4.2.3 Capillary Pressure (Air-Brine)

CAPILLARY PRESSURE
Overburden

Client	Origin Energy Resources Limited	**Air Permeability**	3.90 milliDarcy's
Well	Yolla-3	**Porosity**	22.9 percent
Sample	1		
Depth	2216.10 metres		
Test Method	Air/Brine Porous Plate @ Overburden		
Overburden	3200 psi		

Capillary Pressure (psi)	Brine Saturation (percent)
1.0	100.0
2.0	100.0
4.0	99.6
8.0	85.4
16	68.4
25	62.8
40	57.9

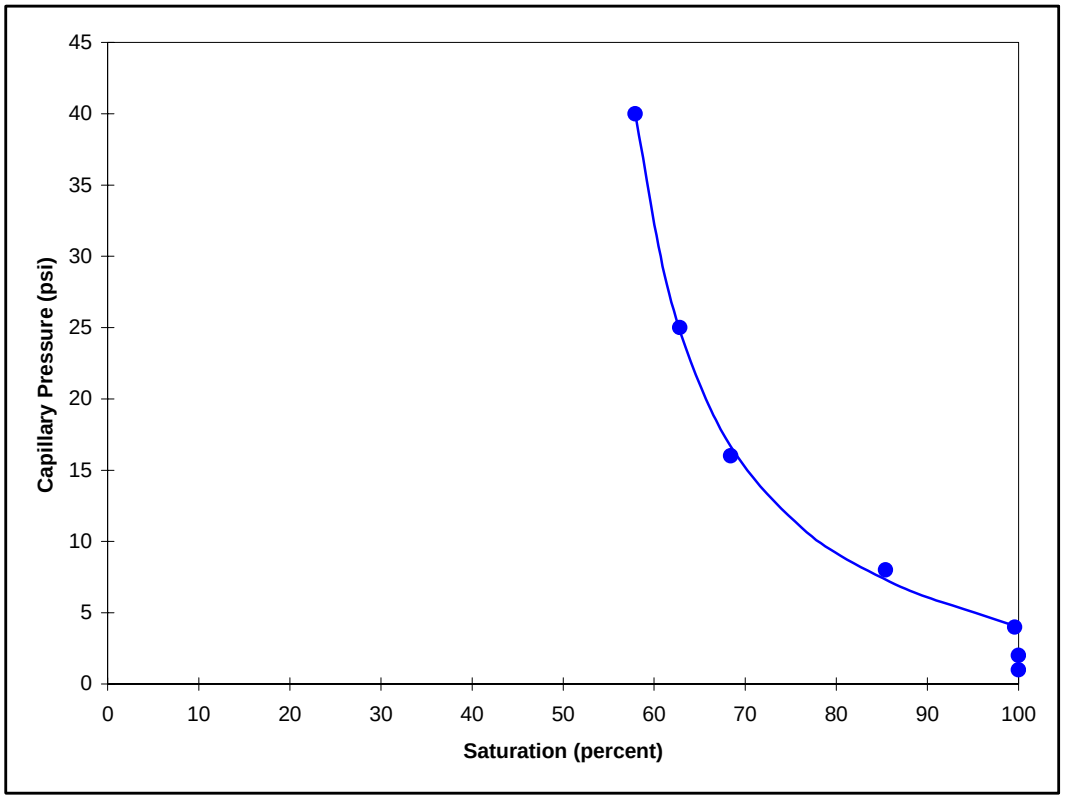

CAPILLARY PRESSURE
Overburden

Client	Origin Energy Resources Limited	**Air Permeability**	1.01 milliDarcy's
Well	Yolla-3	**Porosity**	20.3 percent
Sample	6		
Depth	2217.50 metres		
Test Method	Air/Brine Porous Plate @ Overburden		
Overburden	3200 psi		

Capillary Pressure (psi)	Brine Saturation (percent)
0.50	100.0
1.0	99.1
2.0	98.2
4.0	91.7
8.0	83.4
16	76.0
25	71.4
40	66.4

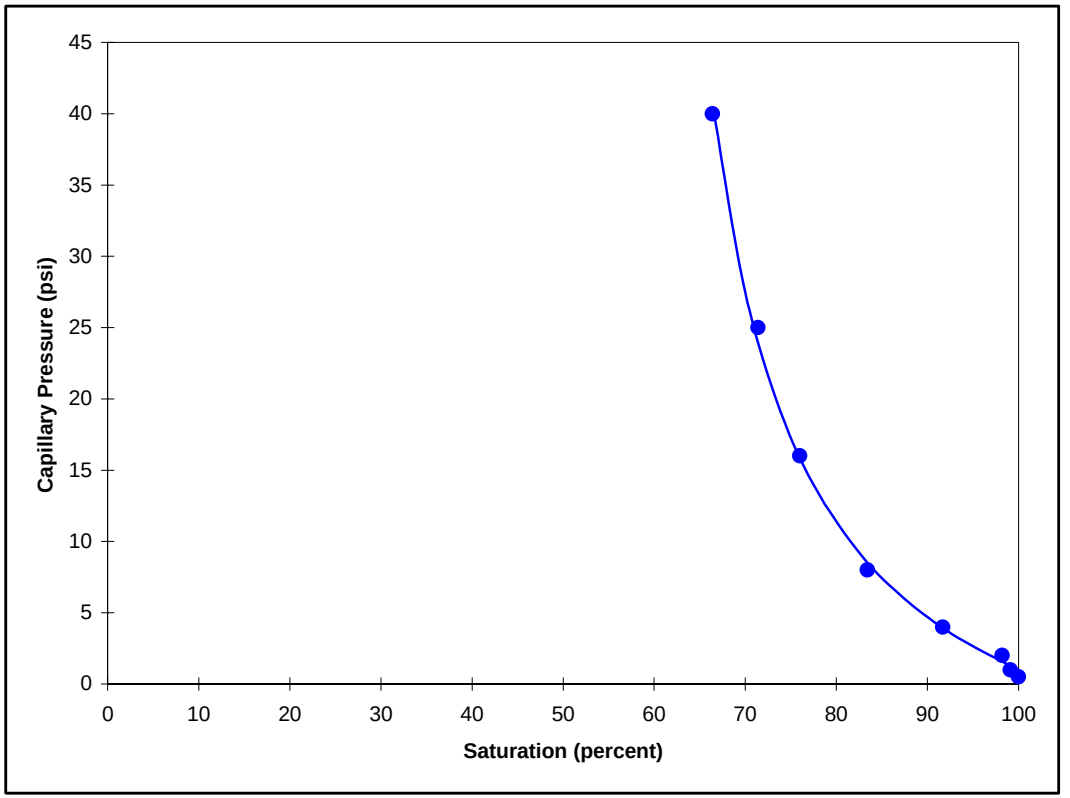

CAPILLARY PRESSURE
Overburden

Client	Origin Energy Resources Limited	**Air Permeability**	171 milliDarcy's
Well	Yolla-3	**Porosity**	33.1 percent
Sample	16		
Depth	2220.58 metres		
Test Method	Air/Brine Porous Plate @ Overburden		
Overburden	3200 psi		

Capillary Pressure (psi)	Brine Saturation (percent)
0.50	100.0
1.0	100.0
2.0	98.3
4.0	56.8
8.0	45.2
16	40.2
25	38.2
40	35.5

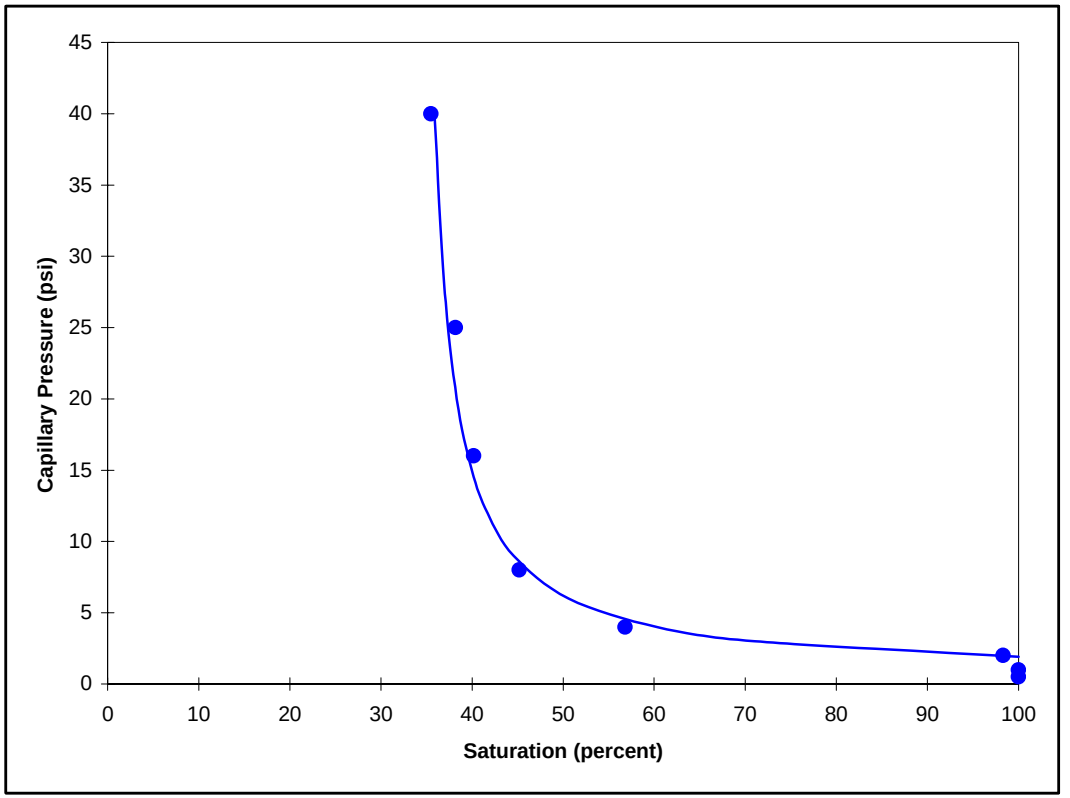

CAPILLARY PRESSURE
Overburden

Client	Origin Energy Resources Limited	**Air Permeability**	23.2 milliDarcy's
Well	Yolla-3	**Porosity**	28.8 percent
Sample	23		
Depth	2222.76 metres		
Test Method	Air/Brine Porous Plate @ Overburden		
Overburden	3200 psi		

Capillary Pressure (psi)	Brine Saturation (percent)
1.0	100.0
2.0	91.8
4.0	80.3
8.0	68.5
16	55.2
25	48.9
40	44.5

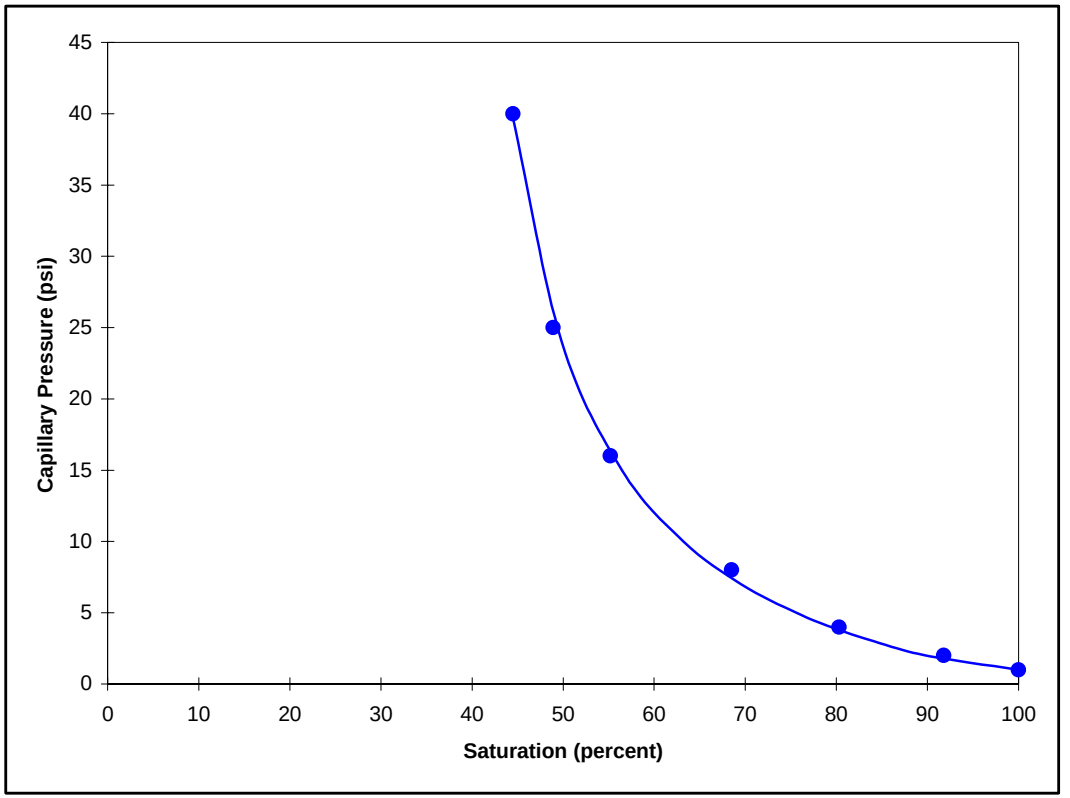

CAPILLARY PRESSURE
Overburden

Client	Origin Energy Resources Limited	**Air Permeability**	38.3 milliDarcy's
Well	Yolla-3	**Porosity**	30.0 percent
Sample	26		
Depth	2223.66 metres		
Test Method	Air/Brine Porous Plate @ Overburden		
Overburden	3200 psi		

Capillary Pressure (psi)	Brine Saturation (percent)
0.50	100.0
1.0	99.4
2.0	98.2
4.0	83.7
8.0	65.7
16	53.6
25	46.4
40	42.8

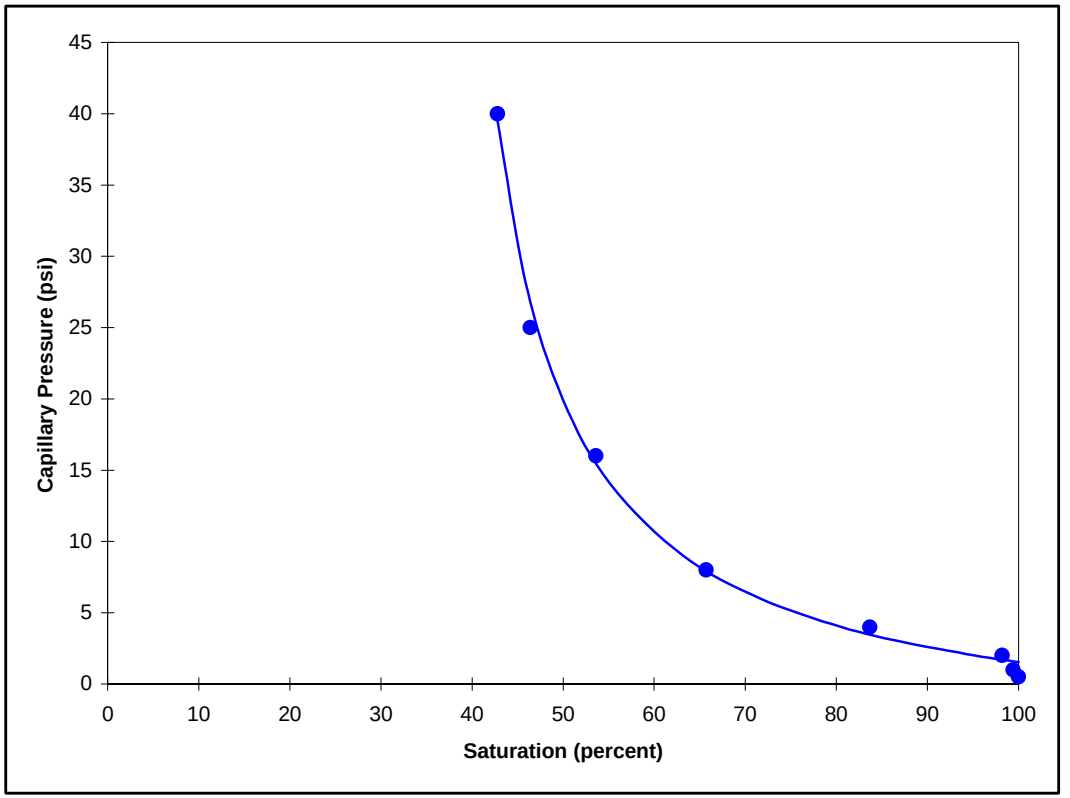

CAPILLARY PRESSURE
Overburden

Client	Origin Energy Resources Limited	**Air Permeability**	78.6 milliDarcy's
Well	Yolla-3	**Porosity**	31.7 percent
Sample	28		
Depth	2224.30 metres		
Test Method	Air/Brine Porous Plate @ Overburden		
Overburden	3200 psi		

Capillary Pressure (psi)	Brine Saturation (percent)
1.0	100.0
2.0	98.0
4.0	78.4
8.0	60.1
16	50.5
25	45.9
40	41.6

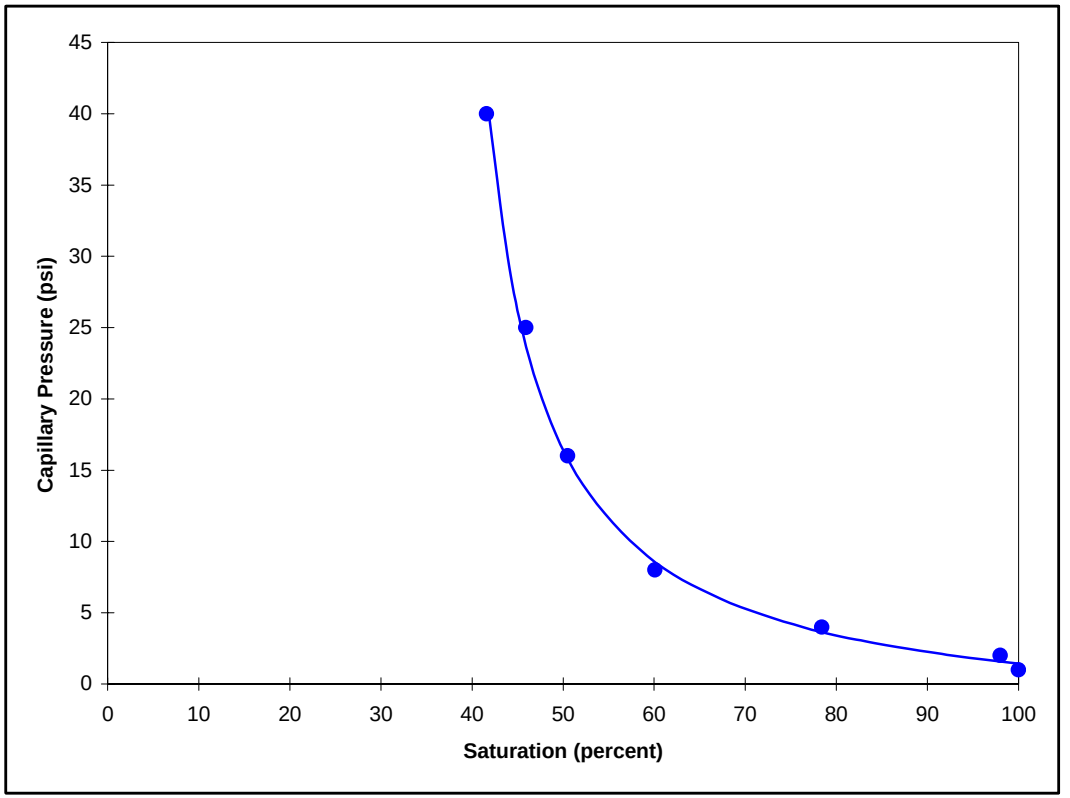

CAPILLARY PRESSURE
Air-Brine

Client Origin Energy Resources Limited
Well Yolla-3

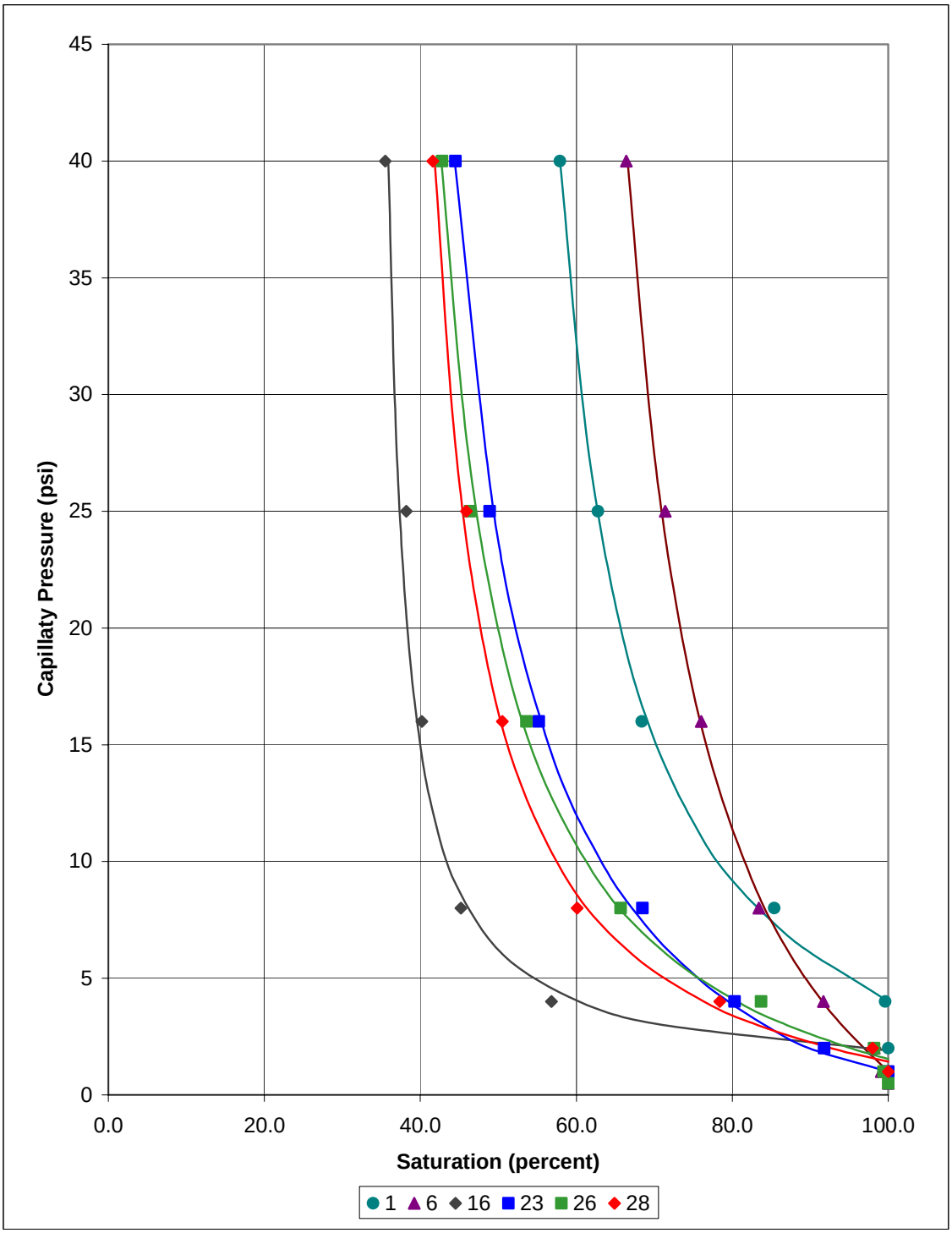

J FUNCTION
Air-Brine

Client Origin Energy Resources Limited
Well Yolla-3

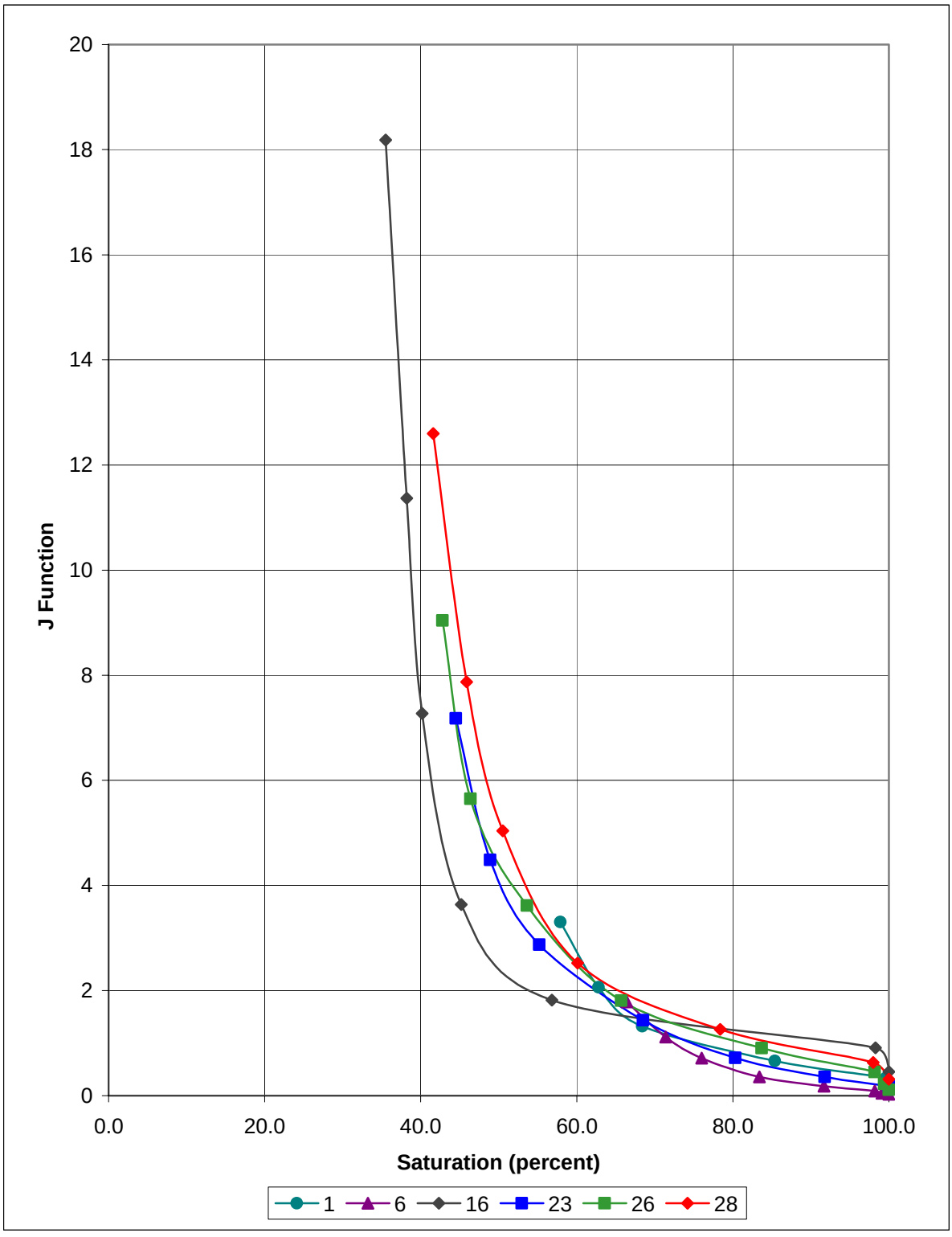

CHAPTER 4

ELECTRICAL PROPERTIES AND CAPILLARY PRESSURE

4.2 Test Results

4.2.4 Capillary Pressure (Oil-Brine)

CAPILLARY PRESSURE
Overburden

Client	Origin Energy Resources Limited	**Air Permeability**	20.2 milliDarcy's
Well	Yolla-3	**Porosity**	27.1 percent
Sample	33		
Depth	2225.77 metres		
Test Method	Oil/Brine Porous Plate @ Overburden		
Overburden	3200 psi		

Capillary Pressure (psi)	Brine Saturation (percent)
0.50	100.0
1.0	100.0
2.0	99.7
4.0	89.7
8.0	69.5
14	62.9
20	59.2

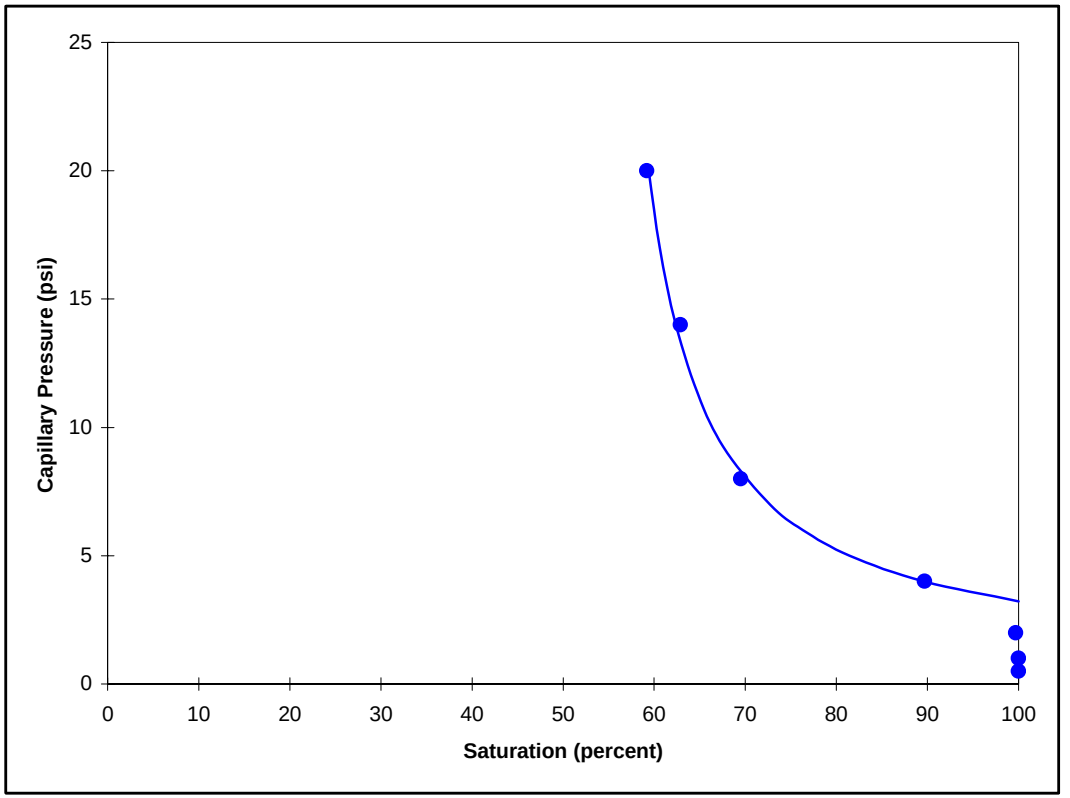

CAPILLARY PRESSURE
Overburden

Client	Origin Energy Resources Limited	**Air Permeability**	149 milliDarcy's
Well	Yolla-3	**Porosity**	33.6 percent
Sample	36		
Depth	2226.67 metres		
Test Method	Oil/Brine Porous Plate @ Overburden		
Overburden	3200 psi		

Capillary Pressure (psi)	Brine Saturation (percent)
0.25	100.0
0.50	100.0
1.0	99.7
2.0	80.4
4.0	54.1
8.0	43.6
14	38.0
20	35.8

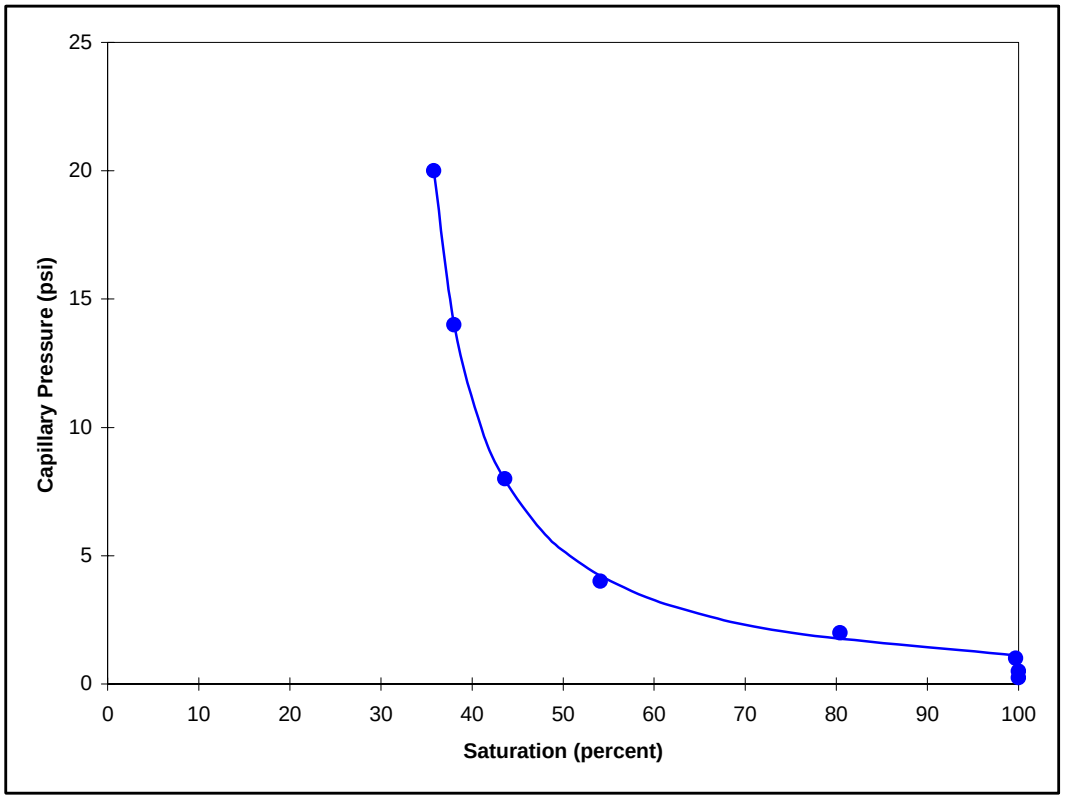

CAPILLARY PRESSURE
Overburden

Client	Origin Energy Resources Limited	**Air Permeability**	97.5 milliDarcy's
Well	Yolla-3	**Porosity**	32.4 percent
Sample	39		
Depth	2227.57 metres		
Test Method	Oil/Brine Porous Plate @ Overburden		
Overburden	3200 psi		

Capillary Pressure (psi)	Brine Saturation (percent)
0.50	100.0
1.0	100.0
2.0	99.7
4.0	64.4
8.0	50.3
14	43.6
20	41.9

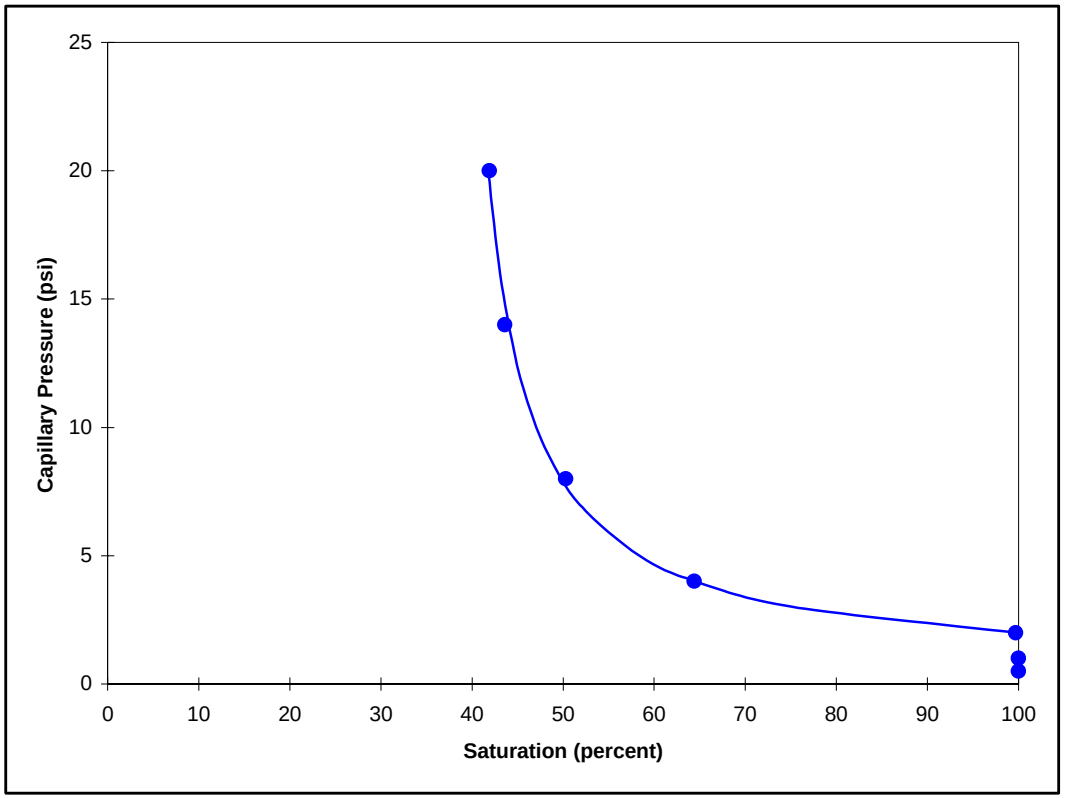

CAPILLARY PRESSURE
Overburden

Client	Origin Energy Resources Limited	**Air Permeability**	102 milliDarcy's
Well	Yolla-3	**Porosity**	32.6 percent
Sample	42		
Depth	2228.49 metres		
Test Method	Oil/Brine Porous Plate @ Overburden		
Overburden	3200 psi		

Capillary Pressure (psi)	Brine Saturation (percent)
0.25	100.0
0.50	100.0
1.0	99.7
2.0	95.0
4.0	65.8
8.0	51.8
14	45.7
20	42.9

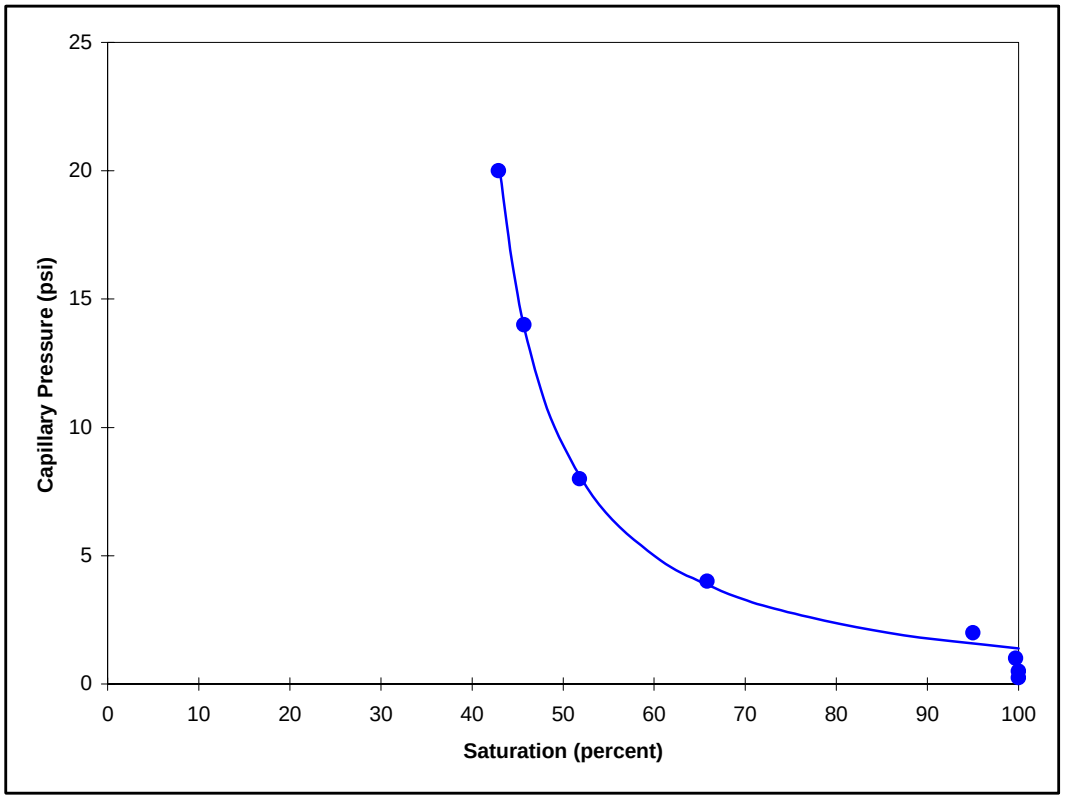

CAPILLARY PRESSURE
Overburden

Client	Origin Energy Resources Limited	**Air Permeability**	333 milliDarcy's
Well	Yolla-3	**Porosity**	36.1 percent
Sample	48		
Depth	2230.27 metres		
Test Method	Oil/Brine Porous Plate @ Overburden		
Overburden	3200 psi		

Capillary Pressure (psi)	Brine Saturation (percent)
0.50	93.3
1.0	74.9
2.0	54.3
4.0	42.3
8.0	31.3
14	25.2
20	22.6

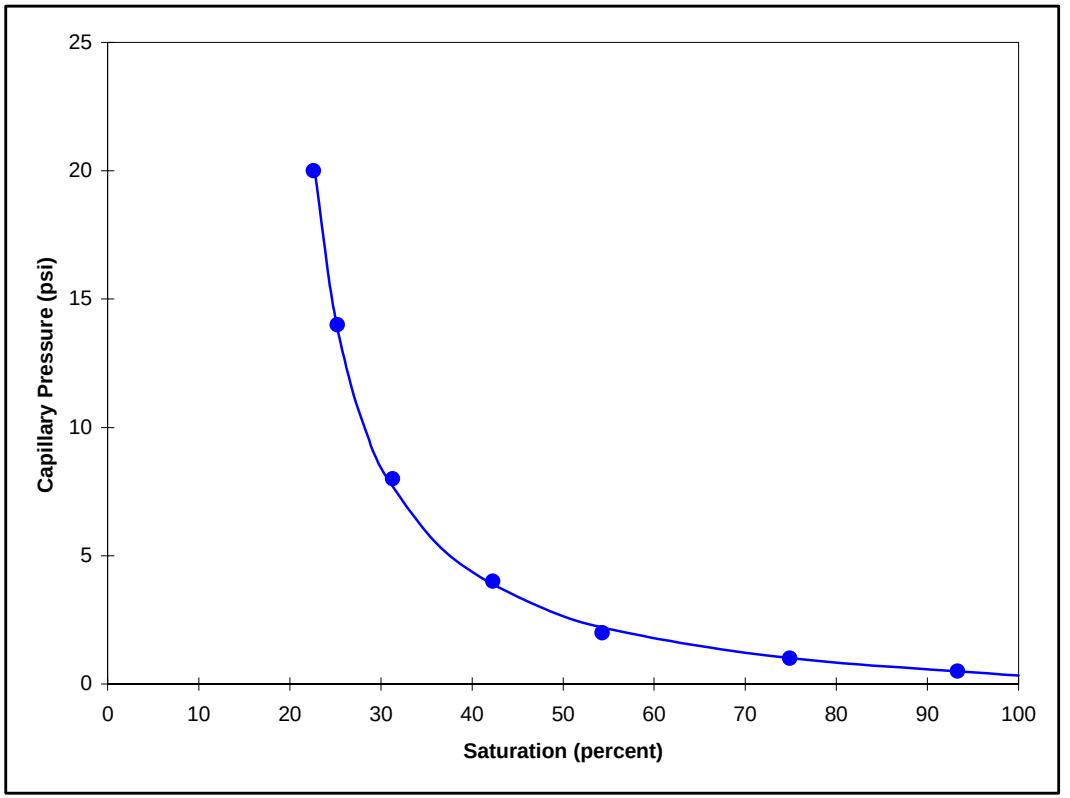

CAPILLARY PRESSURE
Overburden

Client	Origin Energy Resources Limited	**Air Permeability**	7.9 milliDarcy's
Well	Yolla-3	**Porosity**	25.8 percent
Sample	54		
Depth	2232.08 metres		
Test Method	Oil/Brine Porous Plate @ Overburden		
Overburden	3200 psi		

Capillary Pressure (psi)	Brine Saturation (percent)
0.50	100.0
1.0	100.0
2.0	99.7
4.0	90.9
8.0	77.7
14	70.0
20	65.8

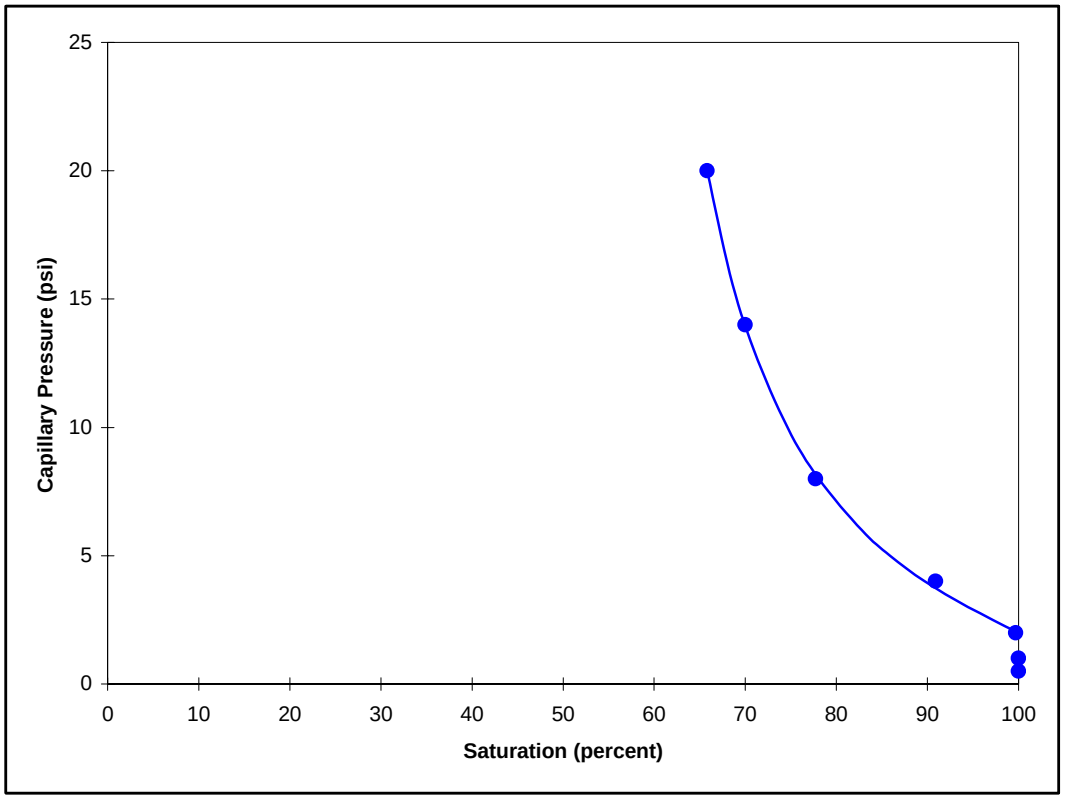

CAPILLARY PRESSURE
Oil-Brine

Client Origin Energy Resources Limited
Well Yolla-3

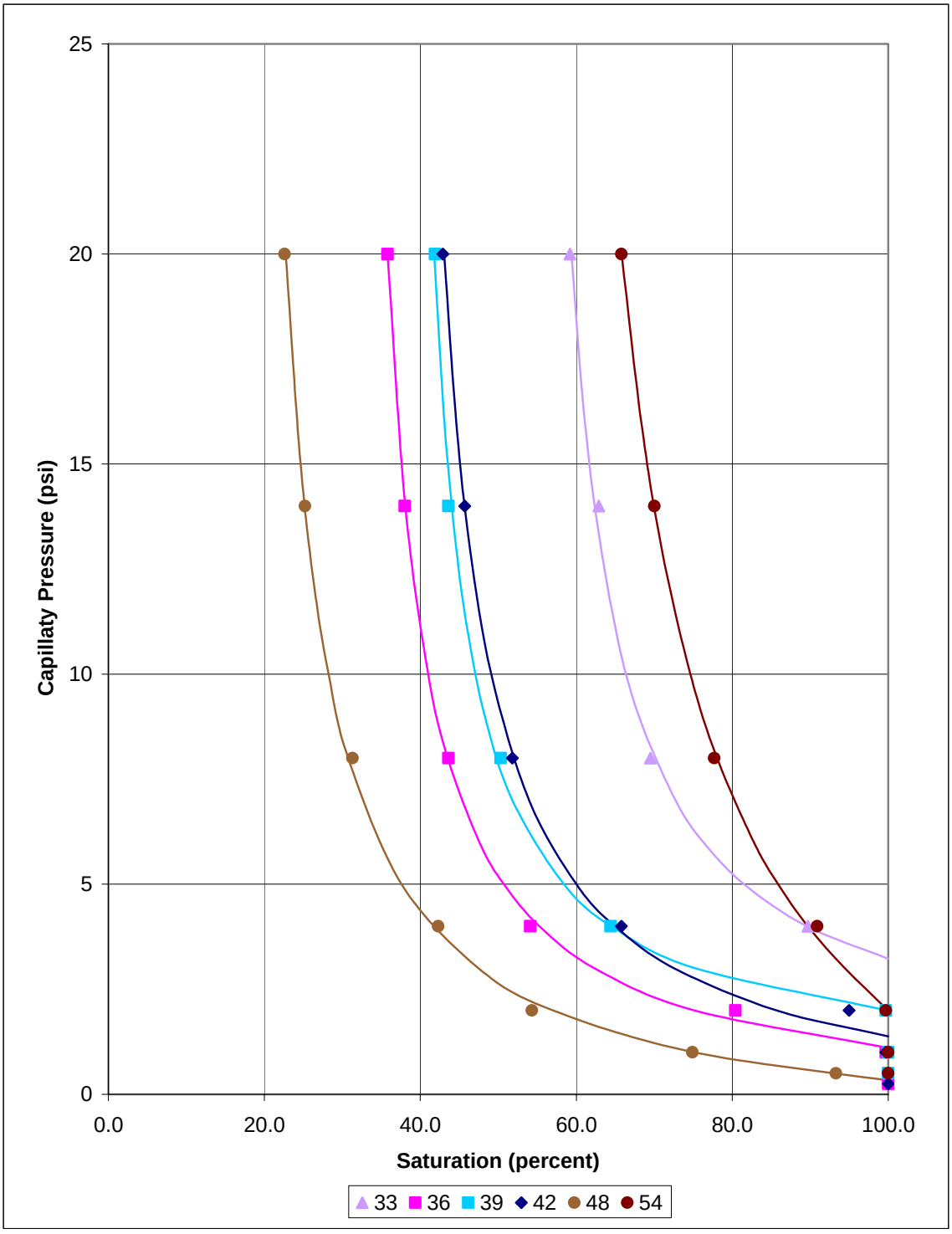

J FUNCTION
Oil-Brine

Client Origin Energy Resources Limited
Well Yolla-3

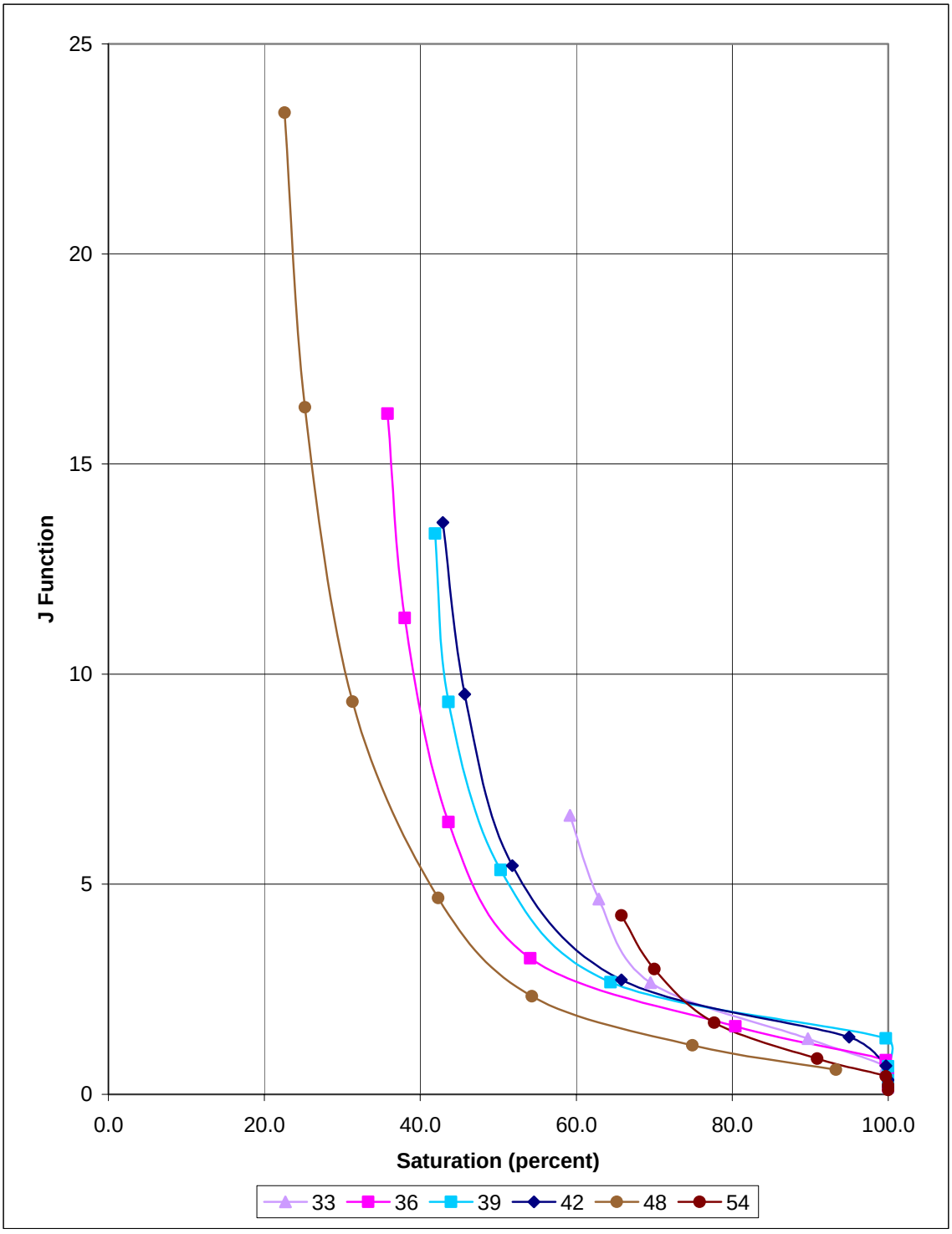

J FUNCTION
Combined Air & Oil-Brine

Client Origin Energy Resources Limited
Well Yolla-3

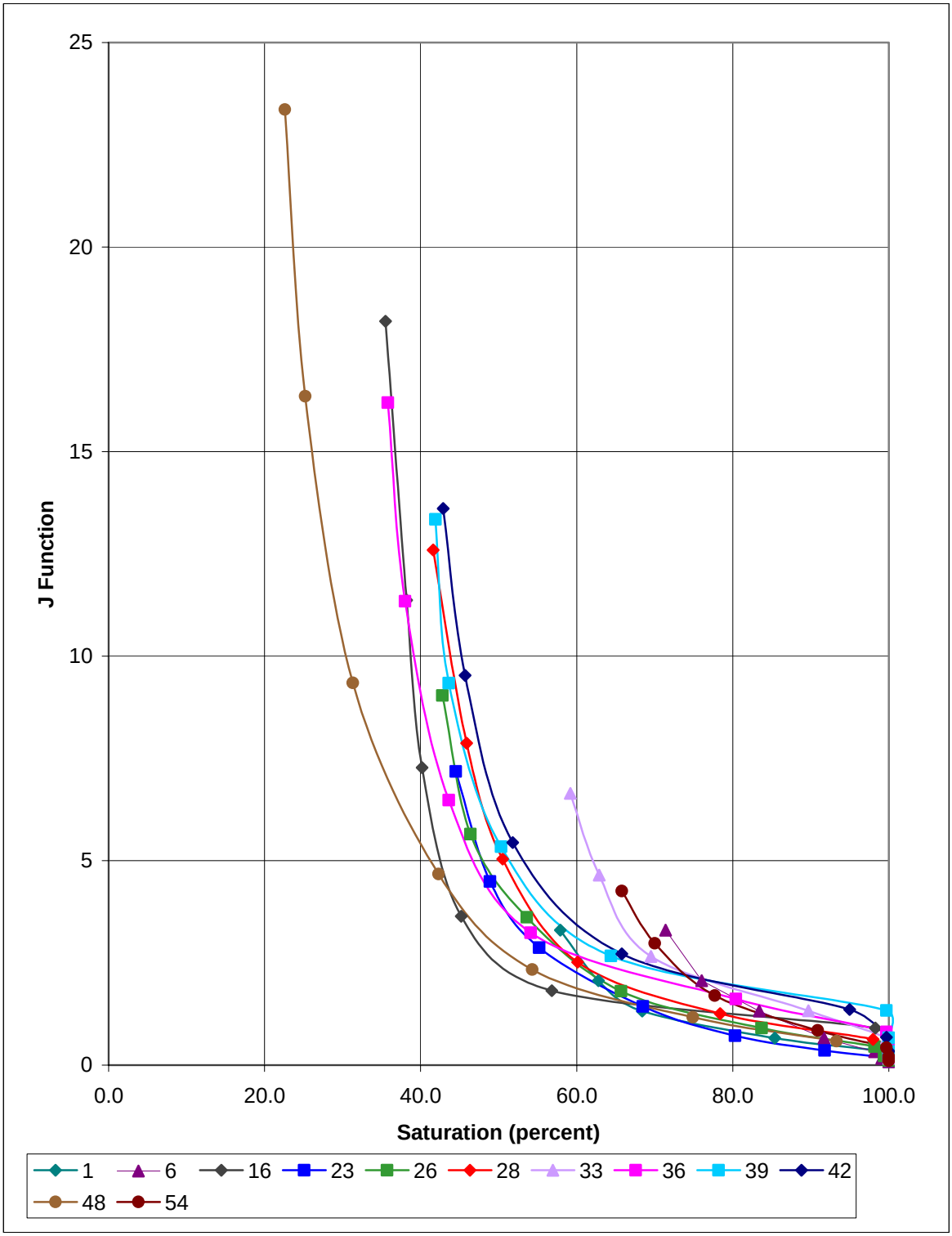

CHAPTER 4

ELECTRICAL PROPERTIES AND CAPILLARY PRESSURE

4.2 Test Results

4.2.5 Cation Exchange Capacity

CATION EXCHANGE CAPACITY

Client Origin Energy Resources Limited
Well Yolla-3

Sample Number	Depth (metres)	Porosity (percent)	Grain Density (g/cm^3)	Cation Exchange Capacity (meq/100g)		Quantity of Cation Exchangeable Clay Qv (meq/cm^3)	
				Uncrushed	Crushed	Uncrushed	Crushed
1	2216.10	23.9	2.64	0.70	1.80	0.06	0.15
16	2220.58	34.2	2.66	2.78	2.88	0.14	0.15
26	2223.66	31.1	2.70	3.62	4.16	0.22	0.25
33	2225.77	28.2	2.68	3.88	4.37	0.26	0.30
39	2227.57	33.5	2.68	3.63	4.04	0.19	0.21
48	2230.27	37.1	2.67	2.37	2.83	0.11	0.13

CHAPTER 4

ELECTRICAL PROPERTIES AND CAPILLARY PRESSURE

4.2 Test Results

4.2.6 Summary

FORMATION RESISTIVITY FACTOR

Client	Origin Energy Resources Limited	**Rw of Saturant**	0.116 at 25ºC
Well	Yolla-3	**Overburden**	3200 psi

Sample Number	Depth (metres)	Permeability to Air (milliDarcy's)	Porosity (percent)	Formation Factor FF	Cementation Exponent m	Saturation Exponent n	Shaley Sand Equivalent † Formation Factor FF*	Shaley Sand Equivalent † Cementation Exponent m*	Shaley Sand Equivalent † Saturation Exponent n*
1	2216.10	3.90	22.9	17.5	1.94	1.72	18.0	1.96	1.75
16	2220.58	171	33.1	7.4	1.81	1.83	7.9	1.87	1.92
26	2223.66	38.3	30.0	9.5	1.87	1.88	10.4	1.95	2.01
33	2225.77	20.2	27.1	11.5	1.87	1.97	12.9	1.96	2.10
39	2227.57	97.5	32.4	7.9	1.83	1.96	8.6	1.91	2.07
48	2230.27	333	36.1	6.2	1.79	1.67	6.5	1.84	1.76

† Calculated from Cation Exchange Capacity

RESIDUAL SATURATION

Client Origin Energy Resources Limited
Well Yolla-3

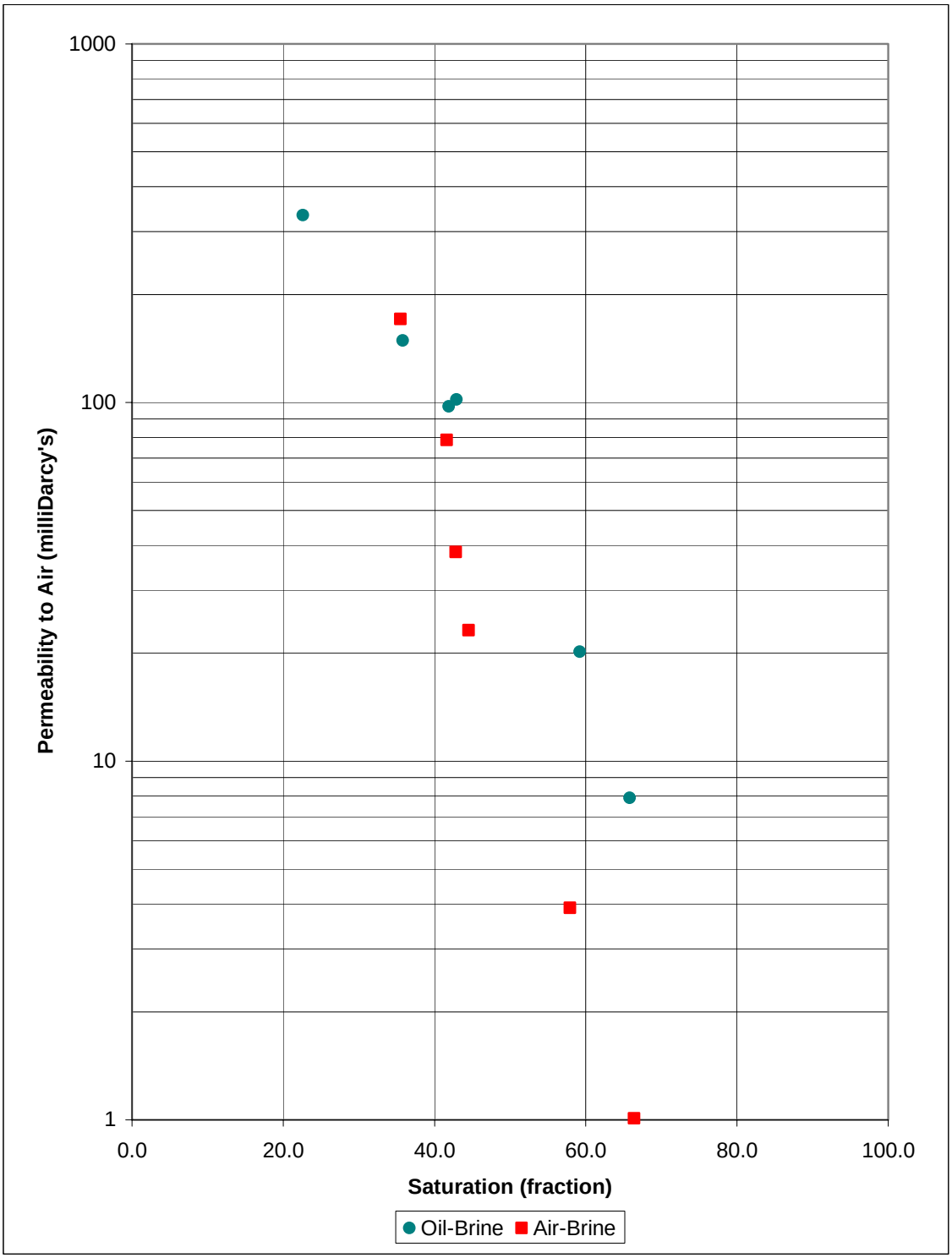

CHAPTER 5

RESIDUAL GAS

5.1 Test and Calculation Procedures

5. RESIDUAL GAS

5.1 Test and Calculation Procedures

5.1.1 Permeability to Air at Residual Water Saturation

On completion of air-brine capillary pressure desaturation the three selected samples at residual water saturation (Swr) underwent effective permeability to air. Each sample was individually placed into a hydrostatic cell with an overburden pressure of 3200 psi applied. A known pressure of humidified air was applied to the upstream face of each sample, creating a flow of air through the core plug. Effective permeability to air was calculated using Darcy's Law through knowledge of the upstream pressure, flow rate, viscosity of air and sample dimensions.

$$Keg = \frac{2000.BP.\mu.q.L}{(P_1^2 - P_2^2).A}$$

where

Keg	=	*effective permeability to air @ Swr (milliDarcy's)*
BP	=	*barometric pressure (atmospheres)*
μ	=	*gas viscosity (cP)*
q	=	*flow rate (cm^3/s)*
L	=	*sample length (cm)*
P_1	=	*upstream pressure (atmospheres)*
P_2	=	*downstream pressure (atmospheres)*
A	=	*sample cross sectional area (cm^2)*

5.1.2 Permeability to Oil at Residual Water Saturation

The three selected samples, on completion of oil-brine capillary pressure determination, were individually mounted into a hydrostatic cell at an overburden pressure of 3200psi. Oil was flowed at a constant rate through each core plug and from upstream pressure, flow rate, viscosity of oil and the sample dimensions, the effective permeability to oil was calculated using Darcy's Law.

$$Keo\ @\ Swir = \frac{14696.q.L.\mu T}{\Delta P.A}$$

where

14696	=	*units conversion*
Keo @ Swir	=	*permeability to oil at residual water saturation*
q	=	*flow rate (cm^3/s)*
ΔP	=	*differential flooding pressure (psig)*
L	=	*sample length (cm)*
A	=	*sample cross sectional area (cm^2)*
μT	=	*oil viscosity (cP) at T (°C)*

5.1.3 Waterflood

The selected samples at residual water saturation were placed into a thick walled rubber sleeve and the assembly loaded into a hydrostatic cell. An overburden pressure of 3200 psi was applied.

Brine was pumped through the samples at a low rate (4 cc/hour). Flow continued until gas or oil production ceased and a brine permeability at residual gas or oil saturation was determined through knowledge of the differential flooding pressure, flow rate, viscosity of brine and the sample dimensions.

$$Kw = \frac{14696.q.L.\mu T}{\Delta P.A}$$

where	*14696*	=	*units conversion*
	Kw	=	*effective permeability to brine*
	q	=	*flow rate (cm^3/s)*
	ΔP	=	*differential flooding pressure (psig)*
	L	=	*sample length (cm)*
	A	=	*sample cross sectional area (cm^2)*
	μT	=	*brine viscosity (cP) at T (° C)*

The flow rate was then increased (to 4cc/min) and further production measured. Once stable gas saturation was reached permeability was measured as per above.

CHAPTER 5

RESIDUAL GAS

5.2 Test Results

WATERFLOOD
Air-Brine

Client Origin Energy Resources Limited
Well Yolla-3

Saturant 60000 ppm
Overburden 3200 psi

Sample Number	Permeability to Air (milliDarcy's)	Porosity (percent)	Initial Brine Saturation (percent)	Permeability to Air @ Swir (milliDarcy's)	Low Rate		Bump Flood		Gas Recovery	
					Residual Gas Saturation (percent)	Effective Brine Permeability (milliDarcy's)	Residual Gas Saturation (percent)	Effective Brine Permeability (milliDarcy's)	Percent of Pore Volume (percent)	Percent of Gas in Place (percent)
1	3.90	22.9	57.9	1.53	13.4	0.61	7.6	1.49	34.5	81.9
16	171	33.1	35.5	141	12.5	5.3	6.3	21.1	58.2	90.2
26	38.3	30.0	42.8	28.9	14.3	3.44	5.8	16.4	51.4	89.9

WATERFLOOD
Oil-Brine

Client Origin Energy Resources Limited
Well Yolla-3

Saturant 60000 ppm
Overburden 3200 psi

Sample Number	Permeability to Air (milliDarcy's)	Porosity (percent)	Initial Brine Saturation (percent)	Permeability to Oil @ Swir (milliDarcy's)	Low Rate		Bump Flood		Oil Recovery	
					Residual Oil Saturation (percent)	Effective Brine Permeability (milliDarcy's)	Residual Oil Saturation (percent)	Effective Brine Permeability (milliDarcy's)	Percent of Pore Volume (percent)	Percent of Oil in Place (percent)
33	20.2	27.1	59.2	14.4	15.2	1.65	13.1	2.61	27.7	67.9
39	97.5	32.4	41.9	94.9	16.8	7.0	15.8	10.1	42.3	72.8
48	333	36.1	22.6	285	19.1	13.0	19.1	47.3	58.3	75.3

APPENDIX I

FLUID PROPERTIES

FLUID PROPERTIES

Brine

60000 ppm NaCl equivalent

Density	=	1.029	g/cm^3 @ 25°C
Resistivity	=	0.116	ohm.m @ 25°C
Viscosity	=	1.015	cP @ 25°C

Oil

Isopar G

Density	=	0.736	g/cm^3 @ 25°C
Viscosity	=	1.00	cP @ 25°C

APPENDIX II

EQUIPMENT SCHEMATICS

POROSIMETER SCHEMATIC

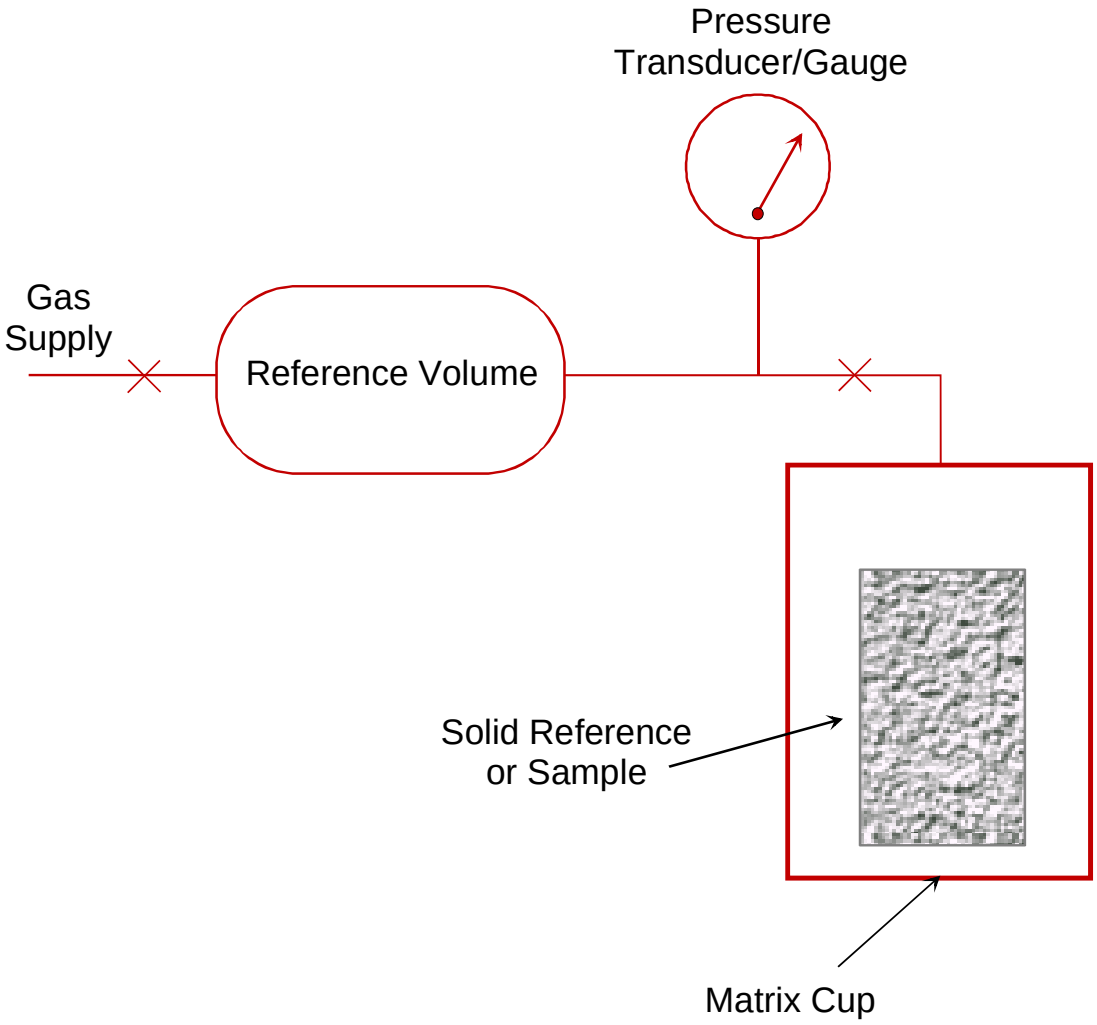

P1.V1 (reference) = P2.V2 (sample)

GAS PERMEAMETER SCHEMATIC (Hydrostatic)

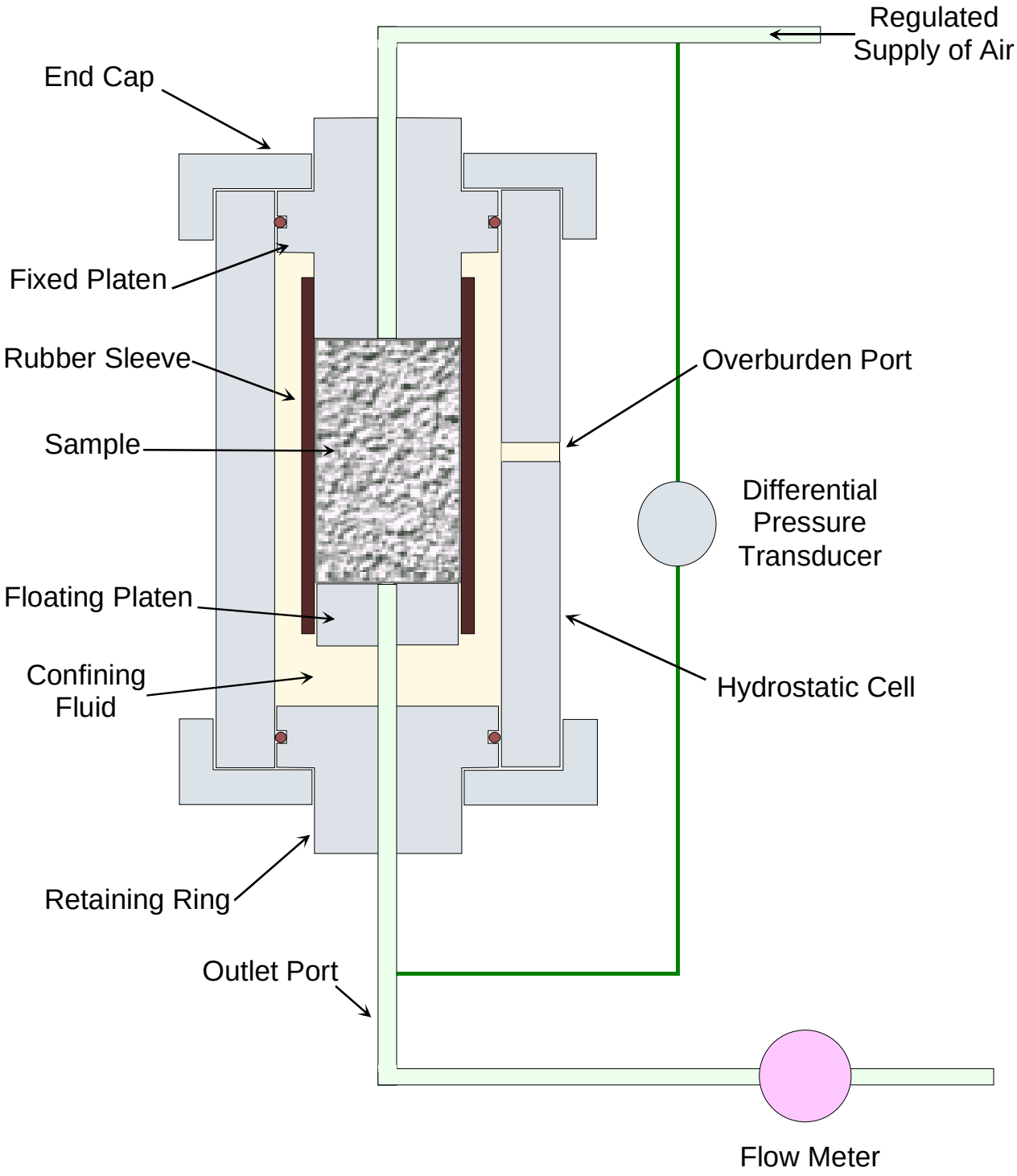

HYDROSTATIC CAPILLARY PRESSURE CELL

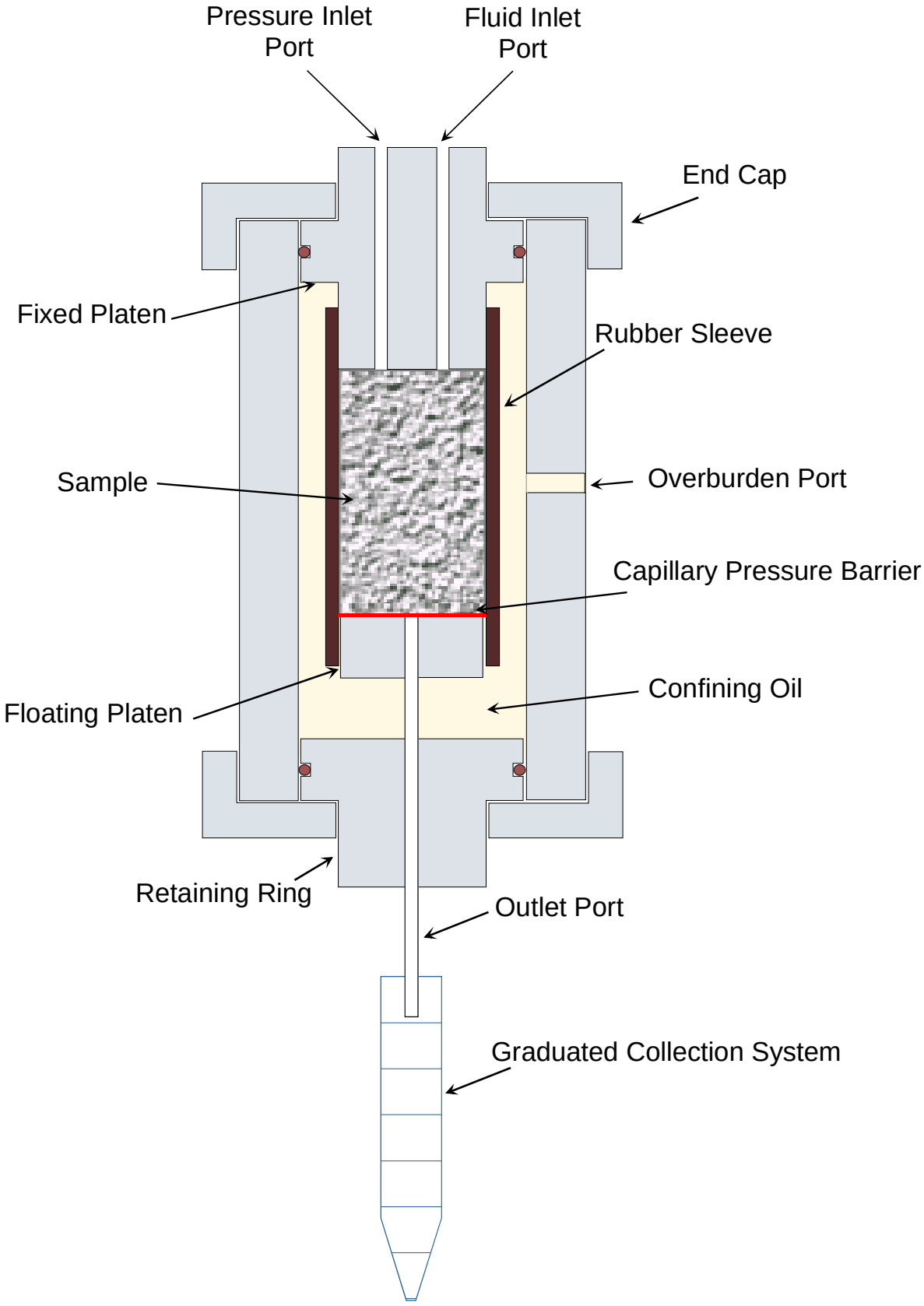

ACS Laboratories Pty Ltd
ABN: 81 008 273 005

CT SCANNER SCHEMATIC

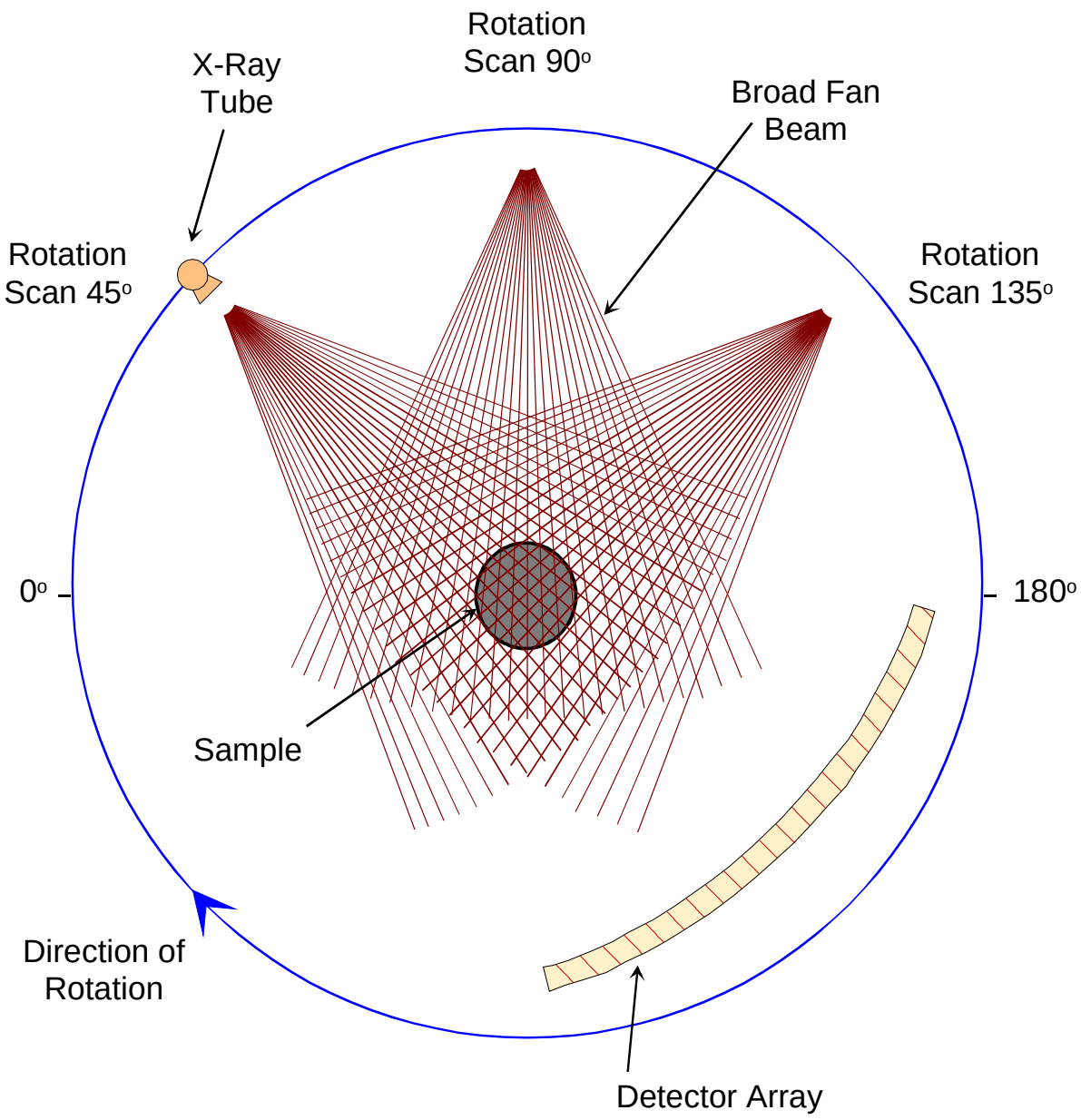

LIQUID PERMEABILITY SCHEMATIC

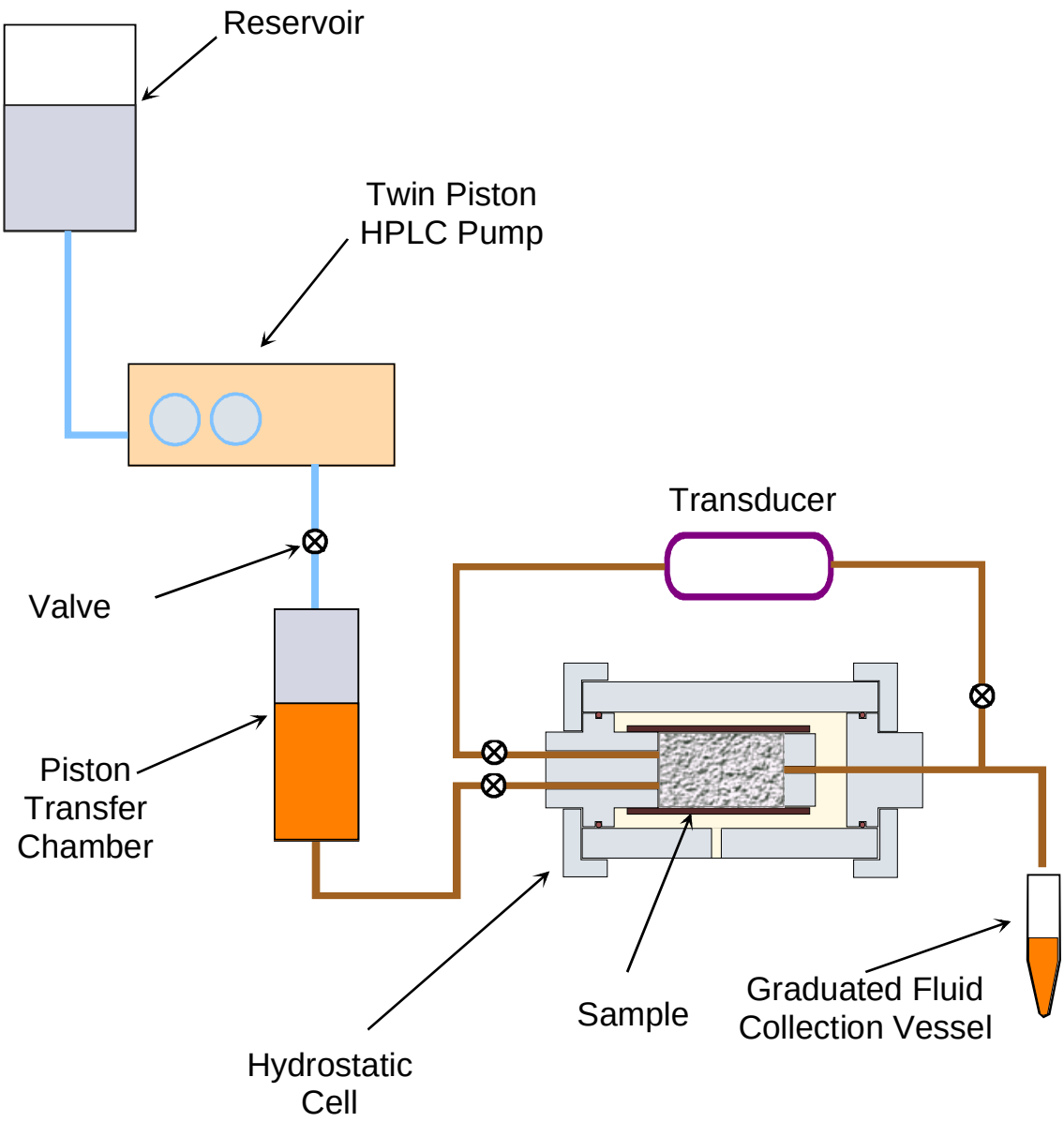

DEAN-STARK APPARATUS

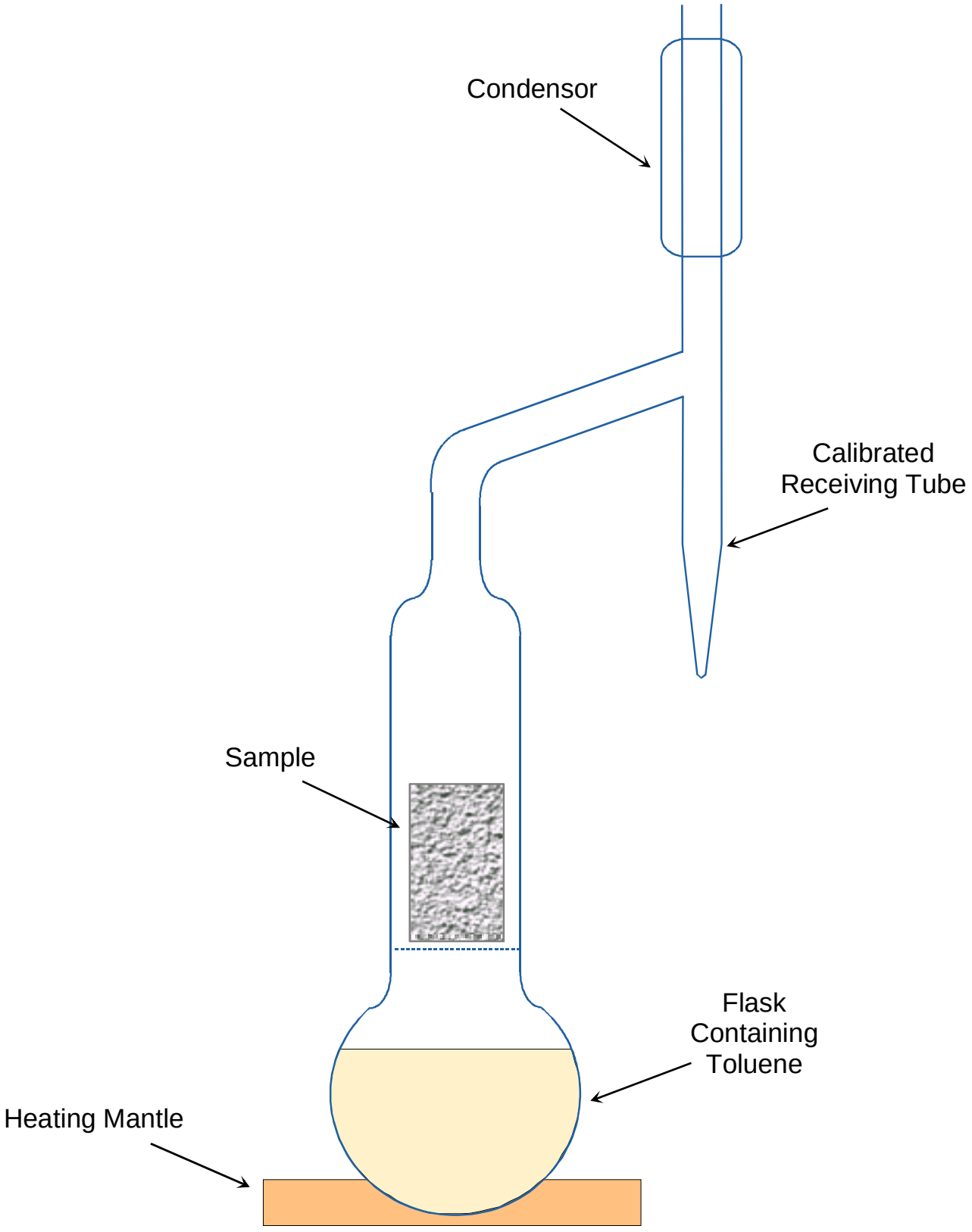

APPENDIX III

CT SCAN IMAGES

Yolla-3
C.T. Scans

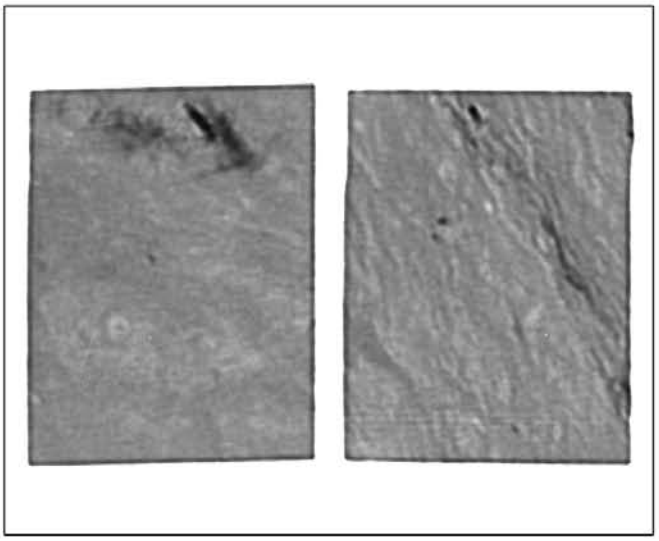

Sample No:	1
Depth:	2216.10 m
Permeability:	5.8 mD
Porosity:	23.9 %

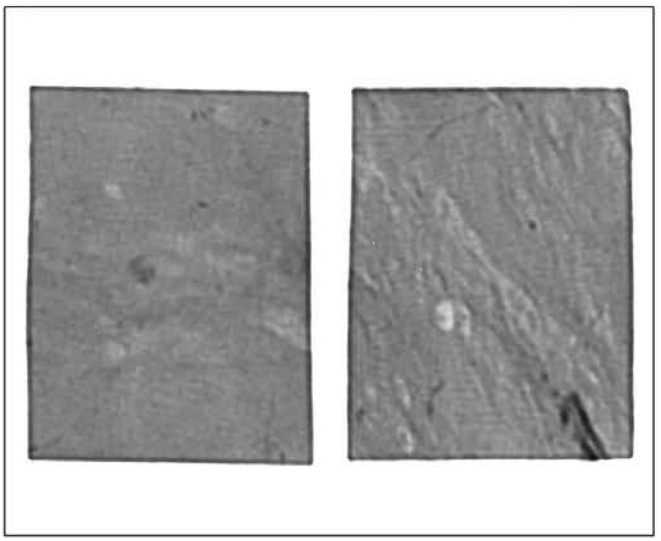

Sample No:	6
Depth:	2217.55 m
Permeability:	1.89 mD
Porosity:	21.4 %

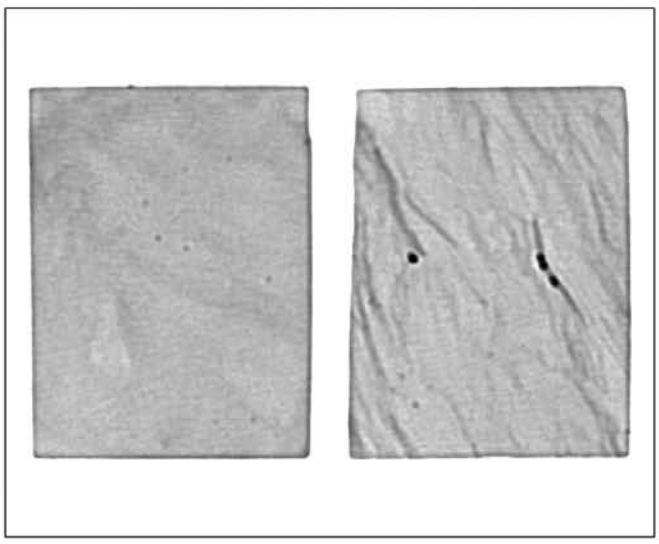

Sample No:	16
Depth:	2220.58 m
Permeability:	196 mD
Porosity:	34.2 %

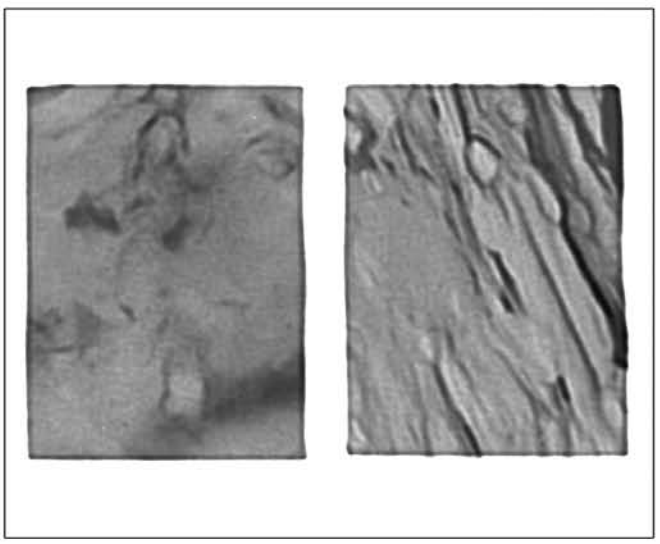

Sample No.:	23
Depth:	2222.76 m
Permeability:	30.1 mD
Porosity:	29.9 %

Yolla-3
C.T. Scans

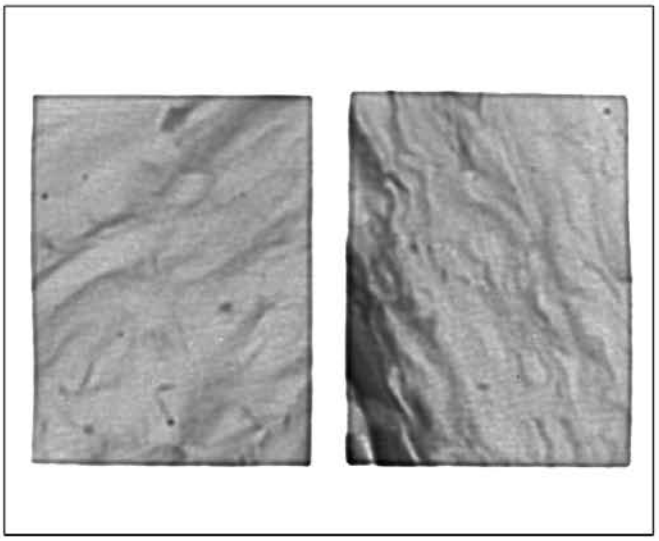

Sample No:	26
Depth:	2223.66 m
Permeability:	47.4 mD
Porosity:	31.1 %

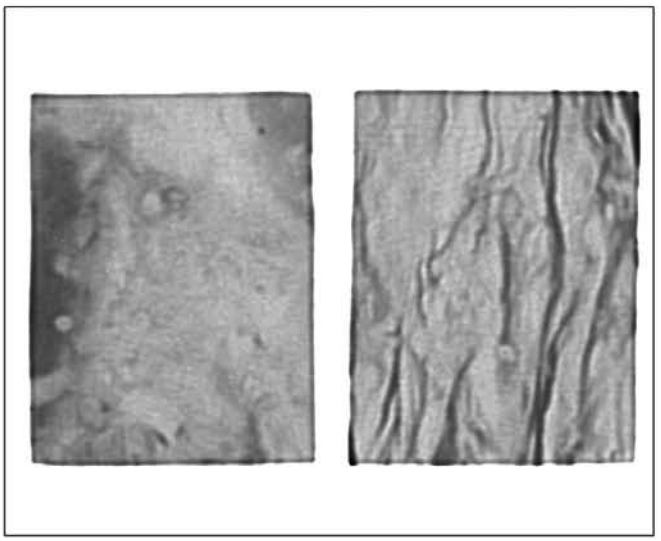

Sample No:	28
Depth:	2224.30 m
Permeability:	90.2 mD
Porosity:	32.7 %

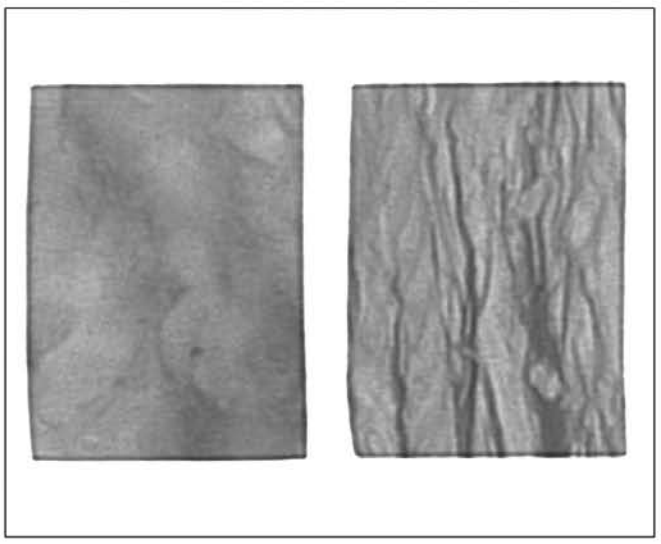

Sample No:	33
Depth:	2225.77 m
Permeability:	25.4 mD
Porosity:	28.2 %

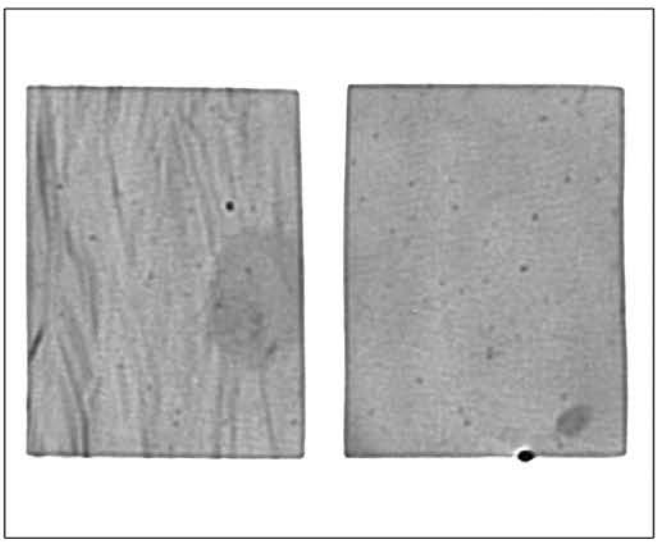

Sample No.:	36
Depth:	2226.67 m
Permeability:	172 mD
Porosity:	34.6 %

Yolla-3
C.T. Scans

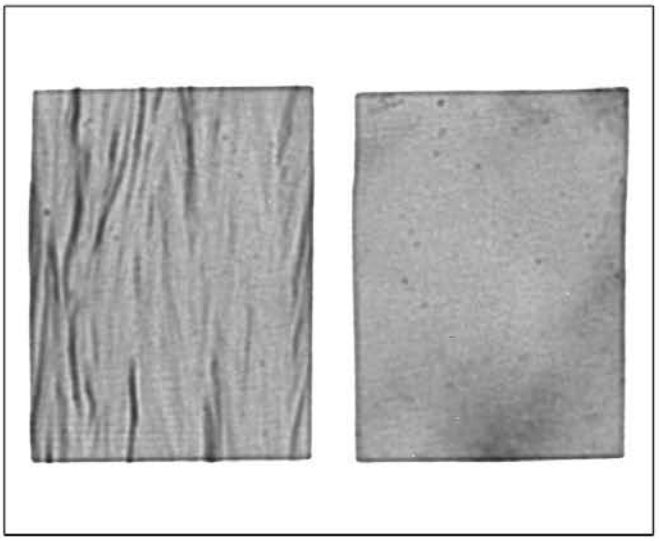

Sample No:	39
Depth:	2227.57 m
Permeability:	114 mD
Porosity:	33.5 %

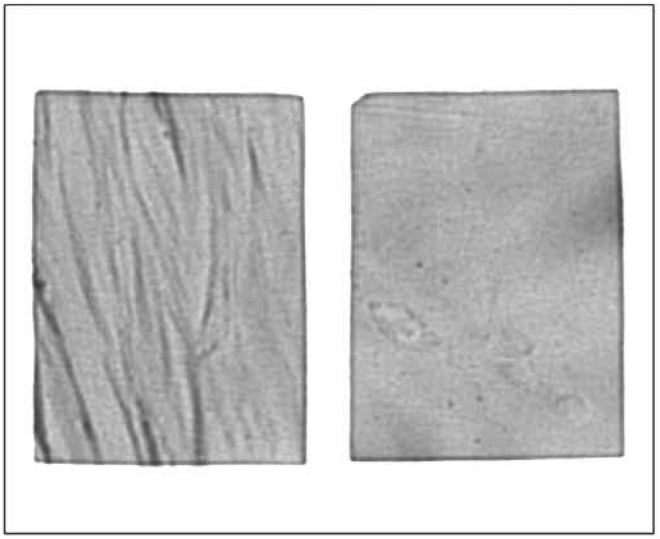

Sample No:	42
Depth:	2228.49 m
Permeability:	120 mD
Porosity:	33.8 %

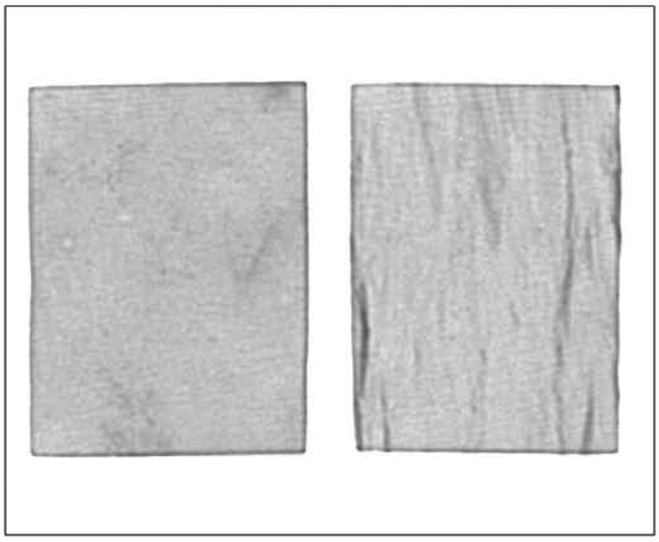

Sample No:	48
Depth:	2230.27 m
Permeability:	387 mD
Porosity:	37.1 %

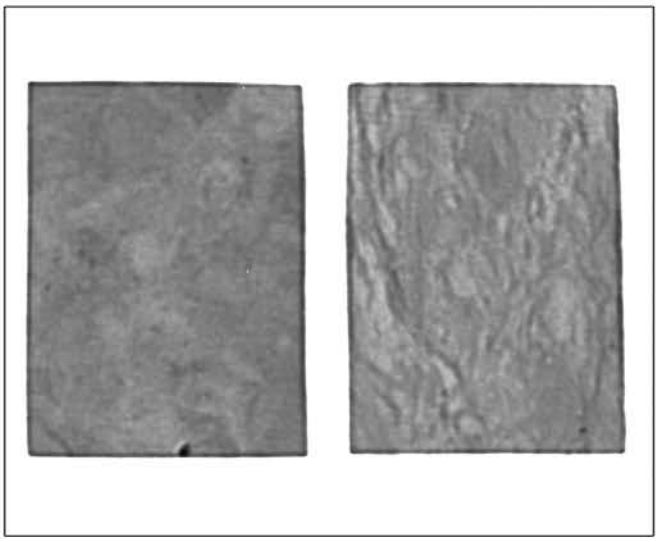

Sample No.:	54
Depth:	2232.08 m
Permeability:	10.2 mD
Porosity:	27.1 %

APPENDIX IV

ABBREVIATIONS

ABBREVIATIONS for CORE PROPERTIES

a	Intercept (assumed = 1)
A	Sample Cross Sectional Area (cm^2)
ABPc	Air-Brine Capillary Pressure
Amb	Ambient Conditions (No Overburden Pressure)
B	Equivalent Conductance of Clay Exchange Cations ($mho/m.cm^2.meq^{-1}$)
β	Beta Factor (ft^{-1})
BF	Basic Flood
BHN	Brinell Hardness Number (kg/mm^2)
BP	Barometric Pressure (atm)
CEC	Cation Exchange Capacity (meq/100g dry sample)
Cent	Centrifuge
Co	Conductivity of Fully Brine Saturated Sample (mho/m)
cP	Centipoise
Cw	Conductivity of Brine (mho/m)
Dr	Drainage (i.e. draining of the wetting fluid - usually brine)
Φ	Porosity
FF	Formation Factor
*FF**	Shaly Sand Equivalent Formation Factor
g	grams
HeInj	Helium Injection
HgInj	Mercury Injection Capillary Pressure
Imb	Imbibition (i.e. imbibition of the wetting fluid - usually brine)
K	Permeability (mD)
Ka	Air Permeability (mD)
Keg	Effective Permeability to Gas (mD)
Keo	Effective Permeability to Oil (mD)
Kew	Effective Permeability to Water (mD)
Kg	Gas Permeability (mD)
KgKo	Gas-Oil Relative Permeability

ACS Laboratories Pty Ltd
ABN: 81 008 273 005

ABBREVIATIONS for CORE PROPERTIES

KgKw	Gas-Water Relative Permeability
Klink or Kl	Klinkenberg Permeability (mD)
Ko	Oil Permeability (mD)
Krg	Relative Gas Permeability
Kro	Relative Oil Permeability
Krw	Relative Water Permeability
Kw	Brine Permeability (mD)
KwKo	Oil-Water Relative Permeability
L	Sample Length (cm)
m	Cementation Factor
*m**	Shaly Sand Equivalent Cementation Factor
mD	milliDarcy's
n	Saturation Exponent
*n**	Shaly Sand Equivalent Saturation Exponent
OB	Overburden Pressure (psig)
OBPc	Oil-Brine Capillary Pressure
P	Pressure (psi)
Pc	Capillary Pressure (psig)
PP	Porous Plate
PvComp	Pore Volume Compressibility
PVR	Pore Volume Reduction (cm^3)
ρ	Density (g/cm^3)
q	Flow Rate (cm^3/s)
θ	Contact Angle (degrees)
Qv	Volume Concentration of Clay Exchange Cations (meq/cm^3)
r	Radius (cm)
Rc	Sample Resistance (ohm)
RCA	Routine Core Analysis

ABBREVIATIONS for CORE PROPERTIES

ResCon	Reservoir Conditions
RI	Resistivity Index
RICP	Resistivity Index & Capillary Pressure
Ro	Resistivity of Fully Brine Saturated Sample (ohm.m)
Rt	Resistivity of Partially Saturated Sample (ohm.m)
Rw	Resistivity of Brine (ohm.m)
S	Saturation
s	Seconds
SCA	Special Core Analysis
Sg	Gas Saturation
Sgr	Residual Gas Saturation
SngPt	Single Point
So	Oil Saturation
Sor	Irreducible Oil Saturation (or Residual Oil Saturation)
SS	Steady State
Sw	Brine Saturation
Swi	Initial Water Saturation
Swir	Irreducible Water Saturation
Swr	Residual Water Saturation
T	Temperature (^{o}C)
USS	Unsteady State
μ	Viscosity (cP)
Vb	Bulk Volume (cm^3)
Vg	Grain Volume (cm^3)
Vp	Pore Volume (cm^3)
ω	Angular Velocity (rad/s)
Wett	Wettability
Wt	Weight (g)

APPENDIX 7: FMI INTERPRETATION REPORT

Origin energy

delivering the goods

Yolla 3

Formation Micro-Imager (FMI) Interpretation Report

T/L1
BASS BASIN

January 2005

by Brett Pidgeon

SUMMARY

This report presents processed and interpreted FMI images from the intervals, 3170 – 3320 m and 3380 – 3440 m within Yolla 3. The studied succession within Yolla 3 is of Palaeocene-Eocene age, and is characterised by variable structural dips, typically in the range 3º-7º, as is listed below. The upper study interval is more structurally complex than the lower interval as reflected in the tectonic tilt that varies over short intervals resulting from fractures and faults.

Structural Zone	Depth Interval	Tectonic Tilt	Comments
3170 - 3320 m			
Zone I	3170 – 3180	3.3°/313°	Fracture or fault bound at 3180 m
Zone II	3180 – 3189.7	3.4°/225°	Change in dip at 3189.7 m
Zone III	3189.7 – 3197.1	5.4°/303°	Fracture or fault bound at 3197.1 m
Zone IV	3197.1 – 3198.9	14.0°/240°	Fracture or fault bound at 3198.9 m
Zone V	3198.9 - 3203	9.6°/037°	Fault bound at 3203 m
Zone VI	3203 – 3204.9	7.6°/122°	Fracture or fault bound at 3204.9 m
Zone VII	3204.9 – 3205.3	2°/061°	Fracture or fault bound at 3205.3 m
Zone VIII	3205.3 – 3206.3	16.6°/225°	Fault bound at 3206.3 m
Zone IX	3206.3 - 3213	6.8°/096°	Change in mudstone dip at 3213 m
Zone X	3213 – 3246.6	5.2°/356°	Change in mudstone overlying sandstone 3246.6 m
Zone XI	3246.6 – 3281.4	6.2°/336°	Change in dip at base of sandstone 3281.4 m
Zone XII	3281.4 - 3313	6.0°/046°	Bounded by erosion surface 3313 m
Zone XIII	3313 - 3320	4.2°/336°	
3380 - 3440 m			
Zone I	3380 – 3409.5	4.2°/336°	Change in mudstone dip at base of sandstone 3409.5 m
Zone II	3409.5 - 3416	10.1°/287°	Change in mudstone dip at top of sandstone 3416 m
Zone III	3416 - 3440	5.6°/338°	

Lithofacies identified from FMI images have been calibrated with cuttings descriptions. Cuttings descriptions match well with lithofacies interpretations derived using wireline log response and FMI image fabrics, and indicate a succession comprising sandstone and mudstone with minor coal. Five lithofacies associations have been identified within the studied section. These are interpreted as having been deposited in a marginal marine / lacustrine (shelf-shoreface?) or fan deltaic setting (prodelta and sub-aqueous shoal water type delta front), and alluvial fans; this setting comprises transverse drainage produced by active faulting within a half-graben. The lithofacies associations identified are summarised as follows:

I. Mudstones that occur at the base of upward coarsening facies successions. (interpreted as either prodeltaic muds, or shelf-shoreface deposits)
II. Heterolithic intercalations of sandstone and mudstone, typically occurring within the lower-mid parts of upward coarsening facies successions (interpreted as either distal fan delta, or shelf-shoreface deposits). When it is interbedded with lithofacies association IV, this implies a sub-aerial setting on a distal alluvial fan.
III. Stratified sandstones with mottled image fabric and low angle (typically <5º) internal bedding surfaces, typically occurring towards the top of upward coarsening facies successions (shoreface deposits).

IV. Successions (often erosively based) of stratified sandstones and pebbly sandstones with dominant internal bedding fabrics inclined at angles <10°, rare intervals of up to 25° dip (distal sheetflood deposits with shallow incised channels).
V. Coals (deposits of swampy coastal plain environments).

Sandstones of Lithofacies Association IV are likely to form the main reservoir intervals. Lithofacies Association III may form a secondary reservoir interval due to these intervals being finer-grained.

Palaeotransport analyses of sandstones from Lithofacies Association III reveals them to be characterised by internal stratification fabrics with very wide ranging sedimentary dip azimuth, suggesting they were originally deposited as "flat lying" strata. Few palaeotransport interpretations can be made for these sandstones. However, in some intervals, a dominant sedimentary dip or cross bedding is present, and may represent onshore migration of fair weather wave formed structures whereas the minor flow direction may represent offshore flow during storm events or rip currents. In most cases, this can broadly be interpreted to have had NE – SE onshore direction and a NW – SW offshore direction.

Palaeotransport analyses of sandstones from Lithofacies Association IV reveals them to be characterised by low angle internal stratification fabrics with variable azimuth. The relationship between intra-set flat lamination, intra-set lamination and coset boundaries suggest that sediment transport occurred normal to the depositional dip i.e. bedforms migrated down fan. Interpreted fan slope drainage directions from low angle laminations are variable and no consistent drainage direction can be inferred. Rare cross bedding within this lithofacies has a general southerly palaeoflow direction and indicates transverse flow derived from intrabasinal highs e.g. footwall of a half graben.

FMI logs were not acquired over the upper Eastern View Coal Measures due to the logging tool hanging up on the intermediate logging run.

TABLE OF CONTENTS

LIST OF TABLES

LIST OF FIGURES

LIST OF ENCLOSURES

		Scale
Enclosure 1	Quality control plot of FMI log, 3170 - 3540 m	1:500
Enclosure 2	Overview structural summary log, 3170 – 3450 m	1:500
Enclosure 3	Data overview plot, 3170 – 3450 m	1:200
Enclosure 4	Sedimentological summary plot, 3170 – 3205 m	1:100
Enclosure 5	Sedimentological summary plot, 3275 – 3320 m	1:100
Enclosure 6	Sedimentological summary plot, 3380 – 3450 m	1:100

INTRODUCTION

The processing and interpretation of the Formation Micro-Imager (FMI) images from Yolla 3 are documented in this report. The detailed sedimentological report is based on FMI images for the intervals 3170 – 3320 m and 3380 – 3440 m.

Objectives

The well details and project objectives for Yolla 3 are summarised in Table 1 with the data that was incorporated into this study.

Table 1. Summary of well details, study objectives and the data set used for this analysis.

Well Details	
Well: Surface Latitude: Surface Longitude: Intervals of interest:	Yolla 3 39° 50' 40.47" S 145° 49' 06.08" E Palaeocene – Eocene succession interpreted as marginal marine/lacustrine – alluvial environment.
Summary of study objectives	
Log Depth Intervals	Objectives
3170 – 3320 m 3380 – 3440 m	Processing of FMI images to provide speed corrected false colour images. QC of images to determine the quantity of information that is interpretable.
3170 – 3320 m 3380 – 3440 m	Summary structural overview using automatic dip calculations, supplemented by manual dip-picking.
3170 – 3320 m 3380 – 3440 m	Overview sedimentological interpretation of features evident within FMI images with the aim of focusing upon variations in palaeocurrent transport directions. This required the manual characterisation of dip features and their interpretation over these intervals.
3170 – 3320 m 3380 – 3440 m	Detailed sedimentological interpretation and lithofacies characterisation.
Data incorporated in study	
3170 – 3320 m 3380 – 3440 m	Open hole logs from Platform Express suite. Raw FMI data in DLIS format.
3170 – 3320 m 3380 – 3440 m	Cuttings description

Depth and directional references

Unless otherwise mentioned, all depths in this report reference log depths. Orientation data is referenced using the standard convention of dip/dip azimuth. For example, 3°/313° indicates a dip of 3° (measured from the horizontal) towards 313° (referenced clockwise from north). Borehole orientation data follows a convention of deviation/azimuth of deviation. For example, 2°/300° indicates an 2° deviation from the vertical towards 300° (SW).

PROCESSING AND QUALITY CONTROL

The Formation Micro-Imager (FMI) tool was run by Schlumberger on 6th September 2004 in the 8½ inch section of Yolla 3 over the interval 2337 – 3494 m.

The Schlumberger Formation Micro-Imager tool is a pad based micro-resistivity imaging device, with an array of 24 measuring electrodes (buttons) on each of pad and flap, with 192 buttons in total. Flaps are offset vertically from the pads by approximately 6 inches. The electrodes are 0.2 inch in diameter and data is sampled at 0.1 inch vertically and horizontally with a bedding resolution of approximately 1 cm. The data is processed to provide 75% coverage of the borehole wall in an 8.5 inch hole. This data also provides 12 Stratigraphical High Resolution Dipmeter (SHDT) tool curves for standard dipmeter processing.

Processing was carried out over the logged interval using Terrasciences TerraStation Formation Viewer module.

The mud system was sea water/Drispac/Soltex with a resistivity of 0.184 Ωm, a viscosity of 98 S and a density of 9.45 lbm/gal. The fluid losses encountered during drilling were minimal (3.1 cm^3). The borehole reached a maximum temperature of 143°C.

An FMI log quality control plot is shown in Enclosure 1. These plots provide detailed information concerning hole orientation, tool orientation, hole condition and FMI operating parameters.

Borehole conditions

FMI image quality is related to borehole condition, which is good throughout the section in Yolla 4 with clear geological detail visible and only minor image artefacts. Borehole deviation is 3.1°/313° at 3165 m and 1.7°/305° at 3310 m, 0.7°/302° at 3368 m, and 0.5°/160° at 3455 m.

A summary of hole conditions is included in Table 2.

Within the upper study interval 3170 – 3320 m the callipers show that the hole is consistently in gauge. There is little difference in the C1 and C2 callipers (typically only 0.25 inch). Intervals of ovalisation (up to 1 inch) are not limited to one direction, but present in both callipers. In the lower interval (3380 – 3440 m) there is limited breakout in either direction, and the C1 and C2 callipers typically overlie.

Table 2. Summary of hole conditions through the study intervals in Yolla 3

Normal Hole Size	Interval Depth	Comments
3170 – 3320 m		
8.5	3170 - 3186	In gauge
	3186 - 3188	1” overgauge
	3188 - 3235	0.5” overgauge
	3235 - 3242	In gauge
	3242 – 3246	0.5” overgauge
	3246 – 3255	In gauge
	3255 – 3274	0.5” overgauge
	3274 – 3278	In gauge
	3278 – 3320	0.5” overgauge
3380 – 3440 m		
8.5	3380 – 3440	In gauge

Data processing

Speed correction

The accelerometer speed correction utility corrects FMI micro-resistivity data for minor variations in recording velocity induced by tool or cable friction. Extremes in velocity variation may occur when the tool is either stationary or rapidly accelerating as a result of being stuck or the logging being stopped for pipe removal. The most important parameter for the speed correction procedure is the zero-sum window, which prevents cumulative build-up of erroneous shifts within a window. Thus all shifts applied by the speed correction should add up to zero within a certain window length. The length of this window is decided by experimenting and the general roughness of the logging run. In the case of Yolla 3, a window of 4 ft was chosen. The speed correction shift curve is calculated by double integration of the Z-accelerometer curve with the cable speed representing the window constant. The resulting shift curve is then applied synchronously to all curves in the log.

Image processing

Before generating the false-colour images from the speed corrected data, the individual curves are transferred back to their physical depth referenced positions. The images are produced with two types of resistivity scaling:

- *Static normalised* images have the same relative resistivity scaling over larger intervals and therefore illustrate large-scale resistivity variations related to lithology and phase changes. Dependent on Emex current variability.

- *Dynamic normalised* images were scaled within a 0.5 m sliding window, thereby maximising the expression of more detailed rock fabrics (and noise).

In this study, the dynamic normalised images were used primarily for bedding, lithofacies and structure identification. Image polarity was correctly matched to openhole resistivity logs.

Block depth shifts

No block depth shifts were applied to the Yolla 3 data.

Dip processing

Two types of dip computation were conducted on the Yolla 3 dataset.

Computed dip correlations were carried out on the SHDT curve sub-set from the loaded interval (Enclosures 1). These correlations use refined least-squares algorithms with regression coefficients cut-offs for each correlation pair. The interval computation parameters were aimed at correlating bedding features using pad-to-pad (PTP) algorithms with the following parameters:

- 60 cm correlation interval, 50 cm step distance and a 70° search angle (referenced to borehole axis) and the cut-off set at 0.2 for individual curve pairs.

This computation also included stacking of three consecutive correlation surfaces. The stacking of dips in this way tends to smooth dip patterns and trends and is a viable method of "quick-look" identification of structural dip. These parameters are referenced as "4X2X70ST3" in Enclosure 1. Detailed interpretation of dip patterns should not be carried out on results from this processing.

Manual dips were computed directly from the images using the TerraStation Formation Viewer (e.g. Enclosure 2). The major advantage of the manual dip technique is that each feature may then be classified into a geological category and that only the results in which the interpreter has confidence are used for further interpretation. A further advantage of manual dip picking is the ability to measure and orientate discordant surfaces such as fractures and faults, which are unlikely to be correlated by standard interval correlation techniques

SEDIMENTOLOGICAL ANALYSIS

Tectonic tilt determination

Prior to detailed sedimentary analyses, it is first required to evaluate structural dip, so that the sedimentary surfaces identified in FMI images can be restored to their original orientation or "sedimentary dip". Structural dip (or tectonic tilt) is the attitude of formations resulting solely from tectonic movements. Structural dip is best determined from beds that were originally deposited as horizontally stratified deposits. These beds can include mudstones, or parallel stratified laminations within heterolithic successions comprising interbedded sandstone-mudstone laminae. The structural dip interpretation within well Yolla 3 was an iterative process involving:

- Initial evaluation of automatic computed dips to identify general data trends.
- Manual picking of shale bed dips to confirm tectonic tilt throughout the studied succession.

Tectonic tilt evaluated on the basis of dip data through shale intervals is summarised in Table 3. Before undertaking a sedimentological interpretation structural dip was removed from the "manual" data set. The structural dip was removed following identification of intervals of strata (structural zones) of consistent structural dip. The structural dips are summarised in Enclosure 2.

Table 3. Tectonic tilt summary of Yolla 3.

Structural Zone	Depth Interval	Tectonic Tilt	Comments
3170 – 3320 m			
Zone I	3170 – 3180	3.3°/313°	Fracture or fault bound at 3180 m
Zone II	3180 – 3189.7	3.4°/225°	Change in dip at 3189.7 m
Zone III	3189.7 – 3197.1	5.4°/303°	Fracture or fault bound at 3197.1 m
Zone IV	3197.1 – 3198.9	14.0°/240°	Fracture or fault bound at 3198.9 m
Zone V	3198.9 - 3203	9.6°/037°	Fault bound at 3203 m
Zone VI	3203 – 3204.9	7.6°/122°	Fracture or fault bound at 3204.9 m
Zone VII	3204.9 – 3205.3	2°/061°	Fracture or fault bound at 3205.3 m
Zone VIII	3205.3 – 3206.3	16.6°/225°	Fault bound at 3206.3 m
Zone IX	3206.3 - 3213	6.8°/096°	Change in mudstone dip at 3213 m
Zone X	3213 – 3246.6	5.2°/356°	Change in mudstone overlying sandstone 3246.6 m
Zone XI	3246.6 – 3281.4	6.2°/336°	Change in dip at base of sandstone 3281.4 m
Zone XII	3281.4 - 3313	6.0°/046°	Bounded by erosion surface 3313 m
Zone XIII	3313 - 3320	4.2°/336°	
3380 – 3440 m			
Zone I	3380 – 3409.5	4.2°/336°	Change in mudstone dip at base of sandstone 3409.5 m
Zone II	3409.5 - 3416	10.1°/287°	Change in mudstone dip at top of sandstone 3416 m
Zone III	3416 - 3440	5.6°/338°	

Cumulative dip azimuth plots for mudstone bedding surfaces within the studied intervals (3170 – 3320 m and 3380 – 3440 m) from Yolla 3 are presented in Figure 1. These plots clearly illustrate the structural subdivisions proposed for this well.

Classification of sedimentary features

Classification of sedimentary surfaces recognised from borehole image logs is a three stage iterative process involving:

- First pass dip picking. This phase of feature identification is carried out in conjunction with examination of wireline logs, and results in a simple 2-fold sub-division of dip features into mudstone and "others".
- Structural dip is removed from the data set using a workstation based stereographic technique to provide sedimentary dips.
- Sedimentary dips are re-classified in the workstation environment. Wireline logs are used to drive lithofacies interpretation. Sedimentary dips within sandstone lithologies are characterised using a hierarchical scheme depending upon their dip and orientation.

The hierarchical scheme applied to Yolla 3 is illustrated in Figure 2 and Table 4 below, and sedimentary dips for the studied intervals 3170 - 3320 m and 3380 - 3440 m are indicated in Enclosures 4 - 6.

Table 4. Classification of surfaces identified from FMI images.

Dip type	Interpreted dip category	Colour	Description
LB	Lithological boundary	Blue green	Low true dip angle surfaces which define a marked resistivity between overlying and underlying beds. Wireline logs indicate a lithological contrast.
LBe	Erosional lithological boundary	Dark green	Erosive surfaces which define a marked resistivity between overlying and underlying beds. Truncation of bedding fabrics beneath the surface may be evident. Wireline logs indicate a lithological contrast.
LBc	Cemented lithological boundary	Pale blue green	Sharply defined highly resistive or conductive bed. Bounding surfaces may define planar or "nodular" features. Normally associated with change in wireline log response.
ISS	Intra set surface	Yellow	Inclined surfaces typically dipping at a true dip angle greater than 5°. Surfaces may be inclined at angles up to 25°-30° (i.e. close to angle of repose), and occur within distinct groups of similar orientation. Surfaces typically show cm-dm scale spacing in borehole image logs. They are discordant to set (or bed) and coset boundaries.
SB	Set (bed) boundary	Brown	Surfaces within sandstone lithologies which are typically (though not exclusively) inclined at sedimentary dip of < 15°. Set boundaries define a group or "set" of intraset surfaces of similar orientation. The set boundary is distinguished from the intraset surfaces by its different orientation. Set boundaries typically occur at dm - m scale spacing in borehole image logs.
CSB	Coset boundary	Cyan	A surface separating a group of sets of similar orientation. Note: Coset boundaries may also define a single bed or set displaying a significantly different internal fabric to those sets surrounding it. Set boundaries are typically identified at m scale spacing in borehole image logs. Note: Coset boundaries may also define a single bed or set at dm scale which displays a significantly different internal fabric to those sets surrounding it.
ISSf	Flat/horizontal	Purple	Near horizontal intraset surfaces with true dip angle (<5°), characterised by resistivity contrast several cm thick. Sedimentary dip azimuth may be variable due to flat lying nature of these beds, and errors associated with fitting dips to such surfaces. Surfaces typically show cm scale spacing in borehole image logs.
PDf	Poorly defined feature	Dark purple	These surfaces may be any of the above but are very poorly defined in terms of continuity around the borehole.
XSB	Small scale cross beds	Red	Cm-dm scale cross stratification fabric, too small to be characterised in detail.
MUDS	Shale bedding	Green	Confident bedding features with consistent magnitudes.
HETS	Heterolithic bedding	Orange	Confident bedding features with approximately consistent magnitudes.

Lithofacies characterisation

Lithofacies identification was first carried out using FMI images in conjunction with openhole log suites. The FMI interpretations were then calibrated against cuttings.

Lithofacies identified from FMI logs.

The sedimentological interpretation of FMI images and dipmeter data were carried out with the aid of gamma ray, density, neutron porosity and sonic logs. Lithofacies were interpreted on the basis of variations in wireline log response in conjunction with fabrics observed in FMI images (Table 5). During interpretation, cuttings descriptions were also used to help provide a guide to lithology, but were found to have only moderate depth resolution (i.e. matching of cuttings description to log /response) due to dispersion of cuttings during circulation of drilling muds. Four broad lithofacies were interpreted as being present, i.e. sandstones, mudstones, finely inter-bedded heterolithic successions and coals. Heterolithic successions comprise centimetre-decimetre scale interbedded sandstone, siltstone and mudstone beds. Coals formed a minor lithofacies within the study intervals, and are clearly recognisable by their low density, high porosity and high resistivity log response (Figure 3).

Lithofacies types were classified according to a simple scheme using mnemonics based upon interpreted lithology and contained fabric, the latter being determined from borehole image log and associated dip data. Examples of identified lithofacies are summarised below in Table 5.

Table 5. Lithofacies identified from FMI images within the study intervals.

Inferred Lithology/Grain Size	Typical Log Response	Image Log Fabrics	Lithofacies Mnemonic
Sandstone	GR <60 API RHO8 2.2 – 2.4 g/cc HTNP 0.12 – 0.20	Laminated	Sl
		Cemented	Sc
		Fine scale mottled or "speckled" texture with poorly defined or disrupted lamination fabric	Sm
		Coarse scale mottled texture with poorly defined or disrupted lamination fabric. Mottling comprises resistivity elements several cm in diameter	Scm
Heterolithics	GR 60 – 110 API RHO8 2.4 – 2.65 g/cc HTNP 0.2 – 0.25	Laminated	Hl
		Mottled with disrupted lamination fabric	Hm
Mudstone	GR 110 – 180 API RHO8 2.65 – 2.75 g/cc HTNP 0.25 – 0.35	Laminated	Ml
		Mottled with disrupted lamination fabric	Mm
Coal	GR variable typically <60 API RHO8 <2.2 g/cc HNTP >0.35	Laminated	Cl
		Mottled	Cm

The hierarchical combinations of different lithofacies mnemonics were used to provide detailed descriptions of lithofacies types. In these descriptions, the enclosure of lithofacies mnemonics in parenthesis was used to denote the minor presence of a lithofacies type, or poor development or preservation of a sedimentary structure, e.g.

- Mm (Ml) mottled mudstones with relict lamination or minor laminated intervals.
- Sm (Sl) mottled sandstone with poorly defined relict lamination.
- Sl (Sm) laminated sandstone with minor fabric loss due to mottling / disruption of lamination etc.

Figures 4 - 8 illustrate examples of different lithofacies types for the lithologies identified, together with their fabric index.

There is uncertainty in the interpretation of the mottled fabrics lithofacies as this fabric in borehole image logs may arise from a number of different mechanisms. These could include:

- Differential cementation or the presence of nodular cements.
- Artefacts such as scattered drilling debris on the borehole wall.
- Textural variations due to biogenic disruption of sediments (bioturbation or rootlets).
- Textural variations associated with dewatering fabrics in sediments.
- The presence of coarse detritus such as pebbles or clay flakes.

Close examination of FMI images reveals that mottled textures are present at 2 distinct scales:

Speckled image texture, in which scattered mottles and speckles occur at *circa* 1 cm scale, and are associated with diffuse bedding fabric. This "fine" scale mottling occurs within a range of lithologies displaying poorly defined lamination, vague and vague mottled texture. These intervals are not characterised by the presence of coarse detritus (pebble clasts etc.).

Strongly mottled image texture, in which mottles are defined by resistivity features of several cm in diameter, so that often, only 2 or three "mottles" may be seen across an individual FMI pad. This "coarse" mottling possibly corresponds to intervals containing granular and pebbly sandstones.

Mottled / disrupted lamination fabrics observed within image logs through mudstone and heterolithic lithologies may reflect bioturbation within sediments. However, in the absence of sufficient core calibration, this interpretation should be treated with caution. Similar fabrics could be generated by a variety of phenomena including nodular cementation patchy sand distribution etc.

Calibration of image log fabrics using cuttings descriptions

Calibration of image log fabrics was carried out using:

- Cuttings descriptions through the logged intervals. Cuttings descriptions are summarised on Enclosure 3.

Image log calibration using cuttings

Generally, cuttings descriptions match well with lithofacies interpretations derived using wireline log response and FMI image fabrics. Cuttings descriptions reveal a succession comprising sandstone, siltstone and claystone with rare intervals of coal.

Characterisation of heterolithic successions comprising individual beds beneath the resolution of wireline logs is difficult. However, image logs revealing extreme resistivity variation within strata containing cm-dm scale bedding fabrics provide some insight as to the presence of these heterogeneous lithologies. Cuttings descriptions through successions interpreted from wireline log and FMI as comprising heterolithic deposits, invariably yield documentation of cuttings of claystone, siltstone and sandstone in varying proportions.

FMI derived lithological fabric index

The hierarchical lithofacies nomenclature scheme applied to description of lithofacies from borehole image logs was also used to provide a simple four-fold fabric index as illustrated for sandstones in Table 6 below. This type of fabric index may be useful for comparison of reservoir properties with image log derived lithological properties. Note, if mottled fabrics identified within sandstones are due to bioturbation, this fabric index may also approximate to a four-fold bioturbation index, which may be useful in construction of sedimentary models using data derived from image logs.

Table 6. Simple fabric index (applied to sandstone lithofacies) based upon mnemonics scheme used for FMI interpretation of lithofacies. Note the fabric index may approximate to a bioturbation index within sandstone lithologies free of granular-pebbly detritus.

Lithofacies	Approximate degree of fabric development within sediments.	Fabric Index
Sl	Minimal <10%	1
Sl (Sm)	approximately 25 %	2
Sm (Sl)	approximately 75 %	3
Sm	near total 100 %	4

The implication of the fabric index is that low indices will result in strongly anisotropic reservoir properties (e.g. Kv > Kh). If due to phenomenon, such as bioturbation, creating mottled image fabric and loss of stratification, higher fabric indices may reflect more homogeneous reservoir properties (e.g. decrease in Kv:Kh ratio due to loss of stratification).

Lithofacies associations

The sedimentary deposits in the intervals 3170 – 3320 m and 3380 – 3440 m within Yolla 3 comprise a heterolithic succession of sandstones and mudstones with minor intervals of coal. The successions can be sub-divided into a number of discrete sub-units based upon log trends and stacking patterns of interpreted lithofacies.

In particular, upward decreasing gamma ray log trends, and NPHI and RHOB log response which trends towards sandstones indicate stacked successions of upward coarsening / upward cleaning deposits that represent parasequences. Sedimentary dips within these upward cleaning successions are typically low (< 12°). However, upward cleaning (and

coarsening) trends are in some cases punctuated by development of sandstones with blocky log character, and elevated sedimentary dips in excess of 12°.

The upward coarsening parasequences described are consistent with a model of deposition in a marginal lacustrine/marine environment, with upward coarsening profiles forming as a result of shoreface or delta front progradation. Blocky sandstones characterised by sedimentary surfaces with elevated dips may represent the deposits of distributary channels or upper shoreface/foreshore environments. The lithofacies identified are described in detail in the following sections. In the absence of core calibration the following discussions are should be considered speculative.

Observed vertical transitions in lithofacies types identified in borehole images have enabled lithofacies to be grouped into genetically related successions of strata or *lithofacies associations*, which have some environmental significance (Walker 1992). Five lithofacies associations were identified within the studied data set, and their distribution within the studied intervals is illustrated in Enclosures 4 - 6. The lithofacies associations identified are summarised below.

Lithofacies Association I

Lithofacies Association I is argillaceous, mainly comprising mudstone lithologies (Ml and Mm), with minor interbedded heterolithic lithologies. The mudstones occur at the base of successions displaying overall upward cleaning (and coarsening) gamma ray log trend (e.g. 3283 –3300 m Enclosure 5) and commonly display a mottled fabric, which decreases in intensity upward through the succession. This may reflect decreasing intensity of cementation mottling upward through the succession.

Generally, Lithofacies Association I forms relatively thick deposits up to several metres thick, and is characterised by blocky to serrate, overall high gamma-ray log response (>110 API), reflecting the presence of a predominantly argillaceous succession of lithofacies types. Gamma ray log response within mudstones typically decreases slightly upward, forming part of an overall upward decreasing trend. Lithofacies Association I typically pass upward into heterolithic lithofacies of Lithofacies Association II.

The mudstones of Lithofacies Association I display low sedimentary dip (typically <10°), except where associated with compaction features and structural features e.g. faults, with wide ranging dip azimuths (covering 360^{o} spread) indicative of their original deposition as parallel stratified sediments upon a flat lying substrate.

Sedimentation within Lithofacies Association I was probably dominated by suspension fallout of argillaceous material, resulting in the accumulation of laminated mudstone lithofacies (Ml, etc.).

As mudstones grade upward into sandier deposits, the degree of mottling, possibly indicating siderite nodules etc., decreases, reflecting changes in environmental conditions.

Lithofacies Association II

Lithofacies Association II comprises heterolithic lithologies. Heterolithic sediments consist of centimetre to decimetre scale interbedded sandstones and mudstones, and often display a highly mottled image fabric. Within the studied intervals, heterolithic deposits may form successions in excess of 5 m thick. Heterolithic deposits predominantly occur towards the base of facies successions which display overall upward cleaning (and

coarsening) gamma ray log trend. This lithofacies association also occurs with lithofacies association IV.

Sedimentary dips within heterolithic deposits are typically characterised by low angle fabrics (inclined typically <10° sedimentary dip). Removal of structural dip reveals these bedding fabrics to be characterised wide ranging (up to 360° spread) dip azimuths, indicative of their original deposition as approximately horizontally stratified sediments.

The heterolithic nature of these deposits suggests deposition via both tractional and suspension processes. In a shallow marine/lacustrine setting, this style of deposition may have occurred at or around fair weather wave base in lower-shoreface setting, or perhaps in the sub-aqueous portion of a shoal water type delta front. When it is interbedded with lithofacies association IV, this implies a sub-aerial setting on a distal alluvial fan.

Lithofacies Association III

Lithofacies Association III mainly comprises sandstone lithologies, with a variety of different internal fabrics (fine scale mottled, well laminated, mottled with relict lamination etc.). Well preserved lamination fabrics are not generally common within images through sandstone lithologies. Lithofacies Association III is characterised by low angle sedimentary dips (typically approximately 10°), and forms successions up to 5 m thick within the studied sections. The sandstones typically rest gradationally upon heterolithic deposits of Lithofacies Association II, in the upper parts of upward coarsening successions. The sandstones of Lithofacies Association III are distinguished from those of Lithofacies Association (IV) discussed below by lower sedimentary dips. The low angle sedimentary dips (typically <10° rarely up to 15°) that are characteristic of this lithofacies association, often display dm to m scale cosets, which may display a relatively tight cluster of unimodal dip azimuths. Flat lying intraset surfaces are also common within this lithofacies association. Few interpretations can be made as to the relative spatial distribution of laminated versus mottled image fabrics within sandstones from this lithofacies association.

The low angle stratification within these sediments is indicative of deposition by traction processes. The occurrence of these sediments within the upper parts of interpreted upward coarsening lithofacies successions, and the often variable orientations of cosets comprising low angle internal stratification that is common within some successions, may be consistent with deposition in a shallow marine/lacustrine environment. In these settings, both unidirectional and oscillatory currents (together forming combined flows) during storms produce variety of 2- and 3-dimensional bedforms. Sedimentary fabrics characterised by sets of low angle stratification of variable orientation may indicate deposition as low amplitude, perhaps strongly 3-dimensional mounded bedforms. In a shallow marine/lacustrine setting, this style of deposition may have occurred above fair weather wave base in shoreface setting. Successions where low angle surfaces display more unimodal distribution of azimuths may indicate the presence of a more significant palaeoslope or sediment transport and deposition under the influence of more unidirectional current systems. Alternately, the low angle parallel lamination fabrics could be consistent with deposition as sands within the upper parts of a shoal water type delta front.

Lithofacies Association IV

This FMI derived lithofacies is sand dominated, mainly comprising Scm, Sm, Sl, Sm(Sl) and Sl(Sm), with minor heterolithic and mudstone lithofacies. Association IV occurs in successions up to 10 m thick within the studied intervals. Three intervals within the studied succession have been assigned to Lithofacies Association IV, and few conclusions can be drawn concerning the spatial distribution of different lithologies within these deposits.

Interpretation of manually picked dips from FMI images indicates the presence of intraset surfaces inclined at angles up to 20°, these steeply inclined surfaces distinguishing this lithofacies association from Lithofacies Association III above. However, both Lithofacies Associations are dominated by Sl, and are differentiated on the basis of position in the succession. Lithofacies Association III occurs at the top of the upward cleaning/upward coarsening successions, whereas, Lithofacies Association IV occurs in thick, amalgamated sandstone units.

The coset boundaries occur at dm to m scale and dip data sets, in places, for Lithofacies Association IV indicate an azimuthal spread of between 90° and 180°, however there is a low azimuthal dispersion within cosets. The coset boundaries within this lithofacies association have similar orientations to the ISSf indicating downfan progradation of sheetflood deposits. Other intervals have variable orientations implying deposition as flat lying sediments.

The cross stratified sediments of Lithofacies Association IV may represent the deposits of channels (fluvial or distributary) within an alluvial setting, however, the dominance of Sl and the thin cross stratified sets indicates unconfined sheetfloods. Evidence of primary stratification within these deposits testifies to the development and migration of bedforms, with the locally cross-bedding indicating dunes and sand waves. Mottled FMI lithofacies Scm reflects the presence of coarse grained pebbly sandstones and mudstone rip up clasts. Finer scale mottling and disrupted lamination / relict internal stratification fabrics within lithofacies Sm may indicate de-stratification a result of sediment de-watering. De-watering may have arisen as a result of pore-pressure adjustments during rapid deposition and burial of sediments, or as a result of a rapid rise / fall in fluvial stage. Alternatively, the mottling could result from biogenic activity (rootlets).

The cosets of strata are typically thin, which indicates unconfined flow and the dominance of Sl imply upper flow regime conditions. Palaeotransport implications for this lithofacies association are discussed in detail in the following sections.

Lithofacies Association V

Coals form a very minor lithology within the studied section, and only present in one interval (3305 – 3307 m). The coal is characterised by high resistivity, low density and high porosity. In images they either display little internal structure, other than rare flat lying internal "bedding" surfaces or have a mottled texture reflecting a lack of internal structure.

Coals occur towards the top of small scale upward coarsening mudstone-heterolithic sandstone successions and in association with thick sandstone intervals.

Summary

The integrated analyses of wireline log signature and FMI fabric allows identification of a variety of different lithofacies types. Calibration with cuttings descriptions has permitted limited lithofacies interpretation from FMI logs. However, in absence of core calibration the environmental interpretations outlined in the following section should be treated with caution as it is only speculative.

Summary of environmental interpretations

A brief summary of the sedimentary successions analysed in detail and their environmental interpretation is provided in the following sections. Detailed discussions of palaeotransport observations are included in the Bedform Orientation and Sediment Dispersal section of this report.

Interval 3400 – 3440 m

Wireline logs and FMI interpretations through this interval indicate that it can be subdivided into four intervals; a lowermost coarsening upward / heterolithic interval, a lower blocky sand interval, a middle heterolithic dominated interval, and an upper coarsening upward interval. The succession is overall heterolithic with mudstone / heterolithics interbedded with sandstone at the base that passes upwards into sandstone. The sandstone is overlain by a sharp based fine grained succession of heterolithics and minor mudstone that passes upwards into heterolithics and sandstone. Details are summarised below in Table 7.

Table 7. Summary of deposits in the interval 3400 – 3440 m

Interval 3400 – 3440 m			
Depth (m)	**Lithofacies Association**	**Brief Description**	**Interpretation**
3433 - 3440	I -> II -> III	Laminated mudstone overlain by heterolithics with thin laminated sandstone at top	Fining upward succession without coals suggesting shallow marine / lacustrine.
3424 – 3433	I, II, III	Heterolithic succession of mudstone, heterolithics and laminated sandstone arranged in metre scale coarsening upward cycles.	Small scale coarsening upward succession is consistent with progradation of shoreface / fan delta deposits.
3417 – 3424	IV	Blocky log response, comprising laminated sandstone.	Blocky sandstone with sharp base and top, low sedimentary dips indicates upper flow regime deposition, possibly as unconfined, low density distal sub-aerial sheetfloods (Benvenuti, 2003). Cross bedded intervals reflect channelised flow.
3410 - 3417	II rare I	Sharp based, blocky log response comprising heterolithics with rare mudstone.	Sharp base reflects rapid abandonment of sub-aerial fan surface and low energy deposition in distal floodplain or offshore environments.
3404 - 3410	I -> II -> III	Upward cleaning (coarsening) succession comprising massive to laminated mudstones, heterolithics and laminated sandstones.	Upward coarsening profile overlying mudstone suggests possible subaqueous fan delta deposition by high density turbidity currents (Benvenuti, 2003), alternatively, possible fan lobe migration in sub-aerial setting.
3400 – 3404	I	Sharp based, massive and laminated mudstones	Thick mudstone interval overlying fan lobe / subaqueous fan delta implies rapid deepening, e.g. offshore transition

Interval 3380 – 3395 m

This interval comprises two stacked upward cleaning (coarsening) successions as identified on wireline logs and FMI interpretations. The succession is heterolithic with the coarsening upward successions typically comprising mudstone at the base overlain by heterolithics and sandstone. The upper boundary of these successions is sharp. Details are summarised in Table 8.

Table 8. Summary of deposits in the interval 3380 – 3395 m

Interval 3380 – 3395 m			
Depth (m)	**Lithofacies Association**	**Brief Description**	**Interpretation**
3380 - 3395	I -> II -> III	Two stacked cleaning (coarsening) upward successions comprising laminated mudstones, heterolithics and laminated sandstones. The succession is dominated by heterolithics. Low angle sedimentary dips (<5°) and wide ranging azimuths indicate flat lying deposition	The upward coarsening profile is consistent with deposition in a prograding shoreface / deltaic environment. Lack of bioturbation (mottling) implies anoxic bottom conditions.

Interval 3270 – 3290 m

Wireline logs and FMI interpretations in this interval suggest that it comprises a heterolithic succession of strata in an upward cleaning (coarsening) succession. Details are summarised in Table 9.

Table 9. Summary of deposits in the interval 3270 – 3290 m

Interval 3270 – 3290 m			
Depth (m)	**Lithofacies Association**	**Brief Description**	**Interpretation**
3270 - 3290	I -> II -> III	Upward cleaning (coarsening) succession comprising massive to laminated mudstones, heterolithics and laminated sandstones.	Upward coarsening profile suggests a progradational shoreface environment.

Interval 3235 – 3265 m

Wireline logs and FMI interpretations through this interval suggest that it comprises a heterolithic succession of strata arranged in an upward cleaning (coarsening) succession at the base, overlain by a blocky sandstone and thin, cleaning (coarsening) upward packages. Details are summarised in Table 10.

Table 10. Summary of deposits in the interval 3235 – 3265 m

Interval 3235 – 3265 m			
Depth (m)	**Lithofacies Association**	**Brief Description**	**Interpretation**
3254 - 3265	I -> II -> III	Upward coarsening interval with high GR sandstone (> 200 API) at top. Massive and laminated mudstones pass upwards into heterolithic and laminated sandstones	Upward coarsening profile suggests a progradational shoreface environment. High GR sandstone may reflect heavy minerals within shoreface / foreshore environment
3247 - 3254	IV	Laminated sandstone with rare intervals of sedimentary dips over 10° record predominantly southerly dip azimuths.	Distal sub-aerial low concentration sheetflood deposits with southerly drainage.
3241.5 – 3247	II	Heterolithic coarsening upward interval	Stratigraphic position implies sub-aerial abandoned alluvial fan lobe
3236 – 3241.5	IV	Laminated to massive sandstone with rare sedimentary dips >10°. Thin mudstone drapes.	The presence of massive and laminated sandstones implies shallow sub-aerial deposition. Mudstone drapes implies waning flow deposition.
3235 - 3236	I	Massive to weakly laminated mudstone	Interval overlies sub-aerial fan deposits and may represent offshore deposition following transgression

Interval 3170 – 3205 m

Wireline logs and FMI interpretations through this interval suggest that it comprises a heterolithic succession of strata, with lithologies comprising mudstones, heterolithics and sandstones. A series of upward cleaning (coarsening) and upward fining trends are evident from log suites. The succession is dominated by heterolithic intervals. Details of interpretations are summarised in Table 11.

Table 11. Summary of deposits in the interval 3170 – 3205 m

Interval 3170 - 3205 m			
Depth (m)	**Lithofacies Associations**	**Brief Description**	**Interpretation**
3199 – 3205	I -> II -> III	Upward cleaning (coarsening) succession comprising massive to laminated mudstones, heterolithics and laminated sandstones	Upward coarsening profile suggests a progradational shoreface environment.
3196 – 3199	I	Laminated to massive mudstone	Sharp base implies rapid transgression into offshore
3192 – 3196	II	Sharp based heterolithic strata	Interval correlates with sub-aqueous fan delta in Core 1 Yolla 4; interpreted as proximal sub-aqueous fan delta. Fining upward trend may indicate lateral migration of active lobe
3188.5 - 3192	VI -> II	Laminated sandstone pass upward into fining upward succession of heterolithic strata	Sharp based laminated sandstone overlain by heterolithic interval implies abandonment / lateral migration of alluvial fan setting.
3180 – 3188.5	II -> VI	Coarsening upward stacking of heterolithic strata and laminated sandstone, rare sedimentary dips up to 20° in sandstones	Coarsening upward stacking with laminated sandstones implies lateral migration of alluvial fan setting
3173 - 3180	I -> II	Massive to laminated mudstones pass upward into a succession of heterolithic strata	Upward coarsening profile suggests possible low energy shoreface or offshore to lower shoreface deposition only
3170 - 3173	I	Weakly laminated mudstone	Occurs at base of thick mudstone interval, possibly representing offshore deposition

BEDFORM ORIENTATION AND SEDIMENT DISPERSAL

Following sub-division of the succession into the five lithofacies associations described above, detailed analysis of the orientation of different bedforms within these successions was undertaken in order to evaluate sediment dispersal, and orientation of the depositional system. Sedimentary dips for the different bedding categories identified are summarised in Enclosures 4 - 6. Cumulative dip azimuth plots for the intervals 3170 – 3320 m and 3380 – 3440 m are shown in Figures 9 – 11.

Lithofacies Associations I, II & III

Sedimentary dips within mudstone and heterolithic lithologies (interpreted as comprising cm-dm scale interbedded sandstone and mudstone laminae) from Lithofacies Associations I and II typically display 360º azimuthal spread, indicative of the original deposition of these lithologies as "flat lying" effectively parallel stratified sediments. These sediments are mainly interpreted to have been deposited in shallow marine / lacustrine settings, in shelf-shoreface or prodelta-fan delta environments. However, in some intervals, e.g. where they occur as part of a well developed overall upward cleaning succession comprising Lithofacies Associations I to III, heterolithic lithologies display a preferred orientation, possibly reflecting palaeoslope.

Sedimentary dips within sandstones of Lithofacies Association III are also typically highly variable, and indicative of original deposition as "flat lying" sediments. This may have occurred within shallow shoreface settings or as sub-aqueous fan deltas. However, intraset surfaces (XBS) and flat lying intraset surfaces (ISSf) do show bimodal orientations with a dominance of surfaces in one direction (NE to SE) with only a minor component oriented at 180° to the main direction. This lithofacies association is interpreted to represent a shoreface environment dominated by wave formed structures. The main flow direction (NE – SE) may represent onshore migration of fair weather wave formed structures whereas the minor flow direction may represent offshore flow during storm events.

Lithofacies Association IV

The low gamma ray log response typical of Lithofacies Association IV, indicates that these successions contain a significant proportion of clean, potentially high reservoir quality sandstones. This lithofacies association within Yolla 3 is interpreted as distal sub-aerial sheetflood deposits on the basis of the dominance of low angle lamination and the spread of palaeocurrent data (90° to 180°).

The dominance of low angle laminations indicates that fan delta / alluvial fan was sheetflood dominated as debris flow dominated fans have chaotic deposits. Sheetfloods result from flashy concentration of runoff over drainage basin colluvial slopes, leading to sediment laden and catastrophic water discharge downslope. Debris flows do not form due to the low concentration of clay in the colluvium, insufficient sediment concentration, or slow rate of sediment entrainment in the flow. Sheetfloods are unconfined flows that expand as they move down fan. They develop when sediment charged flash floods reach a fan and attenuate because of the lack of channel walls, and the multi-directional slope of the fan surface caused by its semi-conical form. The most prevalent sheetflood facies consists of vertically alternating planar bedded couplets pebbly lags (in distal fan environments, termed the distal sand skirt) interstratified with laminated sandstone. The

planar bedded sets have distally decreasing slopes of 2 - 8° parallel to the fan surface, that produce a concave profile (Blair and McPherson, 1994).

Debris flows are initiated by two mechanisms, the most common involves transformation of a colluvial slide into a debris flow by entrainment of air and water through the jostling, deformation and loss of particle individuality as it moves downslope. This transformation requires the presence of water in the colluvium, and is therefore most apt to occur during or immediately after excessive precipitation. The second initiation mechanism occurs where fast moving water intersects a drainage basin slope mantled by abundant sediment. The ensuing reaction, in which the water dissipates its energy by dispersing clasts through mixing, can result in rapid entrainment of sediment, air and water to produce a debris flow. Debris flow dominated alluvial fans have constant slopes with values between 5 and 15° (Blair and McPherson, 1994). See Table 12 for the characteristics of debris flow (Type I) and sheetflood dominated (Type II) alluvial fans.

Sheetflood deposits typically have high porosity, permeability and connectivity of permeable units and this has major implications for volumetrics and production strategies.

The main intervals of sheetflood deposits assigned to lithofacies association IV have been identified within the intervals studied in detail.

The main intervals of sheetflood deposits occur:
3180 – 3192 m
3236 – 3254 m
3417 – 3424 m

The orientation of bedding surfaces within these intervals are summarised in Tables 13 – 15 below.

Table 12. Characteristics of Type I verses Type II alluvial fans (Blair and McPherson, 1994)

Feature	Type I Alluvial Fan	Type II Alluvial Fan
Dominant primary process and facies	Debris flows, especially lobe facies	Sheetfloods, especially couplet facies
Minor primary process	Rockfall, rock slide, rock avalanche, colluvial slide, incised channel	Rockfall, rock slide, rock avalanche, colluvial slide, incised channel, non-cohesive debris flow
Dominant secondary process	Winnowing by overland flows and wind to produce deflation pavements, boulder mantles, gullies and shallow channels	Winnowing by overland flows and wind to produce deflation pavements, gullies and shallow distributary channels
Typical grainsize and sorting	Very poorly sorted clayey boulder, pebble and cobble gravel	Poorly sorted sandy and bouldery, cobble to pebble gravel
Downfan trend in maximum clast size	Relatively constant	Typically decreases from boulders to pebbles or sand
Typical grain shape	Angular	Angular to sub-angular
Typical stratification style	Poorly or subtly stratified except for secondary winnowed surfaces	Well stratified coarse gravel and sandy fine gravel couplets
Presence of granular or sandy interbeds	Rare	Common
Presence of a distal sand skirt facies	Rare	Common
Presence of depositional matrix clay	Common	Rare
Drainage basin size	Small to moderate	Small to large
Feeder channel length	Short to moderate	Moderate to long
Typical bedrock lithology underlying the drainage basin	Pelitic metamorphic rocks, mudstone, aphanitic volcanic rocks, or mafic plutonic rocks; also weathering of granitic or gneissic rocks in humid climate	Quartzite, quartz rich conglomerate or sandstone; also granitic or gneissic rocks weathering in an arid climate
Clay abundance in the drainage basin colluvial slopes	Moderate to abundant	Rare
Common average slope values	5 - 15°	2 - 8°
Downfan slope style	Constant to straight	Distally decreasing or plano-concave
Permeability	Low	High
Porosity	Low	High
Connectivity of permeable units	Low	High

Table 13. Bedding orientations, sheetflood deposits within the interval 3400 – 3440 m

Interval 3400 – 3440 m (Log depth)				
Depth (m)	Orientation of ISSf's	Orientation of XBS's	Orientation of CSB's	Comments
3417 – 3424	Variable	W	SSW	Variable orientation may reflect original flat lying deposition in distal sand skirt facies. CSB (SSW) and SB (SSW) have similar orientations indication downslope progradation

Table 14. Bedding orientations, sheetflood deposits within the interval 3235 – 3265 m.

Interval 3235 – 3265 m (Log depth)				
Depth (m)	Orientation of ISSf's	Orientation of XBS's	Orientation of CSB's	Comments
3236 – 3241	SE Variable	E	NE SB oriented SSW	Variable orientation of low angle bedforms indicates original flat bedding. The presence of XBS may indicate shallow incised channels with lower flow regime deposits. CSBs at high angle to SB may indicate lateral migration of bedforms in shallow channel.
3241 - 3247		ESE	E	XBS oriented in same direction as CSB indicating downslope progradation
3247 - 3254	W Variable		SW	Variable orientation may reflect original flat lying deposition in distal sand skirt facies.

Table 15. Bedding orientation, sheetflood deposits within the interval 3170 – 3205 m.

Interval 3170 – 3205 m (Log depth)				
Depth (m)	Orientation of ISSf's	Orientation of XBS's	Orientation of CSB's	Comments
3180 - 3187	Variable	SE	ENE	Variable orientation may reflect original flat lying deposition in distal sand skirt facies. XBS may indicate shallow incised channels with SE drainage.
3187 - 3192	SE	W	E	Interval dominated by heterolithic strata

Lithofacies Association V

These data sets are too small and biased for orientation analyses.

CONCLUSIONS

1. The studied successions dip at low angles in variable orientations. A number of structural zones have been defined, these are summarised as follows:

Interval 3170 – 3320 m

Zone I	3170 – 3180	3.3°/313°	Fracture or fault bound at 3180 m
Zone II	3180 – 3189.7	3.4°/225°	Change in dip at 3189.7 m
Zone III	3189.7 – 3197.1	5.4°/303°	Fracture or fault bound at 3197.1 m
Zone IV	3197.1 – 3198.9	14.0°/240°	Fracture or fault bound at 3198.9 m
Zone V	3198.9 - 3203	9.6°/037°	Fault bound at 3203 m
Zone VI	3203 – 3204.9	7.6°/122°	Fracture or fault bound at 3204.9 m
Zone VII	3204.9 – 3205.3	2°/061°	Fracture or fault bound at 3205.3 m
Zone VIII	3205.3 – 3206.3	16.6°/225°	Fault bound at 3206.3 m
Zone IX	3206.3 - 3213	6.8°/096°	Change in mudstone dip at 3213 m
Zone X	3213 – 3246.6	5.2°/356°	Change in mudstone overlying sandstone 3246.6 m
Zone XI	3246.6 – 3281.4	6.2°/336°	Change in dip at base of sandstone 3281.4 m
Zone XII	3281.4 - 3313	6.0°/046°	Bounded by erosion surface 3313 m
Zone XIII	3313 - 3320	4.2°/336°	

Interval 3380 – 3440 m

Zone I	3380 – 3409.5	4.2°/336°	Change in mudstone dip at base of sandstone 3409.5 m
Zone II	3409.5 - 3416	10.1°/287°	Change in mudstone dip at top of sandstone 3416 m
Zone III	3416 - 3440	5.6°/338°	

2. The sedimentary succession is highly heterolithic, comprising sandstones, mudstones and heterolithic intervals composed of dm scissile intercalations of sandstone, siltstone and mudstone.

3. Five lithofacies associations have been identified, these comprise:

   I. Mudstones that occur at the base of upward coarsening facies successions. (interpreted as either prodeltaic muds, or shelf-shoreface deposits)
   II. Heterolithic intercalations of sandstone siltstone and mudstone, typically occurring within the lower-mid parts of upward coarsening facies successions (interpreted as either distal fan delta or shelf-shoreface deposits). When it is interbedded with Lithofacies Association IV, this implies a sub-aerial setting on a distal alluvial fan.
   III. Stratified sandstones with mottled image fabric and low angle (typically <5º) internal bedding surfaces, typically occurring towards the top of upward coarsening facies successions (shoreface deposits).
   IV. Successions (often erosively based) of stratified sandstones and pebbly sandstones with dominant internal bedding fabrics inclined at angles <10°, rare intervals of up to 25° (distal sheetflood deposits with shallow incised channels).
   V. Coals (deposits of swampy coastal plain environments).

5. Sandstones of Lithofacies Association IV are likely to form the main reservoir intervals. Lithofacies Association III may form a secondary reservoir interval and typically have over an order of magnitude less permeability than the sheetflood deposits.

6. Palaeotransport analyses of sandstones from Lithofacies Association III reveals them to be characterised by internal stratification fabrics with very wide ranging sedimentary dip azimuth, suggesting they were originally deposited as "flat lying" strata. Few palaeotransport interpretations can be made for these sandstones. However, in some examples, a dominant sedimentary dip is present, and may represent onshore migration of fair weather wave formed structures whereas the minor flow direction may represent offshore flow during storm events. In most cases, this can broadly be interpreted to have had NE – SE onshore direction and a NW – SW offshore direction.

7. Palaeotransport analyses of sandstones from Lithofacies Association IV reveals them to be characterised by low angle internal stratification fabrics with variable azimuth. The relationship between intra-set flat lamination, intra-set lamination and coset boundaries suggest that sediment transport occurred normal to the depositional dip i.e. bedforms migrated down fan. Interpreted fan slope drainage directions are variable and no consistent drainage direction can be inferred.

8. In the absence of a detailed core calibration environmental interpretations are highly subjective. However, observed lithofacies stacking patterns do appear to be consistent with an interpretation of deposition of strata within a marginal marine / lacustrine fan deltaic setting.

REFERENCES

Benvenuti, M., 2003. Facies analysis and tectonic significance of lacustrine fan-deltaic successions in the Pliocene-Pleistocene Mugello Basin, Central Italy. *Sedimentary Geology*, 157, 197-234.

Blair, T.C. and McPherson, J.G., 1994. Alluvial fans and their natural distinction from rivers based on morphology, hydraulic processes, sedimentary processes and facies assemblages. *Journal of Sedimentary Research*, 64, 450-489.

Walker, R.G. 1992. Facies models. *In:* Walker, R.G. and James, N.P. eds. *Facies Models: Response to Sea Level Change*, Geological Association of Canada, Newfoundland, 1-14.

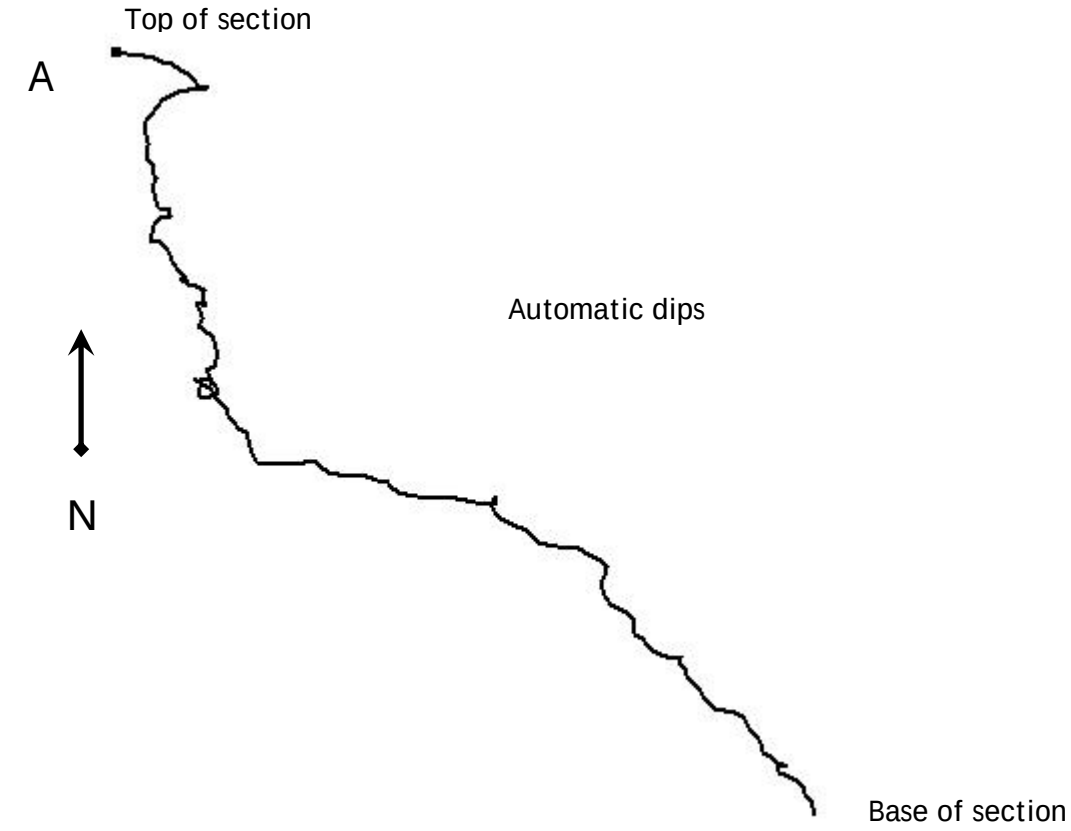
Top of section
A
Automatic dips
N
Base of section

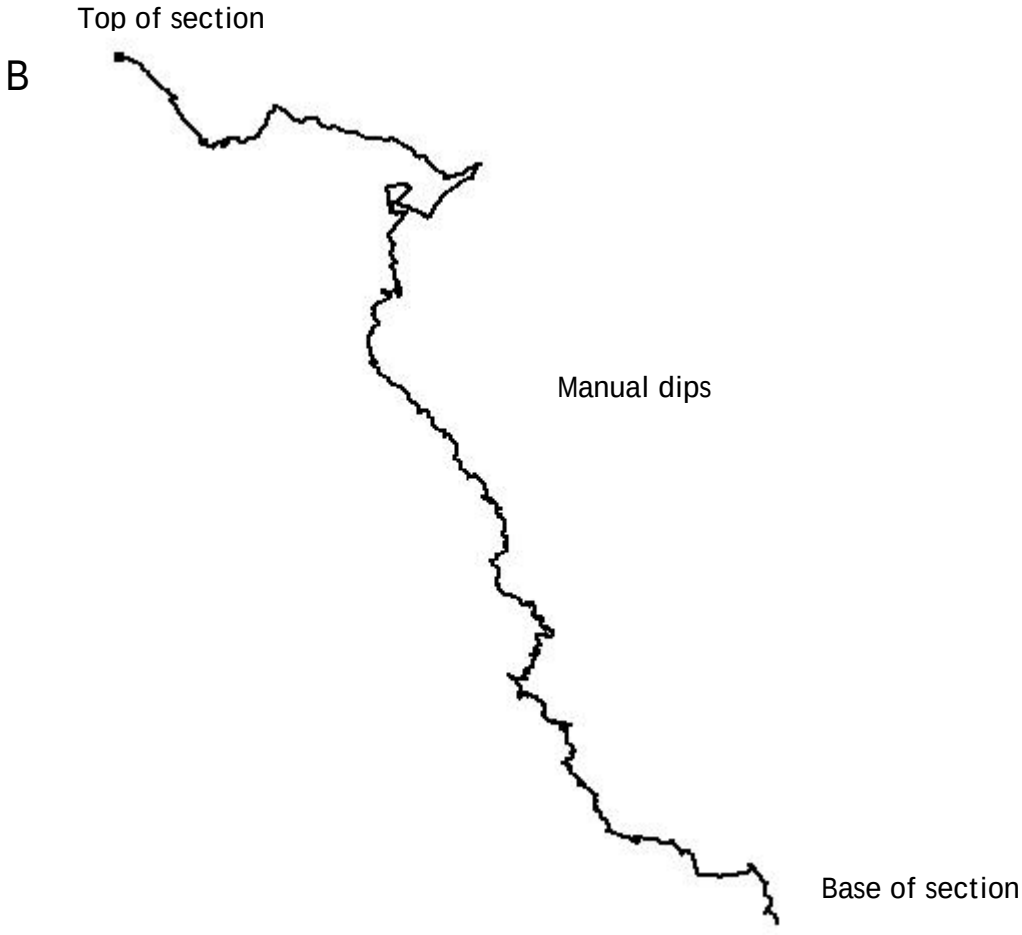
Top of section
B
Manual dips
Base of section

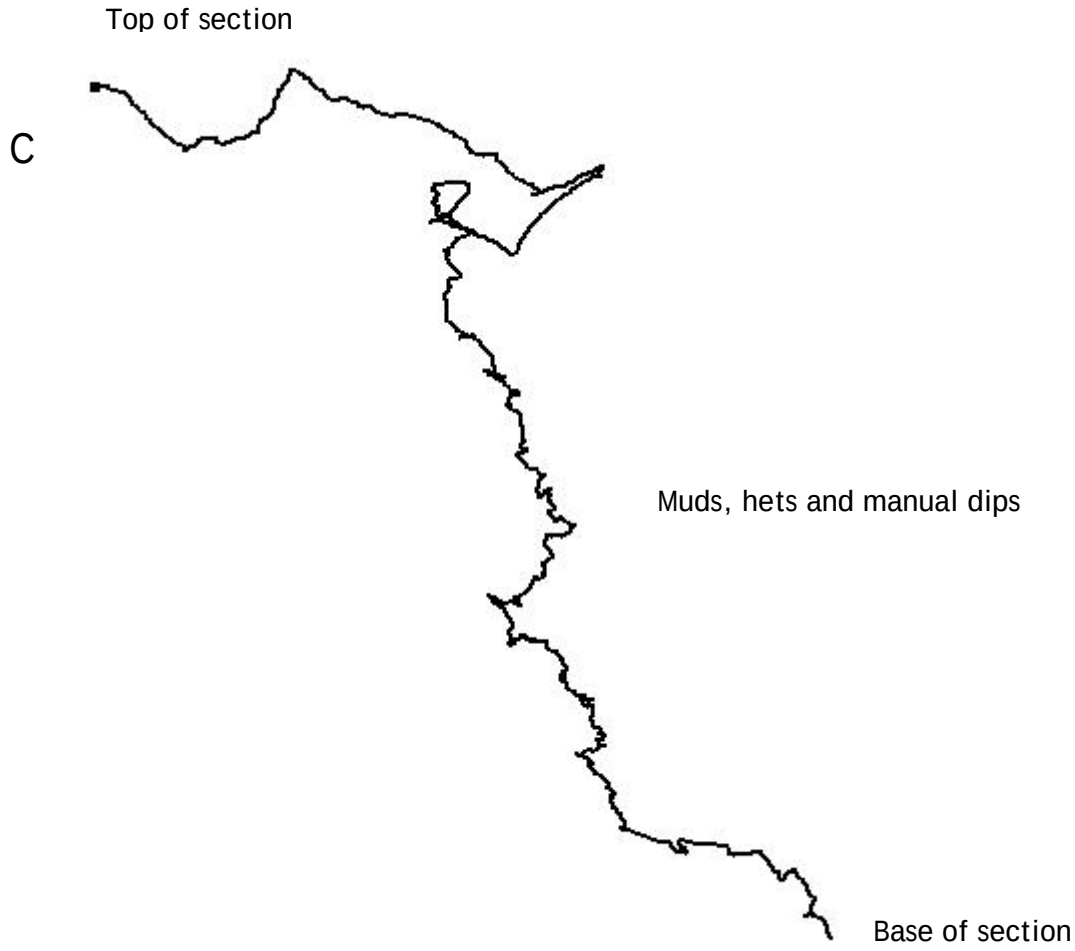

Figure 1. Cumulative automatic, manual and muds and hets, dip azimuth plots for studied section (3170 – 3450 m).

Code	Description	Interpreted category
MUD	Confident bedding features, with consistent magnitudes.	Shale Bedding
HETS	Confident bedding surfaces characterised by high resistivity contrasts.	Inter-bedded dm-scale sand and mud. (Heterolithics)
LB	Low true dip angle (typically less than 5°), marked resistivity contrast with overlying/underlying beds	Lithological boundary
LBe	Low true dip angle (typically less than 5°), marked resistivity contrast with overlying/underlying beds and truncation of underlying beds.	Erosional lithological boundary
LBc	Separates a highly resistive zone from overlying and underlying beds. May be a planar layer or non-planar nodular feature.	Cemented lithological boundary
SB	Surface (typically less than 15°) enclosing a bed that may have internal stratification with consistent dip and azimuth.	Set (bed) boundary
CSB	Surface separating groups of beds or a single bed displaying a significantly different character.	Coset boundary
ISS	Steeply dipping true dip angle (15-40°), highly discordant to set (bed) boundaries, and are characterised by resistivity contrast of cm scale with constant dip azimuth trends.	Intra set, cross-bedding surface
ISSF	Near horizontal surfaces with true dip angle (<5°), characterised by resistivity contrast several cm thick. Azimuth trends may be variable due to the low precision associated with determining the azimuth of flat lying beds.	Flat/horizontal intra set surface
FRAC	Generally discordant plane with moderate to steep dip (resistive or conductive).	Fracture
FAULTR	Generally discordant plane with moderate to steep dip, with identifiable displacement (resistive or conductive).	Fault

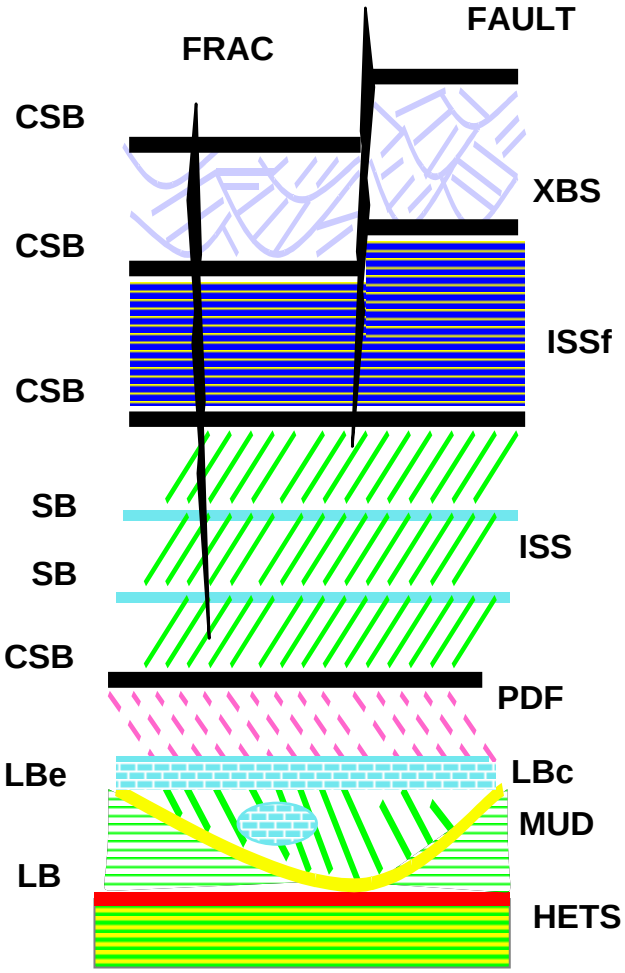

Figure 2. Dip categories used in this study.

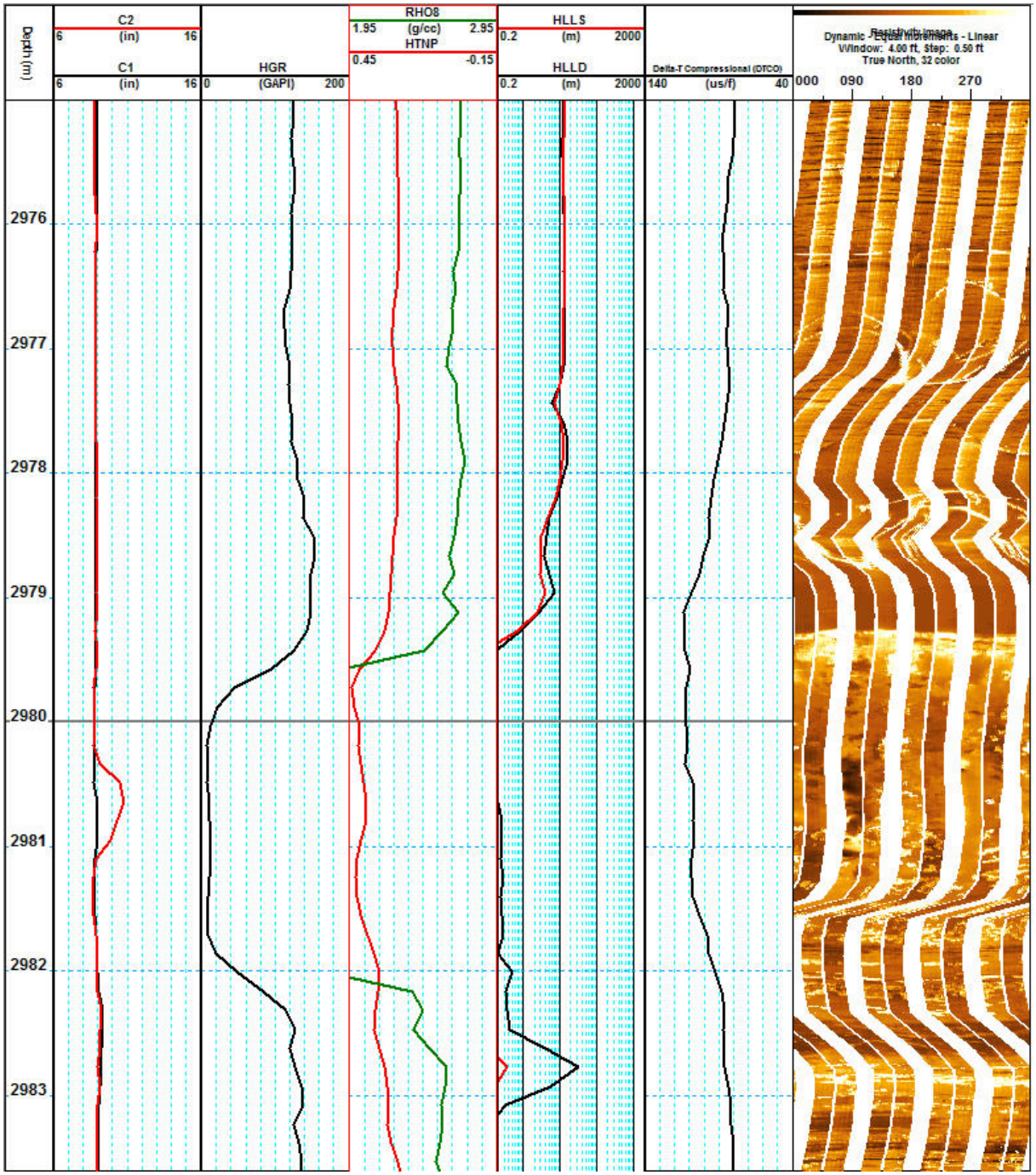

Figure 3. Example of coal (lithofacies VI) in interval 2975 – 2983 m.

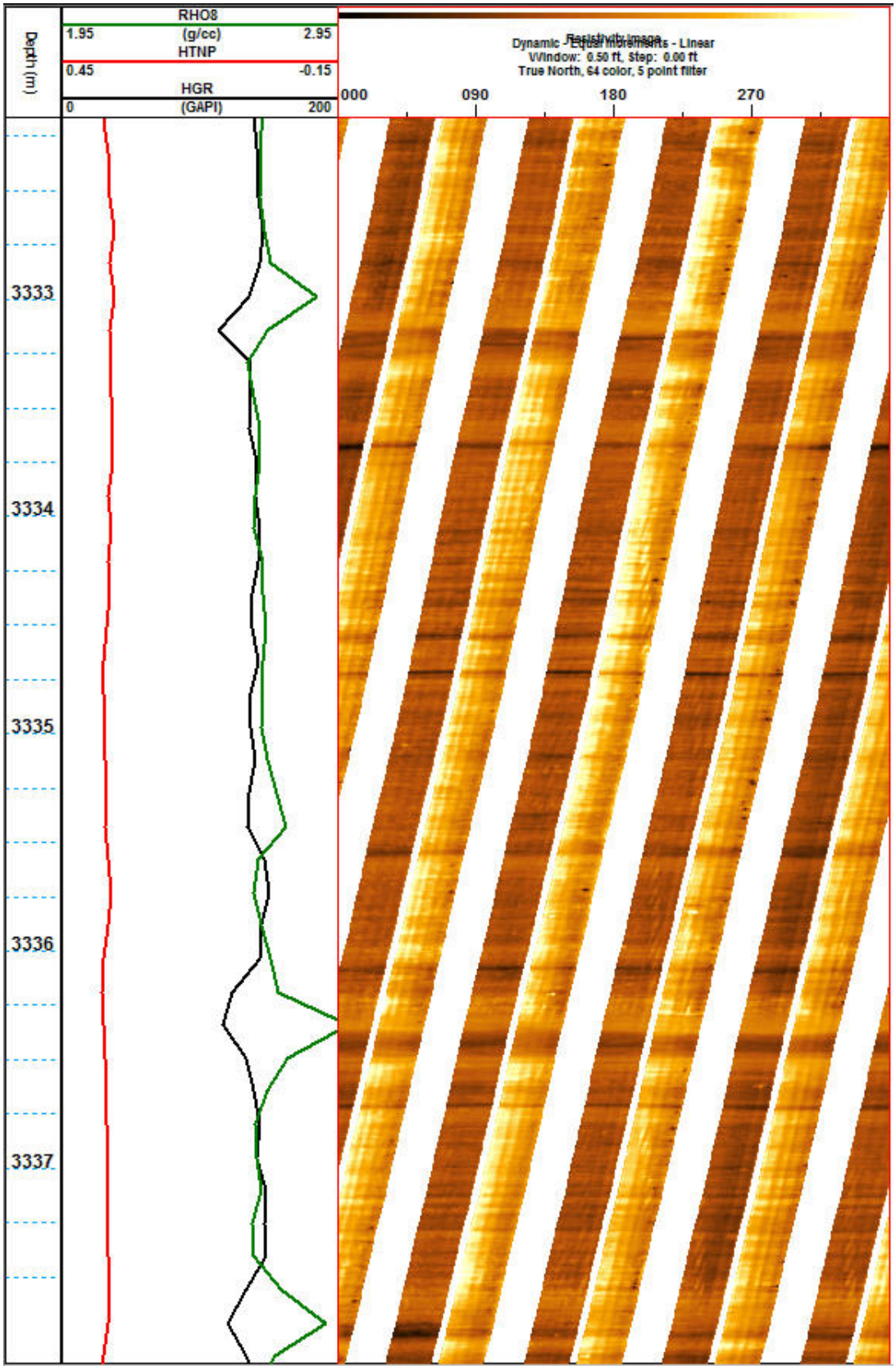

Figure 4 FMI Image through well laminated to massive mudstone (lithofacies Ml & Mm)

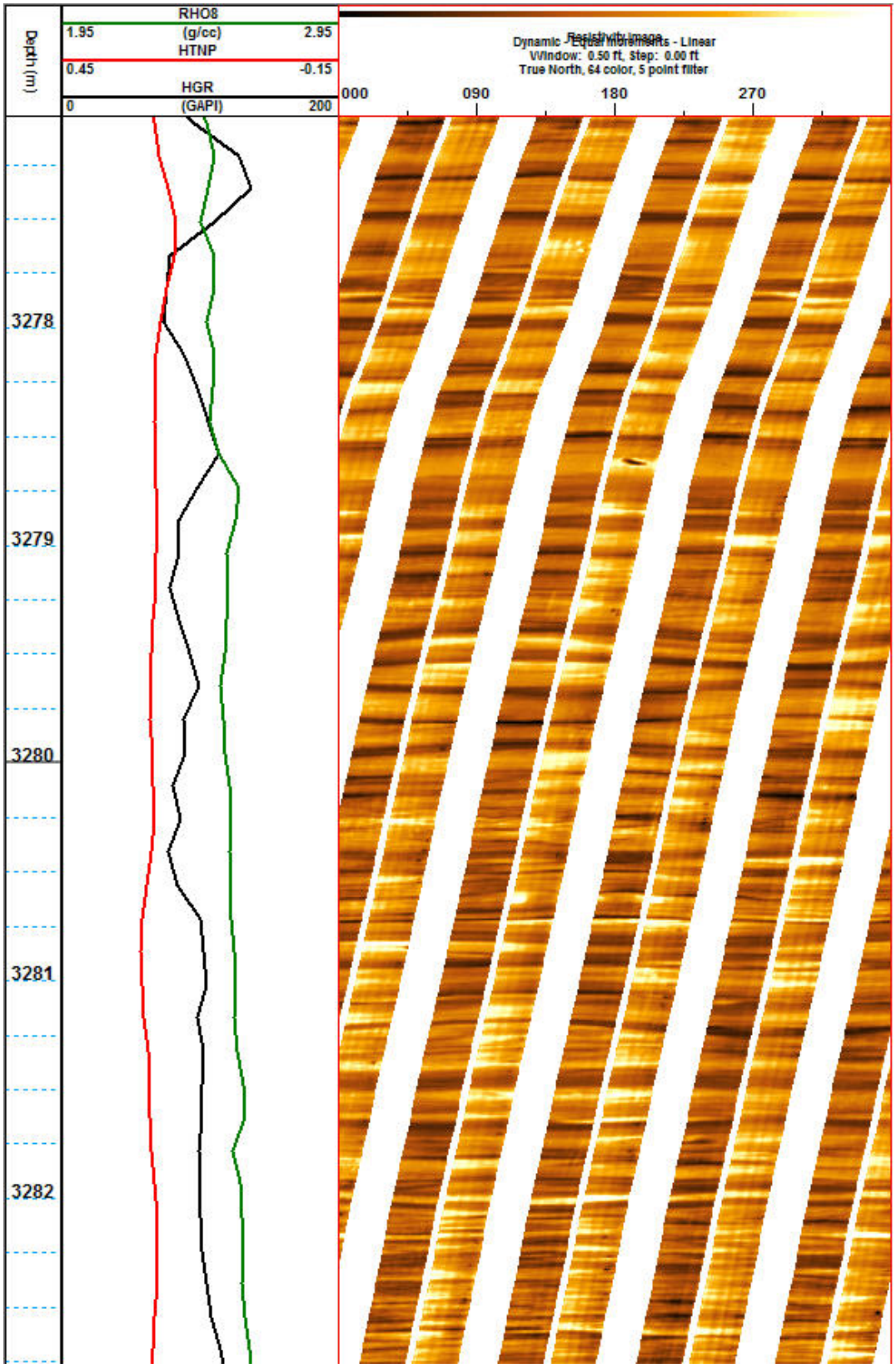

Figure 5. FMI image through dm-scale heterolithic sandstone-mudstone lithofacies with well developed lamination fabric (Hl) becoming less well developed, fabric (Hm), toward the top.

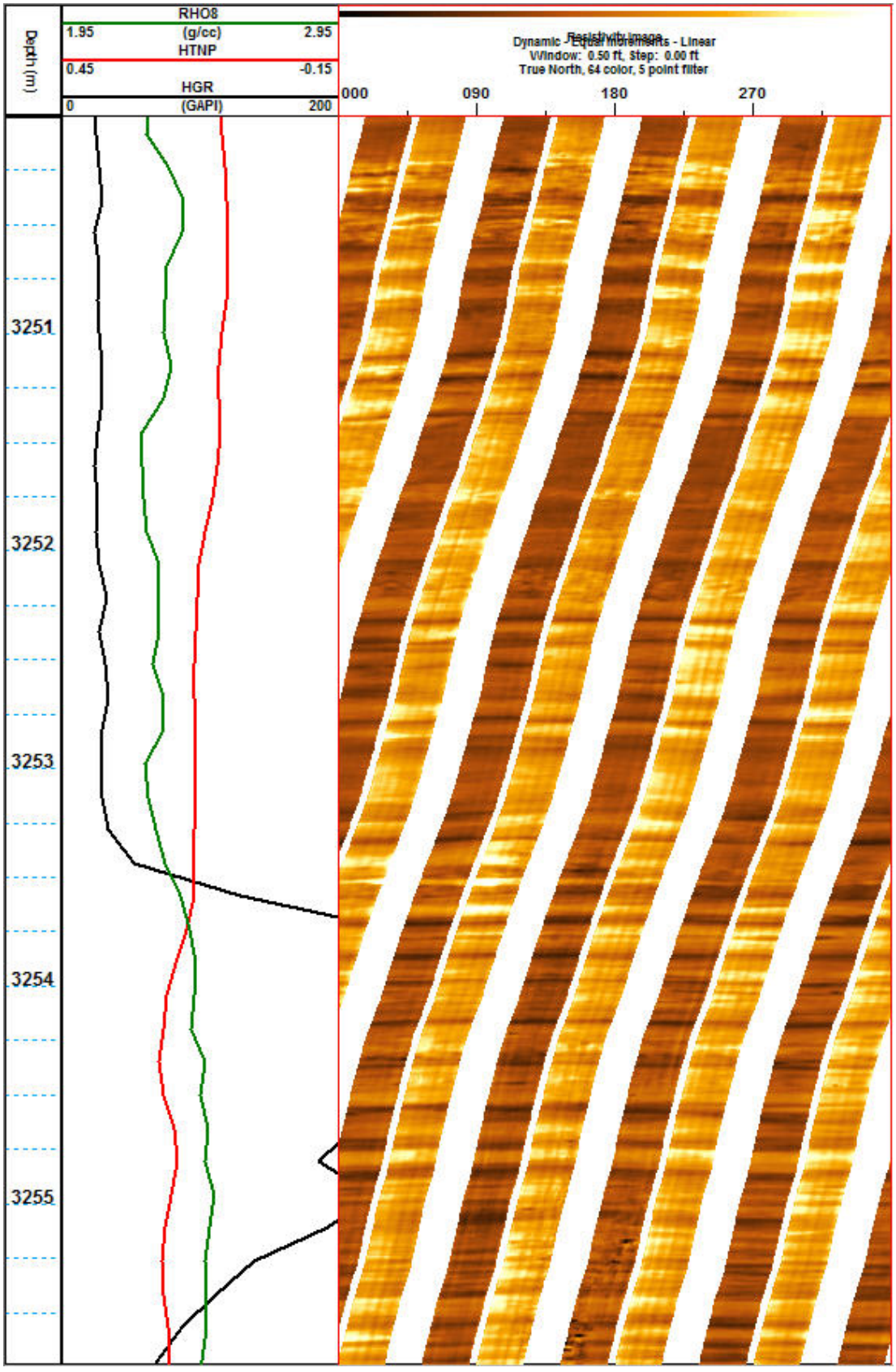

Figure 6. FMI image illustrating well laminated sandstone Sl at the base with thin mottled sandstone with vague lamination Sm(Sl) (3250 – 3253 m). Note the change in texture associated with contact between the high GR Lithofacies Association III and the Lithofacies Association IV at 3253.75 m.

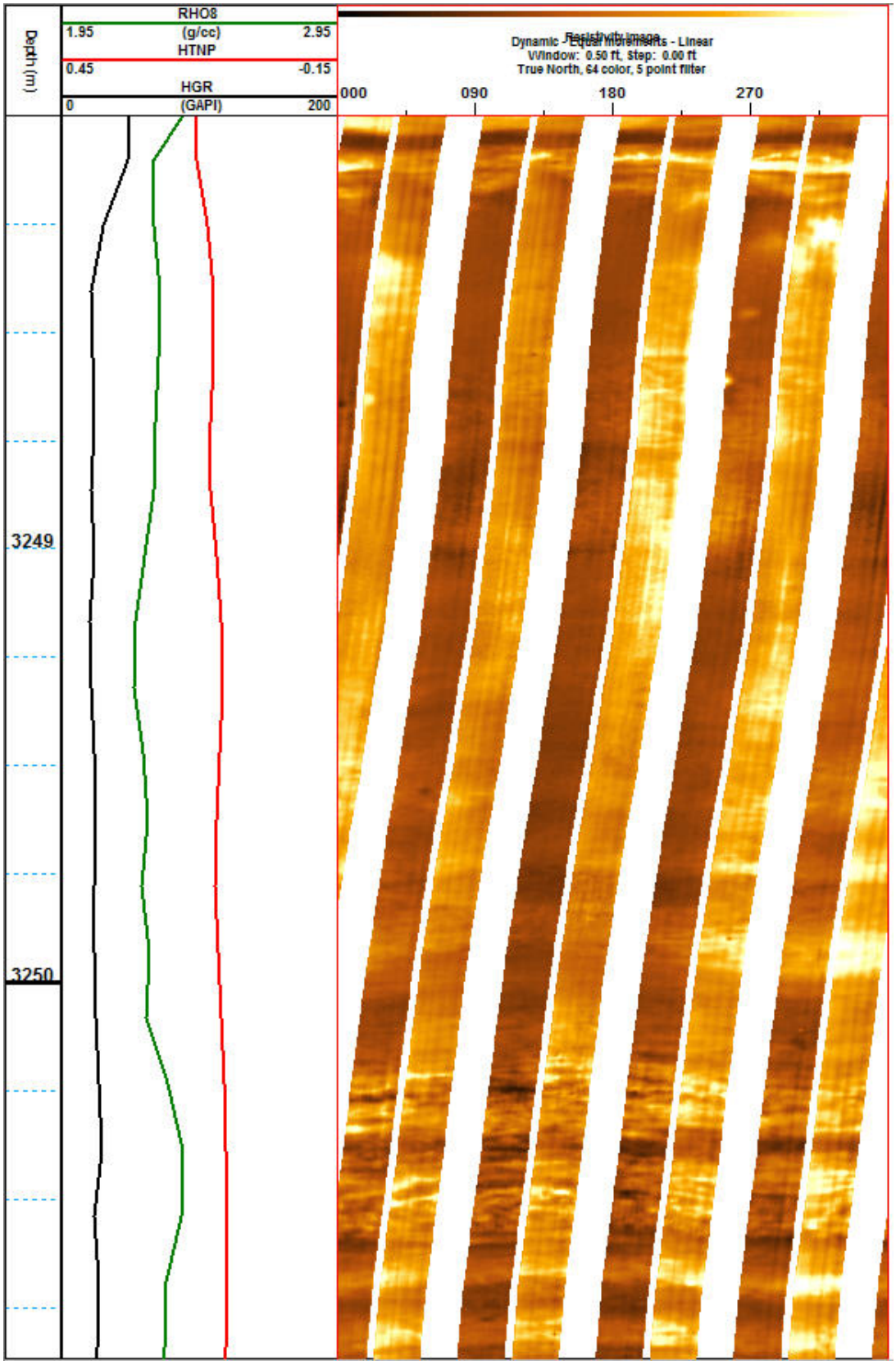

Figure 7. FMI image illustrating sandstone with coarse scale mottled fabric, Scm and massive sandstone (SM).

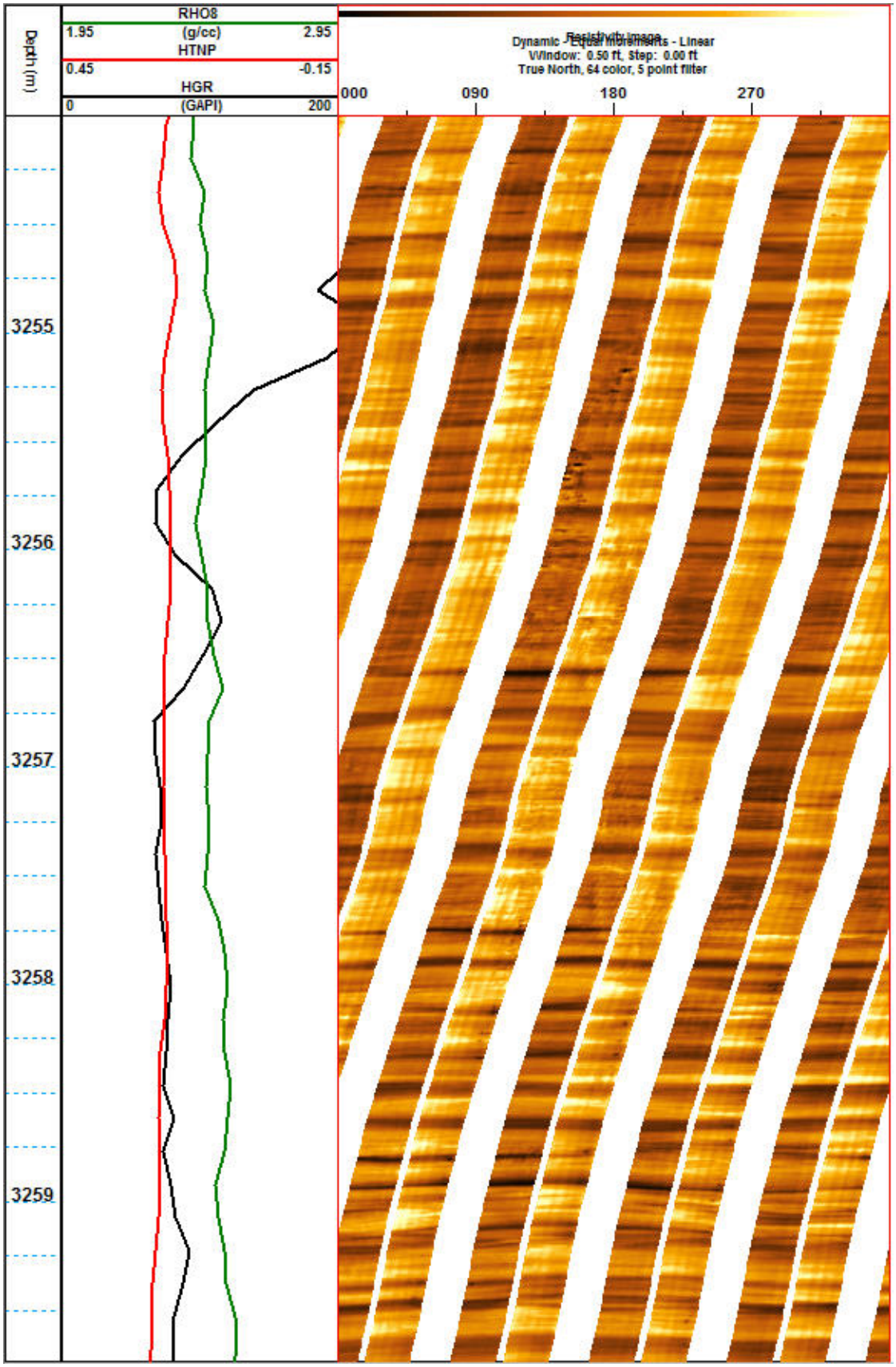

Figure 8. FMI image illustrating laminated sandstone with weak fine scale mottled fabric Sm(Sl).

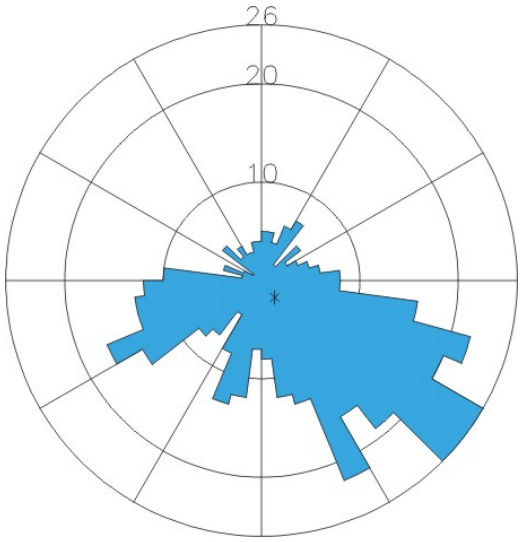

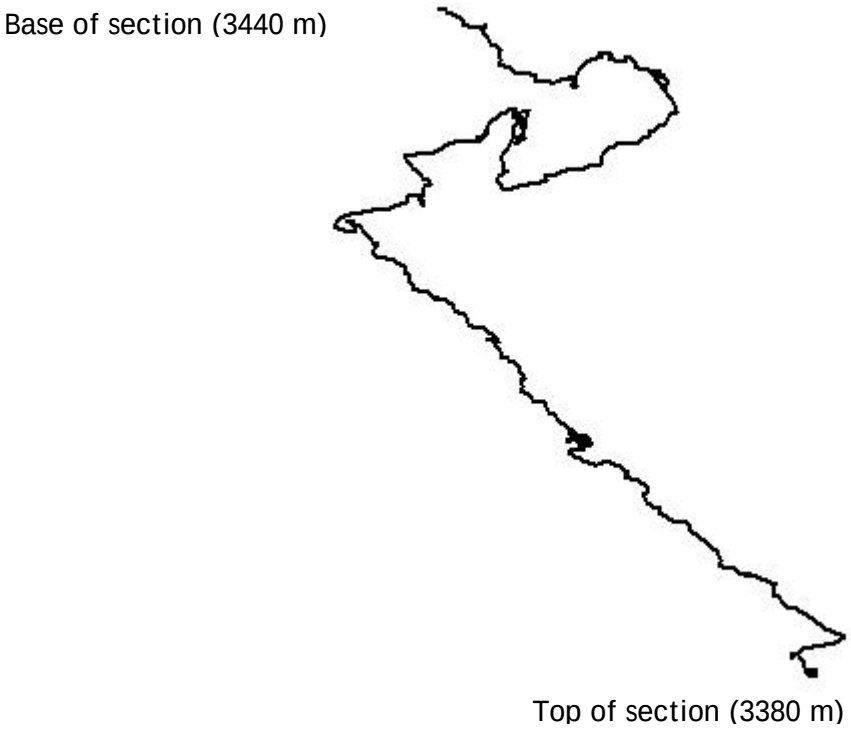

Figure 9. Cumulative dip azimuth plot for the interval 3380 – 3440 m. ISSf and ISS intraset surfaces (flat) are shown with structural dip removed. ISSf surfaces are dominant and large changes in azimuth are associated with these nearly flat lying structures.

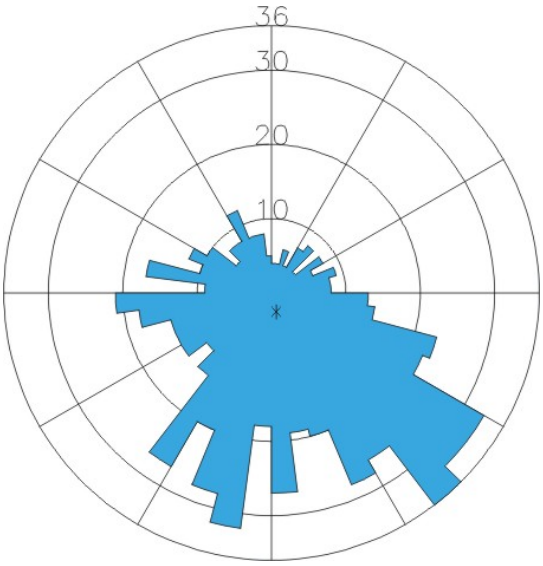

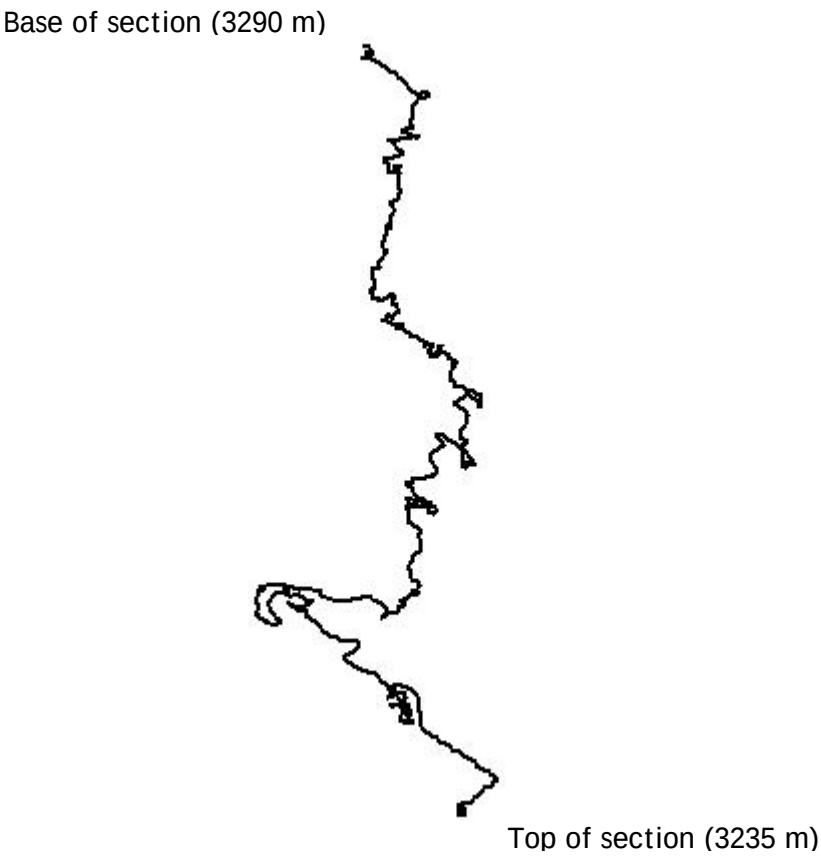

Figure 10. Cumulative dip azimuth plot for the interval 3235 – 3290 m. ISSf and ISS intraset surfaces (flat) are shown with structural dip removed. ISSf surfaces are dominant and large changes in azimuth are associated with these nearly flat lying structures.

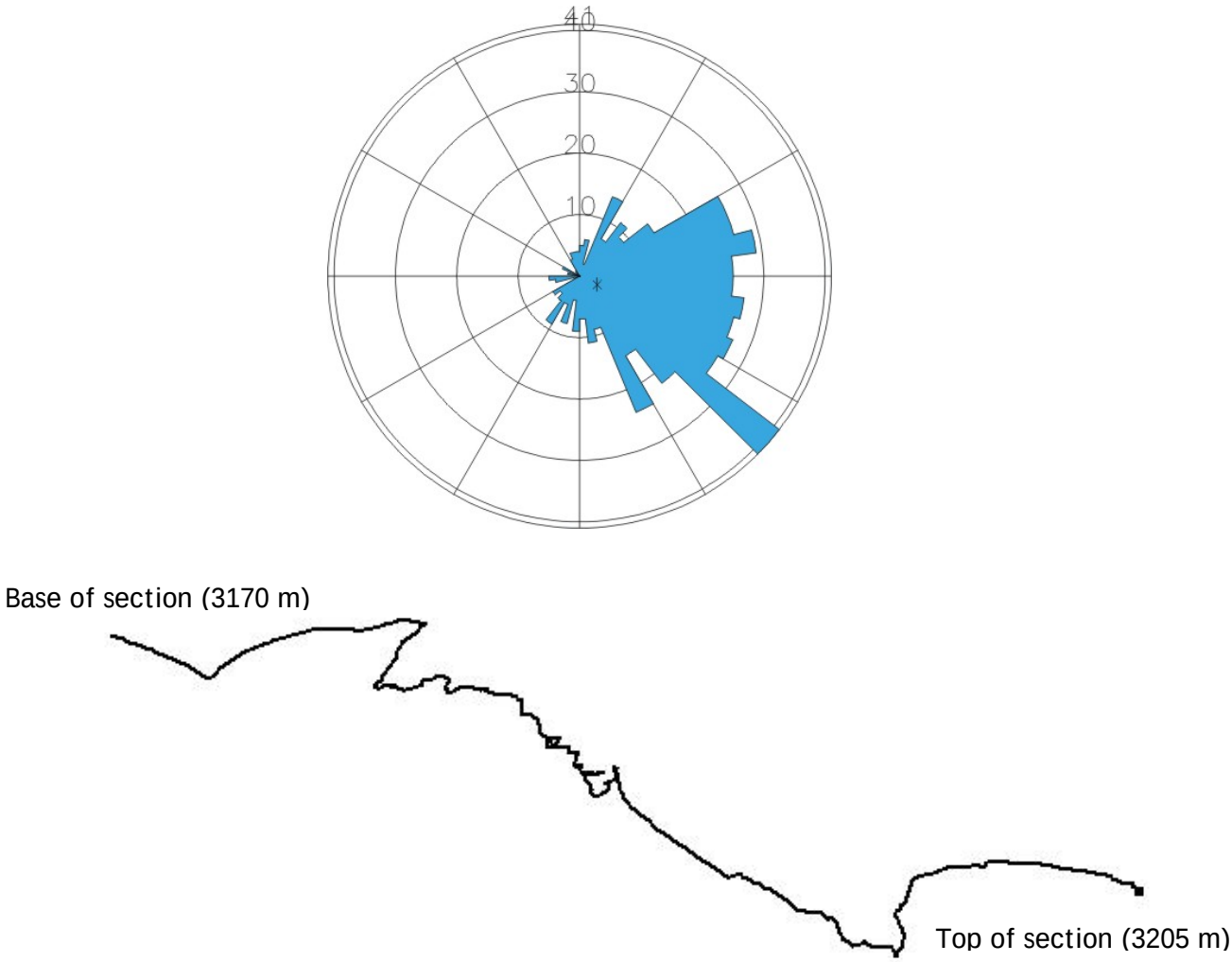

Figure 11. Cumulative dip azimuth plot for the interval 3170 – 3205 m. ISSf and ISS intraset surfaces (flat) are shown with structural dip removed. ISSf surfaces are dominant and large changes in azimuth are associated with these nearly flat lying structures.

ENCLOSURE 1: YOLLA 3 1:500 3170 - 3450 M QUALITY CONTROL PLOT

BIT SIZE: 8.5 IN
BH TEMP: 143 DegC
BOREHOLE SALINTY: 27000 PPM
FLUID LOSS: 3.1 cm3
MUD DENSITY: 9.45 lb/g
MUD pH: 8.9
MUD TYPE: Sea water / Dripsac/Soltex
MUD VISCOSITY: 98 S
SURFACE LATITUDE: 39 50' 40.57" S
SURFACE LONGITUDE: 145 49' 06.08" E
RUN DATE:6-Sept-2004
2337.00 - 3494 METRES

Origin energy
delivering the goods

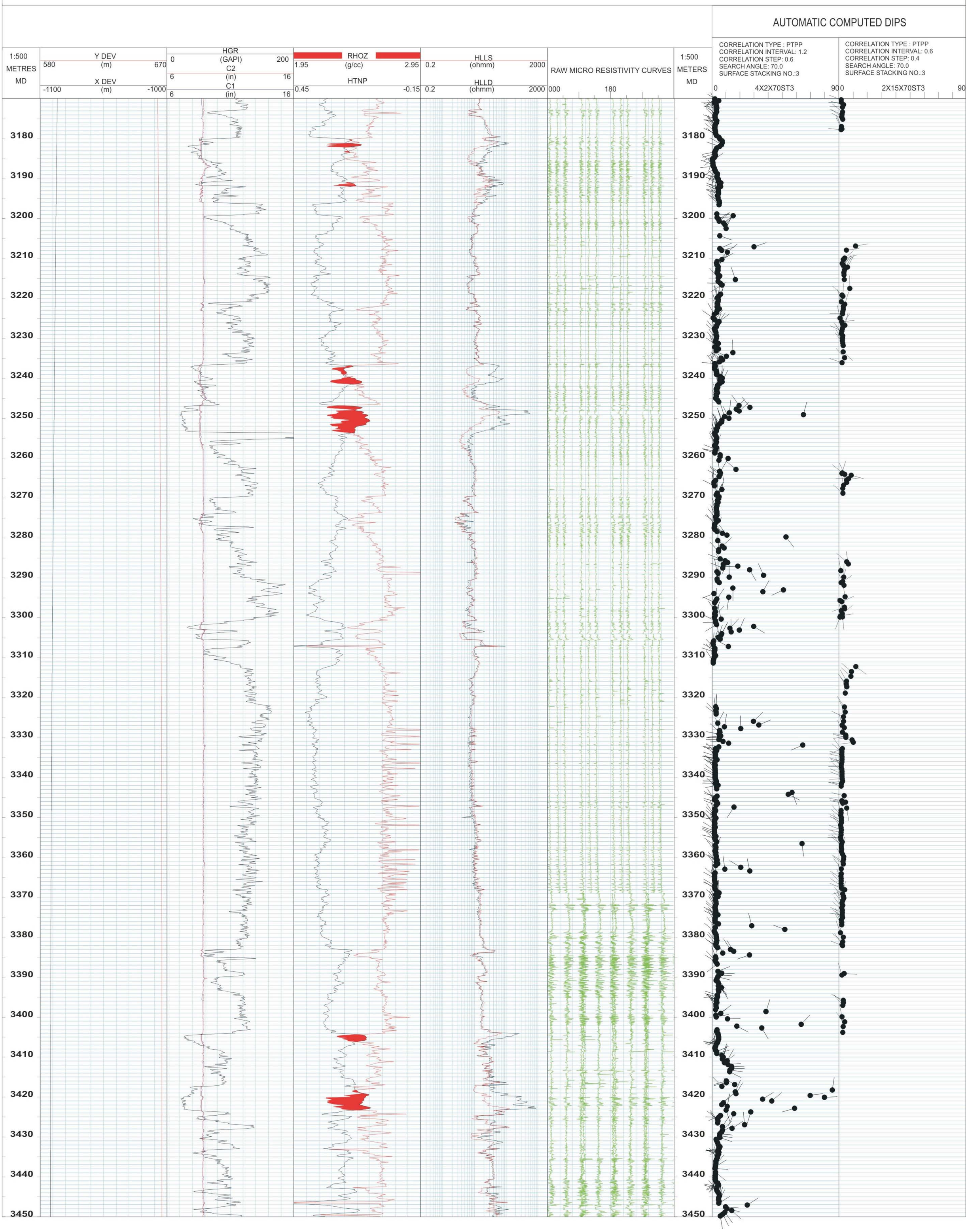

ENCLOSURE 2: YOLLA 3 1:500 3170 - 3450 M STRUCTURAL SUMMARY PLOT

FRACTURE / FAULT STRIKE

ST FRAC
ST FAULT

MANUAL DIPS

LB
LBc
LBe
SB
CSB
ISS
ISSf
XSB
PDf
HETS
MUD
FAULT
FRAC

Origin energy

delivering the goods

1:500 METRES MD

C2 (in) 6 16
C1 (in) 6 16

HGR (GAPI) 0 150

RHOZ (g/cc) 1.95 2.95
HTNP 0.45 -0.15

HLLS (ohm) 0.2 2000
HLLD (ohm) 0.2 2000

Y_FMI_1.pck 0 90

STRUCTURAL ZONES
MUDS
HETS
Y_FMI_1.pck

AUTOMATIC COMPUTED DIPS
4X2X70ST3 0 90

ZONE I 3.3/313 DEG
ZONE II 3.4/225 DEG
ZONEs III to IX
Fractured zones
ZONE X 5.2/356 DEG
ZONE XI 6.2/336 DEG
ZONE XII 6.0/046 DEG
ZONE XIII 4.2/336 DEG
ZONE XIV 9.9/295 DEG
ZONE XV 4.9/349 DEG

3180 3190 3200 3210 3220 3230 3240 3250 3260 3270 3280 3290 3300 3310 3320 3330 3340 3350 3360 3370 3380 3390 3400 3410 3420 3430 3440 3450

ENCLOSURE 3:

YOLLA 3 1:200 3170 - 3450 M DATA OVERVIEW PLOT

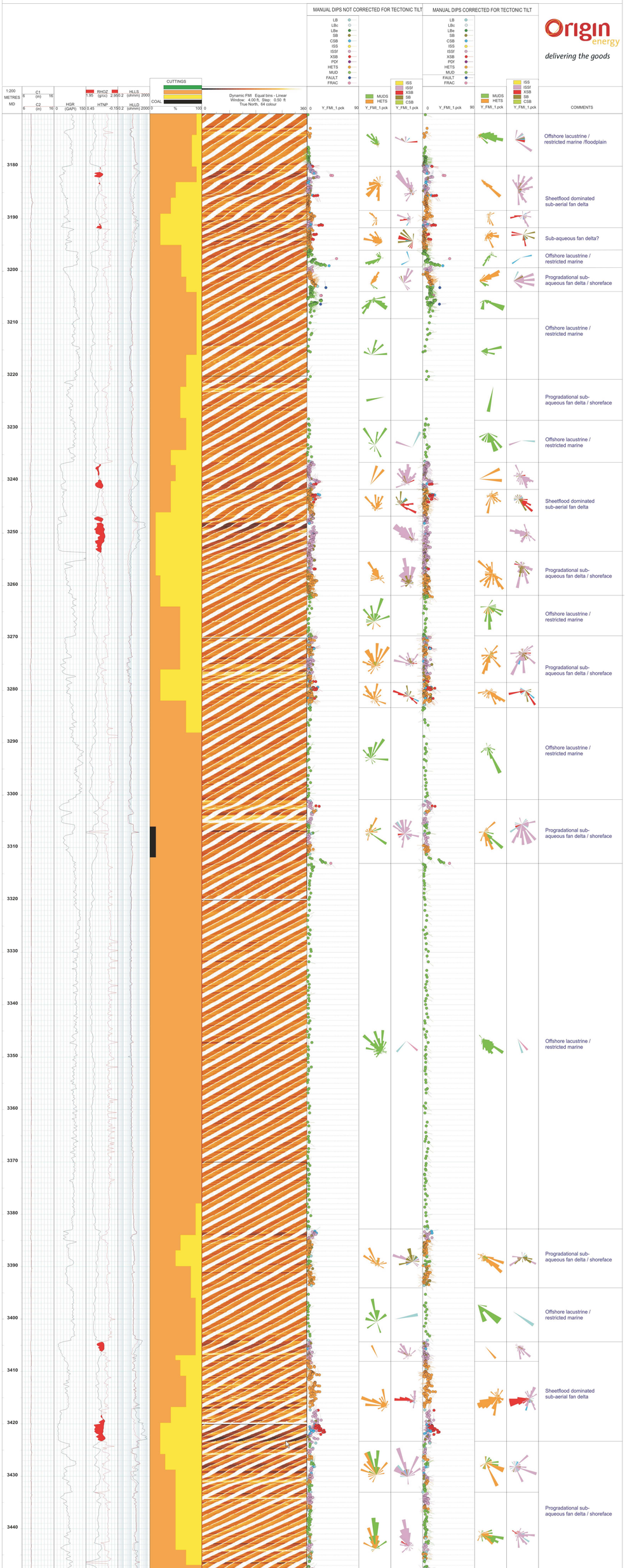

ENCLOSURE 4:

YOLLA 3 1:100 3175 -3205 M SEDIMENTOLOGICAL COMPOSITE PLOT

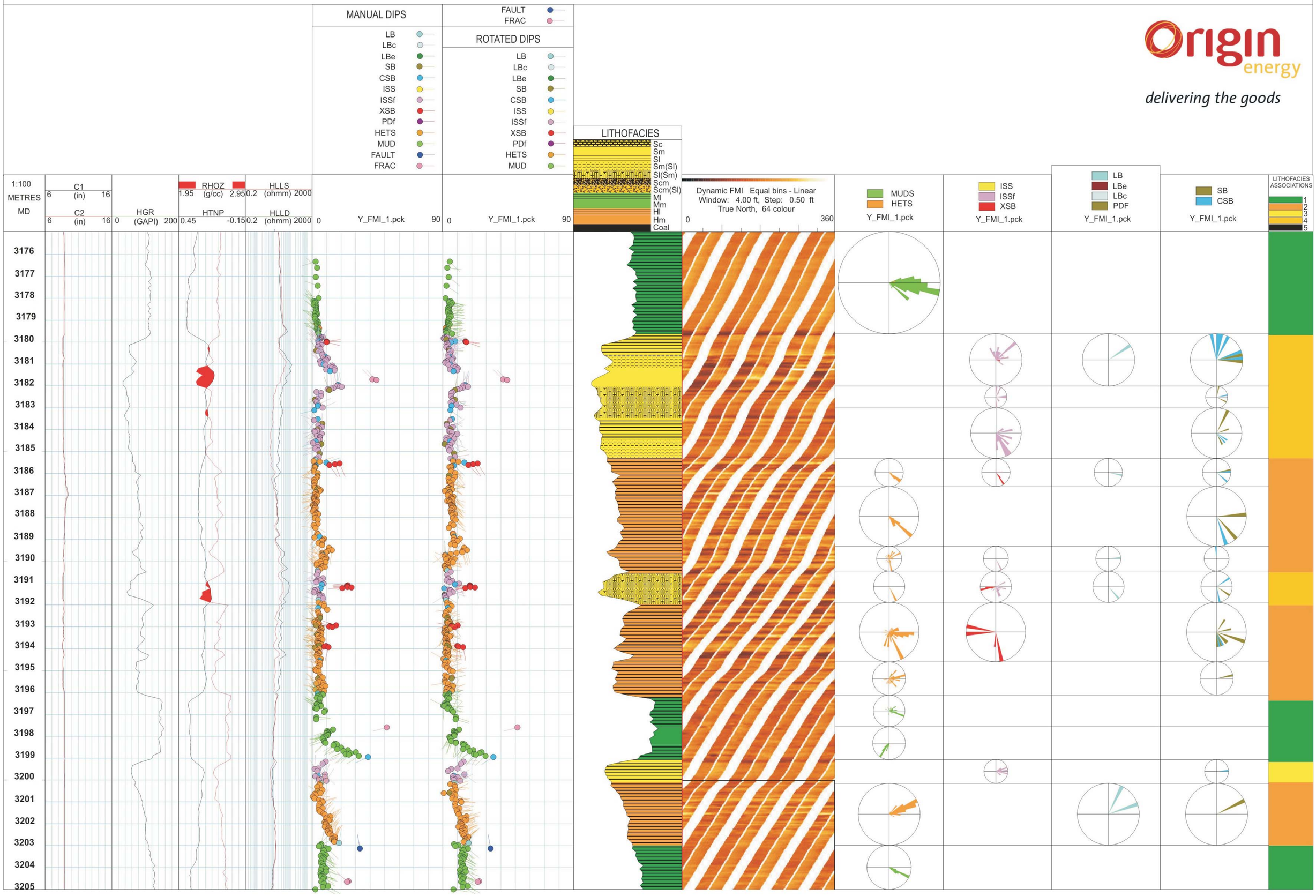

Origin energy

delivering the goods

ENCLOSURE 5:

YOLLA 3 1:100 3275 -3320 M SEDIMENTOLOGICAL COMPOSITE PLOT

Origin energy

delivering the goods

MANUAL DIPS: LB, LBc, LBe, SB, CSB, ISS, ISSf, XSB, PDf, HETS, MUD, FAULT, FRAC

ROTATED DIPS: LB, LBc, LBe, SB, CSB, ISS, ISSf, XSB, PDf, HETS, MUD, FAULT, FRAC

LITHOFACIES: Sc, Sm, Sl, Sm(Sl), Sl(Sm), Scm, Scm(Sl), Ml, Mm, Hl, Hm, Coal

1:100 METRES MD

C1 6 (in) 16 | C2 6 (in) 16 | HGR 0 (GAPI) 200 | RHOZ 1.95 (g/cc) 2.95 | HTNP 0.45 -0.15 | HLLS 0.2 (ohm) 2000 | HLLD 0.2 (ohm) 2000

Y_FMI_1.pck 0 90 | Y_FMI_1.pck 0 90

Dynamic FMI Equal bins - Linear
Window: 4.00 ft, Step: 0.50 ft
True North, 64 colour
0 360

MUDS, HETS — Y_FMI_1.pck

ISS, ISSf, XSB — Y_FMI_1.pck

LB, LBe, LBc, PDF — Y_FMI_1.pck

SB, CSB — Y_FMI_1.pck

LITHOFACIES ASSOCIATIONS: 1, 2, 3, 4, 5

3236 3237 3238 3239 3240 3241 3242 3243 3244 3245 3246 3247 3248 3249 3250 3251 3252 3253 3254 3255 3256 3257 3258 3259 3260 3261 3262 3263 3264 3265 3266 3267 3268 3269 3270 3271 3272 3273 3274 3275 3276 3277 3278 3279 3280 3281 3282 3283 3284 3285 3286 3287 3288 3289 3290 3291 3292 3293 3294 3295 3296 3297 3298 3299 3300 3301 3302 3303 3304 3305 3306 3307 3308 3309 3310 3311 3312 3313 3314 3315 3316 3317 3318 3319 3320

ENCLOSURE 6:

YOLLA 3 1:100 3380 -3450 M SEDIMENTOLOGICAL COMPOSITE PLOT

Origin energy

delivering the goods

MANUAL DIPS: LB, LBc, LBe, SB, CSB, ISS, ISSf, XSB, PDf, HETS, MUD, FAULT, FRAC

ROTATED DIPS: LB, LBc, LBe, SB, CSB, ISS, ISSf, XSB, PDf, HETS, MUD

FAULT, FRAC

1:100 METRES MD

C1 6 (in) 16 | C2 6 (in) 16 | HGR 0 (GAPI) 200 | RHOZ 1.95 (g/cc) 2.95 | HTNP 0.45 -0.15 | HLLS 0.2 (ohm) 2000 | HLLD 0.2 (ohm) 2000

0 Y_FMI_1.pck 90

0 Y_FMI_1.pck 90

LITHOFACIES: Sc, Sm, Sl, Sm(Sl), Sl(Sm), Scm, Scm(Sl), Ml, Mm, Hl, Hm, Coal

Dynamic FMI Equal bins - Linear
Window: 4.00 ft, Step: 0.50 ft
True North, 64 colour
0 360

MUDS, HETS — Y_FMI_1.pck

ISS, ISSf, XSB — Y_FMI_1.pck

LB, LBe, LBc, PDF — Y_FMI_1.pck

SB, CSB — Y_FMI_1.pck

LITHOFACIES ASSOCIATIONS: 1, 2, 3, 4, 5

3381 3382 3383 3384 3385 3386 3387 3388 3389 3390 3391 3392 3393 3394 3395 3396 3397 3398 3399 3400 3401 3402 3403 3404 3405 3406 3407 3408 3409 3410 3411 3412 3413 3414 3415 3416 3417 3418 3419 3420 3421 3422 3423 3424 3425 3426 3427 3428 3429 3430 3431 3432 3433 3434 3435 3436 3437 3438 3439 3440 3441 3442 3443 3444 3445 3446 3447 3448 3449 3450

APPENDIX 8: PVT REPORT 2

A. C. N. # 008 130 667
Adelaide, May 10, 2004
P. O. Box 410
Magill
S. A. 5072

Origin Energy Resources Limited
1 King William Street
PO Box 1199
Adelaide
S.A. 5000

Subject : **Reservoir Fluid Study**
Well: **Yolla # 3 UEVCM**
File: **O – 25012**

Attention: Mr. Joe Parvar

Dear Sirs,

On September 28, 2004 representatives of Petrotech collected isokinetic wellhead samples, from their mini-lab separator, originating from the UEVCM sand of the subject well.

After quality checks and compositional analyses on these samples, reported in our report reference # O – 24037, it was decided to continue with additional work, including a physical recombination and constant mass study on the resulting mixture.

A new mathematical recombination of the separator products into a corrected produced field ratio resulted in the actual produced reservoir fluid composition.

The corrected producing gas - liquid ratio given was 15898 of cubic feet of separator gas for every barrel produced in the separator at 500 psig and 85 °F. In the laboratory this ratio was determined to be equivalent to 22210 standard cubic feet of separator gas for at 14.696 psia and 60 °F., for every stock tank barrel produced.

We then continued with the physical recombination of these samples using the same ratios as used for the mathematical recombination.

This recombined reservoir fluid was charged to a visual P V T cell and thermally expanded to the reservoir temperature of 209 °F. During a constant composition expansion at this temperature, a dew point pressure of 5280 psig was observed.

Since the reservoir pressure of this zone was 2695 psig, it was confirmed that, even though this zone was producing mainly from the gas cap, some black oil reservoir fluid had entered the well

bore.

The sample in the cell was subsequently equilibrated at original reservoir conditions where it was observed to consist of 2.15 volume percent of oil reservoir fluid and 97.85 volume percent of gas cap.

The cell was kept at these conditions and the equilibrium gas and liquid were flashed at atmospheric conditions into two phases. Through measurements of densities, molecular weights, quantities produced and compositions of the evolved stock tank gas and liquid from the flash experiments, we were able to mathematically recombine these products into the equilibrium reservoir fluid compositions.

We thank Origin Energy Resources Limited for the opportunity to be of service. Please do not hesitate in contacting us should you require any further information or if we can assist you in any other way.

Yours Sincerely,

Jan G. Bon
Manager

PETROLAB

FINGERPRINT ANALYSIS
BY CAPILLARY GAS CHROMATOGRAPHY
UEVCM SAND
On Stock Tank Oil from atmospheric flash of sample in cylinder # L - 602 ex TS - 9212

Component		Mol %
Hexanes minus	C6-	17.04
Hexanes	C6	12.89
Heptanes	C7	20.63
Octanes	C8	10.77
Nonanes	C9	9.31
Decanes	C10	6.07
Undecanes	C11	3.68
Dodecanes	C12	2.58
Tridecanes	C13	2.45
Tetradecanes	C14	1.84
Pentadecanes	C15	2.08
Hexadecanes	C16	1.40
Heptadecanes	C17	1.96
Octadecanes	C18	1.11
Nonadecanes	C19	0.88
Eicosanes	C20	0.86
Heneicosanes	C21	0.80
Docosanes	C22	0.69
Tricosanes	C23	0.62
Tetracosanes	C24	0.51
Pentacosanes	C25	0.44
Hexacosanes	C26	0.36
Heptacosanes	C27	0.30
Octacosanes	C28	0.24
Nonacosanes	C29	0.20
Triacontanes	C30	0.09
Hentriacontanes	C31	0.10
Dotriacontanes	C32	0.05
Tritriacontanes	C33	0.05
Tetratriacontanes	C34	0.00
Pentatriacontanes Plus	C35+	0.00
TOTAL		100.00

Molecular Weight Calculated *	:	125.7
Density @ 60 °F Calculated *	:	0.7596

*Calculation based on generalized properties as published by Katz and Firoozabadi

FINGERPRINT ANALYSIS
BY CAPILLARY GAS CHROMATOGRAPHY
UEVCM SAND
On Stock Tank Oil from atmospheric flash of sample in cylinder # L - 602 ex TS - 9212

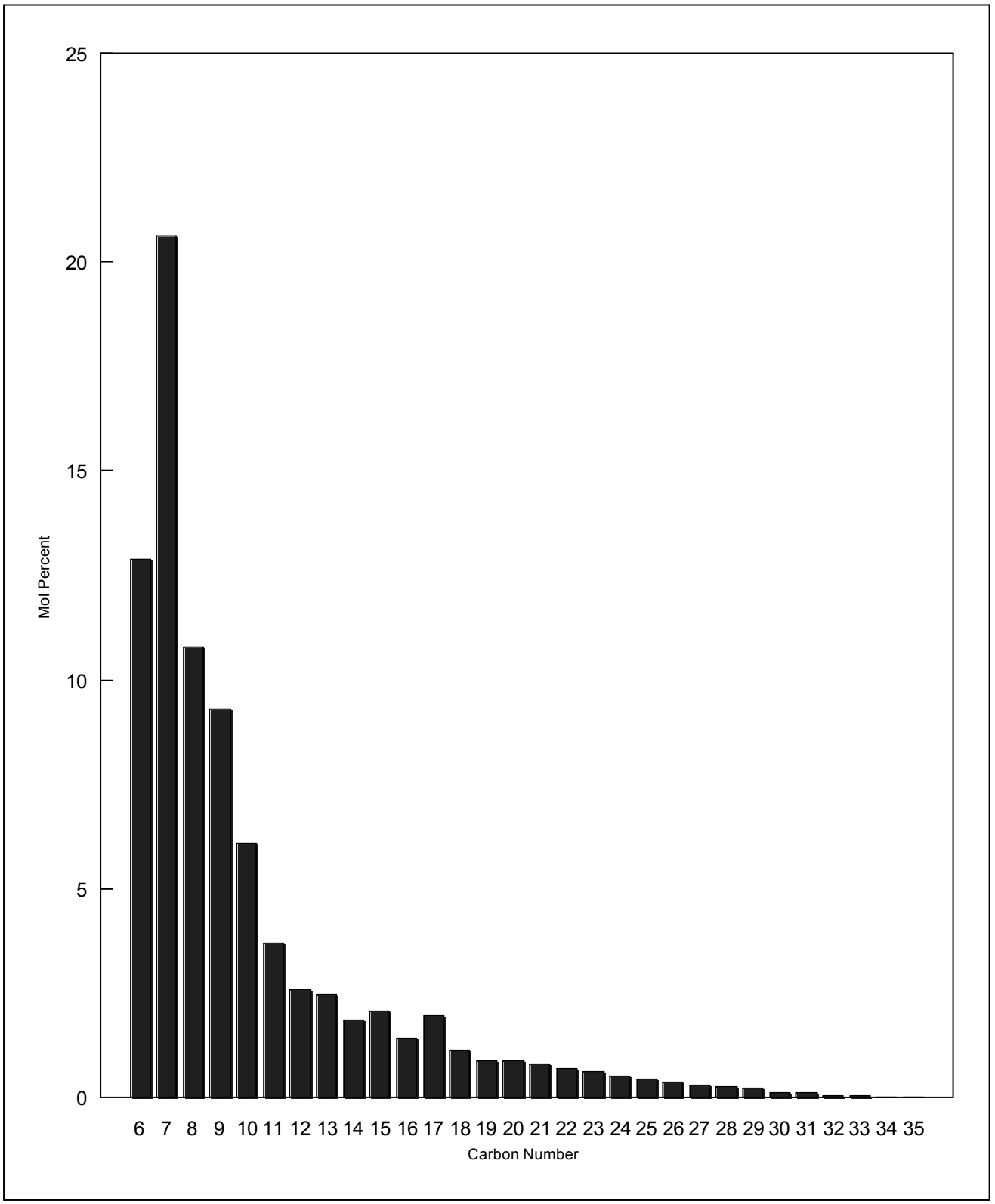

PETROLAB

COMPOSITIONAL ANALYSIS OF SEPARATOR LIQUID

UEVCM SAND

Cylinder # L - 602 ex TS - 9212

Component		Stock Tank Liquid Mol %	Stock Tank Gas Mol %	Separator Liquid Mol %
Hydrogen Sulphide	H2S	0.00	0.00	0.00
Carbon Dioxide	CO2	0.09	5.67	2.49
Nitrogen	N2	0.00	0.08	0.03
Methane	C1	0.17	28.20	12.21
Ethane	C2	0.58	16.12	7.26
Propane	C3	2.95	22.57	11.38
Iso-Butane	iC4	2.29	6.87	4.26
N-Butane	nC4	5.09	10.57	7.45
Iso-Pentane	iC5	4.17	3.24	3.77
N-Pentane	nC5	4.78	2.88	3.96
Hexanes	C6	12.41	2.27	8.05
Heptanes	C7	19.87	1.22	11.85
Octanes	C8	10.37	0.23	6.01
Nonanes	C9	8.96	0.07	5.14
Decanes	C10	5.85	0.01	3.34
Undecanes	C11	3.54	0.00	2.02
Dodecanes Plus	C12+	18.88	0.00	10.78
TOTAL		100.00	100.00	100.00

Ratios				
Molar Ratio	:	0.5702	0.4298	1.0000
Mass Ratio	:	0.8035	0.1965	1.0000
Liquid Ratio (bbl/bbl)	:	1.0000 @ SC	--	1.3970 @ PT*
Gas Liquid Ratio	:	1.0000 bbl @ SC	622 SCF	--
Stream Properties				
Molecular Weight	:	121.5	39.42	86.4
Density obs. (gm/cc)	:	0.7543 @ 60 °F	--	0.6740 @ PT*
Gravity (AIR = 1.000)	:	55.9 °API @ 60 °F	1.380	78.2
GHV (BTU/scf)	:	--	2151	--
Hexanes Plus Properties				
Mol %	:	79.89	3.80	47.19
Molecular Weight	:	136.7	90.1	135.1
Density (gm/cc @ 60 °F)	:	0.7792	0.6753	0.7765
Gravity (°API @ 60 °F)	:	49.9	77.8	50.6
Heptanes Plus Properties				
Mol %	:	67.47	1.53	39.14
Molecular Weight	:	146.4	99.0	145.6
Density (gm/cc @ 60 °F)	:	0.7907	0.6878	0.7894
Gravity (°API @ 60 °F)	:	47.3	74.0	47.6
Decanes Plus Properties				
Mol %	:	28.27	0.01	16.14
Molecular Weight	:	204.4	133.9	204.3
Density (gm/cc @ 60 °F)	:	0.8322	0.7277	0.8321
Gravity (°API @ 60 °F)	:	38.4	62.8	38.4
Undecanes Plus Properties				
Mol %	:	22.42	0.00	12.80
Molecular Weight	:	222.7	--	222.7
Density (gm/cc @ 60 °F)	:	0.8413	--	0.8413
Gravity (°API @ 60 °F)	:	36.5	--	36.5
Dodecanes Plus Properties				
Mol %	:	18.88	0.00	10.78
Molecular Weight	:	236.9	--	236.9
Density (gm/cc @ 60 °F)	:	0.8479	--	0.8479
Gravity (°API @ 60 °F)	:	35.2	--	35.2

* (P)ressure : 500 psig * (T)emperature : 85 °F

PETROLAB

Company : Origin Energy Resources Ltd.	Page : 4 of 12
Well : Yolla # 3	File : O - 24037

COMPOSITIONAL ANALYSIS OF SEPARATOR GAS CYLINDER # 5051-A UEVCM SAND

Component		Mol %	GPM
Hydrogen Sulphide	H2S	0.00	
Carbon Dioxide	CO2	7.35	
Nitrogen	N2	0.49	
Methane	C1	75.84	
Ethane	C2	9.04	2.419
Propane	C3	4.81	1.326
Iso-Butane	iC4	0.79	0.259
N-Butane	nC4	0.99	0.312
Iso-Pentane	iC5	0.23	0.084
N-Pentane	nC5	0.20	0.072
Hexanes	C6	0.15	0.058
Heptanes	C7	0.08	0.034
Octanes	C8	0.02	0.009
Nonanes	C9	0.01	0.005
Decanes	C10	0.00	0.000
Undecanes	C11	0.00	0.000
Dodecanes Plus	C12+	0.00	0.000
TOTAL		100.00	4.578

Pressure Base	:	14.696
Zsc	:	0.997
Mol Weight	:	21.96
Gas Gravity	:	0.761
Pc	:	692.9
Tc	:	402.9
Mol Weight C6+	:	90.9
Density C6+	:	0.6765
Mol Weight C7+	:	100.3
Density C7+	:	0.6895
Mol Weight C10+	:	--
Density C10+	:	--
Mol Weight C11+	:	--
Density C11+	:	--
Mol Weight C12+	:	--
Density C12+	:	--
Heating Value (BTU/ft3)		
Gross	:	1142
Nett	:	1035
Wobbe Index	:	1310
Zpt *	:	0.905

* (P)ressure : 500 psig * (T)emperature : 85 °F

Date Sampled: September 28, 2004 @ 09.53 - 10:10hrs

Laboratory Opening Pressure : 866 psig @ : 110 °F

SEPARATOR SAMPLES QUALITY CHECK

On Separator Samples From Gas Cylinder # 5051-A and Liquid Cylinder # L - 602 ex TS - 9212

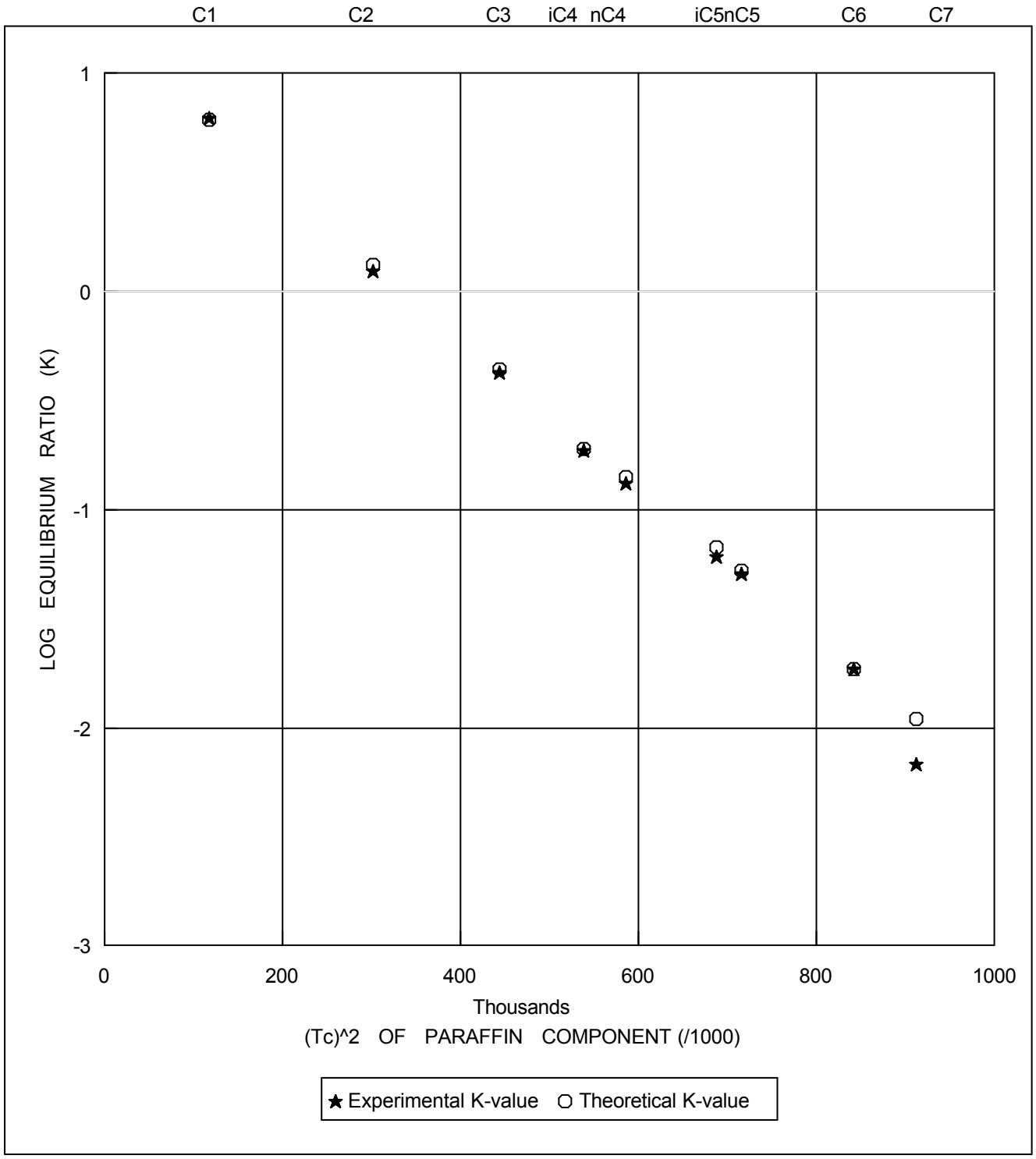

COMPOSITIONAL ANALYSIS OF RECOMBINED RESERVOIR FLUID

Using Separator Samples from UEVCM SAND in

Component		Cyl # L - 602 ex TS - 9212 Separator Liquid Mol %	Cyl # 5051-A Separator Gas Mol %	Recombined Fluid Mol %
Hydrogen Sulphide	H2S	0.00	0.00	0.00
Carbon Dioxide	CO2	2.49	7.35	7.05
Nitrogen	N2	0.03	0.49	0.46
Methane	C1	12.21	75.84	71.94
Ethane	C2	7.26	9.04	8.93
Propane	C3	11.38	4.81	5.21
Iso-Butane	iC4	4.26	0.79	1.00
N-Butane	nC4	7.45	0.99	1.39
Iso-Pentane	iC5	3.77	0.23	0.45
N-Pentane	nC5	3.96	0.20	0.43
Hexanes	C6	8.05	0.15	0.63
Heptanes	C7	11.85	0.08	0.80
Octanes	C8	6.01	0.02	0.39
Nonanes	C9	5.14	0.01	0.32
Decanes	C10	3.34	0.00	0.20
Undecanes	C11	2.02	0.00	0.12
Dodecanes Plus	C12+	10.78	0.00	0.68
TOTAL		100.00	100.00	100.00

Ratios

Molar Ratio	:	0.0613	0.9387	1.0000
Mass Ratio	:	0.2043	0.7957	1.0000
Liquid Ratio (bbl/bbl)	:	1.0000	--	-- @ PT**
Gas Liquid Ratio	:	1.0000 @ PT*	15898 SCF ***	--

Stream Properties

Molecular Weight	:	86.39	21.96	25.91
Density obs. (gm/cc)	:	0.6740 @ PT*	--	-- @ PT**
Gravity (AIR = 1.000)	:	78.24 API @ 60 ° F	0.761	--
GHV (BTU/scf)	:	--	1142	--

Hexanes Plus Properties

Mol %	:	47.19	0.26	3.14
Molecular Weight	:	135.1	90.9	131.7
Density (gm/cc @ 60 °F)	:	0.7765	0.6765	0.7704
Gravity (°API @ 60 °F)	:	50.6	77.5	52.0

Heptanes Plus Properties

Mol %	:	39.14	0.11	2.51
Molecular Weight	:	145.6	100.3	143.7
Density (gm/cc @ 60 °F)	:	0.7894	0.6895	0.7861
Gravity (°API @ 60 °F)	:	47.6	73.5	48.3

Decanes Plus Properties

Mol %	:	16.14	0.00	1.00
Molecular Weight	:	204.3	--	204.3
Density (gm/cc @ 60 °F)	:	0.8321	--	0.8321
Gravity (°API @ 60 °F)	:	38.4	--	38.4

Undecanes Plus Properties

Mol %	:	12.80	0.00	0.80
Molecular Weight	:	222.7	--	222.7
Density (gm/cc @ 60 °F)	:	0.8413	--	0.8413
Gravity (°API @ 60 °F)	:	36.5	--	36.5

Dodecanes Plus Properties

Mol %	:	10.78	0.00	0.68
Molecular Weight	:	236.9	--	236.9
Density (gm/cc @ 60 °F)	:	0.8479	--	0.8479
Gravity (°API @ 60 °F)	:	35.2	--	35.2

* (P)ressure : 500 psig * (T)emperature : 85 °F

** **Dew Point (P)ressure : 5280 psig @ Reservoir (T)emperature : 209 °F**

*** 15898 SCF / SEP BBL @ PT = 22210 SCF / ST BBL

22210 = 22210 * (1.1466 * 1.0512) / (1.1466 * 1.0512)

FINGERPRINT ANALYSIS
BY CAPILLARY GAS CHROMATOGRAPHY
On Stock Tank Oil from atmospheric flash of sample in cylinder # PVT Cell

Component		Mol %
Hexanes minus	C6-	4.71
Hexanes	C6	7.07
Heptanes	C7	22.94
Octanes	C8	18.54
Nonanes	C9	18.84
Decanes	C10	11.90
Undecanes	C11	6.06
Dodecanes	C12	3.53
Tridecanes	C13	2.63
Tetradecanes	C14	1.49
Pentadecanes	C15	1.21
Hexadecanes	C16	0.51
Heptadecanes	C17	0.38
Octadecanes	C18	0.08
Nonadecanes	C19	0.06
Eicosanes	C20	0.02
Heneicosanes	C21	0.01
Docosanes	C22	0.01
Tricosanes	C23	0.01
Tetracosanes	C24	0.00
Pentacosanes	C25	0.00
Hexacosanes	C26	0.00
Heptacosanes	C27	0.00
Octacosanes	C28	0.00
Nonacosanes	C29	0.00
Triacontanes	C30	0.00
Hentriacontanes	C31	0.00
Dotriacontanes	C32	0.00
Tritriacontanes	C33	0.00
Tetratriacontanes	C34	0.00
Pentatriacontanes Plus	C35+	0.00
TOTAL		100.00

Molecular Weight Calculated *	:	117.7
Density @ 60 °F Calculated *	:	0.7535

*Calculation based on generalized properties as published by Katz and Firoozabadi

FINGERPRINT ANALYSIS
BY CAPILLARY GAS CHROMATOGRAPHY
On Stock Tank Oil from atmospheric flash of sample in cylinder # PVT Cell

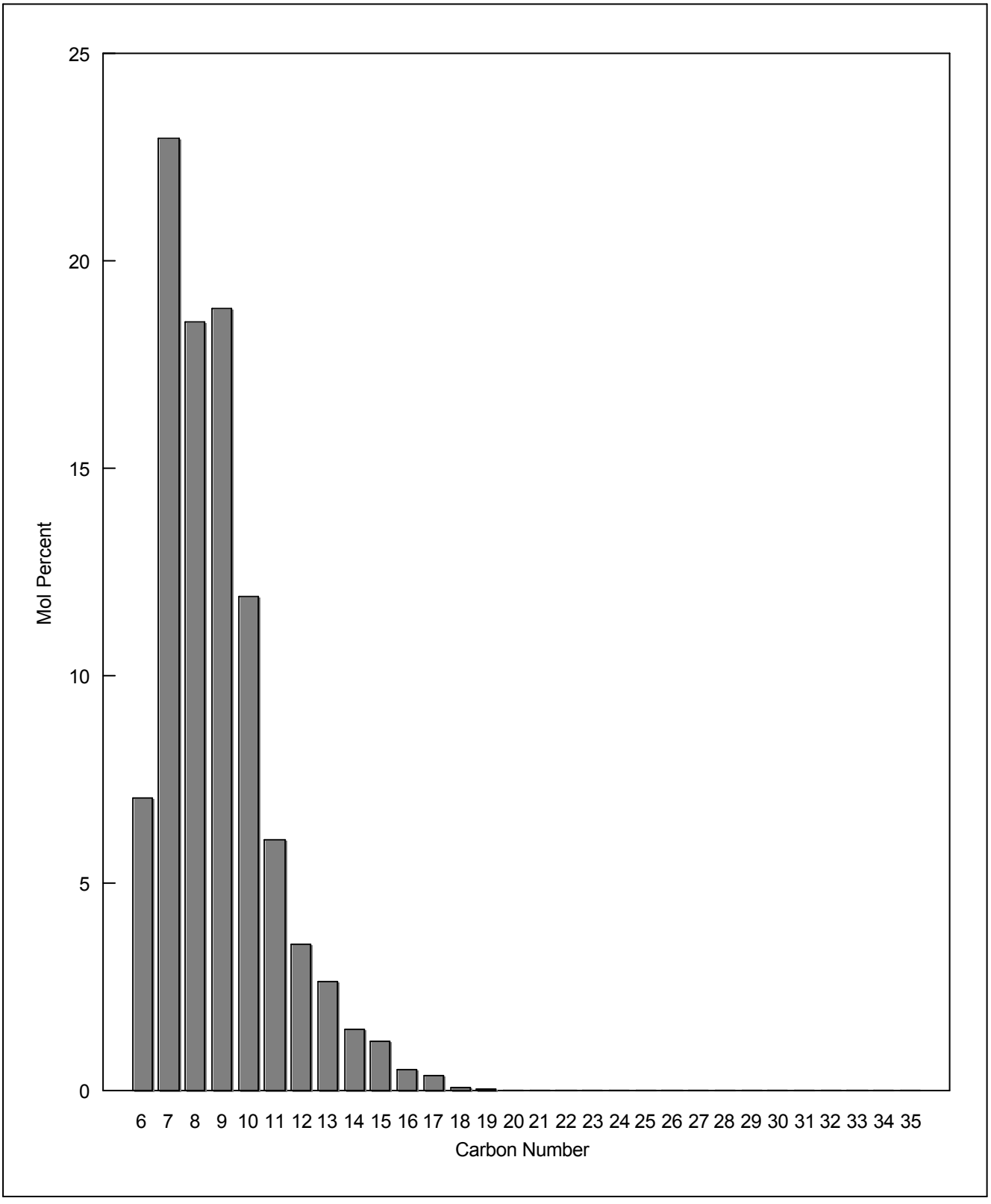

PETROLAB

Company : Origin Energy Limited	Page : 9 of 12
Well : Yolla # 3	File : O-24037

COMPOSITIONAL ANALYSIS OF GAS CAP (97.9 %)

UEVCM SAND

FROM PVT CELL AT 2695 PSIG & 209 °F

Component		Stock Tank Liquid Mol %	Stock Tank Gas Mol %	Reservoir Fluid Mol %
Hydrogen Sulphide	H2S	0.00	0.00	0.00
Carbon Dioxide	CO2	0.10	6.85	6.77
Nitrogen	N2	0.00	0.33	0.33
Methane	C1	0.43	74.05	73.21
Ethane	C2	0.31	8.96	8.86
Propane	C3	0.63	5.16	5.11
Iso-Butane	iC4	0.28	0.92	0.91
N-Butane	nC4	0.59	1.33	1.32
Iso-Pentane	iC5	0.49	0.42	0.42
N-Pentane	nC5	0.63	0.42	0.42
Hexanes	C6	7.16	0.55	0.63
Heptanes	C7	23.24	0.57	0.83
Octanes	C8	18.78	0.23	0.44
Nonanes	C9	19.09	0.15	0.37
Decanes	C10	12.06	0.05	0.19
Undecanes	C11	6.14	0.01	0.08
Dodecanes Plus	C12+	10.07	0.00	0.11
TOTAL		100.00	100.00	100.00

Ratios				
Molar Ratio	:	0.0115	0.9885	1.0000
Mass Ratio	:	0.0548	0.9452	1.0000
Liquid Ratio (bbl/bbl)	:	1.0000 @ SC	--	-- @ PT*
Gas Liquid Ratio	:	1.0000 bbl @ SC	74014 SCF	--
Stream Properties				
Molecular Weight	:	116.9	23.39	24.46
Density obs. (gm/cc)	:	0.7547 @ 60 °F	--	-- @ PT*
Gravity (AIR = 1.000)	:	55.8 °API @ 60 °F	0.811	--
GHV (BTU/scf)	:	--	1235	--
Hexanes Plus Properties				
Mol %	:	96.55	1.56	2.65
Molecular Weight	:	119.2	97.3	106.5
Density (gm/cc @ 60 °F)	:	0.7591	0.6855	0.7181
Gravity (°API @ 60 °F)	:	54.7	74.7	65.4
Heptanes Plus Properties				
Mol %	:	89.38	1.01	2.02
Molecular Weight	:	122.0	104.6	113.4
Density (gm/cc @ 60 °F)	:	0.7636	0.6951	0.7308
Gravity (°API @ 60 °F)	:	53.6	71.9	61.9
Decanes Plus Properties				
Mol %	:	28.27	0.06	0.38
Molecular Weight	:	154.1	136.1	151.0
Density (gm/cc @ 60 °F)	:	0.7961	0.7299	0.7860
Gravity (°API @ 60 °F)	:	46.1	62.2	48.4
Undecanes Plus Properties				
Mol %	:	16.21	0.01	0.19
Molecular Weight	:	169.0	146.9	167.9
Density (gm/cc @ 60 °F)	:	0.8072	0.7399	0.8040
Gravity (°API @ 60 °F)	:	43.6	59.6	44.3
Dodecanes Plus Properties				
Mol %	:	10.07	0.00	0.11
Molecular Weight	:	182.4	--	182.4
Density (gm/cc @ 60 °F)	:	0.8164	--	0.8164
Gravity (°API @ 60 °F)	:	41.7	--	41.7

* (P)ressure : 2695 psig * (T)emperature : 209 °F

FINGERPRINT ANALYSIS
BY CAPILLARY GAS CHROMATOGRAPHY
On Stock Tank Oil from atmospheric flash of sample in cylinder # PVT Cell

Component		Mol %
Hexanes minus	C6-	6.24
Hexanes	C6	5.13
Heptanes	C7	10.34
Octanes	C8	6.37
Nonanes	C9	7.05
Decanes	C10	5.84
Undecanes	C11	4.29
Dodecanes	C12	3.87
Tridecanes	C13	4.32
Tetradecanes	C14	3.83
Pentadecanes	C15	4.79
Hexadecanes	C16	3.82
Heptadecanes	C17	5.07
Octadecanes	C18	3.30
Nonadecanes	C19	2.97
Eicosanes	C20	2.83
Heneicosanes	C21	2.68
Docosanes	C22	2.42
Tricosanes	C23	2.27
Tetracosanes	C24	2.07
Pentacosanes	C25	1.89
Hexacosanes	C26	1.59
Heptacosanes	C27	1.49
Octacosanes	C28	1.20
Nonacosanes	C29	1.13
Triacontanes	C30	0.95
Hentriacontanes	C31	0.83
Dotriacontanes	C32	0.68
Tritriacontanes	C33	0.44
Tetratriacontanes	C34	0.19
Pentatriacontanes Plus	C35+	0.11
TOTAL		100.00

Molecular Weight Calculated *	:	193.5
Density @ 60 °F Calculated *	:	0.8243

*Calculation based on generalized properties as published by Katz and Firoozabadi

FINGERPRINT ANALYSIS
BY CAPILLARY GAS CHROMATOGRAPHY
On Stock Tank Oil from atmospheric flash of sample in cylinder # PVT Cell

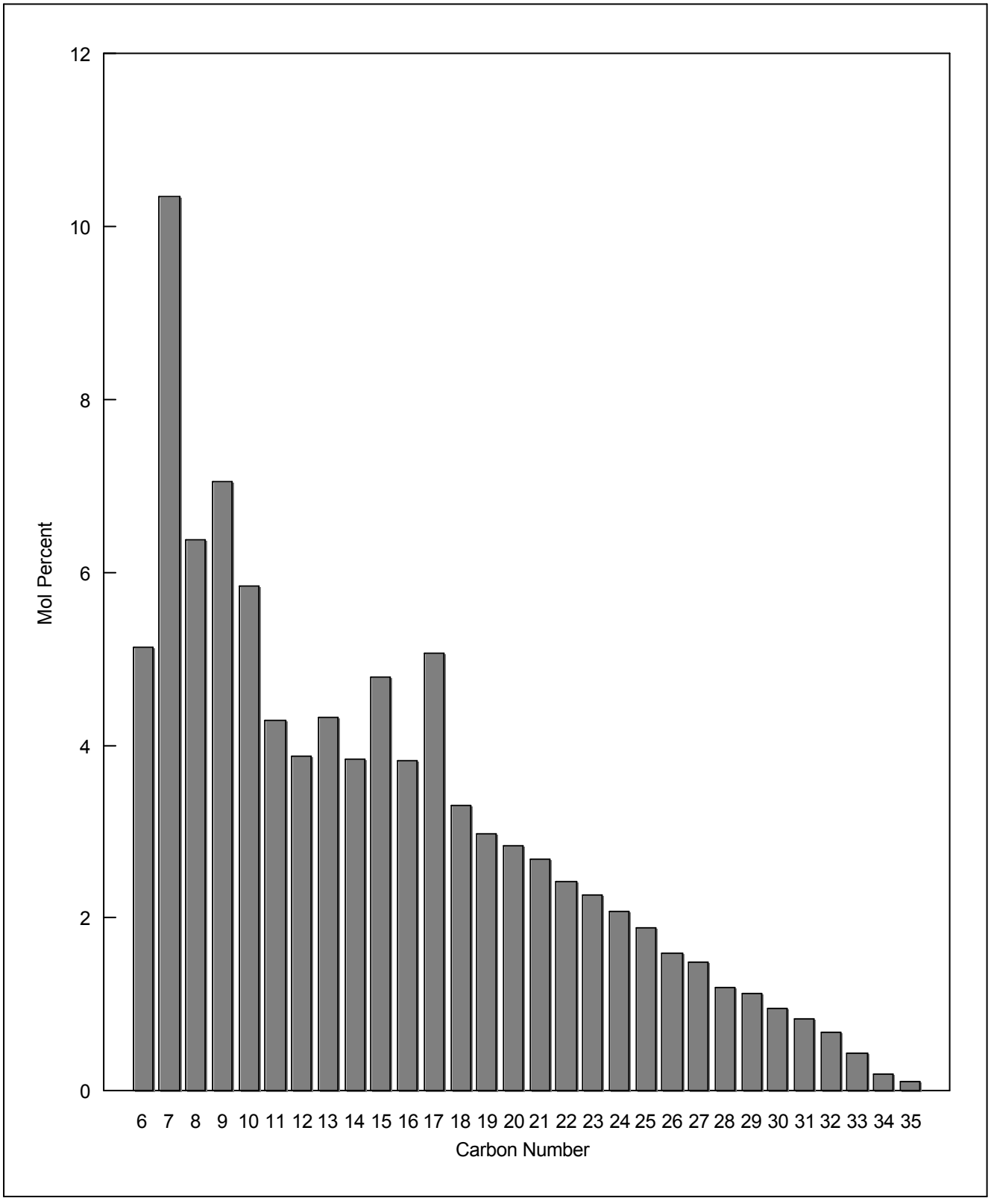

PETROLAB

Company : Origin Energy Limited	Page : 12 of 12
Well : Yolla # 3	File : O-24037

COMPOSITIONAL ANALYSIS OF OIL LEG (2.1 %)

UEVCM SAND

FROM PVT CELL AT 2695 PSIG & 209 °F

Component		Stock Tank Liquid Mol %	Stock Tank Gas Mol %	Reservoir Fluid Mol %
Hydrogen Sulphide	H2S	0.00	0.00	0.00
Carbon Dioxide	CO2	0.11	7.54	4.49
Nitrogen	N2	0.00	0.23	0.14
Methane	C1	0.35	59.64	35.30
Ethane	C2	0.47	13.43	8.11
Propane	C3	1.32	10.59	6.79
Iso-Butane	iC4	0.73	2.31	1.66
N-Butane	nC4	1.53	3.38	2.62
Iso-Pentane	iC5	1.24	1.03	1.12
N-Pentane	nC5	1.44	0.93	1.14
Hexanes	C6	5.08	0.52	2.39
Heptanes	C7	10.24	0.16	4.30
Octanes	C8	6.31	0.13	2.67
Nonanes	C9	6.98	0.08	2.91
Decanes	C10	5.78	0.03	2.39
Undecanes	C11	4.25	0.00	1.74
Dodecanes Plus	C12+	54.19	0.00	22.23
TOTAL		100.00	100.00	100.00

Ratios				
Molar Ratio	:	0.4105	0.5895	1.0000
Mass Ratio	:	0.8303	0.1697	1.0000
Liquid Ratio (bbl/bbl)	:	1.0000 @ SC	--	1.5237 @ PT*
Gas Liquid Ratio	:	1.0000 bbl @ SC	822 SCF	--
Stream Properties				
Molecular Weight	:	191.4	27.25	94.65
Density obs. (gm/cc)	:	0.8237 @ 60 °F	--	0.6518 @ PT*
Gravity (AIR = 1.000)	:	40.1 °API @ 60 °F	0.946	85.4
GHV (BTU/scf)	:	--	1430	--
Hexanes Plus Properties				
Mol %	:	92.81	0.92	38.63
Molecular Weight	:	201.9	94.2	200.4
Density (gm/cc @ 60 °F)	:	0.8317	0.6812	0.8305
Gravity (°API @ 60 °F)	:	38.5	76.0	38.7
Heptanes Plus Properties				
Mol %	:	87.74	0.40	36.24
Molecular Weight	:	208.7	107.4	208.0
Density (gm/cc @ 60 °F)	:	0.8359	0.6986	0.8354
Gravity (°API @ 60 °F)	:	37.6	70.9	37.7
Decanes Plus Properties				
Mol %	:	64.22	0.03	26.36
Molecular Weight	:	246.2	134.0	246.1
Density (gm/cc @ 60 °F)	:	0.8530	0.7278	0.8530
Gravity (°API @ 60 °F)	:	34.2	62.7	34.2
Undecanes Plus Properties				
Mol %	:	58.44	0.00	23.97
Molecular Weight	:	257.3	--	257.3
Density (gm/cc @ 60 °F)	:	0.8573	--	0.8573
Gravity (°API @ 60 °F)	:	33.4	--	33.4
Dodecanes Plus Properties				
Mol %	:	54.19	0.00	22.23
Molecular Weight	:	265.9	--	265.9
Density (gm/cc @ 60 °F)	:	0.8605	--	0.8605
Gravity (°API @ 60 °F)	:	32.8	--	32.8

* (P)ressure : 2695 psig * (T)emperature : 209 °F

ENCLOSURE 1: COMPOSITE LOG

Yolla-3
Composite Well Log

Origin energy

Well Location

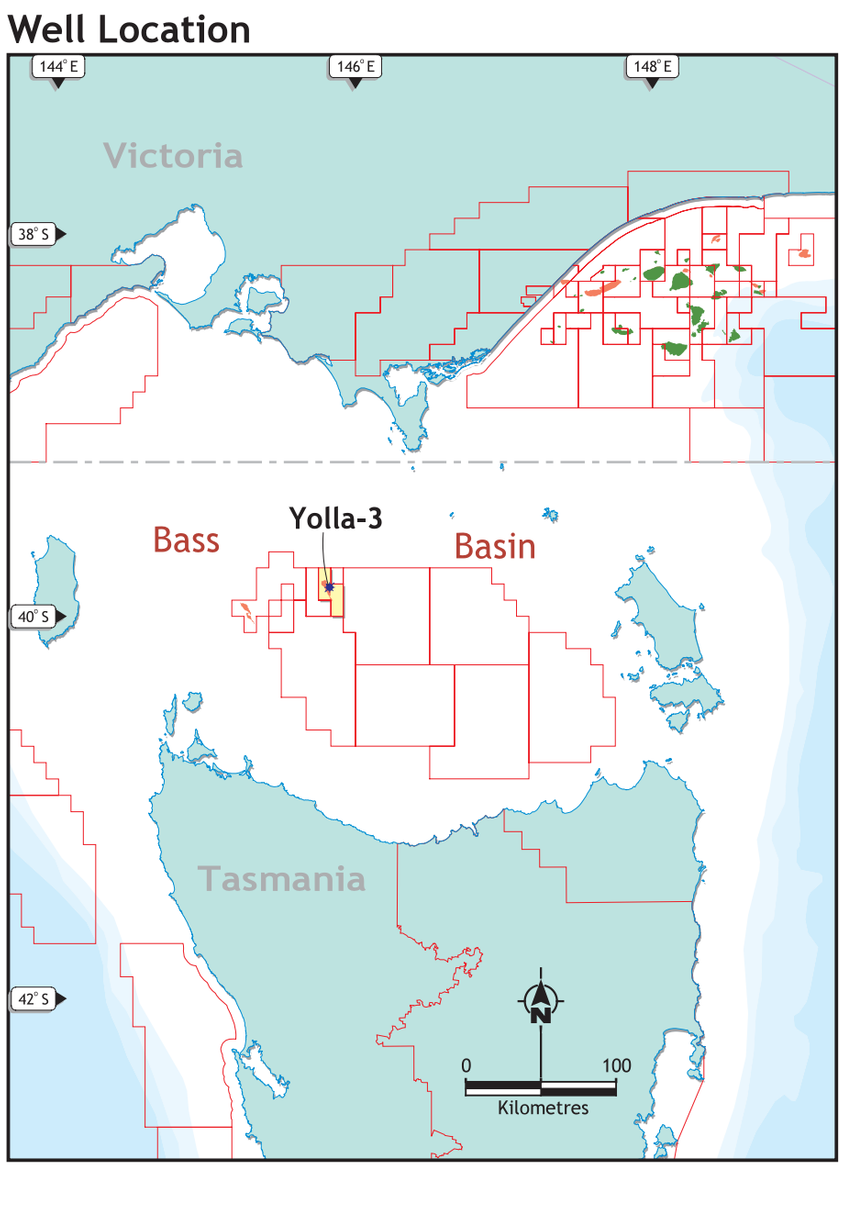

Well Data Card

Well Name:	Yolla 3
Permit:	T/L1 Offshore Bass Basin
Well Path:	Deviated
Top Hole Location:	Latitude: 39° 50' 40.4707" South Longitude: 145° 49' 06.0849" East Easting: 398 905.69 metres Northing: 5 588 825.22 metres (GDA 94; AMG Zone 55, Central Meridian 147° East)
Seismic Location:	Yolla 3D Seismic Survey, In-line 480, X-line 1000
Bottom Hole Location:	664.2m north and 1091.7m west of surface location
Elevation:	43m (RT-sea level)
Water Depth:	80.8m LAT
Total Depth Driller:	3497 mMDRT
(TVD) Driller:	3100 mTVDRT
Rig on tow:	17:30hrs 06/06/2004
Rig on Location:	20:00hrs 06/06/2004
Spud:	03:00hrs 11/08/2004
Reached TD:	11:30hrs 04/09/2004
Rig Released:	10:00hrs 30/09/2004
Total Rig Days:	54
Well Status:	Cased Gas Producer
Permit Interests:	Origin Energy Resources Ltd 32.5% (Operator) Origin Energy Northwest Pty Ltd 5% AWE Petroleum Pty Ltd 30% CalEnergy Gas (Australia) Ltd 20% Wandoo Petroleum Pty Ltd 12.5%
Rig Name:	ENSCO 102 (Jack-up)
Drilling Contractor:	ENSCO Australia Pty Ltd
Approx. Well Cost:	A$23,329,727

Casing Schematic

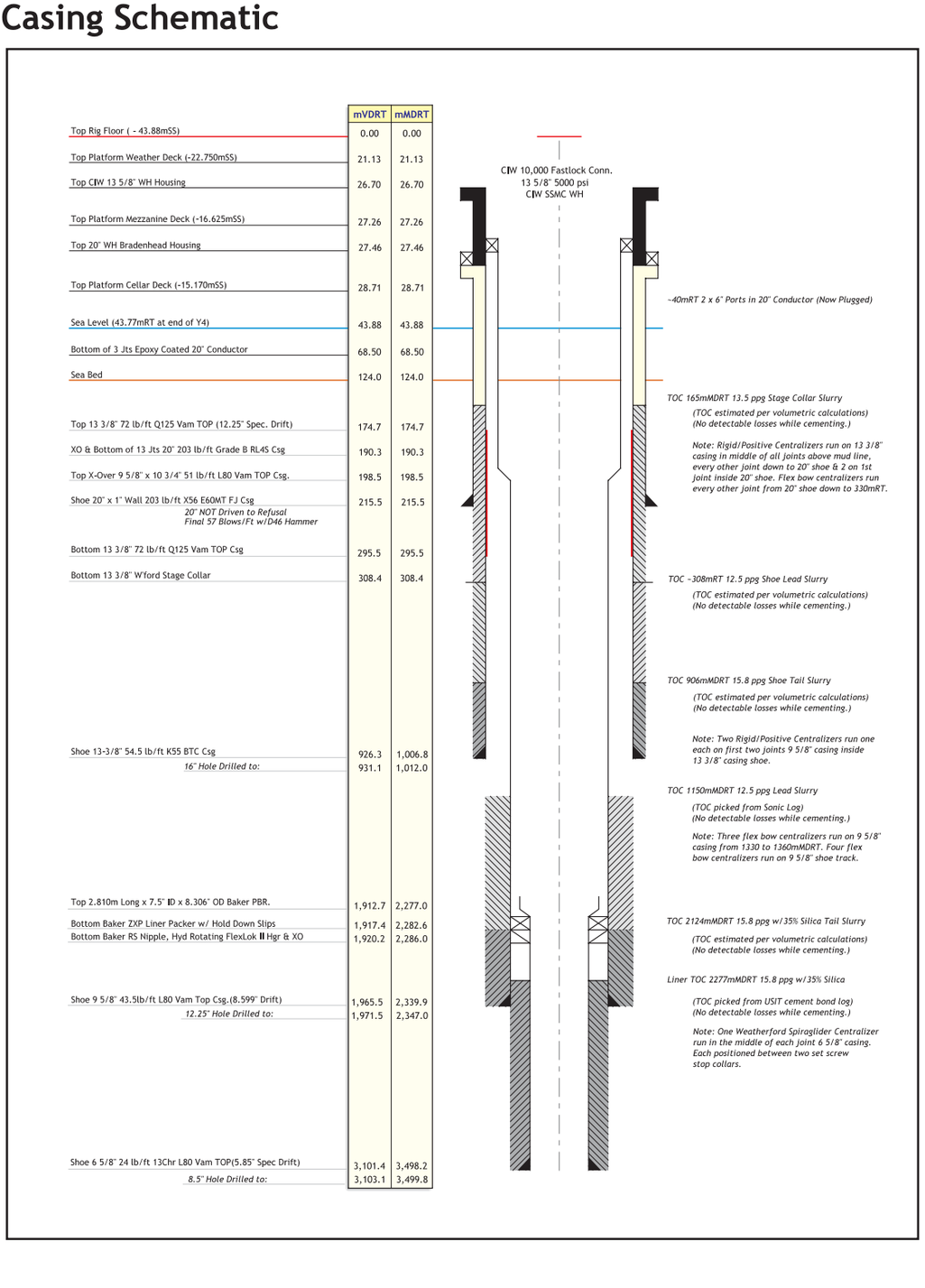

Time vs Depth

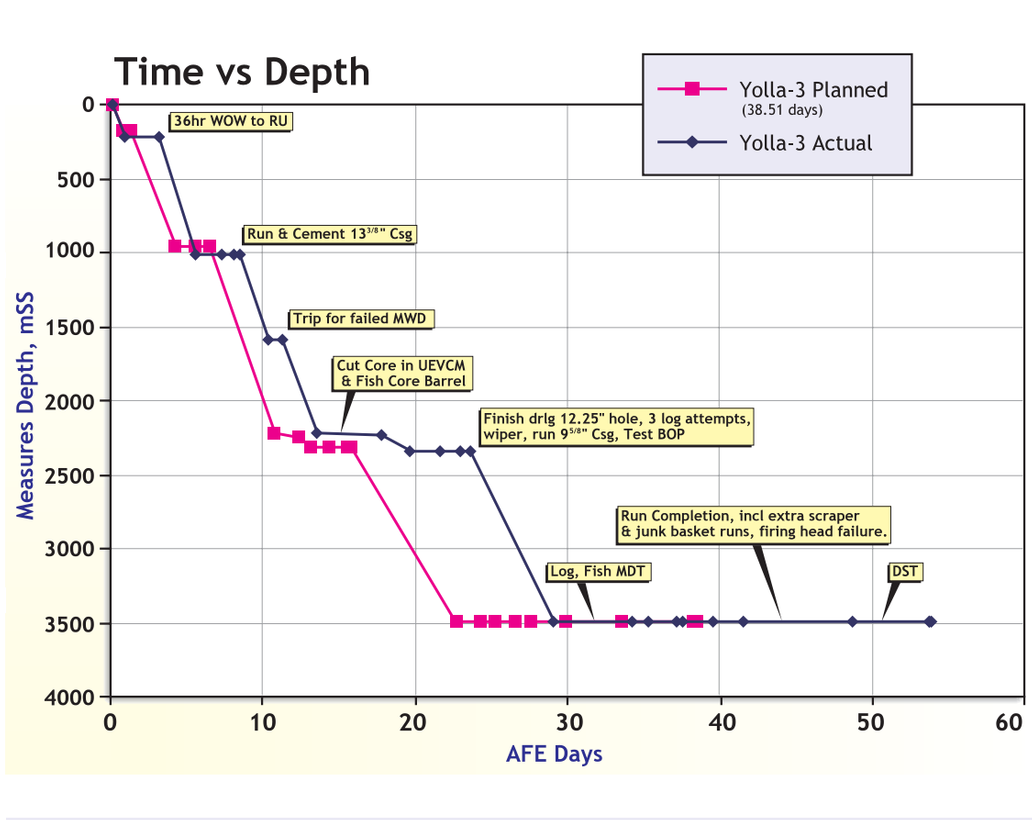

Formation Tops

Formation / Seismic Marker	Tops (m) m MDRT	m TVDSS	THICK (rel to TVD)	TWT (ms)	Remarks/Shows
Torquay Group	123.8	80.8	963.3	128	No Returns 123.8 - 1017.0 mMDRT. Claystone, calcareous.
Upper Angahook Formation	1221.6	1044.1	191.6	868	Claystone, calcareous in part
Angahook Volcanics	1486.0	1235.7	130.0	1028	Volcanic Tuff interbedded with claystone and sandstone and minor siltstone
Angahook Oligocene	1659.0	1365.7	292.3	1136	Interbedded sandstone, siltstone and claystone, grain size decreasing with depth
Demons Bluff Formation	2034.0	1658.0	129.6	1378	Siltstone with minor interbedded sandstone and occasional dolomite
Eastern View Coal Measures	2184.8	1787.6	1233.4	1487	Interbedded Sandstone, coal, siltstone and minor claystone
TEV4	*2217.5*	*1816.0*	*8.2*	*1510*	*Sandstone (oil)*
TEV4 OWC	*2234.7*	*1831.0*	*NA*		
2458 sand	*2902.8*	*2464.4*	*16.3*	*1922*	*Water bearing sand (oil in Yolla 4)*
Igneous Intrusive	*2994.5*	*2555.5*	*64.4*	*1974*	*Gabbro*
2718 sand	*3145.3*	*2705.8*	*8.2*	*2043*	*Water bearing sandstone*
2755 sand	*3179.8*	*2740.2*	*16.2*	*2061*	*Gas-bearing sandstone*
2809 sand	*3236.5*	*2796.9*	*23.4*	*2090*	*Gas-bearing sandstone*
2844 sand	*3269.6*	*2830.0*	*11.0*	*2107*	*Tight Sandstone*
2873 sand	*3300.6*	*2861.0*	*10.3*	*2123*	*Tight sandstone*
2952 sand	*3383.0*	*2943.3*	*10.4*	*2164*	*Tight sandstone*
2973 sand	*3404.1*	*2964.4*	*19.5*	*2174*	*Gas-bearing sandstone*
Basal Volcanics	3460.7	3021.0	36.3+	2202	Volcanics: basalt and weathered basalt
Total Depth	3497.0	3057.3			

Wireline Log Runs

Suite #	Run #	Logs Acquired	Interval (mMDRT)
1	1	PEX-HRLA-CMR-SP-GR-LEHQT	3474 m - surface
1	2	FMI-DSI-HNGS-ECS-LEHQT	3494 - 1000 m (HNGS-DSI to 120)
1	3	MDT-GR (pre-tests)	3479.5 - 3148.6 m
1	4	MDT-GR (sampling)	3420.6 - 3149 m
1	5	USIT-CBL-VDL-GR-CCL	3453 - 2281 m
1	6	USIT-CBL-VDL-GR-CCL	2265 - 1350 m
1	7-11	4 ½", 12 spf, HSD 34JL, Pure Perforating Record	3248.5 - 2210.2 m
1	12-13	CPST Packer Set, Packer Setting Record	3258 - 3258

Logging Parameters

Suite	Run	Bit Size	Fluid Type	Density (lbm/gal)	Viscosity (s)	Fluid Loss (cm3)	pH	RM @ measured Temp (ohm.m@oC)	RMF @ measured Temp (ohm.m@oC)	RMC @ measured Temp (ohm.m@oC)
1	1-4	8 ½"	Sea Water Drispac Soltex	9.45	98	3.1	8.9	0.184 @26°C	0.147 @26°C	0.229 @24°C

Temperature Data Recorded During Wireline Logging

Suite #	Run #	Maximum Recorded Temperature (°C)	Bottom Hole Depth (mRT)	Time Circulation Stopped	Time Logger on bottom
1	1	132	3491	05/09/04 06:00	05/09/04 21:00
1	2	143	3483	05/09/04 06:00	06/09/04 15:05
1	3	148	3479.5	05/09/04 06:00	07/09/04 20:16
1	4	146	3420.6	05/09/04 06:00	08/09/04 02:50

Yolla-3-CWL.dgn 03-05

Lithologies

Shale · Siltstone · Sandstone · Coal · Volcanics · Dolomitic Sandstone

Legend

Cement plug · Casing shoe · Core recovered · MDT Data: Invalid point, Valid point · Side wall cores: Attempted, Recovered · Perforation